

Frontier Areas in Chemical Technologies

Editors

P. MANISANKAR

K. GURUNATHAN

C. SEKAR

T. STALIN

G. GOPU

S. VISWANATHAN



ALAGAPPA UNIVERSITY

(Re-accredited with 'A' Grade by NAAC)

Karaikudi-630 003, Tamil Nadu, India.



Padma bhushan
Vallal Dr. RM. ALAGAPPA CHETTIAR

Frontier Areas in Chemical Technologies

Editors

P. Manisankar

K. Gurunathan

C. Sekar

T. Stalin

G. Gopu

S. Viswanathan



ALAGAPPA UNIVERSITY

(A State University Re-accredited with 'A' Grade by NAAC)

Karaikudi - 630 003

First Impression: 2016

© Alagappa University, Tamil Nadu

Frontier Areas in Chemical Technologies

**A Compendium of Research Papers presented in the International Conference FACTs
2016, March 21-23, 2016**

Conference Organised by:

Department of Industrial Chemistry

Department of Bioelectronics & Biosensors

Department of Nanoscience and Technology

Alagappa University, Karaikudi-6300 003.

ISBN: 978-81-928690-7-0

Price : ` 1,000/- \$ 30

No part this publication may be reproduced or transmitted in any form by any means, electronic or mechanical, including photocopy, recording, or any information storage and retrieval system, without permission in writing from the copyright owners.

DISCLAIMER

The authors are solely responsible for the contents of the papers compiled in this volume. The publishers or editors do not take any responsibility for the same in any manner. Errors, if any, are purely unintentional and readers are requested to communicate such errors to the editors or publishers to avoid discrepancies in future.

Published by

Alagappa University

Karaikudi-630 002.

Typeset by:

Department of Industrial Chemistry

Alagappa University, Karaikudi – 630 003

Printed by:

Poocharam Printers,

Karaikudi – 630 002.

ALAGAPPA UNIVERSITY
(Re-accredited with 'A' Grade by NAAC)
ALAGAPPA NAGAR, KARAIKUDI- 630 003, TAMIL NADU, INDIA.

Prof. S.Subbiah, M.A., M.Ed., M.Phil., Ph.D.,
VICE- CHANCELLOR



Off : 04565 - 225200
Resi : 04565 - 225201
Fax : 04565 - 225202
Mobile: 94890 79080, 94422 82517
E-mail : vicechancelloralu@gmail.com

FOREWORD

This compendium contains extended abstracts of the International Conference on Frontier Areas in Chemical Technologies 2016 (FACTs 2016). The conference is sponsored by Alagappa University, Karaikudi, from Alagappa University Research Fund (AURF). This is a logical sequel to the dynamism exhibited by Alagappa University aligned with its innate technical and research strengths.


Sustained research and development in chemical technologies and their advancements will be helpful in improving the quality of life of the mankind, solving environmental problems and preservation of natural resources. The present expectation is that this field will bring innovation and changes in daily life for sustainable tomorrow. Thus, the development of chemical technologies should be in accordance with the needs and requirements for the next generation. Examining the current practices and determining the policies of the future endeavours is another focal point of the International Conference organised during 21-23 March 2016.

The conference program has featured a wide variety of invited and contributed lectures, oral presentations as well as poster sessions. This conference has brought together researchers and experts working in this field to exchange ideas, share best practices, and discuss critical issues and concerns impacting the implementation and success. It has provided a platform for participants to share and discuss recent findings of their research covering all topics related to chemical technologies and crystallise new ideas. I recognize the importance of this International Conference especially when India is preparing to articulate policies and initiatives for 'MAKE IN INDIA'. Thanks to the experts for their initiatives to strengthen this process reflected in the diversity of subjects and expertise in conjunction with the growing recognition of the issues associated with the phenomenon.

This compendium of research papers presented at the International Conference on Frontier Areas in Chemical Technologies 2016 would serve as an important collection for the divulgation of research in the field of chemical technologies. It is an invaluable resource for researchers, academicians and industrialists being the first compendium of extended abstracts of FACTs 2016. It publishes high-quality articles on fundamental and applied research.

The program for this conference required the dedicated efforts of many people. I wish to congratulate Dr. P. Manisankar, Professor & Head, Department of Industrial Chemistry, Dr.C.Sekar, Professor & Head, Department of Bioelectronics and Biosensors and Dr.K.Gurunathan, Professor & Head, Department of Nanoscience and Technology, Alagappa University, Karaikudi, for taking the initiative to organize the international conference. Secondly, I thank the members of the Program Committee and the reviewers for their diligent and professional work. I thank the invited speakers for their invaluable contribution. I wish all the speakers and delegates a fruitful participation and an unforgettable stay in the town of Karaikudi.

Date : 18.3.2016


(S. Subbiah)

Preface

Chemical technologies involving Green Chemistry, Material Chemistry, Electrochemistry, Textile Chemistry, Nanoscience, Computational Chemistry, etc., are the challenging as well as fascinating branches of advanced technologies and they find applications in almost all areas of Science and Technology. It is important for the researchers, educators and developers from academic institution and industries to know the research and recent developments that have been made on various aspects of Chemical and Electrochemical Sciences and Technologies. The present conference on **Frontier Areas in Chemical Technologies (FACTs-2106)** is the First International Conference organized by the Departments of Industrial Chemistry, Bioelectronics & Biosensors and Nanoscience & Technology to focus on the update of recent advancements in different areas of chemical science and technologies. The aim of this international conference is to provide a forum to all the chemists, physicists, biologists and material scientists and technologists and researchers to discuss their recent findings and information and to promote cooperation both nationally and internationally. The invited talks and papers focus mainly on various advanced aspects of Chemical Technologies such as Electrochemical Technologies, Nanoscience and Technology, Sensor Technologies, Supramolecular and Photochemical Technologies, Green Chemical Technologies and other allied technologies-

It is indeed a matter of great pleasure and satisfaction to the Editors to present this volume containing collection of extended abstracts of the presented in the International FACTS 2016 held at Alagappa University, Karaikudi during 21-23 March 2016. There are about 14 Invited Talks, 119 Oral Presentations and 143 Poster Presentations. In addition, the programme includes open forum discussions. About 250 delegates from various Research Institutes, Universities, Colleges and Industries in India including four Invited Speakers from overseas participate in the conference.

The editors are thankful to **Prof. S. Subbiah**, Vice-Chancellor, Alagappa University, Karaikudi for supporting all the activities of this International Conference and advising in promoting the research culture among the young researchers. Our sincere thanks are to all the **Syndicate Members, Prof. V. Balachandran**, Registrar and Authorities of Alagappa University, Karaikudi for their constant support and encouragement. The editors are pleased to acknowledge all the sponsors. Sincere thanks are due to the Organizing Committee Members of the conference, Faculty Members, Research Scholars and Students of the Departments of Industrial Chemistry, Bioelectronics & Biosensors and Nanoscience & Technology. We also thank all the authors for submitting their extended abstracts in time.

We hope all the delegates had a pleasant stay in Karaikudi and stimulating discussions during the International Conference on FACTS 2016.

Editors

CONTENTS

1.	ELECTROCHEMICAL TECHNOLOGIES	
1.1	Intrinsically microporous polymers and membranes in electrochemistry <i>Frank Marken, Elena Madrid, Yuanyang Rong, Daping He, Richard Malpass-Evans, Mariolino Carta, Neil B. McKeown</i>	1
1.2	Recent trends on the advanced materials for battery application <i>G.A. Pathanjali and M. Nagarajan</i>	1
1.3	Surface engineering of porous metal nanostructures: Synthesis, fabrication and their applications in electro-catalysis and electrochemical biosensors <i>C. Sivakumar</i>	2
1.4	Electrochemical synthetic route for the generation of WO ₃ thin films <i>Akshay V. Salkar, Mamta Prabhugaonkar and Purnakala Samant</i>	2
1.5	Electrocatalytic reduction of dioxygen on 9, 10-anthraquinones-incorporated carbon nano tubes modified glassy carbon electrodes <i>P. Manisankar and S.Valarselvan</i>	3
1.6	Corrosion resistance and bioactivity evaluation of europium substituted hydroxyapatite coating on passivated surgical grade stainless steel for biomedical application <i>S. Sathishkumar, P. Karthikeyan, N. Murugan, M. Chozhanathmisra and R.Rajavel</i>	4
1.7	Structure and cycle stability of LaPO ₄ coated LiMn ₂ O ₄ cathode materials for rechargeable lithium ion batteries <i>P. Mohan and G. Paruthimal Kalaignan</i>	5
1.8	Supercapacitive behaviour of nanofibrous LiFe _x Co _{1-x} O ₂ cathode material by electrospinning technique <i>G. Bhuvanalogini and A. Subramania</i>	6
1.9	Chemical synthesis and characterization nano size poly (Aniline-co-ethyl 4- Aminobenzoate) copolymers <i>R. Sasikumar, V. Sethuraman, P. Muthuraja and P. Manisankar</i>	7
1.10	Study of desalination characteristics of activated carbon electrode prepared from bael fruit shell <i>N. Mohanraj, Sachin Kumar, Shailendera Shukla, Uttam Kumar, Priyanka JP, S. Bhuvaneshwari</i>	8
1.11	Acid doped poly(fluorenyl ether sulfone) with pendent imidazole side groups for high temperature proton exchange membranes application <i>P. Kandasamy, G. Paruthimalkalaignan and K. Tharanikkarasu</i>	9
1.12	Effects of nanofiller on electrochemical properties of polymer electrolytes for lithium batteries <i>S. Edwinraj, R. Kaladevi, M. Ramesh Prabhu</i>	9
1.13	1-allyl-3-methylimidazolium chloride as a corrosion inhibitor on mild steel in 3.5% sodium chloride solution <i>S. Velrani and P. Prakash</i>	11
1.14	Temperature dependent anatase titanium dioxide thin film prepared by electrodeposition technique <i>M. Karthikeyan, N. Anandhan, V. Dharuman, G. Gopu, A. Amali Roselin and S. Viswanathan</i>	12
1.15	Optimization of CeO ₂ dispersoid content in polymer gel electrolyte based on P(S-MMA)12 <i>K. Diwakar, M. Sivakumar, R. Subadevi</i>	
1.16	Structural and morphological characterizations of Li ₂ FeSiO ₄ via solid state method <i>R. Dhanalakshmi, K. Diwakar, P. Rajkumar, R. Subadevi, M. Sivakumar</i>	13
1.17	Structural and morphological studies of sulfur-PEO-MnO ₂ composite for lithium sulfur batteries <i>G. Radhika, M. Sivakumar, R. Subadevi</i>	13
1.18	Electrochemical copolymerization coating on passivated low nickel stainless steel for corrosion protection performance in 0.5M H ₂ SO ₄ medium <i>P. Karthikeyan, S. Sathishkumar, N. Murugan, M. Chozhanathmisra and R. Rajavel</i>	14

1.19	Improved electrochemical properties of LiMn_2O_4 with the La and Sm co-doping for rechargeable lithium-ion batteries <i>K. Kalaiselvi, P. Mohan and G. Paruthimal Kalaigan</i>	15
1.20	Inhibition of aluminium corrosion using agarose in acidic medium <i>R.S. Nathiya and V. Raj</i>	16
1.21	A study of corrosion inhibition effect on mild steel by L-Phenylalanine in 1 M HCl medium <i>G. Jayabharathi and G. Chandramohan</i>	17
1.22	Numerical analysis of specific absorption rate and to protect human brain from microwave radiation using electromagnetic shielding <i>Vakula Paranam S, Vasant Naidu, Senthil Kumar A</i>	18
1.23	Electrochemical synthesis and spectroelectrochemical characterization of poly(3-oxylthiophene-co-3,4-ethylenedioxythiophene) <i>P. Authidevi, D. Kanagavel, J. Peter and C. Vedhi</i>	18
1.24	Study of mediator-less and membrane-less microbial fuel cell system on power generation from dairy wastewater treatment <i>Vidhyeswari. D, Chinchu Elezebeth, A. Surendhar and S. Bhuvaneshwari</i>	19
1.25	Corrosion inhibition of aromatic ring substituted benzimidazole derivatives for mild steel in acidic medium <i>A. Velmurugan, K. Kanmani, G. Muthusankar, G. Gopu</i>	20
1.26	Double layer $\text{SiO}_2\text{-TiO}_2$ Sol-gel coating for corrosion protection of wearables <i>S. Ramasubramanian, P. Prakash</i>	21
1.27	Corrosion behaviour of Mg-Li-Al alloy in chloride media <i>A. Cyril & L. Sudha</i>	21
1.28	Electrochemical properties of organo-montmorillonite clay nanocomposite lithium polymer electrolytes based on PEO/PVdF-HFP blend <i>Pradeepa Prabakaran, Roshini Raju, Sowmya Gurusamy, Ramesh Prabhu Manimuthu</i>	22
1.29	A systematic study on effect of electropolymerisation conditions on the permeability of polyresorcinol films <i>R. Karkuzhali, AR. Pandiselvi, P. Karthika and S. Viswanathan</i>	23
1.30	Corrosion resistance of heat treated Ni-W and Ni-W- TiO_2 nanocomposite coatings <i>K. Arunsunai Kumar, G. Paruthimal Kalaigan and S. Senthilkumar</i>	24
1.31	Structural analyses of $\text{Li}_2\text{FeSiO}_4$ cathode material prepared by sol-gel method <i>R. Dhanalakshmi, P. Rajkumar, R. Subadevi, M. Sivakumar</i>	25
1.32	Studies on sulfur/polyethylene glycol/graphene composite for lithium sulfur batteries <i>K. Krishnaveni, R. Subadevi, M. Sivakumar</i>	26
1.33	Effect of pretreatments of sepiolite for cathode materials in Li-S batteries <i>C. Kalaiselvi, M. Sivakumar, R. Subadevi</i>	26
1.34	Preparation of lanthanum (III) impregnated nano porous activated carbon and its application in electro-chemical oxidation of tannery wastewater <i>M. Ezhilpriya, G. Naveen Kumar, S. Swarnalatha and G. Sekaran</i>	27
1.35	Moringa olifera: Green corrosion inhibitor for mild steel in sulphuric acid medium <i>N. Subasree, J. Arockia Selvi, P. Kamaraj, M. Arthanareeswari</i>	27
2.	NANOSCIENCE AND TECHNOLOGIES	
2.1	Brighter future for cancer therapy with smart theranostics through nanobiotechnology: Efforts and innovations from our laboratory <i>Kaliaperumal Selvaraj</i>	28
2.2	Synthesis, phase transition and thermoelectric properties of bismuth telluride nanostructures <i>M. Arivanandhana, P. Anandanb, D. Rajan Babuc, M. Azhagurajand, R. Jayavela, Y. Hayakawae</i>	28
2.3	Synthesis, characterization and catalytic behavior of nano-silica derived from bamboo rice husk ash <i>Cinnathambi Subramani Maheswari, Appaswami Lalitha</i>	30
2.4	Different dimensional semiconductor nanocomposites <i>G. Ramalingam and K. Gurunathan</i>	31

2.5	Synthesis of nanocrystalline Au substituted hydroxyapatite: Investigation on cytocompatibility and antibacterial efficacy <i>S. Jegatheeswaran, S. Selvam, S. N. Karthick and M. Sundrarajan</i>	31
2.6	Multicomponent effect of Ni-W-MoS ₂ -PTFE nanocomposite coatings prepared by direct and pulse current electrodeposition <i>S. Sangeetha and G Paruthimal Kalaigan</i>	32
2.7	Synthesis and characterization of iron oxide coated nickel oxide nanoparticles <i>R. Krishnaveni</i>	33
2.8	Green synthesis of silver nanoparticles and impregnation on surgical mask & surgical thread for antimicrobial property <i>M. Kavitha and A. Arumugam</i>	34
2.9	Formation and characterisation of electroless silver nanoparticles on aluminium from <i>Solanum melongena</i> leaves extract <i>N. Latha, M. Gowri, K. Sathishkumar, D. Sumathi</i>	35
2.10	Green synthesis and characterization of silver nanoparticles from fruit extract and its antibacterial activity <i>R. Bhuvaneswari, S. Keerthana and D. Ramyadevi</i>	36
2.11	Synthesis, characterization and catalytic properties of CuO nanocrystals <i>E. Bharathia S. Senthilvelan and B. Karthikeyan</i>	36
2.12	Anticancer potential of the synthesized gold nanoparticles against A549 lung cancer cell lines <i>Natarajan Suganthy, Vijayan Sri Ramkumar and G. Archunan</i>	37
2.13	Preparation of sputtering target of Cr ₂ O ₃ :CuO (50:50) and its thin film preparation by RF magnetron sputtering <i>S. Ponmudi, R. Sivakumar, C. Sanjeeviraj and C. Gopalakrishnan</i>	38
2.14	Anti-tumor promoting potential of 3, 3'-Diindoylmethane encapsulated chitosan nanoparticles on 7, 12-dimethylbenz (a) anthracene induced rat mammary carcinoma <i>S. Isabell and S. Mirunalini</i>	39
2.15	Synthesis and characterization of terbium chloride doped polyaniline/ MWCNT nanocomposite <i>J. Dominic and K. K. Satheesh Kumar</i>	40
2.16	Non-enzymatic Biosensor for Dopamine using Graphene oxide-poly (3,4-ethylenedioxythiophene)-Copper Nanoparticles Modified Electrode <i>V. Sethuraman, M. Malathi, M. Akila and P. Manisankar</i>	41
2.17	Adsorption of methylene blue dye by SW-ZnO composite doped polyaniline: Evaluation of the kinetic and isotherm <i>R. Pandimurugan, S. Thambidurai</i>	42
2.18	Green synthesis of gold nanoparticles from <i>Lawsonia inermis</i> seeds extracts <i>Subramani Seethai and Karuppiah Muthu</i>	43
2.19	Nanostructured based on organic – inorganic hybrid composites for high-performance supercapacitor <i>M. Arun Prabhu and K. Gurunathan</i>	44
2.20	Antimicrobial effect of cobalt and manganese codoped tungsten oxide nanoparticles <i>R. Arunadevi, B. Kavitha, M. Rajarajan, A. Suganthy, P. Muthuraj</i>	44
2.21	Preparation of pyridoxine/Cu ₂ O nanocubes and their antimicrobial activity <i>B. Suganya Bharathi, T. Stalin</i>	45
2.22	Electro-optical properties of 2,5-dimethoxy polyaniline with tin oxide nano composites <i>M. Senthil kumar and P. Manisankar</i>	45
2.23	An eco-friendly synthesis of silver nanoparticles using <i>Achyranthus aspera</i> root promising anticorrosion potentials for mild steel in acidic medium <i>B. Gowri Shannkari, S. Siva Bharathi and R. Sayee Kannan</i>	46
2.24	Biosynthesis of silver nanoparticles using <i>Curuma longa</i> and their application of pharmacological and catalytic activity <i>N. Muniyappan, T. K. Dhamodharan S. Baskar and P. Ramar</i>	47
2.25	Enzymatic synthesis of ethyl ferulate using celite immobilized lipase from <i>Bacillus subtilis</i> <i>S. Monisha, M. Sinduja, K. Swetha Laxmi, Anant Achary, S. Karthikumar</i>	47
2.26	A novel cobalt doped Dy ₂ O ₃ nanoparticles synthesized by co-precipitation method <i>C. Suganya, N. Anandhan, M. Karthikeyan, V. Dharuman, G. Gopu, A. Amali Roselin, S. Viswanathan, J. Umadevi</i>	48

2.27	Studies on solid polymer electrolytes added with nano fillers <i>T.M. Amarnath, J. B.A. J. Helen Therese and K. Gurunathan</i>	48
2.28	Analytical studies on polystyrene methylmethacrylate poly(sty-MMA)-poly (vinyl chloride) polymer electrolytes with lithium Salts <i>C. Balalakshmi, J.B.A.J. Helen Thesere and K. Gurunathan</i>	49
2.29	Microrheology – methods and technique <i>Anand Tadas</i>	50
2.30	Enhanced antibacterial activity and low bandgap energy of ZnO/BC nanocomposite material <i>K. Bama, M. Sundrarajan and K. Bharathi</i>	50
2.31	CuO nanostructure: Optical and antibacterial activity against pathogenic bacteria <i>S. Ambika, M. Sundrarajan and V. Magesh Kumar</i>	51
2.32	Synthesis of Pd doped magnetic Fe ₃ O ₄ nanoparticles <i>A. Sangili, M. Sundrarajan and M. Abdul kathir</i>	52
2.33	Catalytic oxygen reduction on silver nanoparticle modified glassy carbon electrode with 2-hydroxy-1,4-naphthoquinone <i>J. Antony Rajam A. Gomathi and C. Vedhi</i>	53
2.34	Preparation and EMI shielding studies on Au-CNT dispersed polyvinylene difluoride nanocomposites <i>R. Kumaran, M.Kesava, and K.Dinakaran</i>	54
2.35	Hydrothermal synthesis and characterization of cobalt oxide nanoparticles; an evaluation of biological activities <i>V. Meenakshi and A. Arumugam</i>	54
2.36	Facile hydrothermal synthesis of iron oxide nanoparticles and their biomedical applications <i>D. Ellakkiya and A. Arumugam</i>	55
2.37	Application of magnesiumoxide nanoparticles in cotton fabric as anantibacterial textile finishes <i>R.Kiruba and A. Arumugam</i>	56
2.38	Synthesis of and characterization of nano metal oxides (NMO) on removal of heavy metals in textile waste water <i>M.Kavitha and A. Arumugam</i>	57
2.39	Mycosynthesized Pd nanoparticles using <i>Nigrospora sp.</i> , for biomedical applications <i>P. Menaka and A. Arumugam</i>	57
2.40	Biosynthesis and characterization of cerium oxide nanoparticles using <i>Nigrospora sp.</i> , <i>S. Gowri and A. Arumugam</i>	58
2.41	One-pot hydrothermal synthesis of Fe ₃ O ₄ /RGO nanocomposites as coupling agents for biomedical applications <i>V. Karthika and A. Arumugam</i>	59
2.42	Eco friendly synthesis of dysprosium oxide nanoparticles and its evaluation of toxicity <i>T. Baranisri, K. Gopinath and A. Arumugam</i>	60
2.43	Facile synthesis of Multiwall carbon nanotube supported Palladiumdoped polypyrrole catalyst <i>M. Balaji, M. Sundrarajan, S. Selvam and G. Selvanathan</i>	60
2.44	Green synthesis of silver nanoparticles from root extracts of <i>Phyllanthus maderaspatensis L.</i> and their biological applications <i>K. Kokila, N. Elavarasan and V. Sujatha</i>	62
2.45	Rapid synthesis of lithium titanate nanocomposites for lithium – ion batteries <i>M. Selvamurugan and S. Karuppuchamy</i>	62
2.46	Synthesis of microemulsion assisted with chitosan/silver-desferrioxamine B (CS/Ag-DFOB) complex for skin disease <i>S.Anandhavelu, A.Yogiananth, M.Murugavelu, V.Sethuraman, S.Thambidurai</i>	63
2.47	Pulse electrodeposition and corrosion properties of Ni-W-ZrO ₂ nanocomposite coatings <i>K. Alex Mary, S. Sangeetha and G Paruthimal Kalaigan</i>	64
2.48	Characterizations of pulsedeposited Ni-W-SiC nanocomposite coatings <i>K.Mohana, S. Sangeetha and G Paruthimal Kalaigan</i>	65
2.49	In situ synthesis of macroporous Fe ₂ O ₃ fiber nanomaterials by cellulose fibers for electrocatalytic oxidation of dopamine <i>Rajesh Madhuvilakku, Shakkthivel Piraman</i>	65

2.50	Manganese dioxide nanoparticles for electrochemical energy storage and conversion applications <i>Srinivasan Alagar, Rajesh Madhuvilakku and Shakkthivel Piraman</i>	66
2.51	Synthesis and characterization of CdSSe/ZnS core shell for photovoltaic application <i>Ishimwe Francoise and K. Gurunathan</i>	67
2.52	Physical and electrochemical performances of pulse electrodeposited Ni-CeO ₂ nanocomposite coatings <i>S. Kasturibai and G. Paruthimal Kalaignan</i>	67
2.53	Improvement of Bagasse based Paper Critical Properties using CaCO ₃ Nanofillers <i>Maruthaiya Karuppaiah, Sasikala Sundar, Manisankar Paramasivam and Shakkthivel Piraman</i>	68
2.54	Vapour phase polymerization of styrene over mesoporous aluminophosphate catalyst <i>M.A. Mary Thangam, S.Usha, Chellapandian Kannan</i>	69
2.55	Synthesis and characterization of hybrid structure of Ni doped ZnO/reduced graphene oxide <i>R. Karthik, S. Thambidurai</i>	69
2.56	Synthesis and characterization of zinc oxide nanoparticles from <i>Azadirachta indica</i> extract <i>T. Revathi, S.Thambidurai</i>	70
2.57	[BMIM] BF ₄ assisted morphological improved synthesis of magnetic Fe ₂ O ₃ nanoparticles <i>S. Nagapriya, S.Jegatheeswaran, M. Balamurali and M. Sundrarajan</i>	71
2.58	Synthesis and antibacterial studies of zinc oxide nanoparticles <i>C.Rani and K.Sanathi</i>	72
2.59	Ag nanoparticles from <i>Nyctanthes arbor-tristis</i> : Synthesis, characterization and application <i>K. Iswarya, K. Bama, J. Anandha Raj and M. Sundrarajan</i>	73
2.60	Facile synthesis of palladium nanoparticles using Punica granatum peel extract: Green chemistry approach <i>S. Tamil Selvi, S. Ambika, S. Angappan and M. Sundrarajan</i>	73
2.61	Synthesis, characterization and antibacterial activity of silver nanoparticles synthesized from <i>Padina boergeresii</i> <i>Arockiam Sagina Rency, Lakkakula Satish, Shanmugaraj Gowrishankar, Manikandan Ramesh</i>	74
2.62	Lyotropic liquid crystal assisted preparation of nanomaterials: A greener approach for the controlled growth <i>R. Umamaheswari, G. Karpagam, S. Umadevi</i>	75
2.63	Synthesis and Physical Characterization of LiCoVO ₄ nano cathode materials for the rechargeable lithium ion batteries <i>V. Jeyanthi, P. Naveenkumar and G. Paruthimal Kalaignan</i>	76
2.64	Development of poly-anionic nano cathode materials for the rechargeable lithium-ion batteries <i>P. Naveenkumar and G. Paruthimal Kalaignan</i>	76
2.65	In-situ synthesis, functionalization and fabrication of flexible electronics using graphene-pani derivative nanocomposites <i>C.Sathya, S.Viswanathan and C.Sivakumar</i>	77
2.66	Synthesis and antibacterial evaluation of amide linked N-formyl-pyrazolines <i>R. Selvi, S. Sudalaimani and L. Pushpa Radhika</i>	78
2.67	Structural and Morphological properties of polypyrrole doped Sb ₂ S ₃ thin films <i>J. Umadevi, N. Anandhan, V. Dharuman, G. Gopu, M. Karthikeyan, A. Amali Roselin, C. Suganya, P. Rajeswari</i>	78
2.68	Facile synthesis and characterization of CeO ₂ particles as function of various precipitation agents by modified co-precipitation method <i>M.Ramachandran, R.Subadevi, M.Sivakumar</i>	79
3.	SENSOR TECHNOLOGIES	
3.1	Biosensors for health and safety monitoring <i>M.S. Thakur</i>	80
3.2	Reduced graphene oxide: Sensing, delivery, therapy <i>Sabine Szunerits</i>	81

3.3	CeO ₂ /Nile blue nanocomposite modified glassy carbon electrode for selective detection of dopamine in presence of ascorbic acid <i>S. Selvarajan, A. Suganthi, M. Rajarajan</i>	81
3.4	Electrochemical guanine sensing based on Ni ion irradiated WO ₃ thin films <i>A.C. Anithaa, K. Asokan, C. Sekar</i>	82
3.5	Room temperature CO gas sensor based on CuO-ZnO loaded polypyrrole nano composite <i>Heiner .A.J and Gurunathan .K</i>	83
3.6	The behavior of binary lipid on different chain length thiol monolayer modified gold electrode <i>Karutha Pandian Divya and Venkataraman Dharuman</i>	83
3.7	Studies of self-assembled binary mixed monolayer for label free DNA hybridization electrochemical sensing on liposome – gold nanoparticle composite tethered on gold transducer <i>Naganathan Dhanalakshmi, Venkataraman Dharuman</i>	84
3.8	An electrochemical biosensor methyl parathion on immobilization of acetylcholinesterase on ironoxide - chitosan nanocomposite <i>S. Muthumariappan and C.Vedhi</i>	85
3.9	Electroanalysis of heavy metals in seaweed using multiwalled carbon nanotubes modified glassy carbon electrode <i>A.Vimala and C.Vedhi</i>	85
3.10	Glassy carbon electrode modified with poly (glutamic acid) as a probe for the voltammetric determination of thymine <i>Jesny S. and K. Girish Kumar</i>	86
3.11	A simple and sensitive fluorescent sensor for the determination of epinephrine <i>Shalini Menon and K. Girish Kumar</i>	88
3.12	Electrochemical sensor for cefotaxime based on gold modified molecularly imprinted polymer <i>P. Karthika, R. Vidhya, C.Rani and S. Viswanathan</i>	89
3.13	Rhodamine based 'OFF-ON' fluorescent probe for Al ³⁺ and S ²⁻ : Synthesis, crystal structure, <i>in silico</i> and live cell imaging <i>M. Maniyazagan, R. Mariadasse, M. Nachiappan, J. Jeyakanthan, N. K. Lokanath, S. Naveen, K. Premkumar, P. Muthuraja, P. Manisankar and T. Stalin</i>	90
3.14	Piperazine based Schiff base for chemosensor and biological applications <i>N. Kavitha and N. Sengottuvelan</i>	90
3.15	A differential pulse voltammetry sensor based on graphene oxide-multiwalled carbon nanotube nanocomposite for the simultaneous determination of carbendazim and isoproturon pesticides <i>C.Vasanthi and R. Saraswathi</i>	91
3.16	Sensitive detection of Hg(II) using carbon dots as fluorophore <i>K. Rubini, K. Sivakumar, B. Sinduja and S. Abraham John</i>	92
3.17	Methyl Parathion Sensor based on Cu doped CeO ₂ nanoparticles <i>Jean Claude Nizeyimana, N. Lavanya, C. Sekar</i>	93
3.18	Polymer based nanobiosensor and its controlled drug delivery for the of detection of glucose <i>J. Nivin, B. Kalyanasundar and C. Sivakumar</i>	94
3.19	Tin dioxide (SnO ₂) nanoparticles based biosensors for monitoring of neurochemical substances <i>N. Lavanya, C. Sekar</i>	94
3.20	Determination of heavy metals on poly(Aniline-Co-Sulfamethazine) modified electrode <i>K. Masilamani, G. Selvanathan, B. Elanchezhian</i>	95
3.21	Controlled growth of single crystalline nanostructured dendrites of α-F ₂ O ₃ blended with MWCNT: a systematic investigation of highly selective determination of L-dopa <i>D. Nathiya and J. Wilson</i>	96
3.22	Properties of SnO ₂ -CNT powdered particles by using hydrothermal method for gas sensors <i>D. Saravanakkumar, B.H. Abbas Shahul Hameed, P. Ponsurya, A. Ayeshamariam and M. Jayachandran</i>	97

3.23	Silver nanoparticles for selective and sensitive sensing of Hg ²⁺ colorimetrically <i>Muthupandi Kasithevar and Prakash Periakaruppan</i>	98
3.24	Highly selective fluorescent chemosensor for the detection of Al ³⁺ using a rhodamine spirolactam and its application in cell imaging <i>R. Manjunath and P. Kannan</i>	98
3.25	Synthesis and characterization of polythiophene-zinc oxide nanocomposite for oxygen sensing application <i>Regina. R, Heiner. A. J and Gurunathan. K</i>	99
3.26	Dynamic sensing of L-Dopa using zinc oxide-reduced graphene oxide film <i>Palinci Nagarajan, Manikandan, Venkataraman Dharuman</i>	100
3.27	Electrochemical investigation of Lead (II) ion using sulphanic acid functionalized mesoporous carbon modified electrode <i>Subramani. S., Sangeetha., C and Thinakaran. N</i>	101
3.28	Determination of Reactive Red 141 dye by stripping voltammetry <i>C. Kavitha and H. Gurumallesh Prabu</i>	101
3.29	Metal-organic framework based ammonia gas sensor <i>T. Ponmuthuselvi and S. Viswanathan</i>	102
3.30	A fluorescent probe based on histidine carbon dots for highly sensitive detection of Hg ²⁺ in aqueous solution <i>M. Jayalakshmi, M. Maniyazagan, T. Stalin</i>	103
3.31	Rhodamine based gold nanoparticles for rapid colorimetric detection of Fe ³⁺ ions in aqueous medium with real sample applications <i>U. Thenmozhi, M. Maniyazagan, T. Stalin</i>	104
3.32	Electrochemical determination of 4-Nitrophenol by single-drop micro extraction <i>S. Sudha, I. Victor Emeka, T. Ponmuthuselvi and S. Viswanathan</i>	104
3.33	Microfluidic biosensor for cholera toxin detection <i>S. Viswanathan, Ja-an Annie Ho, Cristina Delerue-Matos</i>	105
3.34	Organometallic compounds (OMC): A new sensing platform for biomolecules <i>K. Dinesh Christy, S. Prakash, P. Muthuraja, P. Manisankar</i>	106
3.35	Label-free electrochemical immunosensor for egg allergen <i>S. Viswanathan, M.B.P.P. Oliveira, K. Thangapandi, Cristin Delerue-Matos</i>	107
3.36	Highly sensitive and selective fluorescent sensor for unique cadmium ion in aqueous media <i>P. Sakthivel and K. Sekar</i>	108
3.37	Fabrication of p-Cresol sensor for veterinary applications <i>N. Sudhan, C. Manikkaraja, G. Archunan, P. Manisankar, C. Sekar</i>	109
4	SUPRAMOLECULAR AND PHOTOCHEMICAL TECHNOLOGIES	
4.1	Impact of sodium in the photocatalysis of ZnTiO ₃ powder prepared by coprecipitation oxalate method <i>Sirajudheen P</i>	110
4.2	Prolific synthesis of transition metal doped TiO ₂ (TM= Au, Pt), nanoparticles and its photocatalytic activity <i>PR. Kaleeswaran and A. Arumugam</i>	111
4.3	Synthesis and photo physical property of 4, 4' (4, 5-diphenyl-1H-imidazol-1,2-diyl) dianiline and perylene dianhydride based fluorescent polyimide <i>A. Hariharan, K. Subramanian and K. Dinakaran</i>	112
4.4	Folic acid coated carboxymethyl cellulose/casein nanogels loaded with curcumin for skin cancer treatment <i>P. Priya and V. Raj</i>	113
4.5	Microwave synthesis of Sn-WO ₃ photocatalyst <i>K. Santhi, C. Rani and S. Karuppuchamy</i>	114
4.6	Photocatalytic dye degradation of transition metal ions (Co, Cr, Cu) doped TiO ₂ nanocomposites <i>T. Pushpa, R. Kalyani and K. Gurunathan</i>	115
4.7	Wet catalytic degradation of crystal violet dye using Fenton like Co ₃ O ₄ /Zeolite X catalyst <i>N.L. Subbulekshmi and E. Subramanian</i>	115

4.8	Removal of chromium from wastewater using emulsion liquid membrane <i>P. Murugan, B. Manoj Reddy, T. Vinaya Sri, B.V.N.S. Bhavanad, G. Umadevi, S. Bhuvaneshwari</i>	117
4.9	Efficient photocatalytic degradation of Victoria blue by MnWO ₄ - BiSbO ₄ nanocomposite under visible light irradiation <i>D. Rani Rosaline, V. Ramasamy Raja, M. Rajarajan, A. Suganthi</i>	117
4.10	A facile synthesis of magnetic activated carbon/CoFe ₂ O ₄ nanocomposite for the adsorption of Congo Red dye from water <i>P. Karthikeyan, P. Anjana, K.S. Anjali, P.S. Anaghaa B. Ushadevib, S. Vairamb, V. Ranjithkumara*</i>	118
4.11	Effect of annealing temperature on structural and optical properties of BTO thin films for photocatalytic applications <i>A. Amali Roselin, N. Anandhan, G. Gopu, M. Karthikeyan</i>	118
4.12	Synthesis, characterization of hematite NpS decorated N-doped graphene sheet/MoS ₂ nanocomposite for photocatalytic application <i>S. Senthilnathan, S. Sivasakthi and K. Gurunathan</i>	119
4.13	Fabrication of highly flexible dye sensitized solar cell using the electrospun nickel oxide nanofibers based counter electrode <i>K. Sakthi Velu, P. Manisankar and T. Stalin</i>	119
4.14	Inclusion complex of 1,8-Dihydroxyanthraquinone with β-cyclodextrin: Spectral and molecular modeling studies <i>S. Mohandoss and T. Stalin</i>	120
4.15	Electrochemical treatment of Disperse Orange3 found in textile effluents <i>M. AbdulKadir, P. Manisankar and A. Gomathi</i>	121
4.16	Host-guest chemistry of β-Cyclodextrin and plumbagin in aqueous and solid state <i>R. Kavitha and T. Stalin</i>	121
4.17	Salvatochromism and proton transfer kinetics of 5- perylene imide in (5PI) the excited singlet state: A study of electronic spectra <i>Shanmugapriya RM, Gnanamalar K and Radha N</i>	122
4.18	Host-guest interaction of p-sulfonatocalix[4]arene with 1,8-diaminonaphthalene <i>C. Saravanan, M. Senthilkumaran, B. M. Ashwin, J. Karpagam, P. Muthu Mareeswaran</i>	123
4.19	Photocatalytic oxygenation of organic sulfides using earth-abundant metal ions as catalyst and water as oxygen source <i>Thangamuthu Rajendran, Krishnan Senthil Murugan, Gopalakrishnan Balakrishnan, Muniyandi Ganesan, Veluchamy Kamaraj Sivasubramanian, and Seenivasan Rajagopal</i>	123
4.20	Influence of Sm on structural and optical properties of Bi ₂ S ₃ thin films using SILAR method <i>D. Janani, N. Anandhan, V. Dharuman, G. Gopu, M. Karthikeyan, A. Amali Roselin, K. P. Ganesan</i>	124
4.21	Combustion synthesis of nanocrystalline FeWO ₄ and its application towards the photocatalytic degradation of Methylene Blue <i>M. Mohammed Rafic, R. Saraswathi and L. John Berchmans</i>	125
4.22	Biosynthesized silver-nanoshells for catalytic degradation of organic pollutants <i>Balakumar Vellaichamy and Prakash Periakaruppan</i>	126
4.23	Degradation of organic dye in contaminated water by green synthesized CuO nanoparticles using aqueous flower extract of <i>Cordia sebestena</i> Linn <i>S. Prakash, A. Venkatesan, M. Stanely Britto, M. Sowndharya and V. Sujatha</i>	126
4.24	Fabrication of dye-sensitized solar cell using electrospun TiO ₂ /CaCO ₃ nanowires <i>C. Brundha and S. Karuppuchamy</i>	127
4.25	Microwave synthesis of metal doped TiO ₂ for photocatalytic applications <i>J. Maragatha and S. Karuppuchamy</i>	128
4.26	Synthesis, characterization and antibacterial properties of TiO ₂ nanowires <i>M. Nagalakshmi, C. Brundha and S. Karuppuchamy</i>	129
4.27	Facile Synthesis of Barium Titanate Nanopowder by Microwave Assisted Route for Photocatalytic Applications <i>M. Thamima and S. Karuppuchamy</i>	130

4.28	The roles of protic solvents on CdS thin films prepared by chemical bath deposition technique <i>K.Rajeswari, N.Anandhan, V. Dharuman, A.Amali Roselin, M.Karthikeyan, G. Gopu</i>	131
4.29	Synthesis and characterization of Fe-TiO ₂ / polyanilecore-shell nanostructure for photocatalytic hydrogen production <i>C. Meyyathal, R. Kalyani and K. Gurunathan</i>	131
4.30	Fabrication of novel Zn ₂ SnO ₄ / V ₂ O ₅ composite for degradation of Eosin Yellow under visible light irradiation <i>V. Ramasamy Raja, A. Suganthi, M. Rajarajan, D.Rani Rosaline</i>	133
4.31	Visible light sensitisation of TiO ₂ by polyaniline and a photocatalytic water splitting of resulting PANI-TiO ₂ hybrid materials <i>E Subramanian, A Baby Shanthi, J V Anusha</i>	133
4.32	Synthesis and characterisation of core- shell of ZnSSe/ ZnS for solar cell application <i>G. Ganesh Priya, R. Kalyani and K. Gurunathan</i>	134
4.33	Synthesis, characterization and photocatalytic study of cerium oxide/ zeolite-NaX with brilliant green dye degradation <i>G. Sudha and E. Subramanian</i>	135
4.34	Fluorescence spectral studies of some imidazole derivatives <i>T.S.Rajasekar, and N. Srinivasan</i>	136
4.35	Sol-gel based synthesis and characterization of photoactive nanocrystalline ZnO thin films for hydrogen production <i>R. Kalyani and K. Gurunathan</i>	136
4.36	Photolytic degradation of Alizarin Red S by zn doped TiO ₂ in presence of electron acceptor <i>C.Rani and K.Santhi</i>	137
4.37	Comparison of photocatalytic applications of TiO ₂ and Mn(TiO ₃) <i>C. Rani, K.Santhi and Vinothini</i>	138
4.38	Activated carbon derived from <i>Cannabis sativa</i> , interconnected with nanostructured metal oxide for energy storage applications <i>S. Imran Hussain, S. Kalaiselvam</i>	138
4.39	Electrochemical polymerization of poly (aniline) - multiwalled carbon nanotube composite counter electrode for dye sensitized solar cell applications <i>S. Nagaraj, K. Sakthi Velu and T. Stalin</i>	139
4.40	In-situ electrochemical synthesis of poly-(aniline) - graphene oxide composite counter electrode for high efficiency quasi-solid-state dye sensitized solar cell applications <i>A. Saranyadevi, K. Sakthi Velu and T. Stalin</i>	140
4.41	Enhanced solubility, dissolution rate and antimicrobial activity studies of etoposide drug with β-CD by inclusion complexation <i>Arumugam Shanmuga Priya, Jeyachandran Sivakamavalli, Baskaralingam Vaseeharan, Thambusamy Stalin</i>	140
4.42	Electrochemical degradation of Reactive Blue 19 on lead/lead dioxide electrodes <i>S. Anita, J. Anitha Pushparani, P. Karpagavinayagam and C.Vedhi</i>	141
4.43	Synthesis of Cu doped TiO ₂ photocatalyst <i>C. Rani, K.Santhi and R.Latha</i>	142
4.44	Hydrothermal preparation of reduced graphene oxide-ZnO composite for photocatalytic degradation of DY-86 dye <i>R. Rajeswari, H. Gurumalles Prabu</i>	142
4.45	Studies on the removal of colour from textile effluent salt <i>Vishnuprasad, M A Vishnuganth</i>	143
4.46	Sun light assisted photocatalytic degradation of dye <i>P.Karthika, P. Nithya, G. Srinivasan, K.Thangapandi and S. Viswanathan</i>	144
4.47	Design to conductive sulfonated polypyrrole incorporated with hybrid SPVdF- ZnO composite for high energy conversion counter electrode in DSSC <i>A. Sarathkumar Muthuraja, M. Sundrarajan, M. Balaji, S. Jegatheeswaran, A. Sangili, S. Selvam and G. Selvanathan</i>	145
4.48	Investigation of Congo Red decolourization using clay/polymer composite beads <i>S. Vahidhabanu, D. Karuppasamy and B. Ramesh Babu</i>	146

4.49	Structure and vibrational analysis of iloperidone <i>Selvam Karthick, Somasundaram Meenakshisundaram and Gopalakrishnan Gopu</i>	146
4.50	Virtual screening of high affinity guests for cyclophane amides <i>Somasundaram Meenakshisundaram, Selvam Karthick and Gopalakrishnan Gopu</i>	147
4.51	Photophysical behavior of 6-peryene imide (6PI) in different solvents and at various pH <i>Gnanamalar K, Shanmugapriya RM and Radha N</i>	148
4.52	Comparative study on the removal Congo Red using conducting polymers <i>A. Vijayakumar, A. Sakthivel, A. Sarathi, N. Raman and K. Arunsunai Kumar</i>	148
4.53	Enhanced Cr(VI) removal using green synthesized Fe-nanoparticles decorated graphene <i>Baishnisha Amanulla and Sayee Kannan Ramaraj</i>	149
4.54	Preparation of macromolecule derivative with anhydride salts <i>R. Sountharya, B. Nivethetha, S. Karthick, G. Gopu</i>	150
4.55	Synthesis of metal oxide/carbon nanofiber using paraffin wax as precursor for dye adsorption in aqueous media <i>Indiran Muralisankar, Sunderajan Vairam, Ramasamy Narayanasamy</i>	151
4.56	Encapsulation of acenaphthenequinone with p-sulfonatocalix[4]arene <i>M. Senthilkumar, C. Saravanan, B. M. Ashwin, K. Pramila Selas, P. Muthu Mareeswaran</i>	151
5.	GREEN CHEMICAL TECHNOLOGIES	
5.0	Voight Reaction – Recent Advances and Applications <i>H. Surya Prakash Rao</i>	152a
5.1	Synthesis and antimicrobial activity of novel 5, 5-disubstituted pyrrolo- β -carbolines <i>S. Senthilkumar, M. Priya and S. Sudha</i>	153
5.2	Electrocatalytic reduction of oxygen at the surface of poly (3-methylthiophene-co-3,4-ethylenedioxythiophene) modified electrode with 1,8-dihydroxy anthra-9,10-quinone <i>G. Amala Jothi Grace A. Gomathi and C. Vedhi</i>	153
5.3	Green based AgNPs from red seaweed and its defensive effect to control vibriosis in Brine shrimp: An environmental friendly approach <i>Lakkakula Satish, Sivasubramanian Santhakumari, Arokiam Sagina Rency, Shanmugaraj Gowrishankar, Shanmugaiah Karutha Pandian, Arumugam Veera Ravi, Manikandan Ramesh</i>	154
5.4	Green synthesis of 5,6-Bis[(2,4-dinitrophenyl)hydrazinylidene]-1,2,3,4-hexanetetrol using glucose – urea as deep eutectic solvent <i>D. Ilangeswaran and P.G. Ramesh</i>	155
5.5	PEG assisted two-component access to 3-amino-4-arylidene-1-pyrazol-5(4H)-ones under catalyst-free conditions <i>Rathinam Ramesh, Pullar Vadivel, Kaliyan Bhuvaneswari and Appaswami Lalitha</i>	156
5.6	A facile and efficient synthesis of fused-pyridine heterocycles in ionic liquid under microwave irradiation <i>Selvam Chitra, Shanmugam Muthusubramanian and Paramasivam Manisankar</i>	158
5.7	Synthesis of newer thiopyridine derivatives and evaluation of their biological properties <i>P. Muthuraja, S. Prakash, K. Dinesh Christy and P. Manisankar</i>	158
5.8	Anodic bromomethoxylation of styrenes <i>V.M. Shanmugam, K.Kulangiappar, T.Raju and D.Velayutham</i>	159
5.9	Adsorption removal of malachite green dye from aqueous solution by wood apple rind (<i>Limonia acidissima</i>) <i>N. Ramulu, S.Krishnaveni, T.Rajajeyantham and V.Thirumurugan</i>	159

5.10	Kinetic and statistical studies on degradation of reactive orange -16 dye by electrocoagulation method	161
	<i>K.Diana, R.Koushalyaa, T.Srinithi, N.Maheshwari, G.Madhangi Priyadharshini, V.C.Padmanaban</i>	
5.11	Corrosion inhibition studies on carbon steel in sea water using an aqueous seed extract of <i>Lablab purpureus</i>	162
	<i>K Anuradha, R Nandhini, P Govintha Raju and K Velmanirajan</i>	
5.12	Multistep synthesis of newer 3'-(2-methoxyphenyl)-1'H-spiro[piperidine-4, 2'-quinazolin]-4'(3'H)-one derivatives and their biological evaluation	162
	<i>P. Sathiaseelan, P.Muthuraja, Prakash and P.Manisankar</i>	
5.13	Garlic peel derived high capacity hierarchical N-doped porous carbon anode for sodium ion cell	163
	<i>V. Selvamani, R.Ravikumar, V. Suryanarayanan, D. Velayutham and S. Gopukumar</i>	
5.14	Preparation, characterizations and morphological studies of carbonaceous nanoparticle reinforced polymer nano-composites	163
	<i>S. Imthiyas Ahamed, R. Janapriyan, S. Mohammed Asik, R. Mahendran, D. Sridharan, C. Arunmozhidevan</i>	
5.15	Preliminary phytochemical analyses and antioxidant potential of dicranopterislinearis (<i>Burm.f.</i>) Underw. (<i>Gleicheniaceae</i>)	164
	<i>R. Kalpana Devi Rajesh, S. Vasantha and A. Panneerselvam</i>	
5.16	Synthesis of phenyl-2-thiocyanatoacrylic acid derivatives	165
	<i>A. Rajan, P. Prakash</i>	
5.17	Ionic liquid mediated green synthesis of palladium doped nickel oxide to design efficient catalyst	166
	<i>P. Nithya, S. Rajamohamed and M. Sundrarajan</i>	
5.18	Ruthenium (II) catalyzed oxidative C-H activation/annulation: A straightforward route to pyrene fused isoquinolium salts	167
	<i>Shanmugam Karthik, Joseph Ajantha, Shanmugam Easwaramoorthi, Thirumanavelan Gandhi</i>	
5.19	Green synthesis of aryl substituted urea using glucose – urea mixture as deep eutectic solvent	168
	<i>D. Ilangeswaran and I. Gnanasundaram</i>	
5.20	Kinetics and thermodynamics of acid catalysed oxidation of dialkyl sulphides by quinolinium dichromate	169
	<i>M.R.K. Hemalatha and T.K.Ganesan</i>	
5.21	Studies on <i>In-Vitro</i> anti thyroidal and antimicrobial activity of <i>Aegle marmelos</i> and <i>Mukia madaraspata</i>	169
	<i>K. Murugaiah, R. Venkatachalam, B.Muralidharan</i>	
5.22	Primary phytochemical analysis and antioxidant activity of <i>Millingtonia hortensis</i> Linn., stem bark extracts	171
	<i>B. Akilanda Easwari and Karuppiah Muthu</i>	
5.23	Effect of <i>Vigna unguiculata</i> aqueous extract on corrosion inhibition of MS in sea water	172
	<i>K. Anuradha, R. Nandhini, P. Govintha Raju and K. Velmanirajan</i>	
6.	INORGANIC CHEMISTRY	
6.1	A study on DNA binding behaviour of a few Schiff base transition metal complexes bearing triazole moiety	173
	<i>Ponya Utthra Ponnukalai and Natarajan Raman</i>	
6.2	Cu(II) Schiff base metal complex immobilized on MCM-41 material as catalyst for Ullmann-type coupling reactions	173
	<i>M. Malathy, G. Anbarasu and R. Rajavel</i>	
6.3	Metal- based biologically active compounds: Synthesis, spectral, and biological evaluation of some schiff base metal complexes derived from 2,6-diamino pyridine and cuminaldehyde	174
	<i>R. Jayalakshmi and R. Rajavel</i>	
6.4	One-pot synthesis, characterization, HSA and CT DNA binding, <i>in vitro</i> cytotoxicity and cell imaging studies of surfactant Rhenium(I)-polypyridine complexes	175
	<i>T. Rajendran, G. Balakrishnan, K. Senthil Murugan, V.K. Sivasubramanian, M. Ganesan, S. Rajagopal</i>	

6.5	Influence of solvent in synthesis of copper(II) biimidazole complex on geometry and Hirshfeld surfaces <i>A. Jayamani, V. Thamilarasan, S. Nagasubramanian, N. Sengottuvelan</i>	176
6.6	Synthesis, spectral studies and reactivity of Cu(II), Ni(II), Co(II), Zn(II), Cd(II), VO(IV), mixed ligand complexes with 4-oxo-4H-1-benzopyran-3-carboxaldehyde and acetylacetone <i>V. Pushpa Raja, A. Aarthy Samini, N. Nagarjun C. D. Sheela</i>	177
6.7	Studies on Cu(II), Co(II), Zn(II) complexes of novel Schiff base derived from 2, 4-diamino-6-phenyl-1,3,5-triazine and (E)-3-(4-methoxyphenyl)-1-(thiophen-2-yl) prop-2-en-1-one <i>P. Muthukumar, M. Krishnaveni, M. Vathanaruba, P. Tharmaraj</i>	177
6.8	Synthesis, characterization and antibacterial study of Ni(II) Complex of 2-(4, 5-diphenyl-1H-imidazol-2-yl)-phenol <i>E. Elanthamilan, S. Ebinezer, J. Princy Merlin, L. Sarala</i>	178
6.9	Synthesis, DNA interactions and antimicrobial screening of few novel metal(II) complexes with a Schiff base derived from imidazole <i>Ganesan Kumaravel and Natarajan Raman</i>	179
6.10	Comparative analysis of sequences and predicted structures of proteases produced by <i>Bacillus pumilus</i> through <i>in silico</i> Approach <i>Mohana, HariSuthan, Selva Kumar and Geetha K</i>	179
6.11	Synthesis of a new series of Cu(II)-Cu(II) homobinuclear and Cu(II)-Zn(II) heterobinuclear side-off complexes: Spectral analysis and antimicrobial activity <i>S. Indira, G. Vinoth and K. Shanmuga Bharathi</i>	180
6.12	A physiochemical studies of azo dyes: DFT based ES IPT process <i>S. Mohana, and N. Srinivasan</i>	181
6.13	Studies on synthesis, characterization, and biological activity of some transition metal complexes with isoniazid <i>S. Radha, K. K. Mothilal, A. Thamarachelvan and A. Elangovan</i>	182
6.14	Impact of non-aqueous solvent mixtures treatment on the fibre matrix and dyeability of polyester/cotton - a hybrid composite fibre <i>S. Vigneswari, J. Ethiraj, R. Venkatachalam, V. Ramasamy, G. Gopu and B. Muralidharan</i>	182
6.15	Synthesis and catalytic activity of novel Cu(II) Schiff base complex immobilized silica <i>G. Anbarasu, R. Rajavel</i>	183
6.16	Synthesis, analytical, spectral and DNA binding studies of Cu(II) complex with 1-phenyl-2,3-dimethyl-4-aminopyrazole-5-one and benzoate ion <i>K. Rajasekar, T. Gomadurai, P. Manikandan, S. Narasimhavarman and B. Sathiyamoorthy</i>	184
6.17	Comparative study of biological activity of alanine and valine incorporated schiff-base transition metal complexes <i>A. Sakthivel, N. Raman, A. Vijayakumar, K. Arunsunai Kumar and A. Sarathi</i>	185
6.18	Synthesis and spectral characterization of Schiff base complexes of Cu(II), Co(II), Zn(II) and VO(IV) containing 4-(4-aminophenyl)morpholine derivatives: Antimicrobial evaluation and Anticancer studies <i>K. Dhahagani and G. Rajagopal</i>	186
6.19	Synthesis, spectral characterization and biological activities of Co(II), Ni(II), Cu(II) Schiff base complexes <i>K. Mageswari, R. Regina, A. Surya, V. Thamilarasan, N. Sengottuvelan</i>	187
7.	MISCELLANEOUS	
7.1	Cellulose aerogel beads: A promising material for future <i>K. Seeni Meera, G. Kathirvel, Barbara Milow and Lorenz Ratke</i>	188
7.2	Probing the DNA binding and cleavage activities of novel water soluble Cu(II) and Zn(II) complexes having dicarboxylic acids <i>Ganesan Kumaravel, Narayanaperumal Pravin and Natarajan Raman</i>	189
7.3	A study on extraction of natural dye from bougainvillea bracts and its dyeing properties <i>J. Ethiraj, A. Nagarajan, S. Vigneswari, G. Gopu and B. Muralidharan</i>	189

7.4	Feasibility studies on the detection of onset of third phase in the solvent extraction equipment during reprocessing of fast reactor fuels	190
	<i>M Suba, P.Velavendan, N K Pandey and U Kamachi Mudali</i>	
7.5	Decolourization and detoxification of distillery spent wash using bacterial consortia –confirmsthrough structural changes and Ao-Eb fluorescence	191
	<i>Tamilselvi duraisamy, Ramarajan Selvam, Selvakumar Muniraj, Habibunisha Mubarakali and Vasanthi Muthunarayanan</i>	
7.6	Biocatalytic cascade synthesis of fine chemicals-bio-inspired metabolic pathway	192
	<i>Saravanakumar Shanmuganathan</i>	
7.7	Effects of dopant HNO ₃ on the properties of lead nitrate oxidized polyaniline composite prepared via solid-state polymerization	193
	<i>S. Suganya, J. Dominic, P. Karthikeyan, R. Gowshalyadevi, V. Mangala Gowri and K. K. Satheesh Kumar</i>	
7.8	DPPH radical scavenging antioxidant analysis of leaf extracts of <i>Dodonaea viscosa</i>	194
	<i>M. Anandan and H. Gurumalles Prabu</i>	
7.9	Chemical oxidative polymerization of aniline using zirconium oxynitrate as an oxidizing agent	195
	<i>P. Karthikeyan, J. Dominic, S. Suganya, R. Gowshalyadevi, V. Mangala Gowri and K. K. Satheesh Kumar</i>	
7.10	A Study on the effect of azeotropic solvent mixture pre treatment on the crystallinity and dyeing behaviour of polyester/cotton composite fibre	196
	<i>S.Vigneswari, J.Ethiraj, K.Balakrishnan, V.Ramasamy, G.Gopu and B.Muralidharan</i>	
7.11	Soil conditioning potential of cotton stalk biochar	197
	<i>D. Krishnaveni, S. Priyanga, G. Samuvel, A.N. Senthilkumar</i>	
7.12	Strain-free hydrophobic silk fabric coated with Hexamethyldisiloxane (HMDSO) using plasma enhanced chemical vapour deposition (PECVD)	199
	<i>K. Vinisha Rani, Bornali Sarma, and Arun sarma</i>	
7.13	Adsorption kinetics and isotherm removal of chromium (VI) ions from aqueous solution by kottikilangu (<i>Appanogeton natans</i>)	199
	<i>S. Krishnaveni, N. Ramulu, T. Rajajeyagantham and V. Thirumurugan</i>	
7.14	Spectral, NLO, fluorescence, anti-inflammatory and biological screening of thiadiazole based conjugated ligand and their metal(ii) complexes	200
	<i>K. Mahalakshmi, P. Tharmaraj, C.D.Sheela</i>	
7.15	Synthesis, spectral characterization and antifungal activities of Some spiroheterocyclic compounds	201
	<i>Elanchezhian. B, Selvanathan. G and Manivannan. N</i>	
7.16	Physico chemical study on the quality of surface water of Kolavai lake in Kanchipuram District, Tamilnadu -before and after the 2015 floods	202
	<i>Stephen Jayakumar. P and Mary Vergheese. T</i>	
7.17	Studies on statistical modelling of degradation of Reactive Orange 16 dye by ozonation: central composite design	202
	<i>M. Abaranjitha, G. Abarna, S. Gayathri, G. JananiSree, V. C. Padmanaban</i>	
7.18	Quality analysis of groundwater in malur taluk of kolar district used for drinking and domestic purposes	203
	<i>J. Ethiraj, Mohammadi Afshan, A. Nagarajan S. Vigneswari, G. Gopu, B. Muralidharan</i>	
7.19	Extraction and application of eco- friendly natural dye obtained from flower of <i>Acacia eburnea</i> (L.f.) willd on Cotton Fabric	204
	<i>S. Thiyagarajan, K. Balakrishnan, B. Muralidharan</i>	
7.20	Synthesis and characterisation of nylon-6 with p-Cresol resin by solution methodology for the thermally stable hydrophobic polymer	204
	<i>V. Thiruvengadam, M.Malathi</i>	
7.21	Synthesis, spectral and antimicrobial studies of some bis-dimedone derivatives	205
	<i>P. Navamani and N. Srinivasan</i>	
7.22	Biotemplate connected on CdO-polyethylene glycol film for structural and thermal properties	206
	<i>S. Saranya, S. Rajaboopathi, S. Thambidurai</i>	
7.23	Synthesis and characterization of chitosan-SnO ₂ particle intercalated PVP films	206
	<i>S. Anusuya, M. Karpuraranjith, S. Thambidurai</i>	

7.24	Synthesis and characterization of biopolymer connected on copper oxide-polyvinyl alcohol films <i>S. Muthu, T. Revathi, S. Thambidurai</i>	207
7.25	Synthesis and characterization of polyaniline-CdO composite for better thermal and electrochemical properties <i>S. Rajaboopathi, S.Thambidurai</i>	208
7.26	Biotemplate connected on SnO ₂ -graphene hybrid composite for structural, morphological and thermal properties <i>M. Karpuraranjith, S.Thambidurai</i>	209
7.27	Activated carbon-ZnO/Polypyrrole hybrid composite for structural, morphological and thermal properties <i>S. Nathiya, R. Karthik, S. Thambidurai</i>	210
7.28	Synthesis of novel ionic liquid crystal bearing imidazolium salt <i>R. Mangaiyarjkarasi, K. Prabhavathi and S. Umadevi</i>	210
7.29	Physico-chemical characterization and identification of halophenols (DBP's) in drinking water sample <i>Ramarajan Selvam, Selvakumar Muniraj, Tamilselvi Duraisamy, Vasanthi Muthunarayanan, Saravanan Dhandayutham, Ramaswamy Babu Rajendran</i>	211
7.30	Design and performance of a riboflavin-alginate hydrogel beads for <i>in vitro</i> anti-oxidant activity <i>G. Sathya, B. Suganya Bharathi, T. Stalin</i>	212
7.31	Liquid crystal functionalized platforms for electro-optical applications <i>B. Sivarajini, G. Suganya and S. Umadevi</i>	213
7.32	Physico-chemical studies and micronutrients status in coastal agriculture land area of Sirkazhi taluk of Nagapattinam district, Tamil Nadu, India <i>A.Arokiyaraj, N.Pasupathy, A.Vincentraj and D.Sathya</i>	214
7.33	Synthesis and characterization of PVA modified VO ₂ nanocomposites by thermal decomposition method <i>A. Mohamed Azharudeen, B. Kavitha, M. Rajarajan, A. Suganthi</i>	214
7.34	Antimicrobial activity of some newly synthesized copper (II) 2-(1H-benzo[d]imidazole-yl) methylamino)benzoic acid complex on bacterial and fungal pathogens <i>R.T. Rajalakshmi, S. R. Bheeter and T. Dons</i>	215
7.35	Synthesis, structural, morphological and electrical properties of Zn _{1-x} Al _x O nanocrystals for thermoelectric applications <i>T.M.V. Murugu Thiruvalluvan, V.Natarajan, S. Valanarasu, P.Anandan, M.Arivanandhan, R.Chandramohan</i>	215
7.36	The effect of Zn:Ti ratio on the various phase formation and optical properties of zinc titanate nanocrystals <i>P. Chandrasekaran, P.Anandhan, A.Raja, G.Gopu, M.Arivanandhan</i>	216
7.37	Dynamic sensing of ascorbic acid, dopamine and uric acid at electrochemically exfoliated graphene oxide-gold nanoparticle by electrochemical methods <i>Habibulla Imran, Venkataraman Dharuman</i>	217
7.38	Synthesis and characterization of polypyrrole-zirconia-graphene (Ppy-ZrO ₂ -Graphene) nanocomposite for voltammetric nitrite detection <i>M. Ramya and J. Wilson</i>	217
7.39	Cerium doped nickel-oxide nanostructures for riboflavin biosensing and antibacterial applications <i>P. Muthukumaran and J. Wilson</i>	218
7.40	Synthesis and characterization of polyaniline-zirconia-graphene (PANi -ZrO ₂ - Graphene) nanocomposite for voltammetric nitrite detection <i>P. Thivya and J. Wilson</i>	219
7.41	Synthesis of Pyrano-phenazine derivatives and their evaluation biological activities <i>P. Veeramani, V. Sethuraman and P. Manisankar</i>	219
7.42	Ag ₆ Mo ₁₀ O ₃₃ /ZnO nanocomposites with high visible light photocatalytic activity for removal of organic pollutant: Optimization by Genetic algorithm <i>K. Eswaran, B. Kavitha, P. Manikandan, M. Rajarajan, A. Suganthi</i>	220
7.43	Degradation of reactive red 2 dye with novel nanosize active charcoal <i>V. Sreeja, J. Anandha Raj, C. Vedhi</i>	221

7.44 A facile synthesis of magnetic activated carbon/cofe2o4 nanocomposite for the adsorption of congo red dye from water

*P. Karthikeyan, P. Anjana, K.S. Anjali, P.S. Anagha,
B. Ushadevi, S. Vairam, V. Ranjithkumar*

222

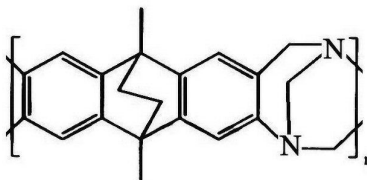
1.1 Intrinsically microporous polymers and membranes in electrochemistry

Frank Marken^a, Elena Madrid^a, Yuanyang Rong^a, Daping He^a, Richard Malpass-Evans^b, Mariolino Carta^b, Neil B. McKeown^b

^aDepartment of Chemistry, University of Bath, Claverton Down, Bath BA2 7AY, UK

^bSchool of Chemistry, University of Edinburgh, West Mains Road, Edinburgh, EH9 3JJ, UK
f.marken@bath.ac.uk

Polymers with Intrinsic Microporosity (PIMs) provide a novel class of structurally rigid ion-selective membrane materials with 3D nanofluidic pores of typically 1-2 nm size. The PIM-EA-TB material (see Figure) employed here is based on a poly-amine with estimated $pK_{A1} = 4.0$ and $pK_{A2} = 0.4$ and therefore in the protonated state an anion-conductor.



The microporous material can be employed to “heterogenise” water-insoluble molecular redox systems in films at the electrode surface [1,2]. When deposited asymmetrically over a 20 μm diameter hole in poly-ethylene-terephthalate (PET) and investigated in a two-compartment electrochemical cell with aqueous electrolyte on both sides, ionic diode effects [3] (associated with pK_{A1}) are observed with potential applications in iontronics and water desalination [4].

References:

- [1]. Y.Y. Rong, R. Malpass-Evans, M. Carta, N.B. McKeown, G.A. Attard, F. Marken, *Electrochem. Commun.* 2014, 46, 26-29.
- [2]. A. Kolodziej, S.D. Ahn, M. Carta, R. Malpass-Evans, N.B. McKeown, R.S.L. Chapman, S.D. Bull, F. Marken, *Electrochim. Acta* 2015, 160, 195-201.
- [3]. E. Madrid, Y.Y. Rong, M. Carta, N.B. McKeown, R. Malpass-Evans, G.A. Attard, T.J. Clarke, S.H. Taylor, Y.T. Long, F. Marken, *Angew. Chem. Int. Ed.* 2014, 53, 10751-10754.
- [4]. E. Madrid, P. Cottis, Y.Y. Rong, A.T. Rogers, J.M. Stone, R. Malpass-Evans, M. Carta, N.B. McKeown, F. Marken, *J. Mater. Chem. A* 2015, 3, 15849-15853.

1.2 Recent trends on the advanced materials for battery application

G.A.Pathanjali^a & M.Nagarajan^b

^{a,b}High Energy Batteries (I) Ltd., Mathur 622 515, Tamil Nadu. info@highenergyltd.com

High Energy Batteries (I) Ltd. (HEB) one of the major power source suppliers for Indian Navy, Air force, Army and Export markets, is engaged in the Development and manufacture of Silver Oxide-Zinc (Primary, Secondary and Reserve batteries), Ni-Cd and Sea water activated batteries like AgCl-Mg, CuCl-Mg. The product range includes a wide spectrum of size, weight and configuration for torpedoes, missile, aero-space and military applications. The batteries should strictly meet the defense specification requirements in terms of performance, life, cyclability, safety and the stringent environmental conditions that will be encountered during storage, handling and operation. HEB is also making commercial Lead acid batteries for automobile, standby applications and also engaged in the design and development of Phosphoric acid fuel cell and Polymer electrolyte fuel cell. HEB is engaged with, not only manufacturing but also involved in research work pertaining to advanced high performance materials and electro catalysts for Batteries and Fuel Cells.

There is a lot of scope for the development work on new material for increasing the endurance of battery and many experiments on battery materials are under progress for reducing the cost and enhancing the performance of the battery. The variety of battery applications have increased multifold, as evidenced by the remarkable growth of the battery market. The recent advancement is focused on Sodium Ion batteries to replace the Lithium Ion batteries due to scarcity of Lithium metal. Design features and manufacturing procedures of high energy density batteries will be presented.

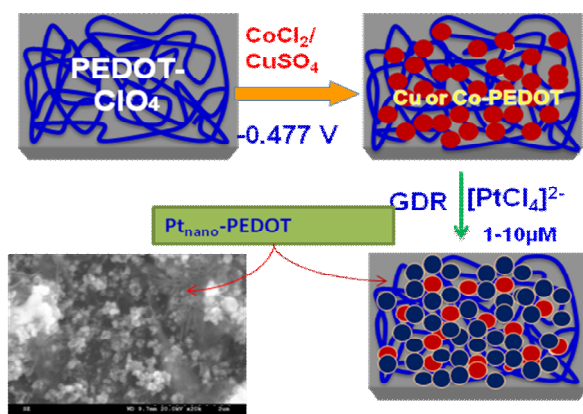
1.3 Surface Engineering of porous Metal Nanostructures: Synthesis, Fabrication and their applications in Electro-catalysis and Electrochemical Biosensors

C. Sivakumar

*Electrodics and Electrocatalysis, CSIR-Central Electrochemical Research Institute, Karaikudi-630 006, Tamil Nadu, India.
E-mail: ccsivakumar@cecri.res.in*

Abstract: Development of ordered/non-ordered porous metal nanostructured catalysts or materials is the cutting edge of present research work especially in the progress of renewable energy generation and conversion fields, electro-catalysis, electrochemical sensor and biosensor applications. To attain superior catalytic activity, complete utilization and maximum usage of nanostructured metal catalysts, different synthetic pathways such as, tailored chemical or electrochemical routes were explored with soft and hard templates for the fabrication of porous metal nanostructured catalysts with definite size and shapes. Various nanostructures of (Pt, Au, and Pd) monometallic or bimetallic or alloy nanocatalysts with controlled morphologies were also evolved using these templates. Further synergistic effect of support such as carbon including CNTs, conducting polymer and graphene matrices is also played crucial role to enhance the catalytic activity of nanostructured metal catalysts. In the present work mainly emphasise that the synthesis and fabrication of Pt based porous nanostructured metallic or bimetallic or alloy catalysts by adopting various routes like i) *in-situ* chemical and electrochemical ii) ion-exchange doping mechanism followed reduction and iii) galvanic displacement reaction (GDR) routes with and without templates. The porous nanostructured catalysts have been tested towards the catalytic hydrogenation of biologically important nitro compounds, ammonia oxidation, electrocatalytic oxidation of C1-C3 organic molecules and electrochemical bio-sensing applications like poly(phenol), glucose and neurotransmitters.

Key Words: Nanostructured metal catalysts, FE-SEM, XRD, Catalysis and Biosensor



Scheme-1: illustrate the methodology of preparing porous nanostructured catalysts

1.4 Electrochemical synthetic route for the generation of WO₃ thin films

^a*Akshay V. Salkar, Mamta Prabhugaonkar and ^bPurnakala Samant

^a*P.G. Department Of Chemistry, St. Xavier's College, Mapusa-Goa*

^b*Department of Chemistry, Govt. College of Arts, Science & Commerce, Sanquelim-Goa
thatsme.mamta@gmail.com, samantpurnakala@gmail.com*

Abstract

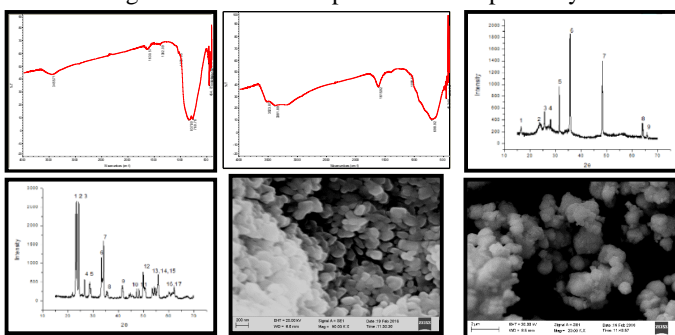
Now a days, thin films are of great importance, due to its special optical, mechanical and electrical/electronic properties. There are several methods for the preparation of thin films. Tungsten trioxide(WO₃), finds large applications in smart windows and switching devices due to its unique electrochromic properties.

In the recent work, WO₃ thin films were electrochemically generated in an aq. solution of tungstic acid by applying a voltage of 1V, with a DC source using sodium tungstate as a precursor. A blue colored thin film was found to appear gradually on a Al substrate. The voltage was applied for 6 minutes in order to develop a uniform layer of blue colored WO₃ on the Al substrate, this was the sample (A). WO₃ was also produced by conventional chemical method using nitric acid for the precipitation of sodium tungstate and calcinating it at 500°C, this was the sample (B). The two samples were characterized using instrumental techniques such as IR, XRD and SEM.

The Figure 1 and 2 displays the FT-IR spectra of the samples A and B respectively. The IR spectra confirms

the formation of WO_3 . FT-IR Spectra recorded at a range of $400\text{--}4000\text{ cm}^{-1}$ showed that stretching vibrations of $\text{W(O}_2)$ and W-O were occurring at 698cm^{-1} and 1615cm^{-1} which assigns the confirmation of formation of WO_3 and are in good agreement with reported values. The X-ray diffraction studies exhibits different XRD patterns for sample A and B as shown in figure 3 and 4 respectively. The XRD peaks of the sample prepared by chemical method are in good agreement with JCPDS file no. 30-1387.

2 theta values obtained indicates the formation of perovskite structure for WO_3 powder prepared from chemical route. The XRD pattern of the sample (A) obtained by electrochemical method can be observed from Fig.3. Data obtained indicates the formation of spinel type structure for WO_3 . The SEM images reveals the highly uniform distribution of particle size. The surface morphology reveals the appearance of typical pentagon shaped particles which remarks the generation of nano sized crystallite of WO_3 , a electrochromic material as shown in figure 5 and 6 for sample A and B respectively.



Present work offers an electrochemical method as a facial technique for preparation of nano sized thin films on aluminium substrate. This method is highly selective in creating spinel type structure

for WO_3 which can be further utilized as smart materials for electrochromic applications and switching devices. The cyclic voltammetric studies in this direction is in progress.

References:

- [1] R. Vijayalakshmi, C. Sanjeeviraja, M. Jayachandran and D. C. Trivedi, Synthesis and Reactivity in Inorganic, Metal-Organic and Nano-Metal Chemistry, 36:89–94, 2006
 [2] H.M.A. Soliman, A.B. Kashyout, A.M. Abosehly, International Journal of Innovative Research in Science, Engineering and Technology, Volume 3, special issue 3, march

1.5 Electrocatalytic Reduction of Dioxygen on 9,10-anthraquinones-incorporated Carbon Nano Tubes modified Glassy Carbon Electrodes

P.Manisankar^a and S.Valarselvan^b

^aDepartment of Industrial Chemistry, School of Chemistry, Alagappa University, Karaikudi-630003, Tamilnadu, India.

^bDepartment of Chemistry, H.H. The Rajah's College(Autonomous), Pudukkottai-622001Tamilnadu, India. svalarselvan@gmail.com

Electrocatalysis of the oxygen reduction reaction continues to command a great deal of interest in modern electrochemistry owing to its technological importance in electrochemical devices such as fuel cells and biosensors [1-3]. Carbon nano tubes have gained considerable attention in recent years due to their unique structural and physicochemical properties [4-6]. Both single walled (SWCNT) and multiwalled CNT's (MWCNT) produced an enhanced electrocatalytic effect in dioxygen reduction process[7].

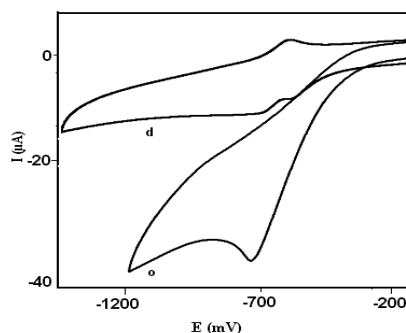


Fig.1. Cyclic voltammogram of 1,4-dihydroxy anthraquinone(1,4-DIHAQ) at GCE / MWCNT in the absence (d) and presence (o) of Oxygen at pH 6.0 at scan rate 40 mVs^{-1}

The electro chemical behaviour of hydroxy derivatives of 9,10-anthraquinone adsorbed on MWCNT modified glassy carbon electrode, the stability and efficiency in dioxygen reduction were examined by cyclic voltammetry, chronoamperometry, chronocoulometry and rotating disk voltammetry along with the determination of diffusional and kinetic parameters. The electrocatalytic reduction of dioxygen by one mono

and four dihydroxy 9,10-anthraquinone derivatives incorporated in multiwall carbon nano tubes (MWCNT) on glassy carbon electrode has been investigated. The electrocatalytic capability of modified electrodes was examined in various pH solution and dioxygen reduction potential exhibited pH dependency. The surface morphology of modified electrode was characterized by SEM. The modified electrode was found to be stable in neutral pH media. The cyclic voltammetric studies of anthraquinone derivatives at different pHs in the presence and absence of O₂ were carried out. Higher shift in oxygen reduction potential and enhancement in peak current was observed at pH 7.0 for all the five anthraquinones and hence it was chosen as the optimum working pH. Chronocoulometric studies revealed the involvement of two electrons in the reduction. The mass specific activity of anthraquinones, the diffusion coefficient of oxygen and the heterogeneous rate constants for the oxygen reduction at the surface of modified electrodes were determined by rotating disk voltammetry.

References

- [1] E.L. Dewi, K. Oyaizu, H. Nishide, E. Tsuchida, J. Power Sources 130 (2004) 286-290.
- [2] T. Ohsaka, L. Mao, K. Arihara, T. Sotomura, Electrochem. Commun. 6 (2004) 273-277.
- [3] P. Manisankar, S. Valarselvan, Ionics 18 (2012) 679-686.
- [4] H. Dai, Carbon nanotubes : opportunities and challenges. Surf. Sci. 500 (2002) 218-241.
- [5] P.M. Ajayan, Nano tubes from carbon, Chem. Rev. 99 (1999) 1787, 1799.
- [6] J. Wang, Carbon nano tube based electrochemical biosensors. A review, Electroanalysis, 17 (2005) 7-14.
- [7] M.D. Rubianes and G.A. Rivas, Electrochem. Commun., 5 (2003) 689-694.

1.6 Corrosion resistance and bioactivity evaluation of europium substituted hydroxyapatite coating on passivated surgical grade stainless steel for biomedical application

S. Sathishkumar^{a,b}, P. Karthikeyan^a, N. Murugan^a, M. Chozhanathmisra^a and R. Rajavel^{a,*}

^aDepartment of Chemistry, Periyar University, Salem 636 011, Tamilnadu, India

^bCentre for Nano science and Nanotechnology, Periyar University, Salem 636 011, Tamilnadu, India

sathish.sskg@gmail.com, rrajavel@periyaruniversity.ac.in

Introduction

The aim and development of multifunctional materials with excellent biocompatibility and bioactivity are the substantial requirement for the biomedical applications. Hydroxyapatite (Ca₁₀(PO₄)₆(OH)₂, HAP) is the main inorganic compound of human bones due to its highly biocompatible and bioactive material [1]. In this work, we modified the composition of CaP by the addition of Eu³⁺ in order to improve the bioactivity [2] and corrosion resistance on the implant materials. The present study deals with successful electrodeposition of europium substituted hydroxyapatite (Eu-HAP) on borate passivated 316L SS for biomedical applications.

Materials and Methods

Type 316L stainless steel substrates of dimension 10 x 10 x 3 mm were thoroughly polished, degreased with acetone and ultrasonication. The 316L SS were potentiostatically held in 0.4 M borate buffer solution (pH 9.3) at 640 mV vs SCE for 1 h. An anodic potential of 640 mV vs SCE was applied after which the electrode was step by step rinsed in acetone and double distilled water and immediately transferred to the analyzing chamber. Electrochemical studies linking potentiodynamic polarization experiments and impedance analysis in Ringer's solution were carried out to determine the corrosion resistance of the coating.

Results

Figure 1 shows the FT-IR spectrum of Eu-HAP coating on passivated 316L SS and all the peaks in the spectrum proved the functional groups of the Eu-HAP coating. The SEM image of Eu-HAP coating obtained on Passivated 316L SS (Fig. 2) at -1400 mV reveals that completely covered a rod-like structure. The electrochemical studies showed an improved corrosion resistance performance and bioactivity for Eu-HAP coatings on passivated 316L SS.

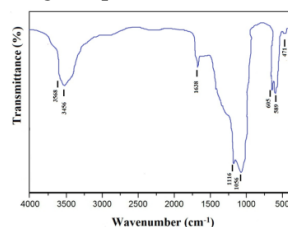


Fig. 1 FT-IR spectrum of the Eu-HAP coated on Passivated 316L SS

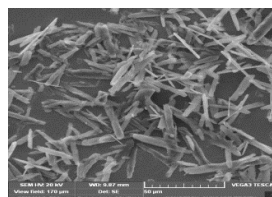


Fig. 2 SEM image of the Eu-HAP coated on passivated 316L SS

Conclusion

In present work, fully covered rod-like structured Eu-HAP coating on passivated 316L SS possessing enhanced corrosion resistance and bioactivity can be a promising candidate for biomedical applications.

Acknowledgment

S. Sathishkumar acknowledges the support received from Periyar University in the form of University research fellowship.

References

- [1] Darcy E. Wagner a, Kathryn M. Eisenmann b, Andrea L. Nestor-Kalinoski c, Sarit B. Bhaduri, Acta Biomaterialia, 9 (2013) 8422–8432.
- [2] Piaoping Yang Zewei Quan , Chunxia Li , Xiaojiao Kang , Hongzhou Lian , Jun Lin, Biomaterials, 29 (2008) 4341–4347

1.7 Structure and cycle stability of LaPO₄ coated LiMn₂O₄ cathode materials for rechargeable lithium ion batteries

P. Mohan^{a*}, and G. Paruthimal Kalaignan^{b*}

^aDepartment of Chemistry, Sree Sevugan Annamalai College, Devakottai – 630 303, India.

^bDepartment of Industrial Chemistry, Alagappa University, Karaikudi – 630 003, India

pmohanic@gmail.com : pkalaignan@yahoo.com

In this paper, we have attempted to synthesize LaPO₄ coated LiMn₂O₄ particles by sol–gel method. The structure and electrochemical properties of the surface modified LiMn₂O₄ materials were characterized by using XRD, SEM, TEM, XPS, Cyclic voltammetry and Charge-discharge techniques. The cycling behaviours of LaPO₄-coated LiMn₂O₄ cathodes were evaluated with various discharge rates between 4.5 and 3.0 V. The effects of coating on the structural and electrochemical properties were investigated in detail.

XRD patterns for LaPO₄-coated LiMn₂O₄ did not show any change in the 2θ value of the peaks, lattice parameters and no impurities were detected. TEM and XPS results revealed that, the LaPO₄ was coated over the surface of the core LiMn₂O₄ powder materials. The initial discharge capacity for LiMn₂O₄ was 125 mAh/g and declines to 70 mAh/g after 100th cycle with a capacity loss of 44%. The fast capacity fading was ascribed to the contribution of Mn³⁺ ions for Jahn-Teller distortion during the cycling process at elevated temperature. The charge/discharge capacities of surface modified LiMn₂O₄ cathode material have little reduced with increasing coating content. This result suggests that even for the LaPO₄-coated spinel phase, only the Mn³⁺ contributes the charge/discharge capacities during the electrochemical reaction. The initial discharge capacities for 1.0, 2.0 and 3.0 Wt.% LaPO₄-coated LiMn₂O₄ are 109, 103 and 93 mAh/g respectively. LaPO₄ coated (1.0, 2.0 and 3.0 Wt.%) LiMn₂O₄ cathode delivers the discharge capacities of 69, 84 and 71 mAh/g after 100 cycles respectively. The 2.0 Wt.% of LaPO₄-coated LiMn₂O₄ exhibits initial discharge capacity of 103 mAh/g, but after 100 cycles only 18% capacity loss was obtained and the discharge capacity still maintains at 84 mAh/g. This cycling behaviour of the LaPO₄-coated LiMn₂O₄ electrodes indicate the impact of LaPO₄ coating significantly which improved the electrochemical performances. On the other hand, 2.0 Wt.% of LaPO₄-coated LiMn₂O₄ shows the similar characteristics of two potential plateaus which were obtained at 3.96 and 4.11 V compared with uncoated electrode (Fig. 1). This indicates that the LaPO₄ coating does not change the intrinsic property of LiMn₂O₄ during insertion and extraction of lithium ions.

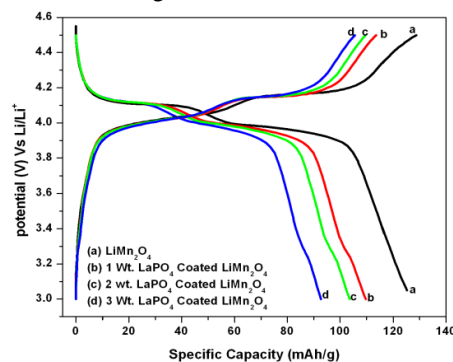


Fig.1 : Charge and discharge curves of pristine, 1.0 Wt.%, 2.0 Wt.% and 3.0 Wt.% of LaPO₄-coated LiMn₂O₄ cathode materials between the range of 3.0-4.5 V at elevated temperature.

From these results, it is believed that the improved cycling performances of LaPO₄-coated LiMn₂O₄ is attributed to the ability of LaPO₄ layer in preventing direct contact of the active material with the electrolyte resulting in a decrease of electrolyte decomposition reactions and dissolution of active materials.

1.8 Supercapacitive behaviour of nanofibrous $\text{LiFe}_x\text{Co}_{1-x}\text{O}_2$ cathode material by electrospinning technique

G. Bhuvanalogini^a and A.Subramania^b

^aDepartment of Chemistry, Sree Sevugan Annamalai College, Devakottai – 630 303, Sivaganga District, Tamil Nadu, India

^bCentre Head, Centre for Nano Sciences & Technology, Madanjeet School of Green Energy Technologies, Pondicherry University, R.V. Nagar, Kalapet, Puducherry-605 014. bhuvanalogini.g@gmail.com

Over the past few years, considerable effort has been devoted to the development of alternative energy storage/conversion devices with high power and energy densities because of the ever-increasing environmental problems and the up-coming depletion of fossil fuels. As an intermediate system between dielectric capacitors and batteries, supercapacitors have attracted a great deal of attention owing to their higher power densities relative to secondary batteries and traditional electric double-layer capacitors. Electrochemical capacitors (so-called supercapacitors), with desirable properties of high power density (10 times more power than batteries), fast charging (with seconds), excellent cycling stability, small size and light weight, have become some of the most promising candidates for next-generation power devices. With characteristics complementary to those of rechargeable batteries and fuel cells, supercapacitors have been used in many applications, such as power back-up, pacemaker, air bags and electrical vehicles.

Currently, most commercial supercapacitors make use of high surface area carbonaceous material in both aqueous electrolyte and organic electrolyte, in which the weight of the whole system is considered.

Therefore, the challenge for current supercapacitor technology is to improve the energy density without sacrificing the power density and the cycle life. An alternative approach to improve energy density is to develop hybrid electrochemical capacitors (so called asymmetric supercapacitors, or ASCs) [1], which can also provide a wider operating potential window compared to symmetric supercapacitors. For an ASC, the active material used in one electrode is usually different from that used in the other electrode in a cell system. Moreover, ASCs can make use of the different potential windows of the two electrodes to increase the maximum operation voltage of the aqueous electrolyte in the cell system, which results in an improved specific capacitance and energy density.

Fe- doped LiCoO_2 nanofibers with non-aggregated morphology have been synthesized by the electrospinning of PVA/LiAc-CoAc/Fe(NO_3)₂ followed by the calcination at an elevated temperature of 500°C for 4 hours. According to X-ray diffraction analysis, the addition of Fe into LiCoO_2 gives rise to a layered structure and similar α - LiFeO_2 with a cubic rock salt structure co-existing with the rhombohedral phase ($R\bar{3}m$). Scanning electron microscopic analyses clearly demonstrated the nanofibers with a diameter of ~40nm and a length of several micrometers. Of special importance is that the present Fe-substituted LiCoO_2 nanofibers show promising electrode performance for supercapacitors superior to those of unsubstituted LiCoO_2 nanofibers. Cyclic voltammetric analysis gave a specific capacitance of 75.8 F/g with a good capacity retention upto 1000 cycles.

Cyclic voltammetry studies

Voltammetry testing was carried out at potentials between 0 and 3 V using 1M LiPF_6 - EC/DMC (1:1v/v) electrolyte for $\text{LiFe}_{0.1}\text{Co}_{0.9}\text{O}_2$ /AC capacitor cell. CV responses recorded for the capacitor cell at different scan rates of 5, 10, 20 and 50 mV/s are presented in Fig.1. The CVs are proximately rectangular-like shape with a steep current change at the switching potential, which is similar to characteristic behaviour of an ideal capacitor. The specific capacitances calculated for the capacitor cell were 75.8, 72.6, 65.5 and 46.6 F/g at the scan rates of 5, 10, 20 and 50 mV/s, respectively. The increasing scan rate, changed the anode and cathode current with the change in voltage. This result was induced by the lithium ion insertion/extraction reaction which takes place at the electrode surface. The dramatic drop in the specific capacitance may also be due to the increasing iR -effect with increasing scan rate. The lack of symmetry of the curves with increasing scan rate is probably due to combination of both double layer capacitance and pseudocapacitance contributing to the total capacitance, and this behaviour indicate the effective utilization of the electrode material by the electrolyte, resulting in better ionic diffusion, and predominantly due to the well-spaced nanofibrous geometry of the material.

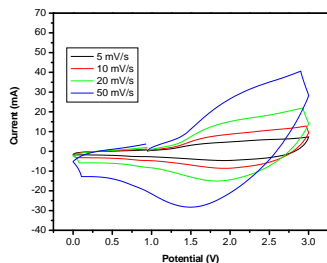


Fig. 1. Cyclic voltammograms of $\text{LiFe}_{0.1}\text{Co}_{0.9}\text{O}_2$ / PP-1M LiPF_6 – EC:DMC (1:1v/v) /AC at the sweep rates of a) 5 mV/s, b) 10 mV/s, c) 20 mV/s and d) 50 mV/s

Based on the present findings, the electrospinning technique provides a powerful method not only to prepare cation substituted LiCoO₂ nanofibers but also to improve the electrode performance of metal oxides through nanostructure fabrication.

References

[1] Xiaocheng Li, Juanjuan Shen, Wei Sun, Xuda Hong, Rutao Wang, Xinhong Zhao and Xingbin Yan, *J. Mater. Chem. A*, 3 (2015) 13244.

1.9 Chemical synthesis and characterization nano size poly (Aniline-co-ethyl 4-Aminobenzoate) copolymers

R. Sasikumar^a, V. Sethuraman^b, P. Muthuraja^b and P. Manisankar^{a,b}

^aDepartment of Physical Chemistry University of Madras, Chennai – 25, Tamil Nadu, India

^bDepartment of Industrial Chemistry, Alagappa University, Karaikudi –3, Tamil Nadu, India
skumaratr@gmail.com.

Abstract

Aniline was copolymerized chemically in presence of five different concentrations of ethyl 4-aminobenzoate using potassium persulphate as an oxidant. The copolymer exhibited good solubility in many organic solvents. Copolymers were characterized by UV-Vis, FTIR, XRD and SEM studies. The formation of copolymer was confirmed by FTIR spectral data. The spectroscopic studies confirmed incorporation of ethyl 4-aminobenzoate units in the copolymers and hence the presence of C=O group in the copolymer chains. The X-ray diffraction studies revealed the formation of nano sized crystalline copolymer. When more ethyl 4-aminobenzoate was incorporated in the copolymer the crystalline nature changed from less to more. The grain size of the copolymer calculated from Scherrer's formula was found nanometer scale. The nano size copolymer formation was also confirmed through surface morphology (100 nm) studies. The electrical property of the copolymer was studied by four-probe conductivity meter.

UV-Vis absorption spectra

The UV-VIS spectral studies were carried out for all poly (ANI-co-EAB) in DMF and DMSO solvents. Peak with wavelength maximum around 295 nm was observed for all copolymers in both the solvents. This peak may be associated with $\pi \rightarrow \pi^*$ transition from conjugated benzenoid band. This confirms the presence of benzene ring in poly (ANI-co-EAB) as in aniline and EAB. Hence it is confirmed indirectly the polymerization of aniline and EAB through amino group. Another absorption band observed at 598 nm indicates the presence of polaronic and bipolaronic radicals in the copolymer backbone (Fig.1).

Conductivity Studies of Copolymers

The electrical conductivity of copolymer was measured, through four-point conductivity meter and the results were summarized in table.1. It is observed that the electrical conductivity is strongly influenced by the EAB incorporation. Compared to the conductivity of aniline, lower values are found for copolymers. As the feed concentration of EAB increased, the conductivity of the copolymer slowly decreased. Similar observations were reported by Wang et al. [1]. This might be caused by the increased separation of the polymer chain due to the presence of side groups.

FT-IR spectral behaviour of copolymers

FT-IR spectral studies of the copolymers were carried out. The spectrum shows two absorption peaks around 3544 and 3346 cm⁻¹ these represents the formation of N-H stretching vibrations bond due to the protonation of nitrogen and NH groups of both monomer units. The quinonoid and benzenoid C=C stretching vibrations are found at 1500 and 1438 cm⁻¹, respectively. The occurrence of these two bands clearly shows that these copolymers contain secondary amine and imine units. The spectra of carbonyl C=O stretching vibrations shows a strong peak at 1662 cm⁻¹ and the peak at 2927 cm⁻¹ is attributed to the C-H stretching vibrations. The symmetric C-N stretching vibration is observed at 1254 cm⁻¹ for all the copolymers. From this spectroscopic investigation, the presence of all the fundamental functional groups present in the copolymer was confirmed qualitatively.

XRD pattern

X-ray diffraction profile of the copolymer indicates substantial degree of amorphous nature in the doped forms. The crystallite size of the copolymer was determined by employing XRD results and Scherrer's formula. The copolymers was determined as 0.02 M EAB (20 nm), 0.03 M EAB (30 nm), 0.1 M EAB (40 nm), 0.2 M EAB (55 nm) and 0.3 M EAB (70 nm) confirming the presence of nano sized copolymers of poly (ANI-co-EAB). Previous studies determined that a copolymer of aniline and 4,4- diaminodiphenyl sulphone had size of 83 nm [2].

SEM analysis of copolymer

The surface morphology was studied for chemical polymerized polymer powder by SEM analysis. Fig.5. shows SEM photograph of copolymer formed from 0.1 M aniline and 0.02 M EAB monomers in 1 M H_2SO_4 medium showed small cavity structures with approximately diameter 50 nm size is observed. The micrograph is different from flake-like surface structure of polyaniline.

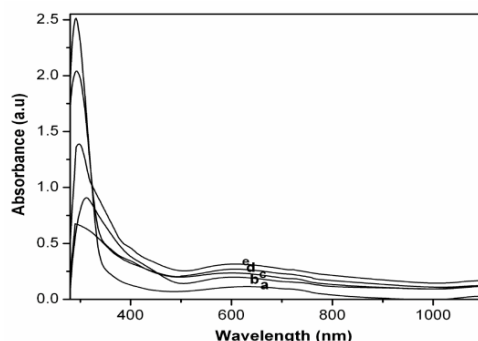


Figure 1. UV-Vis Spectra of Chemically synthesized Poly (Ani-co-EAB)

References

- [1]. Z.H. Wang, A. Ray, A.G. MacDiarmid, A.J. Epstein, Phys. Rev. B, 43 (1991) 4373
- [2]. P. Manisankar, C. Vedhi, G. Selvanathan, J. Polym. Sci. Part A: Polym. Chem. 43 (2005) 1702.

1.10 Study of Desalination Characteristics of Activated Carbon Electrode Prepared From Bael Fruit Shell

N.Mohanraj, Sachin Kumar, Shailendera Shukla, Uttam Kumar, Priyanka JP, S.Bhuvaneshwari*
 Department of Chemical Engineerin, National Institute of Technology, Calicut, Kerala
 nmohanraj2006@gmail.com, *sbuvana@nitc.ac.in

Abstract

Electrosorption, defined as potential-induced sorption on the surface of charged electrode, is a promising method for water purification and desalination. To prepare carbon electrodes assisted electrosorption process at the point of economical and biological view by using bael-fruit shell. Sliced activated carbons were prepared from bael-fruit shells, a biomass material using physical and chemical method. The ability of fine powder formed from bael-fruit shell as low-cost natural adsorbent were investigated for adsorptive removal of cations such as Zn(II), Fe (II) and Cr (VI) ions present in water. The bael-fruit shell was activated chemically and thermally. The activated carbon was prepared as electrode with 10% PVDF and DMA'c method. Improvement of desalination efficiency in capacitive deionization using Carbon electrode coated with an ion-exchange polymer. The prepared electrode has enough mechanical strength, good electrochemical stability and favourable capacitive characteristics for electrosorption process. The effects of operation parameters such as voltage, metal concentration, time on the adsorption properties of activated carbon electrode were measured in a batch process. Also characterization of raw material, activated carbon powder and electrode using BET Surface area analyzer, SEM and EDX analysis has been done. The results under the experimental circumstances studied represents adsorptive performances were good at a fixed concentration of 100 ppm metal solution, keeping voltage constant at 5 Volt and varying the time intervals.

Keywords: electrosorption, desalination, bael fruit shell, carbon electrodes, natural adsorbent

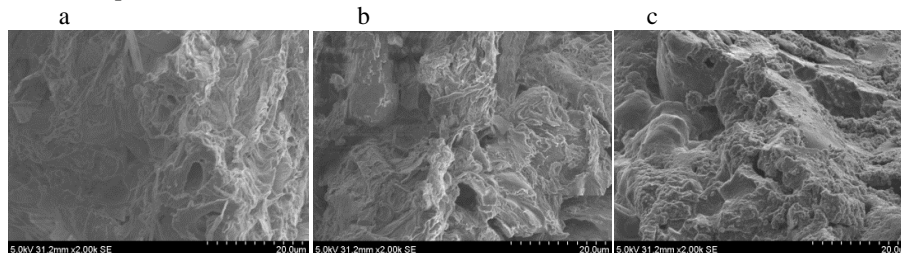


Fig. 1. Bael shell SEM image a) before activation, b) after activation, c) after electrosorption

References

- [1] Anandkumar, J. & Mandal, B., *Journal of Hazardous Materials*, (2009)168(2-3), pp.633–640.
- [2] Chang, L.M., Duan, X.Y. & Liu, W., *Desalination*, (2011)270(1-3), pp.285–290

[3] Hou, C.H. et al., Journal of the Taiwan Institute of chemical Engineers, (2012)43(3), pp.473-479.

[4] Huang, C.C. & He, J.C., Chemical Engineering Journal, (2013.)221, pp.469-475.

[5] Bayram, E. & Ayrançi, E., Separation and Purification Technology, (2012) 86, pp.113-118.

1.11 Acid doped poly(fluorenyl ether sulfone) with pendent imidazole side groups for high temperature proton exchange membranes application

^a P.Kandasamy, G. Paruthimalkalaigan and ^b K. Tharanikkarasu+

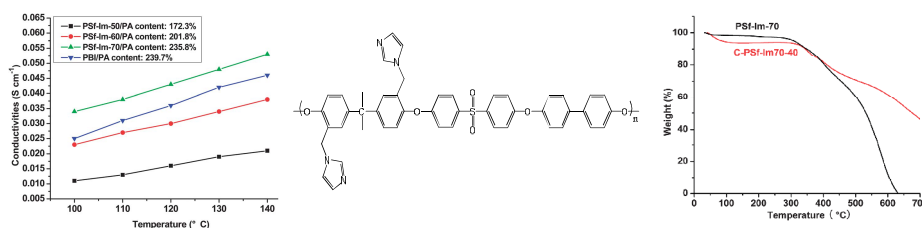
^aDepartment of Industrial Chemistry, Alagappa University, Karaikudi.

^bDepartment of Chemistry, Pondicherry University

Proton exchange membrane fuel cells (PEMFCs) is the promising power sources, has provide clean and efficient energy for stationary, transportation and portable electronics power applications. Proton exchange membrane (PEM) is a key component for fuel cell system 1-8. The existing commercial perfluorosulfonic acid PEM, such as Nafion (DuPont), has excellent chemical stability, good mechanical properties and exhibit high proton conductivities only hydrated condition. Polybenzimidazoles (PBI) membrane found to be high thermal stability, good mechanical property, excellent chemical stability and also easy to form acid-base crosslinking. Moreover the base functional polymer and inorganic acid is an effective method to develop high temperature PEM which is provide proton conductivity by a Grotthus mechanism. The use of ionic liquids, which have recently attracted great attention due to their low volatile anhydrous high proton conductivity, good thermal stability and promising physical properties.

Synthesis of polymers

2,2'-dimethylaminemethylene-9,9'-bis(4-hydroxyphenyl)fluorene imidazole functional monomer was controlled by adjusting molar ratio of aromatic biphenol monomers. 50%, 60%, 70% and 80% molar ratio was prepared. The synthesized monomer characterized by NMR, IR, Elemental Analysis and Mass spectroscopy method. Membranes were cast from the viscous solution onto glass plates with a doctor's knife. The membranes were dried in a vacuum at 80 °C for 24 h. The acid doping level of all the membranes were immersed in aqueous PA (9 M) for 1 day and the absorbed water was removed in an oven at 100 °C until the membrane weight remained unchanged.



Scheme 1. Synthesis of Imidazole: Polymer TGA curves for PSf-Im-70 and C-PSf-Im-70-40 Conductivities of acid doped PSf-Im-x membranes as a function of temperature

High molecular weight poly (arylene ether sulfone) with pendent imidazole groups was successfully synthesized using a novel monomer. The results indicate that the new PAES and PAEB membranes are promising high temperature polymer electrolyte membranes for fuel cell applications.

References

[1] J. Roziere and D. J. Jones, Annu. Rev. Mater. Res., 2003, 33, 503-555.

[2] O. Savadogo, J. Power Sources, 2004, 127(1-2), 135-161.

1.12 Effects of nanofiller on electrochemical properties of polymer electrolytes for lithium batteries

S. Edwinraj, R. Kaladevi, M. Ramesh Prabhu*

School of Physics, Alagappa University, Karaikudi-630 004, Tamil Nadu, India.

kaladevirasu@gmail.com

Abstract

An effect has been made to prepare a poly(ethylene oxide) (PEO), poly(vinyl pyrrolidone) (PVP), complexed with LiClO₄ salt and propylene carbonate (PC) based polymer gel film electrolyte for the application of lithium batteries. Physical characterization by X-ray diffraction (XRD) and Electrical properties were measured as a function of composition and temperature using complex impedance spectroscopy.

Electrochemical performance were studied due to the effect of nanofiller TiO_2 with the addition to gel polymer electrolytes.

Keywords: Polymer electrolytes, nanofiller, Ionic conductivity.

Introduction

Recently, there have been many efforts to develop thin lithium batteries using gel polymer electrolytes. Since light weight, small size and high efficiency of electrical machinery can be achieved lithium polymer batteries are very promising systems in terms of energy density and power density. Polymer gel electrolytes combine good mechanical properties with high ionic conductivity at room temperature. A salt, plasticizing liquid and a filler in polymer gels are expected to increase the ionic conductivity of system [1].

Experimental Procedure

PEO ($M_w \sim 8000$) and PVP ($M_w \sim 3,60,000$) were procured from sigma Aldrich chemicals limited, U.S.A. LiClO_4 (purity > 99.9%) from Aldrich was used as a lithium salt. The nanosized filler TiO_2 (~ 10 nm) were purchased from sigma Aldrich and used without further purification. The polymers PEO and PVP were dissolved in methanol at 50°C and room temperature respectively. Then Li salt, PC and TiO_2 were added and stirred well for 24h. Finally obtained solution was cast on a well cleaned petridishes and free standing films were obtained.

Results And Discussion

X- Ray Diffraction

The ionic conductivity of the polymer electrolytes is found mostly in the amorphous phase of the complexes. The structural analysis was carried out using XRD for all the compositions.

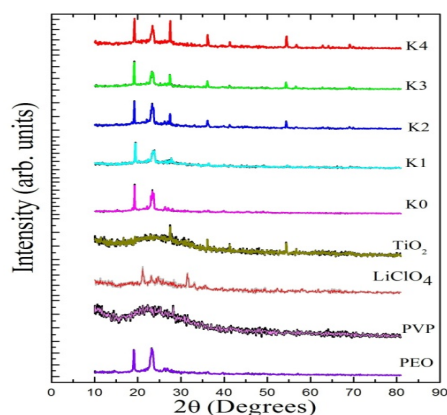


Figure 1. X-ray diffraction spectra of pure and blend electrolytes

Figure 1 shows the diffraction patterns for PEO, PVP, LiClO_4 , TiO_2 and prepared compositions of electrolytes. Two broad peaks are found at $2\theta = 19.2^\circ$ and 23.5° which confirms the semi-crystalline nature of PEO. A peak around 22.7° which is attributed to the amorphous nature of pure PVP. LiClO_4 shows intense peaks at angles $2\theta = 20.9, 22.9, 26.56, 32.75$ and 35.8° which reveal the crystalline nature of ionic salt. It has been observed after the addition of filler TiO_2 to the polymer blend, the intensity of these peaks decreases gradually and becomes relatively broader, suggesting a decrease in the degree of crystallinity of the complex. Absence of peaks and decreasing in intensity in the complexes indicates the complete dissolution of salt, filler and increase in amorphous nature of

the polymer matrix [2].

Electrochemical Impedance Spectroscopy

The behaviour of the electrochemical system can be studied by means of impedance plots over a wide range of frequencies at different temperatures by applying AC voltage or current. The ionic conductivity of a polymer electrolyte depends on the concentration of the conductivity species and their mobility. The intercept of the inclined line with the real impedance (z') axis gives the bulk resistance (R_b) of the polymer electrolytes. The ionic conductivity has been calculated using the equation $\sigma = l/R_b A$, where l is the thickness of the film and A is the surface area of the film. The highest room temperature ionic conductivity is found to be $7.167 \times 10^{-4} \text{ S cm}^{-1}$ for the sample K3.

Conclusion

Polymer electrolytes based on PEO/PVP blend with LiClO_4 , PC with nanofiller TiO_2 were prepared by solvent casting technique. The effect of TiO_2 was studied by XRD which revealed the amorphous nature of the polymer blend complexes that produced greater ionic conductivity. The maximum ionic conductivity of $7.167 \times 10^{-4} \text{ S cm}^{-1}$ at 303K was observed for sample containing 12% of TiO_2 nanofiller. Hence this polymer blend electrolyte is a potential candidate for lithium battery application.

References

- [1]. K. Kesavan, Chitra M. Mathew, S. Rajendran, Materials science and Engineering B, 184 (2014)- 26-33.
- [2]. Changmin Lee, Jin-Hwan Kim, Jin-Young Bae, polymer, 44(2003),7143-7155.

1.13 1-allyl-3-methylimidazolium chloride as a corrosion inhibitor on mild steel in 3.5% sodium chloride solution

S. Velrani^a & P. Prakash^b

^aDepartment of Chemistry, Kamaraj College, Tuticorin, Tamilnadu, INDIA

^bDepartment of Chemistry, Thiagarajar College, Madurai, Tamilnadu, INDIA

velraniprabu@gmail.com

The inhibition ability of 1-allyl-3-methylimidazolium chloride (1-AMIC) against the corrosion of mild steel in 3.5% NaCl solution was studied by using weight loss, potentiodynamic polarization and electrochemical impedance studies. Corrosion rates and inhibition efficiencies were determined and the inhibition efficiency of the studied inhibitor decreases with increase in temperature. The influence of various parameters such as the effect of inhibitor concentration and temperature on the inhibition efficiency of inhibitor was investigated in detail using weight loss technique. The kinetic and thermodynamic parameters for mild steel corrosion and inhibitor adsorption respectively, were determined and discussed. The adsorption of 1-AMIC is physical adsorption. The negative values of ΔG_{ads} indicate the spontaneous adsorption of inhibitor on the surface of mild steel in 3.5% NaCl medium. The adsorption of 1-AMIC on the mild steel surface obeyed Freundlich adsorption isotherm. Inhibition efficiency was found to depend on concentration of the inhibitor.

Electrochemical impedance measurements show that an increase in inhibitor concentration increases the charge transfer resistance (R_{ct}) and decreases double layer capacitance (C_{dl}) values owing to the increased thickness of adsorbed layer. Potentiodynamic polarization results show that 1-AMIC inhibited both anodic and cathodic reactions of mild steel and that the inhibitor act as a mixed type in 3.5% NaCl medium. FT-IR spectroscopic techniques reveal that the protective film consists of Fe-inhibitor complex. SEM images of mild steel specimens in the presence of inhibitor show almost smooth surface indicating the protective action of the inhibitor (1-AMIC) in sodium chloride medium.

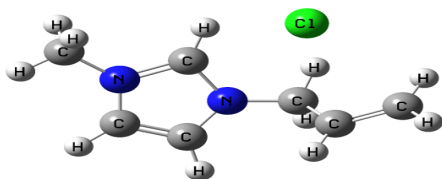


Fig. 1a: Optimized molecular structure of 1-AMIC

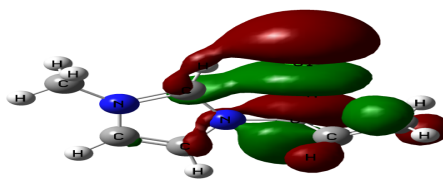


Fig. 1b: HOMO surfaces for 1-AMIC molecule

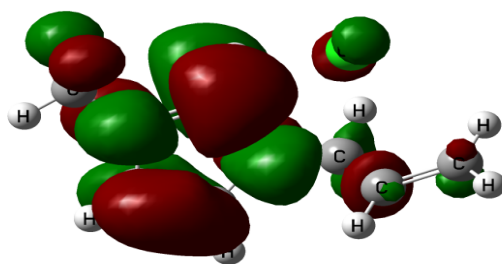


Fig. 1c: LUMO surfaces for 1-AMIC molecule.

The results find good agreement between the values of corrosion inhibition efficiency obtained from weight loss (74.63%), potentiodynamic polarization (71.99%) and impedance measurements (75.08%). Quantum chemical calculations prove that there is a link existing between the inhibitive effect of the inhibitors and the electronic properties of their main constituents. The effect of the presence of N atom in 1-AMIC and its ability act as corrosion inhibitor was investigated by quantum chemical calculations. The electronic properties such as energy of the highest occupied molecular orbital (E_{HOMO}), energy of the lowest unoccupied molecular orbital (E_{LUMO}), energy gap (E) between HOMO and LUMO on the backbone atoms were determined by optimization. The optimized molecular structure of 1-AMIC, HOMO and LUMO surfaces for 1-AMIC molecule are given in Fig. 1a, b & c respectively.

Keywords: 1-allyl-3-methylimidazolium chloride, Corrosion, Impedance, Polarization, Sodium chloride.

References

- [1] I. Ahamad, C. Gupta, R. Prasad M.A. Quarishi, *J. Appl. Electrochem.*, **40** (2010) 2171.
- [2] F. El-TaibHeakal, A.S. Fouda and M.S. Radwan, *Mater. Chem. Phys.*, **125**(2011)26.

- [3] B. Mernari, H. Elattari, M. Traisnel, F. Bentiss, M. Lagrenee, *Corrosion*, 40 (1998) 391.
 [4] S.S. Abd El Rehim, Magdy A.M. Ibrahim, K.F. Khaled, *Mater. Chem. Phys.*, 70 (2001) 268.
 [5] M.M. Hamza, S.S. Abd El Rehim and Magdy A.M. Ibrahim, *Arab. J. Chem.*, (in press).
 [6] S.S. Abd El Rehim, Magdy A.M. Ibrahim and K.F. Khaled, *J. Appl. Electrochem.*, 29 (1999) 593.

1.14 Temperature Dependent Anatase Titanium Dioxide Thin film Prepared by Electrodeposition Technique

M.Karthikeyan¹, N.Anandhan^{1*}, V. Dharuman², G.Gopu³, A.Amali Roselin¹, S.Viswanathan⁴

¹Advanced Materials and Thin film Physics Lab, Department of Physics, Alagappa University, Karaikudi-4, Tamilnadu.

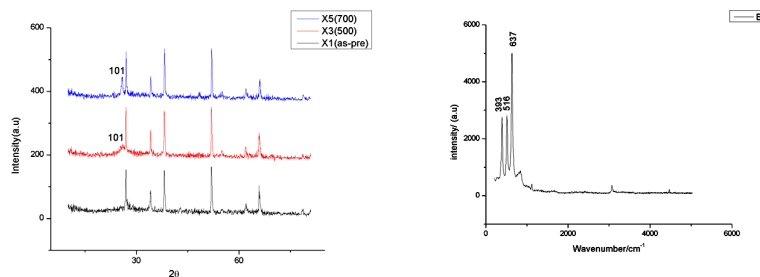
²Molecular Electronics Laboratory, Department of Bioelectronics and Biosensors, Alagappa University, Karaikudi -4,

³Catalytic and Supercapacitor Lab, Department of Industrial Chemistry, Alagappa University, Karaikudi-3, Tamilnadu.

⁴Department of Industrial Chemistry, Alagappa University, Karaikudi-3, Tamilnadu anandhan_kn@rediffmail.com

Abstract

Anatase phase titanium dioxide (TiO₂) thin film has been prepared by electrodeposition technique at lower oxidation potential and low pH below 3 for the first time on FTO glass plate (7 Ω/cm²) [1]. For this, 50 mM TiCl₃ [from 15% of TiCl₃, 10% HCl] solution was used as a precursor and 10% Na₂CO₃ solution is used to adjust the solution pH 2.5. The electrodeposition was carried out using three electrode setup with a platinum counter electrode, an Ag/AgCl reference electrode and FTO as the working electrode. The electrodeposition was performed at +0.45V vs Ag/AgCl for 1 hour at a constant bath temperature 70 °C. The film has been annealed at 500 and 700 °C in a tubular furnace for 2 hour. The X-ray diffraction shows (101) plane confirming anatase form of TiO₂ and observed data is in good agreement observation of wessels et al.,[1]. The Raman peak observed at 516 cm⁻¹ indicate the anatase phase of TiO₂ [2-3]. Band gap energy calculated from UV-absorption analysis. These results suggest that the anatase TiO₂ could be useful for the development of highly efficient solar cell devices.



XRD pattern of asprepared, 500 and 700 °C annealed TiO₂ Raman Spectra of TiO₂

References

- [1]. K. Wessels, M. Wark, T. Okermann, *J. Electrochim. Acta*, 55, 6352- 6357, 2010.
 [2]. H.Z. Zhang, J.F. Banfield, *Am. Mineral.* 84, 528, 1999.
 [3]. G.A. Tompsett, G.A. Bowmaker, R.P. Cooney, J.B. Metson, K.A. Rodgers, J.M. Seakins, *J. Raman Spectrosc.* 26, 57, 1995.

1.15 Optimization of CeO₂dispersoid content in polymer gel electrolyte based on P(S-MMA)

K. Diwakar, M. Sivakumar*, R. Subadevi

#120, Energy Materials Lab, School of Physics, Alagappa University, Karaikudi-630004.Tamil Nadu, India.

susiva73@yahoo.co.in

Abstract

In the present investigation, poly(styrene-methyl methacrylate) P(S-MMA), lithium perchlorate (LiClO₄), ethylene carbonate and propylene carbonate (EC/PC) (50/50) mixture have been taken in the optimized ratio and the Cerium oxide (CeO₂) has been dispersed in various composition in the optimized GPE system using solution casting technique [1]. The samples were characterized using Electrochemical Impedance Spectroscopy (EIS), Fourier Transform Infrared Spectroscopy (FTIR), X-ray Diffraction (XRD) and Scanning Electron Microscope (SEM). The ionic conductivity of the bare GPE has been increased by two orders of magnitude. The ionic conductivity increases with the increase of dispersoid content up to 9 wt%. Further addition of CeO₂ causes aggregation of dispersoid and the free volume has been occupied and constrains the ionic mobility, in turn conductivity. This enhancement is attributed the Lewis acid-base interaction and the

formation of three dimensional networks for ionic conduction. The ionic conductivity of the electrolytes seems to obey Arrhenius relation [2]. The outcomes of XRD and FTIR confirmed the amorphous region and the formation of complex between polymer host and the additives. The SEM images seem that the three dimensional networks formed with dispersion of ceramic fillers into polymer matrix.

Keywords: polymer electrolytes; ionic conductivity; dispersoid; P(S-co-MMA); Characterization.

References

1. S. Rajendran, M. Sivakumar, R. Subadevi, *Mat. Lett.* 58 (2004) 641–649
2. R. Subadevi, M. Sivakumar, S. Rajendran, H-C.Wu, N. L. Wu, *J.Appl.Polym.Sci.* 119 (2011)1-6

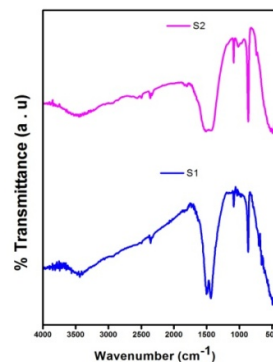
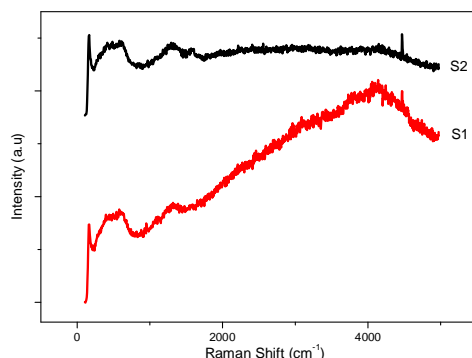
1.16 Structural and morphological characterizations of $\text{Li}_2\text{FeSiO}_4$ via solid state method

R. Dhanalakshmi^{a,b}, K. Diwakar^b, P. Rajkumar^b, R. Subadevi^b, M. Sivakumar^{b,*}

^a Department of Physics, Thiagarajar College, Madurai-625009, Tamil Nadu, India

^b Energy Materials Lab, School of Physics, Alagappa University, Karaikudi-630 004, Tamil Nadu, India.
susiva73@yahoo.co.in

In the research area of lithium-ion batteries (LIBs), great efforts have been devoted to increase the capacity and improving the security of the cathode materials [1]. Among currently available rechargeable battery systems, Lithium-ion (Li-ion) batteries feature high energy density and operating voltage, and long cycle life [2]. Lithium-ion batteries are a promising technology for energy storage. The importance of exploring new low cost and safe cathodes for larger scale lithium batteries has led to increasing interest in $\text{Li}_2\text{FeSiO}_4$ [3]. A novel synthetic method was developed to produce lithium iron silicate cost effectively starting with low cost precursors and basic laboratory equipment. The material was synthesized using a solid state synthesis. The structure and morphology of the obtained materials were characterized by XRD, FTIR, RAMAN and SEM. The crystal structure has been confirmed by powder X-ray diffraction. The functional group vibrations have analyzed using Fourier Transform Infrared Spectroscopy (FTIR). The surface morphology has been studied by Scanning Electron Microscopy (SEM).



Keywords: $\text{Li}_2\text{FeSiO}_4$; electrode; SEM, Raman spectroscopy; XRD.

References:

- [1] R. Dominko, *J.Power Sources*, 184 (2008) 462–468.
- [2] M. Armand, J.M. Tarascon, *Nature*, 451 (2008) 652–657.
- [3] Xiaobing Huang, Xing Li, Haiyan Wang, Zhonglai Pan, Meizhen Qu, Zuolong Yu, *Solid State Ionics*, 181 (2010) 1451-1455.

1.17 Structural and morphological studies of sulfur-PEO- MnO_2 composite for lithium sulfur batteries

G. Radhika, M. Sivakumar^{*}, R. Subadevi

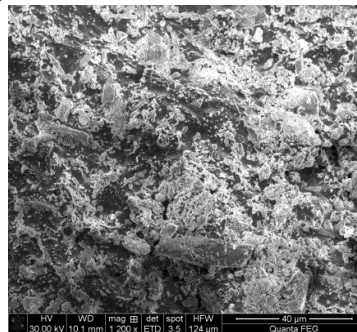
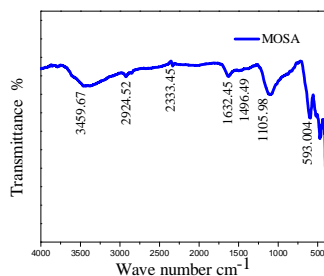
#120, Energy Materials Lab, School of Physics, Alagappa University, Karaikudi-630 004, Tamil Nadu, India
susiva73@yahoo.co.in

Abstract

Lithium sulphur batteries with a higher theoretical capacity of 1672 mAhg⁻¹ than commercial LIB systems can meet the many requirements of day to day life [1]. Metallic oxide is fascinating because it provides higher electrode density than carbon materials [2]. A simple and facile synthesis route for S/PEO/ MnO_2 composite via dry media reaction. The complexation has been investigated using FTIR and RAMAN Analysis.

The XRD data do not show any new phases in the final product, which could be an indication of the absence of chemical reaction between the composites. SEM reveals that most of the sulfur is uniformly dispersed in the MnO_2 . The present study indicates that S/PEO/ MnO_2 composite is a good candidate for the cathode material particularly in Lithium Sulfur Battery.

Keywords: electrode; lithium sulfur battery; composite;



Reference

- [1] R.Demir-cakan, M. Morcrette, babuGanguli, A. Gueguen, R. Dedryvere, J.M. Tarason, *Energy Environ. Sci.* 6(2013) 176-182
 [2] Jeongyeon Lee, taejin Hwang, Yongho Lee, JoongKee Lee, Wonchang Choi, *Material Letters* 158(2015) 132-135.

1.18 Electrochemical copolymerization coating on Passivated Low Nickel Stainless Steel for corrosion protection performance in 0.5M H_2SO_4 medium

P. Karthikeyan^a, S. Sathishkumar^a, N. Murugan^a, M. Chozhanathmisra^a and R. Rajavel*^a

^aDepartment of Chemistry, Periyar University, Salem 636 011, Tamilnadu, India.

*dr Rajavel@periyaruniversity.ac.in; p.karthikeyan.msc@gmail.com

Abstract

Monomer of O-Anisidine (POA), 3, 4 ethylenedioxythiophene (PEDOT) and its Copolymer (P(PEDOT-co-POA)) coating were electrochemical polymerization by cyclic voltammetry as protective coating against corrosion on passivated Low Nickel Stainless Steel (LN SS) surface. It yields to strong adherent and smooth nanopolymer films. The anti-corrosion test was investigated in 0.5M H_2SO_4 solution by electrochemical impedance spectroscopy (EIS) and potentiodynamic polarization study. The result shows that the presence of polymer and copolymer coating on passivated metal considerably reduces the corrosion rate of LN SS. Moreover, Copolymer (P(PEDOT-co-POA)) coating provided higher corrosion resistance coating than PEDOT and POA alone.

Introduction

Stainless steel is extensively used in many fields due to their exceptional corrosion resistance property. The largest part of stainless steel equipment failures are caused by chloride ions, particularly in cooling water systems the pitting and crevice corrosion are still serious problems for stainless steel[1]. In recent times, conducting polymers have received considerable value as corrosion protective coatings for oxidizable metals. It is now well-known that electrochemical polymerization is a effortless and most suitable method for corrosion protection [2-5]. The present work deals with the electrochemical polymerization of PEDOT, POA and Copolymer (P(PEDOT-co-POA)) coating on LN SS in 0.5M H_2SO_4 medium.

Experiment

LNSS specimens of dimension 10 x10 x 3 mm were polished, degreased with acetone and ultrasonicated. The PEDOT, PANI and Copolymer (P(PEDOT-co-POA)) coating on passivated LN SS was carried out using cyclic voltammetry in a three electrode assembly. Electrochemical studies involving potentiodynamic polarization experiment and EIS analysis in H_2SO_4 medium were carried out to determine the corrosion resistance of the coatings.

Results/Discussion

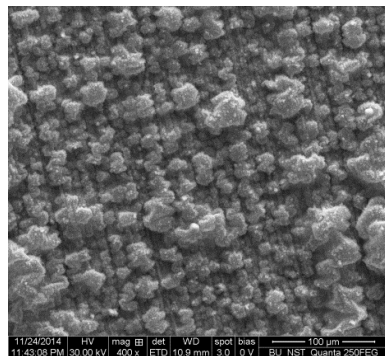


Fig. 1(a)

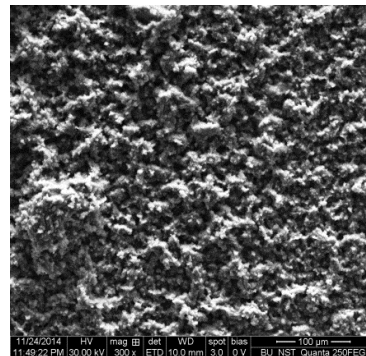


Fig. 1(b)

The surface morphology of the POA coated on passivated LN SS (**Fig. 1(a)**) exhibited the formation of granular and non-uniform nanostructure. **Fig. 1(b)** shows the surface morphology of copolymer (P(PEDOT-co-POA)) coated on passivated LN SS, small granular with uniform nanostructure [6,7].

The nyquist plots of the uncoated and POA, PEDOT and copolymer (P(PEDOT-co-POA)) coated passivated LN SS in 0.5 M H₂SO₄ medium. The I_{corr} value obtained for the uncoated specimen is 0.72 mA/cm². The lower I_{corr} 0.04 mA/cm² value obtained for the copolymer (P(PEDOT-co-POA)) coated passivated LN SS demonstrated that the small granular with uniform like polymer layer covers the metal surface completely and protects against the acid corrosive ions significantly

Conclusion

Electrochemical polymerization of mono and Copolymer coatings on passivated LN SS were successfully carried out by cyclic voltammetric technique. The POA, PEDOT and copolymer (P(PEDOT-co-POA)) coated on passivated LN SS were characterized by potentiodynamic polarization and electrochemical impedance studies. The results are revealed that the 1:2 ratio acts as a better protective layer than that obtained at other on LN SS, against corrosion protection in 0.5M H₂SO₄ medium.

Acknowledgements

P. Karthikeyan acknowledges the support received from Periyar University in the form of University Research Fellowship (URF).

References

- [1] S. Fajardo, D.M. Bastidas, M.P. Ryan, M. Criado, D.S. McPhail, R.J.H. Morris, J.M. Bastidas, *Appl. Surf. Sci.* 288 (2014) 423-429.
- [2] K.M. Govindarajua, V. Collins Arun Prakashb, *Colloids and Surfaces A: Physicochem. Eng. Aspects* 465 (2015) 11–19.
- [3] D. Gopi, P. Karthikeyan, L. Kavitha, M. Surendiran, *Appl. Surf. Sci.* 357 (2015) 122–130.
- [4] SP. Sitaram, JO. Stoffer, TJ. OKeefe, *J. Coatings Technol.* 69 (1997) 65-69.
- [5] P. Karthikeyan, S. Sathishkumar, E. Shinyjoy, L. Kavitha and D. Gopi ISBN 978-93-85477-46-1
- [6] A. Madhankumar, S. Ramakrishna, P. Sudhagar, H. Kim, Y.S. Kang, I.B. Obot, Z.M. Asad Gasem, *J Mater Sci* (2014) 49:4067–4080
- [7] A.T. Ozyilmaz, B. Avsar, G. Ozyilmaz, I.H. Karhan, T. Camurcu and F. Colak, *Appl. Surf. Sci.* doi: 10.1016/j.apsusc.2014.04.177

1.19 Improved electrochemical properties of LiMn₂O₄ with the La and Sm co-doping for rechargeable lithium-ion batteries

K. Kalaiselvi^a, P. Mohan^b and G. Paruthimal Kalaignan^{a*}

^aDepartment of Industrial Chemistry, Alagappa University, Karaikudi – 630 003, India

^bDepartment of Chemistry, Sree Sevugan Annamalai College, Devakottai – 630 303, India.

pkalaignan@yahoo.com

In this work, the pristine LiMn₂O₄ and samarium and lanthanum substituted LiSm_xLa_{0.2-x}Mn_{1.80}O₄ (X = 0.05, 0.10 and 0.15) cathode materials were prepared by using the tartaric acid assisted sol-gel method. The physical and electrochemical properties of the synthesized materials were characterized by using TG/DTA, XRD, SEM, TEM, XPS, cyclic voltammetry, charge/discharge and electrochemical impedance spectroscopy studies.

LiMn₂O₄ samples with and without the Sm and La substitution have similar charge-discharge profiles, exhibiting two charge-discharge plateaus in the potential region of 3.96 and 4.11 V, which are ascribed to the

remarkable characteristics of a well defined spinel LiMn_2O_4 (Fig. 1). Voltage plateaus have suggested the insertion and extraction of lithium-ions occurring in two states. The first voltage plateau at about 3.96 V is attributed to the removal of lithium ions from half of the tetrahedral sites in which Li-Li interaction occurs. The second voltage plateau observed at around 4.11 V is ascribed to the removal of lithium ions from the remaining tetrahedral sites.

The initial discharge capacity for LiMn_2O_4 was 133 mAh/g and declines to 98 mAh/g after 100th cycle with a capacity loss of 26%. This fast capacity fading is ascribed to the contribution of Mn^{3+} ions for Jahn-Teller distortion during the cycling process. LiMn_2O_4 still suffers capacity fading due to Mn^{3+} dissolution resulted from side reactions, which occurred at the interface between electrode and electrolyte during charge-discharge process. In contrast, the $\text{LiSm}_{0.10}\text{La}_{0.10}\text{Mn}_{1.80}\text{O}_4$ electrode has exhibited an initial discharge capacity of 127 mAh/g and 114 mAh/g discharge capacity after 100th cycle with only 10% capacity loss. This cycling behaviour of the Sm and La substitution has significantly improved the electrochemical performances. The samarium and lanthanum substituted $\text{LiSm}_{0.10}\text{La}_{0.10}\text{Mn}_{1.80}\text{O}_4$ electrode has the better cycling performance. Because the substitution of manganese by Sm and La has increased the unit cell volume (In XRD analysis) and the Mn^{3+} ions concentrations which reduce the Jahn-Teller distortion and also reduce the manganese dissolution. It also stabilizes the structural integrity and improves the electrochemical behaviour of Sm and La substituted LiMn_2O_4 electrode. The strength of dual metal-oxygen (Sm-O and La-O) bond is another reason for enhanced cycleability of LiMn_2O_4 electrode.

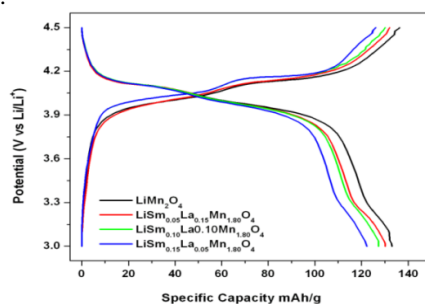


Fig.1 Charge/discharge curves of pristine and $\text{LiSm}_x\text{La}_{0.2-x}\text{Mn}_{1.80}\text{O}_4$ ($X = 0.05, 0.10$ and 0.15) cathode materials between the range of 3.0 - 4.5 V at 0.5 C rate discharge

Small amount of samarium and lanthanum substitution in $\text{LiSm}_{0.10}\text{La}_{0.10}\text{Mn}_{1.80}\text{O}_4$ has developed the structural stability, rate capability and cycling performances of the cathode materials for the rechargeable lithium-ion batteries. These results suggest that, $\text{LiSm}_{0.10}\text{La}_{0.10}\text{Mn}_{1.80}\text{O}_4$ sample is attractive material for battery applications.

1.20 Inhibition of aluminium corrosion using agarose in acidic medium

R.S. Nathiya and V. Raj*

*Advanced Materials Research Laboratory, Department of Chemistry, Periyar University, Salem – 11, Tamil Nadu, India
alaguraj2@rediffmail.com*

Introduction

Aluminium is one of the most important metals which find extensive domestic and industrial applications. Prevention of corrosion using inhibitor is the most applicable and cost effective economical methods. Most of the corrosion inhibitors are synthesized organic heterocyclic and inorganic compounds which are very expensive and toxic. So the development of novel corrosion inhibitors of natural source and non-toxic type of prime important. Bio polymers are chemically stable, biodegradable and eco-friendly macromolecules with unique inhibiting strengths and mechanistic approaches to metal surface and regraded as low cost, renewable and readily available alternatives for the corrosion inhibition. Agarose, a biodegradable polymer, is a seaweed polysaccharide, consists of alternating 3-O-linked d-galactopyranose and 4-O-linked 3, 6-anhydro-l-galactopyranose.

The aim of this study is to investigate the inhibition effect of agarose on aluminium corrosion in 1 M HCl solution by potentiodynamic polarization and electrochemical impedance spectroscopy methods. At the same time, aluminium surfaces were examined by scanning electron microscopy and water contact angle techniques. The performance of the agarose inhibitor on prevention aluminium corrosion has been further ascertained through molecular modeling using density functional theory (DFT).

Results and discussion

The results indicate (Fig.1) inhibition efficiency increases with increase in concentration of the inhibitor but decreases with rise in temperature in 1M HCl. The potentiodynamic polarization results (Fig. 2)

indicate that the agarose acts as a good inhibitor for the corrosion in acidic medium and it behaves as a mixed-type inhibitor. SEM and Water contact angle (Fig. 3) images confirm the protective film formation on the aluminium surface. A quantum chemical computational approach was performed to support the strong adsorption of agarose molecules on the aluminium surface.

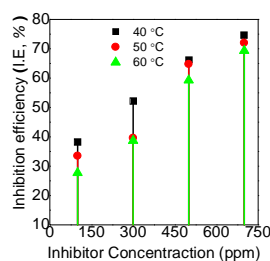


Fig. 1. Effect of inhibition efficiency of agarose in 1M HCl.

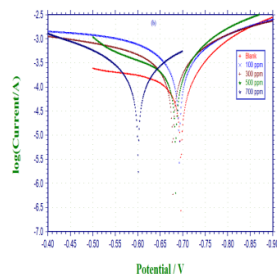


Fig.2. Tafel curve for the corrosion of aluminium in 1 M HCl containing various concentration of inhibitor.

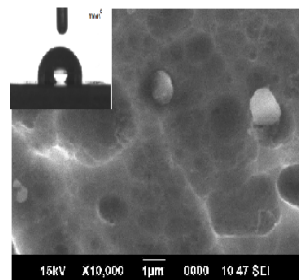


Fig. 3. SEM and WCA images 700 ppm of agarose 1 M HCl

Conclusion

These findings indicate that agarose has potential as green alternative to existing biopolymer corrosion inhibitors.

Reference

- [1]. Quraishi, M. A., Singh, A., Singh, V. K., Yadav, D. K., Singh, A. K., Mater. Chem. Phys., 122 (2010) 114.
- [2]. Tebbji .K, Faska .N, Tounsi .A, Oudda. H, Benkaddour .M, Hammouti. B, Mater. Chem. and Phys., 106 (2007)260.

1.21 A study of corrosion inhibition effect on mild steel by L-Phenylalanine in 1 M HCl medium

G. Jayabharathi^{a*}, and G. Chandramohan^b

^aDepartment of Chemistry, AVVM Sri Pushpam College, Poondi, Thanjavur-613503, TN

^bDepartment of Chemistry, Jairams Arts and Science College, Karur, TN

bharathi.sarju@gmail.com

Abstract

In the present work, corrosion inhibition effect of L-Phenylalanine will be investigated on Mild Steel in 1 M HCl medium by gravimetric method and electrochemical studies. Several parameters like inhibitor concentration, time, temperature and synergistic effect of some salts will also be studied. Literature survey reveals that the increase in concentration of inhibitor will increase the inhibition efficiency [1]. Electrochemical methods like Tafel polarization, Electrochemical Impedance Spectroscopy (EIS), Inductively Coupled Plasma Optical Emission Spectroscopy (ICP-OES) techniques will be followed [2]. Adsorption of inhibitor was found to follow the Langmuir's adsorption isotherm. Adsorption equilibrium constant (K_{ads}) and free energy of adsorption (ΔG_{ads}^0) were calculated and discussed [3]. Surface analysis (SEM) was also carried out to establish the corrosion inhibitive property of inhibitors in 1 M HCl solution [4]. The inhibition efficiency will also be compared with 0.5 M H_2SO_4 medium. It is also planned to use some synthesized Schiff bases to study the inhibition efficiency on mild steel in acid medium.

Key words: L-Phenylalanine, mild steel, Tafel polarization, EIS, ICP-OES

References:

- [1] K. Stanly Jacob and Geetha Parameswaran, *Corrosion Sciences*, **52**(1), (2010), pp. 224-228.
- [2] P. Shanmugasundaram, T. Sumathi, G. Chandramohan and G.N.K. Ramesh Babu, *International Journal of Current Research*, **5**(5), (2013).
- [3] SLA Kumar, P Iniyavan, MS Kumar, and A Sreekanth, *Journal of Materials and Environmental Sciences*, **3**, (2012), p. 461.
- [4] A. Yurta, A. Balabanb, S. Ustün Kandemira, G. Bereketa, and B. Erkb, *Materials Chemistry and Physics*, **85**(2), (2004), pp. 420-426.

1.22 Numerical analysis of specific absorption rate and to protect human brain from microwave radiation using electromagnetic shielding

Vakula Paranam S, Vasant Naidu, Senthil Kumar A

Dept of ECE, Sethu Institute of Technology, Pulloor, Kariapatti-626115, Email: vakulaparanam@gmail.com

Abstract

The utilization of electromagnetic wave in various applications is increasing rapidly because of its advantages. Possibility of the electromagnetic wave impinges in a target, any one or combination of three interactions may occur: beam may be reflected, absorbed or may pass through the object. Only the absorbed fraction is harmful, it cause increase in temperature of human brain. Hence, to provide the shielding towards human brain from microwave radiation, the $\text{TiEr}_x\text{Ho}_y\text{Fe}_{2-x-y}$ material will be used $\text{TiEr}_x\text{Ho}_y\text{Fe}_{2-x-y}$ ferrite with $x=0.15, 0.7$ and $y=0.1, 0.06$ compositions were synthesized through the sol-gel method. These powders are calcined, compacted and sintered in a microwave furnace. The effect of Er substitution on phase composition, nano size structure was analyzed by X-ray diffraction. The nano material mixed with paint and it is coated on the glass surfaces to absorb the electromagnetic radiation. The depth of penetration and shielding effectiveness was measured. Shielding effectiveness increases upto 30 db as a function of frequency. The electrical, porosity studies and structural properties of $\text{TiEr}_x\text{Ho}_y\text{Fe}_{2-x-y}$ have been investigated and numerical analyzing of the reflection loss, dielectric properties for human brain in high frequency range has obtained. Moreover, the dielectric properties and temperature increase are proportional to the power of heating source. The specific absorption rate and the temperature distribution obtained by numerical solution of electromagnetic wave propagation to the human brain during exposure to mobile phone radiation are presented.

Keywords - Specific absorption rate, Electrical Properties, Porosity, and Shielding Effectiveness.

1.23 Electrochemical synthesis and spectroelectro chemical characterization of poly(3-ocylthiophene-co-3, 4-ethylenedioxythiophene)

P.Authidevi^a, D.Kanagavel^{*b}, J. Peter and C.Vedhi^c

^a*Department of Chemistry, Chandy College of Engineering, Thoothukudi.*

^{*b}*Department of Chemistry, Kamaraj College, Thoothukudi.*

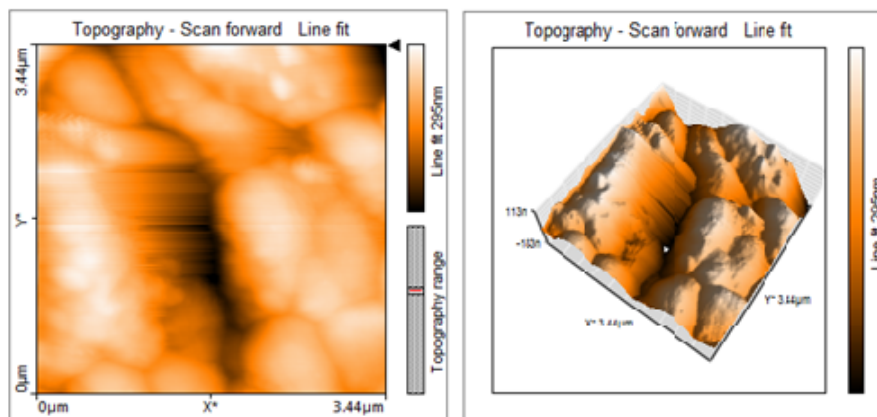
^c*Department of Chemistry, V.O.Chidambaram College, Thoothukudi*

Abstract

Poly(3-ocylthiophene-co-3,4-ethylenedioxythiophene) was electrochemically polymerized in aprotic acetonitrile medium on indium-tin oxide (ITO) plate. The properties of the resulting film were studied by cyclic voltammetry (CV), Fourier transform infrared spectroscopy (FTIR) and UV-visible spectroscopy. The surface morphology of the film was investigated through scanning electron microscopy (SEM) and atomic force microscope (AFM). X-ray diffraction and EDAX experiments were also performed to characterize the structural and composition of the thin film. Spectroelectrochemical properties of the co-polymer were studied through cyclic voltammetry with UV-visible spectroscopy. Spectroelectrochemical study reveals that this co-polymer film exhibits high chromic contrast, comparative switching times, great electrochromic efficiency, and long-term switching stability. The electrochromic properties of this co-polymer motivate for the future application in electrochromic devices.

Growth of Poly(3-ocylthiophene-co-3,4-ethylenedioxythiophene) thin film on ITO surface was carried out in 0.01M EDOT and 0.01M (P3OT) in aprotic acetonitrile medium in the potential range from -600 to 1400 mV at a scan rate of 50 mVs⁻¹. The morphology of the co-polymer film surface was studied by AFM. The film exhibits bundles of nanowire structure. The line roughness parameters of Ra, Rq, Ry, Rp, Rv, Rm are measured to be 62.83nm, 75.47nm, 262.05nm, 92.86nm, -169.18nm, -20.47fm respectively. The area of the film is calculated as 3.44 μm^2 and the area roughness parameters of Sa, Sq, Sy, Sp, Sv, Sm value are measured to be 46.34nm, 58.15nm, 420.04nm, 209.52nm, -210.52nm, -20.47fm respectively.

Key words: poly3-ocylthiophene, poly3, 4-ethylenedioxythiophene, cyclic voltammetry, electrochromic, spectroelectrochemistry.



AFM image of Poly(3-ocylthiophene -co-3,4-ethylenedioxythiophene)

1.24 Study of mediator-less and membrane-less microbial fuel cell system on power generation from dairy wastewater treatment

Vidhyeswari.D^{a*}, Chinchu Elezebeth^b, A.Surendhar^c and S.Bhuvaneshwari^d
^{a,c&d} *Chemical Engineering Department, National Institute of Technology Calicut, Kerala*

^b *Department of Biotechnology, Mep's School of Engineering, Thrissur, Kerala. ^{*}ammudilip@gmail.com*

Increasing human activities are consuming the natural energy sources leading to the depletion of fossil fuels. The present day energy scenario in India and around the globe is precarious. The need for alternate fuel has made us to initiate extensive research in identifying a potential, cheap and renewable source for energy production. Microbial fuel cells (MFCs) are being developed by greater efforts since they are envisaged to be a promising wastewater treatment technology with direct recovery of electric energy. It is a bioreactor that converts chemical energy present in the bonds of organic compounds into electric energy, through the reactions of microorganisms. The principal problem with MFC is that Power generated by the cell may not be enough. It can be solved by increasing the surface area of the electrodes. In this work, graphite rods (of height, 11cm and radius, 0.5cm) were used as electrodes in both chambers. Mixed culture of bacteria were isolated from dairy wastewater and used for this study. Bacterial strains were made to grown in anode material by inoculating organisms in the rod. The entire setup was kept in stirrer at 500rpm for maintaining mass transfer throughout the system and to prevent the formation of sludge at the bottom. After 12 days of operation, the color of wastewater changes from white to transparent. COD and BOD concentrations were reduced by 89% and 85% respectively. Total dissolved solids concentration was reduced by 57.68%. The power density reached 565mW/m². Small portion of the biofilm was scratched from the electrode surface after emptying the MFC. SEM image revealed typical bacterial growth on the surface of anode electrode. A close examination revealed that there were different predominant bacterial morphologies on the electrode.



MFC SETUP

References

- [1]. Alberty, R. a. et al., 2011. *Biophysical Chemistry*, 155(2-3), pp. 89–103.
- [2]. Choi, C. & Hu, N., 2013. *Bioresource Technology*, 133, pp. 589–598.
- [3]. Du, Z., Li, H. & Gu, T., 2007. *wastewater treatment and bioenergy* 25, pp. 464–482.
- [3]. Hernández-Fernández, F.J. et al., 2015. *Fuel Processing Technology*, 138, pp. 284–297.
- [4]. Li, Z., Zhang, X. & Lei, L., 2008. *fuel cell.* , 43, pp. 1352–1358.

- [5]. Oliveira, V.B. et al., 2013. *Biochemical Engineering Journal*, 73, pp. 53–64. [6]. Pinto, R.P. et al., 2010. *Bioresource Technology*, 101(14), pp. 5256–5265. [7]. Potter, M.C., 1911. *Proceedings of the Royal Society B: Biological Sciences*, 84(571), pp. 260–276. [8]. Zheng, S. et al., 2015. *fuel cells*, 284, pp. 252–257.

1.25 Corrosion Inhibition of Aromatic Ring Substituted Benzimidazole Derivatives for Mild Steel in Acidic Medium

A. Velmurugan, K. Kanmani, G. Muthusankar, G. Gopu*
 Department of Industrial Chemistry, Alagappa University, Karaikudi – 630003
 nggopi79@gmail.com, velmurugansuresh26@gmail.com

Acid solutions are widely used for industrial cleaning, oil well acidification and in the petrochemical processes. For Inhibition purpose nitrogen, sulphur or oxygen atoms containing heterocyclic organic compounds are frequently used [1, 2]. In this work the corrosion inhibition ability of synthesized benzimidazole derivatives against the corrosion of mild steel in acid solution was examined. The synthesized derivatives (Fig.1) were characterized by ^1H NMR, ^{13}C NMR spectrum and FT-IR spectrum (Fig.2). The corrosion inhibition ability was studied by using potentiodynamic polarization technique. The obtained results show that the benzimidazole derivatives block both the anodic and cathodic currents in acid medium due to the adsorption of inhibitor on the surface of the mild steel.

To confirm the adsorption phenomena, electrochemical impedance spectrum has studied by varying the inhibitor concentration. During the impedance measurement, the charge transfer resistance (R_{ct}) increases and the double layer capacitance (C_{dl}) decreases in the presence of the inhibitors which implied the adsorption of the inhibitor molecules on the mild steel surface [3]. It was clear that the organic substrate concentration increased the area of adsorption increased, hence the inhibition efficiency increased. The results suggested that Derivative 2 showed higher inhibition than the derivative 1. The adsorption of inhibitor highly related with Langmuir adsorption isotherm.

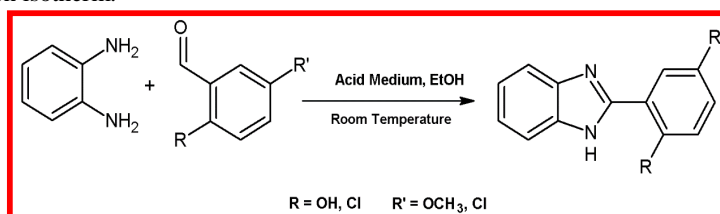


Fig 1: Scheme for the preparation of benzimidazole derivatives

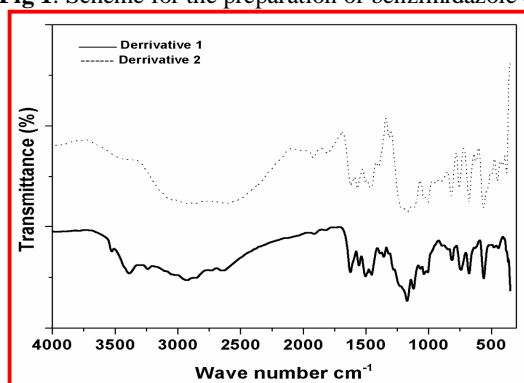


Fig 2: FT-IR spectrum of Benzimidazole Derivatives

Reference:

- [1]. M. Yadav et al. *Journal of Molecular Liquids* 213 (2016) 122–138
 [2]. I.B. Obot, N.O. Obi-Egbedi *Corrosion Science* 52 (2010) 657–660
 [3]. J. Aljourani et al. *Corrosion Science* 51 (2009) 1836–1843

1.26 Double layer SiO₂-TiO₂ Solgel coating for corrosion protection of wearables

S.Ramasubramanian^a, P.Prakash^{b,*}

^aMaterial Engineering Department, Titan Company Limited, Hosur, Tamilnadu, India.

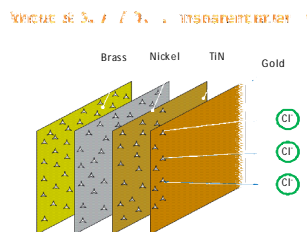
^bDepartment of Chemistry, Thiagarajar College, Madurai-9, Tamilnadu, India. knpprakash@gmail.com

Abstract

This manuscript aims to investigate the corrosion resistance behaviour of SiO₂-TiO₂ solgel coating on gold plated fashion accessories, especially watches. A double layer of SiO₂-TiO₂ with varied concentrations (0.1M - 0.5M) was coated on gold plated accessories by dip coating process. The coating was characterised using Atomic force microscope, Scanning electron microscope and Stylus profilometer. The corrosion behaviour was studied by potentiodynamic polarisation experiments in artificial sweat solution. Coating with 0.3 M of SiO₂-TiO₂ shows higher corrosion inhibition compared to other concentrations. The coated layer retains the lustre and brilliance of the gold with all the above concentrations.

Keywords: Sol gel coating, double layer, fashion accessories, corrosion resistance

Graphical Abstract



Corrosion spots due to meso pores of titanium nitride & gold coated fashion accessories lead to corrosion on brass substrate due to leaching of highly corrosive chloride ion of sweat solution.

1.27 Corrosion behaviour of Mg-Li-Al alloy in chloride media

A.Cyral^{a,*} & L.Sudha^a

^aP.G.&Research Dept.of Chemistry, Raja Duraisingam Govt.Arts College, Sivaganga – 630 561, Tamilnadu, India. * Tel +91-096883-65009

Abstract

In this investigation attempts have been made to understand the corrosion behavior of the Mg-Li-Al light alloy materials, which are widely used in battery and aerospace industry. The performance of the Mg-Li-Al has testified in the aqueous environment of NH₄Cl and MgCl₂ in the concentration range of 0.05 to 2.0 M. The dc, ac and SEM techniques have been adopted for this investigation. Results indicate that the more corrosion prone at NH₄Cl than in MgCl₂ solutions. The dc polarization data shows that corrosion reaction of the alloy is controlled by anodic in NH₄Cl and cathodic reactions in MgCl₂ solutions. From the impedance data, it is found that the corrosion of Mg-Li-Al alloy is controlled by charge transfer process at all concentrations. Surface morphology has been identified by SEM.

Keywords : Corrosion; Mg-Li-Al alloy; Polarization; impedance; SEM

Conclusions

Based on the Tafel slopes, the Mg-Li-Al alloys corrosion reaction is anodically controlled in NH₄Cl solution where as cathodically controlled in MgCl₂ solution. The corrosion current (i_{corr}) is found to increase with increase in concentration of the electrolyte. The aggressiveness of NH₄Cl is reflected in the R_{ct} value, least value is observed in 2.0 M concentration and high value obtained in 0.1 M MgCl₂ solution. Hence NH₄Cl is more aggressive media than the MgCl₂. From SEM, the pit formation is uniform at the surface of higher concentration MgCl₂ than at the lower concentration.

1.28 Electrochemical properties of organo-montmorillonite clay nanocomposite lithium polymer electrolytes based on PEO/PVdF-HFP blend

Pradeepa Prabakaran, Roshini Raju, Sowmya Gurusamy, Ramesh Prabhu Manimuthu*
School of Physics, Alagappa University, Karaikudi-630 004, Tamil Nadu, India.
roshuraju29@gmail.com

Abstract

A study is conducted on the electrochemical properties of nanocomposite polymer electrolytes based on intercalation of montmorillonite (MMT) clay polymer into the galleries of poly (ethylene oxide) (PEO)-poly (vinylidene fluoride-co-hexa fluoro propylene) (PVdF-HFP) . Solution casting technique is employed for nanocomposite formation with varying clay loading from 0 to 4 wt%. Examination with a.c. impedance spectroscopy reveals that the ionic conductivity of the nanocomposite polymer electrolytes increases with increase in clay loading and attains a maximum value of $4.67 \times 10^{-3} \text{ Scm}^{-1}$ for a 4 wt% clay loading at room temperature. The same composition exhibits enhancement in the electrochemical and interfacial properties as compared with that of a clay-free electrolyte system. The change of conductivity with temperature was found to be related to the polymer segmental motion by an Vogel Tamman Fulcher (VTF) relation.

Introduction

Rechargeable lithium batteries with high-specific energies are promising power sources for portable electronic products and electric vehicles [1]. Solid polymer electrolytes (SPE) have many advantages. However, the low ionic conductivity of SPE at ambient temperatures limits their applications. One of the approaches relies upon the addition of nanocomposite sorbents. Nanocomposites based on polymer/layered silicates are promising new material systems with structural and functional advantages. Among the most commonly used inorganic layered hosts, montmorillonite (MMT) is a favoured choice in view of its special features of high aspect ratio (~1000), high cation-exchange capacity (CEC~80 mequiv./100 g), large specific surface area (~31.82 m^2g^{-1}) [2]. Incorporation of nano clays in the PEO matrix may reduce the crystallinity of PEO and thus increase its ionic conductivity. (PVdF-HFP) which possesses lower crystallinity and higher free volume It provides ionic path way which will improve the overall ionic conductivity of the electrolyte system. In the present work, an investigation is conducted on the electrochemical properties of PEO/PVdF-HFP based nanocomposite gel polymer electrolytes

The nanocomposite polymer electrolytes were prepared by solution casting technique. poly (ethyleneoxide)(PEO)/poly(vinylidene fluoride-co-hexafluoropropylene) (PVdF-HFP), Propylene carbonate (PC), Lithium perchlorate salt (LiClO_4) and montmorillonite (MMT) were obtained from Sigma Aldrich, USA. The appropriate quantities of polymer and salt were dissolved separately in acetone and then mixed together with plasticizer and filler. The solution was stirred continuously for 24 hrs to obtain a homogeneous mixture and then it was allowed to evaporate. The jelly solution was cast on to the glass plate to obtain free standing films. The prepared electrolyte were subjected to an ac impedance analysis, in order to calculate the ionic conductivity with the help of stainless steel blocking electrodes using a computer controlled μ -autolab type III potentiostat/Galvanostat in the frequency range 100Hz to 300KHz.

Results and discussion

In figure 1, the influence on conductivity is mainly attributed to the lower the crystallinity of PEO/PVdF-HFP with the addition of LiMMT. The presence of high dielectric constant electronegative silicate layers in the nanocomposite could increase the dissolution of the electrolyte salt (LiClO_4), thereby increasing the ion conduction through the solvent domain surrounding the polymer matrix. The cationic charges on the surface of MMT act as Lewis acid centres and compete with Li^+ cations (strong Lewis acid) to form complexes with the polymer host. This, in turn, may result in: (i) structural modifications and the promotion of Li^+ conducting pathways at the surface of filler, and (ii) lowering of the ionic coupling, which promotes salt dissociation [3]. Figure 2 presents the temperature dependent ionic conductivity, which follows a non-linear trend i.e., VTF behavior. As expected, increase in temperature leads to increase in ionic conductivity due to increase in the polymer chain flexibility producing more free volume, which leads to increased polymer segmental mobility. An interesting effect occurs in the high-temperature range wherein at about 70°C the conductivity of the filler-free polymer electrolyte dramatically decays. This is ascribed to the fact that at this temperature the polymer melts and the film loses its consistency. On the other hand, the materials for high-temperature operation [4].

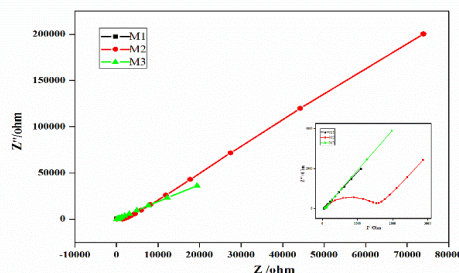


Figure 1. Room temperature complex prepared samples

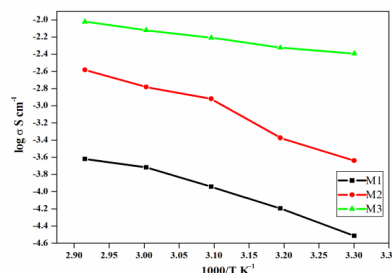


Figure 2. Temperature dependent ionic impedance for the conductivity plot

It is concluded that PEO/PVdF-HFP based clay-composite polymer electrolyte incorporated with 4 wt% MMT looks desirable and promising for lithium battery applications. Since the highest ionic conductivity at room temperature $4.67 \times 10^{-3} \text{ Scm}^{-1}$ was observed for the system

References

- [1] J.M. Tarascon, M.B. Armand, Nature 414 (2001) 359.
- [2] H.-W. Chen, T.-P. Lin, F.-C. Chang, Polymer 43 (2002) 5281–5288.
- [3] J. Xi, X. Qiu, X. Ma, M. Cui, J. Yang, X. Tang, W. Zhu, L. Chen, Composite polymer electrolyte doped with mesoporous silica SBA-15 for lithium polymer battery, Solid State Ionics 176 (2005) 1249–1260.
- [4] V. Gentili, S. Panero, P. Reale, B. Scrosati, J. Power Sources 170 (2007) 185–190.

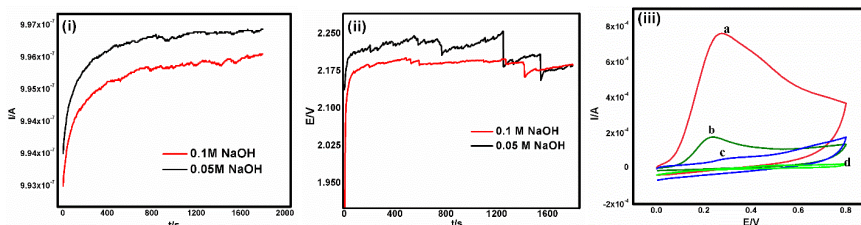
1.29 A systematic study on effect of electropolymerisation conditions on the permeability of polyresorcinol films

*R. Karkuzhali, AR. Pandiselvi, P. Karthika and S. Viswanathan**

Department of Industrial Chemistry, Alagappa University, Karaikudi-630 003, Tamil Nadu, India. rsviswa@gmail.com

Effect of electropolymerisation conditions on the permeability of polyphenolic films deposited on a glassy (GC) carbon electrode was studied [1, 2]. Resorcinol was electro polymerized on a GC electrode using galvanostatic and potentiostatic techniques. Difference in permeability of resulting electro synthesized polyresorcinol films were observed through cyclic voltametric technique. Conditions that allow electropolymerisation to proceed as long as a current is supplied to the electrode and permeability for phenate ions strongly depends on the parameters which are utilized on electro synthesis. Hence conditions to prevent blocking the electrode activity and further removal of phenolic ions were studied. Chronoamperometric deposition of resorcinol yields a nonconductive film on GC electrode. Figure. 1. Shows oxidative electrodeposition response of resorcinol on fixed GC electrode and unstirred electrolyte solution conditions and applied time was 1800 seconds. Influence of hydroxyl anion on electropolymerisation was studied by varying NaOH concentration. In both potentiostatic and galvanostatic studies, films obtained from the solutions containing 0.1M NaOH has limited for electron transfer hence low current/potential values i, e low permeability values are obtained. Permeation of 0.05M and 0.03M resorcinol concentrated ions through such polyresorcinol coated films was also studied by cyclic voltammetry technique (Figure. 1 Right side image).

Figure 1. Potentiostatic I-t curve (i) and Galvanostatic E-t curve (ii) for electro synthesis of polyresorcinol on GC electrode. Conditions: 0.01M Resorcinol, 0.1M Na₂SO₄, 0.1 and 0.05M NaOH. Voltametric response (image - iii) of (a) 0.05M and (b) 0.03M resorcinol on polymeric film synthesized by potentiostatic technique. Applied potential: 1800mv (c) 0.05M and (d) 0.03M are resorcinol on polymeric film synthesized by



galvanostatic technique. Applied current: 2mA. Time of deposition: 1800 seconds. Phenol oxidation currents are limited for polymeric films

synthesized electrodes when compared to bare GC electrode. Potentiostatic technique have appreciable permeability for phenol molecules and phenate ions when compared to films synthesized by galvanostatic method. Thus the influence of the electropolymerisation controllable parameters such as NaOH and phenol concentrations, potential or current applied, electro synthesis time on the permeability of these polymeric films was examined.

Keywords: Electropolymerisation, resorcinol, permeability.

Reference:

- [1] N. B. Tahar, & A. Savall, *Electrochimica Acta* 82 (2012) 427.
[2] M. Ferreira, H. Varela, R. M. Torresi, & G. Tremiliosi-Filho, *Electrochimica Acta* 52(2006) 434.

1.30 Corrosion resistance of heat treated Ni-W and Ni-W-TiO₂ nanocomposite coatings

^aK. Arunsunai Kumar, ^bG. Paruthimal Kalaignan* and ^cS.Senthilkumar
^aDepartment of Chemistry, VHNSN College (Autonomous), Virudhunagar, Tamilnadu.

^bAdvanced Nano Composite Coatings Laboratory, Dept. of Industrial Chemistry,
Alagappa University, Karaikudi – 630 003, Tamilnadu.

^cDepartment of Chemistry, Ayya Nadar Janaki Ammal College (Autonomous), Sivakasi, Tamilnadu
gpkalaignan@gmail.com, arunsunaikumar@vhnsnc.edu.in

Abstract

Ni-W alloy and Ni-W-TiO₂ nanocomposite deposits (PRC) were subjected to heat treatment at various temperatures. Surface morphologies of heat treated nanocomposite coatings were examined by using SEM & AFM studies. SEM images of heat treated electrodeposits prepared by pulse reverse method are shown in Figs 1 (a)&(b). The surface of heat treated Ni-W alloy deposit is compact and has needle sized grain. Heat treated Ni-W-TiO₂ nanocomposite deposits are found to have smaller sized grains. Needle shaped grains disappeared throughout the surface of nanocomposite deposit. These suggest that, TiO₂ particles are uniformly distributed in the Ni-W alloy matrix. Figs 2 (a)&(b) show that, the AFM images of heat treated Ni-W alloy and Ni-W-TiO₂ nanocomposite deposits prepared by Pulse reverse current method respectively. Ni-W-TiO₂ nanocomposites have much smaller particle size. The co-deposited TiO₂ particles are uniformly distributed over the Ni-W alloy matrix. The presence of TiO₂ decreases the size of particles.

XRD measurements were carried out to investigate the structural evolution of heat treated Ni-W alloy deposit and Ni-W-TiO₂ nanocomposite deposits. Before heat treatment, these patterns have revealed the fcc structure of Ni-W alloy with predominant planes (111), (200) and (220). After heat treatment at 600 °C, the precipitate of Ni₄W alloy phase was observed. A thorough phase analysis of the diffraction peaks have identified the formation of NiW and Ni₄W inter-metallic phases [1]. The crystallite sizes of heat treated Ni-W and Ni-W-TiO₂ nanocomposites were calculated using Scherrer equation. The crystallite sizes of heat treated Ni-W alloy deposit and Ni-W-6.66 % of TiO₂ nanocomposite are found to be 85 nm, and 45 nm respectively. The results suggest that, heat treated nanocomposite coatings have smaller crystallites compared to heat treated Ni-W alloy deposit.

The microhardness values for heat treated Ni-W alloy deposit and Ni-W-6.66 % of TiO₂ nanocomposite deposits were studied. The hardness values measurements at different location for each nanocomposite deposits were made and averaged. Increase in hardness values of Ni-W-TiO₂ nanocomposite deposit is due to increase in the annealing temperature of the deposit. The results suggest that, heat treated pulse reverse current deposits have offered enhanced microhardness compared to as deposited nanocomposite deposits.

Corrosion resistances of the electrodeposits were evaluated in 3.5 % NaCl solution by electrochemical methods. Potentiodynamic polarization studies were carried out at a potential of ± 400 mV away from the corrosion potential at a scan rate of 5 mV/s. Corrosion resistances of the electrodeposits were evaluated in 3.5 % NaCl solution by electrochemical methods. The polarization curves obtained by potentiodynamic polarization technique for various heat treated deposits by pulse reverse current method. Corrosion current density values were decreased with increase of heat treatment temperatures of the Ni-W-TiO₂ nanocomposite deposits. Corrosion current density values have decreased in all the heat treated nanocomposite deposits compared to as deposited nanocomposite coatings. The results suggested that, heat treated Ni-W-TiO₂ nanocomposite deposit has lower corrosion current density than as deposited nanocomposite deposits.

Impedance measurement is one of the most useful and effective methods for the corrosion assessment of metal deposit and coated deposits. They are capable of insitu and non-destructively probing relaxation phenomena over a wide frequency range [2]. Charge transfer (R_{ct}) values for Ni-W-TiO₂ nanocomposite deposits have increased and double layer capacitance (C_{dl}) values decreased with increase of heat treatment temperature of Ni-W-TiO₂ nanocomposite deposit. The results Suggest that, all the heat treated Ni-W-TiO₂ nanocomposite deposits were more corrosion resistant than as deposited Ni-W-TiO₂ nanocomposite deposit.

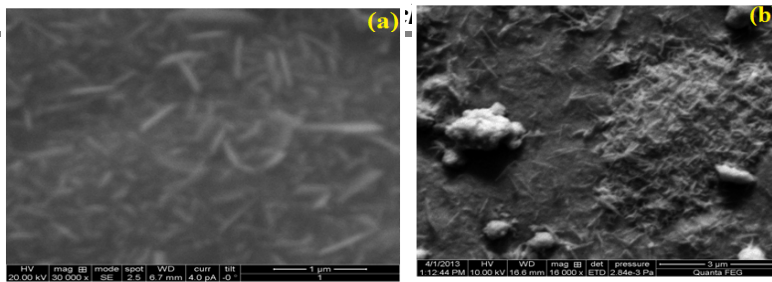


Fig 1 SEM images of (a) Ni-W alloy deposit (b) Ni-W- TiO₂ nanocomposite deposit at 600 °C

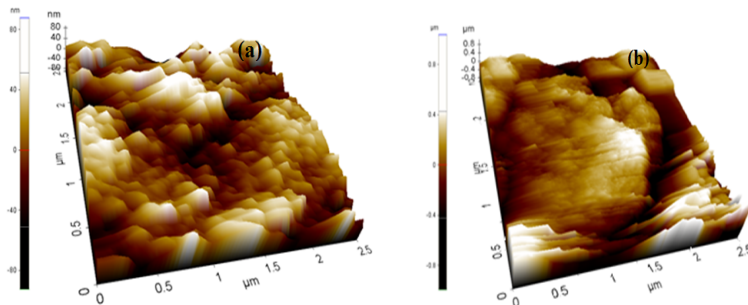


Fig 2 AFM images of (a) Ni-W alloy (b) Ni-W-TiO₂ nanocomposite at 600 °C

Keywords: Nanocomposite, Corrosion resistance, Surface morphology and Microhardness.

References

- [1] H.S.Cho, K.J.Hemker, K.Lian, J.Goettert, G.Dirras, *Sens Actuat a -Phys* 103 (2003) 59.
 [2] Hu JM, Liu XL, Zhang JQ, Cao CN., *Prog Org Coat.*, 55 (2006) 388.

1.31 Structural analyses of Li₂FeSiO₄ cathode material prepared by sol-gel method

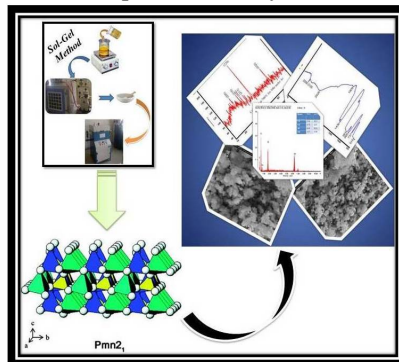
R. Dhanalakshmi^{a,b}, P. Rajkumar^b, R. Subadevi^b, M. Sivakumar^{b,*}

^a Department of Physics, Thiagarajar College, Madurai-625009. Tamil Nadu, India

^b Energy Materials Lab, School of Physics, Alagappa University, Karaikudi-630 004. susiva73@yahoo.co.in- M.Sivakumar

Abstract

Rechargeable lithium-ion batteries (LIBs) have been widely applied in the storage of energy due to their high-power and energy density [1]. Particularly in Li-ion batteries, cathode materials play an important role in the determination of energy density, safety and life cycle [2]. Lithium iron orthosilicate (Li₂FeSiO₄) has been proposed as a promising cathode material owing to its low cost raw materials, environmental friendliness, high safety and electrochemical stability [3]. In the present work, nano-crystalline Li₂FeSiO₄ cathode material has been successfully prepared by sol-gel method. The as-prepared cathode material has been characterized and the results are reported. The crystal structure has been confirmed by powder X-ray diffraction, the prepared Li₂FeSiO₄ has orthorhombic structure with space group of P_{mm}2₁. The functional group vibrations have analyzed using Fourier Transform Infrared Spectroscopy (FTIR). The surface morphology has been studied by Scanning Electron Microscopy (SEM) and the compositional analysis was also carried out through EDX analysis.



Keywords: Lithium electrodes; sol-gel method; Lithium iron orthosilicate; characterization.

References

- [1] J-J Lee, H-C Dinh, S-I Mho, I-H Yeo, W-I Cho and D-W Kim, *Mater. Lett.* 160 (2015) 507-510.
 [2] H Zhou, M-AEinarsrud, FVBruer, *J. Power Sources* 238 (2013) 478-484.
 [3] X Huang, X Li, H Wang, Z Pan, M Qu, Z Yu, *Solid State Ionics* 181 (2010) 1451-1455.

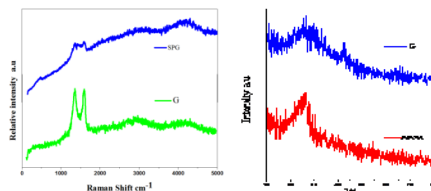
1.32 Studies on sulfur/polyethylene glycol/graphene composite for lithium sulfur batteries

K.Krishnaveni, R.Subadevi, M.Sivakumar*

Energy Materials Lab, School of Physics, Science Block, Alagappa University, Karaikudi-630 004.Tamil Nadu, India. susiva73@yahoo.co.in

Abstract

Lithium Sulfur (Li-S) batteries have been regarded as promising next generation rechargeable energy storage system, due to the high theoretical specific capacity and energy density[1-4].However, several critical problems hinder the wide-scale commercial use of lithium/sulfur system, namely the low electrical conductivity of sulfur, dissolution of polysulfides in electrolyte, and volume expansion of sulfur during discharge [5-7]. In this work, Graphene- coated sulfur/PEG composite was prepared by solvent- less reaction. The composites were characterized by XRD, FTIR, RAMAN and SEM. From XRD pattern, the amorphous nature of the composites visualized that the elemental sulfur was fully dispersed in the Graphene. It also confirms that most of the sulfur was encapsulated by graphene which is elucidated from the SEM analysis. The S/PEG/G composite cathode materials can be served as potential composite cathode material in lithium-sulfur battery.



References

- [1] M. Armand, J.M. Tarascon, Nature 451 (2008) 652–657.
- [2] B. Dunn, H. Kamath, J.M. Tarascon, Science 334 (2011) 928–935.
- [3] P.G. Bruce, S.A. Freunberger, L.J. Hardwick, J.M. Tarascon, Nat. Mater.11 (2012) 19–29.
- [4] D. Bresser, S. Passerini, B. Scrosati, Chem. Commun.49 (2013) 10545–10562.
- [5] L.C. Yin, J.L. Wang, F.J. Lin, J. Yang, Y.N. Nuli, Energy Environ. Sci.5 (2012) 6966–6972.
- [6] W. Ahn, K.B. Kim, K.N. Jung, K.H. Shin, C.S. Jin, J. Power Sources 202 (2012) 394–399.
- [7] Y.S. Su, A. Manthiram, Electrochim. Acta 77 (2012) 272–278.

1.33 Effect of pretreatments of sepiolite for cathode materials in Li-S batteries

C.Kalaiselvi, M.Sivakumar, R.Subadevi*

Energy Materials Lab, School of Physics, Science Block, Alagappa University, Karaikudi-630 004. Tamil Nadu, India. susimsk@yahoo.co.in

Abstract

Lithium sulfur batteries are receiving significant attention owing to its theoretical capacity and specific energy density. However the system suffers from several drawbacks: poor active material conductivity, active material dissolution and use of the highly reactive lithium metal electrode.To overcome these difficulties, a variety of additives were added into the positive electrode material, with an expectation to utilize their high specific surface area and surface groups to adsorb lithium poly sulfide and inhibit its dissolution. Sepiolite is found to be an ideal matrix towards the preparation of cathode materials for lithium sulfur battery. Sepiolite powders were screened through a 200mesh sieve (particle size 76 microns) and subjected to acid and thermal treatment. These treatments were experimented with the expectation to increase the practical capacity and to utilize their specific area and surface groups. Acid activations were carried out using various acids viz., HCl and H₂SO₄(10M) at room temperature for 24 hours. The thermal activation of sepiolite was conducted by calcined at 200,300,400,600 and 900°C for 2h respectively.The XRD patterns and FTIR spectra of the pure sepiolite, sieved, acid treated and thermally treated samples were investigated.It is observed that in acid solutions, the sepiolite structure collapsed and amorphous silica was formed.The intensity of the characteristic diffraction peak of sepiolite at $2\theta = 7.45^\circ$ disappeared in acid thermally activated samples.Also the XRD patterns indicate that the sepiolite amorphous phase did not change with pretreatments.

Keywords: Lithium Sulfur battery; electrode; sepiolite; pre-treatment.

1.34 Preparation of lanthanum (III) impregnated nano porous activated carbon and its application in electro-chemical oxidation of tannery wastewater

M.Ezhilpriya^a, G. Naveen Kumar^b, S. Swarnalatha^a and G. Sekaran^{a*}

^aEnvironmental Technology Division, Central Leather Research Institute, Chennai – 20.

^bMadras Christian College, Chennai - 59

Tanneries in India face survival difficulties owing to occasional noncompliance with pollution regulation policies. Presently this problem is tackled with cost intensive zero liquid discharge technology using membrane separation process. However, the tannery sector confronts with high operational and maintenance cost as the reverse osmosis membranes are bound to high fouling due to the presence of refractory organics that escaped primary and secondary treatment methods. An attempt was made in the present investigation to reduce the refractory organics present in the biologically (Activated Sludge Treatment) treated tannery effluent with three dimensional electro-chemical oxidation followed by Fluidized Immobilized Cell Carbon Oxidation (FICCO) technique. The paper discusses on wet impregnation of rare earth metal ion, Lanthanum (III), onto Nano Porous Activated Carbon (NPAC). The effect of process parameters such as contact time (5, 10, 15, 30, 45, 60, 120, 180, 240 and 300 mins), pH (2, 3, 4, 5, 6, 7, 8, 9, 10, 11 and 12) of the equilibrating mixture (La^{3+} aqueous solution), mass of NPAC (0.2, 0.4, 0.6, 0.8, 1, 1.2, 1.4, 1.6, 1.8 and 2 g per 20 mL of La^{3+} containing aqueous solution), initial concentration of La^{3+} (20, 30, 40 and 50 ppm), and temperature (20, 30 and 40° C) were determined. The La^{3+} impregnated NPAC matrix was subjected to calcination at different temperatures, say, 400° C, 500° C and 600° C under inert atmosphere. The La^{3+} impregnated NPAC catalyst was characterized by SEM, XRD, FTIR and EPR. Batch studies on electrochemical oxidation using La^{3+} impregnated NPAC as third dimensional catalyst was carried out and observed that La^{3+} impregnated NPAC calcined at 500° C is efficient enough to degrade refractory organics in the treated tannery effluent. Further the effect of process parameters such as time, pH and potential on electrochemical oxidation were studied. The secondary treated tannery wastewater after electrocatalytic oxidation was further treated with FICCO reactor. The oxidation process was evaluated using FTIR Spectroscopy, UV – Visible Spectroscopy, Fluorescence Spectroscopy and HPLC.

Key words: impregnation of La^{3+} , three dimensional electro-chemical oxidation, refractory organics, FICCO, tannery wastewater, secondary treated wastewater

1.35 *Moringa olifera*: Green corrosion inhibitor for mild steel in sulphuric acid medium

N. Subasree, J. Arockiaselvi*, P. Kamaraj, M. Arthanareeswari

Department of Chemistry, SRM University, Kattankulathur-603203, Tamil Nadu, India.

arockiaselvi29@yahoo.co.in, suba25692@gmail.com

Abstract

The inhibitive effect of *Moringa Olifera* on mild steel corrosion in 1N and 2N sulphuric acid solution was studied using electrochemical techniques and gravimetric method. The weight loss results showed that the plant extract was an excellent corrosion inhibitor. The inhibition efficiency increased with increase in concentration of the plant extract. The highest inhibition efficiency of 96% was observed with 8ml plant extract in the acid medium. Immersion period was carried out to optimize the period of immersion. The surface studies such as FTIR, SEM and EDAX were carried out to confirm the protective layer formed on the metal surface. The inhibition effect is due to the adsorption of active molecules leading to the formation of a protective layer on the surface of mild steel.

Keywords: Corrosion inhibition, *Moringa olifera*, weight loss method, electrochemical studies, Surface studies.

2.1 Brighter Future for Cancer Therapy with Smart Theronastics through Nanobiotechnology: Efforts and innovations from our laboratory

Kaliaperumal Selvaraj*

Nano and Computational Materials Lab, Catalysis Division, CSIR-National Chemical Laboratory, Dr. Homi Bhabha Road, Pune 411 008, India. k.selvaraj@ncl.res.in

Cancer being the second leading cause of death in most countries as of today, an increasing attention of global nanotechnology researchers is being focused on finding smarter ways to handle this dreadful menace. India has registered a 6% raise in mortality due to cancer between 2012 and 2014 with a staggering number of about 1330 succumbing to cancer each day [1]. Though the entire globe has realized the need of a major thrust on research in this area, India is not yet geared up for this and certainly a front runner with indigenous technologies to effectively encounter the increasingly growing threat. Very scanty picture of nanobiotechnology based research in this regard in Indian R&D sector shows to have confined mostly at laboratory level and not yet progressed beyond. Its further raise up to clinical trials that translates them into viable technologies is too far from the reality. The proposed talk would cover (i) an overview of this with national and international back ground, (ii) recent developments in nanomedicine for smarter cancer therapy and (iii) few example innovations carried out at our research group and its future scope.

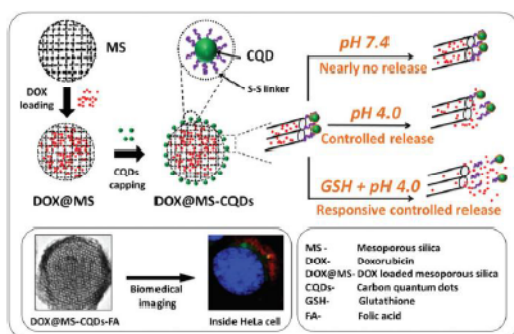


Figure 1. Schematic that illustrates the features and performances in-vitro conditions of a recently developed nanosystem at Nano and Computational Materials Lab (NCML) at NCL.

Our research group, NCML is involved in developing novel multifunctional nanosystems for simultaneously managing various levels of cancer diagnosis and therapy that includes precise advanced diagnosis, targeted and/or triggered chemotherapy and combo therapies that includes photothermal and chemotherapy. Much safer nanostructures of mesoporous silica as recently approved by United States FDA for human trials are being custom synthesized at our laboratory with enhanced properties and used by our group to pack several functionalities in one nanosystem. Novel green fluorescent carbon quantum dots developed in our laboratory has been used as a 'nano-gate' for the drug release. A recent attempt in developing a nanosystem that is bioresponsive and the release is controlled [2] has excitingly encouraged our enthusiasm in testing them under *in-vitro* conditions

with HeLa cancer cell lines. Following patenting, our recent innovative nanosystems are currently under animal testing, a step prior to clinical trials. Future looks promising to convert them into technologies and to successfully contribute in the bigger leaps by India in this field of indigenous research and development.

References

- [1] National Cancer Registry Programme of the India Council of Medical Research (ICMR), <http://www.ndtv.com/india-news/1-300-die-of-cancer-every-day-in-india-763726> as accessed on 10 Mar 2016.
 [2] R. Prasad, S. Aiyer, D.S. Chauhan, R. Srivatsava and K. Selvaraj*, *Nanoscale*, 8, (2016), 4537

2.2 Synthesis, phase transition and thermoelectric properties of bismuth telluride nanostructures

M. Arivanandhan^a, P. Anandan^b, D. Rajan Babu^c, M. Azhagurajan^d, R. Jayavel^a, Y. Hayakawa^e

^aCentre for Nanoscience and Technology, Anna University, Chennai-600025, India

^bDepartment of Physics, Thiru Kolanjiyappar Government Arts College, Vridhachalam-606001, India,

^cSchool of Advanced Sciences, VIT University, Vellore 632014, India.

^dInstitute of Multidisciplinary Research for Advanced Materials, Tohoku University, 2-1-1 Katahira, Sendai 980-8577, Japan

^eResearch Institute of Electronics, Shizuoka University, 3-5-1 Johoku, Naka-Ku, Hamamatsu 432-8011, Japan.

Bismuth telluride (Bi_2Te_3) nanocrystals were synthesized by wet chemical method and pellets of nanocrystals were made by high pressure and high temperature sintering (HPHTS) process. The impact of sintering temperature on phase transformation and morphological evolutions of pelletized nanocrystals were studied. Thermoelectric properties of as-prepared and sintered pellets were measured. Seebeck coefficient of Bi_2Te_3 nanocrystals has increased and the electrical resistivity decreased with sintering temperature. The variations of Seebeck coefficient and power factor is explained by a proposed model.

1. Introduction

The rapidly increasing energy demand and environmental problems are the two major issues for the present and next generation. Thermoelectric (TE) energy conversion is one of the promising ways to convert the waste heat into electric energy. Thermoelectric nanomaterials have received much attention because of its high performance compared to bulk material due to increased phonon scattering at grain boundaries. Bismuth telluride (Bi_2Te_3) is a well-known low temperature TE material, and is commercially available for practical applications. Despite of huge efforts made by the researchers for the preparation of Bi_2Te_3 material, the large scale synthesis using conventional processes such as directional crystallization, is quite complicated as it requires sophisticated systems, due to the volatile nature and high vapour pressure of tellurium [1-4]. Moreover, as per the Bi-Te phase diagram, the compound has several other phases, such as BiTe, Bi_4Te_3 and Bi_3Te_4 , referred to as bismuth telluride alloys (BTAs). All of the BTA structures have similar layered structures with hexagonal symmetry and larger c-axis lattice constants. [3,4] The effect of mixed BTA phases on the TE properties has been rarely investigated. [4,5]. The objective of the present work is to synthesis phase controlled BTA material for thermoelectric applications.

2. Experiment

BTA nanocrystals were synthesized by wet chemical method and pellets of nanocrystals were made by high pressure and high temperature sintering (HPHTS) process. The prepared pellets were sintered at three different temperature under argon atmosphere. The impact of sintering temperature on phase transformations of BTA and morphological evolutions of pelletized nanocrystals were studied by X-ray diffraction analysis (XRD), Field emission scanning electron microscopy (FESEM), Transmission Electron Microscopy (TEM) and X-ray photo electron spectroscopy (XPS). Thermoelectric properties of as-prepared and sintered pellets were measured as a function of temperature.

3. Results and discussion

Figure 1a shows the FESEM image of as synthesised Bi_2Te_3 nanocrystals. The as synthesised materials are spherical in shape and the size in the range of 60 to 70 nm. The nanocrystals grown as a meso crystals during the sintering process. The various phases of the material has been identified by XRD analysis. Seebeck coefficient of the sintered pellets has increased with sintering temperature and the electrical resistivity decreased. The power factor of the material was calculated using the measured resistivity and seebeck coefficient. The high Seebeck coefficient and power factor of the sample sintered at 300 °C is due to combined effect of nano & meso structures and mixed phases of BiTe & Bi_2Te_3 . Moreover, the experimental results were discussed based on the proposed model.

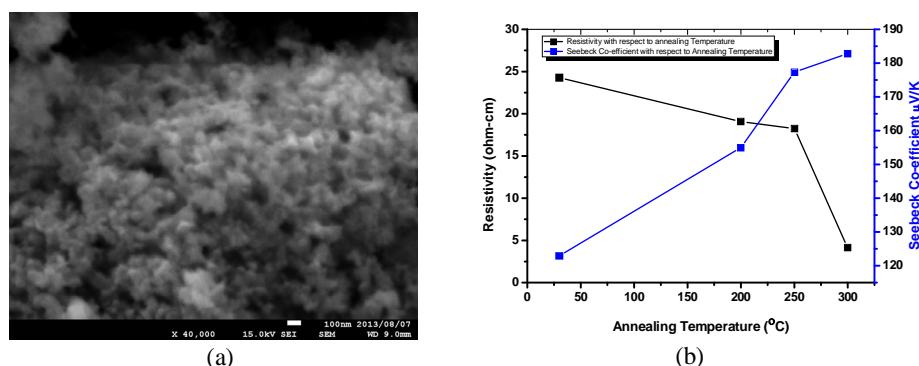


Fig.1: (a) FESEM image of as prepared Bismuth Telluride nanocrystals, (b) Seebeck coefficient and electrical resistivity variation of Bismuth Telluride as a function of sintering temperature.

References:

- [1]. H. Fang, T. Feng, H. Yang, X. Ruan and Y. Wu, *Nano Lett.*, 2013, 13, 2058.
- [2]. C. L. Hsin, M. Wingert, C. W. Huang, H. Guo, T. J. Shih, J. Suh, K. Wang, J. Wu, W. W. Wu and R. Chen, *Nanoscale*, 2013, 5, 4669.
- [3]. D. Jeweldebrhan, V. Goyal and A. A. Balandin, *Nano Lett.*, 2010, 10, 1209.
- [4]. C. Yu, X. Zhang, M. Leng, A. Shaga, D. Liu and F. Chen, *J. Alloys Compd.*, 2013, 570, 86.
- [5]. P. Anandan, M. Omprakash, M. Azhagurajan, M. Arivanandhan, D. Rajan Babu, T. Koyama, Y. Hayakawa, *CrystEngComm*, 2014, 16, 7956.

2.3 Synthesis, characterization and catalytic behavior of nano-silica derived from bamboo rice husk ash

Cinnathambi Subramani Maheswari, Appaswami Lalitha*

Department of Chemistry, Periyar University, Periyar Palkalai Nagar, Salem-636011, Tamil Nadu, India
lalitha2531@yahoo.co.in; csmahesthiya@gmail.com Tel: +91-427-234-5271; Fax: +91-427-234-5124

Abstract

Herein, we have reported the Nano-silica derived from bamboo rice husk ash as an efficient, greener, reusable and biodegradable heterogeneous catalyst towards the synthesis of tetrahydro-4*H*-chromene-3-carbonitriles *via* the one-pot three component reaction of malononitrile with aromatic aldehydes and dimedone. The formation of Nano-silica has been confirmed by IR, SEM, XRD and EDX analytical techniques.

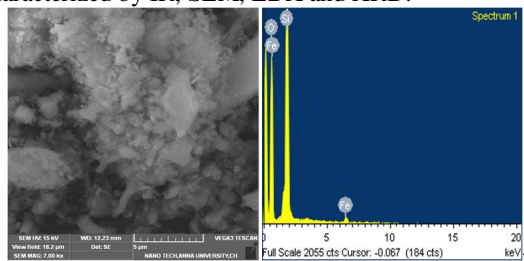
Keywords: Nano-silica, Bamboo rice husk ash, Tetrahydro-4*H*-chromene-3-carbonitriles.

Introduction

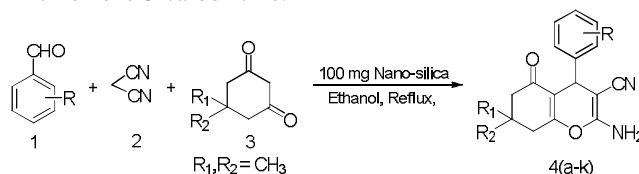
Heterogeneously catalyzed reactions are found to possess various advantages like simple and ease of work-up, mild reaction conditions, improved product yields and selectivity. In addition to that, the main advantage of this heterogeneous catalyst is the easy recovery and reusability of the catalyst [1]. With this background, we have developed a simple and practical approach for the construction of tetrahydro-4*H*-chromene-3-carbonitriles using Nano-silica as an efficient heterogeneous catalyst.

Result and discussion

Initially, we have prepared the Nano-silica from bamboo rice husk ash according to the literature method [2] and completely characterized by IR, SEM, EDX and XRD.



The catalytic activity of the synthesized Nano-silica was checked through the three component synthesis of tetrahydro-4*H*-chromene-3-carbonitrile.



To find out the suitable reaction conditions for this reaction, a model reaction of malononitrile (1 mmol) with 4-chlorobenzaldehyde (1 mmol) and dimedone (1 mmol) was carried out with different solvents like CH_3CN , CH_3OH , EtOH, EtOH/ H_2O and H_2O under reflux conditions as well as under solvent free condition at 80 °C using 100 mg of Nano-silica as a catalyst and found that ethanol was a better reaction medium for this reaction. To optimize the suitable amount of catalyst required for this reaction, we have employed the same reaction with different quantities of catalyst such as, 20, 40, 50 and 100 mg of Nano-silica. When increasing the catalyst amount, the reaction time was decreased with the increased product yield up to 100 mg of the catalyst and after that there was no change in reaction rate and product yield.

Under these optimized reaction conditions (100 mg of catalyst and ethanol as solvent), we have synthesized a variety of tetrahydro-4*H*-chromene-3-carbonitrile derivatives in good yields (Table 1). Next, we have also checked the reusability of the Nano-silica catalysts and found that the Nano-silica catalyst has been efficiently reused for four consecutive runs without any significant loss in its activity.

Conclusion

In summary, we have developed a simple protocol for the synthesis of tetrahydro-4*H*-chromene-3-carbonitrile derivatives from the one pot three component reaction of malononitrile with aromatic aldehydes and dimedone using Nano-silica as an efficient and reusable catalyst under mild conditions. Non-toxic, inexpensive, eco-friendly, easy recovery and reusability of the catalysts are some notable advantages of the present methodology. The recovered Nano-silica was reused for four times without any appreciable change in its catalytic activity.

References

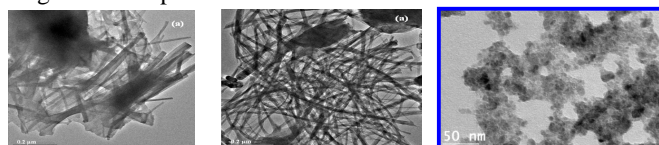
- [1] R. Fricke, H. Hosslick, G. Lischke, M. Richter, *Chem. Rev.*, 100 (2000) 2303.
- [2] F. Shirini, S. Akbari-Dadamahaleh, A. Mohammad-Khah, A. Aliakba, *C. R. Chimie* 16 (2013) 207-216.

2.4 Different Dimensional Semiconductor Nanocomposites

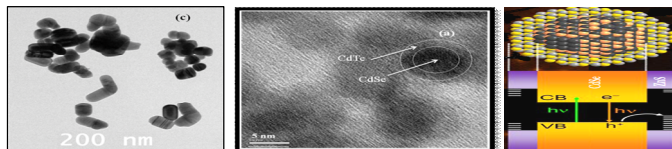
G.Ramalingam^a and K. Gurunathan^b

^{a,b}Department of Nanoscience and Technology, Alagappa University, Karaikudi. ramanloyola@gmail.com

The various semiconductor quantum dots (QDs) of II-VI group metal chalcogenides such as ZnS, CdSe and CdTe have been studied intensively on their quantum confinement effects including size dependent photoemission properties due to the latest development in synthesis leading to high quality QD ensembles with narrow size distribution. The photoluminescence (PL) spectra of these QDs can be tuned over a wide range of the electromagnetic spectrum with the control in size and composition. QDs have many advantages compared to organic dyes, such as high PL intensity with narrow bandwidth and high photo-stability against photo bleaching [1-3]. Due to such excellent properties, these QDs have potential application in light harvesting to biomedical tags. Core/shell particles involving metals, semiconductors or oxide nanocrystals in the core, with shells composed of different materials have been widely investigated [4-6]. The present work focuses on the preparation of semiconducting nanoparticles CdSe along with nanocomposites of CdSe/ZnS, CdSe/ZnSe and CdSe/CdTe by low temperature solution route, different capping agents were used to optimize the experimental conditions suitable for mass production. The synthesis procedures and results of the characterization of these nanoparticles were discussed in details. The as prepared nanoparticles were characterized structurally and optically using powder X-ray diffraction (PXRD), Scanning electron microscopy (SEM), Energy dispersive X-ray analysis (EDAX), transmission electron microscopy (TEM), UV-Vis spectroscopy and photoluminescence (PL) studies. The morphology and size of the obtained different dimensional semiconductor nanocomposite were investigated and reported.



Fig(a): CdSe Nanorods Fig(b): CdSe Nanobelts Fig(c): CdSe/ZnS QDs



Fig(d) CdSe/ZnSe Nanorods, Fig(e & f) CdSe@CdTe core-shell and structure

The coupling of CdSe with ZnSe was achieved by adding CTAB and L-Cysteine. The obtained nanorods diameter is 50-70 nm and the length is 150-175 nm whereas; the spherical shape nanoparticles were achieved within 50-72 nm diameters. The SAED pattern of the CdSe/ZnSe nanorods shows a superimposed pattern from the single crystalline CdSe/ZnSe composite material. Core-shell heterostructures using group II-VI nanocrystals, such as CdSe, CdTe have been of particular interest and the same was developed successfully.

References

- [1] Jr .Bruchez Marcel, Moronne Mario, Gin Peter, Weiss Shimon, and Alivisatos A. Paul., *Science*, 25 (1998) 2013-2016.
- [2] S. Coe, W-K. Woo, M. Bawendi, Bulovic., *Nature*, 420 (2002) 800-803
- [3] J. Lee, A. O. Govorov, and N. A. Kotov., *Nano Lett*, 5 (2005) 2063-2069.
- [4] Protiere and Myriam., *Chemical Communication*, 3 (2007) 399-403.
- [5] Chan Warren and Nie Shuming., *Science*, 281(1998) 2016.
- [6] C. B. Murray, D. J. Norris, M. G. Bawendi., *J. Am. Chem. Soc*, 115 (1993) 8706-15.

2.5 Synthesis of nanocrystalline Au substituted hydroxyapatite: Investigation on cytocompatibility and antibacterial efficacy

S. Jegatheeswaran^a, S. Selvam^b, S. N. Karthick^b and M. Sundrarajan^{a*}

^aAdvanced Green Chemistry Lab, Department of Industrial Chemistry, School of Chemical Sciences, Alagappa University, Karaikudi -3, Tamil Nadu, India.

^bLaser and Sensor Application Laboratory, Pusan National University, Busan 609735, South Korea.

sudrarajan@yahoo.com and sjwaran90@gmail.com

Introduction

Synthetic hydroxyapatite (HAp) is a calcium phosphate based bioceramic, it has been widely applied in the tissue engineering applications. In this work, Au²⁺ cations may replace Ca²⁺ ions in the lattice of HAp structure

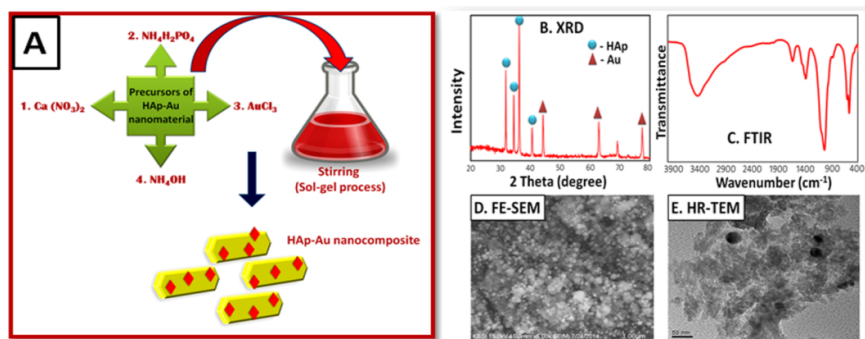
and it possess antibacterial efficacy, which is beneficial for biomedical applications. Au ions incorporated into the apatite structure, inducing modifications in powder crystallinity, particle morphology, lattice parameters and thermal stability. Gold (Au) substituted hydroxyapatite has been focused because of its diverse roles in cytocompatibility and antibacterial properties.

Experimental Details

The experimental details are given below in the Figure A.

Results and Discussion

Figure B shows the XRD pattern of the Au substituted HAp, with the inset showing that of presence of pure HAp and Au. No impurity peaks were observed in the XRD pattern due to the substitution of Au ions and the 2θ values are in agreement with those of pure HAp (JCPDS No. 09-432).



The FT-IR spectrum of HAp-Au nanoparticles are shown in the Figure C. The structure of HAp is characterized by different vibrational modes of the phosphate PO_4^{3-} and hydroxyl OH^- groups. Figure D and E displays the FE-SEM and HR-TEM images of the HAp-Au sample, respectively. The spherical and less agglomerated structures were found for all samples, while the particle sizes did not exceed 100 nm. It reveals that good spherical geometry and high dispersion of Au particles on the surface of the HAp nanoparticles.

Conclusion

In summary, we have developed novel Au substituted nanocrystalline HAp particles. The HAp-Au nanoparticles exhibited interesting crystallinity and good surface morphology. The synthesized Au-HAp nanoparticles has given better antimicrobial activity and cytocompatibility behavior. This nanomaterial is highly suitable for the bone substitute applications.

References

- [1]. M. Sundrarajan, S. Jegatheeswaran, S. Selvam, et al., *Materials and Design* 88 (2015) 1183–1190.
- [2]. D. MubarakAli, N. Thajuddin, K. Jeganathan, M. Gunasekaran, *Colloids and Surfaces B: Biointerfaces* 85 (2011) 360–365
- [3]. S.V. Dorozhkin, *Biomaterials* 31 (2010) 1465–85.

2.6 Multicomponent effect of Ni-W-MoS₂-PTFE nanocomposite coatings prepared by direct and pulse current electrodeposition

S. Sangeetha and G Paruthimal Kalaignan*

Advanced Nanocomposite Coatings Laboratory, Department of Industrial Chemistry, Alagappa University, Karaikudi 630 003, India. Phone No: +91-9443135307, Fax: +914565 225202. pkalaignan@yahoo.com and sangeetha4880@gmail.com

Abstract

In this report, we have investigated both the tribological and electrochemical properties of solid lubricant coatings from MoS₂ and PTFE nanoparticles. Solid lubricants are having many advantages including long life, no contamination and usage in harsh environments. In this study, PTFE was incorporated in the optimized Ni-W-MoS₂ nanocomposite coatings by both direct and pulse current techniques. The surface morphology and microstructure studies were examined by X-ray Diffractometry (XRD), Scanning Electron Microscopy (SEM) and Energy Dispersive X-Ray Analysis (EDAX). PTFE polymer was completely mixed with the bath solution. Crystalline structure of the Ni-W-MoS₂ was not affected even after the addition of PTFE polymer in the bath. The mechanical and tribological characteristics were measured by using Vicker's micro hardness tester, Mitutoyo Surf test SJ-310 (ISO1997) and Scratch tester TR-101-M4. The surface roughness values have decreased with the addition of the PTFE polymer in the coatings. Hence, the two solid lubricant particles have played a vital role to decrease the surface roughness. Similarly, decrease of the coefficient of friction values of the deposits is due to the addition of two solid lubricant fillers such as MoS₂ and PTFE. The corrosion behaviour was measured by using Tafel Polarization and Impedance methods in 3.5% NaCl solution.

The positive shift in the corrosion potential designates the good protection ability of cathode surface against corrosion by the nanocomposite coating. The Pulse current (PC) nanocomposite coatings have offered uniform surface, higher microhardness and excellent corrosion resistance properties than the direct current (DC) composite coatings [1]. When PTFE included as a fourth component in the bath a protective oxide layer was formed on the cathode surface. Moreover, the uniformly incorporated filler particles in the coating have behaved as a passive layer between the deposit surface and corrosive media. Hence, it has been achieved that, the existence of PTFE increases the anticorrosion property of the nano composite coatings [2].

Keywords: Solid lubricant, Pulse current deposition, Coefficient of friction, Microhardness, Corrosion resistance.

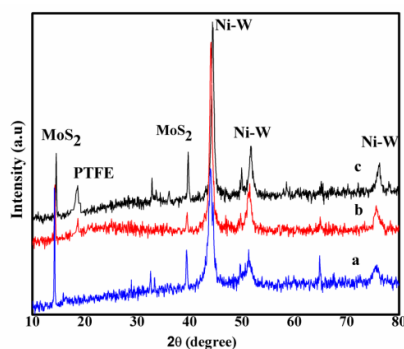


Fig.1. XRD patterns of a) Ni-W-MoS₂ b) Ni-W-MoS₂-PTFE (DC) c) Ni-W-MoS₂-PTFE (PC) nanocomposite coatings

References

- [1] N.Tsyntsar, S.Silkin, *Electrochimica Acta* 188 (2016) 589.
 [2] S.Sangeetha, G.P. Kalaignan, *Applied Surface Science* 359 (2015) 412.

2.7 Synthesis and characterization of iron oxide coated nickel oxide nanoparticles

R. Krishnaveni

Department of Chemistry, Sree Sevugan Annamalai College, Devakottai, TamilNadu. Krishnaa_veni@yahoo.co.in

Abstract

The present work deals with the synthesis of iron oxide coated nickel oxide nanoparticles and its characterization studies was carried out by FTIR, XRD and AFM analysis. The peak appeared at $640\text{-}675\text{cm}^{-1}$ is due to the Ni-O stretching vibration absorption band, the broadness of the peaks is indicates that the particles interrogated for FTIR studies is in nanosize. The crystalline size of 39 nm is observed at the iron oxide coated nickel oxide nanoparticles from XRD. AFM image shows that the synthesized particles are in the range of 25nm-35nm.

Keywords: Iron oxide coated NiO, FTIR, XRD and AFM.

Synthesis of Iron oxide coated Nickel oxide

A 15gms of nickel nitrate was dissolved with 2ml of glycerol in a 250ml glass beaker. Then 2g of urea and required amount of 5% Iron nitrate added and stirred well to get a clear solution. This solution was kept at 60°C till the product was formed. The resulting product was kept at furnace for 3 hours at 500°C and then allowed to cool. The resulting product was tested for different characterization studies like FTIR, XRD and AFM.

Result and Discussions

From FTIR studies (Thermo-Nicolet-380 Madison, USA model) it was observed that the broadband in the region of $430\text{-}450\text{cm}^{-1}$ is due to the stretching mode of NiO nanoparticles [1]. The peak appeared at $640\text{-}675\text{cm}^{-1}$ is due to the Ni-O stretching vibration absorption band, the broadness of the peaks is indicates that the particles interrogated for FTIR studies is in nanosize. The XRD studies were carried out using X-PERT PRO PAN analytical diffractometer system with Cu K α radiation ($\lambda=0.15418\text{ nm}$) with 2θ ranging from 5° to 80° (fig.1)[2]. The well-defined sharp peaks in the spectra indicate that synthesized particles are crystalline. The particle size of 39 nm is observed at the iron oxide coated nickel oxide nanoparticles. AFM studies shows that the particle sizes are in the range of 25nm-35nm. This result well corroborates with the XRD results.

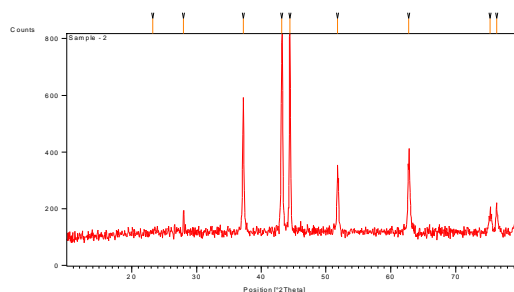


Fig 1. XRD of 5% Iron oxide coated NiO nanoparticles

Conclusion

The magnetic nanoparticles synthesized conveniently through combustion method. The iron oxide is coated on the nickel oxide. The synthesis is confirmed by FTIR. The synthesized particles are in the nm range.

References

- [1] X.Li, X.Zhang, Z.Li and Y.Quan, *Solid State Communications*, 137, (2006) 581.
 [2] Q.Wang, X.Fan, W.Gao and J.Chen, *Carbohydrate Research*, 341, (2006) 2170.

2.8 Green synthesis of silver nanoparticles and impregnation on surgical mask & surgical thread for antimicrobial property

M. Kavitha^a and A. Arumugam^{b*}

^aDepartment of Nanoscience and Technology, Alagappa University, Karaikudi – 630 003. Tamil Nadu, India.

^bDepartment of Botany, Alagappa University, Karaikudi – 630 003. Tamil Nadu, India.

kavisuganya25@gmail.com, sixmuga@yahoo.com

Abstract

Silver nanoparticles (Ag NPs) have been widely used due to its broad spectrum of antibacterial activity while exhibiting low toxicity towards mammalian cells. A nano-silver colloidal solution was prepared by green synthesis of AgNO₃ aqueous solution and leaf extract of *Citrus medica* under vigorous stirring at room temperature. All results of UV, FT-IR, XRD analysis and AFM indicated that Ag NPs had been formed in colloidal solution. Surgical mask & surgical threads were treated with nano-silver colloid by an impregnation method to provide with effective antibacterial properties. In addition, the results of scanning electron microscopy (SEM) confirmed that silver nanoparticles have been fixed and well dispersed on surgical mask and thread surface.

The antimicrobial activity of Ag NPs was influenced by the dimensions of the particles, the smaller the particles, the greater antimicrobial effect. Silver nanoparticles have the ability to anchor to the bacterial cell wall and subsequently penetrate it, thereby causing structural changes in the cell membrane like the permeability of the cell membrane and death of the cell. There is formation of "pits" on the cell surface, and there is accumulation of the nanoparticles on the cell surface. Ag NPs are generally smaller than 100 nm and contain 20-15,000 silver atoms. At nanoscale, silver exhibits remarkably unusual physical, chemical and biological properties and antibacterial activity.

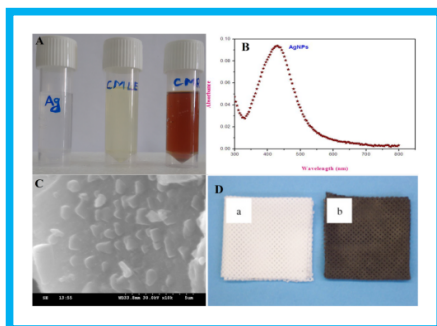


Figure. 1 (A) - Synthesis of Ag NPs, (B) – UV-Vis Spectroscopic analysis of Ag NPs, (C) – SEM analysis of Ag NPs, (D) – Coated & Uncoated AgNPs

Keywords: Silver nanoparticle, *Citrus medica*, Antibacterial, Surgical mask, Surgical thread.

References

- [1]. M.L. Rao, and N. Savithamma, *J. Pharm. Sci. & Res.*, vol.3, (2011). pp.1117-1121.
 [2]. R. Geethalakshmi., D.V. Sarada, *IJIRSET*, vol.2(2010.), pp.970-975.
 [3]. P.C. Nagajyothi, K. Lee, *J.Nano Mat*, vol.10, (2011), pp.1155-2011.

- [4]. B. Mahitha, B. Deva, *J NanomaterBiostruct*, vol.6, (2011) pp.135-142.
[5]. T.Prathna, N. Chandrasekaran, *Colloids Surf B*, vol.82, (2011) pp.152–159.

2.9 Formation and characterisation of electroless silver nanoparticles on aluminium from *Solanum melongena* leaves extract

N.Latha*, M.Gowri, K.Sathishkumar, D.Sumathi.

Department of Chemistry, Kandaswami Kandari's College, Velur - 638 182, Tamil Nadu, India.
lathaankl@gmail.com, gow_chem@yahoo.co.in; Phone : +91 9487427667

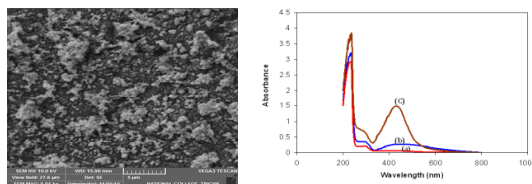
Abstract

A simple and versatile process of electroless silver nanoparticle formed on aluminium by using silver nitrate as a metal ion and *Solanum Melongena* leaves extract as a reducing agent. The formation of silver nanoparticles were confirmed by the colour change of plant extracts from orange to black and it was further confirmed with the help of UV-Vis analysis by changing the bath parameters such as concentrations of the metal ion, volume of plant extract, temperature, pH and deposition time. The functional group, surface morphology, elemental composition and structure were characterized by FT-IR, SEM/EDS and XRD techniques. FT-IR confirmed the presence of functional groups of both leaf extract and silver nanoparticles. SEM revealed that larger number of tiny silver nano particles formed on aluminium and its chemical composition 20.7 Wt.% of Ag was found out from EDS results. From the XRD pattern, the average crystalline size was found to be in the range of 46 nm to 54 nm for the deposition time of 30 sec to 600 sec respectively. This approach is novel, eco-friendly and promising for applications in medicine.

Key Words: Al, *Solanum Melongena* leaves extract, AgNps, UV-Vis, FT-IR, SEM /EDS,

Noble metallic nanoparticles are of particular interest today because of their interesting optical, electrical and possible applications in microelectronics. Silver nanoparticles have good electrocatalytic and lower resistance as compared to the other metal nanoparticles. Silver nanoparticle used in the field of solar energy conversion, environment, water treatment, textiles, cosmetics, batteries, electronics and to fabricate optical devices. For biological and biomedical applications, silver nanoparticles are the primary choice because of their biocompatibility and chemical stability. Many synthesis methods have been adopted for surface metallization of materials. In this electroless plating process uniform deposition of silver on aluminium by without applying any electricity and the driving force for the reduction of metal ions is supplied by reductants in *Solanum Melongena* leaves extract.

UV-Vis results showed the presence of surface plasmon resonance band at pH=5,7 and 9, the peak was found at around 400 nm region, 340 -760 nm and 444 nm respectively. The FT-IR spectrum of *Solanum melongena* leaves extract peaks at 3302 cm^{-1} represents the -NH stretch of primary and secondary amines or amides. It may be due to the -OH stretch of alcohols and phenols. The peaks at 2123 cm^{-1} corresponding to -CN stretch of nitriles and 1636 cm^{-1} indicate -C-C- stretch of alkenes and -NH bend of primary amines. SEM image indicate that the presence of large numbers of tiny nanoparticles are formed on the aluminium surfaces. EDS analysis showed the presence of aluminum and silver. From XRD, the Bragg reflections at 31.56° , 38.03° , 44.26° , 55.28° , 64.60° , 77.72° and 77.99° can be indexed into (111), (111), (200), (220), (220), (311), (311) and (311) orientations, respectively, confirmed the presence of AgNp's. The average crystalline size was found to be in the range of 46 nm, 36 nm and 54 nm for the deposition time of 30 sec, 3 min and 10 min respectively.



SEM image of synthesised AgNP's. UV-Vis spectra of AgNP's a) pH=5.0, b) pH=7.0 c) pH=9.0

2.10 Green Synthesis and characterization of silver nanoparticles from fruit extract and its antibacterial activity

R. Bhuvaneswari, S. Keerthana and D.Ramyadevi*

Department of Chemical Engineering, Anjalai Ammal Mahalingam Engineering College, Kovilvenni – 614 403 India.
dramyachem@gmail.com

Abstract

The synthesis of nanoparticles is in the spotlight in modern nanotechnology. In recent years, the development of competent green chemistry methods for synthesis of metal nanoparticles (NPs) has become a main limelight of researchers. Biological synthesis of nanoparticles using fruit extract is currently under exploitation. The first time in this paper we have reported the green synthesis of silver nanoparticles (AgNPs) by reduction of silver nitrate, using fruit extracts of *Citrullus vulgaris* (water melon); commonly found plant in south East Asia. The reaction process for the synthesis of silver nanoparticles is simple, cost-effective, novel, rapid and eco friendly route using fruit extract of *Citrullus vulgaris*, which acted as a reducing and stabilizing agent simultaneously at room temperature. The bio reduced silver nanoparticle were characterized by UV Vis spectrophotometer, Fourier transform infra-red (FTIR) spectroscopy, particle size analyzer and AFM. The observed peaks in UV a broad spectrum at 430 nm wave length. The FTIR measurement was carried out to identify the ascorbic acid present in the water melon extract is responsible for reduction of silver nanoparticles. Antibacterial property of our synthesized AgNPs was tested against four common bacteria *Bacillus cereus*, *Klebsiella pneumonia*, *Pseudomonas aeruginosa* and *Staphylococcus aureus* by conventional disc diffusion procedure. The inhibition zone formed on the discs in presence of silver nanoparticles, proved effective antibacterial property of these nanoparticles against the tested bacterial strains [1]. The diameter of inhibition zones ranged between 11 and 18 mm. Overall, results highlight a potential low-cost green method of synthesizing AgNPs from fruit extract. Significant bio potentials of synthesized AgNPs could make it a potential candidate for its application in the biomedical, pharmaceutical, cosmetics, and food sectors [2].

Keywords: Green synthesis, Silver nanoparticles, *Citrullus vulgaris* and Antibacterial activity.

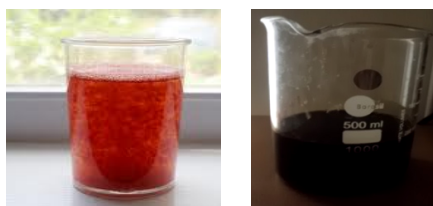


Figure 1. Observation of colour change indicating the synthesis of silver nanoparticles mediated by fruit extract of water melon

A, and B indicate drug, and silver nanoparticles concentrations respectively.

References

- [1]. P.P.N. Vijay Kumar, S.V.N. Pammi, Pratap Kollu, K.V.V. Satyanarayana, U. Shameem, *Industrial crop and products*, 52(2014) 562.
- [2]. K.D. Arunachalam, S.K. Annamalai, *International Journal of Nanomedicine*, 8 (2013) 2375.

2.11 Synthesis, characterization and catalytic properties of CuO nanocrystals

E.Bharathi^a S.Senthilvelan* and B.Karthikeyan

Department Of Chemistry, Annamalaiuniversity, Annamalainagar. elavaranbhrth@gmail.com

Abstract

The G -CuO composite is prepared by precipitation method. Guanine interaction with CuO nanocrystals of various sizes of clusters has been investigated. The binding energy (E_b), binding site, energy gap (E_g), electronic and spectral properties were studied by density functional theory method (DFT). The HOMO-LUMO energies illustrate that charge transfer from ligand to metal (L-M) occurs in (G-CuO) as well as metal to ligand (M-L) transfer occurs in CuO-G. From the transfer we can understand that interaction occur between CuO to G. Physisorption proceeded via formation of the N-Cu bond between guanine and the active Cu^{2+} site on CuO. The Mulliken charges are computed. The prepared G-CuO and CuO nanocrystals were characterized by FT-IR, XRD, FE-SEM, EDAX and FT-RAMAN analysis. The adsorption of G-CuO composite was observed by UV-Vis spectroscopy. The resulting experimental information like microscopic and spectroscopic evidence is also included for understanding the G-CuO interactions. Finally the experimental results are compared with the DFT results.

Optimized structure

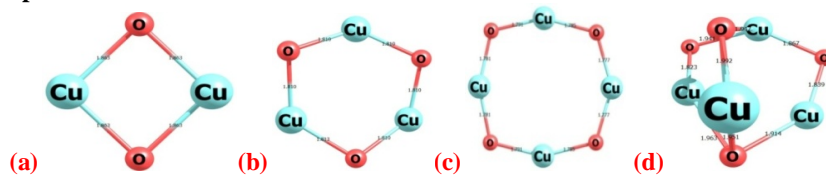


Fig.1 optimized structure of CuO Clusters (a) Cu_2O_2 (b) Cu_3O_3 (c) Cu_4O_4 (R) (d) Cu_4O_4 (w)

The application of nanotechnology in medical applications, commonly referred to as ‘nanomedicine’, delivers a set of tools, devices and therapies for the treatment of human diseases.¹⁻³ The optimized structures of CuO clusters such as Cu_2O_2 , Cu_3O_3 and Cu_4O_4 are shown in Fig.1. Mulliken charge distributions were calculated by determining the electron population of each atom as defined by the basis set.⁴ The Mulliken charge values were calculated using the B3LYP/LanL2DZ levels of theory. The Mulliken atomic charges of CuO clusters are given in For CuO clusters the oxygen atoms exhibit a negative charge, which are donor atoms. Cu atoms exhibit a positive charge, which is an acceptor atom for CuO clusters (Cu_2O_2 , Cu_3O_3 and Cu_4O_4 (R) Cu_4O_4 (w)). The HOMO is the orbital that primarily acts as an electron donor and the LUMO is the orbital that largely acts as the electron acceptor.

Conclusion

We have investigated the electronic structure of different sized CuO clusters (Cu_2O_2 , Cu_3O_3 and Cu_4O_4). According to the value of Table: 1 we have identified the most stable structure Cu_2O_2 Cluster by DFT theory.

References

1. V. Wagner, A. Dullaart, A. K. Bock and A. Zweck, *Nat. Biotechnol.*, 2006, 24, 1211–1217.
2. M. Ferrari, Cancer, *Nat. Rev. Cancer*, 2005, 5, 161–171.
3. R. G. Panchal, *Biochemist. Pharmacol.*, 1998, 55, 247–252.
4. C. Arunagiri, A. Subashini, M. Saranya and P. T. Muthiah, *Molecular Structure, Ind. J. Appl. Res.*, 2013, 3, 78–81.

2.12 Anticancer potential of the synthesized gold nanoparticles against A549 lung cancer cell lines

Natarajan Suganthy^{a*}, Vijayan Sri Ramkumar^b and G. Archunan^c

^aDepartment of Nanoscience and Technology, Science Campus, Alagappa University, Karaikudi-630 003, Tamil Nadu.

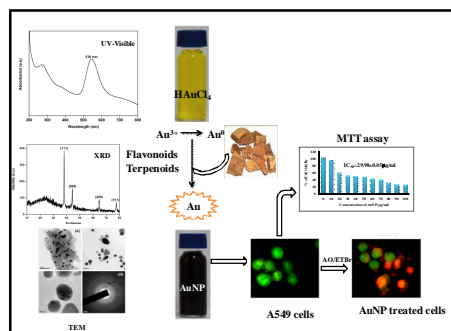
^bDepartment of Environmental Biotechnology & ^cDepartment of Animal Science, Bharathidasan University, Tiruchirappalli, Tamil Nadu, India. suganthy.n@gmail.com

Lung cancer is one of the leading disorders of present scenario that causes higher mortality rate across the world and its effect is increasing day by day. Currently, available chemotherapeutic agents have complications like severe side effects, poor solubility and non-specificity^[1]. Recently, nanoparticles have gained more attention in designing new metal based anticancer therapeutics with an emphasis on their use as drug delivery vehicles for selective targeting of cancer cells. The present study focuses on the biogenic synthesis of gold nanoparticles (AuNPs) using ethanolic extract of *Terminalia arjuna* bark and evaluating its anti-cancer potential against human lung cancer cell line A549.

The synthesized nanoparticles were characterized using UV-Vis spectra, FTIR, XRD and HRTEM analysis. The synthesized AuNPs was assessed for its anticancer potential against human lung cancer cell lines (A549). Cytotoxic activity of AuNPs against A549 cells were evaluated using MTT assay. Mitochondrial membrane potential was measured using Rhodamine 123 stain. Apoptosis was assessed by Acridine orange/Ethidium bromide dual staining technique.

UV-Vis spectra showed a characteristics SPR absorption band for AuNPs at 536 nm^[2]. The high crystallinity of AuNPs with a face-centered cubic phase is evident from XRD patterns. Furthermore, TEM analysis revealed the formation of spherical and triangular shaped AuNPs, and the size of the particles were observed to be in the range of 20-50 nm^[3]. Results of MTT assay showed increased cytotoxicity with increased concentration of AuNPs. IC₅₀ value was observed to be 29.98± 0.05 µg/ml and this concentration was fixed for further studies. Results illustrated that AuNPs (24 h) treated cells showed decreased fluorescence intensity due to the collapse of Δψ_m when compared to control cells. Results of AO/EB dual staining revealed uniform green nucleus in control cells, while yellow (early apoptotic cells) and red fluorescing cells (late apoptosis) were predominantly observed in AuNPs treated A549 cells indicating apoptotic mediated cell death. Acute toxicity studies on Zebra fish convincingly showed that AuNPs are non toxic up to maximum dose of 100 µg/L. Overall, the results conclude that AuNPs exhibited anticancer effect through its anti-proliferative and anti-apoptotic effect.

Anticancer potential of Gold nanoparticles synthesized from Ethanolic bark extract of *Terminalia arjuna*



Reference

- [1] R. Vaikundamoorthy, R. Sundaramoorthy, S. Thirugnana Sampanthan, M. Laxmanan and R. Rajendran, *RSC Adv.*, (2016) DOI: 10.1039/C5RA26781A
 [2] K. Mohan Kuma, B.K. Mandal, M. Sinha, V. Krishnakumar, *Spectrochim Acta A Mol Biomol Spectrosc* (2012), 86:490–494
 [3] SR. Vijayan, P. Santhiyagy, M. Singamuthu, N.K. Ahila, R. Jayaraman, K. Ethiraj, *Sci World J* (2014), Article ID 938272, 10 pages, doi:10.1155/2014/938272

2.13 Preparation of sputtering target of Cr₂O₃:CuO (50:50) and its thin film preparation by RF magnetron sputtering

S. Ponmudi¹, R. Sivakumar^{2,*}, C. Sanjeeviraja¹ and C. Gopalakrishnan³

¹Department of Physics, Alagappa Chettiar College of Engineering and Technology, Karaikudi-630004, India

²Department of Physics, Alagappa University, Karaikudi-630004, India

³Nanotechnology Research Centre, SRM University, Kattankulathur-603203, India krsivakumar1979@yahoo.com

Metal oxide thin films have been attracted much attention because of their various applications in solar cells, gas sensors, anti-reflecting coating, and opto-electronic devices, etc. Copper (II) oxide is one of the well-known non-toxic and abundantly available semiconducting materials. Similarly, chromium (III) oxide is also a most widely used ceramic material on earth. Due to their technologically important behaviors, thin films of Cr₂O₃:CuO (50:50) have been prepared by radio frequency (RF) magnetron sputtering technique at room temperature with the RF power of 100 W. The structural and optical properties of the deposited films were studied.

The powders of Cr₂O₃ and CuO (99.99% purity, Sigma Aldrich) were mixed in equal weight proportion (50:50) and grained thoroughly using the ball miller and the mixed powders were pelletized (2 inch diameter and 5 mm thickness) using hydraulic press. The prepared pellet was sintered at 900°C for 6 hours in vacuum. The structural property of Cr₂O₃ and CuO powders and Cr₂O₃:CuO (50:50) target was studied by X-ray diffraction (XRD) (X'pert-Pro PANalytical using CuK α radiation source with $\lambda=1.5418$ Å operating at 40 kV and 30 mA). The observed 2θ values of Cr₂O₃ powder and CuO powder was compared with standard JCPDS data (Card Nos. 38-1479 and 89-2529), which revealed the existence of rhombohedra phase Cr₂O₃ and monoclinic phase of CuO. Further, the observed deviations in the 2θ values of the XRD patterns of mixed Cr₂O₃:CuO (50:50) target when compared to Cr₂O₃ powder and CuO powder revealed the proper mixing of the two metal oxides.

The sintered pellet was used as a target to deposit Cr₂O₃:CuO thin films on pre-cleaned glass substrate by RF magnetron sputtering unit (HINDHIVAC; Planar magnetron RF/DC sputtering unit; Model-12"MSPT). The distance between the target and the substrate was fixed at 6 cm. During deposition, the RF power and working pressure of the chamber were maintained at 100 W and 1×10^{-3} mbar, respectively. High purity argon gas (99.999%) was used as sputtering gas. The film deposition time was varied as 60 minutes and 90 minutes with the RF sputtering power of 100 W at room temperature. The XRD patterns of the deposited films revealed the amorphous nature. The optical properties of the deposited films were studied by UV-Vis-NIR spectrophotometer (LAB INDIA; UV3000⁺). The transmittance of the prepared films increased with increasing wavelength. The films have approximately 70 to 80% of transmittance throughout the Vis-NIR region. The optical band gap (E_g) of the deposited films was determined using Tauc plot. It is observed that the E_g of the films decreased (3.11 - 2.90 eV) with increasing deposition time. The optical band gap of 3.30 eV was reported for Cr₂O₃ thin film prepared by spray pyrolysis technique [1] and thermal evaporation technique [2]. The optical band gaps of CuO thin films deposited on glass substrate by RF magnetron sputtering technique [3]

and by reactive DC magnetron sputtering technique [4] were reported as in the range of 2.25 – 2.6 eV and 1.6 – 2.54 eV, respectively. The results will be discussed in detail.

References

- [1]. Z.T.KAODAIR, G.A.KAZEM AND A.A.HABEED, IJAP 10 (2012) 83.
- [2]. MD.Julkarnain, J.Hossain, K.S.Sharif and K.A.Khan, J Optoelectron. Adv. M 13 (2011) 485.
- [3]. Riyam A. Hammoodil, Ahmed K. Abbas and Abdulhussein K.Elttayef, IJAIEM 3 (2014) 7
- [4]. Mugwang F.K, Karimi P.K, Njoroge W.K, Omayio O and Waita S.M, IJTFST 2 (2013) 15.

2.14 Anti-tumor promoting potential of 3, 3'-Diindolylmethane encapsulated chitosan nanoparticles on 7, 12-dimethylbenz (a) anthracene induced rat mammary carcinoma

S.Isabella and Dr.S.Mirunalini*

Department Biochemistry and Biotechnology, Annamalai University, Chidambaram, India. isabelladt@gmail.com

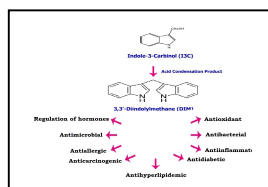


Fig 1. Pharmacological properties of DIM

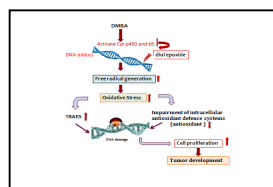


Fig 2. Mechanism action of DMBA

Abstract

The prevalence of breast cancer was reported in 151 countries worldwide. In both the developed and developing countries, breast cancer is a foremost large-scale public health problem and accounts for the highest morbidity and mortality worldwide. [1]. Upon metabolism, DMBA is either metabolized into biologically active metabolites, including diol epoxides free radical intermediates, which bind to cellular DNA forming covalent DNA adducts responsible for mutagenicity and carcinogenicity [2]. In recent years, natural dietary interventions are encouraging and emerging as an acceptable approach for controlling the cancer incidence worldwide. One such dietary bioactive compound 3, 3'-diindolylmethane (DIM), a major acid condensation product of indole-3-carbinol (I3C), is a promising antitumor agent derived from *Brassica* vegetables [3]. Therefore, nano formulation of this drug might play a beneficial role in prevention and treatment of neoplastic and there is still insufficient data on drug targeted action especially against DMBA induced breast cancer.

In this study animals were randomly divided into six groups and each group contains 6 animals. Group 1 animals will serve as control. Groups 2-4 animals will receive 25mg/kg BW of DMBA, In addition groups 3 and 4 will be treated with DIM 10mg /kg bw, DIM @ CS-NP 0.5mg/kg bw respectively. Groups 5-6 will receive bare DIM and DIM @ CS-NP served as drug control. We proposed to screen the lipids (PL, TG, FFA, and TC) in plasma, liver, mammary lipoproteins (HDL, LDL, VLDL) in plasma more over supported by histopathological evaluation of liver in control and experimental animals were carried out. In our study, we observed increased levels of TC and TG in DMBA-induced experimental rats [4]. Whereas decreased levels of PL and FFA found in mammary tissue. This may be due to the increased PL degradation which can results membrane dysfunction. The decreased PL concentration may also be due to the decreased FFA level in mammary tissue [5]. Moreover, DIM@CS-NP treatment group increased the levels of PL, FFA in mammary tissue, whereas significantly decreased TC, TG, PL, and FFA and increased HDL-C, as compare to plain DIM group. This piece of work is paving a way to represent a nano approach of drug may valuable for treatment of cancer. The profound efficacy of DIM@CS-NP indicated it potential application for cancer treatment and the research provided a novel and available method for the application of valuable for cancer.

References

- [1] A.H. Sims, A. Howell, S.J. Howell, R.B. Clarke, *Nat Clin Pract Oncol.* 4 (2007) 516-525.
- [2] Y.U. Hongtao Jian Yan, Yuguao Jiao, P. Peter. *Int J Environ Res Public Health.* 2 (2005)114-122.
- [3] M.D. Gammon, R.M. Santella, A.I. Neugut, S.M. Eng, S.L. Teitelbaum, A. Paykin, *Cancer Epidemiol Biomarkers Prev.* 11 (2002) 677–685.
- [4] K. McGuire, P. Ngoubilly, N.M. Neavyn, S. Lanza-Jacoby, *J. Surg. Res.* 137 (2006) 208-213.
- [5] T.Musumeci, C.A. Ventura, I. Giannone, B.Ruozi, L.Montenegro, R.Pignatello, G.Puglisi, *Int.J.Pharm.* 352 (2006) 172-179.

2.15 Synthesis and characterization of Terbium chloride doped polyaniline/MWCNT nanocomposite

J. Dominic and K. K. Sathesh Kumar*

Department of Chemistry, The Gandhigram Rural Institute – Deemed University, Gandhigram – 624 302, Dindigul, Tamil Nadu, India. dominiccharleschemist85@gmail.com, *k.k.satheeshkumar@ruraluniv.ac.in

Abstract

This article reports, the synthesis and characterization of Terbium chloride doped polyaniline/MWCNT nanocomposite (Tb-MWPAni). The synthesized Tb-MWPAni was characterized by FT-IR studies, scanning electron microscopy (SEM), Elementary dispersion analysis (EDAX) and Conductivity measurements.

Keywords: Nanocomposite, Terbium chloride, Polyaniline, MWCNT and Doping

1. Introduction

Conducting polymers with polyaromatic backbone including polyaniline (PAni), polypyrrole (PPy), polythiophene (PTh), etc., has received great interest for the past three decades. The inorganic-organic nanocomposite is extensively used in various technological applications and in these materials conducting polymers act as an organic counterpart¹. One of the outstanding features of conducting polymers is that it is possible to control the electrical conductivity over a wide range from insulating to metallic by proper doping with suitable dopants. The rare-earth doped polyaniline has a significant role in the area of industrial applications such as positive active materials with large energy density for secondary batteries. PAni interaction with metal ions to give rise to new chemical and physical properties of the formed macromolecules². PAni/MWCNT nanocomposite, which pool to improve conductivity and mechanical properties of MWCNT and high pseudocapacitance property of PAni³. Oxidized π -conjugated PAni possess delocalized charge and provide both steric and electrostatic stabilization to maintain the metal nanoparticles on the surfaces of the MWCNT⁴.

2. Synthesis of Tb-MWPAni nanocomposite

The Terbium chloride doped polyaniline/MWCNT nanocomposite (Tb-MWPAni) was synthesized as follows: 0.5M of aniline was dissolved in 1M HCl and 0.56M of ammonium peroxy disulfate (APS) was dissolved in 1M HCl. The oxidant was added slowly in a dropwise manner and the mixture was continuously stirred for about 6 h. During polymerization, 1 mg of multiwall carbon nanotubes (MWCNT) and 0.1M of Terbium chloride was added by an *in-situ* method. The obtained green precipitate of Tb-MWPAni was washed with 1M HCl. The obtained Tb-MWPAni was dried in an vacuum oven at 80 °C for 24 h.

3. Materials and methods

FT-IR spectra were obtained by using Perkin Elmer 1600 instrument using KBr pellets technique in the range from 4000 to 400 cm^{-1} . The surface morphology of the synthesized Tb-MWPAni was observed by scanning electron microscopy (SEM) and EDAX analysis of C, N, Cl and Tb were measured by using model TESCAN VEGA 3. The conductivity measurement was done by the four-probe method.

4. Result and discussion

The synthesized Tb-MWPAni has been characterized by FT-IR spectroscopy, scanning electron microscopy, elementary dispersion analysis, and conductivity.

4.1. FT-IR spectroscopy

Figure 1 shows FT-IR spectrum of Tb-MWPAni. The peak appears at $\sim 3419 \text{ cm}^{-1}$ due to N-H bond stretching frequency. The characteristic peaks at $\sim 1585 \text{ cm}^{-1}$ and $\sim 1487 \text{ cm}^{-1}$ represent quinoid and benzenoid structures respectively. The corresponding N-H bending of the amine shows the strong band at $\sim 1100 \text{ cm}^{-1}$ and corresponds to the dopant. The peak at $\sim 1024 \text{ cm}^{-1}$ corresponds to the C-H vibration and aromatic in plane bending vibrations. The band at $\sim 800 \text{ cm}^{-1}$ was represented the out-of-plane C-H bending modes of the quinoid units. The TbCl_3 is doped into MWPAni chain or attach itself loosely to the PAni backbone, which makes the peaks of FT-IR spectra of the Tb-MWPAni shifts to higher wavenumber than PAni-HCl⁵.

4.2. Scanning electron microscopy

The surface morphology of the synthesized Tb-MWPAni was observed by scanning electron microscopy (SEM) and EDAX. The inset of Figure 2 shows the elemental compositions of the Tb-MWPAni were found to be C-83%, N-10.97%, Cl-0.29, Tb-0.12% which confirms the formation of Tb-MWPAni nanocomposite. The morphology of the Tb-MWPAni nanocomposite was clearly shown that the polymer chain is well interconnected with MWCNT.

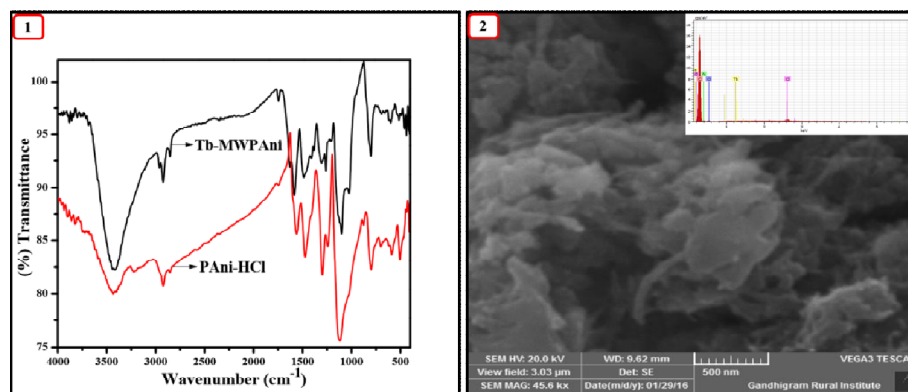


Figure 1. FTIR spectrum of synthesized Tb-MWPAni.

Figure 2. SEM image of Tb-MWPAni. Inset: EDAX analysis of Tb-MWPAni.

5. Conclusion

The synthesized Tb-MWPAni nanocomposite was synthesized by chemical oxidative polymerization at room temperature. FT-IR studies clearly explain the quinoid and benzenoid structure present the polymer chain. The SEM study reveals that the MWCNT interconnected with the PAni. The elementary dispersion analysis shows that terbium, chloride, nitrogen and carbon were present in the Tb-MWPAni nanocomposite.

Acknowledgement

“J. Dominic gratefully acknowledges the financial support from UGC-BSR Fellowship- New Delhi”.

Reference

- [1] Gupta, K.; Chakraborty, G.; Ghatak, S.; Jana, P. C.; Meikap, a. K.; Babu, R. Synthesis, Magnetic, Optical, and Electrical Transport Properties of the Nanocomposites of Polyaniline with Some Rare Earth Chlorides. *J. Appl. Phys.* **2010**, *108* (7), 073701.
- [2] Lv, R.; Tang, R.; Kan, J. Effect of Magnetic Field on Properties of Polyaniline Doped with Dysprosium Chloride. *Mater. Chem. Phys.* **2006**, *95*, 294–299.
- [3] Ubul, A.; Jamal, R.; Rahman, A.; Awut, T.; Nurulla, I.; Abdiryim, T. Solid-State Synthesis and Characterization of Polyaniline/multi-Walled Carbon Nanotubes Composite. *Synth. Met.* **2011**, *161* (19-20), 2097–2102.
- [4] Giri, S.; Ghosh, D.; Malas, A.; Das, C. K. A Facile Synthesis of a Palladium-Doped Polyaniline-Modified Carbon Nanotube Composites for Supercapacitors. *J. Electron. Mater.* **2013**, *42* (8), 2595–2605.
- [5] Lv, R.; Tang, R.; Kan, J. Effect of Magnetic Field on Properties of Polyaniline Doped with Dysprosium Chloride. *Mater. Chem. Phys.* **2006**, *95*, 294–299.

2.16 Non-enzymatic Biosensor for Dopamine using Graphene oxide-poly (3,4-ethylenedioxythiophene)-Copper Nanoparticles Modified Electrode

V.Sethuraman, M.Malathi, M.Akila and P.Manisankar*

Department of Industrial Chemistry, Alagappa University, Karaikudi-630 003, Tamil Nadu, India. pms11@rediffmail.com

Abstract

Several important diseases of the nervous system are associated with dysfunctions of the dopamine system, and some of the key medications used to treat them work by altering the effects of dopamine [1]. Since, the determination of neurotransmitter in human system becomes a need now-a-days, development of sensor using conducting polymers assumes significance. Electropolymerisation of (3,4-ethylenedioxythiophene) in presence of Graphene oxide was carried out by potential cycling method. Graphene oxide was reduced in PEDOT/GO by amperometric method. Further, Cu nanoparticles were deposited on PEDOT/rGO nanocomposite by electrodeposition in a solution containing 10 mM CuSO₄ and 100 mM Na₂SO₄ at a potential of -1.0 V (vs. Ag/AgCl) for 200 s. The modified GCEs are denoted as PEDOT/rGO/GCE and CuNP/PEDOT/rGO/GCE, respectively. Cyclic voltammetric studies of dopamine with modified electrode were carried out at different pHs. Response peak current for the biosensor was investigated at pHs 4-9 for 10 μM of dopamine. Maximum current response was observed at pH 6.0 which was used for further investigation. The cyclic voltammograms was recorded for 10 μM dopamine on plain glassy carbon, polymer and copper incorporated electrodes at pH 6.0 and scan rate 50 mVs⁻¹. Presence of redox peaks indicates that dopamine is electroactive. The quasi-reversible two-electrons and two proton transfer redox processes showed maximum peak current. The copper modified electrode has been successfully utilized for dopamine sensor by running Differential Pulse Voltammograms for different concentrations of dopamine (Fig. 1). This biosensor has exhibited wider linear range 5 × 10⁻⁸ to 1.40 × 10⁻⁵ M. Lower detection limit of 30 nM was obtained. Current

maxima (I_{max}) is 50.37 μ A and Michealis-Menten (K_m) constant is 76.76 μ M. This non-enzymatic biosensor can detect both low and high concentrations of dopamine. The major important interferences such as ascorbic acid, D-glucose and L-glutamic acid were investigated and the result revealed that the present modified electrode has high selectivity towards the detection of dopamine. The proposed biosensor has been successfully applied for the accurate determination of dopamine in the human urine. The selectivity and linear range are better compare to the reports available [2]. The advantages of the present biosensor are simple design, low cost, lower limit of detection, no usage of enzymes and suitable for real sample analysis. We believe that this system is a significant contribution toward the fabrication of dopamine sensor for real world application.

Keywords: Electrochemical, Amperometric, Copper, Sensor, Dopamine.

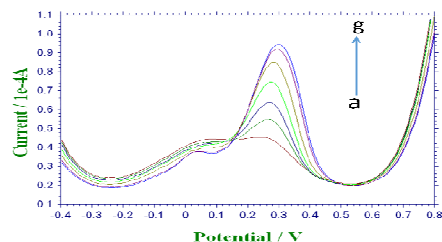


Figure 1. DPV response for the dopamine of prepared electrode

[1] C. Xue, Q. Han, Y. Wang, J. Wu, T. Wen, R. Wang, J. Hong, X. Zhou, H. Jiang, *Biosensor and Bioelectronics* 49(15) (2013), 199-203.

[2] H. Zhang, J. Zhao, H. Liu, L. Renmin, H. Wang, J. Liu, *Microchim Acta* 169 (2010) 277

2.17 Adsorption of methylene blue dye by SW-ZnO composite doped polyaniline: Evaluation of the kinetic and isotherm

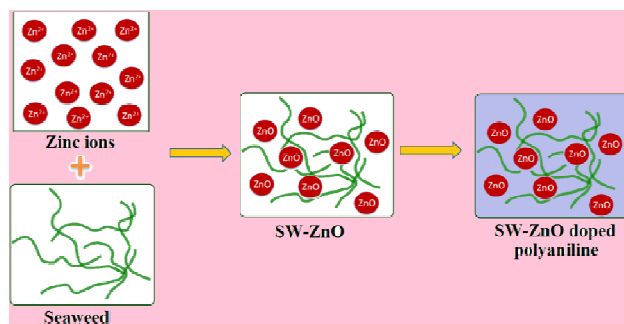
R.Pandimurugan, S.Thambidurai*

Department of Industrial chemistry, School of Chemical Sciences, Alagappa University, Karaikudi-630003, Tamilnadu, India. mpandimurugan1@gmail.com

Abstract

Dye waste water from textile industries are reported to be a major river pollutant. A new hybrid composite consisting of aniline and SW-ZnO composite [1] was prepared by polymerization using an APS as initiator. The SW-ZnO composite have been effectively assembled onto the surface of the synthesized polyaniline via electrostatic attraction. The synthesized material were characterized by using UV-vis, FTIR, XRD, HR-SEM and BET analysis. The results showed that SW-ZnO composite was successfully doped on the surface of polyaniline. The SW-ZnO doped PANI were further applied to remove MB, the effect of pH, initial dye concentration and adsorbent amount of dye adsorbed were investigated using a batch experiment. The pseudo first order and pseudo second order kinetic models were used to describe the kinetic data. It was observed that the pseudo-second-order kinetic model described the adsorption process better than first pseudo-first-order [2,3]. The Langmuir and Freundlich adsorption model were used for the numerical depiction of equilibrium data, and the best fit was obtained using the Freundlich isotherm model [4]. These results indicate that the SW-ZnO doped PANI could be employed as an efficient adsorbent much more than the parent material adsorption of MB dye.

Keyword: Seaweed, Zinc oxide, Polyaniline, composite, high surface area, Isotherm



Scheme 1. Preparation of SW-ZnO doped polyaniline.

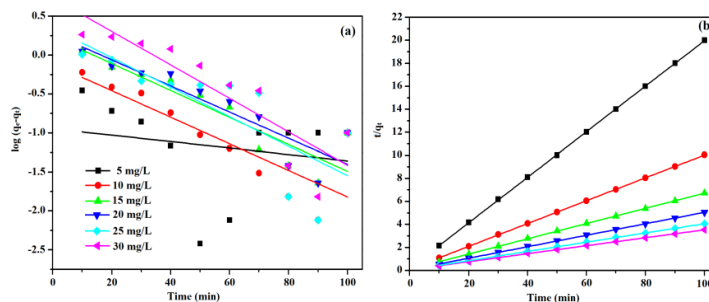


Figure 1. (a) Pseudo-first-order and (b) Pseudo-second-order kinetics for adsorption of methylene blue onto prepared SW-ZnO doped polyaniline.

References

- [1] R.Pandimurugan, S. Thambidurai, J. Appl. Polym. Sci. 131 (2014) 40948.
- [2] Y.S. Ho, G. Mckay, Process Biochem. 34 (1999) 451–465.
- [3] M. Ghaedi, H. Hossainian, M. Montazerzohori, A. Shokrollahi, F. Shojapour, M. Soylak, M.K. Purkait, Desalination 281 (2011) 226–233.
- [4] B.K. Nandi, A. Goswami, M.K. Purkait, J. Hazard. Mater. 161 (2009) 387–395.

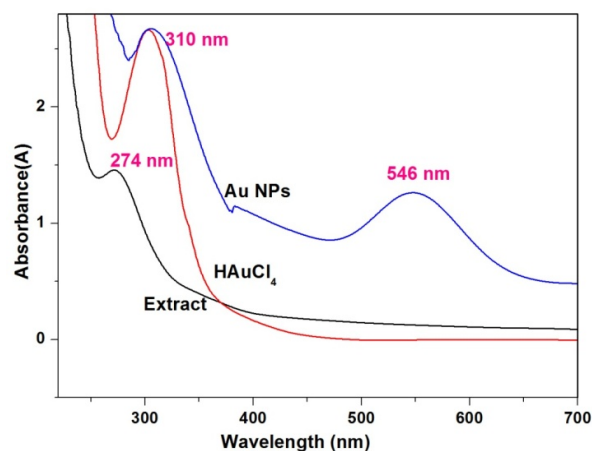
2.18 Green Synthesis of Gold Nanoparticles from *Lawsonia inermis* seeds extract

Subramani Seethai and Karuppiiah Muthu*

Department of Chemistry, Manonmaniam Sundaranar University, Tirunelveli – 627 012. TN, India. karu.muthu@yahoo.com

Abstract

Natural plant mediated synthesized metal nanoparticles (MNPs) were non-toxic, environmental eco-friendly simple process to build up in the Nanosciences and Nanotechnology. The objective of this study is *Lawsonia inermis* seed extracts with increasing order of polarity solvent. The final aqueous extract was concentrated to obtain the orange red (5.211gm) paste. This paste was analysed (present/absent) to primary phytochemical constituents such as steroids, terpenoids, alkaloids, saponins, tannins, phenols, flavonoids, isoflavonoids, amino acids, carbohydrates and glycosides. This selective phyto-compound is effective in the reducing and capping agents for the green synthesis of gold nanoparticles from chloro-auric acid. The pale yellow chloro-auric acid was changed to dark violet colour at 10min after addition of plant extract to visually identify the synthesis of Au NPs. The extract and chloro-auric acid UV-vis spectra of the shorted wavelength region at 274nm and 310nm was shifted in the longer wavelength region at 546nm. The change of surface resonance band at 546nm was confirmed the synthesis of Au NPs. The obtained NPs and extract phytochemical functional groups were characterized by FTIR spectroscopy. The X-ray diffraction results to confirm the formation of Au NPs in crystalline structure. The synthesized Au NPs have been used as a catalyst for the reduction of p-Nitrophenol to p-Aminophenol by NaBH₄.



Reference:

- [1]. W. Raja, M. Ovais and Amit Dubey. International Journal of Microbiological Research, 4(1), (2013) 33-36,
- [2]. D.S. Sheny, J. Mathew and D. Philip. Spectrochimica Acta Part A: Molecular and Biomolecular Spectroscopy 97 (2012) 306–310.
- [3]. J. Kasthuri, S. Veerapandian and N. Rajendiran, Colloids and Surfaces B: Biointerfaces, 68 (2009) 55–60.
- [4]. A. Gangula, R. Podila, M. Ramakrishna, L.Karanam, C. Janardhana, and A.M. Rao. Langmuir, 27 (2011) 15268–15274.

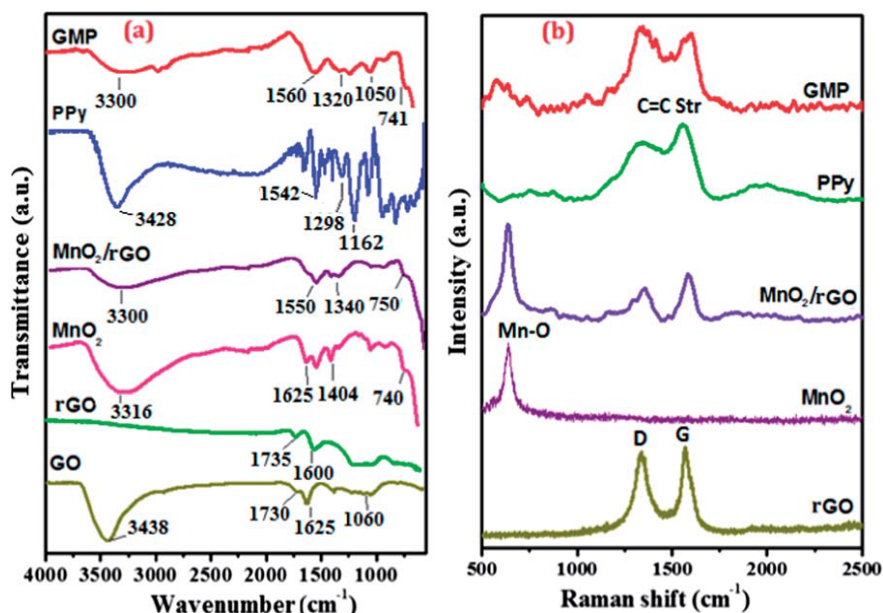
2.19 Nanostructured based on organic – inorganic hybrid composites for high-performance Supercapacitor

M. Arun Prabhu and K. Gurunathan*

Department of Nanoscience and technology, Science Campus, Alagappa University, Karaikudi-630 003.

kgathan27@rediffmail.com

The rational preparation of hierarchical MnO₂/polypyrrole (PPy)/reduced graphene oxide (rGO) nanosheets in a sandwich structure is presented. By co-assembly of MnO₂/GO and PPy/GO into layer-by-layer architecture and reduction of GO, ternary (MnO₂, PPy)/rGO composites were first fabricated. The materials were fully characterized in terms of structure, morphology and electrochemical properties. The unique architecture offers the composites good capacitance by taking advantage of the strong synergistic effect of each component. The good electrochemical performance and long-term cycling stability make this approach attractive in developing multifunctional hierarchical composites for high-performance supercapacitors.



a) FTIR of GO, rGO and metal oxides b) Raman spectrum of GO, rGO and metal oxides

References

- [1]. X. Zhao, B. M. Anchez, P. J. Dobson and P. S. Grant, *Nanoscale*, 2011, 3, 839.
- [2]. L. L. Zhang and X. S. Zhao, *Chem. Soc. Rev.*, 2009, 38, 2520.
- [3]. M. D. Stoller, S. Park, Y. Zhu, J. An and R. S. Ruoff, *Nano Lett.*, 2008, 8, 3498.
- [4]. M. Winter and R. J. Brodd, *Chem. Rev.*, 2004, 104, 4245.
- [5]. Guang qiang Han, Yun Liu, Erjun Kan, JianTang, Lingling Zhang, Huanhuan Wang
- [6]. and Weihua Tang, *RSC adv.*, 2014, 4, 9898.

2.20 Antimicrobial effect of cobalt and manganese codoped tungsten oxide nanoparticles

R. Arunadevi^a, B. Kavitha^a, M. Rajarajan^{a**}, A. Suganthi^{b*}, P. Muthuraj

^aP.G. & Research Department of Chemistry, C.P.A. College, Bodinayakanur, Theni (Dt), Tamil Nadu, India-625513.

^bP.G. & Research Department of Chemistry, Thiagarajar College, Madurai, Tamil Nadu, India -625009.

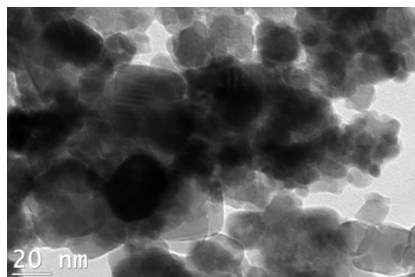
arunarajan3@gmail.com, rajarajanchem1962@gmail.com

Abstract

Semiconductor photocatalysts have been found to kill cancer cells, bacteria and viruses under mild UV illumination, which offers numerous potential applications. This work presents a study about the evolution of Co and Mn codoped WO₃ nanoparticles prepared by simple sonication method using sodium tungstate as precursor and its antimicrobial activities. WO₃, single metal doped WO₃ and codoped WO₃ (Co, Mn-WO₃) nanoparticles were successfully characterized by the following techniques. UV-visible-diffuse reflectance spectroscopy (UV-vis-DRS), fourier transform infrared spectroscopy (FT-IR), X-ray diffraction (XRD), scanning electron microscopy (SEM), energy dispersive X-ray spectroscopy (EDS) and high resolution transmission electron microscopy (HRTEM) techniques. Co, Mn-WO₃, Co-WO₃, Mn-WO₃ and pure WO₃ nanoparticles with an

average crystallite size of 9-14 nm and narrow size distribution are formed after annealing at 400 °C. Co, Mn codoped WO₃ nanoparticles shows plate with needle like morphology. The antimicrobial activity of all the samples was investigated against *Klebsilla pneumonia*, *Staphylococcus aureus*, *Candida albicans* and *Aspergillus niger*. Based on this study, Co, Mn-WO₃ nanoparticles has good antimicrobial activity and can be used as an antibacterial agent for different purposes.

Keywords: Co, Mn-WO₃, sonication method, average crystallite size, antimicrobial effect.



HRTEM image of Co, Mn-WO₃ nanoparticles

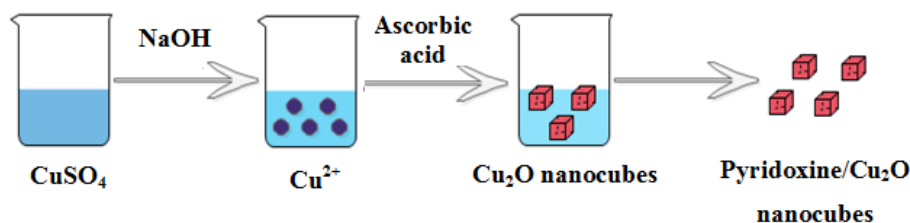
2.21 Preparation of Pyridoxine/Cu₂O Nanocubes and their antimicrobial activity

B. Suganya bharathi, T. Stalin*

Department of Industrial Chemistry, Alagappa University, Karaikudi – 03, Tamilnadu, India.
sbsuganyaa@gmail.com and drstalin76@gmail.com

Abstract:

Highly uniform pyridoxine incorporated Cu₂O nanocube can prepare by precipitation method at room temperature. These nanocubes are prepared in the presence of ascorbic acid as a reducing agent with a well-defined shape. Ascorbic acid plays a vital role in controlling the shape of the Cu₂O nanocubes. Reducing agents are important in determining the samples final morphology structure and composition. It reduces Cu²⁺ ions to Cu₂O quickly in the presence of OH⁻ ion. The size of Cu₂O nanocubes can be modulated by changing the pH of the reaction solution or concentration of the reducing agents. FT-IR spectroscopy, XRD, SEM, UV/vis/NIR spectrometry was employed to characterize the nanostructured Cu₂O samples. The prepared Cu₂O nanocubes are found to have good antibacterial and antifungal activity against both gram positive and gram negative bacteria.



Scheme 1. Schematic representation for the preparation of pyridoxine/Cu₂O nanocubes

Keywords: Pyridoxine (vitamin B6), Cu₂O nanocubes, Ascorbic acid.

References:

- [1]. W. Huang, L. Lyu, Y. Yang and M. H. Huang, *J. Am. Chem. Soc.*, **2012**, 134, 1261.
- [2]. A. Paracchino, J. C. Brauer, J.-E. Moser, E. Thimsen and M. Graetzel, *J. Phys. Chem. C*, **2012**, 116, 7341.

2.22 Electro-Optical Properties of 2,5-dimethoxy polyaniline with Tin Oxide Nano Composites

M.Senthil kumar*¹ and P. Manisankar²

¹Department of Chemistry, Government College of Engineering, Bodinayakanur-625582

²Department of Industrial Chemistry, Alagappa University, Karaikudi-630003. Email: senthilshrivi@gmail.com

2,5-Dimethoxypolyaniline (DPMA)/Tin oxide nano composites, synthesized by incorporation of separately prepared Tin oxide nano particles in acid medium of 2,5-Dimethoxyaniline (DMA) using potassium peroxodisulfate as an oxidant. The crystal structure of the Tin oxide nano particles and 2,5-dimethoxy polyaniline/ SnO₂ nano composites at the annealed temperature of 500°C and 800°C were characterized by X-ray powder diffraction (XRD). Hexagon structure of Tin oxide nano particles, DPMA and DPMA-wt% Tin oxide nano composite was observed by Scanning Electron Microscope (Fig.1) and TEM (Fig.2). UV-Visible

spectroscopy and Impedance spectroscopy characteristics performed the Optical and Electrical conductivity of DPMA and DPMA –wt%SnO₂ and SnO₂ nano composites. Optical and electrical characteristics indicate that the electrical properties of DPMA/SnO₂ composites are dominated by doping SnO₂ nano composite.

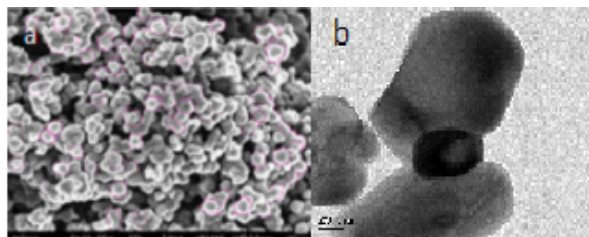


Fig. 1. a) SEM images of SnO₂ b) TEM images of SnO₂ with polymer

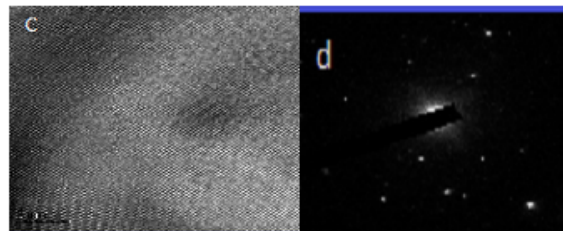


Fig.2 c) Lattices fingers of SnO₂ with polymer d) SAED pattern of SnO₂ with polymer

Keywords: SnO₂ Nanoparticles, DPMA-wt% SnO₂ nano composites, UV, XRD, Impedance spectroscopy, SEM and TEM

2.23 An Eco-Friendly Synthesis of Silver Nanoparticles Using *Achyranthus Aspera* Root Promising Anticorrosion Potentials For Mild Steel In Acidic Medium

B. Gowri Shannkari^{a,b}, S. Siva Bharathi^a and R. Sayee Kannan^{a*}

^aPG & Research Department of Chemistry, Thiagarajar College, Madurai-625 009

^bDepartment of Chemistry, NMSSVN College, Madurai-625010. sayeekannanramaraj@gmail.com

Abstract

In this present work corrosion inhibition of mild steel in Sulphuric acid (1M) by *Achyranthus Aspera* termed as “Rough cheff” Silver nanoparticles was studied by weight loss method. It has been found that the root extract acts as an effective corrosion inhibition action for mild steel in sulphuric acid medium. The inhibition process was attributed to the formation of an adsorbed film of inhibitor on the metal surface which protects the metal against corrosion. The inhibition efficiency (%IE) and surface coverage (Θ) of RAgNP's increased with increase in inhibitor concentration but decreased with increasing temperature. The adsorption of RAgNP's on mild steel surface was to be obeying Langmuir's adsorption isotherm and also obeys Pseudo first order kinetics. The free energy value (G_{ads}) indicated that the adsorption of inhibitor molecules was typical of physisorption. The silver nanoparticles were synthesized using *Achyranthus Aspera* root extract from 1mM AgNO₃ solution. The size and the morphology of the nanoparticles have been examined by UV, XRD and High resolution transmission electron microscopy (HRTEM). The results obtained indicate that the RAgNP's could serve as an excellent green corrosion inhibitor for mild steel in 1M sulphuric acid medium.

Keywords: *Achyranthus Aspera*, Ag-nanoparticles, Carbon steel, UV, XRD and TEM

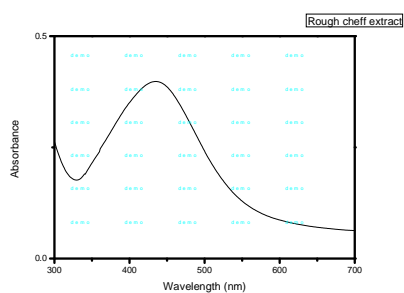


Fig: 1 UV – Visible Spectrum of RAgNp's

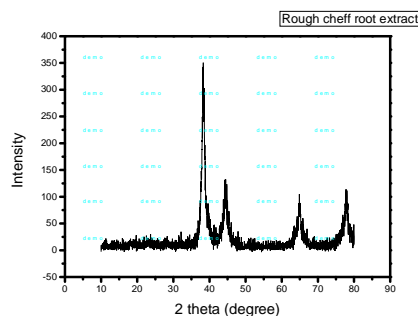


Fig:2 XRD Analysis of RAgNp's

2.24 Biosynthesis of Silver Nanoparticles Using *Curcuma Longa* And Their Application of Pharmacological And Catalytic Activity

N. Muniyappan*, T. K. Dhamodharan S. Baskar and P.Ramar

Department of Chemistry, Saraswathi Narayanan College, Madurai - 625 022, Tamil Nadu, India.

*Correspondence E-mail : nmuniyappan@gmail.com

Abstract

Nanobiotechnology is one of the most interesting areas of research in modern material science. Silver nanoparticles (AgNPs) are emerging as nanoproducts that have interest in the field of nanomedicine because of their unique properties and therapeutic potential in the treatment of innumerable diseases. AgNPs can be synthesized by reduction in solution concentration, chemical and photochemical reaction in reverse micelles, thermal decomposition of silver complex microwave assisted process, polyol and sonochemical methods. It has been observed that plant biosynthesis of silver nanoparticles using a *Curcuma* species has not been carried out earlier and in the present study we have carried out green synthesis of AgNPs by one-pot Microwave synthesis using CLL aqueous extract and also evaluated their *in vitro* antioxidant, anti-inflammatory as well as catalytic activities.

Silver nanoparticles are utilized in drugs because of their pharmacological and catalytic applications and also due to their eco-friendly properties. In the present study stable silver nanoparticles have been synthesized by using aqueous extract of *Curcuma longa* leaves (CLL), used both as a reducing as well as a stabilizing agent. The silver nanoparticles synthesized by Microwave oven for 90 sec were found to be stable in aqueous solution at room temperature over a period of six months. The quantitatively stable silver nanoparticles (AgNPs) formed by treating aqueous solution of AgNO_3 with the aqueous extract of the plant by reduction of Ag^+ ions when monitored by UV – Visible spectroscopic study revealed the Surface Plasmon Resonance (SPR) at 426 nm. FTIR spectrum of the silver nanoparticles showed characteristic bands for corresponds to C–N stretching vibrations of aromatic amine at 1397 cm^{-1} . The band at 1633 cm^{-1} corresponds to C=O stretching of amide band, 2925 cm^{-1} corresponds aldehydic C–H stretching and 3416 cm^{-1} corresponds to –NH stretching in amide and the weak band at 1049 cm^{-1} is characteristic of C–OH stretching of secondary alcohols.

The shape and size of the nanoparticles identified by Transmission Electron Micrography (TEM) were found to be spherical and in the range of $15 \pm 2\text{ nm}$. The study involves a green chemistry approach involving the use of a plant extract material for the generation of stable spherical silver nanoparticles. The evaluation of the antioxidant and anti-inflammatory activities by *in vitro* methods showed that the both the activities increased in a dose dependent manner and CLL-AgNPs showed better antioxidant and anti-inflammatory activities when compared to the standards at all the five test doses of (2, 4, 6, 8 and 10 $\mu\text{g}/\text{ml}$) study. Hence it could be concluded that CLL-AgNPs produced using aqueous extract of CLL possess good antioxidant and anti-inflammatory activities. The reaction mechanism can be reasoned by the inherent hydrogen adsorption, desorption characteristics of silver nanoparticle. The AgNPs shuttle the hydrogen transport between NaBH_4 and 4-nitrophenol. The shuttling behaviors can be reasoned that the AgNPs adsorbs hydrogen from the NaBH_4 and efficiently release during the reduction reaction and hence AgNPs acts as a hydrogen carrier in this reduction reaction. The reduction of nitro group of 4-NP into 4-AP was qualitatively monitored in UV–Vis spectrophotometer. AgNPs showed considerably enhanced catalytic activity.

Keywords: Ultrasonication, Silver nanoparticles, *Curcuma longa*, catalytic activity.

2.25 Enzymatic synthesis of ethyl ferulate using celite immobilized lipase from *Bacillus subtilis*

S.Monisha, M.Sinduja, K.SwethaLaxmi, AnantAchary, S.Karthikumar

Department of Biotechnology, Kamaraj College of Engineering and Technology, S.P.G.C. Nagar, Virudhunagar-626001, Tamilnadu. skarthikumar@gmail.com, enthusiasticsin@gmail.com

Abstract

The unstable nature of the edible oil due to auto oxidation give rise to serious health problems. Direct blending or biotransformation of anti-oxidant to the edible oil reduce the risk of auto oxidation. In the present work, we synthesized ethyl ferulate by the esterification offerulic acid and ethanol bycelite immobilized lipase from *Bacillus subtilis*. The bacterial strain was cultivated in minimal medium and the crude lipase was concentrated by ammonium sulphate precipitation at 80% saturation followed by dialysis. 7 mg of protein sample (Specific activity - 3826.4 U/mg) was immobilized on 1 gm ofcelite by adsorption and crosslinked by 1% glutaraldehyde at 37°C for 2 hours. 85% of immobilization efficiency was achieved. The stability of the immobilized enzyme over wide range of temperature was studied and found that the immobilized enzyme was stable between 37°C and 80°C .The ethyl ferulate was synthesized by esterification of ferulic acid and ethanol at 1:3 molar ratio. The reaction was initiated by adding 25 mg of lyophilized immobilized enzyme and continued

for 12 h at 37°C, 150 rpm. The formation of ethyl ferulate was monitored in fluorescence spectrophotometer and Reverse phase HPLC. The product conversion achieved was 94%.

Key words: *Bacillus subtilis*, Lipase, Celite, Immobilization, Esterification, Ethyl ferulate,

2.26 A novel Cobalt doped Dy₂O₃ nanoparticles Synthesized by co-precipitation method

C. Suganya^a, N. Anandhan^{a*}, M. Karthikeyan^a, V. Dharuman^b, G. Gopu^c, A. Amali Roselin^a, S. Viswanathan^d, J. Umadevi^a

^aAdvanced Materials and Thin film Physics Lab, Department of Physics, Alagappa University, Karaikudi-4, Tamilnadu.

^bMolecular Electronics Laboratory, Department of Bioelectronics and Biosensors, Alagappa University, Karaikudi -4,

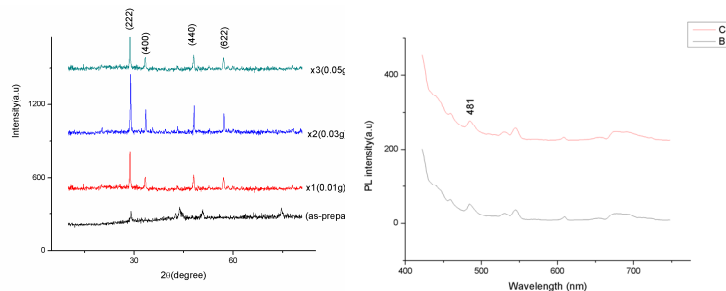
^cCatalytic and Supercapacitor Lab, Department of Industrial Chemistry, Alagappa University, Karaikudi-3, Tamilnadu.

^dDepartment of Industrial Chemistry, Alagappa University, Karaikudi-3, Tamilnadu. anandhan_kn@rediffmail.com

In this present work, a novel nano crystalline Cobalt doped Dy₂O₃ nanopowder was synthesized by co-precipitation method. Dy(NO₃)₃.5H₂O and (CH₃COO)₂Co.4H₂O is dissolved in 25 ml in de-ionized water. The precipitation agent 1N of NaOH solution was added drop-wise to maintain constant pH 12, the obtained solution was allowed to magnetic stirring for 30 minutes, precipitate was obtained. The obtained precipitate was filtered and washed several times by de-ionized water and then ethanol to remove the residual of ammonia and nitrate ions present in it. After washing, the product was dried in hot-air oven 80°C for 7h. Finally, calcined at 550°C for 2h to get Co doped Dy₂O₃ nanoparticles. From the XRD pattern, the sharp and high intensive peak observed at an angle 2θ=29.04° and corresponding to reflection plane is (222), which confirms the Co doped Dy₂O₃ nanoparticles are in cubic nature and crystalline size is 73.4nm [1-2]. As concentration of doping level increases from 0.01g to 0.03g, the intensities of the planes (222), (400), (440), (622) are increases with area but the dopant at 0.05g of Co- Dy₂O₃ is almost reflects similar to Dy₂O₃ due to ionic diameters of Co and Dy ions [3]. The PL spectra of Dy₂O₃ and doped Dy₂O₃ nanoparticles emission peak is observed at 481nm. Surface morphology and vibrational properties of the samples were studied and analyzed by SEM and micro Raman spectroscopy.

Keywords: Cobalt doped Dy₂O₃ nanoparticles, Sol-gel method.

Graphical Abstract



References

- [1]. Bahaa M. Abu-Zied, Abdullah M. Asiri, J. Rare Earths., 32, P.259, (2014)
- [2]. M. Chandrasekhar, H. Nagabhushana, K.H. Sudheerkumar., J.Mater.Res.Bull., 55,237-245 (2014).
- [3]. A. Bandyopadhyay, S. Sutradhar, B.J. Sarkar., J. Appl. Phys. Lett.,100,252411 (2012).

2.27 Studies on Solid Polymer Electrolytes Added With Nano Fillers

T.M. Amarnath, J. B.A. J. Helen Therese and K. Gurunathan *

Nano Functional Materials Research Lab, Department of Nanoscience and Technology, Science Campus, Alagappa University, Karaikudi- 630 003; *E-mail: kgnathan27@rediffmail.com

Abstract

In this work, we report a new composite, poly (styrene-co-methylmethacrylate) based lithium polymer electrolyte containing micro sized, nano porous Al₂O₃ (Alumina) filler synthesized through wet chemical method. The properties of the material leading to a new solvent free electrolyte having unique features in terms of ionic conductivity, lithium ion transference number and thermal behaviour. The polymer films are characterized by XRD, FTIR, RAMAN, IMPEDENCE Spectroscopic studies. Hybrid polymer electrolytes based on Poly(Sty-co-MMA) appear very promising for lithium battery application. Polymer electrolytes are attracting and increasing attention due to promising applications such as solid-state rechargeable Lithium ion batteries, Super capacitors electro-chromic windows and sensors. The main advantage of polymer electrolyte is favourable mechanical properties, ease of fabrication of thin film of desirable sizes and on ability to form

effective electrode electrolyte contacts. The crystalline complexes formed from alkali metal salts with Poly (styrene-co-methylmethacrylate) are capable of demonstrating significant ionic conductivity and highlighted the possible applications as battery electrolytes.

NaHCO_3 and $\text{Al}_2(\text{SO}_4)$ were added with 50 ml of water separately. The solution of Al_2O_3 is injected to the NaHCO_3 solution, after the fizzing stops the obtained white precipitate is filtered by Buchner filter system. The white precipitate is dried in oven at 70°C for 6 h. Then again it is calcinated at 800°C for 3 h. Finally, Alumina NPs were obtained. Several wt% of polymer and salt complexes are weighed and added with nano fillers with aspect ratio combination. And finally the preparation of electrolyte film is prepared by solution casting techniques. The crystal structure of the prepared electrolyte has been analyzed using the X-ray diffractometer. Figure 1 shows the XRD diffraction pattern of the prepared electrolyte samples. A peak at 2θ degrees shows the semi crystalline nature of the prepared electrolyte sample. If its complexed with a metallic salt the crystalline peaks of polymer and the salts are suppressed. This suppressed peaks with amorphous nature helps for ionic conduction within the electrolyte matrix. There are no particular peaks for lithium perchlorate has been obtained. The presence of peak shows the alumina nano particles. This confirms the complex nature of polymer and the lithium perchlorate salt. The chemical structure of the polymer electrolytes are ascertained via Raman Analysis and it is given in Fig.1.B for the samples JB1-JB10. The shift at 2950 cm^{-1} is corresponding to CH_2 stretching of PS-MMA. The shifting has appeared in all complexes. The shifting around 950 cm^{-1} is representing the ClO_4^- anion of LiClO_4 salt.

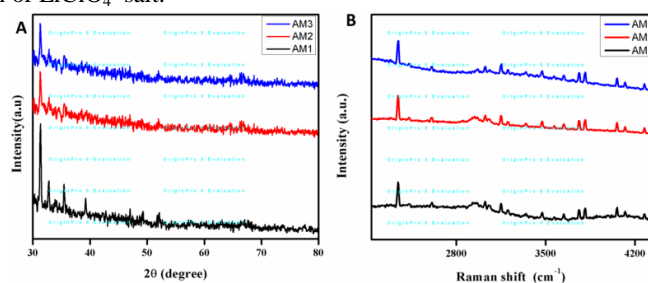


Figure 1.(A) XRD pattern,(B) Raman spectra of synthesized samples.

Reference

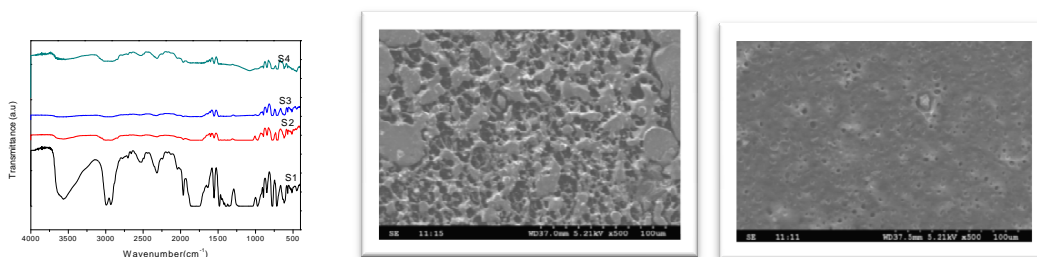
- [1]. J.O. Lundgren, R. Liminga, R. Tellgren, Acta Crystallogr. Sec. B 38(1982) 15.
- [2]. R. A.Nyquist, SE.Settineri, Appl. Spectro. 45 (1991) 1991.
- [3]. S.Rajendran, O.Mahendran, T.Mahalingam, Euro.Polym. J. 38 (2002) 49.
- [4]. M. Raja, M.Sc. project report during 2012-13 in the Dept. Physics, Alagappa University.

2.28 Analytical Studies On Polystyrene methylmethacrylate Poly(Sty-MMA)-Poly(vinyl Chloride) Polymer Electrolytes with lithium Salts

C.Balalakshmi, J.B.A.J. Helen Thesere and K. Gurunathan*

Department of Nanoscience and technology, Science Campus, Alagappa University, Karaikudi- 630 003;
e-mail: kgnathan27@rediffmail.com

The transport properties of gel type ionic conducting membrane consisting of Poly styrene methylmethacrylate P(S-MMA), Poly(vinyl chloride) and LiTFO_2 are studied [1,2]. The polymer films are characterized by FTIR and SEM studies. Blending of polymer is useful method to develop new materials it improved mechanical stability. The problem in choosing polymer blends is the miscibility of the components. By careful selection of the support polymer, there may be the added advantage of lowering the degree of crystallinity. Combination of proton donating and proton accepting polymer can form intermolecular complexes in aqueous or organic media. P(S-MMA) and PVC form one such couple [3,4]. These studies have shown clear evidence of the miscibility of P(S-MMA) and PVC. The FTIR plots of pure P(S-MMA), PVC, LiTFO_2 and polymer electrolyte complexes are shown in fig (a). The specimens for the SEM images of the cross section of the films were prepared by fracturing the films in gel polymer. The electron scanning micrographs (SEM) of the cross section of the polymer films were taken by using the Philips SEM 535M. fig. (b) and (c) shows the SEM images of the cross section of the polymer matrices with various compositions. The good miscibility between PVC and P(S-MMA) was confirmed by a single glass transition behavior of the PVC/P(S-MMA) mixture as shown in fig.a). The micro pore structure was also absorbed in the P(S-MMA)/PVC/ LiTFO_2 film as shown in fig (b)and (c).



References

1. Fenton, D.E., Parker, J.M., Wright, P.V., Complexes of alkali metal ions with poly(ethylene oxide), *Polymer*, 1973, 14, 589.
2. Armand MB (1986), *Annu. Rev. Mater. sci.*, 16, 245..
3. Abraham K M and Alamgir M (1990), 'Li⁺ conductive solid polymer electrolytes with liquid-like conductivity', *J Electrochem Soc.*, 137: 1657-1658
4. M. B. Armand, *Solid state Ionics* (1994), 69, 309

2.29 Microrheology – methods and technique

Anand S Tadas^{1,*}

^{1,*}Malvern Aimil Instruments Pvt Ltd, Naimex House, A-8, Mohan Co-operative Industrial Estate, Mathura Road, New Delhi 110044 Email: anand.tadas@malvernaimil.com

Abstract

Rheology is the study of how complex materials flow and deform under stress. Complex fluids, such as emulsions, suspensions, polymer, and micellar solutions, play a ubiquitous role in everyday life, their microstructures both store and dissipate the deformation energy in a frequency-dependent manner, reflecting viscoelasticity.

The rheological properties of a soft material determines its flow and processing behaviour, and provide a window into its microstructural makeup. Traditional rheometers typically measure the frequency-dependent linear viscoelastic (LVE) relationship between strain and stress on milliliter-scale material samples.

However, mechanical rheometry has fundamental limits, primarily arising from the effects of mechanical inertia, which prevent complete characterization across all complex fluid types.

The term microrheology describes a range of techniques that extract the rheological properties on a micro-scale and remove the inertia limitations. This in turn would enable an experimentalist to perform high frequency measurements that capture short timescale dynamics of low viscosity formulations.

Using a drive force of such low applied stress and sensitivity, the onset of molecular aggregation or denaturation processes can be followed, within the linear regime of the most highly strain-sensitive systems. This gives the ability to probe different material length scales, from bulk properties down to mapping localized spatial dynamics at a microstructural level. The sample volume needed for such studies would be on a micro(litre)-scale indeed a requirement of the time for high value, scarce materials such as biotherapeutic proteins or novel engineered polymers..

This paper looks at the various modes used to study microrheology in general and focuses on the ability and limitations of Dynamic Light Scattering as a preparatory tool for studying micro-rheology.

2.30 Enhanced antibacterial activity and low bandgap energy of ZnO/BC nanocomposite material

K. Bama^a, M. Sundrarajan^{a*} and K. Bharathi^b

^aAdvanced Green Chemistry Lab, Department of Industrial Chemistry, School of Chemical Sciences, Alagappa University, Karaikudi -3, Tamil Nadu, India. Tel: +91 94444 96151

E-mail address: drmsgreenchemistrylab@gmail.com and kbama85@gmail.com

^bDepartment of Chemistry, Poompuhar College (Autonomous), Melaiyur - 609 101, Tamil Nadu, India.

Introduction:

Bentonite clay (BC) is a natural rock material that combines one or more minerals with metal oxides and organic matter. The 2:1 layer of BC consists of an octahedral sheet sandwiched between two tetrahedral sheets. BC materials possess many unique properties and applications such as an ability to swell, cation exchange capacity, large surface area, which leads them exceptional antibacterial for extensive applications [1]. Zinc oxide (ZnO) is an II-VI group semiconductor material and wide-bandgap (3.3 eV) energy. ZnO has

aroused concern due to its better antibacterial activities on a broad spectrum of bacteria. BC has been reported to be effective and deactivating and inhibiting growth of some bacteria. Therefore, combining BC with ZnO nanoparticles (NPs) would enhance the antibacterial activity [2-3]. We describe the synthesis of zinc oxide/bentonite clay nanocomposite (ZnO/BC NC) is very common due to their stable and robust and wide range of applications particularly enhanced biological properties.

Experiment:

In this study, composite of ZnO NPs supported on BC were synthesized by thermal decomposition method up to 600 °C (200, 400 and 600 °C) for use as an antibacterial material.

Results and discussion:

The schematic illustration of synthesized ZnO/BC nanocomposite as shown in Figure 1. The structure and phase composition of ZnO/BC nanocomposite was characterized by X-ray diffraction (XRD), Scanning electron microscope (SEM) with Energy dispersive X-ray spectroscopy (EDX), UV-Visible diffuse reflectance spectroscopy (UV-Vis DRS) and Fourier transform infra-red spectroscopy (FT-IR) techniques, and the results showed that the products exhibited high crystal, large porous surface area and lower band gap energy. The UV-DRS shows the band gap energy of ZnO/BC nanocomposite (2.5 eV) is less than ZnO NPs (3.2 eV) at 600 °C, might be due to the increase temperature with increase the crystal size of nanocomposite [2-3].

Conclusion:

The newly synthesized ZnO/BC nanocomposite has been tested against both gram-negative *Escherichia coli* and gram-positive *Staphylococcus aureus* by well diffusion method. The results show that, compare to pure ZnO nanoparticles, clay and ZnO/BC NC exhibit higher antibacterial behaviour. In overall, many advantages in this synthesis, it is easy to preparation, environmental friendly, cost efficiency, simple facile process and room temperature, ZnO/BC nanocomposite enlarged in this work may find probable applications as a useful inorganic antibacterial agent in the areas of healthcare.

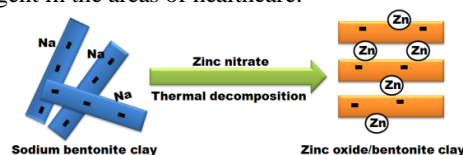


Figure 1: Schematic illustration of synthesized zinc oxide/bentonite nanocomposite

References

- [1] Chengli Huo, Huaming Yang, *Appl. Clay Sci.* 50 (2010) 362-366.
- [2] Sh. Sohrabnezhad, M. J. Mehdipour Moghaddam, T. Salavatiyan, *Spectrochim. Acta Mol. Biomol. Spectrosc.* 125 (2014) 73-78.
- [3] Is Fatimah, *Int. J. Chem. Sci.* 10 (2012)1341-1349.

2.31 CuO nanostructure: Optical and antibacterial activity against pathogenic bacteria

S. Ambika^a, M. Sundrarajan^{a*} and V. Magesh Kumar^b

^aAdvanced Green Chemistry Lab, Department of Industrial Chemistry,
School of Chemical Sciences, Alagappa University, Karaikudi-630003, Tamil Nadu, India.

E-mail: drmsgreenchemistrylab@gmail.com and ambi5373@gmail.com

^bDepartment of Chemistry, Raja Duraisingam Govt. Arts College, Sivaganga-630561, Tamil Nadu, India.

Introduction

Metal oxide nanoparticles have been of great interest due to their unexpected catalytic, optical, magnetic and electrical properties. Among the various metal oxides, copper oxide nanoparticles (CuO NPs) have gained significant interest and attention due to their physical and chemical properties and it is very important in various biomedical fields [1]. Ionic liquids are non-conventional molten salt typically consisting of an organic cation and inorganic anion. Recently ionic liquids are used in the template for nanomaterials synthesis with improved properties like good morphology and less size [2]. *Pongamia pinnata* belongs to the *Fabaceae* family and is also called Pungai in Tamil. All parts of *Pongamia pinnata* are used in the indigenous system of medicine. *Pongamia pinnata* active compounds are phenolic compounds, flavonoids, saponins, terpenoids, tannins and alkaloids [3].

Method:

CuO NPs were prepared by biosynthesis method at room temperature. Copper sulphate was mixed with 25 ml of leaves extract and 1 ml of ionic liquid (1-ethyl-3-methylimidazolium tetrafluoroborate- [EMIM]⁺ BF₄⁻) using a magnetic stirrer for 3 hours at room temperature. The prepared CuO NPs were calcinated at 400 °C and characterized by XRD, SEM with EDX, UV- DRS and FT-IR techniques.

Results:

The schematic representation of the synthesis of CuO NPs with ionic liquid as shown in Figure 1. The

crystalline nature of the CuO NPs with the average size of 27.52 nm was confirmed by XRD analysis. The band gap energy of CuO NPs was found to be 1.77 eV [4]. SEM micrographs of the synthesized CuO NPs showed the aggregated and spherical shape. The maximum zone of inhibition was observed in the synthesized CuO NPs (25 µg/mL) against *Staphylococcus aureus* (17 mm) and *Escherichia coli* (16 mm).

Conclusion:

Green synthesized CuO NPs provides a promising approach can satisfy the requirement of large scale industrial production bearing the advantage of low cost and eco-friendly.

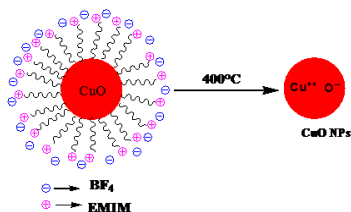


Figure 1: Schematic representation of the ionic liquid assisted synthesis of CuO NPs

References

- [1] Vasudevavendan Chakrapani, Khan Behlol Ayaz Ahmed, V. Vinod Kumar, Veerappan Ganapathy, Savarimuthu Philip Anthony and Veerappan Anbazhagan *RSC Adv* 4 (2014) 33215.
 [2] Małgorzata Swadźba-Kwasny, Chancelier, Shieling Ng, Hareesh G. Manyar, Christopher Hardacre and Peter Nockemann, *Dalton Transactions* 49 (2012) 2019.
 [3] D. Prabhu, C. Arulvasu, G. Babu, R. Manikandan and P. Srinivasan, *Process Biochemistry* 48 (2013) 317-324.
 [4] S. Harish, M. Navaneethan, J. Archana, S. Ponnusamy, C. Muthamizhchelvan and Y. Hayakawa, *Materials Letters* 139 (2015) 59–62.

2.32 Synthesis of Pd doped magnetic Fe₃O₄ nanoparticles

A. Sangili^a, M. Sundrarajan^{a*} and M. Abdul kathir^b

^aAdvanced Green Chemistry Lab, Department of Industrial Chemistry, School of Chemical Sciences, Alagappa University, Karaikudi -3, Tamil Nadu, India.

^bDepartment of Chemistry M.S.S. Wakf Board College, K.K.Nagar, Madurai-20, Tamil Nadu, India. Tel: +91 94444 96151
 E-mail address: drmsgreenchemistrylab@gmail.com and sangili10492@gmail.com

Introduction

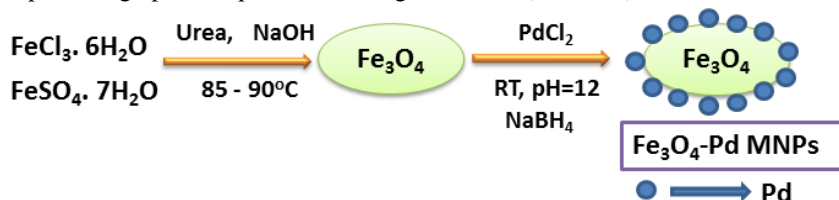
Magnetic iron oxide nanoparticles have attracted much more attention because of their wide applications to supports of catalysts, drug delivery and biosensors. Especially, the magnetic nanoparticles make possible the complete recovery of the catalyst using external magnetic field, which is an important advantage of the use of a magnetically separable catalyst. In this present investigation, palladium (Pd) doped iron oxide (Fe₃O₄) magnetic nanoparticles (MNPs) exhibit many interesting properties that can be used as a catalyst in carbon - carbon reactions, hydrogenation, oxidation and coupling reaction [1].

Experiment

Fe₃O₄ MNPs were prepared from iron chloride and iron sulphate by using sodium hydroxide and urea at 85 to 90 °C. Pd - Fe₃O₄ MNPs were prepared by using Fe₃O₄ and palladium chloride (PdCl₂) in the presence of sodium borohydride by co-precipitation method, and this method is an environmental friendly. Then the palladium was reduced from Pd²⁺ to Pd⁰ in ice bath at -5 °C. The Phase composition and microstructure analysis indicate that the urea have been successfully grafted onto the surface of Fe₃O₄ MNPs [2].

Results and discussion

The synthesized Fe₃O₄ MNPs were characterized and confirmed by X-ray diffraction (XRD), Scanning electron microscope (SEM) with Energy dispersive X-ray spectroscopy (EDX), and Fourier transform infra-red spectroscopy (FT-IR). FT-IR spectrum of Fe₃O₄ MNPs samples absorption bands, shows at 3397 and 1621 cm⁻¹ corresponding to O-H stretching and bending bands respectively. The corresponding adsorption frequencies at low wavenumber 562 cm⁻¹ come from the vibration of Fe-O bond of Fe₃O₄ [3]. Pd doped Fe₃O₄ MNPs were characterized using FT-IR spectroscopy and X-ray photoelectron spectroscopy(XPS). Synthesis of Pd doped magnetic Fe₃O₄ nanoparticles graphical representation as given below (scheme 1).



Scheme 1: Synthesis of Pd doped magnetic Fe₃O₄ nanoparticles

Conclusion:

In summary, we have presented a simple and effective technique to prepared Pd-Fe₃O₄ MNPs, which make Pd-Fe₃O₄ MNPs as a good catalyst for organic reactions. The catalyst could be reused by recycling, which avoids the necessity for a traditional filtration process.

Reference :

- [1]. M. B. Gawande, P. S. Branco and R. S. Varma . *Chem. Soc. Rev.* **2013**.
- [2]. K. V. S. Ranganath, J. Kloesges, A. H. Schfer, and F. Glorius. *Angew. Chem. Int. Ed.* **2010**, *49*, 7786–7789.
- [3]. K. Kumar, B. Smita, K. Cumbal, L. Debut and A. Debut. *J. Saudi. Chem. Soc.* **2014**, *18*, 364-369.

2.33 Catalytic Oxygen Reduction on Silver Nanoparticle Modified Glassy Carbon Electrode with 2-Hydroxy-1,4-Naphthoquinone

J. Antony Rajam¹ A. Gomathi*² and C. Vedhi³

²Department of Chemistry, Sri K.G.S Arts College, Srivaikuntam.

^{1,3}Department of Chemistry, V.O.Chidambaram College, Thoothukudi.

Abstract

The electrochemical reduction of oxygen was studied on silver nanoparticle modified glassy carbon electrode (AgNPs/GCE) with 2-Hydroxy-1,4-naphthoquinone (2-HNQ) in the pH range 1.0 – 13.0. The electrocatalytic ability of the modified electrode for the reduction of oxygen was examined by cyclic voltammetric and chronocoulometric techniques. Cyclic voltammograms recorded for 2-HNQ exhibited a single redox couple in the deaerated condition. On increasing the scan rate, the peak separation also increases which shows the quasi-reversibility of the electron transfer process at AgNPs/GCE. The cathodic peak current (I_{pc}) increased linearly with square root of scan rate ($v^{1/2}$), indicating diffusion controlled mass transfer for 2-HNQ at AgNPs/GCE. The half peak potential $E_{p/2}$ vs pH shows three distinct linear portions with different slopes of 89mV up to pH 4 (two electron three proton), 60mV at intermediate pH (two electron two proton) and 31mV for pH above 10 (two electron one proton) for 2-HNQ.

Under aerated conditions, there is a large enhancement in the cathodic peak current with the disappearance of anodic peak (Figure 1A) which clearly indicates the irreversible electrocatalytic oxygen reduction. As the pH increases, the cathodic peak current for AgNPs/GCE with 2-HNQ increases upto pH 7. The cathodic peak current I_{pc} is linearly proportional to square root of scan rate $v^{1/2}$ which clearly confirms the diffusion controlled process for oxygen reduction. The 1,4-naphthoquinone-adsorbed silver nanoparticle modified glassy carbon electrode possesses excellent electrocatalytic abilities for oxygen reduction with overpotential 402.5 mV greater than that at a bare glassy carbon electrode.

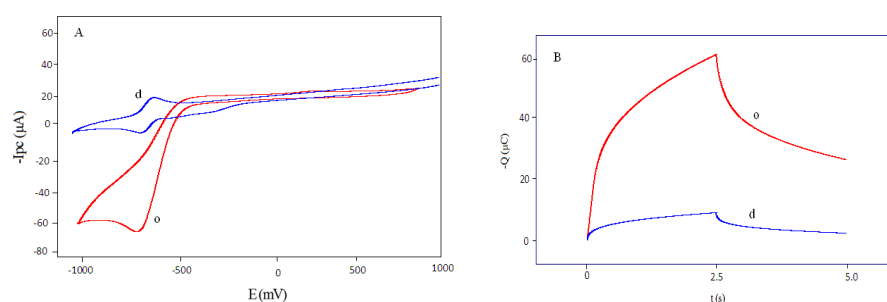


Figure 1: A. Cyclic voltammogram and B. chronocoulomogram of 2-HNQ at AgNPs/GCE in the presence (o) and absence (d) of oxygen at pH 7.

The chronocoulometric behaviour of AgNPs/GCE with 2-HNQ was studied in the absence and presence of O₂ by applying the double potential step technique at an initial and final potential of -100 and -800 mV versus silver electrode in pH 7. Under aeration, a large enhancement in the charge and nearly flat line when the potential was reversed (Figure 1B), prove the irreversible electrocatalytic reduction of oxygen. The number of electrons (n_{NQ}) involved in the reduction of 2-HNQ was calculated from the slope of Q versus $t^{1/2}$ under deaerated condition, which is closer to 2.0. Under aeration, the number of electrons involved in the reduction of oxygen was found to be 2.0.

Keywords: Catalytic reduction, Voltammograms, Silver nanoparticle modified glassy carbon electrode, 1,4-Naphthoquinone, Oxygen reduction.

2.34 Preparation and EMI shielding studies on Au-CNT dispersed Polyvinylene difluoride nanocomposites

R. Kumaran,¹ M. Kesava,² and K. Dinakaran^{2*}

¹Department of Chemical Engineering, Anna University, Chennai-600 025, India.

²Department of Chemistry, Thiruvalluvar University, Serkkadu, Vellore 632115, India

*corresponding E-mail : kdinakaran.tvu@gmail.com

Military, civil and commercial electronic devices have encountered a serious interference from electromagnetic radiation emitted from cell phone towers which affects their efficiency, life time and functionalities. To address this problem, flexible, cost-efficient and lightweight shielding materials have been employed in fabricating the electronic devices which attenuates the undesirable electromagnetic radiation interference.¹ The loading of low amount (3wt%) of Au-MWCNT in PVDF leads to tremendous enhancement of electrical conductivities of MWCNT/PVDF composites resulting from the formation of strong conductive networks. The scanning electron microscopic analysis showed that the Au loaded MWCNT uniformly dispersed in PVDF. The EMI shielding effectiveness of Au NPs/MWCNT/PVDF composites is depicted in Fig.1. The Effective EMI Shielding Effectiveness of pristine PVDF is 1.5 dB at 12 GHz. On incorporation of COOH-MWCNT to PVDF, the EMI shielding value is increased to 16.4 dB at 12 GHz. The addition (3wt %) of MWCNT in PVDF will leads to tremendous enhancement of electrical conductivities of MWCNT/PVDF composites which is credibly attributed to strong conductive networks formed in composites. This conductive network path crosses the percolation threshold,² which is reliable for enhancing shielding value of 21.6 dB. The conductive networks formed in the polymer composites is mainly accounts for interacting EM waves which in turn responsible for ionic conduction and dipolar polarization relaxation. On incorporation of Au nanoparticles on MWCNT in PVDF matrix, there found an enhancement of shielding values. The Au NPs integrated with MWCNT in PVDF matrix is mainly reliable for the free charge carriers in the composites which in turn the credit worth cause for enhancing the shielding values. Another credit worth cause for enhancing EMI shielding value is the impedance match between the materials and air, which in turn reflects the EM radiations from the surface.³ Return loss is the transmission of electromagnetic radiation through the materials. This accounts the satisfactory enhancement of effective EMI shielding values in the composites. Our composites reach EMI shielding value of 26.71 dB at 12 GHz which meets the commercial value of 20 dB evidently propose that it is feasible for protecting electronic devices from harmful electromagnetic radiations.

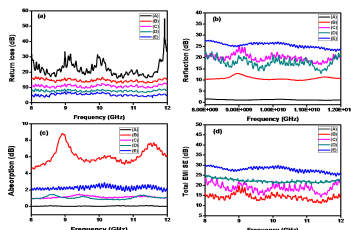


Figure 1a-e shows the Return loss, Reflection, Absorption and Total EMI SE at 12 GHz respectively for (A) Pristine PVDF, (B) 1wt% MWCNT-PVDF, (C) 3wt% MWCNT-PVDF, (D) 1wt% Au Np-MWCNT-PVDF, (E) 3wt% Au Np-MWCNT-PVDF.

References

- (1) Li, X.; Zhang, B.; Ju, C.; Han, X.; Du, Y.; Xu, P. *J. Phys. Chem. C* **2011**, *115*, 12350–12357.
- (2) Luna, A.; Yuan, J.; Neri, W.; Zakri, C.; Poulin, P.; Colin, A. *Langmuir* **2015**, *31* (44), 12231–12239.
- (3) Liu, C.; Xu, Y.; Wu, L.; Jiang, Z.; Shen, B.; Wang, Z. *J. Mater. Chem. A* **2015**, *3*, 10566–10572.

2.35 Hydrothermal synthesis and characterization of cobalt oxide nanoparticles; an evaluation of biological activities

V. Meenakshi^a and A. Arumugam^{b*}

^aDepartment of Nanoscience and Technology, Alagappa University, Karaikudi – 630 003. Tamil Nadu, India.

E-mail: raji.chess@gmail.com

^{b*}Department of Botany, Alagappa University, Karaikudi – 630 003. Tamil Nadu, India.

E-mail: sixmuga@yahoo.com

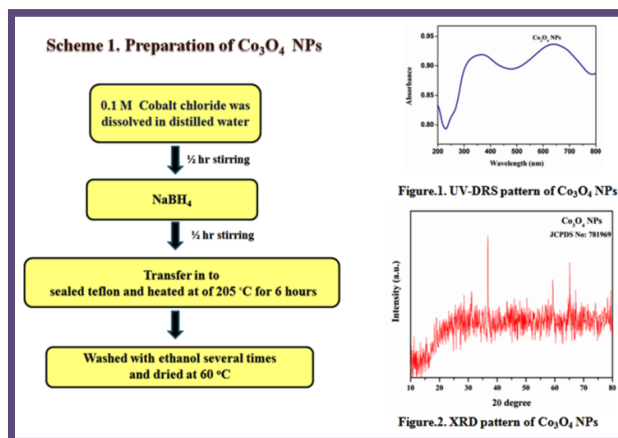
Abstract:

Synthesis of cobalt oxide nanoparticles (Co₃O₄ NPs) using hydrothermal route and were characterized by UV-VIS-DRS, FT-IR, XRD and SEM with EDX analysis. The prominent peaks in XRD result indicate that the average crystalline size of the Co₃O₄ NPs is about 25 nm (JCPDS card no:781970). UV-Vis-DRS peaks showed at 364 and 641 nm. The average size of Co₃O₄ NPs was determined by SEM analysis and it was found to be around 20 nm. Further, we have investigated the antimicrobial activity. Antibacterial activity against two

Gram positive (*Staphylococcus aureus* and *Bacillus subtilis*) and two Gram negative (*Pseudomonas aeruginosa* and *Escherichia coli*) bacterial strains. Antifungal activity against *Candida albicans*, *Aspergillus niger* and *Trichoderma viride* were evaluated. It had been analyzed that the antimicrobial activity showed higher zone of inhibition at low concentration of Co_3O_4 NPs. The *in vitro* cytotoxicity studies of nanoparticles were tested in human breast cancer cell line (MCF-7).

Key Words:

Cobalt oxide nanoparticle, Biomedical applications, Antimicrobial activity, Cytotoxicity activity, Cancer cell line.



References

- [1] M.D. SubrataKundu, b. Mukadam, S.M. Yusufb, M. Jayachandran, *J. CrystEngComm*, 15 (2013) 482.
- [2] E. Lester, G. Aksomaityte, J. Li, S. Gomez, J. Gonzalez-Gonzalez, M. Poliakoff, *Progcryst growth ch.58* (2012) 3.
- [3] Q. Yuanchun, Z. Yanbao, W. Zhishen, *Mater Chem Phys*. 110 (2008) 457.
- [4].R.A. Bohara, N.D. Thorat, H.M. Yadav, S.H. Pawar, *New J.Chem*. 38 (2014) 2979.

2.36 Facile hydrothermal synthesis of iron oxide nanoparticles and their biomedical applications

D. Ellakkiya^a and A. Arumugam^{b*}

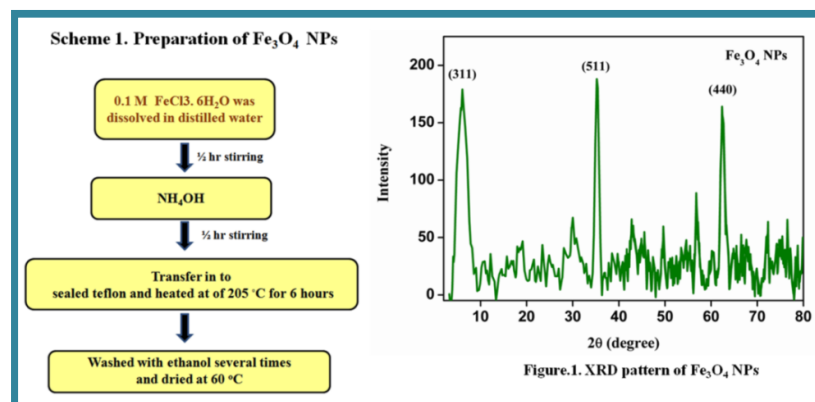
^aDepartment of Nanoscience and Technology, Alagappa University, Karaikudi – 630 003. Tamil Nadu, India.

^{b*}Department of Botany, Alagappa University, Karaikudi – 630 003. Tamil Nadu, India.

E-Mail:elakkiyadurai15@gmail.com/ sixmuga@yahoo.com

Abstract:

Iron oxide nanoparticles with appropriate surface chemistry can be used for numerous *in vivo* applications, such as MRI contrast enhancement, tissue repair, immuneassay, detoxification of biological fluids, hyperthermia, drug delivery, and cell separation. All of these biomedical applications require nanoparticles because of high magnetization values, a size smaller than 100 nm, and a narrow particle size distribution. In this attempt, Iron oxide nanoparticles (Fe_3O_4 NPs) were synthesized by hydrothermal method, confirmed by UV-



Visible spectroscopy and the average crystalline size was determined by X-ray diffraction (XRD). Morphology of the synthesized Fe_3O_4 NPs was identified using Scanning Electron Microscopy (SEM). Further Fe_3O_4 NPs was characterized by FTIR and TGA. Biological activity of Fe_3O_4 NPs was examined through antimicrobial studies against Gram positive *Staphylococcus aureus*,

Bacillus subtilis and Gram negative *Pseudomonas aeruginosa* and *Escherichia coli*. In addition, the antifungal activity of synthesized Fe_3O_4 NPs was assessed against fungi strains namely: *Candida albicans*, *Aspergillus niger* and *Trichoderma viride*. Further, cytotoxicity was tested against human breast cancer cell lines using MTT assay.

Key Words: Hydrothermal method, Fe_3O_4 nanoparticles, antimicrobial activity, anticancer activity.

References

- [1]. R. Qiao, C. Yang and M. Gao, *J. Mater. Chem*, 19 (2009) 6274.
- [2]. H. Li, Z. Lu, G. Cheng, K. Rong, F. Chen, *R. Chen, RSC Ad. 5* (2015) 5059.
- [3]. L. Ren, S. Huang, W. Fan, T. Liu, *Appl Surf Sci.* 258 (2011) 1132.
- [4]. G. Wang, X. Zhang, A. Skallberg, Y. Liu, Z. Hu, X. Mei, K. Uvdal, *Nanoscale*, 6 (2014)
- [5]. C. Yang, J. Wu, Y. Hou, *Chem Commun*, 47 (2011) 5130.

2.37 Application of Magnesium Oxide Nanoparticles in Cotton Fabric as an Antibacterial Textile Finish

R. Kiruba^a and A. Arumugam^{b*}

^aDepartment of Nanoscience and Technology, Alagappa University, Karaikudi – 630 003. Tamil Nadu, India.

E-mail: kirubanano19@gmail.com

^bDepartment of Botany, Alagappa University, Karaikudi – 630 003. Tamil Nadu, India. E-mail: sixmuga@yahoo.com

Abstract

The impact of nanotechnology in the area of textile cotton fabric finishing has brought up innovative finishes along with new application techniques. Coating the surface of textiles and clothing with nanoparticles (NPs) is an approach to the production of highly active surfaces to have UV-blocking, antimicrobial, flame retardant, water repellent and self-cleaning properties. When nano metal oxides coatings are applied to fabrics, the nanoparticles readily form bonds with the fibers of the materials. In this work we mainly concentrated on the synthesis of Magnesium Oxide nanoparticles (MgO NPs) exhibiting antibacterial activity on textile fabrics. MgO plays a very prominent role based on surface properties. An interesting property of MgO nanoparticles is their ability to adsorb and retain for a long time. Simple and cost effective synthesis of magnesium oxide nanoparticles were prepared by co-precipitation method. The Magnesium hydroxide precipitates at room temperature followed by calcinations at 450°C. The synthesized metal oxide nanoparticles have been characterized by UV-Visible, FT-IR spectroscopy, XRD analysis. MgO NPs were impregnated into cotton fabric to impart antibacterial properties was confirmed by scanning electron microscope coupled with high energy dispersive X-Ray spectroscopy analysis (SEM-EDX). The MgO NPs loaded with cotton fabrics showed excellent antibacterial activity against one gram positive (*Bacillus megaterium*) and five Gram-negative bacteria (*Aeromonashydrophila*, *Escherichia coli*, *Enterobacter cloacae*, *Moraxella spand Pseudomonas aeruginosa*).

Keywords

MgO NPs, Antibacterial, Cotton fabrics, Textile finishing.

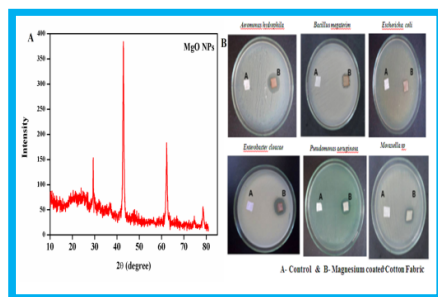


Figure.1 Synthesis of MgO NPs (A) - XRD analysis (B) - Antibacterial activity for MgONPs coated fabric

References

- [1] Y. Gao, *Textile Research Journal*, 78, (2008). 160–72.
- [2] V. Isaeva, M. Aizenshtein, A review, *Fibre Chemistry*, 29 (5), (2007). 269-281.
- [3] M. Tel, D. Shrish Kumar, *Journal of the Textile Association*, (2007). 21-30.
- [4] Y. Lai, *Journal of Polymer Science Part A*, 6, (1997). 1039–1046.
- [5] D. Radic, L. Gargallo, *Copolymers. Macromolecules*, 30, (1997). 817-825

2.38 Synthesis of and Characterization of Nano Metal Oxides (NMO) on Removal of Heavy Metals in Textile Waste Water

M.Kavitha^a and A. Arumugam^{b*}

^aDepartment of Nanoscience and Technology, Alagappa University, Karaikudi – 630 003. Tamil Nadu, India.

E-mail: kavithanano24@gmail.com

^bDepartment of Botany, Alagappa University, Karaikudi – 630 003. Tamil Nadu, India.

E-mail: sixmuga@yahoo.com

Abstract

Different contaminants are released to environment including heavy metal ions, organics, bacteria, viruses and so on that are serious harmful to environment and human health. Among all water contaminations, heavy metal ions, such as Pb²⁺, Cd²⁺, Zn²⁺, As, Ni²⁺, Cr and Hg²⁺, have high toxic and non-biodegradable properties. Aluminium oxide (Al₂O₃) have been studied in the removal of heavy metal ions from aqueous solutions and the results indicates that it show high adsorption capacity. They are present in different forms, such as particles, tubes and others. The size and shape of NMOs are both important factors to affect their adsorption performance. Efficient synthetic methods to obtain shape-controlled, highly stable, and monodisperse metal oxide nanomaterials have been widely studied during the last decade. Here the metal oxides used as nanosorbents themselves should be nontoxic. For ensuring the nontoxic nature, the metal oxide NPs have tested for antibacterial assay. Al₂O₃ NPs provide high surface area and specific affinity and are characterized by UV, FT-IR, XRD and SEM analysis. The present work mainly focuses on NMOs preparation, their physicochemical properties, adsorption characteristics and mechanism as well as their application in heavy metal removal.

Keywords: Al₂O₃, Antimicrobial, Nanosorbents, Waste water, Heavy metal removal.

XRD Analysis for Al₂O₃

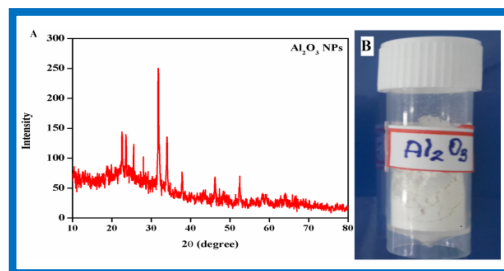


Figure 1. (A) – XRD - analysis of Al₂O₃ NPs, (B) – Synthesized Al₂O₃ Nanopowder.

References:

- [1] G. Oberdörster, *Environmental health perspectives* 113, (2005), 823-839.
- [2] V. Colvin, *Nature Biotechnology*, 21(2003), 1166–1170.
- [3] J. Carmichael, V. DeGra, *Cancer Research*, 47, (1987), 936–942.
- [4] W. J. Lukiw, M. Percy, T. Kruck, *InorgBiochem*, 99, (2005), 1895–1898
- [5] S. Hussain, J. Frazier, *Toxicological Sciences*, 69, (2002) 424–432.

2.39 Mycosynthesized Pd nanoparticles using *Nigrospora* sp., for Biomedical Applications

P. Menaka^a and A. Arumugam^b

^a. Department of Nanoscience and Technology, Alagappa University, Karaikudi-630 003, Tamil Nadu, India.

E-mail: menaka1993nano@gmail.com

^bDepartment of Botany, Alagappa University, Karaikudi – 630 003, Tamil Nadu, India. E-mail: sixmuga@yahoo.com

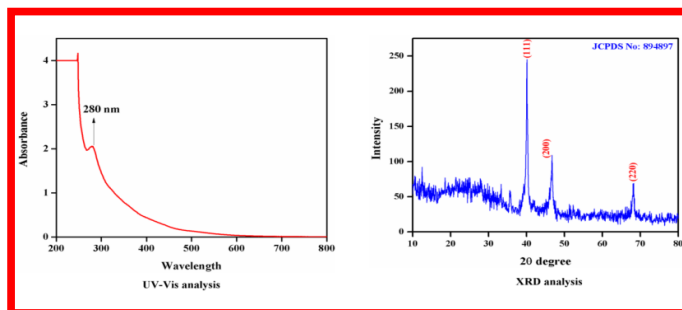
Abstract

The present studies demonstrates an Eco- friendly for synthesis of palladium nanoparticles (Pd) were synthesized by using *Nigrospora* sp., culture. Synthesized Pd NPs were characterized by UV- visible, Fourier transform spectroscopy, X- ray diffraction Transmission Electron Microscopy. Furthermore the Pd NPs was also tested for its antimicrobial activity. The UV- visible spectrum of the fungal culture filtrate containing Pd

nanoparticles showed peak at 279 nm and the functional groups present in the fungal filtrate responsible for the synthesis of NPs analysed by FT-IR. The X- ray analysis showed the confirmation of crystalline nature of the Pd nanoparticles. TEM analysis showed the nanoparticles were spherical in shape with the size of 5-20 nm. The antimicrobial activity of Pd nanoparticles examined two Gram positive and two Gram negative bacteria and one fungus by disk diffusion method. The results showed better results in Gram positive bacteria compared to Gram negative bacteria.

Key words: *Nigrospora* sp., Palladium Nanoparticles, Fungal filtrate, TEM, Antimicrobial activity,

Figure 1. UV –Vis spectroscopy and XRD analysis of Pd NPs.



References

- [1] P. Dauthal and M. Mukhopadhyay, *Acs publications*52 (2013) 18131.
- [2] V.Mazumder and S.Sun, *Acs publications*131 (2009) 4588.
- [3] A. Balanta, C. Godard and C.Claver, *Chem..Soc.Reviews* 40 (2010) 4973.
- [4] X. Chen, J.Wang, X. Jing and Y. Zheng, *Materials letter* 165 (2016) 29.

2.40 Biosynthesis and Characterization of Cerium Oxide Nanoparticles using *Nigrospora* sp.,

S. Gowri^a and A. Arumugam^b

^aDepartment of Nanoscience and Technology, Alagappa University, Karaikudi-630 003, Tamil Nadu, India.

E-mail: sgowri.shs@gmail.com

^bDepartment of Botany, Alagappa University, Karaikudi – 630 003, Tamil Nadu, India. *E-mail: sixmuga@yahoo.com

Abstract

The present study, biosynthesis of cerium oxide nanoparticles (CeO₂) was achieved by a novel, biodegradable and convenient procedure using *Nigrospora* sp. as reducing and capping agent. CeO₂ nanoparticles were synthesized by using *Nigrospora* sp., fungal culture filtrate. Bio-Synthesized CeO₂ NPs were characterized by UV- visible, X- ray diffraction, Raman spectroscopy, Transmission Electron microscopy and Scanning Electron Microscopy with Energy Dispersive X- ray Spectroscopy. Furthermore the CeO₂ were apply for antimicrobial and bioimaging applications. The UV- vis absorbance peak was showed at 295 nm. XRD revealed the crystalline structure of the synthesized CeO₂ with face centered cubic. Further, the Raman spectroscopy was exhibited a strong intense band at 450 cm⁻¹. TEM studies of CeO₂ NPs were found to be spherical in shape with the average size of 10 – 20 nm. SEM results exhibited the homogenous distribution of CeO₂ NPs. Then the applications of the synthesized CeO₂ NPs were investigated such as Antibacterial activity which shows a significant inhibition towards both gram positive and gram negative bacterial strains. The pollen germination activity was performed different concentration in *G.superba* pollen grains with the help of Confocal microscopy.

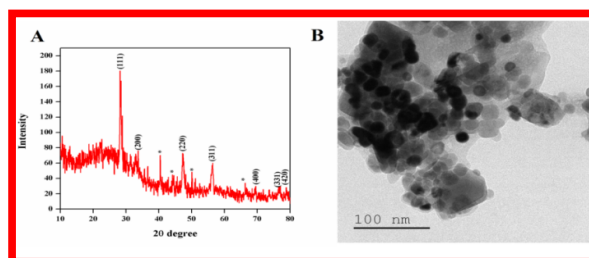


Figure 1: (A) UV- Vis analysis of CeO₂ NPs, (B) : XRD analysis of CeO₂ NPs

References

- [1] J.J. Miao, H. li, R. Zhu and J.M. Zhu, *J. Cryst.Growth* 281(2005) 525.
- [2] S. Maensiri, S. Labuayai, P. Laokul and J. Klinkeawnarong, *J. Appl. Phys* 53(2014) 6.
- [3] C. Sundaravadivelan, M. NaliniPadmanabhan, P. Sivaprasath and L. Kishmu, *Parasitol. Res* 112(2013) 303.
- [4] K.Kashar, P. Fornesiero and M. Grazini, *Catal. Today* 50 (1999) 285.

2.41 One-pot hydrothermal synthesis of Fe₃O₄/RGO nanocomposites as coupling agents for biomedical applications

V. Karthika^a and A. Arumugam^{b*}

^aDepartment of Nanoscience and Technology, Alagappa University, Karaikudi-630 003, Tamil Nadu, India.

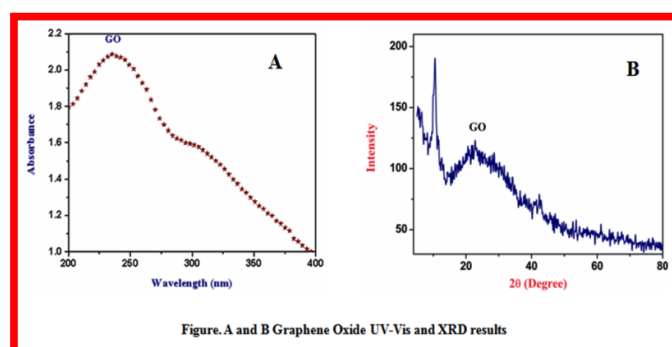
E-Mail: vkarthikanano@gmail.com

^bDepartment of Botany, Alagappa University, Karaikudi – 630 003, Tamil Nadu, India. *E-mail: sixmuga@yahoo.com

Abstract

Graphene based nanocomposites have been extensively explored in worldwide range of medicinal and industrial fields in recent years. Fe₃O₄/RGO nanocomposites used environmental application such as capacitors, solar cells, sensor and biological application for antimicrobial activity, cytotoxic activities and hyperthermia. In our work, the synthesized a multifunctional super paramagnetic iron oxide/reduced graphene oxide hybrid nanocomposite via one pot hydrothermal approach. The synthesized nanocomposite characterized by X-ray diffraction (XRD), UV-Visible spectroscopy (UV-Vis), Fourier transform infrared spectroscopy (FT-IR), Vibrating sample magnetometer (VSM), Field emission scanning electron microscopy (FE-SEM), High resolution transmission electron microscopy (HR-TEM). The biological activities were systematically evaluated. Binding of these composites with calf thymus DNA was investigated by UV-Vis, fluorescence spectroscopy and viscosity measurements. Composites also exhibit a good binding propensity to bovine serum albumin (BSA). The cytotoxicity studies of composites were tested *in vitro* on human cervical cancer cell line (HeLa) and they found to be active and antimicrobial activities were also carried out. Hence, from these findings, compositewas suggested to demonstrate better activity and further evaluation of *in vivo* anticancer activities and biosensor application of compositesis in progress.

Key Words: Fe₃O₄/RGO nanocomposites, Antimicrobial activity, Cytotoxicity study, Cervical cancer, DNA binding study.



References

- [1]. S. Goenka , V. Sant , S. Sant, *J Control Release.* 173 (2014) 75.
- [2]. K. Yang, S. Zhang, G Zhang, X. Sun, S.T. Lee, Z. Liu, *Nano Lett.* 10 (2010) 3318.
- [3]. Q.L. Jiang , S.W. Zheng , R.Y. Hong , S.M. Deng , L. Guo , R.L. Hu , B. Gao ,M. Huang , L.F. Cheng, G.H. Liu , Y.Q. Wang, *Appl Surf Sci.* 307 (2014) 224.
- [4]. Y. Zhang, B. Chen, L. Zhang, J. Huang, F. Chen, Z. Yang, J. Yaoc, Z. Zhang, *Nanoscale.* 3(2011)14.
- [5]. L. Ren, S. Huang, W. Fan, T. Liu, *Appl Surf Sci.* 258 (2011) 1132.

2.42 Eco friendly synthesis of Dysprosium oxide nanoparticles and its evaluation of toxicity

T. Baranisri^a, K. Gopinath^a and A. Arumugam^{b*}

^aDepartment of Nanoscience and Technology, Alagappa University, Karaikudi - 630 003. Tamil Nadu, India.
E-mail: baranianu93@gmail.com

^bDepartment of Botany, Alagappa University, Karaikudi - 630 003. Tamil Nadu, India.
*E-mail: sixmuga@yahoo.com

Abstract

We describe a simple approach for the synthesis of Dysprosium oxide nanoparticles (Dy₂O₃ NPs) using *Terminalia arjunabark* extract. The formation of Dy₂O₃ NPs was confirmed by UV-VIS-DRS, ATR-FT-IR, PL, Raman, XRD and TEM analysis. UV-Vis-Diffused Reflectance Spectrum clearly showed the absorption peak at 355 nm and band gap value of 4.8 eV. ATR-FT-IR analysis was performed to analyze the biomolecules responsible for formation of Dy₂O₃ NPs. Photoluminescence measurements obtained at the broad green emission bands at 417, 486 and 510 nm. Micro Raman spectrum analysis clear showed the peak at 373 cm⁻¹. XRD result confirmed the presence of Dy₂O₃ NPs with body centered structure. Transmission electron microscopy images clearly showed that average particles size in the range of 20 to 50 nm. Synthesized NPs was evaluated for anti cancer activity in HeLa cell line.

Key words

Terminalia arjuna, Bark extract, Dysprosium oxide Nanoparticle, HeLa cell line, Anti-cancer.

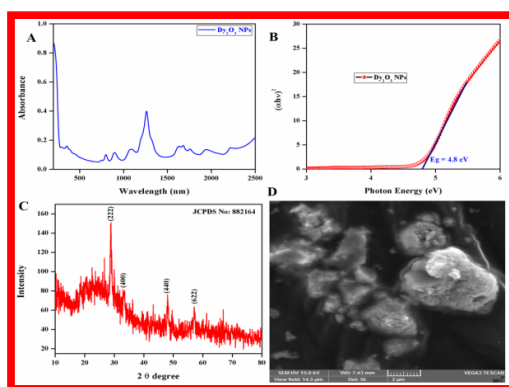


Figure 1. Dy₂O₃ NPs (A) - UV-VIS-DRS analysis, (B) - Band gap value of Dy₂O₃ NPs, (C) - XRD analysis, (D) - SEM analysis

References

- [1] A. Zelati, A. Amirabadizadeh, A. Hosseini, *Int J Ind Chem.* 5 (2014) 69.
- [2] H.A.I.Y. Tok, F.Y.C. Boey, R. Huebner, S.H. Ng, *J Electroceram* 17 (2006) 75.
- [3] K. Kattela, J.Y. Parka, W. Xua, H. G. Kima, E. J. Leea, B. A. Bonya, W. C. Heoa, S. Jinb, J.S. Baeckb, Y. Changb, T. J. Kimc, J. E. Baed, K. S. Chaed, G. H. Leea, *Biomaterials.* 33 (2012) 3254.

2.43 Facile synthesis of Multiwall carbon nanotube supported Palladiumdoped polypyrrole catalyst

M. Balaji^a, M. Sundrarajan^{a*}, S. Selvam^b and G. Selvanathan^c

^aAdvanced Green Chemistry Lab, Department of Industrial Chemistry, School of Chemical Sciences, Alagappa University, Karaikudi-600 003, Tamil Nadu, India.

^bLaser and sensor Application Laboratory, Pusan National University, Busan 609735, South Korea.

^cDepartment of Chemistry, AVC College, Mayiladuthurai- 609 305, Tamil Nadu, India.
drmsgreenchemistrylab@gmail.com and mbalaji.chem@yahoo.com

Introduction

Carbon nanotubes (CNTs) have a chemical stability, electronic conductivity, thermal stability, capability to functionalize with chemically or electrochemically active species for that reason it is promising material for catalysis [1]. Catalytically active palladium (Pd) nanoparticles (NPs) on a multiwall carbon nanotube (MWCNT) with enhanced nucleation and stability have been demonstrated through introduction of electron-conducting polypyrrole (PPy) via non-covalent functionalization to bridge the Pd nanoparticles and

MWCNT walls with the presence of palladium-nitride(Pd-N) bonding and π - π bonding [2, 3].

Need for non-covalent functionalization and cause of catalyst formation

Covalent functionalization in most cases alters the intrinsic properties of CNT such as conductivity and mechanical strength since it destroys the regular graphene-type structure [4-6]. Noncovalent functionalization of CNTs with polymers is an effective way to disperse the tubes in aqueous and non-aqueous solvents without damaging their unique structure and thus preserving their intrinsic properties[7-9]. The Pd colloids were prepared through sodium borohydride reduction under the protection of polypyrrole, Pd-N interactions and polymeric stabilization play a key role in the formation of stable and highly dispersed Pd NPs on the conducting composite material PPy/MWCNT. The MWCNT was dispersed well with the existence of pyrrole in the solution, and pyrrole was polymerized in the presence of a protonic acid (HCl) and an oxidant ($\text{NH}_4\text{S}_2\text{O}_8$).

Preparation of catalyst Pd-PPy/MWCNT

Polypyrrole functionalized multiwall carbon nanotube (PPy/MWCNT) was prepared with the help of previous literature [9-12]. Prepared PPy/MWCNT (500 mg) was suspended in H_2O (100 mL) with ultrasonic treatment for 30 min and was stirred mechanically for another 30 min. PdCl_2 (154 mg) was then added to the solution. Pd nanoparticles formed and were anchored on the support after adding a mixture of NaBH_4 (85 mg, 2.25 mmol) and Na_2CO_3 (85 mg, 0.8 mmol) in water (20 mL) at room temperature and was stirred for another 1 hour. The resulting samples were filtered, washed with distilled water, and dried at 80°C overnight.

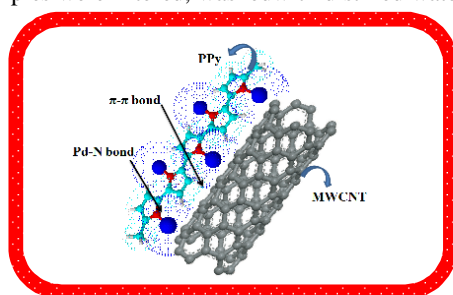


Figure1: Polypyrrole functionalized MWCNT- palladium

Confirmation Analysis for prepared catalyst

The synthesized PPy is found to wrap around the MWCNT as a result of π - π bonding, and highly dispersed Pd nanoparticles are loaded onto the MWCNT with narrowly distributed particle sizes ranging from 20- 40 nm due to the polymer stabilization and existence of Pd-N bonding. These are confirmed by XRD due to three peaks at around 40.1° , 46.8° and 68.3° correspond to plane (111)(200) and (220)[10- 12]. In FT-IR spectrum the characteristic peak observed of monosubstituted arene with two other peaks at 761 and 701 cm^{-1} due to C=C-H out-of-plane bending. The characteristic bipolar bands at 1222 and 939 cm^{-1} and the broad band at 1578 and 1054 cm^{-1} indicates the formation of PPy in its doped state [13, 14]. The MWCNT/PPy/Pd (figure-1) catalysts are excellent stability, reusability and high dispersibility of palladium, therefore promise potential applications in carbon-carbon coupling reactions and hydrogenation reactions.

Reference

- [1] S. Iijima, Nature, 354 (1991) 56-58.
- [2] Daping He, Chao Zeng, Cheng Xu, Niancai Cheng, Huaiguang Li, Shichun Mu, and Mu Pan, Langmuir, 27 (2011) 5582-5588.
- [3] Jinzhu Chen, Wei Zhang, Limin Chen, Longlong Ma, Hui Gao, and Tiejun Wang, ChemPlusChem 78 (2013) 142-148.
- [4] M. S. Dresselhaus, G. Dresselhaus and P. Avouris, Carbon Nanotubes: Synthesis, Structure, Properties and Applications, 7 (2000) 153-159.
- [5] G. Sakellariou and A. Avgeropoulos, RSC Adv, 34 (2013) 234-238.
- [6] M. S. Dresselhaus, G. Dresselhaus and P. C. Eklund, Science of Fullerenes and Carbon Nanotubes, Academic Press, (1996).
- [7] P. M. Ajayan, L. S. Schadler, and P. V. Braun, Nanocomposite Science and Technology, Wiley(2003).
- [8] C. A. Cooper, R. J. Young and M. Halsall, Compos. Part A., 2001, 32A, 401-411. G. Gao, T. Cagin, and W. A. Goddard, Nanotechnology, 9 (1998) 184-191.
- [9] J. M. Thomassin, R. Jerome, C. Jerome and C. Detrembleur, Surface Modification of Nanotube Fillers, First Edition, Wiley (2011).
- [10] W. Liang, G. Zhang, H. Sun, Z. Zhu and A. Li, RSC Advances, 3 (2013) 18022-18027.
- [11] J. F. Mike and J. L. Lutkenhaus, J. Polym. Sci. Part B: Polym. Phys, 51 (2013) 468-480.
- [12] Y. Kou, Y. H. Xu, Z. Q. Guo and D. L. Jiang, Angew. Chem, 50 (2011) 8753-8757
- [13] Syuji Fujii, Soichiro Matsuzawa, Hiroyuki Hamasaki, and Yoshinobu Nakamura Langmuir 28 (2012) 2436-2447
- [14] Syuji Fujii, Soichiro Matsuzawa, Yoshinobu Nakamura, Atsushi Ohtaka, and Takuto Teratani Langmuir 53 (2010) 6230-6239.

2.44 Green Synthesis of Silver Nanoparticles from Root Extract of *Phyllanthus maderaspatensis* L. and their Biological Applications

K. Kokila, N. Elavarasan and V. Sujatha*

Department of Chemistry, Periyar University, Salem-636 011, Tamil Nadu, India. email id: chemsujatha888@gmail.com

Introduction

Green synthesis of metal nanoparticles is a raising research area because of their vital role in the nanomedicines. The synthesis of silver nanoparticles (AgNPs) is a suitable, cheap and environmentally safe approach, when compared to chemical synthesis. In the present investigation, we have synthesized silver nanoparticles using the aqueous extract of *Phyllanthus maderaspatensis* L. root by reducing 10mM silver nitrate (AgNO_3) solution. AgNPs are characterized by UV-vis spectroscopy (UV), Fourier infrared spectroscopy (FT-IR), X-ray diffraction (XRD), Energy-dispersive X-ray spectroscopy (EDX) and Scanning electron microscopy (SEM) techniques. The synthesized AgNPs were also evaluated for its antioxidant and antibacterial activities.

Results and Discussion

The result indicates the water soluble phytoconstituents present in the *Phyllanthus maderaspatensis* root extract were mostly responsible for the reduction of Ag^+ ions to nanosized Ag^0 particles. UV-Vis spectral analysis was observed the band at 479 nm. The presence of bioactive compounds present in the biomass before and after reduction was identified by FT-IR. The presence of elements such as silver (74%) and oxygen (26%) was characterized by EDS. The morphology and size of the nanoparticles were determined by SEM, and X-ray diffraction studies which showed the average particle size in the ranges from 3-10 nm (Fig.2), as well as shows their face centered cubic structure. The biosynthesized silver nanoparticles might serve as a potent antioxidant as revealed by DPPH assay. AgNPs was more effective against pathogens like *Staphylococcus aureus* (14mm), *Bacillus subtilis* (17mm) and *Escherichia coli* (16mm).

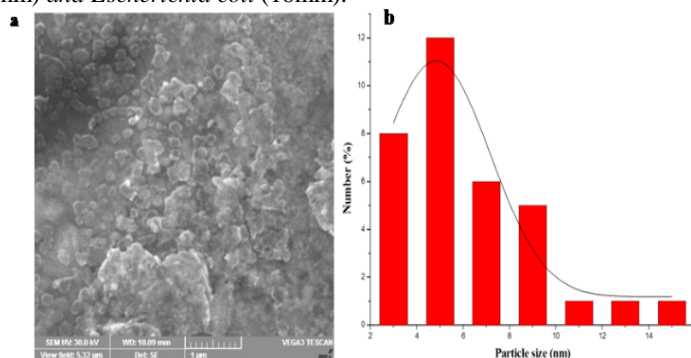


Fig.2. a) SEM image and b) Histogram of AgNPs

Conclusion

The obtained result reveals that silver nanoparticles synthesized from *Phyllanthus maderaspatensis* L. root may serve as a potential antioxidant and antibacterial agent, inferring its pharmacological property.

Key words: *Phyllanthus maderaspatensis*; AgNPs; antioxidant; antibacterial activity. **Acknowledgements:** T

he 'INSPIRE fellowship' is gratefully acknowledged for the award of 'DST-INSPIRE fellowship' to K. K [IF.120748] and ADTWD-Scholarship to N. E.

2.45 Rapid Synthesis of Lithium titanate Nanocomposites for Lithium – Ion Batteries

M. Selvamurugan and S. Karuppuchamy*

Department of Energy Science, Alagappa University, Karaikudi, Tamil Nadu-630003

E.mail: skchamy@alagappauniversity.ac.in

Abstract

Lithium titanate composites have been synthesized by simple peroxo solution growth technique for lithium ion battery applications. The structural characterization was carried out using advanced techniques. XRD pattern confirms the formation of lithium titanate. FT-IR spectroscopy confirms the presence of asymmetric stretching vibrations of Ti-O bond.

Introduction

Spinel $\text{Li}_4\text{Ti}_5\text{O}_{12}$ has been accepted as a novel anode material for lithium ion battery instead of carbon and graphite anodes because it can release lithium ions constantly for swift recharging of high current. Among all the anode materials, $\text{Li}_4\text{Ti}_5\text{O}_{12}$ has been identified as one of the most capable anode candidates for the next-

generation extensive power lithium-ion batteries. In this work, we report the synthesis and characterization of Lithium titanate composites by simple solution growth route.

Experimental Section

All chemicals used were of analytical grade and used without any further purification. Titanium oxysulphate and Lithium hydroxide ($\text{LiOH}\cdot\text{H}_2\text{O}$) was dissolved in distilled water separately. Then, it was stirred continuously for 2 hour and then the two solutions were mixed. Then, few drops of H_2O_2 were added into the above precursor solution and subsequently yellow colored precipitate was quickly obtained. The precipitate was collected and dried at 80°C for 12 h in hot air oven and finally the precipitate was annealed at high temperatures.

Results and Discussion

XRD patterns of synthesized titanate powders sintered at 700°C for 4 h are shown in Fig. 1. The appeared peaks are matches well with the JCPDS card no: 38-0270. This clearly indicates the formation of $\text{Li}_4\text{Ti}_5\text{O}_{12}$. The average crystallite size of 48 nm was obtained for the synthesized materials. The vibrational frequencies of elements present in Lithium titanate nanoparticles are obtained from Fourier Transform Infrared (FTIR) spectroscopy. The FT-IR spectra of Lithium titanate nanoparticles are shown in Fig.2. The peaks seen at 456 and 678 cm^{-1} are ascribed to the Ti-O-Ti stretching vibrations of lithium titanate [1,2].

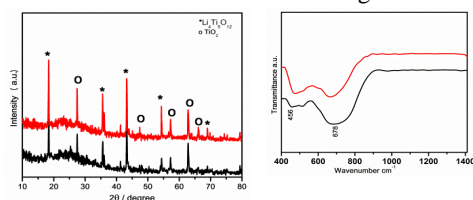


Fig. 1 XRD pattern of $\text{Li}_4\text{Ti}_5\text{O}_{12}$.

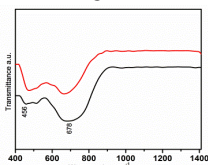


Fig. 2 FT-IR spectra of $\text{Li}_4\text{Ti}_5\text{O}_{12}$.

Conclusions

Lithium titanate and titanium oxide nanocomposites were successfully synthesized by simple solution growth method from aqueous solution. XRD studies confirmed the formation of lithium titanate. FT-IR spectroscopy confirms the presence of asymmetric stretching vibrations of Ti-O bond.

Reference

1. R.Xu, J. Li, A. Tan, Z. Tang, Z. Zhang, J. Power. Sources 196 (2011) 2283–2288.
2. Y. Ren, J. Zhang, Y.Liu, H.Li, H.Wei, B. Li, X.Wang, ACS Appl. Mater. Interfaces 4 (2012) 4776–4780.

2.46 Synthesis of microemulsion assisted with Chitosan/Silver-Desferrioxamine B (CS/Ag-DFOB) complex for skin disease

S.Anandhavelu¹,A.Yogiananth¹,M.Murugavelu¹,V.Sethuraman²,S.Thambidurai²

¹Department of Chemistry, Vel Tech Multi Tech., Chennai-600062, Tamilnadu, India.

²Department of Industrial Chemistry, Alagappa University, Karaikudi-630003,TN, India.

Abstract

In this work, Novel chitosan based Silver-Desferrioxamine B complex was prepared using Microemulsion as well as potentiometrically done the reaction. The development of pharmaceutically relevant microemulsions using DFOB and chitosan was used as the surfactant since it forms stable microemulsions without the need of co-surfactants. These w/o microemulsions were used as reactors for the synthesis of silver nitrate and acetate nanocrystals. The reaction is hypothesized to proceed via diffusion controlled mass transport of emulsified water droplets containing either silver acetate or nitrate. This project was motivated by results from earlier work that demonstrated increased biological effectiveness of a smaller particle size CS/Ag-DFO product and stabilization of these smaller particles by adsorbed surfactant. Further size reduction of CS/Ag-DFO particles may result in greater biological effectiveness based, in part, on enhanced solubility of CS/Ag-DFO due to the Kelvin effect. The Prepared complex was characterized using FT-IR, UV-Vis Spectroscopy and compound confirmation using (LC-MS) Mass Spectroscopy.

Keywords: Chitosan, Microemulsion, Desferrioxamine B, Skin Disease.

Introduction

Microemulsions can be easily prepared and have demonstrated desirable biopharmaceutical properties due to their unique physico-chemical characteristics.^{8,9} Chemical engineers and material science groups have used such microemulsions as reactors for synthesizing magnetic particles,^[1] semiconductors,^[2] and polymeric nanoparticles ^[3]. The microemulsions reported in the cited works used dioctyl sodium sulfosuccinate (DOSS) with organic solvents such as iso-octane and n-hexane. The desferic molecule (Desferrioxamine) (**Figure 1**) is a hexadentate ligand consisting of three bidentate hydroxamic groups. The residual chain includes two

secondary amide groups and an aliphatic chain. The saturated amine group on one edge of the linear molecule gives the molecule a positive charge in acid to slightly alkaline solutions.

Different hydrophilic and lipophilic drugs have been incorporated into microemulsion formulations and evaluated for delivering therapeutic agents via the oral, topical, and parenteral routes. In most cases, further product development of the evaluated systems for human use was hampered by concerns about the toxicity of components in the formulations.

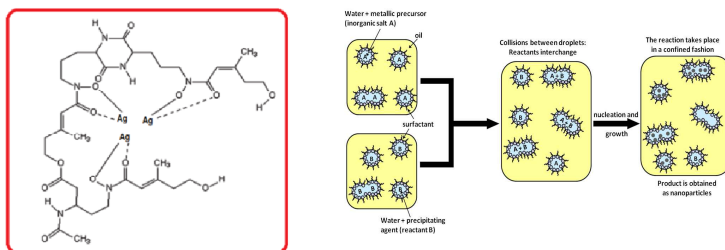


Figure.1 synthesis of metal complex nanoparticle using micro-emulsion technique A brief description of the synthesis of CS/Ag-DFOB complex in W/O microemulsions.

The above prepared samples were characterized using Functional group by FTIR, UV-vis spectroscopy and prepared (CS/Ag-DFOB) compound identification by (LC-MS) Mass Spectroscopy.

References

1. Li S, John VT, O'Conner C, Harris V, Carpenter E. 2000. J Appl Phys 87:6223–6225.
2. Sato H, Ohtsu T, Komasa I. 2000. J Colloid Interface Sci 230:200–204.

2.47 Pulse electrodeposition and corrosion properties of Ni-W-ZrO₂ nanocomposite coatings

K. Alex Mary, S. Sangeetha and G Paruthimal Kalaignan*

Advanced Nanocomposite Coatings Laboratory, Department of Industrial Chemistry, Alagappa University, Karaikudi.

Corresponding Author Phone No: +91-9443135307, Fax: +914565 225202.

Email id: pkalaignan@yahoo.com and sangeetha4880@gmail.com

Abstract

Ni-W-ZrO₂ nanocomposite coatings were deposited on a mild steel substrate by pulse current electrodeposition from the Watt's bath containing uniformly dispersed zirconium oxide (ZrO₂) particles. Pulse plating with optimum pulse current parameters have some advantages such as smaller grain size, uniform deposition, less absorption of hydrogen, higher deposition rate and improved corrosion resistance [1]. Ni-W alloys are considered as a substitute to hard chromium deposition, which also having a better abrasion resistance [2]. The crystallographic structures, surface morphology and chemical compositions were analyzed by means of X-ray Diffraction analysis (XRD), Scanning Electron Microscopy (SEM) and Energy Dispersive X-Ray Analysis (EDAX). The peaks corresponded to the Ni-W alloy matrix has face centered crystalline structure and the predominant planes are (111) (200) and (220). JCPDS card number (65-4828) has confirmed this pattern. The crystallite sizes of the deposits were calculated by Debye Scherrer's equation. Incorporation of ZrO₂ particles into the alloy matrix has modified the Ni-W crystal growth. The microhardness value of the Ni-W alloy matrix was ~ 460 HV. After the inclusion of ZrO₂ particles the microhardness value was increased to ~ 568. The improvement of microhardness can be due to more second-phase particle dispersion which tends to have superior mechanical properties of the nanocomposite coatings. The Potentiodynamic polarization and electrochemical impedance methods were used to calculate the corrosion resistance properties of Ni-W-ZrO₂ nanocomposite coatings in 3.5% NaCl solution. The increase in R_{ct} value is ascribed to the formation of protective layer on the metal/solution interface. The decrease in C_{dl} values was due to the gradual replacement of water molecules by the adsorption of the second phase ZrO₂ particles. A significant grain refinement, higher microhardness and improved corrosion resistance were occurred at the pulse current electrodeposition for Ni-W-ZrO₂ nanocomposite coatings.

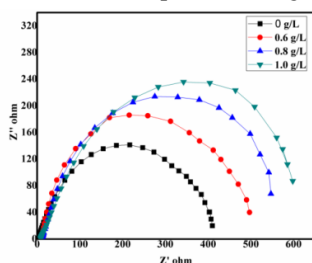


Fig.1. Nyquist plots (Z'' vs Z') obtained for Ni-W-alloy matrix and various amounts of ZrO₂ incorporated into Ni-W-ZrO₂ nanocomposite coatings

References

- [1] G. Soroor, G. Wei, *J. alloys comp*622 (2015) 918.
[2] E.B. Lehman, P. Indyka, A. Bigos, M.J. Szczerba, *Mater Design* 80 (2015) 1.

2.48 Characterizations of pulsedeposited Ni-W-SiC nanocomposite coatings

K.Mohana, S. Sangeetha and G Paruthimal Kalaignan*

Advanced Nanocomposite Coatings Laboratory, Department of Industrial Chemistry, Alagappa University, Karaikudi.
Phone No: +91-9443135307, Fax: +914565 225202. Email id: pkalaignan@yahoo.com and sangeetha4880@gmail.com

Abstract

In the present study, SiC reinforced Ni-Wnanocomposite coatings were deposited on a mild steel substrate using pulse current electrodeposition process employing a nickel sulphate bath. Pulse electrodeposition is one of the important technological techniques for co-depositing fine (micro or nano) particles with a metal or alloy matrix to generate composite coatings for potential engineering applications [1]. Ni-W alloys are well-known to display better mechanical and chemical properties than Ni coatings [2]. The surface morphology, chemical composition and crystallographic orientation were characterized using scanning electron microscopy (SEM), energy dispersive analysis of x-ray (EDAX), and X-ray diffractometry (XRD). Microhardness of the coating was measured by using Vicker's microhardness tester. The preferred growth process of the Ni-W alloy matrix in crystallographic directions $\langle 111 \rangle$, $\langle 200 \rangle$ and $\langle 220 \rangle$ is strongly influenced by SiC nanoparticles. The average crystallite size was calculated by using X-ray diffraction analysis and it was ~ 46 nm for electrodeposited Ni-W and ~ 34 nm for Ni-W-SiC nanocomposite coatings. The crystallite structure was fcc for electrodeposited Ni-W and Ni-W-SiC nanocomposite coatings. Incorporation of SiC nanoparticles into the electrolytic bath does not affect the crystalline structure of the alloy matrix. Co-deposited SiC nano-particulates were uniformly distributed in the Ni-W alloy matrix. The mean value of Vicker's microhardness of the Ni-W alloy coating has been found at about ~ 460 HV, while the hardness for that of Ni-W-SiC nanocomposite coatings is in the range of ~ 580 HV. The higher microhardness of the nano composite coatings is due to a grouping of the particle reinforcement and the change of Ni-W alloy arrangement. The corrosion behaviour was measured by using Tafel Polarization and Impedance methods with 3.5% NaCl solution. Ni-W-SiC nanocomposite coatings have shown a positive shift in the potential and decreased corrosion current. The incorporation of SiC nanoparticles into the Ni-W alloy matrix was found to enhanced the corrosion resistance than the Ni-W alloy matrix.

Keywords: Pulse deposition, Corrosion, Microhardness, Impedance.

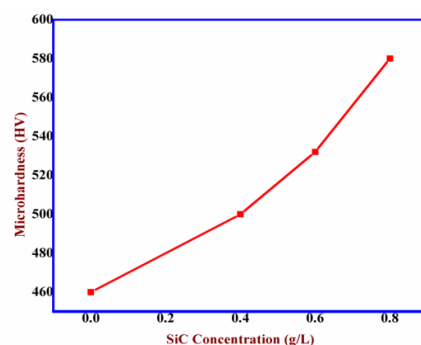


Fig.1. Microhardness values of Ni-W-SiC nanocomposite coatings

References

- [1] S.A. Lajevardi, T. Shahrabi, *Appl. Surf. Sci*256 (2010) 6775.
[2] M.F. Cardinal, P.A. Castro, J. Baxi, *Surf. Coat. Technol*204 (2009) 85.

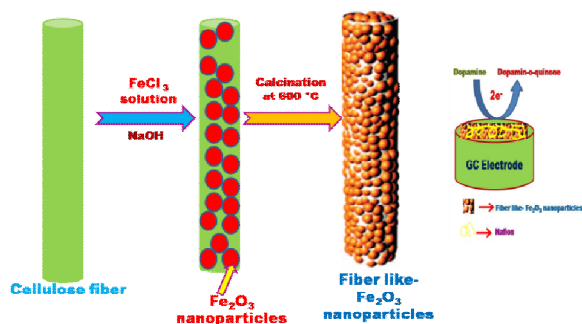
2.49 In situ Synthesis of Macroporous Fe₂O₃ Fiber Nanomaterials by Cellulose Fibers for Electrocatalytic Oxidation of Dopamine

Rajesh Madhuvilakku, Shakkthivel Piraman*

Sustainable Energy and Smart Materials Research Lab, Department of Nanoscience and Technology, Alagappa University, Karaikudi. Email: apsakthivel@yahoo.com / nanorajesh9626@gmail.com

Abstract:

Nanocomposite fiber is one of the most fascinating materials with broad applications. In the present work, nanocomposite fibers were prepared by using a low-cost, simple and “green” process. Fiber-like



Fe_2O_3 macroporous nanomaterials have been prepared by in-situ synthesis of Fe_2O_3 nanoparticles using the cellulose fibers. The interpenetrated porous structure in the cellulose fibers served as templates for the preparation of Nanoparticles. The structure and properties of the Fe_2O_3 nanomaterials were characterized with X-ray Diffraction, Scanning electron microscopy and electrochemical studies. The Fe_2O_3 nanomaterials exhibited one dimensional (1D) fiber-like morphology with macroporous structure. The results revealed that the Nanomaterials displayed

high purity of $\alpha\text{-Fe}_2\text{O}_3$ and possessed large specific surface area. The electrocatalytic activity towards the oxidation of dopamine was investigated by cyclic voltammetry (CV) and differential pulse voltammetry (DPV). The results showed that the modified electrode exhibited excellent electro catalytic activity towards the electrochemical oxidation of DA compared to bare glassy carbon electrode (GCE). The good analytical performance and long-term stability of the proposed sensor can be attributed to the synergistic effect of 1D- $\alpha\text{-Fe}_2\text{O}_3$ nanomaterials with retention of the macropore structure, which have potential applications in electrochemical analysis.

Keywords: Fiber-like Fe_2O_3 macroporous, cellulose matrix, One Dimensional (1D) fiber, Dopamine, Differential Pulse Voltammetry (DPV)

2.50 Manganese dioxide Nanoparticles for Electrochemical Energy Storage and Conversion Applications

Srinivasan Alagar, Rajesh Madhuvilakku and Shakkthivel Piraman*

Sustainable Energy and Smart Materials Research Lab, Department of Nanoscience and Technology, Alagappa University, Karaikudi-630003. E-Mail: sbn.chem@gmail.com / apsakthivel@yahoo.com

Abstract

Supercapacitors are used as an electrochemical energy storage and conversion devices, continuously serving for human life. The electrochemical performance of supercapacitors mainly depends on active materials present in the electrodes. Cubic structure of MnO_2 electrode materials are rationally synthesized via simple and facile precipitation. The synthesized products were characterized by powder X-ray diffraction, Fourier Transform Infrared spectroscopy and Field Emission Scanning Electron Microscopy analysis. Cyclic voltammetry, impedance spectroscopy and Chronopotentiometry charge-discharge cycling were used to evaluate the electrochemical performance of the synthesized electrode materials. The initial discharge capacities were found to be 302 Fg^{-1} in 1 M LiNO_3 at a current density of 1 Ag^{-1} . The higher specific capacitance in the electrolyte with a bivalent cation is attributed to the reduction of Mn^{4+} to Mn^{3+} by each of the bivalent cations present in the electrolyte. This novel strategy provides a promising route to design high performance supercapacitors with high energy density for next-generation storage devices.

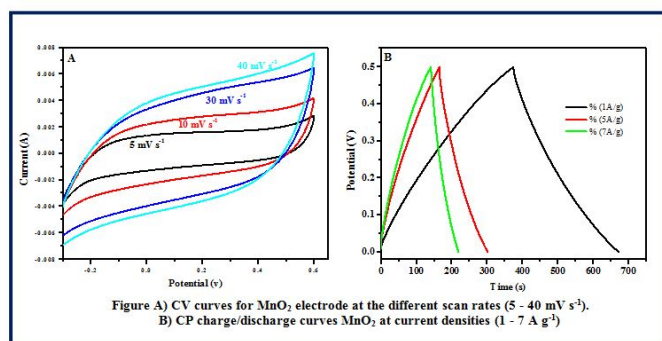


Figure A) CV curves for MnO_2 electrode at the different scan rates ($5 - 40 \text{ mV s}^{-1}$).
B) CP charge/discharge curves MnO_2 at current densities ($1 - 7 \text{ A g}^{-1}$)

The initial discharge capacities were found to be 302 Fg^{-1} in 1 M LiNO_3 at a current density of 1 Ag^{-1} . The higher specific capacitance in the electrolyte with a bivalent cation is attributed to the reduction of Mn^{4+} to Mn^{3+} by each of the bivalent cations present in the electrolyte. This novel strategy provides a promising route to design high performance supercapacitors with high energy density for next-generation storage devices.

Keywords: Manganese dioxide, Energy Storage, Supercapacitor, charge-discharge, specific capacitance

2.51 Synthesis and characterization of CdSSe/ZnS core shell for photovoltaic application

Ishimwe Francoise and K. Gurunathan*

Nano Functional Materials Lab, Science Campus, Department of Nanoscience & Technology, Alagappa University, Karaikudi- 630 003; e-mail:kgnathan27@rediffmail.com

In this paper, co-precipitation method for synthesis of cadmium sulfoselenide was introduced followed by the investigation of structural and electrical properties CdS_xSe_{1-x} and the synthesis of CdSSe/ZnS core shell. The general method of synthesis was as follows: 150ml of distilled water was added into 0.015 $CdNO_3$ to form a solution which was added drop wise into solution of 0.0111 M of Na_2S , 0.00387 M of Se and 0.184 M of NaOH stirred for several hours then aging for 12 hours the red precipitate obtained was centrifuged, heated, and crushed into fine powder. After the synthesis of CdS_xSe_{1-x} the structural and electrical properties were investigated as follow: The complete solution of CdSSe were synthesized by vacuum fusion of stoichiometric proportion of obtained CdS_xSe_{1-x} . X-ray diffraction data revealed that they possess the hexagonal wurtzite structure. The unit cell lattice constants vary linearly with the composition parameter x, following Vegards law. Thin film of CdSSe solid solution could be deposited onto glass substrates by thermal evaporation of bulk material in 10^{-4} pa vacuum.

In the end CdSSe/ZnS was synthesized by taking 0.1 g of CdSSe was dispersed in 12.5 ml of distilled water then 0.7189 g of $ZnSO_4$ was added and 0.1878 g of thioacetamide was added followed by the addition of 0.2 g NaOH the precipitate was obtained heated, dried and crashed into fine powder. Figure 1 shows the XRD spectra of the core/shell structure.

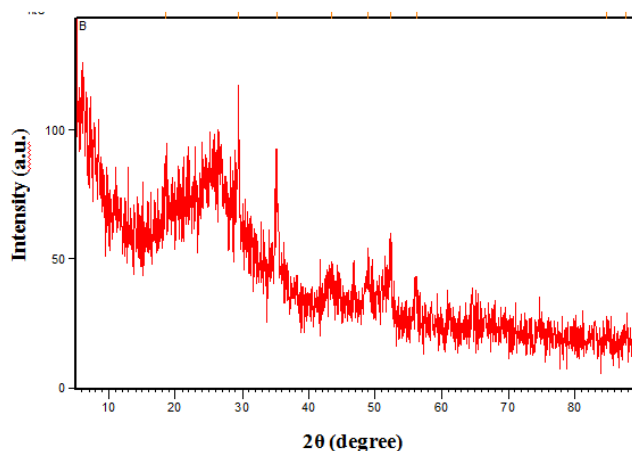


Figure 1. XRD pattern of CdSSe/ZnS core-shell material.

References

- [1]. Alivisatos, A. P., *Semiconductor clusters, nanocrystals, and q 1*. Underwood, D. F.; Kippeny, T.; Rosenthal, S. J., *Ultrafast carrier dynamics in CdSe nanocrystals determined by femtosecond fluorescence upconversion spectroscopy*. *Journal of Physical Chemistry B* 2001, 105, (2), 436-443.
- [2]. Brus, L., *Electronic Wave-Functions in Semiconductor Clusters - Experiment and Quantum dots*. *Science* 1996, 271, (5251), 933-937.
- [3]. Colvin, V. L.; Schlamp, M. C.; Alivisatos, A. P., *Light-Emitting-Diodes Made from Cadmium Selenide Nanocrystals and a Semiconducting Polymer*. *Nature* 1994, 370, (6488), 354-357.

2.52 Physical and Electrochemical performances of Pulse electrodeposited Ni-CeO₂ nanocomposite coatings

S. Kasturibai^A and G. Paruthimal Kalaigan^{B*}

^A Dept of Chemistry, Alagappa Government Arts College, Karaikudi-630 003, Tamilnadu, India

^B Dept of Industrial Chemistry, Alagappa University, Karaikudi-630 003, Tamilnadu, India

E mail: pkalaigan@yahoo.com and kasturibai2007@gmail.com

Abstract

The development of modern technology requires metallic materials with better surface properties. In the present investigation Ni-CeO₂ reinforced nanocomposite coatings were prepared under pulse current method using nickel acetate bath. The use of pulse-electrodeposition technique permits electrolysis with a very high

current density for a short period of time, i.e., a very high deposition rate is achieved during the on-time [1, 2]. The crystal grains on the surface of Ni- CeO₂ composite coating are compact. The preferred growth direction was also influenced by cerium oxide nano-particles. Therefore, the preferred growth process of the nickel matrix in crystallographic directions <111>, <200> and <220> is strongly influenced at a concentration of 9 g/l. The structure of electrodeposited nickel and nickel nanocomposite coatings were face centered cubic (fcc). It was confirmed from ICDD- JCPDS standards [87-0712]. The effect of incorporation is maximum at a current density of 8 A/dm². The microhardness values of the Ni- CeO₂ nanocomposite coatings (810HV) were higher than that of pure nickel (310HV) due to dispersion-strengthening; matrix grain refining and increased with the increase of incorporated CeO₂ particles content. The corrosion rates of Ni- CeO₂ nanocomposite coatings (1.98milliinch/yr) were lower than that of electrodeposited nickel coating (67.69milliinch/yr) in 3.5% NaCl solution. The impedance spectra has showed a depressed semicircle at the centre of real axis, which has been attributed to the roughness and inhomogeneity of the solid surfaces. The charge transfer resistance (R_{ct}) values for Ni-CeO₂ nanocomposite coatings were increased and the constant phase element (CPE) values decreased with increased CeO₂ content in the composite coatings due to the distribution of relaxation times as a result of inhomogeneities present at a micro level or nano level such as the surface roughness and porosity. The enhancement in the corrosion resistance may be due to physical barriers produced by CeO₂ to the corrosion process by filling crevices, gaps, and micron holes on the surface of the composite coatings.

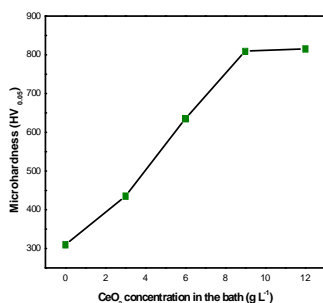


Fig.1 Effect of CeO₂ content on hardness of coatings

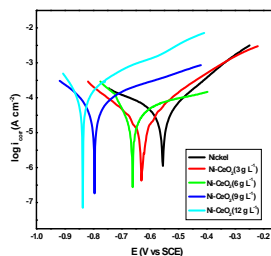


Figure.2 Potentiodynamic Polarization curves for Nickel and Ni-CeO₂ nanocomposite coatings

References

- [1] S.A.Lajevardi T. Shahrabi *Appl. Surf. Sci.* 256 (2010) 6775
- [2] S Kasturibai, G Paruthimal Kalaignan *Bull. Mater. Sci.*37 (2014) 721.

2.53 Improvement of Bagasse based Paper Critical Properties using CaCO₃ Nanofillers

Maruthaiya Karuppaiah¹, Sasikala Sundar¹, Manisankar Paramasivam² and Shakkthivel Piraman^{1*}

¹Sustainable Energy and Smart Materials Research Lab, Department of Nanoscience and Technology, Science Campus,

²Department of Industrial Chemistry, Alagappa University, Karaikudi-630003

Email: apsakthivel@yahoo.com / maruthaiya.k@tnpl.co.in

Abstract

The benefits associated with the use of fillers are attractive to the paper industries mainly include cost and energy savings, improvement in the paper properties. In this research article, the use of inorganic fillers particularly, the synthesized and commercially available Calcium Carbonate nanofillers were used to improve the paper qualities of the refined bagasse and hardwood pulp mixed paper, notably the filler and cellulose fibers showed synergistic effect on the optical, mechanical and surface properties. Here, the effect of fillers content both Micro GCC and Nano PCC on the filler findable factor and paper strength properties, have been investigated. The XRD and FT-IR studies were confirmed the formation of Calcium carbonate with calcite phase with average crystalline size of 48nm and 220 nm for the Nano and Micro calcium carbonate respectively. The surface and optical properties were increased remarkably up to 20% nanofiller (Nano CaCO₃) addition, promising method for paper making to improve the paper properties.

Keywords: Bagasse, Calcium carbonate, Micro GCC, Nano PCC, Paper making

2.54 Vapour Phase Polymerization of Styrene over Mesoporous Aluminophosphate Catalyst

M.A. Mary Thangam, S.Usha, Chellapandian Kannan*

Department of Chemistry, Manonmaniam Sundaranar University, Thirunelveli -12, India. *Corresponding author: Fax: +91 462 2322973, 2334363, Tel: +91 462 2333887; E-mail: chellapandiankannan@gmail.com

Abstract

Styrene polymerization has been carried out over mesoporous AlPO_4 catalyst. The reaction conditions like effect of contact time, temperature, monomer dosage, time on stream has been optimized for maximum conversion.

1.Introduction

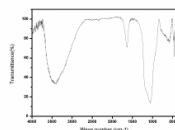
Aluminophosphate materials are a class of zeolite like crystalline sieve materials showing a broad range of physiochemical properties of potential application in the field of catalysis.^[1] Its porous nature and thermal stability are important parameter for carrying out vapour phase reactions.

2.Experimental

Phosphoric acid, aluminium hydroxide and CTABr are mixed in water and stirred for 24 hours. The molar ratio of the gel is 0.1 $\text{Al}(\text{OH})_3$:0.1 H_3PO_4 :0.5CTABr:300 H_2O . The final product was washed with water, dried and calcinated at 873K to remove CTABr. Polymerization of styrene was carried out in the vapour phase over AlPO_4 . The monomer is vaporized above their boiling point and the vapour is passed to the catalytic bed.

3. Result and Discussion

The synthesised catalyst is characterized by FT-IR spectrum (Fig1). The stretching appear near 1100cm^{-1} , 670cm^{-1} and 460cm^{-1} are confirmed the formation of



AlPO_4 molecular sieves Fig1: FT-IR spectrum of AlPO_4

The reaction conditions like effect of contact time, temperature, monomer dosage and catalyst dosage has been optimized and observed that 3 hr contact time, 200°C , 30ml per 3hrs, 0.5g are suitable for maximum conversion of styrene. By adopting these conditions, time on stream (Fig3) has been carried out up to 5 hrs and observed that, the conversion remaining constant above 3 hrs. The polymer is characterized by FT-IR and the stretching 2900 to 2850cm^{-1} and 1250cm^{-1} confirmed the formation of polystyrene (Fig 2).

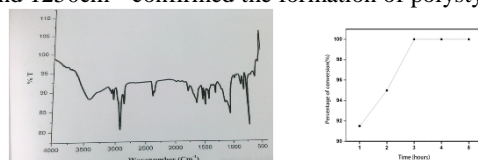


Fig 2: FT-IR spectrum of poly styrene, Fig3: Time on stream for polymerization of styrene

Conclusion

The synthesised AlPO_4 is calcinated and characterized by FT-IR, it proves the formation of tetrahedral framework of the molecular sieves. The polymerization reaction has been carried out at various conditions like contact time (3hrs), the temperature (200°C), the monomer dosage (30ml per 3 hours) and catalyst dosage is 0.5g. These conditions provides the maximum conversion of styrene. The polystyrene formation is confirmed by FT-IR.

References:

1. C.Kannan et al., Research Journal of chemical science, vol 2(7), 27-35, 2012.
2. C.Kannan et al., Materials Letters, vol 113, 93-95, 2013.

2.55 Synthesis and characterization of hybrid structure of Ni doped ZnO/reduced graphene oxide

R.Karthik, S.Thambidurai*

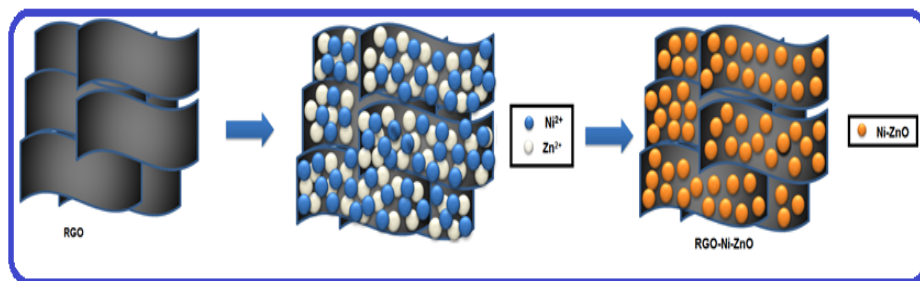
Department of Industrial Chemistry, School of Chemical Sciences, Alagappa University, Karaikudi-630 003, Tamil Nadu, India. Email: karthikchem2013@gmail.com

Abstract

Graphene, a two-dimensional sheet of covalently bonded carbon atoms, has attracted interest as a material with potential use in various applications such as touch panels, p-n junction materials, flexible thin-film transistors,

and solar cells [1]. The perfect structure of graphene shows low chemical reactivity, but one graphene derivative, reduced graphene oxide (RGO) contains a range of reactive oxygen functional groups and is widely used for chemical functionalization. Metal oxide-deposited RGO sheets show promise for applications in the fields of chemical sensors and energy storage devices. The ZnO nanoparticles (band gap of 3.3 eV) have been used for numerous applications such as optics, optoelectronics, sensors, and actuators due to their semiconducting, piezoelectric and pyroelectric properties. ZnO-decorated reduced graphene oxide (ZnO-rGO) sheets display distinct optoelectronic characteristics compared to pure ZnO nanoparticles [2].

Nickel oxide, as one of the most important transition metal oxide, has received increasing attention as materials of supercapacitors due to its merits of high theoretical capacitance, low-cost, high natural abundance [3]. In the past few years, great progress has been made in the preparation of NiO with different morphology and structure such as spheres [4], nanotubes [5], nanorings, nanowires, and nanorods. Flower-like NiO was also prepared using a solution process with the help of some surfactants.



We aimed to develop Ni doped ZnO/reduced graphene oxide (RGO) surface by a chemical precipitation method using nickel nitrate, zinc nitrate, NaOH, and RGO as precursors. Fourier transforms spectroscopy (FTIR), X-ray diffraction spectroscopy was employed to characterize the presence of functional group and crystallinity of the hybrid composite. Homogeneously distributed metal oxide particles are viewed and observed by scanning electron microscope (SEM). Elemental composition of the hybrid composite was investigated by EDXA. Finally, electrochemical properties of Ni doped ZnO/RGO hybrid composite was investigated by cyclic voltammetry and electrochemical impedance spectroscopy. This results indicate that the synergistic effect of Ni doped ZnO/RGO hybrid composite enhance the electrical behavior. From the data, it is observed that the Ni doped ZnO/RGO exhibits good electrical behavior which is highly useful for energy applications.

References

- [1] J. Wu, W. Pisula, K. Mullen, *Chemical Reviews*, 107 (2007) 718.
- [2] G. Singh, A. Choudhary, D. Haranath, A.G. Joshi, N. Singh, S. Singh, *Carbon* 50 (2012) 385.
- [3] YZ. Zheng, ML. Zhang, *Mater Letts* 61 (2007) 3967.
- [4] SJ. Ding, T. Zhu, JS. Chen, ZY. Wang, CL. Yuan, XW. Lou, *J. Mater. Chem.* 21 (2011) 6602.
- [5] HJ. Liu, TY. Peng, DE. Zhao, K. Dai, ZH. Peng, *Mater. Chem. Phys.* 87 (2004) 81.

2.56 Synthesis and characterization of zinc oxide nanoparticles from *Azadirachta Indica* extract

T. Revathi, S.Thambidurai*

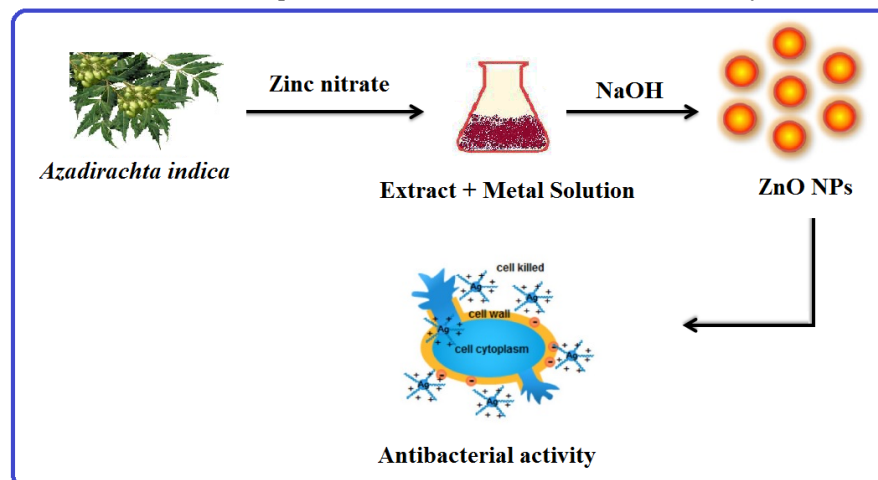
Department of Industrial Chemistry, School of Chemical Sciences, Alagappa University, Karaikudi - 630003, Tamil Nadu, India. *Email:* revathimahesh22@gmail.com

Abstract

The field of Nanotechnology is one of the most active researches nowadays in modern material science and technology. Nanoparticles are particles that have at least one dimension that is 100 nm or less in size. Physical and chemical methods are more popular for nanoparticles synthesis. An eco friendly green mediated synthesis of inorganic nanoparticles is a fast growing research in the limb of nanotechnology. *Azadirachta indica* is commonly known as neem. This plant is mostly available in India and each part of this tree has been used as a household remedy against various ailments from antiquity and for treatment against viral, bacterial and fungal infections. The zinc oxide nano powders are an important metal oxide due to its interesting properties and widely used in various applications.

In the present study, zinc oxide nanoparticles (ZnO NPs) were synthesized by simple precipitation method using neem (*Azadirachta indica*) extract. The functional group peaks of neem extract and zinc oxide nanoparticles confirmed by the FT-IR analysis. In UV-Vis spectrometry, the maximum peak of ZnO was observed at 368 nm. The XRD pattern of ZnO NPs indicated hexagonal wurtzite crystal structure with an average crystal size of 24 nm. The HR-SEM analysis shows that the synthesized ZnO NPs have rod like structure. Finally, the antibacterial activity of ZnO NPs evaluated against gram positive and gram negative microorganisms.

Keywords: *Azadirachta Indica*, ZnO nanoparticles, XRD, HR-SEM, Antibacterial activity.



Scheme 1. Synthesis of ZnO nanoparticles from *Azadirachta Indica* extract

References:

- [1] V.U. Omoja, A. O. Anaga, I.R. Obidike, Asian Pac J Trop Med. 4 (2011) 337-341.
- [2] Z. Deng, M.Chen, G. Gu, L.Wu, Journal of Physical Chemistry B 112 (2008) 16-22.
- [3] A.M. Awwad, B. Albiss, A.L. Ahmad, Adv.Mat.Lett.5 (2014) 520-524.

2.57 [BMIM] BF₄ assisted morphological improved synthesis of magnetic Fe₂O₃ nanoparticles

S. Nagapriya^a, S.Jegatheeswaran^a, M. Balamurali^b and M. Sundrarajan^{a*}

^aAdvanced Green Chemistry Lab, Department of Industrial Chemistry, School of Chemical Sciences, Alagappa University, Karaikudi -3, Tamil Nadu, India.

^bDepartment of Chemistry, Alagappa Government Arts College, Karaikudi - 3, Tamil Nadu, India

E-mail: sundrarajan@yahoo.com and priyajesus024@gmail.com

1. Introduction

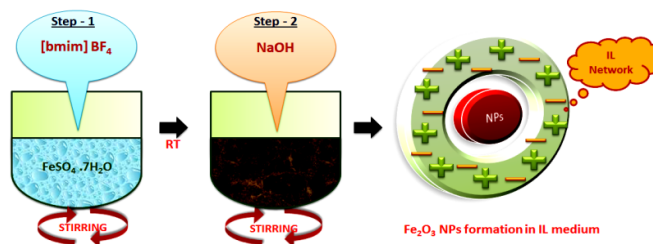
As an abundant, inexpensive, environmentally benign and most stable phase of iron oxide has attracted a great deal of attention for their peculiar properties and potential applications in fields of adsorbent, catalysis, gas sensors and magnetic storage. Therefore, studies on the shape controllable synthesis of nanomaterials are of great interest and are actively being pursued. A new type of green alternative to conventional organic solvents, ionic liquids have found wide spread application in synthesis of inorganic materials. Due to the asymmetry of volume, ionic liquids have some distinctive features like low melting point, negligible vapor pressure, non-volatility, high thermal stability and high ionic conductivity. Therefore, ionic liquids can be referred to as “designed liquids” with tunable properties by adjusting their cations and anions.

2. Morphological synthesis of Fe₂O₃ nanoparticles and characterization studies

Fe₂O₃ nanoparticles was prepared through sol-gel method. 2 mL of Ionic liquid ([bmim] BF₄) was added in the 50 ml of Iron (II) sulphate heptahydrate (0.5 mol/L) solution and magnetically stirred for 15 minutes at room temperature. Then, NaOH (0.1 mol/L) was added in the above mixture. The brown colour precipitate formed immediately after the addition of NaOH confirmed that the formation of iron oxide nanoparticles.

The synthesized Fe₂O₃ nanoparticles were characterized by XRD, FTIR and SEM analyses. The XRD Patterns are confirmed that the well crystalline nature and FTIR can indicated that formation of pure Fe₂O₃ and also be removal of impurities from IL after sintering. SEM images are displayed the morphological improvement and influence of IL during the synthesis.

3. Scheme of the Work



4. Conclusion

In this study, demonstrates polar features and low interface tension of IL has increased the nucleation rate of Fe_2O_3 nanoparticles. The hydrogen bond and π - π stack mechanism is used to be responsible for the present self-assembly of the [bmim] BF_4 ionic liquid in the reaction systems for the formation of the Fe_2O_3 with improved morphology.

5. References

1. J. Lian, X. Duan, J. Ma, P. Peng, T. Kim, W. Zheng, ACS Nano 3 (2009) 3749-3761.
2. M. Ramalakshmi and M. Sundrarajan, Materials Research Bulletin 48 (2013) 2758-2765.
3. M. Smiglak, J.M. Pringle, X. Lu, L. Han, et al., Chemical Communications 50 (2014) 9228-9250.
4. Z. Li, Z. Jia, Y. Luan, T. Mu, Current Opinion in Solid State and Materials Science 12 (2008) 1-8.

2.58 Synthesis and antibacterial studies of zinc oxide nanoparticles

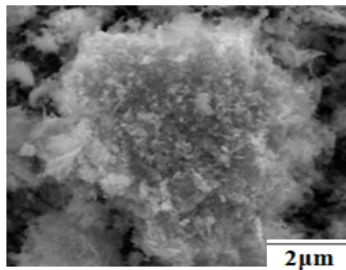
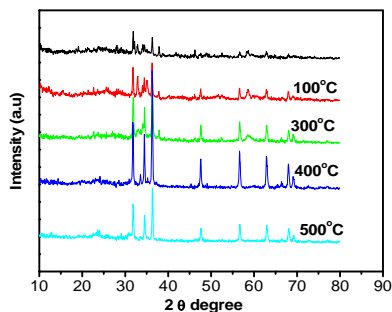
C.Rani* and K.Santhi

Department of chemistry, Alagappa Govt. Arts college, Karaikudi – 630003, India. E-mail: viswanathanrani@gmail.com

Inorganic antimicrobial agents, such as metal oxides, have received increasing attention in food applications because they are not only stable in harsh food-processing conditions, but they are also generally regarded as safe for human beings and animals relative to organic substances. One part of this work focuses on the application of inorganic nanoZnO, with good antimicrobial activity. The antibacterial mechanism of ZnO nanoparticles is most likely due to disruption of the cell membrane and oxidative stress in bacterium. Nano-sized particles of ZnO have more pronounced antimicrobial activities than large particles, since the small size (less than 100 nm) and high surface-to-volume ratio of nanoparticles allow for better interaction with bacteria. Recent studies have shown that these nanoparticles have selective toxicity to bacteria but exhibit minimal effects on human cells. ZnO nanoparticles have been shown to have a wide range of antibacterial activities against both Gram-positive and Gram-negative bacteria, (*Escherichia coli* O157:H7, *Salmonella*, *Listeria monocytogenes*, and *Staphylococcus aureus*). Since there is no more information available on their antibacterial effect against plant pathogens, it is important to focus on the use of ZnO particles as a potential safety intervention technology to effectively control plant pathogens like *Xanthomonas axonopodispv. citri* and *X. campestrispv. malvacearum*.

Synthesis and characterization of ZnO nano particles

Zinc oxide nano particles have prepared by chemical precipitation method. The powder obtained from the above method was calcinated at different temperatures ranges from 100°C to 500°C for 2hrs. The structure and morphology of prepared materials was examined by X-ray diffraction, scanning electron microscopy (SEM) and energy dispersive X-ray diffraction (EDX) techniques. Our results showed that with increasing calcination temperature from 100°C to 500°C the intensity of peaks increases and the diffraction peaks become sharper and narrower. This indicates the enhancement of the crystallinity due to the size enlargement of the nuclei. From the microscopic studies the particles formed were found to be micro nano crystalline in nature.



XRD pattern of ZnO
Antibacterial studies

SEM image of ZnO

The antibacterial assay was carried out using the agar diffusion technique. The assay was carried out on 1.5 % nutrient agar medium. ZnO in DMSO and nutrient medium is smeared with 0.05 ml of bacterial culture in exponential phase of 1.0 OD at 590 nm and incubated at 28°C for 48 hours. The diameters of the agar clear zones of bacterial inhibition around the discs as a result of diffusion of active substances were measured in millimeters as a measure of antibacterial activity. The best antibacterial activity was displayed by ZnO with an inhibition zone of 26 mm against both the plant pathogens.

Key words: Nano particles, Antibacterial activity.

2.59 Ag nanoparticles from *Nyctanthes arbor-tristis*: synthesis, characterization and application

K. Iswarya, K. Bama, J. Anandha Raj and M. Sundrarajan*

Advanced Green Chemistry Lab, Department of Industrial Chemistry, School of Chemical Sciences, Alagappa University, Karaikudi-630 003, Tamil Nadu, India. *Corresponding author: Tel: + 91 94444 96151.

E-mail: drmsgreenchemistrylab@gmail.com

Introduction

In recent years noble plasmonic metal nanoparticles have been focused in biomedical research, due to their unique chemical, electronic, optical, mechanical, magnetic, large specific surface area, quantum confinement effects, and antibacterial properties that are significantly different from those of bulk materials. Biogenic synthesis of plasmonic silver nanoparticles reduction of Ag ions by various natural substances and plant extracts such as *Nyctanthes arbor-tristis* [1]. Preparation of silver nanoparticles in aqueous solution using reducing properties of 3, 4, 5-trihydroxybenzoic acid is one of many possibilities of their “green synthesis”. The environmental issues compared with some of the physicochemical methods and can be used to large scale production of nanoparticles with well-defined size, morphology, very environmentally friendly because they are prepared without using hazardous chemicals [2].

Experiment

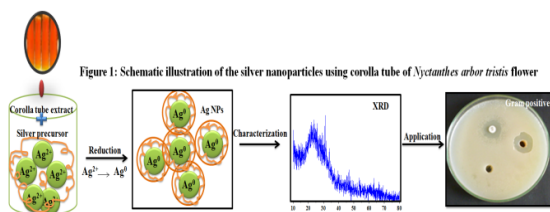
In this study, freshly corolla tubes of the *Nyctanthes arbor-tristis* flower (1.0 g) was extracted in 100 ml at 60 °C for 15 minutes. Ag nanoparticles were synthesized employing the aqueous extract of corolla tubes of *Nyctanthes* as a reducing and stabilizing agent [3] at room temperature for 5 hours. At the same time, the colour of the solution slowly turned into pale yellow, indicating the reduction of the Ag ions into Ag nanoparticles (Figure. 1) after employing for further characterization.

Results and discussion

The synthesis of Ag nanoparticles were characterized by XRD, UV-visible, SEM and FT-IR. The peaks were reflected at $(2\theta) = 38.1^\circ, 44.3^\circ, 64.4^\circ$ and 77.4° for Ag which can be attributed to the (111), (200), (220) and (311) crystallographic planes of face-centered cubic (FCC) of Ag crystals and well matching with JCPDS card No. 89-3722.

Conclusion

A novel and exciting green synthesis of silver nanoparticles employing an eco-friendly approach. The aqueous extract of *Nyctanthes* was successfully used as a reducing and stabilizing agent without any aided supportive chemicals. Ag nanoparticles showed significant activity against *S. aureus* (18 ± 2 mm) and *E. Coli* (15 ± 2 mm). The strong antibacterial activity of Ag nanoparticles using *Nyctanthes* extract, due to may be attributed to their large surface area and small size of nanoparticles. This study provides a platform to synthesize most effective and non-toxic antibacterial agent by a green method for use in pharmaceutical industry.



References

- [1] Abolghasem Abbasi Kajani, Abol-Khalegh Bordbar, Sayyed Hamid Zarkesh ESfahani, Ahamad Reza Khosropour and Amir Razmjou, *RSC Advances*, (2014).
- [2] Aftab Ahmad, Fatima Syed, Akram Shah, Zahid Khan, Kamran Tahir, Arif Ullah Dhan, Qipeng Yuan, *RSC Advances*, (2015).
- [3] S. Meghashri, S. Gopal, *J. Pharm. Bioall. Sci.* 4 (2012).

2.60 Facile synthesis of palladium nanoparticles using *Punica granatum* peel extract: Green chemistry approach

S. Tamil selvi^a, S. Ambika^a, S. Angappan^b and M. Sundrarajan^{a*}

^aAdvanced Green Chemistry Lab, Department of Industrial Chemistry, School of Chemical Sciences, Alagappa University, Karaikudi-630003, Tamil Nadu, India. *Corresponding author: Tel: + 91 94444 96151

E-mail: drmsgreenchemistrylab@gmail.com and tstamilselvi5@gmail.com

^bCentral Electrochemical Research Institute, Karaikudi 630006, India.

Introduction

Metal nanoparticles (NPs) have all kinds of benefits in many fields because of their unique properties compared to bulk materials [1, 2]. *Punica granatum* (Punicaceae), commonly called pomegranate, its peel serves as a mild, renewable and non-toxic reducing agent. The *Punica granatum* contains polyphenols, ellagic acid, ellagitannins, gallic acid and punicalin and it is used for antioxidant and anticarcinogenic agent.

Methods:

In this work, Pd NPs were prepared via reduction of palladium chloride (Pd²⁺) into (Pd⁰) NPs using *Punica granatum* extract as a bioreductant and a capping ligand without the addition of any other external reducing agent. The immediate change in color from pale yellow to red indicates the reduction of nanoparticles. The synthesized nanoparticles were confirmed by UV-Vis, XRD and FT-IR analysis. The synthesized Pd NPs were tested against the *Staphylococcus aureus* and *Escherichia coli* by agar diffusion method.

Results and discussion:

X-ray diffraction (XRD) analysis showed that Pd NPs were well matched with JCPDS-72-0710 with average crystalline size of 61 nm having hexagonal crystal lattice with primitive geometry. FTIR analysis of Pd NPs indicated the involvement of hydroxyl, amine and amino groups in the biosynthesis and stabilization of Pd NPs. UV-Vis shows that as the time interval increases, the absorbance peak was reduced due to the functional group of extract as well as Pd NPs were formed from (Pd²⁺) ion. The zone of inhibition was observed in the synthesized Pd NPs against *Staphylococcus aureus* (17±3 mm) and *Escherichia coli* (15±4 mm). The schematic representation of the synthesis of Pd NPs is shown in Figure 1.

Conclusion:

This one-step strategy using *Punica granatum* peel extract to synthesize Pd NPs is simple, cost-effective and environmentally benign, making possible the large-scale production of Pd NPs. In conclusion, the bioreduction of (Pd²⁺) into Pd NPs by the extract of *Punica granatum* has been demonstrated.

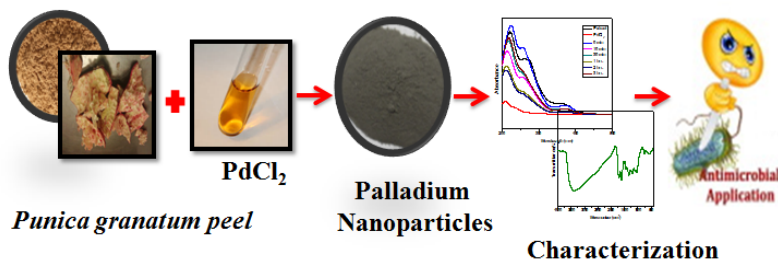


Figure 1: Schematic representation of the synthesis of Pd NPs

References

- [1] Aruna Jyothi Kora, Lori Rastogi, *Arabian Journal of Chemistry* (2015).
 [2] Mahmoud Nasrollahzadeh, S. Mohammad Sajadi, Rushdy S. Othman, *Journal of Colloid and Interface Science*, 462 (2016) 243–251.

2.61 Synthesis, characterization and antibacterial activity of silver nanoparticles synthesized from *Padina boergesensii*

Arockiam Sagina Rency, Lakkakula Satish, Shanmugaraj Gowrishankar, Manikandan Ramesh*

Department of Biotechnology, Science campus, Alagappa University, Karaikudi - 630 004.

E-mail: mrbiotech.alu@gmail.com

Abstract

Nanoscale materials hold great promise for both industrial and biomedical applications. In this study, the silver nanoparticles (AgNPs) were synthesized from *Padina boergesensii* seaweed by a green synthesis method. The synthesized AgNPs were confirmed by formation of dark brown color and characterized by UV-Visible spectroscopy, Fourier Transform Infrared Spectroscopy (FT-IR), X-ray diffraction (XRD), Scanning electron microscopy (SEM), Transmission electron microscopy (TEM), and Atomic force microscopy (AFM).

The antibacterial activity of the AgNPs were tested against clinical bacterial pathogens and confirmed through Light microscopy (LM), SEM and Confocal laser scanning microscopy (CLSM).

Introduction

Seaweeds are macroscopic benthic marine algae is one of the commercially important renewable marine living resources. Seaweeds are rich in several bioactive compounds against human pathogenic viruses, bacteria and fungi. Nanoparticles especially (gold & silver) are extensively used as medicinal agents for treating several diseases. Synthesis of nanoparticles from seaweeds is one of the emerging field because of its cost effectiveness, eco-friendly, easily scaled up for large scale synthesis. Current study discusses the AgNPs synthesized by the aqueous extract of sea weed *P. boergesensii* and its characterization and antibacterial activity.

Experimental Section

Ten gram of the dried seaweed powder was mixed with 100 ml of sterile deionised water and boiled for 15 min and filtered through Whatman no 1 filter paper. Then 1 mM AgNO₃ solution was added to the filtrate and incubated the mixture at room temperature and the dark brown color formation indicates the synthesis of AgNPs.

Results and Discussion

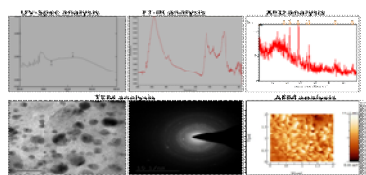


Figure.1

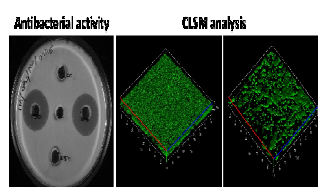


Figure. 2

The colorless reaction mixture turned dark brown color and showed UV-visible spectra of AgNPs. FTIR, XRD, SEM, TEM, AFM observation revealed the predominance of AgNPs (Fig. 1). AgNPs of *P. boergesensii* ($\mu\text{g/ml}$) significantly inhibited the biofilm formation and antibiofilm potential confirmed through LM, SEM and CLSM analysis (Fig.2).

Conclusion

Green synthesized AgNPs from *P. boergesensii* could be a starting point for the development of promising anti-pathogenic agent against the biofilm-associated infection.

Reference: Dhanalakshmi PK, Azeez R, Rekha R, Poonkodi S, Nallamuthu T (2012) Synthesis of silver nanoparticles using green and brown seaweeds. *Phykos* 42(2):39-45.

2.62 Lyotropic Liquid Crystal Assisted Preparation of Nanomaterials: A Greener Approach For The Controlled Growth

R.Umamaheswari, G.Karpagam, S.Umadevi*

Department of Industrial Chemistry, Alagappa University, Karaikudi, Tamilnadu, India.

E-mail: umadevilc@gmail.com and umanatarajan.2012@gmail.com

Lyotropic liquid crystals (LLCs) are interesting class of liquid crystal compounds which are formed by mixing an amphiphilic compound, generally a surfactant and water at a particular concentration. LLCs exhibit different phase structures namely hexagonal, cubic, reverse hexagonal and lamellar arrangements depending on the composition of the amphiphile and temperature. These phases display remarkable properties such as long range order and mobility at the nanoscale level which offer potential platform for the controlled syntheses and organization of nanomaterials. Indeed, LLC have been successfully employed as template for the synthesis of mesoporous materials, ordered metals, semiconducting nanomaterials, nanoscale polymers etc. [1] Recently, we have reported the preparation of gold nanoparticles in a hexagonal LLC phase that consists of water and the non ionic surfactant, triton X-100. [2] Interestingly, star shaped anisotropic nanoparticles with long well-defined thorns were obtained on carrying out the preparation in the LLC medium. Further, the nanostar dispersion in the LLC medium was stable for several months. Extending the work, herein we report our further studies on the influence of the LLC medium for the nanoparticle preparation. Both hexagonal and lamellar phase structures of the triton X-100 and water binary system are evaluated for the gold and silver nanoparticle preparation. The surfactant, Triton X-100, at a concentration ranging from 32.5 to 59.5wt% in water exhibits a hexagonal LLC phase at 25°C. The gold nanoparticles were prepared in the hexagonal phase at 25°C by reducing the chloroauric acid with a mild reducing agent ascorbic acid in presence of silver nitrate. On addition of the reagents, the yellow colour of the gold salt solution turned to deep blue colour. The colour change indicated the formation of nanoparticles which was confirmed through UV-Vis spectroscopy. The blue coloured nanoparticle dispersion

showed an absorption in the visible region with a maximum at 560nm (Figure 1i). Similarly, triton X-100 at a concentration 68-78% in water shows lamellar phase at 5°C. Reduction of silver nitrate with ascorbic acid in the lamellar phase at 5°C yielded a turbid white coloured solution. This solution showed an absorption in the visible region with a maximum situated at 400nm (Figure 1ii) indicating the formation of silver nanoparticles. The morphological studies of both gold and silver nanoparticles through transmission electron microscopy and scanning electron microscopy are underway. The above described method of nanoparticle preparation is simple, one pot preparation and more importantly a green approach since it does not involve any organic solvents or hazardous chemicals.

References

- [1] S. Saliba, C. Mingotaud, M. L. Kahn and J. Marty, *Nanoscale* 5(2013) 6641.
- [2] S. Umadevi, H.C. Lee, V. Ganesh, X. Feng and T. Hegmann, *Liq. Cryst.* 41(2014)265.

2.63 Synthesis and Physical Characterization of LiCoVO₄ nano cathode materials for the Rechargeable Lithium ion batteries

V. Jeyanthi, P. Naveenkumar and G. ParuthimalKalaigan*

Advanced Lithium-Ion Batteries Laboratory, Department of Industrial Chemistry, Alagappa University, Karaikudi-630 003.

*Corresponding Author phone No: +91-9443135307, Fax: +914565 225202.

Email id: pkalaigan@yahoo.com and naveenperumal@yahoo.com

Abstract

LiCoVO₄ cathode material was synthesized by the citric acid assisted Sol-Gel method. Stoichiometric amounts of Lithium acetate, Cobalt acetate, Ammonium meta-vanadate and citric acid were dissolved in triple distilled water and the p^H of the solution is set to be 1 with the help of the dil. HCl. It was stirred at 60°C for 24 hours to get viscous gel. The gel was dried at 120°C for about 12 hours and grinded to make a fine powder. The dried powder was calcined at 500°C in air for 5 hours in a muffle furnace. The final product was grounded well to get the nano powder of LiCoVO₄ cathode material. The phase purity and crystallinity of the synthesized samples was confirmed by XRD studies. UV-Visible spectroscopy was used to calculate the band gap energy of the synthesized cathode materials. The surface morphology and composition of the LiCoVO₄ were identified by SEM image and EDAX analysis respectively.

Key Words: LiCoVO₄, Sol-Gel Method, and Lithium-ion Batteries.

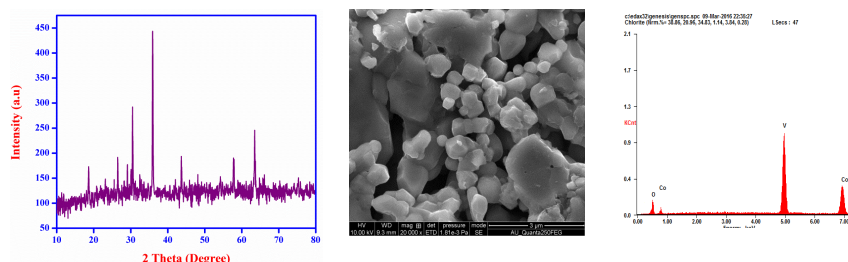


Figure 1. XRD patterns for pristine LiCoVO₄ Figure 2. SEM image of LiCoVO₄ with EDAX

References

1. G. T. K. Fey, W. Li, J. R. Dahn. *J. Electrochem. Soc.* 141 (1994) 227.
2. G. T. K. Fey, C. S. Wu. *Pure Appl. Chem.* 69 (1997) 2329.
3. S. T. Myung, K. Izumi, S. Komaba, Y. K. Sun, H. Yashiro, N. Kumagai. *Chem. Mater.* 17 (2005) 3695.
4. C. Julien, M. Massot, C. P'erez-Vicente, *Mater. Sci. Eng. B75* (2000) 6.

2.64 Development of Poly-anionic nano cathode materials for the Rechargeable Lithium-ion batteries

P. Naveenkumar and G. ParuthimalKalaigan*

Advanced Lithium-Ion Batteries Laboratory, Department of Industrial Chemistry,
Alagappa University, Karaikudi - 630 003, India.

*Corresponding Author phone No: +91-9443135307, Fax: +914565 225202.

Email id: pkalaigan@yahoo.com and naveenperumal@yahoo.com

Abstract

Li₂CoSiO₄ nano cathode material was synthesized by citric acid assisted Sol-Gel method. Thermal

decomposition and phase transition of the dry powder was analyzed by TG/DSC techniques. The dry powder was calcined at 800°C for 10 hours in nitrogen atmosphere. The phase purity of the synthesized samples was confirmed by XRD. FT-IR spectral data was confirmed the presence of SiO₂ in Li₂CoSiO₄ nano cathode materials. UV-Visible spectroscopy data was used to calculate the band gap energy of the cathode materials. The surface morphology and composition of the Li₂CoSiO₄ were studied by SEM with EDAX. The coin cell was assembled using Lithium foil anode, Li₂CoSiO₄ powder as a cathode material, polypropylene separator and LiPF₆ in Ethylene carbonate / Dimethyl carbonate (1:1 v/v) as Electrolyte. The performance of the coin cell was tested by electrochemical methods. Cyclic voltammetry study was revealed the reversibility of the electrode during charge/discharge process. Electrochemical Impedance spectroscopy results were used to calculate the diffusion coefficient of Li⁺ ions during the Intercalation/de-intercalation process. The charge/discharge studies were carried out in the voltage window of 1.5 to 4.5V at 1C rate. The coulombic efficiency and capacity retention parameter were derived from the charge/discharge results.

Key Words: Lithium Cobalt silicate, UV-DRS, EIS and Poly-anionic Cathode Materials.

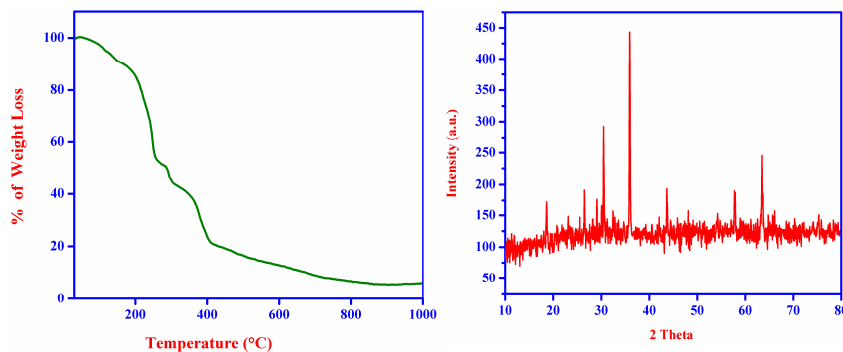


Figure 1. Thermo gravimetric Analysis of the Pristine Li₂CoSiO₄, Figure 2. XRD Analysis of the Pristine Li₂CoSiO₄.

References

- [1]. Michał Świątosławski, Marcin Molenda, Piotr Natkański, Piotr Kuśtrowski and Roman Dziembaj, *Functional Materials Letters*, 7, 6 (2014) 1440001.
- [2]. M. K. Devaraju, Q. D. Truong and I. Honma, *RSC Advances*, 3, (2013) 20633.
- [3]. D. Santamaría-Pérez, U. Amador, J. Tortajada, R. Dominko, and M. E. Arroyo-de Dompablo, *Inorganic Chemistry*, 51, (2012) 5779 – 5786.

2.65 In-Situ Synthesis, Functionalization And Fabrication of Flexible Electronics Using Graphene-PANI Derivative Nanocomposites

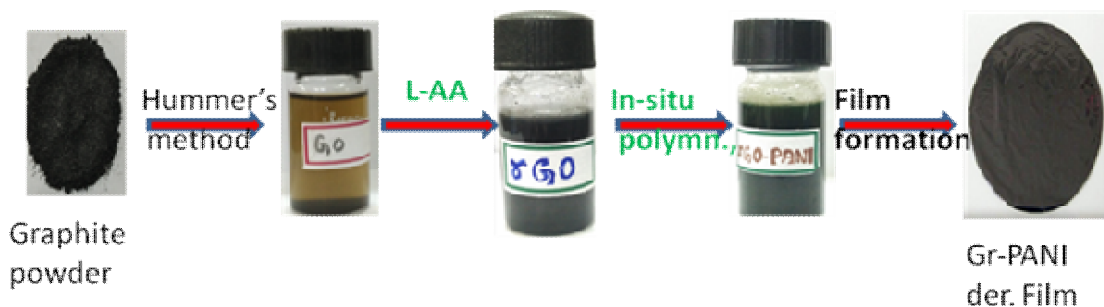
C.Sathya^a and S.Viswanathan^a and C.Sivakumar^b

^aDepartment of Industrial Chemistry, Alagappa University, Karaikudi-630003. ^bElectrodics and Electrocatalysis, CSIR-Central Electrochemical Research Institute, Karaikudi-630 006, Tamil Nadu, India.

*Corresponding Author E-mail: rsviswa@gmail.com

Abstract

Functionalization of graphene with conducting polymer is an attractive research for the fabrication of flexible materials in the field of nano-electronics, display and energy storage devices. Various methods have been reported for the preparation of flexible pristine graphene and its derivative using tailored chemical, electrochemical and photochemical methods [1, 2]. In the present work, functionalized graphene-PANI derivative nanocomposites have been successfully synthesized by simple two step procedure. First reduced graphene oxide (rGO) was prepared from graphite powder by modified Hummer's method. In the second step, functionalization and *in-situ* polymerization were done by using chemical route. By controlling the reaction conditions, various flexible graphene-PANI derivative films were obtained (scheme-1) and these functionalized rGO-PANI derivative nanocomposites were characterized through different spectral tools like UV-Visible, FT-IR & Raman, XRD, and SEM. Electrochemical characterizations and electrical conductivity were performed towards its ready to end-user application. This synthetic route provides a general route for preparing transparent flexible electronics through graphene based conducting polymer films.



Scheme-1: Illustrate the fabrication graphene-PANI derivative film Graphite powder

Key words: Graphene, PANI Derivative, insitu synthesis and flexible electronics

Reference:

- [1] M. J. McAllister, J. L. Li, D. H. Adamson, H. C. Schniepp, A. A. Abdala, J. Liu, M. Herrera-Alonso, D. L. Milius, R. Car, R. K. Prud'homme, I. A. Aksay, Chem. Mater. 19 (2007) 4396.
 [2] Q. Du, M. Zheng, L. Zhang, Y. Wang, J. Chen, L. Xue, W. Dai, G. Ji, J. Cao, Electrochim. Acta 55 (2010) 3897.

2.66 Synthesis and antibacterial evaluation of amide linked N-formyl-pyrazolines

R. Selvi*, S. Sudalaimani and L. Pushpa Radhika

Department of Chemistry, Manonmaniam Sundaranar University, Tirunelveli – 627 012, Tamilnadu, India.

E-mail: cheselvrams@gmail.com

Abstract

Nitrogen containing five membered heterocyclic compounds are biologically active in nature. Among the nitrogen containing compounds, pyrazolines and their derivatives have been reported to possess diverse pharmacological activities such as antimicrobial¹, antioxidant², and antibacterial³. Benzamide containing compounds are widely used in pharmaceuticals⁴ and possess potent antiproliferative activity⁵. In view of these observations we are inspired to synthesize amide linked N-formyl-pyrazoline analogues as antibacterial agents.

In the present study, we report the synthesis of amide substituted N-formyl-pyrazolines from the reaction of amide linked chalcone with hydrazine hydrate and formic acid in good yields. The structures of the synthesized compounds were characterized by spectral methods. All the synthesized compounds exhibit significant antibacterial activity against Klebsiella pneumonia, Escherichia coli, Staphylococcus aureus, Pseudomonas aeruginosa, Bacillus subtilis and Malolactic bacteria.

References

1. J. Rangaswamy, H. Vijay Kumar, S. T. Harini and N. Naik. *Bioorganic & Medicinal Chemistry Letters* 22 (2012) 4773–4777.
2. A. Kumar, B. G. Varadaraj, R. K. Singla. *Bulletin of Faculty of Pharmacy* 51 (2013) 167–173.
3. B. S. Kitawat and M. Singh. *New Journal of Chemistry* 38 (2014) 4290–4299.
4. V. R. Pattabiraman and J. W. Bode. *Nature* 480 (2011) 471–479.
5. M. H. Kim, M. Kim, H. Yu, H. Kim, K. H. Yoo, T. Sim and J. M. Hah. *Bioorganic and Medicinal Chemistry* 19 (2011) 1915–1923.

2.67 Structural and Morphological properties of polypyrrole doped Sb₂S₃ thin films

J. Umadevi^a, N. Anandhan^{a*}, V. Dharuman^b, G. Gopu^c, M. Karthikeyan^a, A. Amali Roselin^a, C. Suganya^a, P. Rajeswari^a

^aAdvanced Materials and Thin film Physics Lab, Department of Physics, Alagappa University, Karaikudi-4.

^bMolecular Electronics Laboratory, Department of Bioelectronics and Biosensors, Alagappa University, Karaikudi -4.

^cCatalytic and Supercapacitor Lab, Department of Industrial Chemistry, Alagappa University, Karaikudi-3.

E-mail: anandhan_kn@rediffmail.com

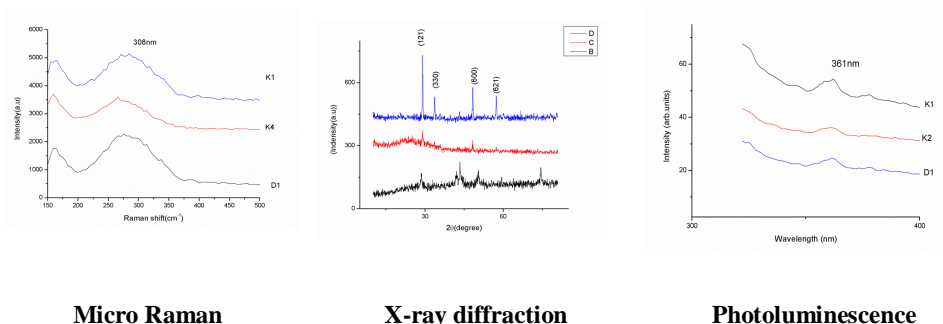
Abstract

Polypyrrole doped Sb₂S₃ thin film has been deposited on stainless steel substrate by electrodeposition technique. Procedure involves preparation of acidic solution consisting of acetic acid (glacial, CH₃CO₂H) and Na₂S₂O₃ as the sulphide source. Preparation of antimony precursor solution involves mixing of 0.01 M SbCl₃, 0.1 M Na₂S₂O₃ and 0.025 M EDTA. The Antimony precursor solution is mixed again with 15 mL of sulphite solution. Cyclic voltammetry characterization was made using conventional three electrode system to identify

the redox potential of antimony sulphide and reduction potential of -0.5 V is found to be optimal potential for doping Sb_2S_3 in polypyrrole matrix [1] and the pH is maintained at constantly at 1.68. The surface is studied by X-ray diffraction (XRD), Scanning electron microscope (SEM), micro Raman, and Fourier transform infrared spectroscopy (FTIR) techniques. The X-ray diffraction pattern of the film showed that the deposited film is being orthorhombic crystal structure that showed a diffraction peak at an angle $2\theta=29.04^\circ$ corresponding to the reflection plane (021) [2]. The PL spectra of $\text{Sb}_2\text{S}_3/\text{polypyrrole}$ exhibits emission peak at 361nm, [3], and ascertained to blue green emission region. Hence, these devices can be used for chemical and biosensor applications and discussed.

Keywords: Polypyrrole, Sb_2S_3 thin films, Electrodeposition method .

Graphical Abstract:



Micro Raman

X-ray diffraction

Photoluminescence

References

- [1]. Rajpure K.Y., Bhosale C.H. J. Physics and chemistry of Solids, 61, 561-568, 2000.
- [2]. Subramanian .S, Chithra lekha, Physica B, 405,925-931, 2010.
- [3]. Srikanth.S, Suriyanarayanan .N, optoelectronics and advanced materials- rapid communications, 4, 2057-2058, 2010.

2.68 Facile synthesis and characterization of CeO_2 particles as function of various Precipitation agents by Modified Co-Precipitation method.

^{1,2}M.Ramachandran, ²R.Subadevi, ²M.Sivakumar*

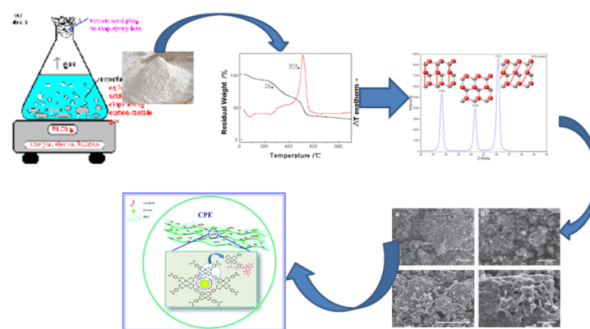
¹Department of Physics, Arumugam Pillai SeethaiAmmal College, Tiruppattur 630211, India

²School of Physics, Alagappa University, Karaikudi, India

(Email: susiva73@yahoo.co.in – M.Sivakumar)

Abstract

As one of the most reactive rare-earth metal oxides, ceria (CeO_2) has concerned extensive interest recently due to the hope it raises for many technological applications in a wide range of fields. The three-way catalysts, oxygen sensors, solid fuel cells, and UV blockers are just a few representative examples [1]. In this attempt, the crystalline phase of pure CeO_2 with various morphologies has been directly synthesized using Cerium nitrate as a raw material and Sodium hydroxide (NaOH), Potassium hydroxide (KOH), sodium carbonate (Na_2CO_3) and Ammonia (NH_3) as a precipitating agent at room temperature by simple green modified Co-precipitation method [2]. The thermal history of the prepared precursors was analyzed by TG/DTA analysis.



During structural characterization techniques, including X-ray diffraction (XRD), Fourier infrared (FTIR), scanning electron microscopy (SEM) were performed on the final product. The X-ray diffraction patterns of the

obtained samples were confirmed with a cubic structure of cerium oxide with space group Fm-3m which was in agreement with the JCPDS No: 81-0798. The infrared spectrum showed that a strong band below 700 Cm^{-1} due to the Ce-O-Ce stretching vibrations. The microstructure of the SEM images seems to be ultra-small and agglomerated. The as prepared CeO_2 particle will be used as filler in the Composite polymer electrolyte.

Key words: CeO_2 , Co-precipitation method.

References:

- [1] Y Chen, T Liu, CL Chen, WWGuo, RSun, ShuhuiLv, M Saito, S Tsukimoto, ZC Wang; Ceramic International 39(2013) 6607-6610.
- [2] M Razaeei, S.M Alavi, S Sahebdehfarand FYZi; J.Porous Mater. 15(2008) 171-179.

3.1 Biosensors for health and safety monitoring

M.S. Thakur

Visiting Professor, Center for Material Science and Technology, University of Mysore, Mysore 570006

E-mail: msthakur@yahoo.com

Applications of biosensors for health, food, environment and defence have increased in recent years. **Biosensor** systems are emerging as one of the advanced diagnostic tools for molecular diagnostics due to their rapidity, specificity, ease of mass fabrication, economics and field applicability. They obtain their specificity and sensitivity from biological binding reactions such as antigen/antibody, enzyme/substrate/cofactor, receptor/ligands and nucleic acid hybridization in combination with a range of physical transducers. The market for the biosensors is US \$ 12 billion and it is growing rapidly. Several commercial biosensor devices for diabetic diagnostics have taken major market share. Many companies in the world over manufacturing biosensor based on optical phenomenon such as surface Plasmon resonance, fluorescence, reflectance, chemiluminescence, bioluminescence, Electrochemical principle such as potentiometric, amperometric and conductometric, quartz crystal microbalance, cantilever based systems, MEMS (micro-Electro-mechanical systems) have been used to fabricate biosensors. Recently, nano technology-based systems becoming more popular for sensitive detection and affordable diagnostics.

Nano-biotechnology has advanced in the field of biosensor through the use of novel materials such as gold nanoparticles, carbon nanotubes and quantum dots (QD). Small size, high photo-stability and size tunable emission properties make QD highly attractive materials in the field of biological analysis allowing high sensitivity and rapid analysis. These particles can be synthesized by physical as well as chemical processes. These particles have characteristic size, high photo-stability and size tunable emission properties make them highly attractive materials in the field of biological analysis with high sensitivity and rapid analysis for many bioassays.

Studies on the immobilization of antibodies for on Nanoparticles to detect pathogens, pesticides and toxins have recently been reported using fluorescence and Surface Plasmon resonance (SPR). Quantum Dots (QDs) can be used as suitable fluorescent labels/probes for their application in immunoassays for the detection of small biomolecules (biomarkers of pesticide exposure) in place of conventional dyes. The spectral properties of QD allow the multi-analyte detection of the targets. Therefore, the bioconjugation of these QDs for biological fluorescent labeling may be of interest as compared to organic fluorescent dyes. These intrinsic properties of QDs have been used for the sensitive detection of target analytes. The application of water-soluble bio-conjugated QDs for the detection of food contaminants such as pesticides, pathogenic bacterial toxins and for the development of oligonucleotide-based microarrays were done to detect these analytes at very low concentrations. Furthermore, the utilization of significant changes in the spectral behavior of QDs and nanoparticles due to resonance energy transfer/Bioluminescence resonance energy transfer and localized surface plasmon resonance with bio-conjugation has potentials in future nanobiosensor development.

Biophotonics is an emerging area employing the photonic based emission system from biological source. Light generation by the biological elements such as luciferase enzyme systems, alkaline phosphatase, horse radish peroxidase and luminol system, have numerous applications in health, food hygiene, sanitation, toxin and pathogen diagnosis. These biomolecules being specific and highly sensitive find better prospects in future in the field of bioimaging, studying host pathogen interaction and developing ultrasensitive biomarkers.

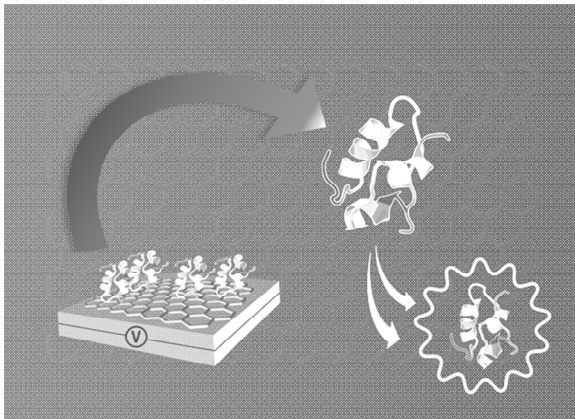
The *lux cassette* is an array of genes that codes for bacterial bioluminescence. Recombinant bacteriophages carrying *lux cassette* is selective for a bacterium. Hence based upon the light emission selective bacterial pathogens can be quantified. The antibodies against food toxins can be generated into animal models such as poultry to get IgY antibodies. These antibodies have affinity towards its corresponding toxin. The bio-conjugation of luciferase enzymes with these antibodies can quantify the amount of toxin present in a sample through the intensity of light emission unlike conventional ELISA based methods. This method is popularly known as bioluminescent immunoassay (BLEIA). Further the *lux* marker gene has also been inserted into certain pathogenic microbes and its pathogenicity in animal models has been studied extensively elsewhere. Thus host pathogen interaction study may find immense help in drug discovery. Concluding, biophotonics based biosensor systems has dramatically improved the present state of available diagnostic methods and is futuristic.

3.2 Reduced graphene oxide: Sensing, delivery, therapy

Sabine Szunerits

Institut d'Electronique, de Microélectronique et de Nanotechnologie (IEMN), UMR CNRS 8520, Université Lille1, Avenue Poincaré-BP 60069, 59652 Villeneuve d'Ascq, France. E-mail : Sabine.Szunerits@univ-lille1.fr

Graphene and its derivatives (graphene oxide, reduced graphene oxide) have drawn tremendous attention from the scientific community as a promising nanomaterial with applications ranging from optoelectronics, high-energy physics, to material science and biomedicine. Different methods have been reported for the preparation of the different graphene-based matrixes. In the sensing area, the choice of the way graphene is obtained is crucial and will influence strongly electron transfer rates, the shape and position of plasmonic bands but will also impact on sensitivity and selectivity to solution analytes. Besides careful



functionalization of graphene, emphasis has to be put on the optimization of the interface design. The majority of electrochemical sensors are produced by simple drop casting with a reduced graphene oxide (rGO) suspension, a method far away from a carefully designed electrode with an optimal structure.

In the first part of this presentation, I will discuss different strategies employed for the formation or reduced graphene oxide (rGO) and rGO-based composite materials. A special focus will be on the use of electrophoretic based approaches for the deposition of rGO and hybrid materials. The use of such interfaces for sensing applications, electrochemically release of drugs and its photo-thermal activity will be presented in addition.

References:

- [1]. Kaminska et al. Chem. Commun. 2012, 48, 1221-1223 (cover page)
- [2]. Kaminska et al. ACS App. Mater. & Interfaces, 2012, 4, 1016-1020
- [3]. Kaminska et al. ACS App. Mater. & Interfaces, 2012, 4, 5386-5393
- [4]. Kaminska et al. Biosensors and Bioelectronics, 2013, 50, 331-337
- [5]. P. Subramanian et al. Biosensors and Bioelectronics, 2013, 50, 239-243
- [6]. K. Turcheniuk et al. RSC Adv. 2014, 4 (2) 865-875.
- [7]. P. Subramanian et al. ACS Applied Materials & Interfaces 2014, 6, 5422-5431
- [8]. P. Subramanian et al. J. Mater. Chem. A 2014, 2, 5525-5533
- [9]. O. Zagorodko et al. Anal. Chem. 2014, 86, 11211-11216
- [10]. G. Daradbhara et al. J. Mater. Chem. B, 2015, 3, 20254-20266
- [11]. K. Turcheniuk et al. J. Mater. Chem. B 2015, 3, 375-386
- [12]. F. Teodorescu et al. Chem. Commun, 2015, 51, 14167

3.3 CeO₂/Nile blue nanocomposite modified glassy carbon electrode for selective detection of dopamine in presence of Ascorbic Acid

S. Selvarajan^a, A. Suganthi^{a*}, M. Rajarajan^b

^a PG & Research Department of Chemistry, Thiagarajar College, Madurai - 625009, Tamilnadu, India.

^b PG & Research Department of Chemistry, Cardamom Planter Association College, Bodinayakanur - 626513, Tamilnadu.

E-mail: suganthicarts@gmail.com, selvarajancy@gmail.com

Abstract

A novel Organic-inorganic nanocomposite of nileblue (NB) and CeO₂ was synthesized and successfully characterized by UV-vis-diffuse spectroscopy, X-ray diffraction (XRD), scanning electron microscopy (SEM) and infra-red spectroscopy. The as-prepared CeO₂/NB modified GCE was applied for highly selective and sensitive detection of dopamine (DA) in the presence of ascorbic acid (AsA) in 0.1M PBS (pH7.0) by DPV (Differential Pulse Voltammetry) technique. The separation of the oxidation peak potentials for DA-AsA was about 0.194 V. This excellent electrochemical performance can be attributed to the unique structure of CeO₂/NB composite. The response of the electrochemical sensor varies linearly with the DA concentration ranging from 5µM to 50µM with a detection limit of 0.050µM (S/N=3). Moreover, CeO₂/NB modified glassy carbon electrode (GCE) exhibits an excellent catalytic activity, long-term stability and reproducibility.

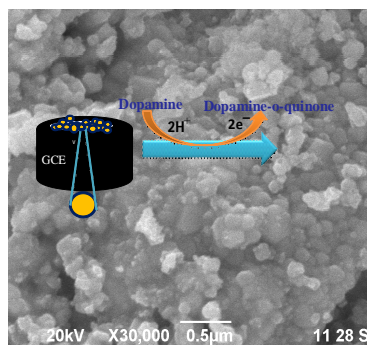


Figure.1. Mechanistic route for the electrochemical detection of dopamine.

Keywords: CeO₂, Nile blue, Differential Pulse Voltammetry, Dopamine.

References

- [1] A. Noorbakhsh, A. Salimi, *Electrochimica Acta*, 54 (2009) 6312–6321.
 [2] S. Saha, S.K. Arya, S.P. Singh, V. Gupta, *International J of Electrochem*, 2011. Article ID 823734, 6 pages.

3.4 Electrochemical guanine sensing based on Ni ion irradiated WO₃ thin films

A.C. Anithaa^a, K. Asokan^b, C. Sekar^{a*}

^aDept. of Bioelectronics and Biosensors, Alagappa University, Karaikudi 630003, TN, India

^b Materials Science Division, Inter-University Accelerator Centre, New Delhi 110067, India

Tel.: +91 9442563637; * E-mail: Sekar2025@gmail.com

Abstract

Deoxyribonucleic acid (DNA) analysis plays an ever-increasing role in food technology, disease diagnosis, genetic mutations, drug discovery and forensics. Guanine (2-amino-1, 7-dihydro-6H-purin-6-one) is the most readily oxidized component of the nucleic acid bases in DNA. It is mostly found in physiological fluids, tissues and cells related to the nucleic acids, the enzymatic degradation of tissues and dietary habits. Therefore, changes in the concentration of guanine are considered as important parameter for diagnosis of cancers, AIDS, myocardial cellular energy status, disease progress and therapy responses. Therefore, the determination of guanine is important in physiology and clinic fields. Although many electrochemically modified electrodes have been reported for guanine detection, still there is a need to develop new method with high efficiency and convenience for the precise determination of guanine [1-3]. Here we propose a new strategy of using the swift heavy ion (SHI) irradiated (Ni¹¹⁺, 150 MeV) tungsten trioxide (WO₃) thin films spin coated on indium tin oxide (ITO) electrodes and its application for electrocatalytic oxidation of guanine (Fig. 1). Ni ions with various fluences (5x10¹¹ to 5x10¹³ ions/cm²) were irradiated on WO₃ films and its influence on surface morphology, structural and electrical properties of WO₃ has been investigated. Powder XRD results reveal the variation in crystallite size and strain with the change in fluences but the monoclinic structure of WO₃ remained unchanged. AFM and Hall Effect studies showed that the films irradiated at high ion fluence have vertical standing needle-like or hillock morphology with increase in roughness which is directly related to the increase in density of defects. Cyclic voltammetry and electrochemical impedance spectroscopy of redox electrolyte were investigated and the results displayed an enhanced conductivity for 5x10¹² ions/cm² irradiated WO₃ modified ITO when compared with non-irradiated films. Differential pulse voltammetric (DPV) studies of SHI-WO₃/ITO exhibited improved electrocatalytic activity towards the oxidation of guanine in 0.1 M phosphate buffer solution (PBS, pH 7.0). A linear curve between current response and guanine concentration was established over a wide linear range of 0.005-160 μM, and the lowest detection limit was found to be 2.3 nM (S/N = 3). The fabricated guanine sensor showed an excellent anti-interference ability against potentially coexisting electroactive species, good stability and excellent reproducibility. The proposed sensor was successfully applied to the detection of guanine in milk, plasma and urine samples with satisfactory recovery.

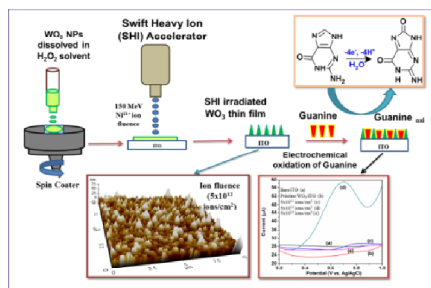


Fig. 1. Schematics showing the approach used for the determination of guanine based on swift heavy ion irradiated WO₃ thin films spin coated on ITO substrate.

Keywords: Swift heavy ion, irradiation, fluence, WO₃ thin films, guanine, biosensor.

References

- [1]. S. Amanpreet, S. Ajnesh, S. Narinder, Dalton Trans. 43 (2014) 16283-16288.
- [2]. R. Vairamuthu, S. Jayachandran, R. Panchanathan, RSC Adv. 4 (2014) 33874-33882.
- [3]. A.C. Anithaa, N.Lavanya, K. Asokan, C. Sekar, Electrochim. Acta167 (2015) 294-302.

3.5 Room Temperature CO Gas Sensor based on CuO-ZnO loaded Polypyrrole Nano Composite

Heiner.A.J and Gurunathan.K*

Nano Functional Materials Lab, Dept. of Nanoscience & Technology, Science Campus, Alagappa University, Karaikudi, Tamilnadu, India – 630 003. e-mail: kgnathan27@rediffmail.com

Nanomaterials have high impact in research field due to its enhanced electrical and electronic properties. In the field of gas sensors, many researchers are focusing on the conducting polymer- metal oxide nano composites because of its high sensitivity and selectivity towards hazardous gases at room temperature. Carbon monoxide (CO) is one of the most hazardous gases and it has many negative impacts on both environment and living organisms. Inhalation of carbon monoxide reduces the oxygen level in blood and continuous inhalation leads to even death of human beings. It has also responsible for formation of smog and ground level ozone. So detection of Carbon monoxide in atmosphere is essential to reduce toxicity level of environment. Hetero junctions formed by Zinc oxide and Copper oxide have high sensitivity towards the carbon monoxide. Presence of π – electrons in polypyrrole leads to room temperature operation of the nano sensor. The sensor electrode formed by the polypyrrole – metal oxide nano composite has improved sensitivity and selectivity towards carbon monoxide at room temperature. The synthesized nano composite were characterized by UV-visible absorption spectroscopy, Fourier Transform Infrared (FTIR) Spectroscopy, X-ray Diffraction, Scanning Electron Microscopy (SEM) and Transmission Electron Microscopy (TEM).

CuO – ZnO nano composite was synthesized by one pot sol – gel method. Polypyrrole was synthesized by Chemical Polymerization method. Metal oxide nanocomposite synthesized by sol – gel method was included in the polymerization process to incorporate the nano- composite with the conducting polymer. Metal oxide nano composites were added in different weight ratios (10%, 30% and 50%) with polypyrrole to analyze the gas sensing property of the nano composites with different compositions. Comparative study of the gas sensing property of the nano composite material with different weight ratio was carried out to conclude the composite ratio with high sensing capability.

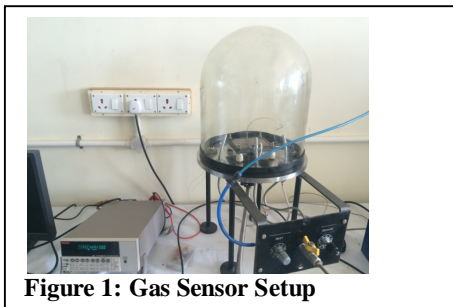


Figure 1: Gas Sensor Setup

When the sensing electrode was exposed to the gas, the resistivity of the material gets altered. This change in resistivity can be monitored using Four-Probe technique. In this method, constant current was given as input to the material. During exposure of gas, the change in resistance was measured by monitoring the output voltage across the material. Response time and Recovery time of the sensing electrode was recorded by using homemade gas sensor setup. Synthesized Nano composites exhibits improved Stability, Selectivity, Sensitivity, Response time and Recovery time towards hazardous Carbon Monoxide gas.

Reference:

- [1]. M.A. Chougule, D.S. Dalavi, Sawanta Mali, P.S. Patil, A.V. Moholkar, G.L. Agawane, J.H. Kim, Shashwati Sen, V.B. Patil, Measurement 45 (2012) 1989–1996
- [2]. Nianqiang Wu, Minhua Zhao, Jian-Guo Zheng, Chuanbin Jiang, Ben Myers, Shuoxin Li, Minking Chyu and Scott X Mao, Nanotechnology 16 (2005) 2878–2881
- [3]. H. Gong, J.Q. Hu, J.H. Wang, C.H. Ong, F.R. Zhu, Sensors and Actuators B 115 (2006) 247–251

3.6 The behavior of binary lipid on different chain length thiol monolayer modified gold electrode

Karutha Pandian Divya and Venkataraman Dharuman*

Molecular Electronics Laboratory, Department of Bioelectronics and Biosensors, Science Block, Alagappa University, Karaikudi – 630 004. E-mail: dharumanudhay@yahoo.com

Cationic liposomes have been studied for various applications in nanobiotechnology, drug delivery and

analytical chemistry. Literature strongly indicates that the effectuality of cationic liposome increases when combined with a zwitterionic liposome. The behavior of binary lipid mixture on solid surface is attempted for the first time. The cationic liposome N-[1-(2,3-Dioleoyloxy)propyl]-N,N,N-trimethylammonium propane (DOTAP) and the zwitterionic liposome 1,2-Dioleoyl-sn-Glycero-3-Phosphoethanolamine (DOPE) have been mixed together and immobilized on three different chain length thiol monolayers such as Cysteamine (Cyst), Mercapto propionic acid (MPA) and Mercapto undecanoic acid (MUDA). Among the three monolayers studied, MPA accounts for the spherical structure of binary lipid which is well established through the sigmoidal curve provided by Cyclic Voltammetry (CV) Fig 1. The structure control of binary lipid is attributed by the use of gold nanoparticle. The DOPE-DOTAP-AuNP is applied for electrochemical label free DNA sensing for the first time. The complementary target (named as cDNA), non-complementary target (un-hybridized named as ncDNA) and single base mismatch target (named as SMM) hybridized surfaces are discriminated sensitively and selectively in presence of $[\text{Fe}(\text{CN})_6]^{3-/4-}$, Fig.2. The result establishes an effective method of electrochemical label free DNA sensing using the binary lipid.

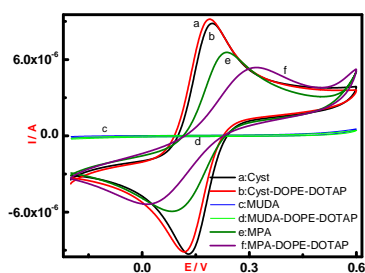


Fig 1

Fig 1: CV behavior of three thiol monolayers (curve a-Cyst) (curve c-MUDA) (curve e-MPA) sequentially modified with binary lipid mixture (curve b, curve d, curve f)

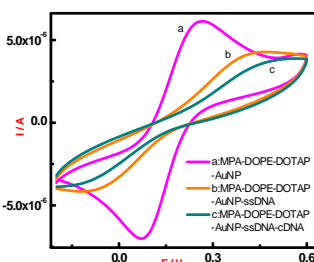


Fig 2

Fig 2: CV behavior of the gold transducer sequentially modified with MPA-DOPE-DOTAP-AuNP (curve a), ssDNA (curve b) and cDNA (curve c)

Keywords : Liposome, DNA sensing, Gold nanoparticle, Cyclic Voltammetry

3.7 Studies of self-assembled binary mixed monolayer for label free DNA hybridization electrochemical sensing on liposome – gold nanoparticle composite tethered on gold transducer

Naganathan Dhanalakshmi, Venkataraman Dharuman*

Molecular Electronics Laboratory, Department of Bioelectronics and Biosensors, Science Block, Alagappa University, Karaikudi – 630 004. E-mail: dharumanudhay@yahoo.com

Liposomes are composed of phospholipids and its biocompatible character helps in DNA sensing, drug delivery and gene therapy application. The spherical liposome structures undergo rupture and vesicle fusion to form bilayer structure on the solid electrode surface. Hence, it is a great challenge to anchor liposome in the spherical shape on electrode surface. Comparison of literature reports on the lipid layer formation on short chain monolayer facilitate defective layer on surface and long chain monolayer create negative effect on charge transport kinetics. In this work, binary mixed monolayer mixture of short chain diluent and long chain diluent is used as a platform for investigating the structural changes of the lipid layer. The cationic liposome N-[1-(2,3-Dioleoyloxy)propyl]-N,N,N-trimethylammonium propane (DOTAP) is placed in-between the binary mixture of short and long chain monolayer. Target self-assembled binary mixed monolayer is constructed by simple sequential adsorption of thiol capped 6-mercapto-1-hexanol (MCH) and 3-mercaptopropionic acid (MPA) diluents and studied for spherical nature of liposome-gold nanoparticle composite (Fig.1) and applied for detection of DNA hybridization sequence by electrochemical method.

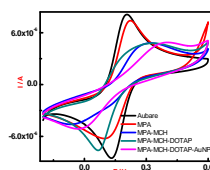


Fig.1 Cyclic voltammetry behavior of liposome-gold nanoparticle composite on binary mixed monolayer modified gold electrode

3.8 An Electrochemical biosensor methyl parathion on immobilization of acetylcholinesterase on Ironoxide - Chitosan nanocomposite

S. Muthumariappan and C.Vedhi*

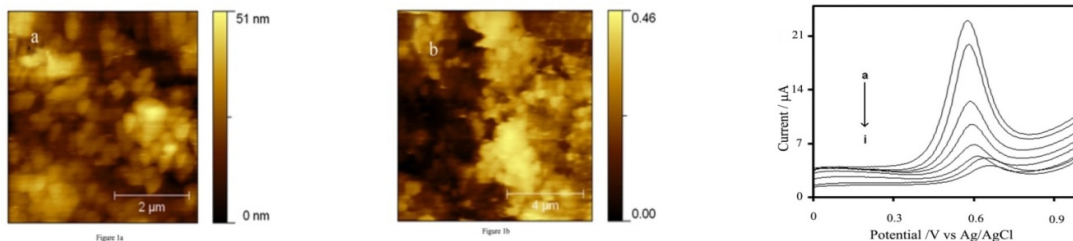
PG & Research Department of Chemistry, V.O.Chidambaram College, Tuticorin –628008, Tamilnadu, India

*E-mail: cvedhi@rediff.com, s.muthumariappan@yahoo.com

Abstract

Biosensing of methyl parathion (MP) based on acetylcholinesterase (AChE) immobilization on iron oxide – chitosan modified glassy carbon electrode was studied. Iron oxide – chitosan acts as a biocompatible immobilization matrix for AChE. The fabricated biosensor device is characterized by AFM and FT-IR. AFM of ironoxide-chitosan composite was exhibits nanosized particle surface. Immobilization of AChE on GCE/ Fe₃O₄ - chitosan was confirmed through AFM and FT-IR studies. Electrochemical oxidation of acetylthiocholine chloride occurs at 0.7V vs. Ag/AgCl at iron oxide – chitosan/AChE modified electrode in pH 7. Various experimental parameters such as effect of scan rate, MP concentration, effect of substrate concentration, enzyme loading and incubation time have been studied. The calibration curve has been constructed using square wave voltammetry in the concentration range 2×10^{-9} M and 70×10^{-9} M with good reproducibility and stability. The sensor is found to have an estimated detection limit of 1×10^{-9} M for an S/N =3 and a 3 % relative standard deviation. The biosensor has been applied for the determination of methyl parathion spiked into vegetable sample of carrot.

Keywords: Biosensor, Acetyl cholinesterase, Methyl parathion, Iron oxide, chitosan



AFM images of (a) GCE/iron oxide – chitosan (b) GCE/iron oxide-chitosan/AChE (c) Square wave voltammetric of various concentration of methyl parathion ranging from (a)10 nm (b)50 nm (c)100nm (d)200 nm (e)300 nm (f)400 nm (g)500 nm (h)750 nm

3.9 Electroanalysis of heavy metals in seaweed using multiwalled carbon nanotubes modified glassy carbon electrode

A.Vimala and C.Vedhi*

Department of Chemistry, V.O.Chidambaram College, Tuticorin – 628008, Tamilnadu, India

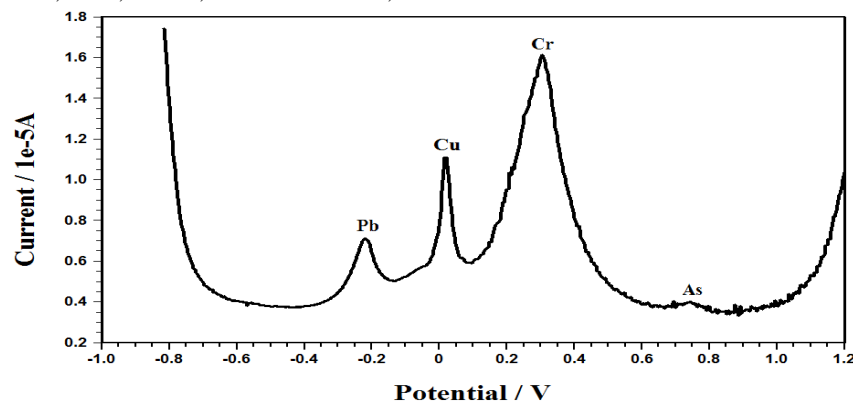
Tel: +91 4612310175, +91 9092368104, *E-mail: cvedhi@rediffmail.com (or) cvedhi23@gmail.com

Abstract

Fourier Transform Infrared (FT-IR) Spectroscopy was recorded to identify the heavy metals of Pb, Cu, Cd, Ni and Cr in seaweed. The ability of the ICP/OES (Inductively Coupled Plasma/Optical Emission Spectroscopy) system was to perform traces of multielement analyses in the seaweed sample. From atomic absorption spectroscopic (AAS) studies was observed Co and Ni trace, Pb, Cr and Cu minor and Fe major amount in seaweed. Image based analysis of phase angle distribution of heavy metals from seaweed across a surface was interpreted through atomic force microscopy. Voltammetry is recognized as one of the most powerful tools in trace and ultra trace analysis of metal ions because it provides wide linear dynamic range, low detection limit and multi-element analysis capability. The potential is varied in some systematic manner to cause electro active chemical species to be reduced or oxidized at the electrode. Multiwalled carbon nanotubes modified glassy carbon electrode (MWCNTs / GCE) have been developed in this investigation for the trace analysis of heavy metals. The resultant current is proportional to the concentration of metal. Under the optimum conditions, the electrochemical behavior of cyclic voltammetry (CV), linear sweep anodic voltammetry (LSAV), and

differential pulse anodic voltammetry (DPAV) were studied on modified glassy carbon electrode. The cyclic voltammetric behavior at different scan rates revealed the adsorption controlled oxidation of heavy metals. The peak current showed increasing trend with increase in concentration. By varying the concentration from 2000 to 3125ppm was studied at a constant scan rate of 50mV/s by LSAV. Two well defined anodic peaks may be representing Cu and As. Square wave anodic voltammetric studies of seaweed on modified glassy carbon electrode showed the four well defined anodic peaks representing Pb, Cu, Cr and As. From the straight line with good correlation, the linear dependence of peak current with concentration was understood. Differential pulse anodic voltammetric studies on MWCNTs modified GCE also revealed the same four well defined anodic peaks around 0.223V (Pb), 0.0152V (Cu), 0.3047V (Cr) and 0.7377V (As). R^2 values of Pb, Cu, Cr and As were found to be 0.988 (Pb), 0.989 (Cu), 0.985 (Cr) and 0.979 (As) respectively. The modified GCE was found to very high current values for all the four metals.

Key words: FTIR, AAS, DPAV, MWCNTs / GCE, Sea weed



DPAV behaviour of 3125ppm *Caulerpa scalpelliformis* on MWCNTs / GCE at pH 7

3.10 Glassy Carbon Electrode modified with poly (Glutamic Acid) as a probe for the Voltammetric Determination of Thymine

Jesny S.^{a,b} and K. Girish Kumar^b

^a Department of Applied Chemistry, Cochin University of Science and Technology, Kochi-22, Kerala, India.
giri@cusat.ac.in

^b Department of Chemistry, Sree Narayana College, Cherthala, Kerala, India. jesnysmail@gmail.com

Thymine or 4-methyl Uracil is a pyrimidine base found in DNA. Together with Adenine, Guanine and Cytosine, it is a major monomer unit of DNA. Any uncharacteristic change in concentration of any of these nucleotides is an indication of mutation or disease or disruption in the immune system. Hence the individual determination of these nucleotides is of significance [1].

Electrochemical methods are fast techniques which provide convenient and inexpensive determinations using miniature instruments [2]. Chemically modified electrodes with conducting polymers electropolymerised on to the electrode surface can accelerate electronic transmission through the electrode surface thereby offering high sensitivity and selectivity. In addition, electrochemical polymerisation ensures controllable and homogeneous formation of the conducting polymer which strongly adheres to the electrode surface [3].

Here we discuss a poly Glutamic acid (pGA) modified Glassy Carbon Electrode (GCE) as a probe for the determination of Thymine in alkaline media. Glutamic Acid was polymerized on to the surface of a cleaned GCE using a procedure reported elsewhere [4]. The thickness of the pGA layer on the GCE surface was optimized by studying the response towards oxidation of 100 μ M Thymine. The pGA layer formed from 2 mM Glutamic acid in PBS pH 7 by cycling the potential between -800 mV to 2000 mV for 20 cycles was found to give the best response in 0.1N NaOH for the electro-oxidation of 100 μ M Thymine.

The oxidation of 100 μ M Thymine on a bare GCE took place at 780 mV with a current of 9.6 μ A whereas on the pGA modified GCE the oxidation peak shifted to 760mV with peak current 22.2 μ A in 0.1M NaOH (Figure 1).

The origin of this electro catalytic effect was investigated using SEM imaging and cyclic voltammetry studies. A study of the effect of scan rate on the reversible peak currents of 2 mM Potassium Ferricyanide using

cyclic voltammetry, provides a method for the determination of surface area of the electrodes. The surface area of the bare electrode was obtained as 0.1248 cm^2 and that of the modified electrode was obtained as 0.1976 cm^2 . The SEM image of the modified electrode indicates that the electropolymerisation of pGA has roughened the surface of the glassy carbon electrode, thereby increasing its surface area (Figure 2a and 2b). These two observations point out to the surface modification of GCE by pGA.

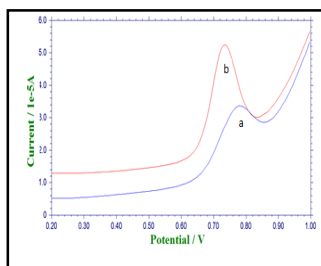


Figure 1. Oxidation peak of 100 μM Thymine on a) bare GCE and b) pGA modified GCE in 0.1 M NaOH

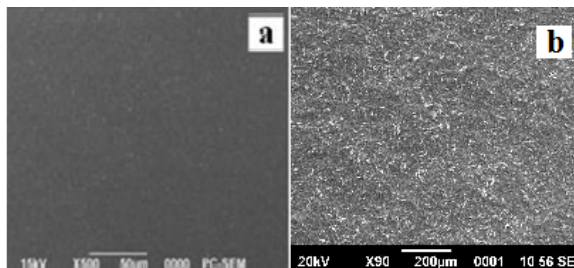


Figure 2. SEM image of a) bare GCE and b) pGA GCE

The variation of anodic peak current for the electro-oxidation with concentration of thymine was studied using Square wave voltammetry and was seen that the relationship between current and concentration was linear in the range $30 \mu\text{M}$ to $1000 \mu\text{M}$ (Figure 2a and 2b) with a detection limit of

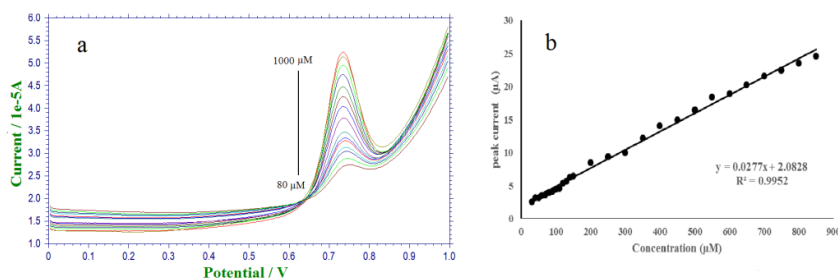


Figure 2 a) Overlay of Square Wave voltammograms of electro oxidation of Thymine from $80 \mu\text{M}$ to $1000 \mu\text{M}$ concentrations at the pGA GCE in 0.1M NaOH. **2b)** Calibration plot from $30 \mu\text{M}$ to $1000 \mu\text{M}$

Linear Sweep voltammetry was used to study the dependence of the oxidation peak parameters on the scan rate (v) in the range from 10 - 100 mVs^{-1} . The plot of peak current versus square root of scan rate was found to be linear pointing to the fact that the electro-oxidation is a diffusion controlled process [6]. A linear relationship was also found between the peak potential (E) and $\ln v$. The slope of the plot of E vs $\ln v$ was used in the Laviron's equation to determine the number of electrons involved in the electro-oxidation process [5]. The number of electrons involved in the process was calculated to be 0.86 which indicates that the electro-oxidation process follows a one electron pathway.

The effect of the other DNA bases on the oxidation peak of thymine on the pGA modified GCE was studied and it was observed that Guanine, Cytosine and Uracil did not interfere with the determination of Thymine when present up to 10 fold excess concentrations. The interference produced by adenine was well below 5% when present in 1:1 molar ratio. The utility of the pGA modified GCE for the determination of Thymine was tested in thermally denatured Herring Sperm DNA using the standard addition method. The results obtained were in good agreement with the theoretical value.

Acknowledgement: The Authors would like to thank the University Grants Commission, India for the financial assistance in the form of Teacher Fellowship and One Time Grant respectively.

References.

- [1] H. Han, J. Li, Y. Li, X. Pang, *Ionics* 19 (2013) 989
- [2] D. Kato, N. Sekioka, A. Ueda, R Kurita, S. Hirono, K. Suzuki, O Niwa *Angew. Chem.Int. Ed.* 47 (2008) 6681
- [3] S. Hou, N. Zheng, H. Feng, X. Li *Analytical Biochemistry* 381 (2008) 179.
- [4] A. Yu, H. Chen *Analytica Chimica Acta* 344(1999) 181

- [5] D. Thomas A. E. Vikraman, T. Jos, K. Girish Kumar *LWT Food Sci. Technol.* 63 (2015) 1294.
- [6] A.E. Vikraman, Z. Rasheed, L. Rajith, L.A. Lonappan, K. Girish Kumar *Food Anal Methods* 6 (2013) 775.

3.11 A Simple and Sensitive Fluorescent Sensor for the determination of Epinephrine

Shalini Menon and K. Girish Kumar

Department of Applied Chemistry, Cochin University of Science and Technology, Kochi
Email: salini.smn@gmail.com, giri@cusat.ac.in

Introduction

Epinephrine (EP), a hormone produced by the adrenal medulla, is also a significant neurotransmitter in the central nervous system of mammals[1]. Vital responses like blood pressure, respiratory rate etc. and also essential body functions can be controlled by the hormone epinephrine[2]. Regulation of EP levels is significant for the maintenance of the homeostasis of the body[3]. Anxiety disorders are a result of increased concentration level of catecholamines and their metabolites. Hence, the determination of EP has attracted much attention and is of clinical interest, especially in the diagnosis of Parkinson's disease, extracranial solid cancer in children, hypertension and benign tumor [2]. Here, we explore the emission properties of the probe PEG₆₀₀₀ coated carbon nanoparticles (PCN) which were synthesized from honey and its use as a turn-on type fluorescent reporter of EP. The introduced method is based on the interaction of EP with PCN resulting in the fluorescence enhancement of PCN.

Results and Discussions

PCN which were synthesized by a procedure as reported elsewhere[4] were characterized by UV-Vis spectrometry, fluorescence spectroscopy, FT-IR and Transmission Electron Microscopy (TEM). The addition of EP to PCN results in an enhancement of its fluorescence intensity. In order to evaluate the performance of the assay, the fluorescence intensity of PCN in presence of EP solutions of varying concentrations ranging from 9.90×10^{-9} M and 1.07×10^{-7} M was measured. A gradual increase in fluorescence intensity was observed with increase in concentration of EP (Figure 1). The calibration plot with concentration of EP against I/I_0 values was highly linear in this range ($R^2 = 0.998$) and the limit of detection (LOD) was found to be 7.59×10^{-10} M (Figure 1 inset).

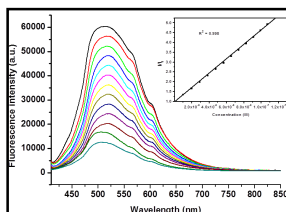


Figure 1. Effect of concentration of EP on the fluorescence intensity of PCN. Inset shows the plot of I/I_0 against Concentration of EP

In order to study the interaction of EP with PCN, TEM analysis was carried out. TEM image of PCN (Figure 2) clearly shows the aggregation of these nanoparticles in the presence of EP. Aggregation effect is shown to block the nonradiative decay process thereby increasing the rate of radiative electron hole recombination which causes enhancement of fluorescence. Also, NH_2 and OH groups present in EP can provide electrons to the fluorophore and thereby bind with the surface defects present on it leading to the removal of the local trap states and formation of more radiative centres on the surface.

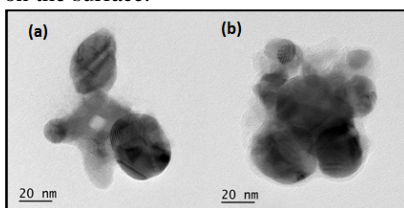


Figure 2. TEM images of (a) PCN (b) PCN in presence of EP

To check the selectivity of the system, the fluorescence intensity of PCN was measured in the presence of some biologically important compounds such as EP, norepinephrine (NE), homovannilic acid (HA), creatinine (CR), ascorbic acid (AA) and uric acid (UA). Among these only EP was found to effectively enhance the fluorescence intensity of the probe whereas all others cause weak fluorescence variations. Thus this fluorescent sensor can be used for the selective determination of EP.

The application of the proposed method was tested by using it for the practical analyses of EP in spiked urine samples. The results are shown in Table 1 and indicate recovery efficiencies between 97.9% and 104.4%. Based on five replicate measurements, the RSD for EP determination in the examined urine samples was found to be 3.2%. Results clearly indicate that proposed method is in good agreement with those provided by the HPLC method.

Acknowledgements

Shalini Menon would like to acknowledge Kerala State Council for Science, Technology and Environment (KSCSTE) for research fellowship. Krishnapillai Girish Kumar would like to express his gratitude to University Grants Commission (UGC), Govt. of India for financial assistance in the form of 'One Time Research Grant'.

References

- [1] S. S. Sharath, S. B. E Kumara, *Int. J. Electrochem. Sci.* 9 (2014)1321.
- [2] S. Masoomeh, L. Jamshid, Manzooria, J. Abolghasem, *Iranian Journal of Pharmaceutical Sciences*3 (2007) 111.
- [3] Y. Jinghe, Z. Guiling, W. Xia, H. Fang, L. Cunguo, C. Xihui, S. Limei, D. Yuanju, *Anal. Chim. Acta*, 363 (1998) 105.
- [4] S. Menon, E. V. Anuja, S. Jesny, G. K. Krishnapillai, *J Fluoresc.*26 (2016) 129.

3.12 Electrochemical sensor for cefotaxime based on gold modified molecularly imprinted polymer

P. Karthika¹, R. Vidhya¹, C.Rani² and S. Viswanathan^{1*}

^aDepartment of Industrial Chemistry, Alagappa University, Karaikudi-630 003

^bDepartment of chemistry, Alagappa Govt. Arts college, Karaikudi – 630003. E-mail: rviswa@gmail.com

Molecularly imprinted polymer (MIP) based electrochemical sensor was prepared for the electrochemical detection of cefotaxime, a widely using antibiotics which also causes serious damage for human health. MIP film was electrochemically polymerized on glassy carbon (GC) electrode in presence of pyrrole and cefotaxime as monomer and template molecules respectively. A careful removal of cefotaxime creates complimentary cavity, which used for specific recognizing towards target in analytical samples. Such analyte bound MIP electrode was employed as working electrode for voltametric sensing [1,2]. Gold nanoparticles (AuNPs) were incorporated using controlled electrochemical tools to improve analytical performance. MIP and MIP/AuNPs were characterized through cyclic voltammetry (CV), AC impedometry and Scanning electron microscope (SEM) techniques. SEM image (Fig. 1) confirms the average size of the gold nanoparticles on GC electrode was found to be in the range of ~ 15-25nm and spherical in shape. Imprinted Polypyrrole film was resulted as sphere like particles and its size was ~ 200nm.

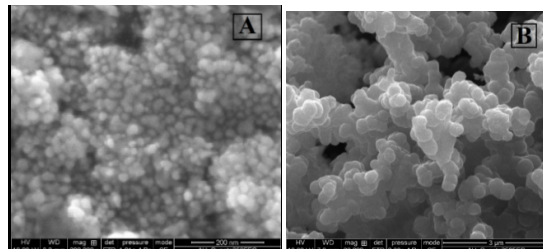


Figure 1. SEM image of AuNPs (A), and MIP coated on AuNPs

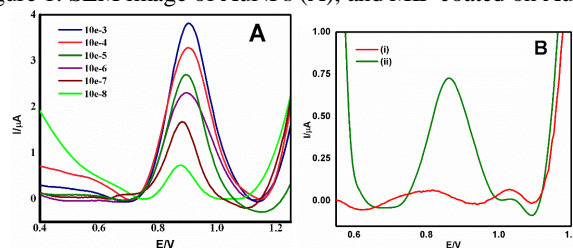


Figure 2. Differential Pulse voltammograms for standard samples of cefotaxime (A) and for Urine samples (B) on MIP/AuNPs/GC electrode.

Differential Pulse voltametric (DPV) studies show linear peak current intensity for 1×10^{-3} to 1×10^{-8} M. Oxidation peak at 0.87 V indicates that the electro-oxidation of Cefotaxime on MIP/AuNPs/GC electrode surface which confirms the successful rebinding of Cefotaxime in polymer imprints (Fig. 2 A). Urine samples were spiked with known amount Cefotaxime and analysed recovery studies. In Fig. 2 B (i) & 2B(ii) are blank and cefotaxime spiked urine samples respectively. Thus the developed molecularly imprinted polymeric sensor offers improved sensitivity, reproducibility, stability and it can be used to quantify cefotaxime in real samples.

Keywords: Electrochemical sensors, Molecularly imprinted polymers (MIPs), Cefotaxime.

Reference:

- [1] H.Silva, J.P. Grosso, S. Viswanathan, C. Delerue-Matos, *Biosensors and Bioelectronics*, 52 (2014) 56-61
 [2] G. Yang, F. Zhao, B. Zeng, *Biosensors and Bioelectronics*, 53(2014)447-452.

3.13 Rhodamine based 'OFF-ON' fluorescent probe for Al³⁺ and S²⁻: Synthesis, crystal structure, *in silico* and live cell imaging

M. Maniyazagan[†], R. Mariadasse[‡], M. Nachiappan[‡], J. Jeyakanthan[‡], N. K. Lokanath[⊥], S. Naveen[⊥], K. Premkumar[‡], P. Muthuraja[†], P. Manisankar[†] and T. Stalin^{†,*}

[†] Department of Industrial Chemistry, School of Chemical Sciences, Alagappa University, Karaikudi-03, Tamil Nadu, India.

[‡] Structural Biology and Bio-computing Lab, Department of Bioinformatics, Alagappa University, Karaikudi-04.

[⊥] Cancer Genetics and Nanomedicine Laboratory, Department of Biomedical Science, Bharathidasan University, Tiruchirappalli, Tamil Nadu, India.

[⊥] Dept. of Studies in Physics, University of Mysore, Mansangangotri, Mysore-06, India

* E-mail address: drstalin76@gmail.com (Dr. T. Stalin)

Abstract

We have synthesized a new 4-bromothiophene functionalized rhodamine derivative RBD2 which specifically binds to Al³⁺ in the presence of excess of other competing metal ions with colour changes in their absorption and fluorescence spectral studies [1-3]. These spectral changes are sufficient to detection of Al³⁺ ions in the visible region of the spectrum and thus support naked eye detection. The fluorescent probe, RBD2, could be active as a Fluorescence resonance energy transfer (FRET) based sensor for detection of Al³⁺ based on the process involving the donor thiophene and the acceptor Al³⁺ bound xanthene fragment [4-5]. The aforesaid studies reveal that RBD2-Al³⁺ complex is highly selective and fully reversible in presence of sulphide anions [6]. Besides, the fluorescence microscopic studies confirmed that the fluorescent probe RBD2 could be used as an imaging probe for detection of uptake of Al³⁺ ion in HepG2 human liver cancer cells.

Keywords

Chemosensor; Fluorescence; Rhodamine; Al³⁺ ion; Cell imaging.

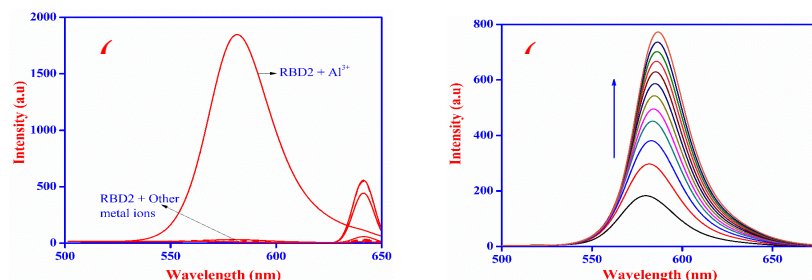


Figure 1. (a) Changes of the fluorescence emission of RBD2 (10 μM) observed upon addition of metal ions (nitrate salts of Na⁺, Mg²⁺, K⁺, Ca²⁺, Fe²⁺, Co²⁺, Ni²⁺, Cu²⁺, Fe³⁺, Pb²⁺, Pd²⁺ and Al³⁺) (10 equiv) in a ACN/HEPES buffer (1 mM, pH 7.3; 1:4 v/v). (b) Fluorescence titration spectra of RBD2 (10 μM) upon addition of 5 equiv of Al³⁺ in ACN/HEPES buffer (1 mM, pH 7.3; 1:4 v/v) λ_{ex} = 495 nm.

References

- [1]. A. W. Czarnik, *Fluorescent Chemosensors for Ion and Molecule Recognition*, American Chemical Society, Washington DC, 1993.
 [2]. A. P. de Silva, H. Q. N. Gunaratne, T. Gunnlaugsson, A. J. M. Huxley, C. P. McCoy, J. T. Rademacher and T. E. Rice, *Chem. Rev.*, 1997, 97, 1515.
 [3]. B. Valeur and I. Leray, *Coord. Chem. Rev.*, 2000, 205, 3.
 [4]. R. Martı́nez-Mañez and F. Sancenón, *Chem. Rev.*, 2003, 103, 4419.
 [5]. J. F. Callan, A. P. de Silva and D. C. Magri, *Tetrahedron.*, 2005, 61, 8551.
 [6]. L. Basabe-Desmonts, D. N. Reinhoudt and M. Crego-Calama, *Chem. Soc. Rev.*, 2007, 36, 993.

3.14 Piperazine based Schiff base for chemosensor and biological applications

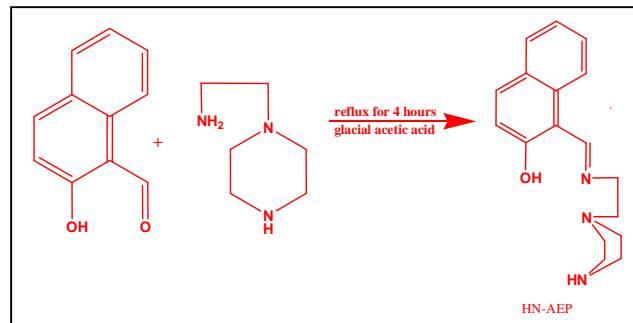
N. Kavitha and N. Sengottuvelan*

Department of Industrial Chemistry, Alagappa University, Karaikudi- 630 003

* nsvelan@gmail.com, nkavita0729@gmail.com

Schiff base is widely studied for its synthetic flexibility, selectivity and sensitivity towards the central metal ion. The presence of azomethine group(-N=CH-) imports in elucidating the mechanism of transformation and racemization reaction biologically. Schiff bases have been used as drugs and possess a wide variety of

biological activities such as antibiotic, antifungal, anticancerous and pharmacological properties. A variety of fluorescent chemosensors have been developed using Schiff base compounds due to the restriction in C=N isomerization. These Schiff base compounds also find its application in cell imaging. 2-Hydroxy-1-naphthaldehyde and aminoethylpiperazine is used to synthesis a Schiff base receptor HN-AEP [1-((Z)-(2-(piperazin-1-yl)ethylimino)methyl)naphthalen-2-yl)] which acts as luminescent chemosensors for Al^{3+} and Br^- . The synthesized ligand HN-AEP was characterized by $^1\text{H-NMR}$, ESI-Mass and FTIR. The selectivity of HN-AEP receptor was investigated upon addition of several metal ions such as Li^+ , Na^+ , K^+ , Ca^{2+} , Mg^{2+} , Sn^{2+} , Cu^{2+} , Co^{2+} , Mn^{2+} , Mg^{2+} , Li^{2+} , Ni^{2+} , Zn^{2+} , Ba^{2+} , Cd^{2+} , Hg^{2+} , Cr^{3+} and Al^{3+} in methanol. Its higher sensitivity and selectivity towards Al^{3+} ion and Cu^{2+} were studied through absorption and emission channels, with a detection limit of $10 \times 10^{-6} \text{ M}$ was established. Selectivity of chemosensor is explained for Al^{3+} based on the excited-state intra molecular proton transfer (ESIPT). The selectivity for anion binding with HN-AEP was also done with I^- , Br^- , Cl^- , F^- , CN^- , ClO_4^- , HSO_4^- in methanol. It was found that the ability for Br^- enhancement was more than 10 fold than the receptor.



Scheme 1 Chemical Structure of synthetic route of HN-AEP

Further, the *in vitro* antibacterial activity of this compound was carried out using two Gram-positive and two Gram-negative bacterial pathogens. Test concentration of HN-AEP for screening was fixed to be 10mg/100 μl . The antibacterial activity was confirmed for two Gram-positive bacteria (*Bacillus subtilis*, *Streptococcus pneumoniae*) and one Gram-negative bacteria (*Proteus vulgaris*). Significant zone of inhibition was found in *B. subtilis* whereas *S. pneumoniae* showed moderate zone of inhibition, *P. vulgaris* showed minimum zone of inhibition and *Escherichia coli* did not show any antibacterial activity. HN-AEP activity against human bacterial pathogens was tested by varying dosage of the compound and compared with standard antibiotic. In addition, anti-biofilm activity of HN-AEP is underway. Thus, the Schiff base HN-AEP is a new antibacterial agent to treat biofilm associated bacterial infection in humans.

References

- [1]. Abhijit Ghosh and Debasis Das, Dalton Trans., 2015, 44, 11797–11804
- [2]. Y.K. Jang et al. Dyes and Pigments 99 (2013) 613
- [3]. R. Azadbakht and S.Rashdi. Spectrochimica Acta Part A: Molecular and Bio molecular spectroscopy 127(2014)329-334
- [4]. Kai Wu et al . Anal. Methods, 2014, 6, 3560–3563

3.15 A differential pulse voltammetry sensor based on graphene oxide-multiwalled carbon nanotube nanocomposite for the simultaneous determination of carbendazim and isoproturon pesticides

C.Vasanthi and R. Saraswathi*

Department of Materials Science, School of Chemistry, Madurai Kamaraj University, Madurai 625 021, Tamil Nadu, India
vasash03@gmail.com and drrsaraswathi@gmail.com

Introduction

Carbon nanotubes (CNTs) has long been recognized as a promising electrode material in the field of electrochemistry due to its capability of direct electron transfer, high electrical conductivity, large surface area and chemical stability but the lack of dispersibility of pristine CNTs in water has made the electrode fabrication quite a challenging task [1]. Graphene oxide (GO) has received immense interest due to its low manufacturing cost, large specific surface area, amphiphilic nature and long term stability. GO possesses abundant oxygen containing functional groups such as epoxide, hydroxyl, carboxylic groups which can significantly affect the van der Waals interaction existing between nanosheets and thus it is water dispersible [2]. The hydrophilic properties of GO can enable the formation of a stable dispersion of GO-CNT nanocomposite material, through

π - π stacking interactions for fascinating electrochemical applications. Several recent studies have demonstrated the superior performance of the GO-CNT nanocomposite as an electrode modifier in comparison to the CNTs modified surface [3]. Herein, the application of GO-MWCNT towards the sensitive and simultaneous determination of two pesticides, viz. carbendazim and isoprotruron is reported for the first time. Carbendazim is a systemic fungicide used to control a wide range of fungal diseases in crops of fruits and vegetables while isoprotruron is widely used as a herbicide. The threshold safe limits of carbendazim and isoprotruron have been declared as 0.02 ppm and 0.1 ppm respectively [4,5]. Therefore it is essential to develop a simple, rapid, sensitive and selective methodology for the determination of these pesticide residues in soil and water resources.

Results and Discussion

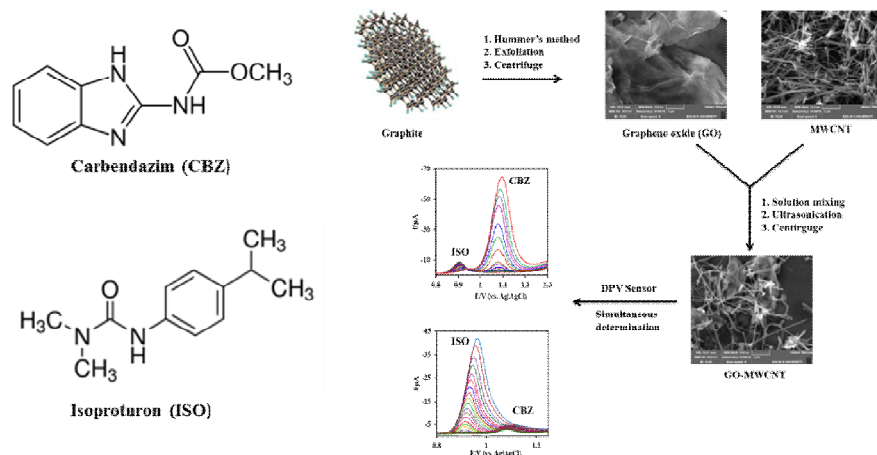


Fig. 1 Schematic representation of preparation of GO-MWCNT and its differential pulse voltammetric response towards the simultaneous determination carbendazim and isoprotruron pesticides

The XRD pattern of the GO-MWCNT shows two typical peaks at $2\theta = 11.62^\circ$, 26.32° corresponding to GO and MWCNT respectively present as components in the nanocomposite. The SEM image indicates the presence of randomly oriented nanotubules on the GO nanosheets. Cyclic voltammetry studies on GO-MWCNT modified surface in H_2SO_4 (pH 2) suggest a good electrocatalytic activity towards oxidation of carbendazim and isoprotruron and an excellent synergy with respect to MWCNT/GCE and GO/GCE. The linear dependence of oxidation peak current against scan rate indicates a diffusion controlled reaction. The optimum pH is observed as pH 2. A differential pulse voltammetric sensor has been developed for the simultaneous determination of carbendazim and isoprotruron using GO-MWCNT/GCE electrode in which the concentration of one analyte is varied while that of the other analyte is kept constant (50 μM). Linear calibrations are obtained for carbendazim in the concentration range of 0.05 to 800 μM with a detection limit of 30.77 nM and a current sensitivity of $1.16 \mu\text{A} \mu\text{M}^{-1} \text{cm}^{-2}$ and for isoprotruron in the concentration range of 0.1 to 700 μM with a detection limit of 12.62 nM and a current sensitivity of $1.11 \mu\text{A} \mu\text{M}^{-1} \text{cm}^{-2}$.

Conclusion

For the first time, a GO-MWCNT based nanocomposite was used for the simultaneous determination of carbendazim and isoprotruron. The electroanalytical performance of the GO-MWCNT/GCE for this study has been assessed in comparison to bare GCE, GO/GCE and MWCNT/GCE by cyclic voltammetry and DPV at pH 2. The GO-MWCNT electrode modifier is found to be competitive to other nanocomposites reported in literature for the simultaneous determination of carbendazim and isoprotruron.

References

- [1] Q. Zhang, S. Yang, J. Zhang, L. Zhang, P. Kang, J. Li, J. Xu, H. Zhou and X. M. Song, *Nanotechnology* 22 (2011) 494010.
- [2] X. Qiua, L. Lua, J. Lenga, Y. Yua, W. Wanga, M. Jianga and L. Baia, *Food Chemistry* 190 (2016) 889.
- [3] B. Dinesh, V. Mani, R. Saraswathi and S. M. Chen, *RSC Advances* 4 (2014) 28229.
- [4] W. F. Ribeiro, T. M. G. Selva, I. C. Lopes, E. C. S. Coelho, S. G. Lemos, F. C. D. Abreu, V. B. D. Nascimento and M. C. U. D. Araujo, *Analytical Methods*, 3 (2011) 1202.
- [5] P. Noyrod, O. Chailapakul, W. Wonsawat and S. Chunuwatanakul, *Journal of Electroanalytical Chemistry* 719 (2014) 54.

3.16 Sensitive Detection of Hg(II) Using Carbon Dots as Fluorophore

K. Rubini, K. Sivakumar, B. Sinduja and S. Abraham John*

Centre for Nanoscience and Nanotechnology, Department of Chemistry, Gandhigram Rural Institute, Gandhigram-624 302, Tamil Nadu, INDIA. e-mail: s.abrahamjohn@ruraluniv.ac.in

Introduction

Carbon dots (CDs) and graphene quantum dots (GQDs) have recently emerged as superior fluorophores because of their interesting properties including excellent photostability, small size, biocompatibility and highly tunable photoluminescence (PL) property. Besides, fluorescent CDs possess rather strong ability to bind with other organic and inorganic molecules due to their abundant surface groups. Thus, CDs can be manipulated via a series of controllable chemical treatments and satisfied the demands in the photocatalytic, biochemical, and chemical sensing, bioimaging, and drug carrier. Currently, the researches of fluorescent CDs mainly focus on two aspects; one is developing rapid, simple preparation method of fluorescent CDs, and the other is expanding the application field. The present study aims to address the synthesis, characterization and application of CDs. The CDs were prepared from asparagines by a simple hydrothermal method and then characterized by FT-IR, UV-vis and spectrofluorimetry. Finally, the CDs were utilized for the sensitive determination of Hg(II).

Experimental

Asparagine was purchased from Sigma-Aldrich. All other chemicals used in this study were of analytical grade and used directly without further purification. Double distilled water was used to prepare the solutions in the present work. Carbon dots were prepared as follows. 0.5 g of asparagine was heated in a heating mantle about 100°C. It was liquated after 10 min and the color was changed to brown within 20 min. The brown color solution was then dissolved in 100 ml of NaOH and stored in refrigerator. Absorption spectra were measured by using JASCO V-550 UV-vis spectrophotometer. Fluorescence spectral measurements were performed on JASCO FP 8500 spectrofluorimeter at room temperature.

Results and Discussion

The synthesized CDs are green-blue luminescent (insert of Fig.1). They show absorption maximum at 207 nm, corresponding to π - π^* transition and a shoulder band at 273 nm due to n - π^* transition. While exciting at 348 nm, they show emission maximum at 441 nm. It was found that the emission maximum was independent of excitation wavelength. This suggests that the size and surface states of CDs are uniform. While adding several toxic metal ions in the milli molar range including Pb(II), Cd(II) and Cu(II), the emission maximum remains unchanged. However, the emission was quenched while adding Hg(II) in the micro molar range. Fig. 1 shows the emission spectra of CDs in the presence of different concentrations of Hg(II). While adding 1 μ M Hg(II), the emission intensity was decreased. Further addition of 1 μ M each increment, the emission was quenched systematically. After the addition, 36 μ M Hg(II), the emission intensity was drastically quenched. The detailed results will be discussed in the poster.

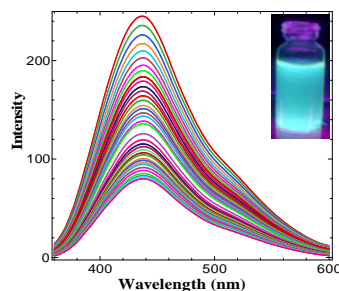


Fig.1. Emission spectra of CDs in the presence of 1-36 μ M Hg(II) (each 1 μ M increment). Inset: Photograph of CDs under UV light.

3.17 Methyl Parathion Sensor based on Cu doped CeO₂ nanoparticles

Jean Claude Nizeyimana, N. Lavanya, C. Sekar*

Department of Bioelectronics and Biosensors, Alagappa University, Karaikudi-630 003.

*Email: Sekar2025@gmail.com

Ceria (CeO₂) is an important rare earth oxide and has been widely investigated in the automotive exhaust purification, oxygen storage and release catalysis, and solid oxide fuel cell applications. The electronic structure and physico-chemical properties of CeO₂ can be easily altered by introducing oxygen vacancies via appropriate chemical doping with transition metal ions [1].

In the present work, Cu doped CeO₂ nanoparticles were prepared by microwave irradiation (2.45GHz) method which permits us to produce gram quantity of homogeneous nanoparticles in just 20 min. Powder XRD results confirmed that both pure and Cu doped CeO₂ form in cubic fluorite structure with the space group Fm3m (ICDD card no. 34-0394) [Fig. 1A]. Raman spectra reveal that the most intense peak at 456 cm⁻¹ correspond to the symmetrical stretching mode (F_{2g}) of the Ce-8O vibration unit [2] [Fig. 1B].

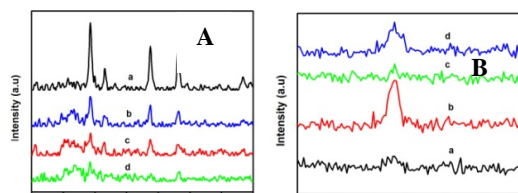


Fig. 1 (A) XRD pattern, (B) Raman spectra of (a) pristine CeO₂, (b) 3 wt% Cu, (c) 5wt% Cu and (d) 10wt% Cu

doped CeO₂ NPs

We have fabricated methyl parathion (MP) electrochemical sensor based on Cu-CeO₂ NPs modified glassy carbon electrode (GCE) without any electron mediators. MP is a restricted-use organophosphorus insecticide throughout the world which is being used on a number of economically important crops such as cotton, soybeans, cereals, fruits, sugar cane, etc. Poisoning with MP leads to cholinergic overstimulation, with signs of toxicity including sweating, dizziness, vomiting, diarrhea, convulsions, cardiac arrest, respiratory arrest, and, in extreme cases, death. The determination of residues of MP in waters is very important.

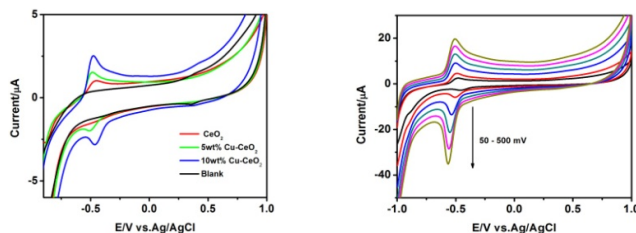


Fig. 2 (A) CV response of 100 μM MP in 0.1 M KNO₃ at bare GCE, pristine CeO₂, 5wt% and 10 wt% Cu-CeO₂ modified GCE recorded at a scan rate of 50 mV/s and (B) CV of 10wt% Cu-CeO₂/GCE in 100 μM MP at different scan rates (50-500 mV/s).

It can be seen that the Cu (10 wt%) doped CeO₂ exhibit improved catalytic activity toward the detection of MP when compared to that of bare GCE and pristine CeO₂. The effect of scan rate, pH and various concentrations of MP were studied. The results and a possible mechanism will be presented in detail.

References:

- [1] Y. Temerk H. Ibrahim, *Sens. Actuat. B* 224 (2016) 868-877.
- [2] K. S. Ranjith, P. Saravanan, S.H. Chen, C.L. Dong, C.L. Chen, S.Y. Chen, K. Asokan, R. T. Rajendra Kumar, *J. Phy. Chem.*, 116 (2014) 27039-27047.

3.18 Polymer based nanobiosensor and its controlled drug delivery for the of detection of glucose

J. Nivin, B. Kalyanasundar and C. Sivakumar*,

Electrodics and Electrocatalysis Division, CSIR-Central Electrochemical Research Institute, Karaikudi-630 006, Tamil Nadu, India. E-mail: ccsivakumar@cecri.res.in

Abstract

Glucose biosensor based on conducting polymer, poly(2,5-dimethoxy aniline) (PDMA) film on Au electrode was constructed. Glucose oxidase (GOx, from *aspergellius*) was physically entrapped during electro polymerization of the monomers (DMA) in 0.5 M sulphuric acid (H₂SO₄). The amperometric responses of the nanobiosensor electrodes were measured in the absence of a mediator and are characterized by cyclic voltammetry, amperometry, SEM, FTIR and XRD. Polymer based controlled drug delivery system was synthesized using β-cyclodextrin and PEG 6000 for diabetes. The Glimepiride drug complex was synthesized by kneading method and characterized by in vitro dissolution study and FTIR. Highly sensitivity and selective glucose sensor was developed by using PDMA on Au electrode, Good controlled release of the Glimepiride coupled with biodegradable of polymer provides a prospective controlled release dosage form to deliver the drug in the therapy of diabetes. Our polymer based biosensor and control drug delivery will find a new path for the growing market of nanotechnology in drug delivery systems.

Keywords: Nanobiosensor, Durg-nanocomplex, Type II diabetes and Programmed drug delivery.

3.19 Tin dioxide (SnO₂) nanoparticles based biosensors for monitoring of neurochemical substances

N. Lavanya, C. Sekar*

*Department of Biosensors and Bioelectronics, Alagappa University, Karaikudi-630003, TN. *Sekar2025@gmail.com*

Nanostructured tin dioxide (SnO₂), a stable n-type semiconductor (E_g = 3.6 eV at 300 K), has been

extensively studied as a promising material for biosensor applications. Performance of the sensors could be improved by adopting different strategies such as chemical doping, surfactant mediation, composite formation and gamma ray irradiation [1,2] of the sensing element. In the present work, an electrochemical sensor has been fabricated based on CTAB assisted SnO₂ nanoparticles modified glassy carbon electrode (GCE) for simultaneous determination of epinephrine (EP) and norepinephrine (NEP) in the presence of ascorbic acid (AA) and uric acid (UA). Catecholamine neurotransmitters such as EP and NEP play essential role in the mammalian central nervous system (CNS). These molecules are involved in a large variety of neurophysiological processes including learning, sleep, memory and appetite. Damage in secretion or uptake of neurotransmitters is known to cause neurodegenerative diseases, drug addiction, and depressive syndromes.

Surfactant assisted SnO₂ NPs were synthesized by microwave irradiation method [3] and the products were characterized using powder XRD, TEM, UV-Vis absorption, CV, EIS and SWV. XRD and HRTEM studies confirmed the formation of rutile structure with space group (P₄₂/mnm) and nanocrystalline nature of the products with spherical morphology. [Fig.1]. The optical absorbance spectra indicate that the absorption edge shifts to higher wavelengths implying a red shift in band gap with respect to bulk SnO₂.

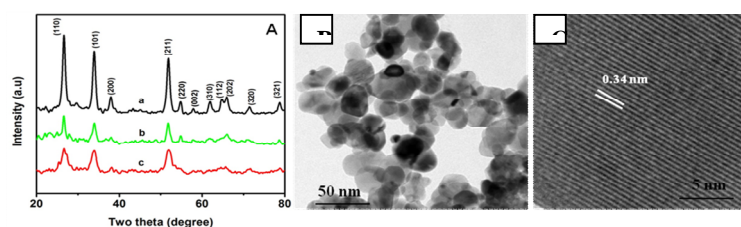


Fig. 1 (A) XRD pattern of (a) pristine SnO₂, (b) EDTA and (c) CTAB assisted SnO₂ NPs and (B, C) TEM and HRTEM image of CTAB-SnO₂ NPs.

A mediator-free electrochemical sensor was fabricated for simultaneous determination of EP and NEP based on surfactant assisted SnO₂ modified glassy carbon electrode. When compared to the pure SnO₂, CTAB-SnO₂ nanoparticles exhibited excellent electron transfer properties for the simultaneous detection of EP and NEP [Fig.2A]. The effect of scan rate and pH of the electrolyte was studied. Under optimum conditions, the calibration curves for EP and NEP were obtained over the wide concentration range of 0.1–300 μM and 0.1–250 μM with the detection limits of 0.01 and 0.019 μM respectively [Fig.2B]. The developed sensor showed an excellent anti-interference ability against electroactive species such as ascorbic acid and uric acid and metal ions and proved to be useful for the determination of EP and NEP in human urine samples with satisfactory results. These sensors are essential for non-invasive disease diagnosis and pharmaceutical applications.

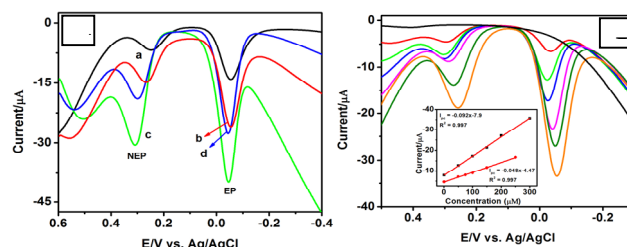


Fig. 2 SWVs obtained for the mixture of 500 μM each EP and NEP in 0.1 M PBS (pH 5.0) at (a) bare GCE, (b) pristine SnO₂, (c) CTAB-SnO₂ (d) EDTA-SnO₂ modified GCE and (B) SWVs obtained for various concentrations of EP (1 to 300 μM) and NEP (1 to 250 μM) at CTAB-SnO₂/GCE in 0.1 M PBS (pH 5.0) and inset shows plots of the reduction peak currents as a function of various concentrations of EP and NEP.

References

1. N. Lavanya, S. Radhakrishnan, C. Sekar, *Biosensors and Bioelectronics*, 36 (2012) 41.
2. N. Lavanya, E. Fazio, F. Neri, A. Bonavita, S. G. Leonardi, G. Neri, C. Sekar, *Sensors & Actuators B: Chemical* 221 (2015) 1412
3. N. Lavanya, C. Sekar, S. Ficarra, E. Tellone, A. Bonavita, S. G. Leonardi, G. Neri, *Materials Science & Engineering C* 62 (2016) 53.

3.20 Determination of Heavy Metals on Poly(Aniline-Co-Sulfamethazine) Modified Electrode

K. Masilamani¹, G. Selvanathan², B. Elanchezhian²

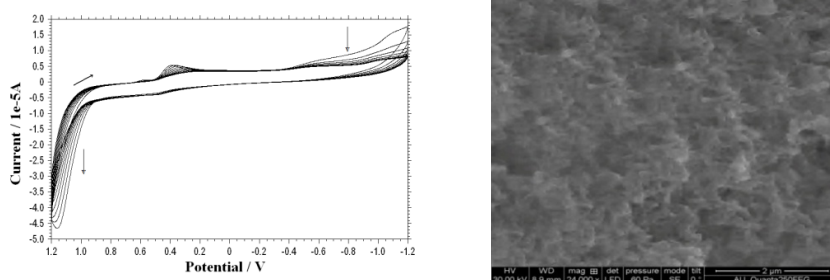
¹Govt High School, A. Kalayamputhur, Palani-624615, Tamil Nadu, India

²Department of Chemistry, A.V.C College (Autonomous), Mannampandal, Mayiladuthurai -609305, Tamil Nadu, India

Abstract

Sulfamethazine (SMZ), 4-amino-N-(4,6-dimethyl-2-pyrimidine) benzene sulfonamide is a commonly used drug in veterinary medicine. Thin film of Poly (aniline-co-sulfamethazine) was synthesized by using cyclic voltammetry in 0.1M aqueous sulfuric acid on the surface of the Glassy carbon electrode at different monomer concentrations [1-3]. The copolymer was characterised by UV, IR, NMR, XRD and SEM. The suitability of this novel copolymer modified electrode was applied for the detection and determination of first transition metals from vanadium to zinc in various pH media using Square Wave Stripping Voltammetry and Differential Pulse Stripping Voltammetry. The optimum parameters were arrived and calibration plots were done. Good response was observed for the metal ions of Cu, Mn and Co. All modified systems led to the determination upto ppb level with good correlations.

Keywords: Sulfamethazine, Glassy carbon electrode, Square Wave Stripping Voltammetry and Differential Pulse Stripping Voltammetry



Left: Cyclic voltammetric behaviour of 0.01 M aniline and 0.0025M sulfamethazine on GCE in 0.1M H₂SO₄, scan rate 100 mV/s, Right: SEM micrograph of the copolymer

References

1. Bagheri. A; Nateghi, M.R ; Massoumi A, Synthetic Metals, 97 (1998) 85.
2. Manisankar.P, Vedhi.C, Selvanathan.G and Somasundaram.R.M, Journal of Chem. Mat., 17 (2005) 1722-1727.
3. Shaolin.M, Synthetic Metals, 143 (2004) 259.

3.21 Controlled growth of single crystalline nanostructured dendrites of α -Fe₂O₃ blended with MWCNT: a systematic investigation of highly selective determination of L-dopa

D. Nathiya and J. Wilson*

*Polymer Electronics lab, Dept. of Bioelectronics & Biosensors, Alagappa University, Karaikudi – 630004.

Email: nathiyad725@gmail.com

Research on the development of high surface area materials for the sensing of biomolecules by electrochemical method is becoming a hot area of research due to their high sensitivity, selectivity and convenience. In that metal oxides doped with MWCNT plays a vital role because of its different physical, chemical and enhanced electronic properties. Recently, a variety of dendritic structures of metals, metal oxides and chalcogenides have been extensively investigated for various applications [1,2]. Among them, α -Fe₂O₃ has been identified as a suitable material for a variety of applications in magnetic devices, catalysis, biosensors, photo electrodes, lithium ion batteries and pigments [3,4]. In sensing of biomolecule like L-dopa, a precursor of dopamine is an important neurotransmitter which is commonly used for the treatment of neural disorders such as Parkinson's syndrome. In this work, we have synthesized α -Fe₂O₃ dendritic nanostructures by hydrothermal method and then blended with MWCNT to construct a biosensor for the determination of L- dopa.

The structure of the new material was characterized by transmission electron microscopy (TEM), Scanning Electron Microscopy (SEM). In that, the surfactant assisted α -Fe₂O₃ exhibited uniform dendritic shaped nanostructures with hierarchical arrangement of a well-defined main trunk, branches and sub-branches. The crystallinity of a material is characterized by X-ray diffraction (XRD) pattern which results rhombohedral structure and also reflection of graphic represents α -Fe₂O₃/MWCNT composite. The electrochemical behavior of L-dopa through a fabricated α -Fe₂O₃/MWCNT composite onto the surface of glassy carbon electrode was also studied by cyclic voltammetry (CV), differential pulse voltammetry (DPV) and amperometry in phosphate buffer solution (PBS) at pH 7.2. From the experimental results α -Fe₂O₃ blended with MWCNT composite has shown 3-fold increase of the oxidation peak current as compared to bare electrode. The DPV current responses of L-dopa were increased linearly in the range from 5.0×10^{-8} to 3.8×10^{-6} M with a lower detection limit of 30 nM (3σ). Thus the present work exhibited good sensitivity, selectivity and stability towards the determination of neurotransmitter with low detection limit.

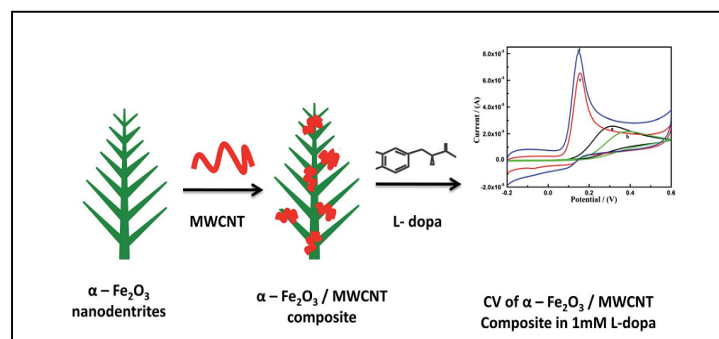


Fig 1. Schematic diagram for L-dopa sensing of α -Fe₂O₃/MWCNT composite

References:

- [1] L. Fan and R. Guo, Cryst. Growth Des., 2008, 8, 2150–2156
- [2] Y. Zhang, H. Sun and C. F. Chen, Phys. Lett. A, 2009, 373, 2778–2781
- [3] T. A. Anhoj, B. Bilenberg, B. Thomsen, C. D. Damsgaard, H. K. Ramussen, C. S. Jacobsen, J. Mygind and S. Morup, J. Magn. Mater., 2003, 260, 115–130
- [4] Y. Jiao, Y. Liu, F. Qu and X. Wu, CrystEngComm, 2014, 16, 575–581.

3.22 Properties of SnO₂-CNT powdered particles by using hydrothermal method for gas sensors

D. Saravanakumar¹, B.H. Abbas Shahul Hameed², P. Ponsurya³, A. Ayeshamariam^{4*} and M. Jayachandran⁵

¹R&D Centre, Bharatiyar University, Coimbatore.

²Department of Mechanical Engineering, SMR East Coast College of Engineering and Technology, Somanathapattinam, Thanjavur District, 614 612, India

³Department of Mechanical Engineering, Loyola ICAM College of Engineering and Technology, Nungambakkam, Chennai-34, India

^{4*}Department of Physics, Khadir Mohideen College, Adirampattinam, 614701, India

⁵ECMS Division, (CSIR) Central Electro Chemical Research Institute, Karaikudi, 630003. aismma786@gmail.com

Crystalline SnO₂:CNT powdered particles were prepared by source materials of tin acetate and SWCNT using a precursor containing these solution, as prepared particles were undergone the annealing two different temperatures of 150° C and 300⁰ C. The structural, morphological and optical properties have been investigated. X-ray diffraction analysis showed that the as-prepared were well crystallized and polycrystalline with cubic structure having (111) preferred orientation. SEM results showed the nanocrystalline nature of the SnO₂:GO powders. The electrical parameters like the bandgap, transmittance and absorbance were found. Carbon based on hybrid carbon nanotube-SnO₂ gas sensors is described. The hybrid gas sensors were fabricated using by hydrothermal synthesis. The instrument employs feature extraction techniques including integral and primary derivative, which lead to higher classification performance as compared to the classical features (ΔR and $\Delta R/R_0$). It was shown that doping of carbon nanotube (CNT) improves the sensitivity of gas sensors, while quantity of CNT has a direct effect on the selectivity to volatile organic compounds, i.e., methanol (MeOH) and ethanol (EtOH). The sensor applications of this pelletized tablets of SnO₂:GO were also demonstrated. Based on the proposed methods, this instrument can monitor and classify 1 vol% of MeOH contamination in whiskeys.

Keywords: Structural, morphological, sensor and EtOH.

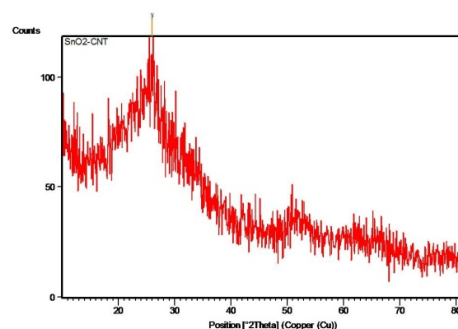


Figure 1. XRD spectrum of SnO₂-CNT as-prepared powdered particle

References

- [1] I.T. Jolliffe, Principal Component Analysis, *Springer*, 2002.
 [2] S. Roussel, G. Forsberg, V. Steinmetz, P. Grenier, V. Bellon-Maurel, *J. Food Eng.* 37 (1998) 207–222.
 [3] S. Zhang, C. Xie, D. Zeng, Q. Zhang, H. Li, Z. Bi, *Sens. Actuators B, Chem.* 124 (2007) 437–443.

3.23 Silver nanoparticles for selective and sensitive sensing of Hg^{2+} colorimetrically

Muthupandi Kasithevar and Prakash Periakaruppan*

Department of Chemistry, Thiagarajar College, Madurai – 09, Tamilnadu, India

E-mail: kmpprakash@gmail.com, k.muthupandi26@gmail.com

Abstract

The present study reports an eco-friendly process for the synthesis of silver nanoparticles (Ag-NPs) using aqueous leaf extract of *Talvergia Latibokiya* (TVLB). The structural and morphological characteristics of synthesized Ag-NPs were investigated by UV-visible, FT-IR, XRD, HR-TEM and EDX analysis. The green synthesized Ag-NPs were tested for selective and sensitive sensing of Hg^{2+} colorimetrically, which show an excellent selectivity and sensitivity in the presence of interfering metal ions. A spectrophotometric method has been established for sensing of Hg^{2+} in the range from 0 to 1000 nm, with a limit of detection (LOD) as low as $7.6 \times 10^{-9} \text{ mol L}^{-1}$. The mechanism for green synthesis of Ag-NPs and detection of Hg^{2+} are discussed.

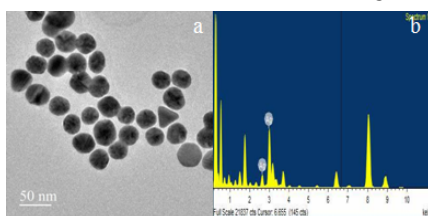


Fig. 1 (a) TEM image of Ag-NPs and (b) EDX spectrum of Ag-NPs

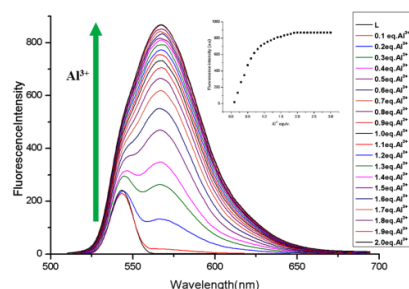
Key words: Green synthesis, Silver nanoparticles, mercury, colorimetric sensing

3.24 Highly Selective Fluorescent Chemosensor for the Detection of Al^{3+} using a Rhodamine Spirolactam and its application in cell imaging

R. Manjunath and P. Kannan*

Department of Chemistry, Anna University, Chennai-600025 India. E-mail: rmanju.chem@gmail.com

A highly selective and sensitive rhodamine based fluorescent and colorimetric chemosensor for Al^{3+} was synthesized. The structures of synthesized compounds were confirmed by using $^1\text{H-NMR}$, $^{13}\text{C-NMR}$, IR, UV-Vis spectrometer and ESI-mass spectral data and its optical properties were studied by UV-Visible and fluorescence spectroscopy. Chemosensing behavior of the synthesized chemosensor were tested with various metal ions such as Zn^{2+} , Cd^{2+} , Ni^{2+} , Co^{2+} , Hg^{2+} , Li^+ , K^+ , Mg^{2+} , Na^+ , Ca^{2+} , Mn^{2+} , Cu^{2+} , Pb^{2+} in aqueous solution. The chemosensor displays an excellent selective and sensitive response towards Al^{3+} ions over other tested metal ions in the aqueous medium. Chemosensor L was colorless and non-fluorescent in the absence of Al^{3+} ions while addition of Al^{3+} ion pink color with strong fluorescence was observed. This process is mainly attributed by spirolactam ring-opening process of rhodamine dye. The colorimetric and fluorescent response of Al^{3+} ion can be conveniently detected even by naked eye and can serve as a naked-eye chemosensor for Al^{3+} ion. The association constant for $\text{L}+\text{Al}^{3+}$ was calculated as $2.03 \times 10^3 \text{ L mol}^{-1}$ with binding mode of 1:2 stoichiometric fashions. In addition, fluorescence imaging experiments of Al^{3+} ions in living cells demonstrate its value in practical applications in biological systems.



Fluorescence spectra of chemosensor with increasing concentration of Al^{3+} (0 - 2equiv.) in aqueous medium.

References:

- [1]. J.Y. Kwon, Y.J. Jang, Y.J. Lee, K.M. Kim, M.S. Seo, W. Nam, J. Yoon, *J. Am. Chem. Soc.* 127 (2005) 10107-10111.
- [2]. Hrishikesan, C. Saravanan, P. Kannan, *Ind. Eng. Chem. Res.* 50 (2011) 8225-8229.
- [3]. R. Balamurugan, C.C. Chien, B.C. Chen and J.H. Liu, *Tetrahedron.* 69 (2013) 235-241.
- [4]. M. Zhao, X. F. Yang, S. He, L. Wang, *Sens. Actuators B: 135* (2009) 625-631.
- [5]. K. Huang, H. Yang, Z. Zhou, M. Yu, F. Li, X. Gao, T. Yi, C. Huang, *Org. Lett.* 10 (2008) 2557-2560.

3.25 Synthesis and characterization of polythiophene-zinc oxide nanocomposite for oxygen sensing application

Regina. R, Heiner. A. J and Gurunathan. K*

Nano Functional Materials Lab, Dept. of Nanoscience & Technology, Science Campus, Alagappa University, Karaikudi, Tamilnadu, India – 630 003. E-mail: kgnathan27@rediffmail.com

Oxygen is an essential element for all living organisms. It has widely used in industries, medical field, space research, space & scuba suits etc. High fraction of inspired oxygen has been associated with several effects on lung tissues. Nano particles have vital role as the sensing electrode in gas sensing system due to its large surface area. Nanocomposites of polythiophene (PTh) and zinc oxide (ZnO) nanoparticles (NPs) have high sensitivity and selectivity towards oxygen gas. Preparation of the nano composite was done by oxidative polymerization method. In this method, the nano composite was synthesized by polymerization of thiophene with ammonium per sulfate (APS) as oxidizing agent with ZnO particles. Prepared nanocomposites were characterized by Fourier transform infrared (FTIR), Scanning Electron Microscope (SEM), Atomic Force Microscopy (AFM), Transmission Electron Microscopy (TEM), X-ray diffraction (XRD) and UV-Vis techniques, which proved the polymerization of thiophene monomer and the strong interaction between polythiophene and ZnO NPs. When the oxygen gas exposed to the material, the composite was oxidized by the oxygen. Due to the oxidation process, carrier concentration of the electrode gets changed. This change leads to change in resistivity. Resistance of the sensor electrode was measured using Four-probe technique. In typical experiment, 2.5ml of thiophene, 1g sodium lauryl sulfate (SLS) and 9.5ml triethanolamine (TEA) and in addition to the above solution, ZnO in 30ml of DDI water was mixed in a reaction vessel containing a magnetic stirrer. Simultaneously, ammonium persulfate (APS) was dissolved in 20ml of DDI water and added into the reaction mixture solution. The molar ratio of APS (5.3g) to thiophene monomer was 1.15. After 24hours, dark brown colour precipitate was collected and washed several times with DDI water and methanol. These nanocomposite products were dried in a vacuum oven at 80°C for 10 hours to get powder form of nanocomposite. The nano composite thin films were prepared by sol-gel spin coating method on glass substrate. The solution was prepared by using an organic solvent NMP solution. The well cleaned substrate was kept in the spinner. The spinner rotated at a constant speed of 3000 rpm. The evenly coated thin film was taken out from the spinner base and dried at vacuum oven at 70°C for 2 hours.

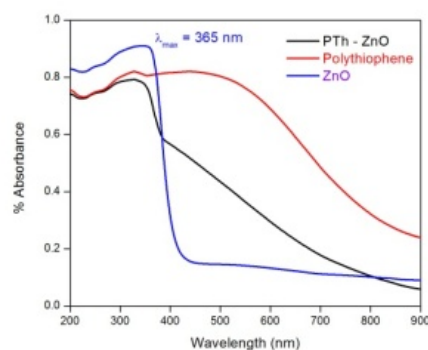


Fig 1: UV-visible spectra of nanocomposites

Reference:

- [1] Mostafa Nasrollahzadeh, Mohsen Jahanshahi, Mehdi Salehi, Mahdi Behzad and Hossein Nasrollahzadeh, Synthesis and characterization of nanostructured polythiophene in aqueous medium by soft-template method, *Journal of Applied Chemistry*, 8 (2013) 27.
- [2] T. V. Kolekar, S. S. Bandgar, S. S. Shirguppikar and V. S. Ganachari, Synthesis and characterization of ZnO nanoparticles for efficient gas sensors, *Arch. Appl. Sci. Res.* 5(6) (2013) 20-28.
- [3] S. Sakthivel and A. Boopathi, Synthesis and Fabrication of Polythiophene/Zinc Oxide Nanocomposites Thin film and Characterizations, *Nano Vision*, 5 (4-6) (2015) 77-82.

3.26 Dynamic sensing of L-Dopa using zinc oxide-reduced graphene oxide film

Palinci Nagarajan, Manikandan, Venkataraman Dharuman*

Molecular Electronics Laboratory, Department of Bioelectronics and Biosensors, Science Block, Alagappa University, Karaikudi – 630 004. E-mail: dharamanudhay@yahoo.com

Dynamic sensing of L-dopa (L-3,4-dihydroxyphenylalanine) using Zinc oxide-reduced graphene oxide to modify platinum electrode without using any enzyme. Graphene oxide was prepared by the modified Hummer's method and following its reduction using ascorbic acid/H₂SO₄. The zinc oxide-graphene interaction is confirmed by X-Ray Diffraction (XRD), Fourier Transform Infra-Red (FTIR) and Ultraviolet visible (UV-Vis) spectroscopic techniques. The 2 θ peak at 10.4° (111) indicates the chemical exfoliation of graphite resulting in graphene oxide formation from graphite (002) at 28.32°. The crystallite size of ZnO, ZnO-GO and ZnO-rGO are 60, 88 and 43 nm respectively. The decreasing crystallite size of ZnO-rGO composite indicates the ZnO anchoring on GO. FTIR peaks at 1086 cm⁻¹ (C-O), 2923 cm⁻¹ (C-H), 3450 cm⁻¹ (O-H) observed for GO and these peaks are decreased for reduced GO. The Zn metallic peak is observed at 440 cm⁻¹ for ZnO, ZnO-GO and Zn-rGO. The decreased IR bands for the ZnO-rGO are attributed to the reduced the C-O and O-H functional groups of GO. That is, the intensities of C=O group is completely disappeared in presence of ZnO on the rGO indicating the presence of lesser number of functional groups. UV-Vis peak of GO is blue shifted from 227 nm to 200 nm for the rGO. The GO-ZnO and rGO-ZnO were prepared in water using ultra-sonication for 1 hour. The band gap energy of ZnO, ZnO-GO and ZnO-rGO are 3.72, 4.45 and 3.03eV respectively. These modified electrodes are investigated by cyclic voltammetry (CV) and electrochemical impedance spectroscopy (EIS) in the presence of 1mM of [Fe(CN)₆]^{3-/4-} prepared in phosphate buffer saline (PBS) at pH 7.4 and applied for L-dopa detection selectively. ZnO-rGO composite enhances oxidation of L-dopa compared to ZnO-GO.

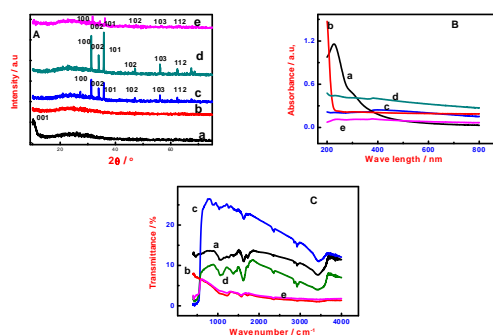


Fig.1 (A) XRD, (B) UV-Vis and (C) FTIR characterizations of (curve a) GO, (curve b) rGO, (curve c) ZnO, (curve d) GO-ZnO and (curve e) rGO-ZnO.

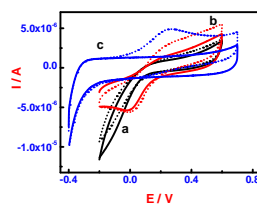


Fig.2 CV behavior of (curve a) ZnO, (curve b) GO-ZnO and (curve c) rGO-ZnO in the absence (solid line) and presence of 0.2 mM of l-dopa prepared in 100 mM PBS at pH 7.4

Key words: Electrochemical techniques (CV, EIS, CA), XRD and FTIR

3.27 Electrochemical Investigation of Lead (II) ion using Sulphanilic acid functionalized mesoporous carbon modified electrode

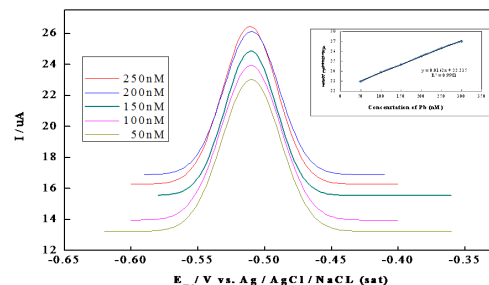
Subramani. S. E¹, Sangeetha. C¹ and Thinakaran. N^{1*}

Environmental Research Lab, PG & Research Department of Chemistry, Alagappa Government Arts College, Karaikudi-630003. Email: thinakaran2k@yahoo.com

Abstract

Most of the heavy metal ions are carcinogens and lead to serious health concerns by producing free radicals. Hence, fast and accurate detection of metal ions has become a critical issue. In this study a new sensitive electrochemical sensor, glassy carbon electrode modified with functionalized mesoporous carbon was constructed to detect the lead metal ions. Mesoporous carbon was synthesized by soft templating technique using resorcinol-formaldehyde-pluronic 127. The prepared mesoporous carbon was functionalized by sulphanilic acid (SAMESO). Lead ion detection was carried out by using square wave anodic stripping voltammetry (SWASV) technique without the removal of oxygen. The morphology of SAMESO was investigated by SEM, and the presence of the amino and sulphonic acid groups & pore size were confirmed using FTIR and XRD techniques. Among the various supporting electrolytes studied acetate buffer gives the good response for the detection of lead metal ions. Cyclic voltammetry technique was used to calculate the active surface area of electrode and diffusion coefficient of the electrolyte. The limit of detection of the modified electrode was found out by various concentrations of lead II ions. The functionalized mesoporous carbon modified glassy carbon electrode has excellent response, good selectivity, low detection of limit and long term stability. The effect of accumulation potential and time were investigated and optimized. The SAMESO electrode was found to be suitable for selective determination of Pb(II) in the solutions containing the mixture of heavy metal simultaneously and individually, including Cd(II), Pb(II) and Cu(II) ions. The limits of detection (LOD) were 13.75 nM for Pb²⁺. Additionally, the repeatability, reproducibility, anti-interference ability and application were also investigated and the proposed electrode exhibited excellent performance. The proposed method could be extended for other heavy metal determination.

Key Words : Mesoporous Carbon, Cyclic Voltammetry and Square Wave Anodic Stripping Voltammetry (SWASV)



Effects of various concentrations of Pb (From 50nM to 250nM) on the response of the SAMESO/GC electrode and its calibration Curve in acetate buffer at pH 4.5 under optimal conditions: accumulation potential -0.64V, accumulation time 120s

3.28 Determination of Reactive Red 141 Dye by Stripping voltammetry

C. Kavitha and H. Gurumallesh Prabu*

Department of Industrial Chemistry, School of Chemical Sciences, Alagappa University, Karaikudi - 630 003, India
Tel.: +919443882946; Fax: +91 4565225202 E-mail: hgprabu2010@gmail.com, hgprabhu@alagappauniversity.ac.in

Abstract

Stripping Voltammetry (SV) is a very sensitive method for the analysis of trace concentrations of electroactive species in test solution. Reactive Red 141 (RR 141) is bis azo class dye. Cyclic Voltammetry (CV) analysis showed that the RR 141 dye was electroactive species. pH of the solution was varied from 1 to 13, a pH of 7 gave good peak responses at peak potential around 0.5 V. In CV, when the scan rate was varied from 0.010 to 0.5V/s, the peak current increased (Fig.1). Similarly, when the concentration was varied from 100 µl to 1000 µl, the peak current (i_p) also increased, but peak potential (E_p) maintained around 0.5 V. From the CV data, plot of $\log i_p$ versus $\log v$ slope yielded a value of 0.3134, hence the reaction is termed as diffusion controlled. From the CV analysis of RR 141 dye, the reduction process was found to be irreversible and the diffusion co-efficient value $5 \times 10^{-10} \text{ cm}^2/\text{s}$ was obtained. An optimum pH of 7 and cathodic reduction peak of 0.5 V were considered and used for further analysis under SV.

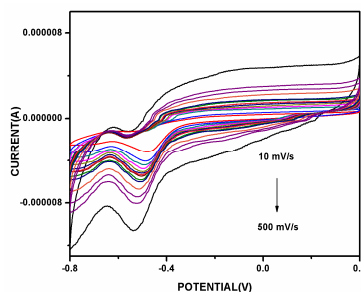


Figure 1: Cyclic voltammogram of RR141 dye with increasing scan rate from 10 mV/s to 500 mV/s. The analyte concentration from 10^{-6} to 10^{-9} M was used for the stripping analysis. The current in SV increased while increase the concentration of analyte. Stripping voltammogram of the dye in buffer with an adsorption time of 60 s, exhibits a well-defined peak which has attributed to the reduction of the bis azo group of RR 141 dye.

Key words: Cyclic voltammetry, Stripping voltammetry, Reactive Red 141 dye.

References

- [1] M.V.B. Zanon, P.A. Carnciro, M. Furlan, E.S. Duarte, C.C.I. Guaratin, A.G. Fogg, *Analytica chimica acta* 385 (1999) 385.
 [2] C.C.I. Guaratini, A.G. Fogg, M.B. Zanoni, *Dyes and pigments* 50 (2001) 211.

3.29 Metal-organic framework based ammonia gas sensor

T. Ponmuthuselvi and S. Viswanathan*

Department of Industrial Chemistry, Alagappa University, Karaikudi-630 003, Tamil Nadu, India.

E-mail: rviswa@gmail.com

Metal-Organic Frameworks (MOFs) are a class of novel porous, three-dimensionally linked coordination network materials, which are composed of metal ions and organic ligands by strong coordination bonds. MOFs have similar structure contrasted to zeolites or alumina silicates. Unlike zeolites which are purely inorganic, MOFs are hybrids of inorganic and organic materials. MOFs have greater advantage than well-known nanoporous zeolites because of its structural and functional group tenability [1]. MOFs have been used for storage, purification, separations of gases, for drug release/delivery, heterogeneous catalysis and sensing [2]. Composites containing copper MOF with reduced graphene oxide (Cu-MOF-rGO) were synthesized by Solvothermal method from the precursors of copper nitrate, benzene tricarboxylic acid (BTC) and graphene oxide. As prepared Cu-MOF and Cu-MOF-rGO was characterized by SEM to investigate the surface morphology. Crystallinity and the functional group's presence in the MOF samples was successfully proved by powder XRD and ATR-FTIR spectroscopy respectively.

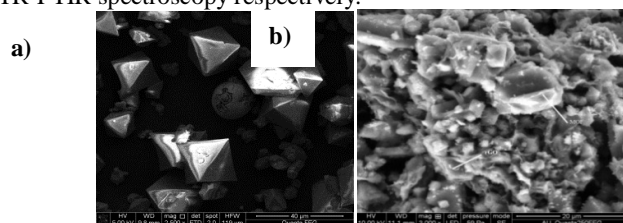


Fig: 1 SEM image of a) Cu-MOF b) Cu-MOF-rGO by solvothermal method

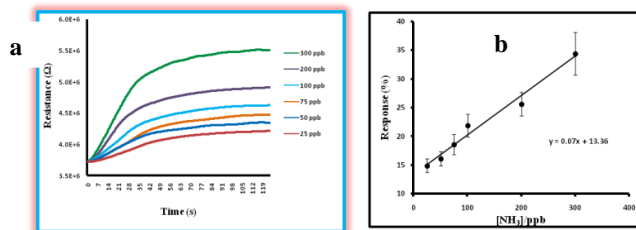


Fig:2 a) Electrochemical response and b) Error bars representing the standard deviation from the mean for ammonia sensing at different concentrations of 25 ppb to 300 ppb using Cu-MOF-RGO hybrid materials

As prepared Cu-MOF-rGO materials was utilized for ammonia (NH_3) gas sensor. NH_3 molecules are absorbed

into the cavity of Cu-MOF-rGO by chemisorption and there is an electron donation through the organic linker (BTC), would result in a decrease in their conductivity, due to the depletion of the charge carriers (holes) (3). The change in normalized resistance upon the exposure of different concentrations of ammonia was monitored by amperometric technique. The graph plotted between Time vs Resistance indicates the reliable linearity of Cu-MOF-rGO composite over a range of concentrations from 25-300 ppb. The recovery of composite from each experiment can be done by activating it through 150°C for 30 minutes.

Keywords: Metal-organic framework, Solvothermal method, amperometric technique.

References:

[1] E. Lauren Kreno, Kirsty Leong, K. Omar, Farha, Mark Allendorf, P. Richard, Van Duyne, and T. Joseph, Hupp, *Chem. Rev.* 112, (2012) 1105–1125

[2] Nikolina A. Travlou, Kavindra Singh, Enrique Rodríguez-Castellón and Teresa J. Bandosz, *J. Mat. chemistry*. 2015, 1-3.

3.30 A fluorescent probe based on histidine carbon dots for highly sensitive detection of Hg²⁺ in aqueous solution

M. Jayalakshmi, M. Maniyazagan, T. Stalin*

Department of Industrial Chemistry, School of Chemical Sciences, Alagappa University, Karaikudi-03, Tamil Nadu, India.

*E-mail address: drstalin76@gmail.com

Abstract

A facile and green hydrothermal method was developed for the preparation of highly fluorescent carbon dots (CDs) by using histidine and urea as carbon source and nitrogen source, respectively. Compared with previous hydrothermal method, the proposed method is performed at comparatively lower temperature and results in 20~30 nm size [1]. As-obtained CDs show a strong emission at 405 nm with an optimum excitation at 265 nm, and exhibit high photostability. Because of the Hg²⁺-induced fluorescence quenching of carbon dots (CDs), such CDs can be used as an effective fluorescent probe for highly selective and sensitive detection of Hg²⁺ in aqueous solution, with a limit of detection (LOD) as low as 5.85 nM in a linear range of 0–50 nM. The CDs showed high sensitivity and selectivity for Hg²⁺ relative to other competitive metal ions such as Na⁺, Ni²⁺, Co²⁺, Ag⁺, Mn²⁺, Cd²⁺, Pb²⁺, Fe³⁺, K⁺, Zn²⁺, Al³⁺, Cu²⁺, and Fe²⁺, by reducing the fluorescence emission at 405 nm [2]. The fluorescence studies of the CDs in the presence of Hg²⁺ revealed that the mechanism of quenching involves complexation and that dynamic quenching dominates over static quenching [3]. The CDs have been successfully applied to the analysis of tap water sample and we believe its simplicity, sensitivity and selectivity will make it promising for monitoring mercury pollution in the environment.

Keywords: Histidine, Carbon dots, Fluorescence, Hg²⁺, Sensor, Off-On.

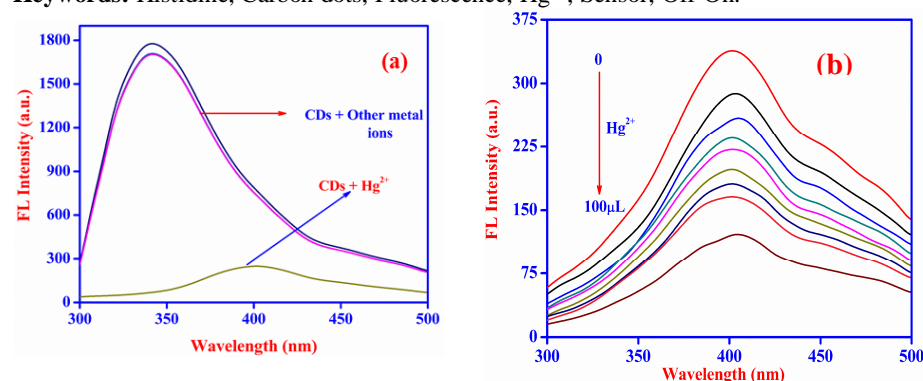


Figure 1. (a) Fluorescence spectra of the CDs aqueous solution in the presence of different metal ions (Na⁺, Ni²⁺, Co²⁺, Ag⁺, Mn²⁺, Cd²⁺, Pb²⁺, Fe³⁺, K⁺, Zn²⁺, Al³⁺, Cu²⁺, and Fe²⁺). (b) The fluorescence titration spectra of CDs upon addition of different concentration Fe³⁺.

References

[1]. Y. Zhang, Y. H. He, P. P. Cui, X. T. Feng, L. Chen, Y. Z. Yang and X. G. Liu, *RSC Adv.*, 5, 2015, 40393.

[2]. Y. Liang, H. Zhang, Y. Zhang and F. Chen, *Anal. Methods*, 7, 2015, 7540-7547.

[3]. Z. Gao, Z. Lin, X. Chen, H. Zhong and Z. Huang, *Anal. Methods*, 8, 2016, 2297-2304.

3.31 Rhodamine based gold nanoparticles for rapid colorimetric detection of Fe³⁺ ions in aqueous medium with real sample applications

U. Thenmozhi^a, M. Maniyazagan^a, T. Stalin^{a,*}

^aDepartment of Industrial Chemistry, School of Chemical Sciences, Alagappa University, Karaikudi-03, Tamil Nadu, India.
E-mail address: drstalin76@gmail.com

Abstract

In this study, a simple rhodamine based gold nanoparticles analytical system is presented for the detection of Fe³⁺ with a wide concentration range, which is respectively based on the fluorescent and colorimetric properties of rhodamine gold nanoparticles [1]. This dual-functional system can work directly for aqueous medium and expand efficiently a wide detection range for Fe³⁺ determination. By using the fluorescence method, the lowest concentration for quantification of Fe³⁺ ions is 2.60×10^{-7} M, and the sensitivity is good enough for the determination of Fe³⁺ ions in drinking water. To recognize higher concentration of Fe³⁺ ions for industrial sewage monitoring, the colorimetric behavior can be used as an alternating tool for field tests from naked eye [2]. The system also provides an excellent selectivity towards Fe³⁺ ions over other common interfering Na⁺, Ni²⁺, Co²⁺, Ag⁺, Mn²⁺, Cd²⁺, Pb²⁺, Hg²⁺, K⁺, Zn²⁺, Al³⁺, Cu²⁺, and Fe²⁺ ions, thus enabling the ability to monitor Fe³⁺ ions contamination in environmental samples [3]. Furthermore, several real water samples spiked with Fe³⁺ ions, including tap water, drinking water, were analyzed, and the experimental results demonstrated that this sensing system exhibited excellent recoveries for these practical water samples. Our attempt may provide a cost-effective, rapid and simple solution for the recognition and determination of different levels of Fe³⁺ ions contamination in aqueous samples.

Keywords: Gold, Nanoparticles, Fe³⁺ ion, Fluorescence Sensor, Wide-Range Detection.

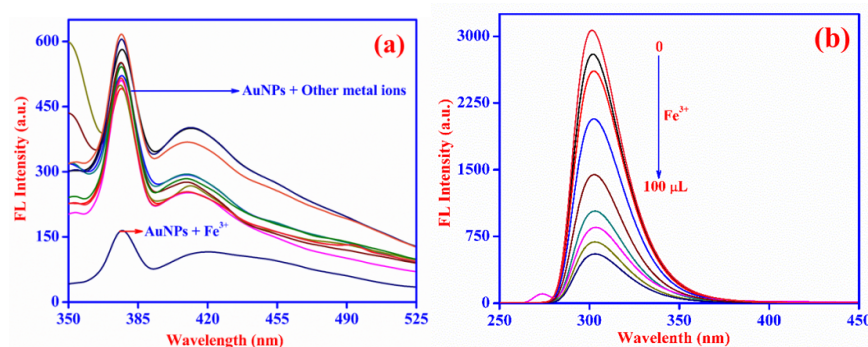


Figure 1
Fluorescence spectra of bare AuNPs in the presence of various metal ions (3 μM)
(a). Absorption spectral changes of bare AuNPs in the presence of different concentrations of Fe³⁺ ions (0–3 μM)
(b).

References

- [1] S. Kubik, *Chem. Soc. Rev.* 39 (2010) 3648–3663.
- [2] D. T. Quong, J. S. Kim, *Chem. Rev.* 110 (2010) 6280–6301.
- [3] J. F. Zhang, Y. Zhou, J. Yoon, J. S. Kim, *Chem. Soc. Rev.* 40 (2011) 3416–3429.

3.32 Electrochemicaldetermination of 4-Nitrophenol by Single-Drop Micro Extraction

S. Sudha, I. Victor Emeka, T. Ponmuthuselvi and S. Viswanathan*

Department of Industrial Chemistry, Alagappa University, Karaikudi-630 003, TN, India. *E-mail: rsviswa@gmail.com

Abstract

4-Nitrophenol (4-NP) has been considered a toxic pollutant causing slow photosynthetic reactions carcinogenicity and other related serious harmful effects toward human and aquatic life [1]. A novel single-drop micro extraction (SDME) method for nitro phenol pesticides determination by using Voltammetric technique was developed [2]. The successful synthesis of graphene oxide (GO) and reduced graphene oxide (rGO) are characterized by using Scanning electron microscopy (SEM), Atomic force microscopy (AFM), X-ray diffraction method and UV-Visible spectroscopy. rGO modified glassy carbon electrode (GCE) was prepared by drop cast method.

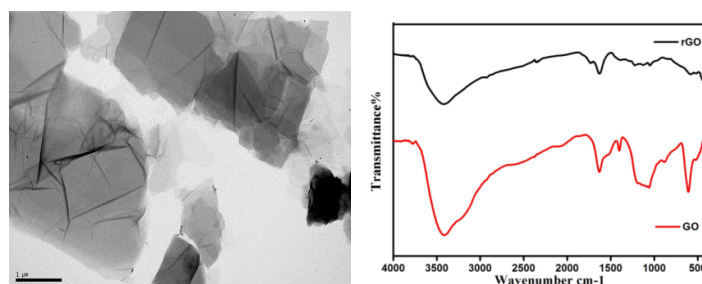


Fig: 1 a) SEM and b) IR image of rGO and GO by Hummers method

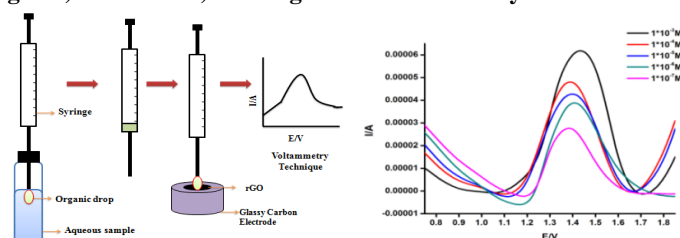


Fig 2 a) Schematic representation of SDME b) DP anodic voltammograms of SDME extracts in various concentration of 4-NP at rGO modified GCE

The modified electrodes were investigated using of Cyclic Voltammetry and Electrochemical impedance spectroscopy technique. Electrochemical behavior of 4-NP on rGO modified GCE outcomes in enhanced anodic and cathodic peak potentials at +1.2V and -0.492 V respectively. An effective preconcentration method for the extraction and determination of traces of multi-residue pesticides was developed using SDM extraction and differential pulse voltammetry (DPV). Extracts obtained using 10 μ l of dichloromethane (DCM) from 4-NP pesticides aqueous sample were drop casted on rGO modified GC electrode. Differential pulse voltammetry was applied to observe corresponding oxidation peak of phenol group at +1.42V. The effects of exposure time and organic drop volume were optimized. The detection limit was observed by 4-NP concentration range from 1×10^{-3} to 1×10^{-7} M.

Keywords: Nitro phenol pesticides, SDME, Differential pulse voltammetry.

References:

- [1] W. Ahmad, A. A. Al-Sibaai, A. S. Bashammakh, H. Alwael, and M. S. El-Shahawi. *TrAC Trends in Analytical Chemistry* 72 (2015) 181-192.
 [2] Virgínia Fernandes, S. Viswanathan, Nuno Mateus, Valentina F. Domingues, and Cristina Delerue-Matos. *Microchimica Acta* 178(2012) 195-202.

3.33 Microfluidic Biosensor for Cholera Toxin Detection

S. Viswanathan^{a,b*}, Ja-an Annie Ho^c, Cristina Delerue-Matos^b

^aDepartment of Industrial Chemistry, Alagappa University, Karaikudi - 630003, Tamilnadu.

^bREQUIMTE - Instituto Superior de Engenharia, Instituto Politécnico do Porto, Rua Dr. António Bernardino de Almeida 431, 4200-072 Porto, Portugal.

^cBioanalytical chemistry and Nanobiomedicine Laboratory, Department of Biochemical Science and Technology, National Taiwan University, No. 1, Sec. 4, Roosevelt Road, Taipei 10617, Taiwan.

Contact: email: rviswa@gmail.com

Cholera is an epidemic diarrheal disease characterised by extreme diarrhoea, vomiting and cramps, often leading to death. The Indian subcontinent is endangered to this disease due to its vast coastlines with areas of poor sanitation, unsafe drinking water, and population. Climatic conditions also play a major role in the persistence and spread of cholera. Cholera is also changing epidemiologically. Multiple antibiotic resistant strains of *V. cholerae* have emerged along with the El Tor variants that produce the cholera toxin of the classical biotype that has spread into Asia and parts of Africa. The severity of the disease appears to be intensifying and recent cholera outbreaks in various places, including Zimbabwe, have run a more protracted course. The severe dehydration can cause death within 3-4 h in cases of untreated patients. The causative agent of this disease is cholera toxin (CT) produced from the bacteria *Vibrio cholerae*. Nowadays, the conventional laboratory diagnosis of cholera is performed by culturing the bacteria from a patient's specimen, which requires 1-2 days. This method might be too long for immediate treatment. Moreover, some strains may not produce the toxin which can result in false positives. We have therefore investigated to develop sensitive microfluidic immunosensors for the detection of cholera toxin. This biosensor was previously developed and tested in

conventional electrochemical setup only, using electrochemical detection strategies [1, 2]. In this work microfluidic channel was made from polydimethylsiloxane and this integrated with gold screen printed electrode. Cholera toxin subunit B (CTB)-specific monoclonal antibodies Fab part immobilized onto screen printed gold electrode and ganglioside GM1-containing liposomes with redox label were used for CTB recognition in the detection system. The cross-reactivity of electrochemical microfluidic CTB- immunosensors was investigated by the heat-labile Escherichia coli toxin and was found to be negligible. A limit of detection smaller than 5 ng mL^{-1} was achieved. The developed microfluidic integrated electrochemical immunosensor fulfil the requirement of low cost and quick reply of the assay and are expected to enable field screening, prompt diagnosis and medical intervention without the need of specialized personnel and expensive equipment, a perspective of special relevance for use in developing countries.

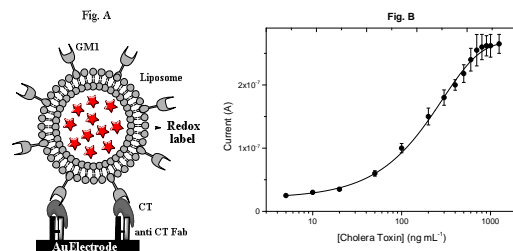


Fig. A Scheme of liposome amplified electrochemical detection of Cholera Toxin B; Fig. B Cholera Toxin concentration-dependent peak current responses versus concentration (ng mL^{-1}) on semi log plot.

Key words: cholera toxin, liposome, immunosensor, microfluidic

References:

- [1]. S.Viswanathan, L.C. Wu, M.R. Huang, J. A. Ho, *Analytical chemistry*, 78 (2006) 1115-1121.
- [2]. N.Bunyakul, C.Promptmas, A. J.Baemner, *Analytical and bioanalytical chemistry*, 407(3) (2015) 727-736.

3.34 Organometallic compounds (OMC): a new sensing platform for biomolecules

K. Dinesh Christy, S. Prakash, P. Muthuraja, P. Manisankar*

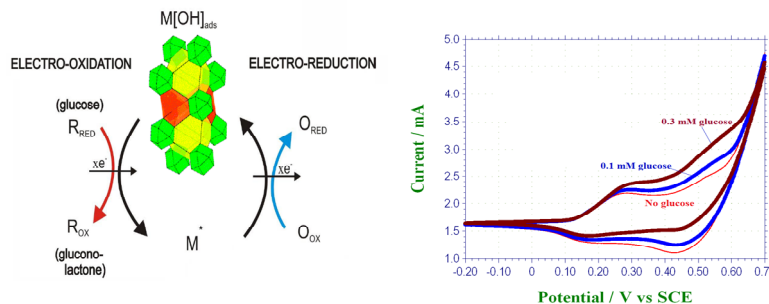
Department of Industrial Chemistry, Alagappa University, Karaikudi-630006, India.

*Email: manisankarp@alagappauniversity.ac.in

Organometallic compounds (OMC) are represents a new class of hybrid material built from metal ions with well-defined coordination geometry and organic bridging ligands. The structure of these crystalline nanoporous materials is composed of metal ions joined by a variety of rigid-rod-like organic ligands through strong covalent bonds¹. This type of structure not only provides OMC with tunable options, organic functionality, high thermal and mechanical stability, open metal sites in the skeleton, large pore sizes, and high surface areas, but also enables easy preparation in one-pot². Due to these fascinating features,³ they have been widely applied in gas storage,⁴ separation,⁵ imaging,⁶ catalysis⁷ and drug delivery⁸. In OMCs, the ligands usually contain a conjugated p- electron system⁹ allowing for binding biomolecules. Additionally, some metal ions are usually used as the coordination centers and open sites, which have intrinsic fluorescence quenching properties¹⁰. Hence, prepared OMCs may have an ability similar to the above carbon nanostructures. We synthesized cobalt based organic compounds for application of enzymeless glucose sensing. The prepared OMC were characterized by scanning electron microscopy (SEM), powder X-ray diffraction (XRD), and FT-IR methods. The structural characterization revealed that the OMC were composed of the organic moiety and inorganic moiety mixed. Moreover, a good synergetic effect between organic moiety and inorganic moiety was confirmed. The enzymeless biosensing properties of as prepared electrodes based on glassy carbon (GCE) were studied and the results indicated that the sensing properties of OMC electrodes were significantly improved. It also showed outstanding long term stability, good reproducibility, excellent selectivity and accurate measurement in synthetic sample.

A schematic illustration of the Incipient Hydrous Oxide Adatom Mediator' (IHOAM) model in which M^* is the reductive metal adsorption site, and $M[OH]_{ads}$ is the oxidative adsorbed hydroxide radical. The scheme shows how both oxidative and reductive processes are catalysed at the metal surface. CVs of prepared OMC electrode for sensing of glucose at different concentrations.

Keywords: Organometallics, Glucose, Non-enzymatic, Electrochemistry



References

- [1] G. Férey, Chem. Soc. Rev., 2008, 37, 191.
- [2] D. N. Dybtsev, H. Chun and K. Kim, Angew. Chem., Int. Ed., 2004, 43, 5033.
- [3] S. Kitagawa, R. Kitaura and S. Noro, Angew. Chem., Int. Ed., 2004, 43, 2334.
- [4] R. Banerjee, A. Phan, B. Wang, C. Knobler, H. Furukawa, M. O'Keeffe and O. M. Yaghi, Science, 2008, 319, 939.
- [5] L. Q. Ma, J. M. Falkowski, C. Abney and W. B. Lin, Nat. Chem., 2010, 2, 838.
- [6] K. M. L. Taylor-Pashow, J. Della Rocca, Z. G. Xie, S. Tran and W. B. Lin, J. Am. Chem. Soc., 2009, 131, 14261.
- [7] L. Q. Ma, J. M. Falkowski, C. Abney and W. B. Lin, Nat. Chem., 2010, 2, 838.
- [8] P. Horcajada, C. Serre, G. Maurin, N. A. Ramsahye, F. Balas, M. Vallet-Regi, M. Sebban, F. Taulelle and G. Férey, J. Am. Chem. Soc., 2008, 130, 6774.
- [9] Y. J. Cui, Y. F. Yue, G. D. Qian and B. L. Chen, Chem. Rev., 2012, 112, 1126.
- [10] J. W. Liu and Y. Lu, J. Am. Chem. Soc., 2007, 129, 9838.

3.35 Label-Free Electrochemical Immunosensor for Egg Allergen

S. Viswanathan^{a,b,*}, M. B. P. P. Oliveira^c, K. Thangapandi^a, Cristin Delerue-Matos^b,
^aDepartment of Industrial Chemistry, Alagappa University, Karaikudi - 630003, Tamilnadu.

^bREQUIMTE - Instituto Superior de Engenharia, Instituto Politécnico do Porto, Rua Dr. António Bernardino de Almeida
 431, 4200-072 Porto, Portugal.

^cREQUIMTE/Departamento de Ciências Químicas, Faculdade de Farmácia, Universidade do Porto, Rua de Jorge Viterbo
 Ferreira, 228, 4050-313 Porto, Portugal.
 E-mail: rsviswa@gmail.com

The development of electrochemical immunosensor for rapid detection of egg-related allergens in baby food products is herein described. Ovalbumin (OVA) was chosen as the target protein to be monitored due to its major constituent in the egg white powder, a typical ingredients used by the baby food industries to promote nutrient value [1]. A label free electrochemical immunoassay was designed, basing on the use of polyclonal anti-OVA antibody as bio-specific receptor. With the aim of optimizing the assay conditions, different parameters able to influence the final biosensor response were carefully investigated. After the fine tuning of these parameters, the assay was tested in the direct analysis of OVA in baby food products artificially contaminated with egg white powder at different concentration levels in order to assess the reliability of the biosensor in detecting traces of OVA in complex matrices. Gold nanoelectrode ensembles (GNEE) electrode, Pt wire counter and Ag/AgCl reference electrodes were used to perform the electrochemical measurements. Self-assembled mixed monolayer is formed on the GNEE using 6-Mercapto-1-hexanol and 11-Mercaptoundecanoic acid solution. Polyclonal anti-OVA antibody was used to attach with COOH terminal by coupling agents N-hydroxysuccinimide (NHS) and 1-(3-Dimethylaminopropyl)-3-ethylcarbodiimide methiodide (EDC).

Scanning Electron Microscopy (SEM) surface image of the membrane shows gold nanowires with an average diameter of 50 nm and a length of 180 ± 20 nm. With antibody exposing out of the self-assembled monolayer on GNEE, anti-OVA antibody (OVA-Ab) undergoes immunoreactions. A selective binding with OVA-Ab occurs between OVA in solution. After the formation of immunocomplex the electrode surface is found inhibited. The developed label free immunosensor showed advantages over the available methods for determination OVA in food samples.

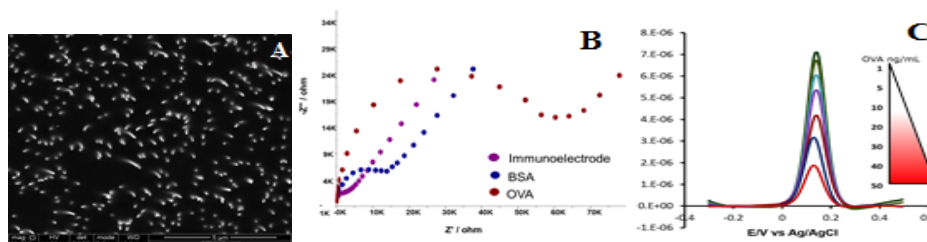


Figure 1. A. Scanning electron microscopic image of a GNEE; B. Comparison of Nyquist plots of immunoelectrode before and after incubated with BSA and OVA and C. Square wave voltammetry of OVA Biosensor (base line subtracted)

Key words: immunosensor, egg allergen, Ovalbumin, nanoelectrode

Reference:

[1]. S.Eissa, L.L.Hocine, M.Siaj, M. Zourob, *Analyst*, 138(15) (2013) 4378-4384.

3.36 Highly sensitive and selective fluorescent sensor for unique cadmium ion in aqueous media

P. Sakthivel, and K. Sekar*

Department of Chemistry, Anna University, University College of Engineering - Dindigul, Dindigul - 624 622, Tamilnadu, India. *E-mail address: karuppannasekar@gmail.com

Abstract

The designed for selective and sensitive sensors able to monitor in real-time the concentration of analytes of Biological, clinical, and environmental interest is nowadays generally accepted. Recognition of metal ions with high specificity under physiologically relevant conditions is an important aspect in the design of fluorescent chemosensors for biological and environmental applications. Cadmium, an important natural element¹, is widely used in many fields, such as industry, agriculture, military affairs, etc., but people have come to realize the toxic effects of exposure to excessive cadmium. Chronic cadmium² exposure can cause renal dysfunction and calcium metabolism disorders, prostate cancer. Recently, Rhodamine-B based fluorescent dyes have attracted extensive interest for current researchers owed their excellent photo-physical properties³, high fluorescence quantum yield and visible-wavelength excitation. Above and beyond, it is well known that rhodamine derivatives with a spirolactam structure are non-fluorescent; on the other hand, when rhodamine derivatives bind to metal ions or protons, ring-opened amides give rise to strong fluorescence emission. In view of that, the design of fluorescent molecular sensors with improved selectivity is the focus of many research groups follows a line of investigation. In the present study, we report the synthesis and metal-binding properties of new Rhodamine B Hydrazide-Diaminomaleonitrile (RBHDM) based fluorescent sensor. The new fluorescent probe was obtained from two stage reaction, first one synthesis of (E)-2-((3',6'-bis(diethylamino)-3-oxospiro[isoindoline-1,9'-xanthen]-2-yl)imino) acetaldehyde, after the final fluorescent probe RBHDM was condensation method of the over aldehyde and Diaminomaleonitrile under reflux condition.

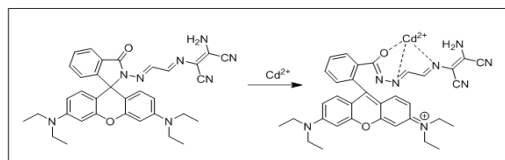


Fig 1: Synthesis of the Compound RBHDM.

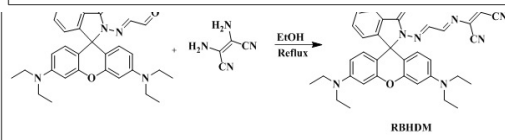


Fig 2: Proposed binding mechanism of RBHDM and Cd^{2+} ion.

It was designed for naked-eye detection of Cd^{2+} , which displayed high selectivity in the presence of other competitive metal ions. The rhodamine B derivative with a spirolactam group, the free RBHDM remained colorless and did not exhibit apparent absorption above 500 nm in CH_3CN/H_2O (v/v = 7: 3, 10 μM) Upon addition of Cd^{2+} (1.0 equiv.) to a solution of RBHDM in CH_3CN/H_2O , the absorption at around 527 nm was significantly enhanced, along with an obvious color change from colorless to red and this indicated that the spirolactam form was opened. Thus, by employing RBHDM Probe - Cd^{2+} can be distinguished easily and further studies of various techniques such as NMR, Mass, and Fluorescence spectra, cell imaging have been adopted for the detection of the new fluorescence sensor compound.

References

[1] Tae Geun Jo, Yu Jeong Na, Jae Jun Lee, Myoung Mi Lee, Sun Young Lee and Cheal Kim, *J. Mater. Chem. B*, 2 (2014) 7918–7926.

[2] Krishnendu Aich, Shyamaprosad Goswami, Sangita Das, Chitragada Das Mukhopadhyay, Ching Kheng Quah, and Hoong-Kun Fun, *Inorg. Chem.* 54 (2015) 7309–7315.

[3] Yang Ma, Fang Wang, Srinivasulu Kambam, Xiaoqiang Chen, *Sensors and Actuators B* 188 (2013) 1116–1122.

3.37 Fabrication of p-Cresol sensor for veterinary applications

N. Sudhan^a, C. Manikkaraja^b, G. Archunan^b, P. Manisankar^c, C. Sekar^{a*}

^aDepartment of Bioelectronics and Biosensors, Alagappa University, Karaikudi-630003

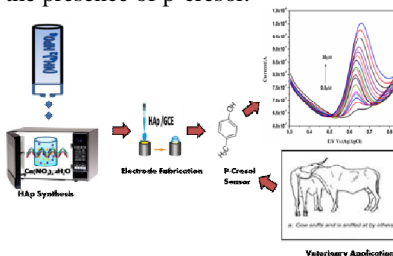
^bDepartment of Animal Science, Bharathidasan University, Tricity-620024.

^cDepartment of Industrial Chemistry, Alagappa University, Karaikudi-630003.

Email: Sekar2025@gmail.com

Many mammalian species are known to use olfactory communication to coordinate their reproductive and social activities. The pheromone signals secreted through urine, feces, vagina, saliva, and specialized scent glands including the hair and wool during estrous cycle indicates the timing of the physiological event of ovulation [1]. The detection of estrus and diagnosing early pregnancy are important problems in farm animals, particularly in buffalo. Effective use of assisted reproductive techniques like artificial insemination, in vitro fertilization/embryo transfer in cattle mainly depends on the time of estrus it is inseminated. The other problems like irregular or prolonging of the estrous cycle, anestrus, fighting behavior among young ones, mother-young bond, unmotivated males, and poor farm animal management including stress are considered as major issues in farm animals that need to be addressed [2]. Detection of pheromone compounds have been used as one of the strategies for the purpose of enhancing livestock production. para-Cresol is one of the significant pheromone compounds in mammalian reproduction systems and it is shown to be prominently high in concentration in buffalo during its estrous period. It is being detected in urine samples of buffalo by mass spectrometry and gas chromatography which are time consuming, expensive and labor intensive. Here, we report the fabrication of a novel electrochemical sensor based on hydroxyapatite (HAp) nanoparticles for the detection of p-cresol.

Hydroxyapatite ($\text{Ca}_{10}(\text{PO}_4)_6(\text{OH})_2$, HAp), the main component of mineral bone, exhibits excellent biocompatibility with various kinds of cells and tissues making it suitable for applications in dental, orthopedic, and tissue engineering applications. In recent years, great efforts have been made in developing nanostructured HAp for applications in the field of biosensors [3, 4]. HAp nanoparticles were synthesized by a simple microwave irradiation method and structural and morphological studies have been carried out by using XRD, FT-IR, and SEM. A novel electrochemical sensor has been fabricated based on HAp NPs modified glassy carbon electrode (GCE) for the selective detection of p-Cresol in phosphate buffer solution (PBS, pH 6.0) for the first time by differential pulse voltammetry (DPV). Under optimum conditions, the anodic peak current is proportional to the concentrations of p-Cresol over a wide linear range of 0.5 μM to 30 μM with the lowest detection limit of 300 nM. The developed sensor displayed high sensitivity, good stability and reproducibility which were attributed to the good affinity and the ion exchange ability of HAp nanoparticles. The fabricated sensor was applied to detect p-Cresol in the buffalo urine collected during estrus cycle and diestrus period and the quantity of p-cresol was estimated. Interestingly, similar studies on male buffalo urine, non-estrus buffalo urine and human urine did not show the presence of p-cresol.



References

- [1]. Rekwot P.I, Ogwu D, Oyedipe E.O, Sekoni V.O. *Anim. Reprod. Sci.* 65 (2001) 157.
- [2]. Patra M.K, Barman P, Kumar H. *Agri. Rev.* 3 (2012) 82.
- [3]. N.Lavanya, N.Sudhan, P.Kanchana, S.Radhakrishnan, C.Sekar, *RSC Adv.* 5 (2015) 52703.
- [4]. P. Kanchana, N. Lavanya, C. Sekar, *Mater. Sci. & Engg. C* 35 (2014) 85.

4.1 Impact of Sodium in the Photocatalysis of ZnTiO₃ Powder Prepared by Coprecipitation Oxalate Method

Sirajudheen P

Department of Chemistry, WMO Imam Gazzali Arts and Science College, Kerala- 670721, India,
E-mail: sirajpallyalil@gmail.com

Abstract.

The coprecipitation oxalate method is used for the preparation of Zinc titanate (ZnTiO₃). Zinc nitrate and titanium (IV) isopropoxide are used as the starting materials; The mole ratio of Zn:Ti is taken as 1:1. The synthesized powder is calcined at 900°C for 3 hours in muffle furnace. The atomic absorption spectra (AAS) are used to study the stoichiometry of the zinc titanate. The phase transformation of ZnTiO₃ powder is studied by using X-ray diffraction analysis (XRD), both hexagonal and cubic phase of ZnTiO₃ powder are attained after calcination at 800°C and hexagonal phase alone obtained at 900 °C. The bonding characteristics of ZnO and TiO₂ are analyzed by using FT-IR. By means of Thermogravimetric analysis decomposition temperature is analyzed. The photocatalytic activity of ZnTiO₃ is measured based on the photo bleaching of methyl orange (MO) in aqueous solution in presence of metallic sodium. The dye exhibited better photocatalytic activity in visible range radiation.

1. Introduction

The study aimed to synthesize zinc titanates, by a simple coprecipitation oxalate method and to analyze the phase transitions by various characterization techniques, to investigate phase transformation for predicting the formation of zinc titanate, and also, to analyze the photocatalytic degradation of methyl orange with ZnTiO₃ in presence of metallic sodium in visible range irradiation.

2. Materials and Methods

2.1. Materials

Zinc nitrate and titanium isopropoxide are the preliminary materials. Oxalic acid, hydrogen peroxide and ammonium hydroxide solutions from Merck are also used without further purification. By using AAS, XRD, FTIR spectra and TGA, the physicochemical characters are analyzed. The decolorization of methyl orange was measured by using UV-Visible Spectrophotometer of Shimadzu at 465 nm by incorporating the dye solution with zinc titanate in metallic sodium.

2. 2. Preparation of the sample

The zinc titanate powder was prepared by the coprecipitation method in presence of oxalic acid solution. The first Solution, Zn(NO₃)₂.6H₂O was prepared by dissolving it in deionized water. The second Solution TiO(C₃H₇)₄, was mixed with NH₄OH to form white precipitate of Ti(OH)₄ and it was converted in to TiO₂(NO₃)₂ by dissolving Ti(OH)₄ in 6M HNO₃ and 30% H₂O₂ solution [1]. The two homogeneous solutions were mixed together with continuous stirring, oxalic acid and NH₄OH was added to the above mixed solution.

3. Result and Discussion

3.1. Structural and thermal analysis

The X-ray diffraction patterns of prepared ZnTiO₃ calcinated at different temperatures are shown in Figure.1. Neither ZnO nor TiO₂ phases are observed. Both hexagonal and cubic phase of ZnTiO₃ powder are attained after calcination at 800°C and a distinct hexagonal phase obtained at 900 °C [2]. it is difficult to distinguish between the cubic ZnTiO₃ and hexagonal ZnTiO₃, because the cubic phase ZnTiO₃ peaks and the hexagonal peaks are appeared in a narrow 2θ range and overlap each other. The intensity of ZnTiO₃ peaks increased with increased calcination temperature.

The differential thermal analysis (DTA) curve (Figure. 2) reveals two endothermic peaks at 120 and 380°C and two exothermic peaks at 450 and 540 °C. The exothermic peaks arise due to the combustion of the organic residues and the endothermic effects can be ascribed to the dehydration of the compound [3].

In the FT- IR spectra (figure. 3), the peaks at ~640 cm⁻¹ and ~530 cm⁻¹ may be due to Ti-O stretching vibrations, peaks at ~619 cm⁻¹ and ~432 cm⁻¹ corresponding to the stretching vibrations for the Ti-O and Zn-O bonds [2]. A characteristic band 735 cm⁻¹ appeared at 800°C and then decreases gradually till 900 °C. This can be assigned to the Zn-O-Ti bond structure in cubic ZnTiO₃ which is formed at 700°C, remains as a major phase up to 800°C.

3.2. Photocatalytic activity

Figure.4 shows the photobleaching of methyl orange, with different amount of zinc titanate in presence of 0.02g of metallic sodium, exposed to visible light irradiation for different duration [4]. As the concentration of zinc titanate increased, more absorption of photon from the visible light leads to more degradation of the dye [5]. The concentration of methyl orange was decreased to 2.0 ppm when solution containing 0.2% of zinc titanate under the visible light exposure of 5 hours.

4. Conclusion

The zinc titanate powders are prepared by co- precipitation oxalate method and its physical properties are analyzed. The prepared zinc titanate contains about 40 percentage of zinc and 23.68 percentage of titanium

and the compound displays dominant cubic structure at 800 °C and hexagonal structure at 900 °C. The concentration of methyl orange is diminished from 10.0 ppm to 0.2ppm by introducing 0.2% zinc titanate in presence of 0.02g of sodium exposed to sun light for 5 hour. The photo bleaching of the dye in visible light with ZnTiO₃ and metallic sodium confirms the photocatalytic activity of zinc titanate under visible light irradiation.

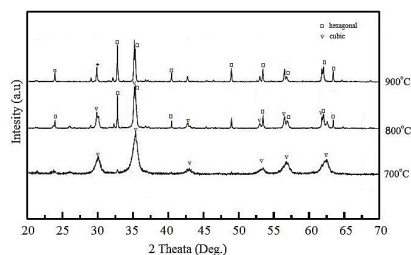


Fig.1. XRD patterns of ZnTiO₃

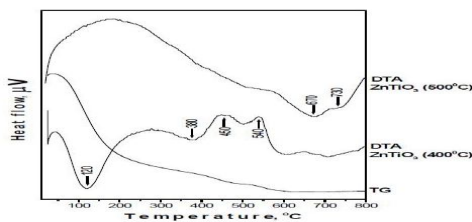


Fig.2. DTA curves of zinc titanate

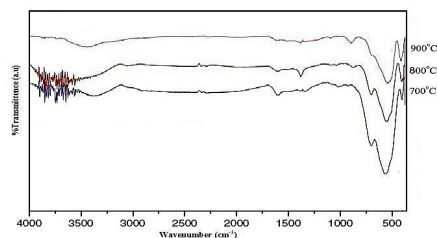


Fig.3. FT-IR spectra of ZnTiO₃

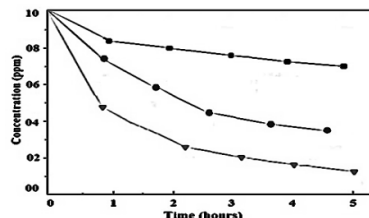


Fig.4. Photo degradation of Methyl orange solution with different concentration of ZnTiO₃
(■- 0.05, ●- 0.1, △-0.2 %) in metallic sodium

References

- [01] P Pookmanee, J Yotasing, S Phanichphant: Adv. Mate. Res. Vols. 55-57, (2008), pp 65-68.
- [02] L Budigi, M R Nasina, K Shaik, S Amaravad, J. Chem. Sci. Vol. 127, No. 3, (2015), pp. 509–518.
- [03] S F Wang, F Gu, M K Lu; Mater, Res, Bull, (2003), 38, 1283-1288.
- [04] N Daneshvar, D Salari and A R Khataee. Journal of Photochem. and Photobio. A: Chemistry. (2003), 157: 111–116.
- [05] Y Li, S Sun, M Ma, Y Ouyang and W Yan. Chem. Eng. Journal, (2008), 142: 147–155.

4.2 Prolific Synthesis of Transition Metal doped TiO₂ (TM= Au, Pt), nanoparticles and its Photocatalytic activity

PR. Kaleeswaran^a and A. Arumugam^{b*}

^aDepartment of Nanoscience and Technology, Alagappa University, Karaikudi-630 003, Tamil Nadu, India.

^bDepartment of Botany, Alagappa University, Karaikudi – 630 003, Tamil Nadu, India.

E-mail: kaleeswaran@gmail.com / sixmuga@yahoo.com

Abstract

Green synthesis and characterization of TiO₂, Au-TiO₂ and Pt-TiO₂ nanoparticles (NPs) were carried out by *Terminalia arjuna* leaf extract. Synthesized NPs were characterized by UV-VIS-DRS, FT-IR spectroscopy, XRD and SEM analysis. UV-VIS-DRS analysis was performed to study the optical property and band gap values at 3.05, 2.95 and 3.00 eV for TiO₂, Au-TiO₂ and Pt-TiO₂ NPs respectively. XRD analysis revealed that tetragonal crystalline nature of synthesized NPs. In further investigation, synthesized NPs used for photocatalytic degradation of Methylene Blue (MB), under visible irradiation. The tested results indicate that Au doped TiO₂ NPs showed a more significant effect towards photocatalytic degradation of MB within 30 min when compared with pure and Pt doped TiO₂ NPs for 140 and 160 min subsequently. Au-TiO₂ NPs play a pivotal role due to its high absorbance coefficient value because of its low band gap energy (i.e 2.95 eV), it also has high surface plasma resonance. Au doped TiO₂ ensures that, this material can be used for other industrial effluent treatment.

Keywords: Green synthesis, *Terminalia arjuna*, Leaf extract, Dye degradation, Industrial Effluent and Surface Plasma Resonance.

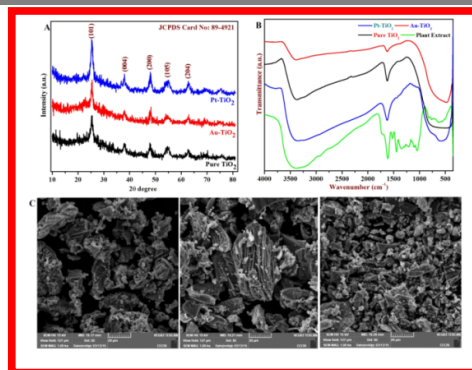


Figure.1 Synthesis of TiO₂, Au-TiO₂, Pt-TiO₂ (A) - XRD analysis (B) - FT-IR analysis (C) : SEM analysis

References:

- [1] N. Chander, P. Singh, A.F. Khan, V. Dutta, V.K. Komaral, *Thin Solid Films* 568 (2014) 74.
 [2] S. Muduli, O. Game, V. Dhas, K. Vijayamohan, K.A. Bogle, N. Valanoor, S.B. Ogale, *Sol. Energy* 86 (2012) 1428.
 [3] Q. Wang, T. Butburee, X. Wu, H. Chen, G. Liu, L. Wang, *J. Mater. Chem.* 1 (2013) 13524.

4.3 Synthesis and Photo physical Property of 4, 4' (4, 5-diphenyl-1H-imidazol-1,2-diyl) dianiline and perylene dianhydride based fluorescent polyimide

A. Hariharan,¹ K. Subramanian^{1*} and K. Dinakaran^{2*}

Department of Chemistry, Anna University, Chennai – 600 025.

Department of Chemistry, Thiruvalluvar University, Vellore – 632 115.

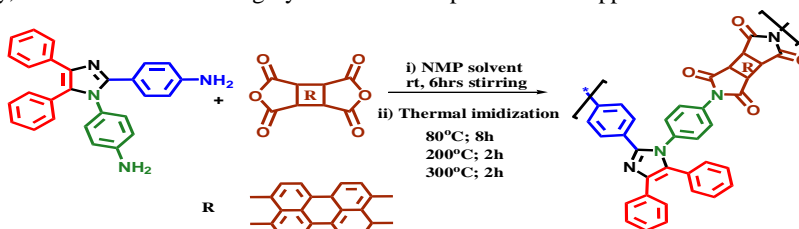
Email: kdinakaran.tvu@gmail.com

Introduction

Heteroaromatic compound based electron-donor and acceptor polymer architectures have attracted growing interest for wide angle application of optoelectronic device such as solar energy, OLED, electrochromic device, memory elements, and etc. Particularly, researcher's consideration on the development of various organic conjugated polymers, due to its efficient intramolecular charge transfer (ICT). Hetero aromatic backbone Organic conjugated polymers acknowledged that the use of appropriate stability, and thermal and solubility essential to device fabrication, which depends on the systems chemical structures, and the donors-acceptors environment of the p-conjugated bridge.

Aromatic polyimides are commercially important materials used extensively in a wide range of optoelectronic applications due to their excellent chemical, thermal, and dielectric properties. Despite their outstanding properties, most of the conventional aromatic polyimides have high melting or glass-transition temperatures (*T_g*) and limited solubility in most organic solvents because of their rigid backbones and strong interchain interactions. Thus, polyimide processing is generally carried out via poly(amic acid) precursor, and then converted to polyimide by vigorous thermal or chemical cyclodehydration. However, this process has inherent problems such as emission of volatile by-products and storage instability of poly(amic acid) solution. To overcome these problems, many attempts have been made to the synthesis of soluble and processable polyimides in fully imidized form while maintaining their excellent properties.

In this work, we report on the synthesis of new tetra substituted imidazole and confirm its structure through IR, NMR, and MASS spectroscopies. Incorporation of tetra substituted imidazole units into the polyimide backbone is a donor-acceptor system. Especially Tetra substituted imidazole used as electron donor in many fundamental studies of organic optoelectronics. The polyimide were synthesized through thermal cyclodehydration between 4,4' (4, 5-diphenyl-1H-imidazol-1,2-diyl)dianiline and aryl di-anhydride. The UV-Vis and photoluminescence spectroscopic property of polyimides have been extensively studied. The most important electrochemical property of aromatic polyimide, such as perylenedianhydride, is the existence of a stable thermal property, which makes them a highly attractive for optoelectronic applications.



Scheme-1: Synthesis of Polyimide

A new diamine monomer, 4,4'-(4,5-diphenyl-1H-imidazol-1,2-diyl) dianiline, was synthesized by a two step procedure according to the synthetic route shown in **Scheme 1**. Condensation of benzil with aromatic aldehyde and ammonium acetate is well known as a classical but convenient synthetic method for preparation of tetra aryl imidazole based amine. The structures of 1,2 -bis(4-nitrophenyl)-4,5-diphenyl -1H-imidazole were characterized by FT-IR, ^1H NMR and 4, 4' (4, 5-diphenyl-1H-imidazol-1,2-diyl) dianiline were confirmed by FT-IR, ^1H NMR and MASS analyses. Spectral data from the FT-IR and ^1H NMR and MASS analysis show the effective formation of the respective imidazole based nitro and corresponding amine group.

The optical properties, absorption and emission of the studied polyimides were analyzed by UV-vis and photoluminescence (PL) spectroscopy in THF solution. Photoluminescence Quantum yield and Band gap of PI-1, PI-2 and PI-3 were calculated by UV-Vis and Photoluminescence spectroscopy. Rhodamine 6G ($\phi_{\text{PL}} = 0.95$) was used as a reference.

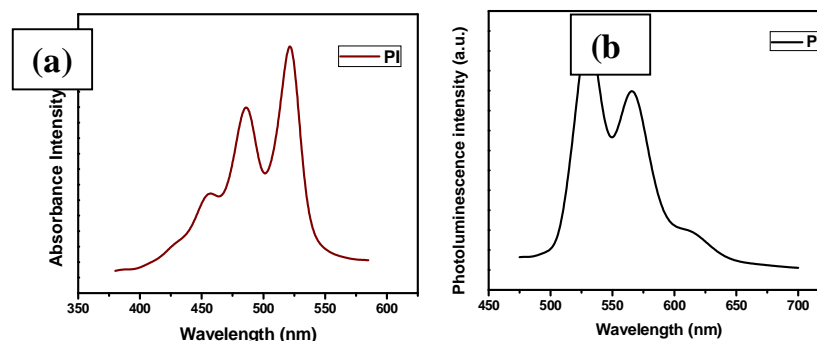


Figure 1- (a) UV-Vis spectra of polyimide, (b) Photoluminescence spectra of Polyimide.

Conclusion:

The new Imidazole containing aromatic diamine monomer was successfully synthesized with high purity and characterized. The amine monomer thermal polymerized with perylenedianhydride. The novel thermally stable aromatic polyimide exhibit excellent solubility in various organic solvents. The PI shows low band gap and good quantum yield property. This makes them a highly attractive for optoelectronic applications.

4.4 Folic acid coated carboxymethyl cellulose/casein nanogels loaded with curcumin for skin cancer treatment

P. Priya and V. Raj*

Department of Chemistry, Periyar University, Salem-636 011, Tamil Nadu, India. email id: alaguraj2@rediffmail.com

Introduction

Skin cancer, a cutaneous malignancy is one of the most prevalent forms of cancer and can result in disfigurement and even in death if not treated early. Treatment of melanoma involves some combination of surgery, chemotherapy, radiation therapy, immune therapy and targeted therapy. Drug delivery through the transdermal route is one of the most important modes of drug administration for skin cancer. Few nanogels made up of polysaccharide such as chitin nanogels, PEG-chitosan nanogels have been reported for skin cancer. But further to improve the transfection and targeting ability and retention property of therapeutic agent within the tumor tissue we have coated the prepared nanogels with folic acid. Nanogels made up of polysaccharide and protein is of particular interest due to biocompatibility, biodegradability and excellent loading capacity. The current work was planned with the aim of preparing curcumin (CUR) loaded carboxymethyl cellulose (CMC)-casein (CA) nanogels coated with folic acid (FA) which may enhance bioavailability of curcumin and cytotoxicity in human melanoma cancer cells. The synthesized nanogels were characterized by Fourier transform infrared spectroscopy (FT-IR), particle size, zeta potential and Field emission scanning electron microscopy (FE-SEM) techniques. The encapsulation efficiency and release properties of nanogels were analyzed using UV technique. The cytotoxicity of the nanogels were analyzed on A375 cell lines.

Results and Discussion

The results indicated that the FA coated CMC-CA nanogels loaded with CUR can be used for treatment of melanoma. The chemical structure of nanogels and drug encapsulation into nanogels was analyzed by FT-IR to verify the intermolecular interactions between CMC and CA. The prepared nanogels have smooth surface and spherical shape with a diameter of 75 nm as shown by SEM image (**Fig. 1a**) and particle size ranges from 50-95 nm as determined by DLS analysis (**Fig. 1b**). The drug release is found to be higher at acidic pH 4.5 almost 80 % of drug is released within 24 h compared to basic pH 7.4 where only 38 % of drug is released as shown in **Fig. 2a**. The nanogels showed toxicity towards melanoma cancer cells represented in **Fig. 2b**.

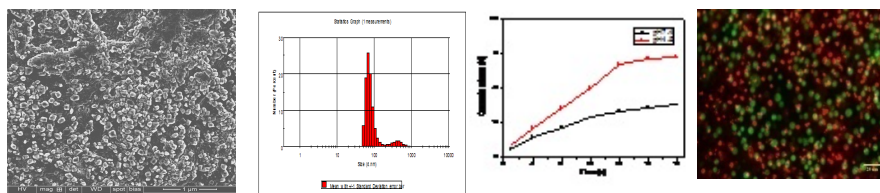


Fig.1. a) FE-SEM image and b) particle size of FA-CMC-CA-CUR nanogel; Fig.2. a) Invitro drug release b) cytotoxicity image of FA-CMC-CA-CUR

CONCLUSION

The obtained results reveals that the FA coated CMC-CA nanogels loaded with CUR can be used for treatment of melanoma or other skin cancer.

Key words: Nanogels, curcumin, skin cancer, cytotoxicity.

Acknowledgements: The 'INSPIRE fellowship' is gratefully acknowledged for the award of 'DST-INSPIRE fellowship' to P.Priya [IF150169].

4.5 Microwave synthesis of sn-wo₃ photocatalyst

K. Santhi^a, C. Rani^a and S. Karuppachamy^{b*}

^aDepartment of Chemistry, Alagappa Govt. Arts College, Karaikudi, Tamil Nadu-630 003, India

^bDepartment of Energy Science, Alagappa University, Karaikudi, Tamil Nadu-630 003, India

E-mail: skchamy@gmail.com

Abstract

Sn-WO₃ photocatalyst was prepared by microwave irradiation method and subsequently it was characterized using advanced techniques. The photocatalytic activity of Sn-WO₃ nanomaterial was studied by degrading methylene blue dye and 100% dye removal efficiency was achieved within 150 min. Photocatalytic degradation processes using semiconductor metal oxide have been attracted as an alternative method for degradation of organic pollutant [1]. Metal has been doped to reduce the recombination of charge carriers and improving the photocatalytic activity of WO₃ [1]. Microwave irradiation method is one of the low cost method to prepare Sn doped WO₃ nanomaterials.

Experimental: Tungstic acid and tin chloride were dissolved in 100 ml of sodium hydroxide solution and then stirred for 1 hr. The obtained precipitate was irradiated by microwave using the power of 160 W for 10 (a), 20 (b) and 30 (c) min. The photocatalytic activity of the synthesized Sn-WO₃ nanomaterial was studied. Photocatalytic degradation experiment was carried out in the 200 ml capacity photo-reactor and decomposition of methylene blue dye was recorded using UV-vis spectrophotometer.

Results and Discussion: Fig. 1 shows the X-ray diffraction pattern of the microwave irradiated samples and it confirms the formation of orthorhombic Sn-WO₃ nanomaterials. The average crystallite sizes of a, b and c samples were calculated as 34.56, 33.64 and 34.04 nm, respectively. The photocatalytic activity of Sn-WO₃ nanomaterials (0.05 g) was studied using decomposition of methylene blue dye (10 mg/l). The higher colour removal efficiency (100%) was achieved using (a) photocatalyst within 150 min. Fig. 2 shows the UV-Vis spectra of methylene blue dye (665 nm) in the presence of (a) sample under UV light.

Conclusion

Photocatalytic activity of the synthesized Sn-WO₃ nanomaterials was studied by degradation of the methylene blue dye under UV light irradiation. The maximum colour removal efficiency of 100 % was achieved within 150 minutes by the addition of (a) photocatalyst.

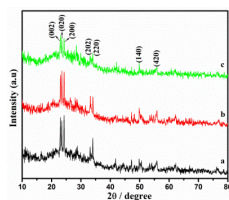


Fig. 1. XRD patterns of Sn-WO₃ nanomaterials prepared by microwave irradiation of various time (a) 10 min (b) 20 min and (c) 30

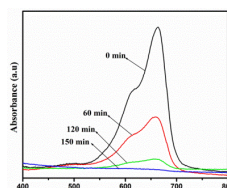


Fig. 2. UV-Vis spectra of methylene blue in the presence of Sn-WO₃ (a)

References

1. K. Santhi, C. Rani, R.D. Kumar and S. Karuppachamy, *J. Mater. Sci. Mater. Electron.* 26 (2015) 10068

4.6 Photocatalytic Dye Degradation Of Transition Metal Ions (Co, Cr, Cu) Doped Tion Nanocomposites

T. Pushpa, R. Kalyani and K. Gurunathan*

*Nano Functional Materials Lab, Department of Nanoscience & Technology,
Alagappa University, Karaikudi-630 003. *E-mail:kgnathan27@rediffmail.com*

This study examines the photocatalytic degradation of three commercially available dyes Methylene blue (MB), Malachite green (MG) and Rose Bengal (RB) using a novel nano composite of N-doped TiO₂, N-doped Co-TiO₂, N-doped Cr-TiO₂, N-doped and Cu-TiO₂. These novel nanocomposites have high photocatalytic activity which is reactive under UV- visible light allowing more efficient usage of solar light. The above samples were characterized by X-ray diffraction, FTIR, UV- Vis spectroscopy and SEM (Scanning Electron Microscope).

The N-doped titania nanocatalysts were prepared by sol-gel method. Specifically, the nitrogen-doped TiO₂ nanocrystals were synthesized by slowly adding 9 ml of titanium isopropoxide to 150 ml of acetone in 5 ml of aqueous ammonia solution. Grey powder was obtained after centrifugation and removing the solvent under air oven for several hours at 60 °C. After calcination at 400 °C for 3 hours a light yellow powder was obtained.

Likewise, N-doped Co-TiO₂, N-doped Cr-TiO₂ and N-doped Cu-TiO₂ were synthesized by adding 150 ml of acetone. After 15 minutes, 9 ml of titanium isopropoxide was added to the above solution. After 30 minutes, metal precursors (1.4 g of cobalt nitrate, 1 g of chromium nitrate and 0.84 g of copper chloride dehydrate) were dissolved in 50 ml of distilled water. The color of the solution changed into light pink for Co-TiO₂, pale green for Cr-TiO₂ and blue color for Cu-TiO₂. Then 5 ml of ammonia solution was added to the above mixture. The above mixture was heated at 80 °C.

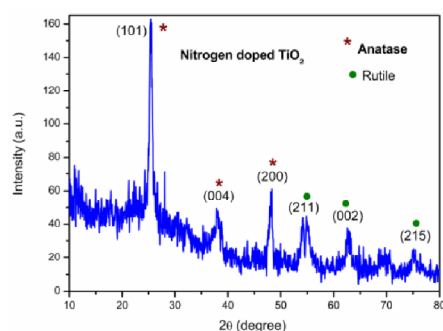


Figure 1. XRD pattern of N-doped TiO₂

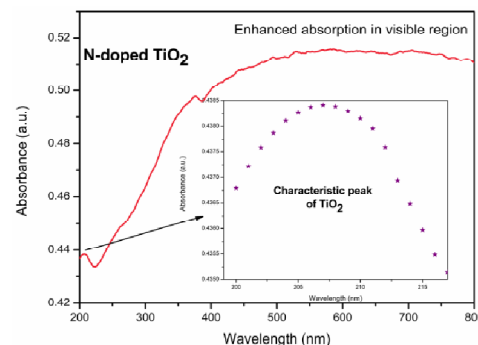


Figure 2. UV-Vis spectra of N-doped TiO₂.

The XRD pattern of N-doped titania is shown in Figure 1. The XRD pattern matches with the JCPDS card No. 04-0477. The pattern shows a mixture of anatase and rutile. The anatase phase of TiO_{2-x}N is tetragonal shaped having body-centric lattice having lattice parameters $a=3.783\text{Å}$ and $b=9.51\text{Å}$. Rutile phase of TiO_{2-x}N has tetragonal primitive structure with lattice parameters $a=4.593\text{Å}$ and $c=2.959\text{Å}$.

Figure 2 shows the UV-Vis spectra of N-doped TiO₂. The spectrum shows absorption in both UV and Visible region. Undoped TiO₂ has the characteristic absorption at UV region. Similarly, this spectrum also shows characteristic absorption of TiO₂ in the UV region near 220 nm and due to the doping of TiO₂ with nitrogen the spectra shows enhanced absorption in the visible region. This result shows that the synthesized material has better photocatalytic property.

This photocatalyst is used to degrade Methylene blue, Malachite green and Rose Bengal. The above prepared photocatalyst degrades the dye more efficiently.

4.7 Wet catalytic degradation of crystal violet dye using Fenton like Co₃O₄/Zeolite X catalyst

N.L. Subbulekshmi and E. Subramanian*

*Department of Chemistry, Manonmaniam Sundaranar University, Tirunelveli - 627 012, Tamilnadu, India.
E mail: anandlekshmi@gmail.com, esubram@yahoo.com*

1. Introduction

Environmental problems associated with synthetic dyes in various industrial processes and their remediation have attracted much attention. Among advanced oxidation processes (AOPs), catalytic wet peroxide oxidation (CWPO) is prominent and effective¹. In this regard, zeolite has a focus of intense research in recent years¹. In this work, spinel cobalt oxide incorporated cheap coal fly ash converted zeolite X is synthesized and its CWPO performance of cationic dye crystal violet (CV) is evaluated.

2. Experimental

Preparation of coal fly ash (CFA) zeolite X (FAZ) was similar to the literature method² which involved hydrothermal treatment of fly ash with 0.1 M Co^{2+} and calcination at 450°C for 4 h. 50 mg Co_3O_4 -FAZ powder dispersed in 200 ml CV solution (100 mgL^{-1}) at natural pH (6.8) with 1 ml H_2O_2 was under continuous magnetic stirring. After 20 min time intervals, the mixture was centrifuged, and the dye supernatant was estimated spectrophotometrically at 588 nm.

3. Results and discussion

In XRD the characteristic high intense peaks at $2\theta = 26.6^\circ$ and 40.9° together with other major peaks (Fig. 1a) are indicative of the presence of Quartz (Q) and Mullite (M) in CFA. The diffraction peaks at $2\theta = 10.1, 11.8, 15.5, 18.4, 20.09, 23.3, 31.1^\circ$ etc (Fig. 1b) confirm the formation of zeolite X. Co_3O_4 peaks are identified on FAZ catalyst however, the peaks are weaker and broad on Co_3O_4 /FAZ (Fig. 1c). This result and a comparison with XRD of pristine Co_3O_4 (Fig. 1d) suggest that Co_3O_4 has spinel structure, a coverage over FAZ and mutual interaction with FAZ. FTIR spectrum of FAZ (Fig. 2) shows characteristic broad peak with high intensity at 983 cm^{-1} and a small peak at 752 cm^{-1} . The band at 1635 cm^{-1} suggests vibration of O-H in hydrated aluminium silicates². The band at 983 cm^{-1} in FAZ is shifted to 1027 cm^{-1} and indicates exchanging of Na^+ by Co^{2+} cations in Co_3O_4 /FAZ.

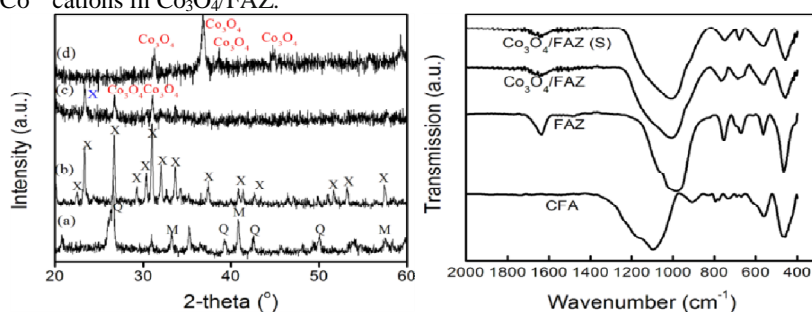


Fig. 1 XRD patterns of (a) CFA (b) FAZ (c) Co_3O_4 -FAZ and (d) Pristine Co_3O_4

Fig. 2 FTIR spectra of (a) CFA (b) FAZ (c) Co_3O_4 -FAZ and (d) Co_3O_4 -FAZ (spent)

FAZ and Co_3O_4 exhibit 30% and 25% CV dye degradation respectively after 180 min of reaction time while the combination Co_3O_4 /FAZ amazingly shows 100% activity at the same condition. This suggests high dispersion of Co_3O_4 crystallites on FAZ with more active sites on Co_3O_4 /FAZ (deduced from XRD) which enhance the catalytic activity. Absorption of CV at 588 nm gets decreased rapidly with reaction time indicating its degradation.

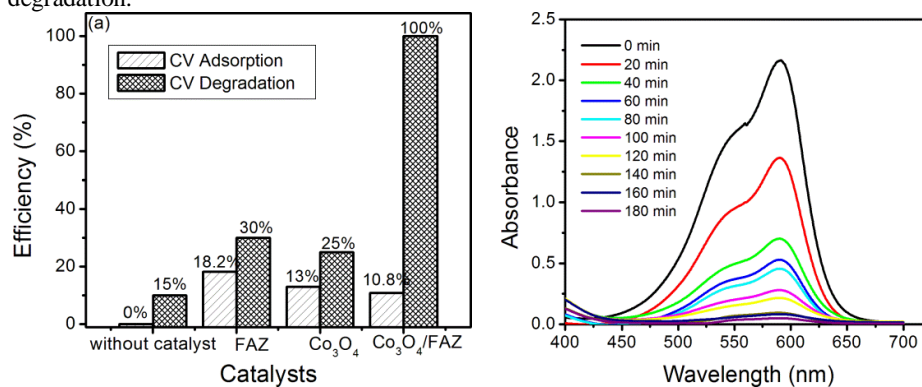


Fig. 3 Various catalysts on CV wet hydrogen peroxide degradation

Fig. 4 Spectral changes of CV dye during CWPO

The developed Co_3O_4 /FAZ is an effective Fenton catalyst for generating hydroxyl radicals in the presence of H_2O_2 to degrade CV. In view of environmental and economic aspects, this novel catalyst being derived from waste coal fly ash, is cost effective to commercial zeolite and is a highly stable, ecofriendly, non-hazardous and reusable catalyst.

References

- [1] M. Chen, W. H. Ding, J. Wang and G. W. Diao, *Ind. Eng. Chem. Res.*, 2013, **52**, 2403.
- [2] K. Ojha, N. C. Pradhan and A. Samanta, *Bull. Mater. Sci.*, 2004, **27**, 555–564.

4.8 Removal of chromium from wastewater using Emulsion liquid membrane

P. Murugan^a, B. Manoj Reddy^b, T. Vinaya sri^c, B. V. N. S. Bhavana^d, G. Umadevi^e, S. Bhuvaneshwari^f
 Department of Chemical Engineering, National Institute of Technology Calicut, Kozhikode – 673 601, Kerala, India
 muruga.tech86@gmail.com

Abstract

This present study is to remove the chromium (VI) from synthetic wastewater using emulsion liquid membrane (ELM) techniques. The importance of emulsion stability for the removal of chromium (VI) has been highlighted. The ELM consists of Aliquat-336 and methyl isobutyl ketone (MIBK), as a carrier for pungai oil and coconut oil as organic solvent respectively. Span 80 has been used as surfactant agent, sodium hydroxide and deionized water were used as stripping phase. The important factors studied for the ELM stability and removal of chromium (VI) were the concentrations of surfactant (2–10% v/v), carrier (2–10% v/v), internal phase NaOH (0.2M), stir time (5–25 min) and the effect of volume ratio of the oil phase to the internal phase (O/A) (1:1–4:1). At the optimum condition it was possible to remove 99.71 and 99.83% of chromium (VI) respectively.

Keywords: ELM, Chromium (VI), Surfactant, Solvent, Stripping phase.

References

- [1] R. A. Kumbasar, *journal of membrane science*, 325 (2008) 712–718.
- [2] M. A. Hasan, Y. T. Selim, and K. M. Mohamed, *journal of hazardous materials* 168 (2009) 1537–1541.
- [3] R. A. Kumbasar, *journal of hazardous materials* 167 (2009) 1141–1147.
- [4] B. Sengupta, M. S. Bhakhar, and R. Sengupta, *Hydrometallurgy* 99 (2009) 25–32.
- [5] J. Berrios, D. L. Pyle, and G. Aroca, *journal of membrane science* 348 (2010) 91–98.
- [6] K. Chakrabarty, P. Saha, and A. K. Ghoshal, *journal of membrane science* 360 (2010) 34–39.
- [7] Y. S. Ng, N. S. Jayakumar, and M. A. Hashim, *journal of hazardous materials* 184 (2010) 255–260.
- [8] L. Zhao, D. Fei, Y. Dang, X. Zhou, and J. Xiao, *journal of hazardous materials* 178 (2010) 130–135.
- [9] A. L. Ahmad, A. Kusumastuti, C. J. C. Derek, and B. S. Ooi, *Chemical Engineering journal* 171 (2011) 870–882.
- [10] A. L. Ahmad, A. Kusumastuti, C. J. C. Derek, and B. S. Ooi, *Desalination* 287 (2012) 30–34.

4.9 Efficient Photocatalytic degradation of Victoria blue by MnWO₄- BiSbO₄ nanocomposite under visible light irradiation

D. Rani Rosaline^a, V. Ramasamy Raja^a, M. Rajarajan^{b*}, A. Suganthi^{a*}
 PG & Research Department of Chemistry, Thiagarajar College, Madurai-625 009, Tamilnadu, India.
 PG & Research Department of Chemistry, C.P.A College, Bodinayakanur-626 513, Tamilnadu, India.
 Corresponding author e-mail: suganthicarts@gmail.com

Abstract

A Novel MnWO₄-BiSbO₄ nanocomposite in two different molar ratios (2%, 5% of MnWO₄- BiSbO₄) were synthesized successfully by precipitation-deposition method and their photocatalytic activity towards Victoria Blue was studied. The phase purity, crystallite size and strain were ascertained by powder X-ray diffraction (XRD) analysis. Further, the synthesized photocatalysts were characterized by Fourier transform infrared spectroscopy (FT-IR), Scanning electron microscopy (SEM), Energy dispersive x-ray spectroscopy (EDAX), UV-Vis diffuse reflection spectroscopy (DRS) and photoluminescence spectroscopy (PL). The efficiency of the photocatalysts was evaluated from the photodegradation of Victoria blue, a target textile pollutant, under visible light irradiation. The photocatalytic activity of the synthesized MnWO₄- BiSbO₄ nanocomposite photocatalyst was found to be more efficient than that of individual components. The composite with molar ratio of 5% MnWO₄- BiSbO₄ photocatalyst shows an excellent photocatalytic activity than the nanocomposite with molar ratio 2% MnWO₄- BiSbO₄. The band edges of the materials have been theoretically calculated on the basis of Mulliken electronegativity of atoms. The effects of operational parameters such as pollutant concentration, pH, catalyst dosage and OH⁻ radical trapping, COD have been investigated in detail. The Kinetics of the photodegradation reaction was correlated with the pseudo-first-order model. A possible mechanism has been proposed for the photocatalytic degradation using MnWO₄- BiSbO₄.

Keywords: Photocatalysis, Visible Light, MnWO₄- BiSbO₄ Nanocomposite, Victoria Blue

References

1. K. Vignesh^a, R. Priyanka^b, R. Hariharan^c, M. Rajarajan^{c*}, A. Suganthi^{a*} *Journal of Industrial and Engineering Chemistry* 20 (2014) 435–443
2. Hoang, Luc Huy; Hanh, Pham Van; Phu, Nguyen Dang; Chen, Xiang Bai; Chou, Wu Ching, *Journal of Physics and Chemistry of Solids*, 02/2015 ; 77; 122–125.

4.10 A facile synthesis of magnetic activated carbon/CoFe₂O₄ nanocomposite for the adsorption of congo red dye from water

P. Karthikeyan^a, P. Anjana^a, K.S. Anjali^a, P.S. Anagha^{aa}, B. Ushadevi^b, S. Vairam^b, V. Ranjithkumar^{aa*}

^aDepartment of Chemistry, Kongunadu Arts and Science College, Coimbatore – 641029, Tamil Nadu, India

^bDepartment of Chemistry, Government College of Technology, Coimbatore – 641013, Tamil Nadu, India

email: mcranjith@gmail.com Tel: 04222642095 & Fax: 04222644452

Abstract:

Activated carbon(AC)/CoFe₂O₄ nanocomposite have been prepared by a simple pyrolytic method using a mixture of oxalates of iron(III) and cobalt (II) was investigated by batch technique. The synthesized nanocomposites were characterized by Fourier transform infrared spectroscopy (FT-IR), X-ray diffraction (XRD), scanning electron microscopy (SEM), energy dispersive x-ray spectroscopy (EDX), transmission electron microscopy (TEM), and vibrating sample magnetometry (VSM). The size of cobalt ferrite nanoparticles formed from oxalate of iron (III) and cobalt (II) precursor was in the range of 6-27 nm. The saturation magnetization (M_s), remanence (M_r) and coercivity (H_c) of the magnetic carbon nanocomposite were found to be 0.2717emu/g, 0.0308emu/g and 338.06 Oe, respectively. The resulting nanocomposite shows extraordinary adsorption capacity and fast adsorption of removal of organic dye, congo red (CR), in water. The adsorption kinetics and isotherm studies were investigated and the results show that the as-prepared AC/CoFe₂O₄ nanocomposite could be utilized as an efficient, magnetically separable adsorbent for the environmental cleanup.

Keywords: Carbon nanocomposites, Magnetic properties, Congo red, Adsorption

4.11 Effect of annealing temperature on Structural and Optical properties of BTO thin films for Photocatalytic applications

A.Amali Roselin¹, N. Anandhan^{1*}, G. Gopu², M. Karthikeyan¹

¹Advanced Materials and Thin film Physics Lab, Department of Physics, Alagappa University, Karaikudi-4, Tamilnadu.

²Catalytic and Supercapacitor Lab, Department of Industrial Chemistry, Alagappa University, Karaikudi-3, Tamilnadu.

*Corresponding author:, E-mail: anandhan_kn@rediffmail.com

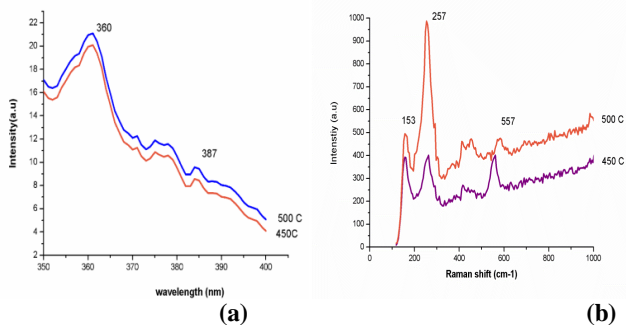
Abstract

In this paper, we report the synthesis of bismuth titanate (Bi₄Ti₃O₁₂) (BTO) thin films using sol-gel spin coating method with various annealing temperature. The X-ray Diffraction (XRD), Micro Raman Spectroscopy, Photoluminescence (PL) and Ultra violet-visible spectroscopy (UV-Vis) techniques were employed to study the structural, vibrational, luminescence and optical properties of BTO thin films. In this study, we also described the correlation between crystallite size and optical gap energy with different annealing temperature of BTO thin films. XRD pattern revealed a preferred orientation (117) of the crystallites along the c-axis [1]. The crystallite size is found to be increase with the increasing annealing temperature. The vibrational modes of the BTO films were examined by Micro Raman Spectrometry, the phonon mode observed at 153cm⁻¹ reflected the vibration of A-site Bi³⁺ ions in layered-structured perovskite [2]. The prepared BTO thin films are showed excellent transparency in visible region [3]. The observed direct optical band gap (E_g) suggests that, the crystallite size of the films is predominantly influenced by the band gap energy with increase in annealing temperature. From these results, we ascertained that, the BTO thin films can be used in visible light photo catalytic applications for energy conversion.

Keywords:

BTO, thin films, crystallite size, visible light photocatalytic activity.

Graphical representation



References

1. JCPDS Card No.89-7500
2. M.S. Tomar, R.E. Melgarejo, S.P. Singh, Leakage current and ferroelectric memory in Nd and Sm substituted $\text{Bi}_4\text{Ti}_3\text{O}_{12}$ films, *Micro.Elect.J.*, 36 (2005) 574-577.
3. Yongyuan Zhang, Dn Xie, Yu Chen, Tuning the Structural and Optical properties of Bismuth Titanate by different Nd substitution content, *Integ.Ferroelec.*, 134 (2012) 1-8.

4.12 Synthesis, Characterization of Hemetite Nps Decorated N-Doped Graphene Sheet/MoS₂ Nanocomposite For Photocatalytic Application

S.Senthilnathan, S. Sivasakthi and K.Gurunathan*

*Nano Functional Materials Lab, Dept.of Nanoscience and Technology, Science Campus, Alagappa University, Karaikudi.
e-mail:kgnathan27@rediffmail.com*

Herein, we report a new nanocomposite material which consist of hematite nanoparticles($\alpha\text{-Fe}_2\text{O}_3$ NPs) decorated Nitrogen doped graphene sheet (NGs)/Molybdenum disulfide (MoS_2). Initially graphene oxide synthesis by conventional improved Hummer's Modified method. Then, the composite was fabricated by simple two step hydrothermal method without stencil.The properties of as-prepared nanocomposite characterized by X-Ray Diffraction(XRD), Raman Spectroscopy, UV-vis Spectroscopy, Field Emission Scanning Electron Microscopy(FESEM), Photoluminesnce (PL), N_2 adsorption-desorption test etc. In this composite Nitrogen has been doped with graphene sheet by Melamine that is one of the protein aminoacid. Nitrogen doping enhances the surface area of the graphene sheet. Thus, it was increased electron holding properties of the composite material and hence that can lag recombination process of electron-hole. Moreover, molybdenum disulfide has layered structure that also increased the surface area of the composite material. It also improves the speed of electrons transfer.N-Gs/ MoS_2 contains hematite NPs shows enhanced catalytic activity and high light harvesting properties.Surface area of the composite material explored by N_2 adsorption-desorption test and recombination process of the composite determined by PL. Surface morphological studies of the prepared materials are shown in Fig.1.

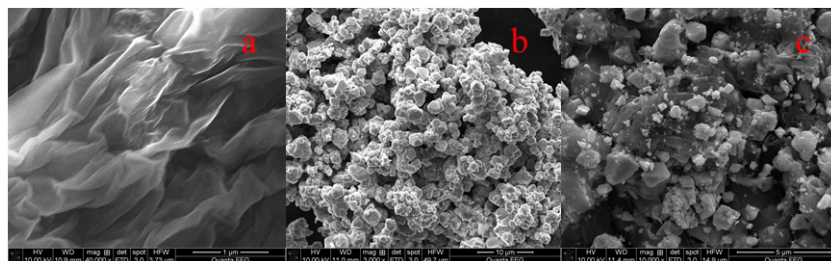


Fig.1: FESEM images a. N-Gs, b. $\alpha\text{-Fe}_2\text{O}_3$ c. $\alpha\text{-Fe}_2\text{O}_3$ @N-Gs/ MoS_2

References

- [1] T. Sadhasivam and K. Gurunathan, *J. Nanosci. Nanotechnol.* 2014, Vol. 14, 1-8.
- [2] Zhen-Huan Sheng, Lin Shao, Jing-Jing Chen, Wen-Jing Bao, Feng-Bin Wang, and Xing-Hua Xia, *ACS Nano*, 2011, 5 (6), pp 4350-4358.
- [3] R.KalyaniandK.Gurunathan, *Int.J.LightElectronOpt.*(2015), <http://dx.doi.org/10.1016/j.ijleo.2016.01.203>
- [4] Gajendra Kumar Pradhan, Deepak Padhi, and kulamani Parida *ACS Appl. Mater.interfaces*, DOI:10.1021/am402487h.
- [5] Quanjum Xiang, Jiaguo Yu, and MietekJarinić J, *Am, Chem, soc.*, 2012,134,6575-6578
- [6] Wingkei Ho, Jimmy C.Yu, Jun Lin Jiaguo Yu, and Puishan ACS, *Langmuir* 2004, 20, 5865-5869.
- [7] Chengbin Liu, Longlu Wang, Yanhong Tang, ShenglianLuo, Yutang Liu, Shuqu Zhang, YuziX *Applied Catalysis B: Environmental* 164(2015) 1-9.

4.13 Fabrication of highly flexible dye sensitized solar cell using the electrospun Nickel Oxide nanofibers based counter electrode

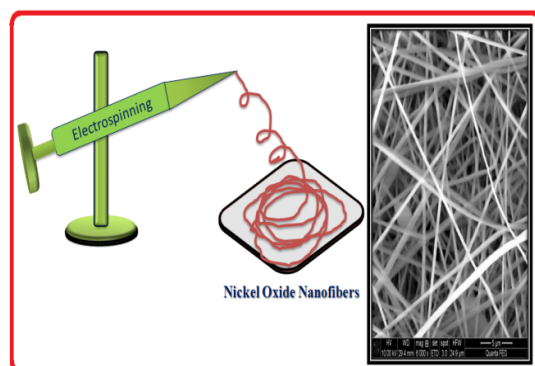
K.Sakthi Velu, P. Manisankar and T.Stalin*

Department of Industrial Chemistry, Alagappa University, Karaikudi-03, Tamilnadu-India.

Abstract

We have prepared the Nickel Oxide (NiO) nanofibers by electrospinning method as a counter-electrode (CE) for a dye sensitized solar cell (DSSC). Scanning electron microscopy images (SEM) and X-ray diffraction analysis clearly indicated the formation of NiO nanofiber in 240nm. The electro-chemical properties

of NiO nanofibers CE are studied by cyclic voltammetry (CV) and electrochemical impedance spectroscopy (EIS). In particular, current-voltage measurements indicated superior power conversion efficiency (PCE) of 7.63% of the NiO-nanofibers CE compared to 6.72% for the platinum (Pt). The superior photovoltaic performance and low cost of the NiO nanofibers counter electrode can be potentially exploited as a new counter-electrode in DSSCs.



Keywords:

Electrospinning Method, Nickel Oxide Nanofibers, Counter electrode, FE-SEM Image, Dye sensitized solar cell.

References:

1. Zhang Z, Shao C, Li X, Wang C, Zhang M, Liu Y. ACS Appl Mater Interfaces:2010; (2) 2915–2923.
2. Kim YS, Yua B-K, Kim D-Y, Kim WB. Sol Energy Mater Sol Cells: 2011; (95) 2874–2879.

4.14 Inclusion complex of 1,8-Dihydroxyanthraquinone with β -cyclodextrin: Spectral and molecular modeling studies

S. Mohandoss and T. Stalin*

Department of Industrial Chemistry, School of Chemical Sciences, Alagappa University, Karaikudi – 03, Tamilnadu, India.
E-mail: smohandoss2020@gmail.com and drstalin76@gmail.com

Abstract

Inclusion complex behaviour of 1,8-Dihydroxyanthraquinone (1,8-DHAQ) with β -cyclodextrin (β -CD) were analysed by UV-visible and fluorescence spectroscopy. The stoichiometric ratio of the inclusion complexes was found to be 1:1 and the binding constant was evaluated using the Benesi-Hildebrand equation. The inclusion interaction was examined and the thermodynamic parameter (ΔG) of inclusion process is also determined. The experimental results indicated that the inclusion process is an exergonic and spontaneous process. A mechanism is proposed to explain the inclusion process [1]. Stable solid inclusion complex were prepared using co-precipitation method by characterised by Fourier transform infrared spectroscopy (FTIR), X-ray diffraction (XRD), Differential scanning calorimetry (DSC), Scanning electron microscopy (SEM) and molecular modeling methods. FT-IR, XRD, DSC and SEM results confirmed the formation of inclusion complex [1]. The β -CD:1,8-DHAQ inclusion complex obtained by molecular docking studies is in good correlation with the results obtained through experimental methods using PatchDock and FireDock servers as shown in Figure 1. PM3 calculations suggest that orientation B is more favored than orientation A for 1,8-DHAQ [2]. The hydrophobic and H-bond interaction between 1,8-DHAQ and β -CD plays an important role in the inclusion complex.

Keywords : 1,8-DHAQ, β -CD, Inclusion complex, Docking study and PM3 calculation

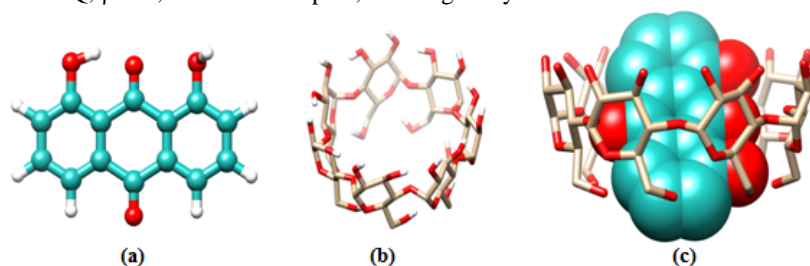


Figure 1. Ball and stick representation of (a) 1,8-DHAQ (b) β -CD (c) β -CD:1,8-DHAQ inclusion complex. The carbon atoms are shown as cyan and sandal, oxygen atoms are shown as red and hydrogen as white color balls.

References

- [1] S. Mohandoss, J. Sivakamavalli, B.Vaseeharan, T. Stalin, RSC Adv. 5 (2015) 101802.
[2] ADB. Yaseen, A. Moala, Spectrochim. Acta Part A. 131 (2014) 424.

4.15 Electrochemical Treatment of Disperse Orange 3 found in Textile Effluents

M.AbdulKadir^{*1}, P.Manisankar² and A.Gomathi³

^{*1}Department of Chemistry, M S S Wakf Board College, Madurai,

²Department of Industrial Chemistry, Alagappa University, Karaikudi- 630003, India.

³Department of Chemistry, Sri K.G.S Arts College, Srivaikuntam – 628619, India.

Abstract

The electrochemical destruction of the dye Disperse orange 3 (DO 3) in synthetic effluent was carried out using batch static electrolytic cell containing graphite as working electrode, stainless steel mesh as counter electrode and standard calomel as reference electrode. The effectiveness of the quantity of electricity passed on the rate of dye degradation was studied without adjusting the pH of the synthetic effluent. The optimum quantity of electricity required was found out as 0.5 Ahr, where maximum COD reductions were achieved. UV-VIS spectral studies of the dye and determination of percentage of COD reduction were carried out to ascertain the removal of dye during electrolysis. The influence of pH on the electrolysis was studied by carrying out electrolysis at various pH values ranging from 1.0 to 11.0. The samples were drawn for every half an hour for the product analysis. The maximum COD reduction (89.6%) was observed at pH 1.0 for the current density of 4.2 A/dm² and hence the optimum pH for significant removal of DO 3 was chosen as 1.0. The cell potential values were measured at constant interval of half an hour during the course of electrolysis at the current density of 4.2 A/dm² and they remained almost constant over an extended period demonstrating that the electrochemical cell is highly stable.

The UV-VIS spectra of the dye before and after the treatment were subjected to the entire UV-VIS range and the spectra are presented in fig.1 Maximum % of absorbance reduction, 95.4% was obtained at pH 1.0 and current density 4.2 A/dm². Square wave stripping voltammetry (SWV) was employed to study the completeness of the electrolysis at pH 1.0 using glassy carbon electrode. The voltammogram of the initial and final samples are presented in fig. 2. The cathodic peak disappeared in the SWV of treated sample indicates the absence of the dye after treatment.

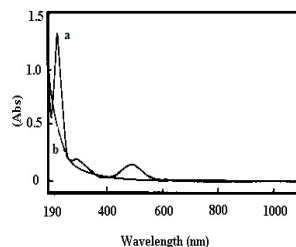


Fig. 1. UV-Visible spectrum of DO3 (a) before and (b) after treatment

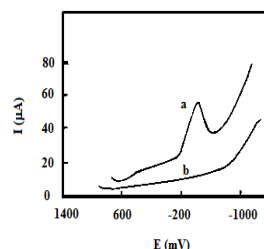


Fig. 2. Square wave stripping voltammogram of DO3 at pH 7.0 (a) before and (b) after treatment

The conclusions derived from the electrochemical treatment of DO3 proved the technical feasibility of the application of electrochemical processes to the treatment of dyes in industrial effluent streams.

Key Words: Electrochemical treatment, Disperse Orange 3, Electrolysis, COD reduction, UV-VIS spectra, Absorbance reduction.

4.16 Host-guest chemistry of β -Cyclodextrin and plumbagin in aqueous and solid state

R. Kavitha^b and T. Stalin^{a,*}

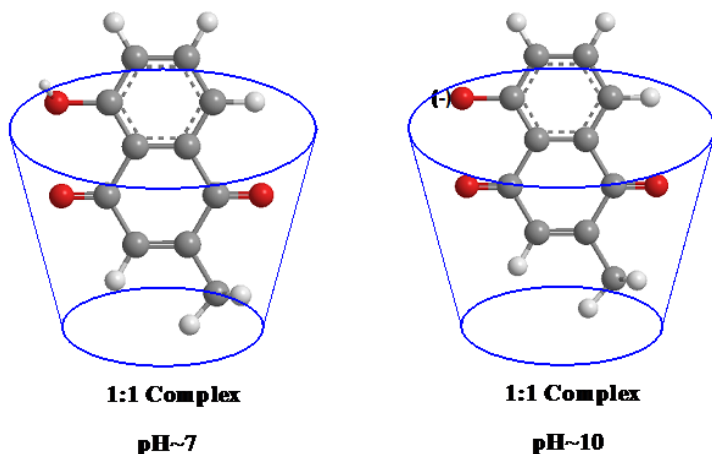
^a Department of Industrial Chemistry, Alagappa University, Karaikudi- 630 003, Tamilnadu, India.

^b Department of Chemistry, Mahendra College of Engineering, Salem Campus, Salem-636016, Tamilnadu, India.

Abstract

An important derivative of 1,4-naphthoquinone is plumbagin (5-hydroxy-2-methyl-1,4-naphthoquinone), a natural quinonoid constituent. The inclusion complexation behavior, characterisation and binding ability of 5-hydroxy 2-methyl 1,4-naphthoquinone (5HMNQ) with β -cyclodextrin (β -CD) has been investigated both in solution and solid state by means of absorption, fluorescence, FT-IR, ¹H NMR, SEM and

XRD methods. The spectral shifts revealed that the part of naphthoquinone ring of 5HMNQ is entrapped in the β -CD cavity. The stoichiometric ratio and binding constant were determined by Benesi-Hildebrand plots and spectroscopic studies respectively. The structure and complex mode of the inclusion complex of 5HMNQ with β -cyclodextrin was investigated by FT-IR and ^1H NMR methods. FT-IR and ^1H NMR results indicated that the naphthoquinone ring of 5HMNQ molecule was partly included into the β -CD cavities.



Scheme 1. The proposed structure of inclusion complexes of 5HMNQ with β -CD. The oxygen atoms are shown as red, carbon as grey and hydrogen atoms as white colours.

References

- [1]. H. Benesi, J. Hildebrand, J. Am. Chem. Soc. 71 (1949) 2703–2707.
- [2]. T. Wang, Y. Bai, L. Ma, X.P. Yan. Org. Biomol. Chem. 6 (2008) 1751–1755.
- [3]. J. Szejtli. Chem. Rev. 98 (1998) 1743-1753.
- [4]. T. Stalin, K. Srinivasan, K. Sivakumar. Spectrochim. Acta Part A 94 (2012) 89– 100.

4.17 Solvatochromism and proton transfer kinetics of 5- perylene imide in (5pi) the excited singlet state: A study of electronic spectra

Shanmugapriya RM^a, Gnanamalar K^a and Radha N^b

^aResearch scholar, PG and Research Department of Chemistry, Alagappa Govt.Arts College, Karaikudi - 3, India.

^bAsst. Professor, PG and Research Department of Chemistry, Alagappa Govt.Arts College, Karaikudi - 3, India.

Abstract:

A study of solvent and pH effects on absorption and fluorescence of 5-Perelene imides' has been carried out. Solvatochromic shift of 5PI different from that of 6PI both in ground and excited states. The difference is more in S1 state. The single molecule spectra of 5PI, 5NI and 6PI reveal three different types of emitters, two of which are not observed at the ensemble level. The nature of these two emitter types is not fully uncovered, but evidence is presented that one emitter type is most probably a result of photo-oxidation. Following a suggestion in the literature, the last emitter type may be attributed to twisted conformations in which the amino group is perpendicular to the beryline core. Computational estimation of such conformations, however, casts doubt on this explanation.

- The shape of the emission spectra that are observed in dropcast or spincoated films with a high dye concentration resembles that of the emission spectra in solution.
- The rigidity of the embedding polymer matrix limits the solvatochromic sensitivity, unfortunately, to the extent that the spectra in chemically different polymers are only slightly different. Finally, preliminary results of single molecule excited state deprotonation and reprotonation experiments are presented.

Keywords: Electronic Spectra, Fluorophore, Photophysical behavior, solvatochromism.

4.18 Host-guest interaction of p-sulfonatocalix[4]arene with 1,8-diaminonaphthalene

C. Saravanan, M. Senthilkumar, B. M. Ashwin, J. Karpagam, P. Muthu Mareeswaran*
Department of Industrial Chemistry, Alagappa University, Karaikudi.
E-mail: saravanangri92@gmail.com

Introduction

The p-SC4 is proposed as a promising host molecule due to their simple one-pot preparation, preorganization of functional groups, unique structural properties and its capacity to co-operate the guest binding site rapidly by low energy conformation change, and has been used as building blocks in the construction of more sophisticated molecular systems in supramolecular chemistry. The ease of shape tunability of calix[4]arene makes this molecule useful in synthesis of wide range of receptors with recognition ability towards guest molecules. There are many reports on the binding of p-SC4 with biologically important molecules, like amino acids, peptides and proteins. 1,8-diaminonaphthalene is an important class of Schiff base ligands in coordination chemistry and find extensive application in different fields. Schiff bases metal complexes including 1,8-diaminonaphthalene have been widely studied because of their industrial, antifungal, antibacterial and biological applications. Schiff bases based on 1,8-diaminonaphthalene can be used to obtain optical materials and conducting polymers. 1,8-diaminonaphthalene is seems to be suitable candidates for further chemical modifications and may be optical communication and optical devices. In this present work, we focused on the binding study of biologically important Schiff base ligand with p-SC4 using optical and electrochemical techniques.

Experimental section

The host-guest association in solution was analyzed using UV-vis spectrometric titration, fluorescence titrations. The binding constant value calculated from UV- visible spectrum using Benesi-Hildebrand equation and then the binding constant from emission studies using modified Stern-Volmer equation.

Result and Discussions

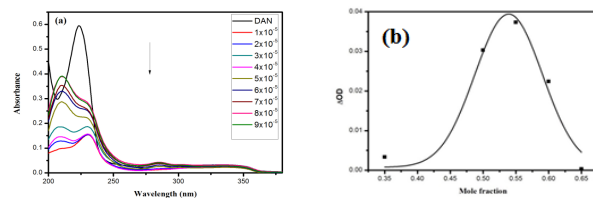


Figure.1 (a) UV-visible absorption spectrum of 1,8-diaminonaphthalene in the presence of p-SC4 (b) Job's plot for host-guest interaction of p-SC4 with 1,8-diaminonaphthalene.

When we increase the concentration of p-SC4 the absorbance intensity of 1,8-diaminonaphthalene decreases. It shows that there is a binding occurs between p-SC4 and 1,8-diaminonaphthalene. The Job's plot shows peak at 0.5 mole fraction. This confirms the 1:1 binding of p-SC4 with 1,8-diaminonaphthalene.

Conclusion

The binding constant value from UV-Visible absorption technique is $2.6 \times 10^3 \text{M}^{-1}$. The binding constants around 10^3M^{-1} shows efficient binding of 1,8-diaminonaphthalene with p-SC4. The binding constant value from emission spectral technique is $7.69 \times 10^1 \text{M}^{-1}$. It is also indicated the binding is occurred or host-guest complex is formed. Therefore, p-SC4 is an efficient host molecule to bind the guest molecule of 1,8-diaminonaphthalene.

4.19 Photocatalytic oxygenation of organic sulfides using earth-abundant metal ions as catalyst and water as an oxygen source

Thangamuthu Rajendran,^{*a,b} Krishnan Senthil Murugan,^a Gopalakrishnan Balakrishnan,^a Muniyandi Ganesan,^a Veluchamy Kamaraj Sivasubramanian,^{a,c} and Seenivasan Rajagopal^a

^aPost Graduate and Research Department of Chemistry, Vivekananda College, Tiruvadakam West, Madurai- 625 234, India.

^bDepartment of Chemistry, PSNA College of Engineering & Technology, Dindugul-624 622.

^cDepartment of Chemistry, K.L.N. College of Engineering, Pottapalayam, Sivagangai-630 612.

*trajan602012@gmail.com, ksenthil.chemistry@gmail.com

Abstract

We report a new dyad photocatalyst incorporating a Fe(III)-salen as catalytic component and a Ru(II)-polypyridine as photosensitizer component for the selective oxidation of organic sulfides to sulfoxides using water as an oxygen source and 4-nitrobenzenediazonium tetrafluoroborate as one-electron oxidant. In the present

study, the catalytic activity of Ru(II)-salen-Fe(III) dyad is compared with the previously reported Ru(II)-salen-Mn(III) dyad. The dynamics and mechanism of sequential electron transfer processes is followed by using nanosecond laser flash photolysis technique and the iron(IV)-salpyr species, $[\text{Fe}^{\text{IV}}(\text{salpyr}^+)]$ is proposed to involve in the catalytic cycles of sulfoxidation reaction. Herein we also present a more comprehensive approach for the photocatalyzed sulfide oxidation reaction using water as an oxygen atom source by the photochemically generated high-valent metal-salen catalysts. The photocatalytic system designed in our lab seems to be a good artificial photosynthetic system using earth abundant metal ions, Fe, Mn and Co as the catalysts and water as the oxygen source promising sustainability of the catalytic activity.

References

- [1] [Krishnan Senthil Murugan](#), [Thangamuthu Rajendran](#), [Gopalakrishnan Balakrishnan](#), [Muniyandi Ganesan](#), [Veluchamy Kamaraj Sivasubramanian](#), [Jeyaraman Sankar](#), [Andivelu Ilangoan](#), [Perumal Ramamurthy](#) and [Seenivasan Rajagopal](#), *J. Phys. Chem. A* 118 (2014) 4451.
 [2] W. Iali, P.-H. Lanoe, S. Torelli, D. Jouvenot, F. Loiseau, C. Lebrun, O. Hamelin, S. Menage, *Angew. Chem. Intd. Ed.* 54 (2015) 8415.

4.20 Influence of Sm on structural and optical properties of Bi_2S_3 thin films using SILAR method

D. Janani¹, N. Anandhan^{1*}, V. Dharuman², G. Gopu³, M. Karthikeyan¹, A. Amali Roselin¹, K. P. Ganesan¹

¹Advanced Materials and Thin film Physics Lab, Department of Physics, Alagappa University, Karaikudi-4, Tamilnadu.

²Molecular Electronics Laboratory, Department of Bioelectronics and Biosensors, Alagappa University, Karaikudi-4, Tamilnadu.

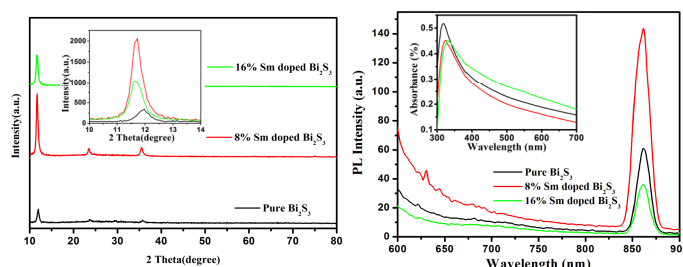
³Catalytic and Supercapacitor Lab, Department of Industrial Chemistry, Alagappa University, Karaikudi-3, Tamilnadu.

E-mail: anandhan_kn@rediffmail.com

Abstract

In this present work, pure and samarium (Sm) doped bismuth sulfide (Bi_2S_3) thin films were grown on glass substrates by successive ionic layer adsorption and reaction (SILAR) method. The prepared thin films were characterized by X-ray diffraction (XRD), UV-visible spectrometer (UV-Vis), photoluminescence (PL) spectroscopy. The X-ray diffraction patterns reveal that the pure and Sm doped Bi_2S_3 thin films are crystalline nature and when Sm is doped at 8 and 16%, the angle of the diffraction is shifted towards lower diffraction angle sides which is indication of Sm well-doped with Bi_2S_3 . Crystalline size, dislocation density and micro strain are determined using XRD data. From UV-spectra, we could be observed that, the absorption peak at 317nm for Bi_2S_3 thin film. After doping of Sm in Bi_2S_3 , the absorption peak is red shifted to 326 and 330nm for 8 and 16% respectively. The band gap value of pure 8% and 16% Sm doped Bi_2S_3 films is found to be 3.7, 3.87, 3.9eV respectively [1]. PL spectra present that 8% of Sm doped Bi_2S_3 thin film exhibits high exciton emission peak at 861nm than pure and 16%, which represents 8% of Sm doped Bi_2S_3 thin film having better optical quality[2]. The thickness of the pure 8% and 16% Sm doped Bi_2S_3 are 6.10 μm , 0.95 μm , 1.36 μm respectively.

Keywords: Bismuth sulfide, SILAR method and Excitation emission.



References

- [1] A. Hussain, Optical and electrical properties of bismuth sulfide thin films prepared in PVA matrix by chemical drop method. *J. Optoelectron. Advance. Mat.*, 12 (2010) 1019–1023.
 [2] Xuelian Yu, Synthesis and photoluminescence properties of Bi_2S_3 nanowires via surfactant micelle-template inducing reaction. *Solid State Commun.*, 134 (2005) 239–243.

4.21 Combustion synthesis of nanocrystalline FeWO₄ and its application towards the photocatalytic degradation of methylene blue

^aM.Mohammed Rafic, ^aR.Saraswathi* and ^bL.John Berchmans

^aDepartment of Materials Science, School of Chemistry, Madurai Kamaraj University, Madurai - 625 021.

^bCentral Electrochemical Research Institute, Karaikudi – 630006

e-mail: chemrafic@gmail.com; drrsaraswathi@gmail.com; berchmans@cecri.res.in

Introduction

Photocatalytic degradation is an advanced oxidation process, widely used for the degradation of organic dyes. TiO₂ (P25, Degussa) is a standard photocatalyst because it is an environmentally friendly, relatively inexpensive and chemically stable material. However, the large band gap of TiO₂ limits its application to the ultraviolet region of the solar spectrum (5 %). In order to make better use of sunlight, photocatalysts that are active to visible light are being explored [1]. Herein, we report for the first time, the application of iron (II) tungstate (FeWO₄) as an effective photocatalyst towards the degradation of methylene blue dye under visible light irradiation.

Experimental

FeWO₄ was synthesized by combustion method using stoichiometric amounts of iron nitrate and sodium tungstate precursors and urea as fuel. The product was used after annealing at 450°C for 30 minutes. The structural, morphological and physicochemical properties of the prepared sample were characterized by X-ray diffraction (XRD), FT-IR, UV-visible diffuse reflectance spectroscopy and scanning electron microscopy. Photocatalytic experiments were carried out in a standard photoreactor equipped with a tungsten halogen lamp as visible light source. A sodium nitrite solution was used as a UV filter to eliminate light < 390 nm. About 100 mg of the catalyst was placed into 250 mL of aqueous solution of methylene blue (2 x 10⁻⁵ M) solution under vigorous and constant stirring for 30 minutes. After dark absorption, the solution containing the catalyst was irradiated with visible light and the changes in dye concentration during photodecomposition were measured by the absorbance at 664 nm as a function of irradiated time. Parallel experiments were carried out with P25 for direct comparison.

Results and Discussion

X-ray diffraction pattern of the combustion synthesized FeWO₄ shows several diffraction peaks which match very well with that of monoclinic FeWO₄ (JCPDS 71-2391). The most prominent peaks are observed at 2θ = 17.87°, 23.64°, 29.65° and 36.14° corresponding to the crystal planes (100), (011), (111) and (200) respectively. Applying the Debye Scherrer equation, the crystallite size corresponding to the high intensity plane (011) is calculated to be 37 nm. The FT-IR spectrum shows the characteristic vibrational bands corresponding to the metal-oxygen bonds. The bands at 615 cm⁻¹ 860 cm⁻¹ can be assigned to the W-O and W-O-W vibration modes respectively while that at 513 cm⁻¹ corresponds to Fe-O bond [2,3]. The scanning electron microscopy image shows a highly porous morphology. The UV-visible diffuse reflectance spectral data are used to generate the Tauc plot ((αhν)^{1/2} vs hν) and from this plot, the band gap of the material is calculated to be 2.04 eV. Figure 1A shows the absorption spectra of methylene blue solution before and after visible light irradiation for different exposure time in the presence of FeWO₄. The characteristic absorption band of methylene blue at 664 nm is significantly decreased in intensity with increasing irradiation time. The normalized temporal concentration changes (C/C₀) are plotted against the irradiation time (Fig.1B). Parallel experiments with the standard photocatalyst (TiO₂, P25) have been carried out and the results show that FeWO₄ can effectively degrade about 80 % of methylene blue dye in 150 minutes in contrast to 51 % for P25 for the same time. Further experiments are in progress to understand the mechanism of photodegradation of methylene blue by FeWO₄.

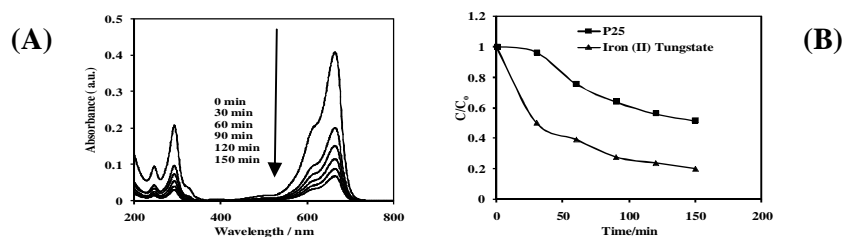


Fig. 1 (A) Absorbance vs wavelength as a function of illumination time for the photocatalytic degradation of methylene blue on FeWO₄ under visible light illumination (B) Plot of normalized concentration of methylene blue against irradiation time for FeWO₄ and P25 photocatalysts.

Conclusion

A new visible light active photocatalyst viz. FeWO₄ has been developed for the photocatalytic degradation of methylene blue dye which shows an efficiency of about 80 % under the conditions employed.

References

- [1] M. D.Hernandez-Alonso, F.Freshno, S.Suarez and J. M.Coronado, *Energy & Environmental Science* 2 (2009) 1231 – 1257.
 [2] J. Zhang, Y.Zhang, J. Y. Yan, S. K. Li, H. Wang, F. Z. Huang, Y. H. Shen and A. J. Xie, *Journal of Nanoparticle Research* 14 (2012) 796-805.
 [3] P. Cambier, *Clay Minerals* 21 (1986) 191 – 200.

4.22 Biosynthesized silver-nanoshells for catalytic degradation of organic pollutants

BalakumarVellaichamy and PrakashPeriakaruppan*

Department of Chemistry, Thiagarajar College, Madurai-625 009, Tamil Nadu, India.

E-mail: kmpprakash@gmail.com, chembalakumar@gmail.com

Abstract

A fastest way to degradation of industrial effluents is reported herein using silver-nanoshells (Ag-NSs) as a green catalyst. Ag-NSs was synthesized using *Crataeva Religiosa* leaf extract as both reducing and stabilizing agents and characterized by UV-visible spectroscopy, FT-IR spectroscopy, XRD, HR-TEM and EDX analysis. The green synthesized Ag-NSs catalyzes in a minute the degradation of organic dye pollutants namely methylene blue and methyl orange from aqueous environment using NaBH_4 . Ag-NSs is able to be conveniently separated from aqueous environment after catalytic dedying and reusable even after five cycles. The formation of Ag-NSs and dedyeing mechanism have also been investigated and discussed.

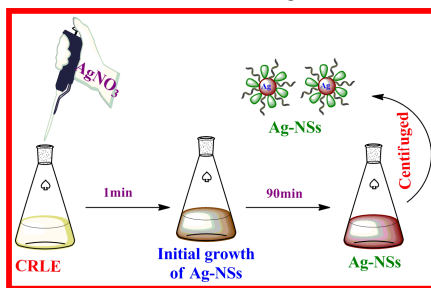


Fig.1 Mechanistic route for the formation of Ag-NSs.

Keywords: green synthesis, silver-nanoshells, catalytic degradation, methylene blue, methyl orange

References

1. V. Balakumar and P. Prakash, *RSC Adv.*, 2015, **5**,105917–105924.
 2. M. Zhu, C. Wang, D. Meng, G. Diao, *J. Mater. Chem. A* 2013, **1**,2118–2125.

4.23 Degradation of Organic Dye in Contaminated Water by Green Synthesized CuO Nanoparticles Using Aqueous Flower Extract of *Cordia sebestena* Linn

S. Prakash, A. Venkatesan, M. Stanely Britto, M. Sowndharya and V. Sujatha*

Department of Chemistry, Periyar University, Salem-11, Tamil Nadu, India. e-mail: chemsujatha888@gmail.com

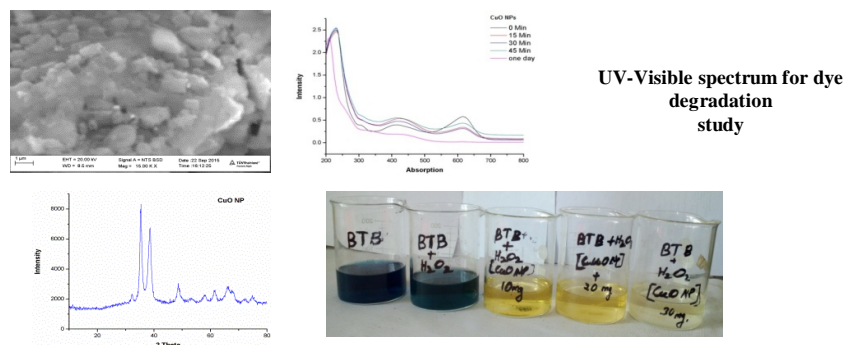
Abstract

Waste water from dyeing and dye related industries contain residual dyes such as organic compounds, which are not readily biodegradable and major causatives for water pollution. Various physical, chemical and biological treatments including ozonization, chlorination and filtration have been developed for alleviating the negative environmental impact of toxic water and pollutants. In current years, metal/metal oxide nanoparticles has been used to degradation of tough dye by its large surface area and surface plasmon resonance. Among that, CuO nanoparticles (CuO NPs) having deep vision for quenching the dye molecules due to consist large number of highly reactive sites and low toxicity, environmental acceptability and inexpensive. Synthesis of metal nanoparticles through green route is an ecologically friendly, cost effective method without use of rough chemicals. Hence focus of the study *Cordia sebestena* (Family: *Boraginaceae*) is ornamental plant flowers aqueous extract was used to synthesis of CuO NPs as bioreducing agent. Synthesized CuO NPs were characterized by UV-Visible, FT-IR, XRD, SEM and EDX techniques. The photodegradation activity was examined for bromothymol blue dye in contaminated water by CuO NPs catalyzed by hydrogen peroxide reaction conditions.

Result and Discussion

UV-Visible spectrum of biosynthesized CuO NPs showed two bands at 270 and 670 nm indicating the formation of CuO NPs. FT-IR analysis revealed the presence of organic molecules in the range $4000\text{--}400\text{ cm}^{-1}$

and peaks at around 500 to 600 cm^{-1} confirming the formation of CuO NPs. The XRD data displayed the monoclinic structure (JCPDS card: 89-2529) using Debye-Scherrer's equation the average particle size depicted is 7 nm. The SEM image showed the presence of some large particles, which can be attributed to aggregation or overlapping of small particles. EDX analysis exhibited the chemical composition of CuO NPs is Cu 4%, O 42%, C 40% and K, Mg, Ca, Cl are detected in insignificant percentage. Degradation of bromothymol blue was assisted by various amount of CuO NPs (10, 20, 30 mg) catalyzed by H_2O_2 and simultaneously the degradation activity was monitored in UV-Visible spectroscopy at the graduated time interval. The *Cordia sebestena* flower aqueous extract mediated green synthesized CuO NPs exhibited efficient activity for degradation of dye in all tested volumes.



Conclusion

Synthesis of CuO NPs through the green synthesis method using *Cordia sebestena* flower extract is very effective, cost free, faceable and risk free avenue to the growing nano materials fields. From this study, the degradation efficient of CuO NPs for organic dye contaminated waste water is strongly suggested to break down the deleterious dyes and organic molecules into toxic free contents and to provide the waste water as bio aptable aquatics for protection of green earth.

4.24 Fabrication of dye-sensitized solar cell using electrospun $\text{TiO}_2/\text{CaCO}_3$ nanowires

C. Brundha and S. Karuppuchamy*

Department of Energy Science, Alagappa University, Karaikudi, Tamil Nadu-630 003, India. Email: skchamy@gmail.com

Abstract

$\text{TiO}_2/\text{CaCO}_3$ nanowires have been synthesized using electrospinning method and subsequently the synthesized nanofibers were characterized using various advanced techniques. Dye-sensitized solar cell was fabricated using electrospun $\text{TiO}_2/\text{CaCO}_3$ nanowires and the highest efficiency was achieved for the cell with CaCO_3 compared with bare TiO_2 .

Introduction

Dye sensitized solar cells (DSCs) are very attractive and promising alternative to conventional silicon solar cells due to their low cost production and easy manufacturing process [1,2]. TiO_2 shows superior performance for electron transfer compared to other metal oxides such as MgO , SnO_2 , Nb_2O_5 and ZnO . In this work, $\text{TiO}_2/\text{CaCO}_3$ nanowires were prepared by electrospinning method. The prepared $\text{TiO}_2/\text{CaCO}_3$ was used to fabricate the DSCs. The performance of the DSCs was also investigated and discussed by comparing with the DSCs prepared using bare TiO_2 .

Experimental Section

A mixture of Polyvinylpyrrolidone and titanium(IV) isopropoxide (TIP) dissolved in ethanol, glacial acetic acid, dimethylformamide (DMF) was used as precursor for the preparation of TiO_2 . The precursor solution was loaded into a syringe under an applied voltage of 8-9 kV. The electrospun TiO_2 was collected on Al foil. The flow rate was controlled by a syringe pump. The needle to collector distance was maintained at approximately 9 cm. The obtained TiO_2 were calcined at 450°C for 1.5 hrs.

Results and discussion

Fig. 1 Indicates the XRD pattern of the synthesized TiO_2 and $\text{TiO}_2/\text{CaCO}_3$ nanomaterials. The overall crystalline structure displays an anatase phase with preferred (101) orientation at $2\theta = 25.2^\circ$ other peaks are assigned to CaCO_3 such as 29° and 43° . Fig. 2 SEM clearly shows the formation of TiO_2 nanowires with homogeneous morphology.

Conclusion

The metal doped TiO₂ photocatalyst was successfully synthesized by microwave irradiation method. The XRD pattern confirms the formation of monoclinic TiO₂. The prepared metal doped TiO₂ photocatalyst was successfully decomposed the methylene blue dye under UV light irradiation.

References

1. A. M. H. Milad, L. J. Minggu, M. B. Kassim, W. R. W. Daud, *Ceramics Inter.* 39 (2013) 3731–3739.
2. R. Dhilip Kumar, S. Karuppuchamy, *J. Mater. Sci.: Mater. Elect.* 26 (2015) 6439–6443.

4.26 Synthesis, Characterization and Antibacterial Properties of TiO₂ Nanowires

M. Nagalakshmi, C. Brundha and S. Karuppuchamy*

Department of Energy Science, Alagappa University, Karaikudi, Tamil Nadu – 630 003, India

*Email: skchamy@alagappauniversity.ac.in

Abstract

Titanium dioxide (TiO₂) nanowires have been successfully prepared by electrospinning method and the resulting material was characterized by XRD and SEM. The antibacterial activity of TiO₂ nanowires was investigated by disc diffusion method against bacterial strains and found good antibacterial effects.

Introduction

Titanium dioxide (TiO₂) nanowires were synthesized by electrospinning which is a simple and low cost technique [1]. Electrospinning allows the production of nanomaterial from various materials, e.g. inorganics and organics in different configurations and assemblies. It has been demonstrated that fibrous structure is preserved even after annealing when the precursor of inorganic (or) organic compound is introduced into the polymer solution. In the present work, we synthesized the TiO₂ nanowires by electrospinning method and then characterized the materials by XRD and SEM. We also investigated the antibacterial activity of the synthesized TiO₂ against bacterial strains such as *Klebsiella pneumonia* and *Bacillus cereus* [2].

Experimental section

A mixture of PVP dissolved in ethanol, glacial acetic acid, dimethylformamide and titanium (IV) isopropoxide were used as precursor for the electrospinning of TiO₂. The precursor solution was loaded into a syringe under an applied voltage of 8-9 kV. The electrospun TiO₂ was collected on Al foil. The obtained TiO₂ was calcined at 450°C for 1.5 hrs. Moreover, the antibacterial activity of TiO₂ nanowires was carried out by disc diffusion method against *Klebsiella pneumonia* and *Bacillus cereus*. The antibacterial study was carried out using different concentrations (20, 40 and 60 µl) of dispersed TiO₂.

Results and discussion

Fig 1 shows the XRD pattern of the TiO₂ nanomaterials. The anatase structure was confirmed from the sharp peaks appeared at 2θ = 25.0°. Fig. 2 shows the SEM image of TiO₂ electrospun nanowires. The antibacterial activity of TiO₂ nanowires was carried out using various concentrations of TiO₂ against *Klebsiella pneumonia* (26mm) and *Bacillus cereus* (25 mm) and maximum zone of inhibition was observed at 60 µl (Fig. 3). It was observed that the increase of inhibition zone during the increase of concentration of TiO₂ nanowires.

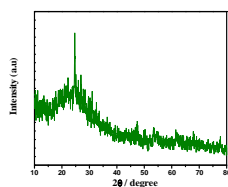


Fig. 1 XRD spectra of TiO₂

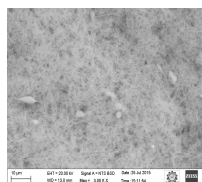


Fig. 2 SEM image of TiO₂



Fig. 3 Zone of Inhibition

Conclusions

In this study, nanowires of TiO₂ were produced by electrospinning method. XRD confirms the formation of crystalline TiO₂. The formation of homogeneous morphology of the TiO₂ nanowires was also observed by SEM. It was found that the electrospun TiO₂ nanowires can be good antimicrobial agents.

References

- [1] S. Karuppuchamy and C. Brundha, *Appl Mech and Mater.*, (2015) 3-7
- [2] N. C. J. Packia Lekshmi, *J. Microbiol. Biotech. Res.*, (2012) 115-119

4.27 Facile Synthesis of Barium Titanate Nanopowder by Microwave Assisted Route for Photocatalytic Applications

M. Thamima and S. Karuppuchamy*

Department of Energy Science, Alagappa University, Karaikudi, Tamilnadu-630003

E.mail: skchamy@alagappauniversity.ac.in

Abstract

Novel perovskite based BaTiO₃ nanocomposite was successfully synthesized by simple microwave irradiation route. The prepared materials were characterized using advanced spectroscopic analytical techniques. Photocatalytic study was also carried out using prepared BaTiO₃ and confirms the photocatalytic performance under UV light irradiation.

Introduction

BaTiO₃ material has perovskite (ABX₃) structure, which is widely used in capacitors, sensor, optoelectronic devices, electronic industry, and photocatalytic applications due to its low tangent losses and high dielectric constant [1]. There are several synthetic routes are available for the preparation of BaTiO₃ such as wet chemical route, hydrothermal, sol-gel, microwave, molten salt etc. Among all the methods, microwave assisted wet chemical route is preferred for synthesis of BaTiO₃ due to its low cost and eco-friendly nature [2]. In this paper, we report a new route to develop BaTiO₃ nanopowder by peroxy route. The synthesized BaTiO₃ nanoparticles were used as photocatalyst for degrading methylene blue (MB) dye under UV light irradiation.

Experimental Section

In a typical procedure, stoichiometric ratio of Ba(OAc)₂, TiOSO₄ was dissolved in the H₂O₂ and water mixture under constant stirring to form a peroxy complex. After 1 h stirring, 10 ml of NaOH solution was added for avoiding the formation of BaCO₃. The colloidal pale yellow colour precipitate was obtained and it was heated at 95 °C for 30 min and the precipitate was washed with distilled water and ethanol and subsequently treated under microwave radiation for 10 min, 20 min and 30 min. The obtained powder was used for photocatalytic dye degradation studies.

Result and Discussion

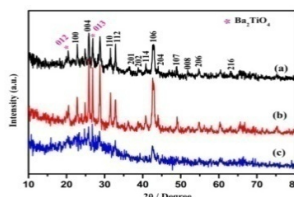


Fig. 1.

1. XRD patterns of the microwave irradiated BaTiO₃ samples: (a) 10 min, (b) 20 min, (c) 30 min

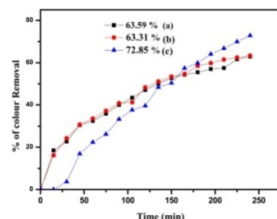


Fig. 2.

2. Photocatalytic degradation of MB in BaTiO₃

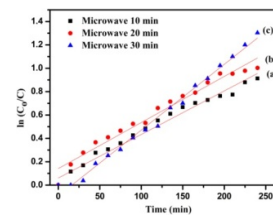


Fig. 3.

3. Kinetic study for the degradation of MB in presence of BaTiO₃

XRD pattern of the synthesized powder confirms the presence of BaTiO₃ and the peak matches well with the JCPDS (card number # 821175) of BaTiO₃. The photocatalytic performance of the microwave irradiated sample (30 min) show higher efficiency of 72.8 % compared to the other samples. The kinetic studies exhibit K= 0.00421, 0.004178 and 0.005432 min⁻¹ for 10 min, 20 min and 30 min microwave irradiated BaTiO₃ samples, respectively.

Conclusions

We have successfully synthesized nanocrystalline BaTiO₃ by microwave method. XRD results suggest that the presence of hexagonal phase BaTiO₃ nanoparticles. The photocatalytic MB dye degradation efficiency of 72.85% was achieved by BaTiO₃.

References

1. S. Fuentes, R.A. Zárate, E. Chávez, P. Muñoz, M. Ayala, R. E. González and P. Leyton, *J. Alloy. Compd.*, 505 (2010) 568–572.
2. M. Thamima and S. Karuppuchamy, *J. Mater. Sci. Mater Electron.*, 27 (2015) 458–465.

4.28 The roles of protic solvents on CdS thin films prepared by chemical bath deposition technique

K.Rajeswari¹, N.Anandhan^{1*}, V. Dharuman², A. Amali Roselin¹, M.Karthikeyan¹, G.Gopu³

¹Advanced Materials and Thin film Physics Lab, Department of Physics, Alagappa University, Karaikudi-4, Tamilnadu.

²Molecular Electronics Laboratory, Department of Bioelectronics and Biosensors, Alagappa University, Karaikudi -4.

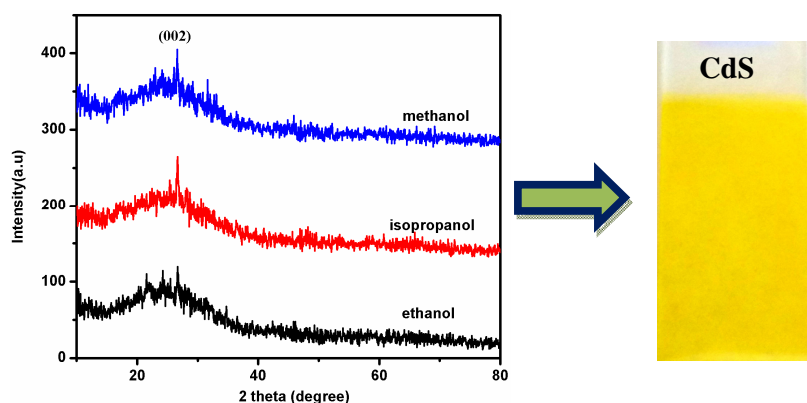
³Catalytic and Supercapacitor Lab, Department of Industrial Chemistry, Alagappa University, Karaikudi-3, Tamilnadu

*Corresponding author; E-mail: anandhan_kn@rediffmail.com

Abstract

In this present work, cadmium sulfide (CdS) thin films were grown on glass substrates by chemical bath deposition technique (CBD). The role of protic solvents (ethanol, isopropanol and methanol) on structural, vibrational and optical properties was studied by using X-ray diffraction (XRD), micro Raman and UV visible spectroscopy. XRD patterns revealed that the prepared CdS thin films exhibit hexagonal structure with preferentially oriented along the (002) plane [1]. Crystalline size, dislocation density and micro strain were determined from XRD data. In micro Raman spectra, the appearance of intensive peak at 313cm^{-1} (1LO) mode confirmed that CdS films were in single crystal and it also indicated high degree of crystallinity [2]. The optical absorbance spectra showed that, the CdS thin film prepared using isopropanol hold more absorbance compared to other protic solvents. The band gap value of the CdS film prepared using ethanol, isopropanol and methanol was found to be 2.10, 2.02 and 2.12 eV, respectively. CdS film thickness was measured 960, 620 and 1003 nm for ethanol, isopropanol and methanol by profilometer. In this present work, it can confirm that CdS thin film prepared using isopropanol is able to use the window layer for photovoltaic applications.

Keywords: Cadmium sulfide, Chemical bath deposition, Protic solvents.



References

1. Pin-Chuan Yao, Chun-Yu Chen, Effect of Protic solvents on CdS thin film prepared by Chemical bath deposition. Thin Solid films, 579 (2015) 103-109.
2. Y-J.Chang, Growth, Characterization and application of CdS thin films deposited by chemical bath deposition, Surface and Interface Analysis, 37 (2005) 398-405.

4.29 Synthesis and Characterization of Fe-TiO₂ / Polyanilinecore-Shell Nanostructure for Photocatalytic Hydrogen Production

C. Meyyathal, R. Kalyani and K. Gurunathan*

Nano Functional Materials Lab, Department of Nanoscience & Technology,
Alagappa University, Karaikudi- 630 003; e-mail:kgnathan27@rediffmail.com

In the present work, TiO₂, Fe-TiO₂ and Fe-TiO₂/PANI nanoparticles were synthesized and its photocatalytic activity was evaluated. The typical synthesis procedure of TiO₂ are as follows: The TiO₂ nanoparticles (Nps) are synthesized by using Titanium Tetraisopropoxide (TTIP), 2-propanol and ammonia as starting materials. In this, 0.049M of TTIP and 1.304 M of 2-propanol are mixed together with constant stirring, meanwhile 0.033M ammonia was added at a constant rate at room temperature. Upon the addition of ammonia, the clear solution turns into white emulsion which was stirred for about 1 hour. The solvent in the mixture was evaporated at 60 °C. The obtained precipitate was filtered under reduced pressure. The filtrate was washed with distilled water and then dried by convection at 105 °C for 18 hours. It was then calcinated at 800 °C for 2 hours. The synthesis of Fe-TiO₂ were done by the following method: 0.6963g of titanium tetra isopropoxide

(TTIP) was dissolved in 50ml of 2-propanol and stirred for 30min. 0.027036g of Iron (III) chloride hexahydrate was dissolved in 100ml of 2-propanol, added at a rate of 5 ml/min. After half an hour, 15ml of ammonia was added at a rate of 1ml/min for 30min. The solution was heated at 60 °C in a water-bath using a condenser. The precipitate was filtered, centrifuged and dried in oven at 105 °C for 18hours and calcinated.

The synthesis of Fe-TiO₂ were prepared by the following method: 0.6963g of titanium tetra isopropoxide (TTIP) was dissolved in 50 ml of 2-propanol and stirred for 30 min. 0.027036 g of Iron (III) chloride hexahydrate was dissolved in 100 ml of 2-propanol, added at a rate of 5 ml/min. After half an hour, 15 ml of ammonia was added at a rate of 1 ml/min for 30 min. The solution was heated at 60 °C in a water bath using a condenser. The precipitate was filtered, centrifuged and dried in oven at 58 °C for 24 h.

The core-shell of Fe-TiO₂/PANI was synthesized by 0.003 mol (0.704 g) of CSA is taken as solution A and 0.05 mol (4 g) of aniline is taken as solution B and 0.1 g Fe-TiO₂ is added to the above solutions. The solutions were mixed in 200 ml of distilled water and stirred for 2 h. After that the solutions were pre-cooled to 0 °C in an ice bath. 50 ml of aqueous solution and 0.04 mol (9 g) of APS were added dropwise to the above mixture, brown color precipitate was formed and stirred for 4 h, finally dark green color precipitate was formed. This is the first evidence of formation of polyaniline. The mixture was centrifuged and dried for 12 h. Fe-TiO₂/PANI powder of polymer was confirmed by further XRD and UV-Vis characterizations.

The proposed work was further characterized by XRD, FTIR, UV, RAMAN and SEM analysis. This photocatalyst was studied for hydrogen production using water splitting reaction and dye degradation studies are also performed to evaluate the photocatalytic activity.

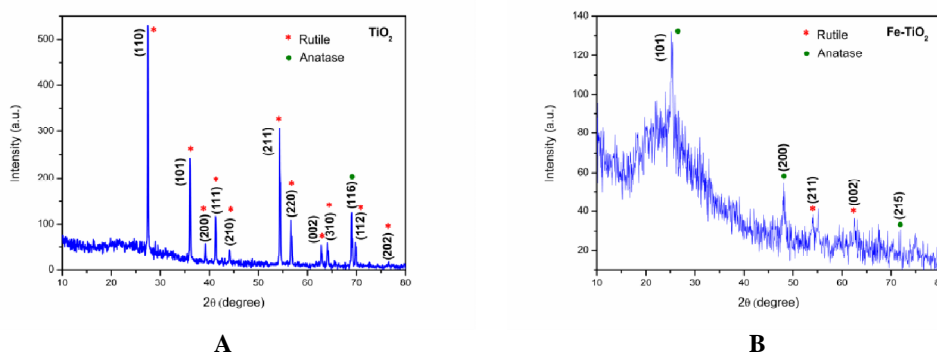


Figure 1. XRD pattern of (a) TiO₂ nanoparticles (b) Fe-TiO₂ nanoparticles

XRD data as shown in Figure 1 reveals the presence of TiO₂ and matches with JCPDS 89-8303. The obtained TiO₂ has tetragonal phase with primitive lattice having cell parameters $a=4.593\text{Å}$, $c=2.959\text{Å}$ with average particle size of about 86.94 nm and specific surface area of 16.917 m²/g. The morphology index of the sample is 0.825. The XRD spectra of Fe-TiO₂ matches with JCPDS 21-1272 having tetragonal body centered lattice with lattice parameters $a=3.785\text{Å}$ and $c=9.513\text{Å}$. The average crystallite size is 29.13 nm having specific surface area of 66.15 m²/g with morphology index of 0.571.

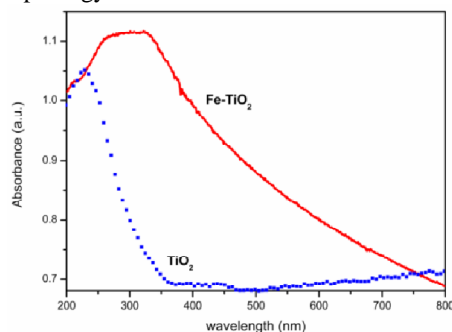


Figure 2. UV-Vis. Absorption spectra of TiO₂ and Fe-TiO₂ nanoparticles.

Figure 2 shows the UV-Visible spectra of TiO₂ and Fe-TiO₂ nanoparticles. UV spectrum shows the absorbance of the sample in the UV region with continuous absorption spectrum extending to the visible region. Compared to the absorption range of TiO₂, Fe-TiO₂ shows a good absorption range in the UV-Visible region.

The above results show that the materials have good crystallinity and optical property which can be used as photocatalyst for hydrogen production and dye degradation.

4.30 Fabrication of Novel Zn₂SnO₄ / V₂O₅ Composite for degradation of Eosin Yellow under Visible light irradiation

V. Ramasamy Raja^a, A. Suganthi^{a*}, M. Rajarajan^{b*}, D.Rani Rosaline^a

PG & Research Department of Chemistry, Thiagarajar College, Madurai-625 009, Tamilnadu, India.

PG & Research Department of Chemistry, C.P.A College, Bodinayakanur-626 513, Tamilnadu, India.

Corresponding author e-mail: suganthicarts@gmail.com

ABSTRACT

A Novel Zn₂SnO₄-V₂O₅ composite in three different molar ratios (1%, 3%, 5% of Zn₂SnO₄-V₂O₅) were synthesized successfully by precipitation-deposition method and its photocatalytic activity towards Eosin Yellow was studied. The phase purity, crystallite size and strain were ascertained by powder X-ray diffraction (XRD) analysis. Further, the synthesized photocatalysts were characterized by Fourier transform infrared spectroscopy (FT-IR), Scanning electron microscopy (SEM), Energy dispersive x-ray spectroscopy (EDAX), UV-Vis diffuse reflection spectroscopy (DRS) and photoluminescence spectroscopy (PL). The efficiency of the photocatalysts was evaluated from the photodegradation of Eosin Yellow, a target textile pollutant, under visible light irradiation. The photocatalytic activity of the synthesized Zn₂SnO₄-V₂O₅ composite photocatalyst was found to be more efficient than that of individual components. The composite with molar ratio of 3% Zn₂SnO₄-V₂O₅ photocatalyst shows an excellent photocatalytic activity than the composite with molar ratio 1% Zn₂SnO₄-V₂O₅, and 5% Zn₂SnO₄-V₂O₅. The band edges of the materials have been theoretically calculated on the basis of Mulliken electronegativity of atoms. The effects of operational parameters such as pollutant concentration, pH, catalyst dosage and OH· radical trapping, COD have been investigated in detail. The Kinetics of the photodegradation reaction was correlated with the pseudo-first-order model. A possible mechanism has been proposed for the photocatalytic degradation using Zn₂SnO₄-V₂O₅.

Keywords: Photocatalysis, Visible Light, Zn₂SnO₄-V₂O₅ composite, Eosin Yellow

References

1. K. Vignesh,^a A. Suganthi,^{a**} M. Rajarajan,^{b**} R. Sakthivadivel,^a Visible light assisted photodecolorization of eosin-Y in aqueous solution using hesperidin modified TiO₂ nanoparticles. Applied Surface Science 258 (2012) 4592–4600.
2. PatcharananJunploy,^a Somchai Thongtem,^{a**} Titipun Thongtem,^{b**} Anukorn Phuruangrat,^a Photocatalytic activity of Zn₂SnO₄-SnO₂ nanocomposites produced by sonochemistry in combination with high temperature calcinations Superlattices and Microstructures 74 (2014) 173–183.

4.31 Visible light sensitisation of TiO₂ by polyaniline and a photocatalytic water splitting of resulting PANI-TiO₂ hybrid materials

E Subramanian^{*}, A Baby Shanthi, J V Anusha

Department of Chemistry, Manonmaniam Sundaranar University, Tirunelveli

E-mail: anushachem412@gmail.com; esubram@yahoo.com

Introduction

TiO₂ is an attractive catalyst in photocatalysis due to its low cost, high photocatalytic activity, stability in aquatic systems and low environmental toxicity [1]. However, it is active in the UV region only (E_g = 3.2 eV; λ ≤ 387 nm). The present work aims to make TiO₂ an efficient and favourable photocatalyst in the visible region by coupling conducting polyaniline (PANI) to TiO₂ and to investigate the hybrid material performance in photocatalytic water splitting to produce hydrogen.

Experimental Section

Chemical oxidative polymerization reported elsewhere [2] was adopted in the synthesis of PANI. 0.1 ml of PANI mixture was added to 100 mg TiO₂ for *ex situ* coating by stirring the mixture uniformly and simultaneously drying for 7 days. The resulting hybrid material washed with 25 ml distilled water and dried at 80°C for 3 h. The same procedure was used for the synthesis of 0.2, 0.3, 0.4 and 0.5 ml PANI coated TiO₂ photocatalyst materials. Photocatalytic water splitting performed under visible light irradiation for 5 h (CFL lamp 20W) using 50 mg of PANI-TiO₂ (0.1 ml, 0.2 ml, 0.3 ml, 0.4 ml and 0.5 ml) and spent 0.5 ml PANI-TiO₂ at pH = 3.5 under room temperature. Hydrogen production was monitored at a regular time interval of 20 min by using manometer.

Results and Discussion

The synthesized materials were characterized by FTIR, XRD, DRS and SEM techniques. The XRD spectra (Fig. 1) confirm the crystal phase of anatase TiO_2 (JCPDS card no. 71-1767) in all the synthesized photocatalysts. The SEM (Fig. 2) images of pristine TiO_2 and 0.5 ml PANI- TiO_2 displays that all the materials have a uniform distribution of nanoparticles of size 100 nm and some agglomeration of primary nanoparticles.

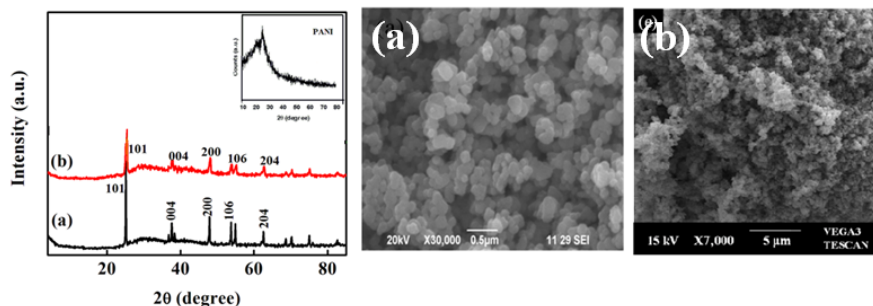


Fig. 1 XRD spectra of (a) TiO_2 , (b) PANI- TiO_2 Fig. 2 SEM images of (a) TiO_2 , (b) PANI- TiO_2 0.5 ml

Conclusion

The PANI- TiO_2 materials were successfully synthesized and characterized. All the PANI- TiO_2 materials showed hydrogen generation activity indicating that TiO_2 could be sensitized in visible region by PANI.

References

1. C. Murugan, E. Subramanian. *J. Adv. Chem. Sci.* **2015**, 1(3): 107-109.
2. O. Legrini, E. Oliveros, and A.M. Braun. *Chem. Rev.* **1993**, 93: 671-698.

4.32 Synthesis And Characterisation of Core- Shell of ZnSse/ Zns For Solar Cell Application

G. Ganesh Priya, R. Kalyani and K. Gurunathan*

*Nano Functional Materials Lab, Department of Nanoscience & Technology, Science Campus, Alagappa University, Karaikudi- 630 003; *e-mail:kgnathan27@rediffmail.com*

In this communication, a hydrothermal method for synthesizing ZnSse/ZnS cre-shell structures was introduced. The general synthesis procedure for ZnSse is as follows: The ZnSse nanoparticles were synthesized by using selenium dioxide (SeO_2) and sodium hydroxide (NaOH) as starting materials. 0.5548 g of SeO_2 was added to 50 ml of distilled water with constant stirring. Then 0.2 g of NaOH was added drop wise to the above solution. After 30 minutes of constant stirring, the product NaSeO_2 was obtained. 1.4377 g of ZnSO_4 was added dropwise to the above solution. After 30 minutes of constant stirring, 0.3756 g of Thioacetamide was added dropwise to the above solution. It turns into yellowish color. After 3 hours, red color precipitate was formed. The precipitate was centrifuged for three times and the obtained product was dried in an air oven at 60°C . Finally core was formed. 0.1 g of ZnSse was dispersed in 12.5 ml of distilled water, ultrasonicated for 1 hour. To this, 25 ml of 0.1 M zinc sulfide was added dropwise and after 10 minutes, 0.1 M NaOH was added dropwise to the above solution when it reached pH 12 and then heated at 80°C for 30 minutes. Further the precipitate was centrifuged at 8000 rpm and dried in oven at 60°C for 5 hours. Finally, core-shell was formed and assigned as sample 1. The same procedure was followed for the synthesis of sample 2 just by varying the temperature to 100°C .

Figure 1 shows the XRD pattern of (a) ZnSse-core and (b) ZnSse/Zns-core/shell. The XRD spectra of ZnSse at 60°C (Fig 1.a) shows the peak at 2θ value which matches with JCPDS no. 02-0479 for ZnSe having FCC structure and the peaks for ZnS matches with JCPDS no. 89-7386. It shows the sample has good crystallinity and also it reveals the nanocrystalline nature of the samples with the average crystallite size of 63.30 nm having morphology index of 0.733. The average surface area of the nanocomposite is $17.98\text{ m}^2/\text{g}$. The XRD spectra of ZnSse at 100°C is also shown in the Figure 1(b). It indicates the amorphous nature of the sample.

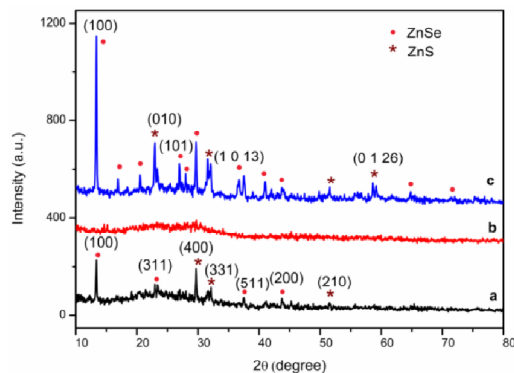


Figure 1. (a) Core of sample 1 (60 °C), (b) Core shell of sample 1 (60 °C) and (c) Core of sample 2 (100 °C).

4.33 Synthesis, characterization and photocatalytic study of cerium oxide/zeolite-NaX with brilliant green dye degradation

G. Sudha and E. Subramanian*

Department of Chemistry, Manonmaniam Sundaranar University, Tirunelveli 627 012, Tamil Nadu, India

Email: sudhachem84@gmail.com; esubram@yahoo.com*

1. Introduction

The incorporation of heteroatoms (Ti and other transition metals) in the framework of zeolites could make the structure photoactive¹. In the present work cerium oxide incorporated zeolite-NaX is synthesized from coal fly ash and its photocatalytic activity is investigated.

2. Experimental

Zeolite-NaX (Zeo-NaX) was synthesized from coal fly ash by alkali fusion and hydrothermal treatment². A mixture of 2 g of synthesized zeolite, 2 g of $(\text{NH}_4)\text{Ce}(\text{NO}_3)_6$ dispersed in water was stirred at 60 °C for 2 h. The product was filtrated, washed, dried at 100 °C overnight. Finally the sample was calcined at 550 °C for 4 h to get cerium oxide loaded fly ash derived zeolite NaX.

The synthesized materials were characterized by FTIR and SEM techniques. The photoactivity of Zeo-NaX and $\text{CeO}_2/\text{Zeo-NaX}$ was studied by the degradation of dye brilliant green (BG) under visible light irradiation maintaining the condition of $T = 30^\circ\text{C}$, $\text{pH} = 6.8$, catalyst dose = 100 mg, $[\text{BG}] = 10 \text{ ppm}$

3. Results and discussion

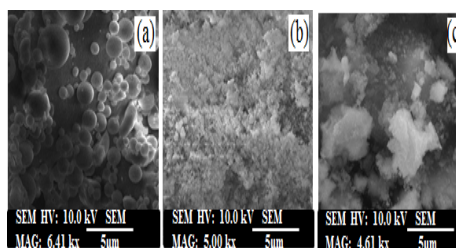
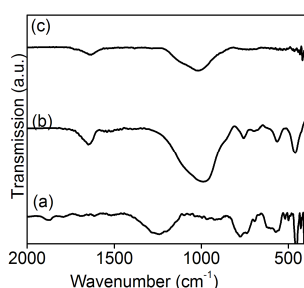


Fig. 1 FTIR spectra of (a) fly ash, (b) Zeo-NaX, (c) $\text{CeO}_2/\text{Zeo-NaX}$ and Fig. 2 SEM images of (a) fly ash, (b) Zeo-NaX, (c) $\text{CeO}_2/\text{Zeo-NaX}$

The FTIR spectra are shown in Fig. 1. The band at 980 cm^{-1} represents Si-O-Al vibration in fly ash². Cerium oxide/Zeolite-NaX exhibits the characteristic peaks at $433, 465, 533, 741, 1018$ and 1634 cm^{-1} . The spectra confirm formation of Zeo-NaX and $\text{CeO}_2/\text{Zeo-NaX}$ from fly ash. The SEM images (Fig. 2) reveals that fly ash particles are predominantly spherical in shape with relatively smooth surface (image a). Image b shows the single phase formation of zeolite with uniform orientation of spherical particles and morphology. The image c shows the formation of agglomerated Ce particles in Zeo-NaX.

4. Conclusion

A novel visible light active photocatalyst CeO₂/Zeo-NaX was designed, successfully synthesized and characterized. Its visible light degradation efficiency is found to be higher in BG dye degradation.

References

1. G. Yanan, Z. Baiyi, D. Xincun, *J. Thermodyn. Catal.* 4 (2) (2013) 1-2.
2. P.T. Amalathas, S.S. Thavamani, *Adv. Matt. Let.* 4 (2013) 688-695.

4.34 Fluorescence spectral studies of some imidazole derivatives

T.S.Rajasekar,^{a,b} and N. Srinivasan.^{a,c*}

^a Research and Development Centre, Bharathiar University, Coimbatore- 641 046, Tamilnadu,

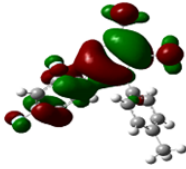
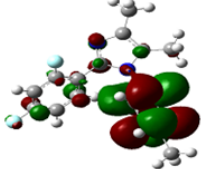
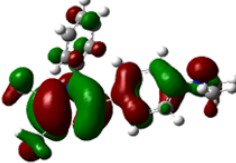
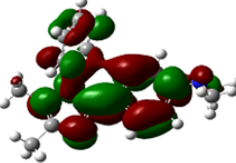
^b Department of Chemistry, Pachaiyappa's College for Men, Kanchipuram-631 501, Tamilnadu,

Abstract

The photophysical properties of imidazole derivatives namely 2-(2, 4-difluorophenyl)-4,5-dimethyl-1-p-tolyl-1H-imidazole and N, N-dimethyl-4-(4,5-dimethyl-2-phenyl-1H-imidazol-1-yl)benzenamine, synthesized from an unusual four components assembling, were studied in several solvents. Polarization also plays major role in the increase of excited-state dipole moment (μ_e). From the spectral results, it was found that there is equilibrium between neutral species and monocationic (MC) species in polar aprotic and polar protic solvents. The basicity of the solvent, C_β or C_{SB} has a negative value, suggesting that the absorption and fluorescence bands shift to lower energies with increasing electron-donating ability of the solvent. Therefore, resonance structures 1b & 2b has the positive charge located at the nitrogen atom stabilized in basic solvents. Study of photophysical properties of heterocyclic organic molecules has achieved a considerable importance recently because of many of these molecules form an integral part of intermediates, fine product for drugs and pesticides, colour industries, redox systems for solar energy, organized assemblies, laser dyes and complex forming agents. Imidazole derivatives have attracted considerable attention because of their unique optical properties. These compounds play very important role in chemistry as mediators for synthetic reactions, primarily for preparing functionalized materials. Imidazole nucleus forms well-known components of human organisms and used as laser, polymer stabilizer.

The present study on the photophysical properties of the imidazole derivatives is a continuation of our earlier work. Based on earlier studies, imidazole derivatives should be quite polar and can lead to greater interactions with the polar solvents. In order to confirm the above-mentioned facts, absorption, fluorescence excitation and fluorescence spectroscopy, as well as, time-dependent spectrofluorimeter have been used. Effect of pH on the spectral characteristics has also been investigated. Characterization of ionic species has been carried out by doing the electronic structural calculations using Gaussian 03 program. The solvent effects on the absorption and fluorescence bands were analyzed by a multi-component linear regression in which several solvent parameters are simultaneously analyzed.

Keywords: Imidazole derivative; Kamlet-Taft; Catalan parameters; Geometrical change.

Cmpd.	HOMO	LUMO
1		
2		

4.35 Sol-Gel Based Synthesis And Characterization of Photoactive Nanocrystalline ZnO Thin Films For Hydrogen Production

R. Kalyani and K. Gurunathan*

Nano Functional Materials Research Lab, Department of Nanoscience and Technology, Science Campus, Alagappa University, Karaikudi- 630 004. *E-mail corresponding author: kgnathan27@rediffmail.com

Zinc Oxide thin films (ZnO) with varying precursor concentrations were successfully synthesized and deposited on glass substrate by sol-gel dip coating method. X-Ray Diffraction (XRD) and Scanning Electron Microscope (SEM) techniques were used to study the structural properties of ZnO thin films. The Optical

properties of ZnO thin films were investigated using UV visible Spectrophotometer and Photoluminescence (PL) studies. The ZnO films showed hexagonal structure with c-axis orientation along (002) plane and the SEM image shows granular surface. The UV visible spectral study showed good transmittance in the visible region with a direct band gap value in the range of 3.15 eV to 3.3 eV for the prepared Zinc Oxide thin films. The PL spectra of ZnO sample gives emission peak centred at 380 nm and 480 nm. The ZnO thin film was used for H₂ production.

In the preparation of ZnO thin films, Zinc acetate dihydrate (Zn(CH₃COO)₂ · 2H₂O), ethanol and mono ethanolamine (MEA) were used as starting material, solvent and sol stabilizer respectively. Zinc acetate (0.25 M) was first dissolved in ethanol at room temperature, the resulting mixture was stirred at 60 °C for an hour and MEA was added into the solution drop by drop (molar ratio of MEA and zinc acetate was maintained at 1.0). Finally, a clear homogeneous solution was obtained. The ZnO solution was aged for 24 hours at room temperature and then ZnO thin films were prepared by dip-coating method on cleaned and dried glass substrates. Every time the substrate was withdrawn from the ZnO solution and kept in furnace, allowed to dry and subjected for pre-heat treatment at 300 °C for 5 minutes. The procedure from dip-coating to drying was repeated six times. At last, ZnO thin film was annealed at 550 °C in air for an hour. Two more samples were also prepared by varying the molarities of zinc acetate as 0.25, 0.3, 0.35 and 0.4M.

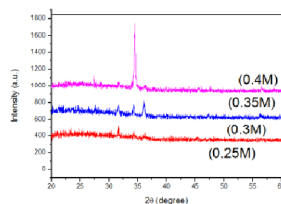


Figure -1. X-Ray diffraction spectra of ZnO thin films for (a) 0.25 M, (b) 0.3 M, (c) 0.35 M and (d) 0.4 M concentrations.

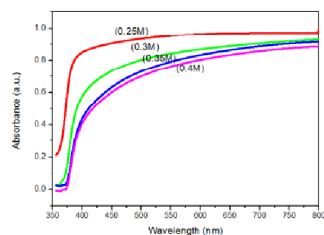


Figure -2. Optical transmittance spectra of ZnO thin films for (a) 0.25 M (b) 0.3M (c) 0.35M and (d) 0.4 M.

References

- [1] J.Xie, H.Deng, Z.Q.Xu, Y.Li and J.Huang, *Journal of Crystal Growth*, 292 (2006) 227.
- [2] E.W.Seelig, B.Tang, A.Yamilov, H. Cao and R.P.H.Chang, *Material Chemical Physics*, 80 (2003) 257.
- [3] N.Megan, M.Tomar, V.Gupta, and A.Mansingh, *Optoelectronic Materials*, 27 (2004) 241.

4.36 Photolytic Degradation of Alizarin Red S By Zn Doped TiO₂ in Presence of Electron Acceptor

C.Rani* and K.Santhi

Department of chemistry, Alagappa Govt. Arts college, Karaikudi – 630003, India

E-mail: viswanathanrani@gmail.com

TiO₂ photocatalytic activity has been improved by doping the transition metal ions used in its formation, such as Zn²⁺, Fe²⁺, Mn²⁺, etc. A novel binary microstructured Zn/TiO₂ was prepared by sol-gel method. Morphological studies like scanning electronic microscopy and EDAX shown in figure 1 and figure 2 confirms the micro crystallinity of the material formed. Many researchers have shown that doped Zn into TiO₂ by various processing methods, increases photocatalytic activity of TiO₂. Figure 2 shows the degradation rate of the catalyst prepared. The degradation ratio of Alizarin red could be up to 75% for Zn doped TiO₂, compared with TiO₂ catalyst. The usage of electron acceptors (H₂O₂ and peroxydisulphate (S₂O₈²⁻) was also tried and found to be enhance the dye degradation rate, because of the electron scavenging processes and the production of oxidizing species during the course of reaction.

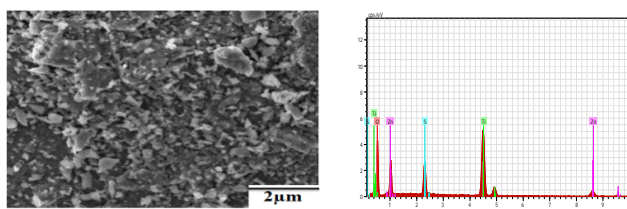


Figure 1. SEM image Zn doped TiO₂ Figure 2. EDX of Zn doped TiO₂

Key words: Photocatalysis, electron acceptor

References

1. T. Dietl, H. Ohno, F. Matsukura, J. Cibertand D. Ferrand, *magnetic semiconductors*, *Sci.* 287 (2000) 1019-1022.
2. H. M. Konyar, C. Yatmaz, K. Öztürk, *Appl. Surface Sci.* 258 (2012) 7440–7447

4.37 Comparison of photocatalytic applications of TiO₂ and Mn(TiO₃)

C. Rani*, K. Santhiand Vinothini

Department of Chemistry, Alagappa Govt. Arts College, Karaikudi, Tamil Nadu-630 003, India

E-mail: viswanathanrani@gmail.com

To increase the photocatalytic efficiency of TiO₂, we tried to extend the absorption light wavelength to visible region by adding manganese into titanium dioxide. TiO₂ nanoparticles were prepared using TiOSO₄ as a precursor solution with sufficient amount of capping agent PVP. The obtained precipitate was calcinated at 5000C for 2 hrs. The same process was used for preparing Mn(TiO₃) materials. Manganese acetate was used as a precursor for Mn. Synthesized TiO₂ and Mn(TiO₃) nanomaterials were characterized by X-ray diffraction spectroscopy (XRD) and Scanning electron microscopy (SEM). XRD pattern confirms the presence of TiO₂/Mn(TiO₃) with small crystallite size. Photocatalytic activity of the synthesized materials was carried out by employing the Alizarin Red S dye as a model pollutant under UV-light irradiation.

Photocatalytic degradation experiment was carried out in the 200 ml capacity photo-chamber and degradation of Alizarin Red S dye was recorded using UV-vis spectrophotometer.

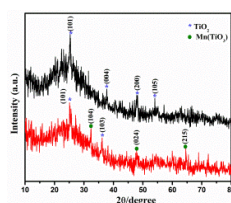


Figure. 1

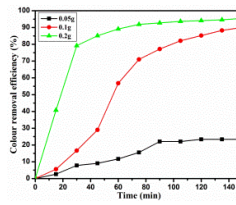


Figure.2

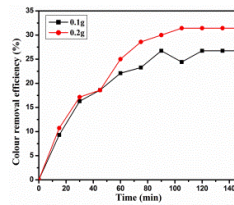


Figure.3

Fig. 1 shows the X-ray diffraction patterns of the synthesized samples and it confirms the formation of anatase TiO₂ and pyrophanite Mn(TiO₃) nanomaterials. The average crystallite sizes of TiO₂ and TiO₂/Mn(TiO₃) samples were calculated as 45.19 and 13.78 nm, respectively. Fig. 2, 3 shows the photocatalytic activity of synthesized nanomaterials. The photocatalytic activity of synthesized nanomaterials was studied using decomposition of Alizarin Red S dye (10 mg/l). The higher colour removal efficiency (95.47%) was achieved using TiO₂ photocatalyst within 150 min.

References

1. G.V. Khade, M.B. Suwarnkar, N.L. Gavade, K.M. Garadkar, Green synthesis of TiO₂ and its photocatalytic activity, *J. Mater. Sci. Mater. Electron.* 26, (2015) 3309–3315.
2. L. Zhang, D. He, P. Jiang, MnO₂-doped anatase TiO₂ – An excellent photocatalyst for degradation of organic contaminants in aqueous solution, *Catal. Commun.* 10, (2009) 1414–1416.

4.38 Activated carbon derived from cannabis sativa, interconnected with nanostructured metal oxide for energy storage applications

S. Imran Hussain¹, S. Kalaiselvam^{1,2}

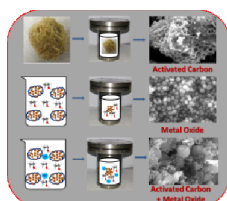
¹*Department of Applied science and Technology, AC Tech Campus, Anna University, Chennai, India.*

²*Department of Mechanical Engineering, College of Engineering Guindy, Anna University, Chennai.*

Climatic change and decrease in the availability of fossil fuels necessitate the society to move towards

the new sustainable and renewable source of energy. Therefore there is an increase in production of energy from renewable sources like sun and wind, which could be used to drive electric vehicles. But the derivation of energy from sun during night and the wind which does not blow on demand makes the society to move towards development of electrical energy storage devices like batteries and supercapacitors. However there is increase in demand to increase the performance of these energy storage devices to meet the requirements of high performance devices ranging from portable electronic devices to high electric devices, for advancing the electrochemical understanding at the nanoscale by developing new materials. Recently electrochemical capacitor (EC) has attracted attention, because that can be charged and discharged in few seconds, also it has much higher power delivery which can be achieved for shorter times. EC have complementing batteries which help to provide uninterrupted power supplies and load leveling.

Activated carbon was prepared from the agricultural bio wastes like hempbast fiber by hydrothermal treatment it shows in the figure. The resultant carbonaceous product that is biochar were activated by potassium hydroxide. The figure illustrated the synthesis and characterization (SEM) of as prepared materials. The bio fuels are also taken from the biochar but there are lot of researchers are concentrated on to produce the bio fuels also lot of other applications too. The carbon is interconnected with metal oxides and it has a better physical and chemical property. The controlled morphology nanostructures will be prepared by suitable method using activated carbon @ metal oxide semiconductor (Fig.1) with high porosity, large surface to volume ratio, and high charge discharge capacity. Because of this property will get a better conductivity and also it has more advantages such as easy production, low cost and compact size. The increase in the active surface area can provide more electrochemical active sites and surface conductivity modulation. The smaller in sized will improve the electronic diffusion length. Porous structure can improve the cycle performance by diffusion of electrolyte. The structural studies carried out by x-ray diffraction (XRD), optical studies by ultraviolet visible spectroscopy (UV-Vis Spec), and electron charge density distribution by maximum entropy method (MEM)/Rietveld. Morphologies studies was examined by field emission scanning electron microscopy (FE-SEM). Specific surface area measured by Brunauer-Emmett-Teller (BET) nitrogen adsorption-desorption isotherm. Electrical conductivity measurement for analyzing electron charge transport behavior and electrochemical performance will calculate by using cyclic voltammetry (CV), and electrochemical impedance spectroscopy (EIS).



Keywords: Bio char, Nanoparticles, Energy Storage, Metal Oxide, Carbon

4.39 Electrochemical polymerization of poly (aniline) - Multiwalled carbon nanotube composite counter electrode for dye sensitized solar cell applications

S. Nagaraj, K. Sakthi Velu and T. Stalin*

Advanced Photo-electrochemistry lab, Department of Industrial Chemistry, Alagappa University, Karaikudi-03. Tamilnadu.

Email ID: tstalinphd@rediffmail.com

Abstract

Poly (aniline) - Multiwall Carbon nanotube composite counter electrode was successfully prepared by simple electro-oxidative polymerization method. PANI-MWCNT composite counter electrode was further characterized by the X-ray diffraction pattern, FT-IR analysis, UV-Visible spectroscopy, Electrochemical impedance spectroscopy (EIS), Cyclic Voltammetry (CV), FE- SEM images and I-V characterization. The XRD pattern analysis was confirmed the Poly (aniline) - Multiwall carbon nanotube counter electrode in amorphous structure. The FT-IR spectroscopy result was observed in the region of 3406 cm^{-1} assign to NH_2 group of Poly(aniline)- Multiwall Carbon nanotube composite and also the peak appears in the region of $1600, 2942, 1700, 600\text{ cm}^{-1}$ was corresponding to C-H bending, C-H, C=O, OH groups, respectively. The UV-visible spectrum was shows the absorption peak at 300 cm^{-1} that is related to $\pi - \pi^*$ transition mode of PANI-MWCNT. The highest ionic conductivity of Poly (aniline)-Multiwall Carbon nanotube counter electrode achieved in the range of $4.014 \times 10^{-3}\text{ Scm}^{-1}$ by electrochemical impedance spectroscopy. The electrocatalytic activity of as prepared PANI- MWCNT counter electrode characterized the cyclic voltammetry the highest electrocatalytic of shows the -0.2 to 1.4 mV . The Dye sensitized Solar cell was assembled with the

electropolymerized Poly (aniline)- Multiwall Carbon nanotube counter electrode give the 7.04% of energy conversion efficiency.

Keywords:

Electropolymerization, Poly(aniline)-Multiwall carbon nanotube, XRD pattern, FE-SEM images, Electrochemical impedance spectroscopy, Counter electrode, Dye sensitized Solar cell.

Reference:

1. Haiphong Niu, Shengxian Qin, and Shiding Miao. *Electrochimica Acta*: 121 (2014) 285– 293.
2. Huihui Zhang, Benlin He, Qunwei Tang, and Liangmin Yu. *Bifacial Journal of Power Sources*: 275 (2015) 489-497.

4.40 In-situ electrochemical synthesis of poly-(aniline) - graphene oxide composite counter electrode for high efficiency quasi-solid-state dye sensitized solar cell applications

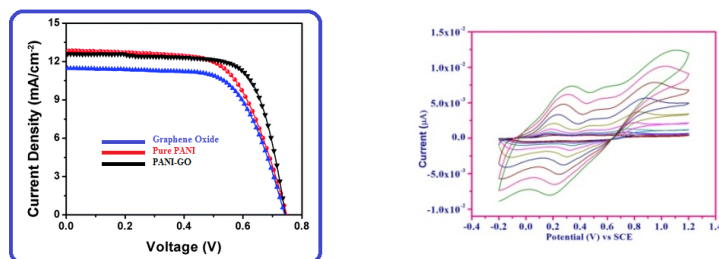
A. Saranyadevi, K. Sakthi Velu and T. Stalin*

Department of Industrial Chemistry, Alagappa University, Karaikudi-03, Tamilnadu - India.

Email: drstalin76@gmail.com

Abstract

The fabrication of Quasi-solid-state dye sensitized solar cells was assembled with the in-situ electrochemical synthesis of pristine polyaniline, graphene oxide, polyaniline-graphene oxide as counter electrode. The graphene oxide was prepared by the Hammers method. The polyaniline (PANI) -graphene oxide (GO) was further characterized the XRD, ATR-FTIR, Electrochemical Impedance spectroscopy, cyclic voltammetry (CV) and I-V characterization.



X-ray diffraction pattern of PANI-GO revealed on sharp peak at $2\theta = 20^\circ$ corresponding to graphitic structure of GO in poly (aniline)-graphene oxide counter electrode. The functional group presence in the composite of poly (aniline)-graphene oxide) counter electrode confirmed the ATR-FTIR spectroscopy. The peaks at 3373, 1718, 1591 and 1015cm⁻¹ for GO attributed to the OH, C=O, C-N, C-O in PANI-GO. The ionic conductivity of PANI-GO in the range of 4.213×10^{-4} was achieved by the electrochemical impedance spectroscopy. The electrocatalytic activity of polyaniline-graphene oxide was observed in cyclic voltammogram of two anodic peaks and two cathodic peaks, which is corresponding to I⁻/I³⁻ redox couple regeneration process of Quasi-solid-state dye sensitized solar cell. Finally, the polyaniline – graphene oxide composite counter electrode was used as counter gave 7.02% of sunlight-into-electrical energy conversion efficiency, which is almost equal to that platinum based quasi-solid-state dye sensitized solar cell fabrication efficiency.

Keywords: Quasi-solid-state dye sensitized solar cell, Electrochemical Polymerization, counter electrode, Poly (aniline), Graphene Oxide and Cell Efficiency.

References:

1. Benlin He, Qunwei Tang, and Shuangshuang Yuan. *ACS Appl. Mater. Interfaces*; 2014, 6, 8230–8236.
2. Yu-Chen Hsu & Guan-Liang Chen & Rong-Ho Lee. *J Polym Res*; (2014) 21:440.

4.41 Enhanced Solubility, Dissolution rate and antimicrobial activity studies of etoposide drug with β -CD by inclusion complexation

Arumugam Shanmuga Priya^a, Jeyachandran Sivakamavalli^b, Baskaralingam Vaseeharan^b, Thambusamy Stalin^{a*}

^a *Department of Industrial Chemistry, School of Chemical Sciences, Alagappa University, Karaikudi 630 003, Tamil Nadu.*

^b *Crustacean Molecular Biology and Genomics Lab, Department of Animal Health and Management, Alagappa University, Karaikudi 630 003, Tamil Nadu, India. E-mail: priyamahachem85@gmail.com*

Abstract

The slightly water soluble anticancer drug Etoposide(EPS) and its inclusion complex with β -cyclodextrin(β -CD) was investigated. Phase solubility studies demonstrated the ability of β -CD to complex with

EPS and increase drug solubility. According to this drug EPS with β -cyclodextrin was classified as A_L type. Stability constant with 1:1 molar ratio was calculated from the phase solubility diagram. The solid inclusion complex of EPS with β -CD were prepared by physical mixture, kneading method and solvent evaporation method. The solid state formation were characterized by FT-IR, ^1H NMR, DSC, XRD and SEM analysis. The dissolution profile of inclusion complex was determined and compared with drug alone. The Dissolution rate of EPS was appreciably increased by complexation as compared with pure drug. The *in vitro* antimicrobial and antibiofilm activity of EPS sensible microorganisms was significantly increased by on inclusion complexation process. This trend of inclusion complexation can be used to expand the applications of EPS drug in pharmaceutical industries.

Key words: Etoposide, β -cyclodextrin, Inclusion complex, Dissolution rate, Antimicrobial activity.

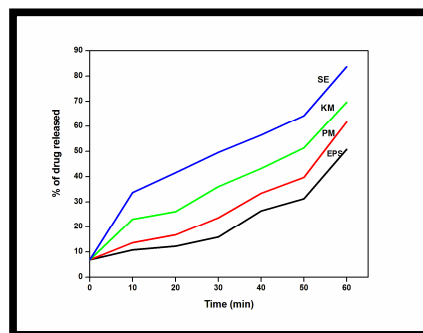


Figure 1. Dissolution profile of (a) drug EPS, (b) physical mixture, (c) inclusion complex by kneading method and (d) inclusion complex by solvent evaporation method.

References

- [1] K. Uekama, F. Hirayama, T. Irie, Chem. Rev. 98 (1998) 2045–2076
- [2] X. Wen, F. Tan, Z. Jing, Z. Liu, J. Pharm. Biomed. Anal. 34 (2004) 517–523.
- [3] J. Szejtli, Chem. Rev. 98 (1998) 1743–1753.
- [4] T. Higuchi, K. Connors, Adv. Anal. Chem. Instrum. 4 (1965) 117–212.
- [5] P. Mura, M.T. Faucci, G.P. Bettinetti, Eur. J. Pharm. Sci. 13 (2001) 187–194.

4.42 Electrochemical Degradation of Reactive Blue 19 on Lead/Lead Dioxide Electrodes

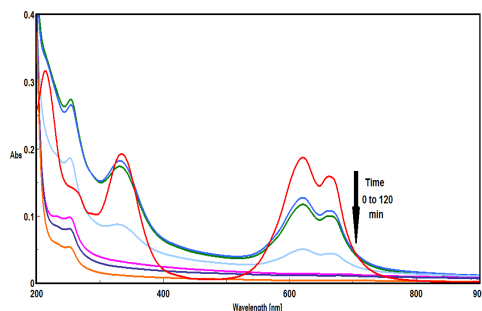
S. Anita, J. Anitha Pushparani, P. Karpagavinayagam and C.Vedhi*

Department of Chemistry, V.O.Chidambaram College, Tuticorin – 628008, Tamilnadu, India

* correspondence: +91 4612310175, +91 9092368104, e-mail: cvedhi@rediffmail.com (or) cvedhi23@gmail.com

Abstract

Effluents of a large variety of industries usually contain important quantities of synthetic organic dyes. The discharge of these coloured compounds in the environment causes considerable non-aesthetic pollution and serious health-risk factors. Since conventional wastewater treatment plants cannot degrade the majority of these pollutants, powerful methods for the decontamination of dyes wastewaters have received increasing attention over the past decade. The electrochemical treatment of wastewater is considered as one of the advanced oxidation processes, potentially a powerful method of pollution control, offering high removal efficiencies. In the present study, electrochemical degradation experiments were conducted to degrade a synthetic textile dye



effluent namely reactive blue 19 (RB-19). The influence of electrodes like stainless steel and lead on decolorization efficiency of synthetic reactive blue 19 is explained. The electrolytic process was monitored by the UV–visible spectrometry. The influence of pH, current density, time of electrolysis, temperature, addition of supporting electrolyte (KCl) and the initial dye concentrations were critically examined. The results of electrochemical degradation of dye showed that it could be used as efficient and environmental friendly technique for the complete degradation of recalcitrant organic pollutants into lower molecular compounds and increases the chances for the

reuse of wastewater. The UV-Vis spectrum of dye solution (25 ppm) shows two peaks in visible region and two peaks in UV region. As time increases, the intensity of peak decreases indicating the degradation of reactive blue 19 dye. Electrochemical degradation reaction was carried out in neutral condition (pH = 7) and the flow of current is maintained from 0.04 A to 0.1 A. The formed final sludge was characterised using UV-Vis, FT-IR, AFM techniques.

4.43 Synthesis of Cu Doped TiO₂ Photocatalyst

C. Rani*, K.Santhi and R.Latha

Department of Chemistry, Alagappa Govt. Arts College, Karaikudi, Tamil Nadu-630 003, India

E-mail: viswanathanrani@gmail.com

Exploring the properties of TiO₂ for improving its efficiency is still an emerging area of research. Modifications of intrinsic properties of TiO₂ have been done by doping with other semiconductor oxides such as CeO₂, SnO₂, SiO₂, WO₃, ZnO and CuO etc. Specially copper(Cu) was found to be one of the most considerable element among those oxides because of its notable effects on the activity of titanium dioxide.

Cu doped TiO₂nanomaterial wassynthesized and subsequently characterization was carried out using X-ray diffraction spectroscopy (XRD), Scanning electron microscopy (SEM) and UV-Visible spectroscopy. Photocatalytic degradation of Alizarin Red S dye was studied using synthesized Cu doped TiO₂ material. In this work, we synthesized Cu doped TiO₂nanomaterials and surface characterization was carried out. The photocatalytic degradation of Alizarin Red S dye was also studied and compared with undopedTiO₂.

XRDpatternsconfirms the formation of anatase TiO₂(Fig. 1) and all phases of the sample exhibited anatase phase diffraction peaks and no characteristic peak of Cu metal or oxides, which imply that the copper ions incorporated into the lattice of the anatase TiO₂. The photocatalytic degradation of Alizarin Red S dye (10 mg/l) was studied using synthesized TiO₂ and Cu doped TiO₂ nanomaterials (0.1 g). The higher colour removal efficiency (93%) was achieved using Cu doped TiO₂photocatalyst within 150 min. Hence, the existence of Cu species at TiO₂ matrix was found to play an important role on the activity, since copper could influence the particle size as well as the number of intermediate active species on the surface of TiO₂. And Copper ions acts as electron trappers facilitating the separation of electrons and holes on the surface of TiO₂ nanoparticles, which allows more efficiency for the photodegradation of alizarin red S.

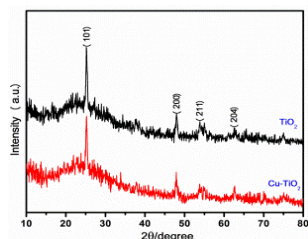


Figure. 1

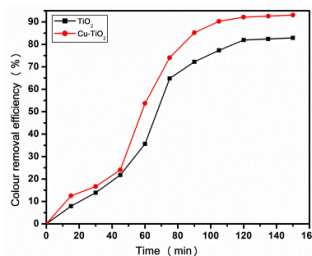


Figure.2

References

1. M. Hussain, R. Ceccarelli, D.L. Marchisio, D. Fino, N. Russo, F. Geobaldo, Chem. Eng. J. 157 (2010) 45–51.
2. B.Xin, P.Wang, D.Ding, J.Liu and H.Fu .Appl.Surf. Sci. (2008), 2569-2574.

4.44 Hydrothermal preparation of reduced Graphene oxide-ZnO composite for photocatalytic degradation of DY-86 dye

R.Rajeswari, H.Gurumallesh Prabu*

Department of Industrial Chemistry, School of Chemical Sciences, Alagappa University, Karaikudi - 630003, Tamil Nadu.

*Corresponding author, Tel: +919443882946; Fax: +914565225202

Email: hgrabhu2010@gmail.com, hgrabhu@alagappauniversity.ac.in

Abstract

Graphene is a flat monolayer consisting of carbon atoms with perfect sp² hybridized two dimensional structure. It has high electron mobility, conductivity and high specific surface area which makes it useful for functional applications. Graphene is a good substrate to produce graphene based composites. Zinc oxide is a semiconducting [1] multifunctional material [2] due to its high surface area and finds applications in photocatalytic and medicinal fields. In the present work, hydrothermal method is employed to prepare reduced

graphene oxide -Zinc oxide composite (RGO-ZnO). This method is a powerful tool for the synthesis of inorganic nanocrystals with high crystallinity at an elevated temperature with high pressure. The raw materials such as Zinc nitrate hexahydrate and graphite flakes were used to synthesize the nanocomposite. Hydrazine solution was added to reduce the graphene oxide. The morphology and properties of RGO-ZnO composite was characterized by XRD, Raman spectroscopy, FT-IR, SEM with EDAX, and UV-Vis Spectroscopy. The emission of photo electrons from ZnO was effectively accepted by the RGO. UV-Vis spectrum shows a characteristic peak at 229nm, corresponding to $\pi-\pi^*$ transition of the C=C bonds for the dispersion of graphene oxide (GO). After hydrothermal treatment, the peak to be appeared at 229 nm was shifted to 269 nm. This may be due to the reduction of GO. UV-Vis spectrum of RGO -ZnO composite exhibited an absorption peak at 386 nm. The XRD characterization of the pristine GO showed peak at 11.2° . This peak was vanished in all RGO-ZnO composite, revealing that the GO has been successfully reduced during the hydrothermal treatment. The diffraction peaks at 31.46° was indexed to hexagonal wurtzite ZnO. These observations indicated the formation of RGO-ZnO composite. The Raman spectroscopy displayed the crystal structures of carbonaceous materials. GO exhibited D line at 1356cm^{-1} and G line at 1810cm^{-1} [3]. After the reduction of GO, the D line (I_D) and G line (I_G) were shifted to 1498cm^{-1} and 1596cm^{-1} respectively. The intensity ratio (I_D/I_G) was observed as 0.94 for GO and 1.09 for RGO. The higher value of I_D/I_G and band shift indicated the formation of RGO-ZnO composite during hydrothermal reduction. FT-IR analysis showed various peaks for GO at 1076, 1232, 1402, and 1731cm^{-1} corresponds to C-O, C-OH, CO-H, C=C stretching peaks. The peak of Zinc oxide was observed at 500cm^{-1} . The photocatalytic degradation efficiency of synthesized RGO-ZnO composite was subjected against Direct Yellow-86 (DY-86); it showed better catalytic activity than with of pristine GO and ZnO.

Keywords : Reduced graphene oxide, Photodegradation, Hydrothermal Direct Yellow-86

References:

- [1] J. Gomez, O. Tigli, J. Mater. Sci. 48 (2) (2013) 612–624.
- [2] H. Li, Y. Ni, J. Hong, Scr. Mater. 60 (7) (2009) 524–527.
- [3] X. Wang, Q. Zhang, Q. Wan, G. Dai, C. Zhou, B. Zou, J. Phys. Chem. C 115 (6) (2011) 2769–2775.

4.45 Studies on the Removal of Colour from Textile Effluent Salt

Vishnuprasad, M A Vishnuganth

Department of Chemical Engineering, National Institute of Technology Calicut, Kerala, India
vishnuchem12@gmail.com, vishnuprasad215@gmail.com.

Abstract

Textile industry is one of the largest producers of wastewater capable of creating serious environmental threats. Textile wastewater is usually treated with conventional methods which suffer from a few limitations related to cost, efficiency and sludge generation. In textile effluent treatment plants, in order to achieve the zero liquid discharge, the treated waste water is sent to evaporation unit. Recovery of the salts and water are the vital functions of the evaporator and these salts can be used again for the dyeing of the fabrics. But the recycled salts have grey or brown in color. Hence it cannot be used lucratively for the dyeing purpose due to its low binding capacity in the fabrics.

Methodology

The salt mixture having a colour of 121.177 Haz at 100000 ppm is maintained and treated by adsorption method. Because the concentration of treated wastewater enters the centrifuge in the common effluent treatment plant has almost equal concentration of our mixture. Fixed bed column studies were carried out using a glass column of 3.75 mm diameter with 300mm height. The three adsorbents are filled inside the column with a bed height of 10 cm each such in a way that the least effective at the top. The tank is equipped with a pipe and a flow meter to maintain the required flow rate.

Results and Discussions

The effect of feed flow rates on the colour removal using fixed bed column at flow rates of (5 to 12) mL min^{-1} at constant initial concentration of 100000mg L^{-1} is studied in this research. By analyzing the results, it was optimized that the flow rate of 8mL min^{-1} gives the better efficiency than others. Similarly, the effect of initial concentration of the salt solution on the breakthrough curve at the optimized flow rate of 8mL min^{-1} was studied and optimized in this research. The kinetic analysis of the packed column adsorption was done using Thomas – BDST Model and Yoon & Nelson Model. Thomas rate constant K_T depends on both the flow rate and initial concentration of the salt solution [1,2]. Yoon and Nelson model is based on the assumptions that the rate of decrease in the probability of adsorption is directly proportional to the probability of adsorbate breakthrough on the adsorbent [2].

Conclusion

In the continuous studies, the experiments were carried out using a packed bed column. The three adsorbents are filled inside the column in such a way that the least effective at the top. In these studies the

influence of parameters such as flow rate and initial colour of the salt solution on the breakthrough curves were studied. The experimental results show that, when the flow rate increases the breakthrough curve becomes steeper. This result was anticipated because of the residence time of the adsorbate in the column which is long enough for adsorption equilibrium to be reached at high flow rate. When the initial concentration gets increases, the availability of molecules to the adsorption sites become more and leads to the higher uptake of molecules. Therefore the breakthrough time is shorter than at lower concentrations. The maximum adsorption capacity increases with increase in flow rate and initial concentration. From the final observations, the continuous column gives 70% colour removal of salt and it gets gradually decreases after the breakthrough starts.

References

- [1] Ali Naghizedeh, Simin Nasser, Amir Hosain and Ramin Nabizedah, *Journal of Environmental Health Science & Engineering* (2013) 11-14.
 [2] Nwabbanne J.T and Igbokwe .P.K, *International Journal of Applied science and Technology* 2 (2012) 245-254.

4.46 Sun Light Assisted Photocatalytic Degradation of Dye

P.Karthika¹, P. Nithya¹, G. Srinivasan², K.Thangapandi¹ and S. Viswanathan^{1*}

¹Department of Industrial Chemistry, Alagappa University, Karaikudi-630 003, Tamil Nadu, India.

²Anna University (BIT Campus), Tiruchirappalli-620 024. E-mail: rsviswa@gmail.com

Photocatalytic processes have been used to demonstrate several aspects of organic pollutant removal and renewable energy production. Many photocatalysts have been found to be very useful in the wastewater treatment for the broad range of organic pollutants. Among many developed photocatalysts, TiO₂ based materials are still in the mainstream of the studies because of their availability, low cost, high and tunable photocatalytic activity. Wide bandgap of Anatase TiO₂'s only utilizes ultraviolet irradiation of the solar radiation. Thus, how to increase the absorption by utilizing the visible spectrum becomes an important issue. In this work, synthesis of Bi-doped TiO₂ nanotubes and sun light assisted dye degradation by Bi-doped TiO₂ nanotubes was described. TiO₂ nanotubes (TNT) were grown on titanium plate by electrochemical anodization. TiO₂ porous layers were grown by anodization in acidic electrolytes with the help of fluoride anions. Ti plate was anodized at 20 V in the electrolyte composition 1 M H₂SO₄ + 0.5 wt % NaF + 75% Glycerol for 20 min. The mechanism of TiO₂ nanotubes formation is related to oxidation and dissolution kinetics. The formation of TiO₂ nanotube in fluoride-ion based electrolytes is said to occur simultaneous process of following: a) Passivation of TiO₂ layer on the Ti surface, b) Formation of pits on the passivated TiO₂ layer at applied constant voltage, c) Growth of Pit with respect to anodization time to form a nano pore. d) Development of nanopores into nanotubes on the Ti surface at specified time and at constant voltage. As a result of this process, TiO₂ nanotubes were formed which appear as nano porous layer and used for implementation. TNTs were dipped in an aqueous solution of Bi (NO₃)₃ solution (1 mM) followed by annealing at 500 C for bismuth doping on TNTs surface. Surface morphology were characterized through TNTs by AFM, XRD and SEM techniques. SEM analysis shows that average diameter of TNT is approximately 80nm. Methyl red solutions are exposed to sunlight in presence of Ti plate, TNTs and Bi - doped TNTs. Corresponding time intervals as contact time was 0-25 min. Since the photo degradation efficiency of methyl red is affected by the pH of the solution, the optimization of pH was carried out. At acidic pH the surface charge of photo catalytic particles are well suited for degrading reactions. Under acidic condition the surface of titania can be protonated hence it shows higher efficiency. Using bismuth metal as dopants improves the performance of TiO₂ Nanotube. Bi-doped TiO₂ nanotubes photocatalysts that utilize the visible spectrum will have great potential application in wastewater treatment, and they can be separated easily from aqueous solutions after being used.

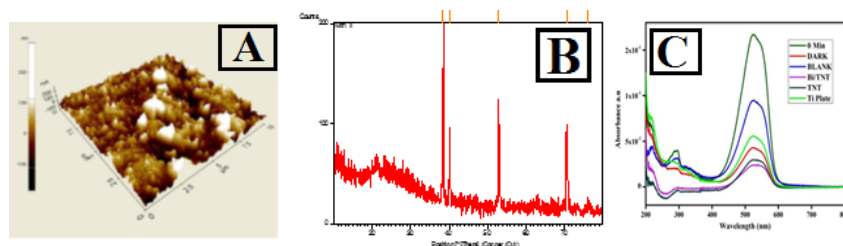


Figure. 1. (A) AFM Scan in 3D image and (B) XRD spectrum TiO₂ Nanotubes, (C) UV-Visible spectrum of MR dye solutions treated with different photo catalytic materials. Dye contact time: 25 Min.

Keywords: TiO₂ nanotube, Bi-TiO₂ nanotubes, Anodization, photo catalyst, Methyl Red

4.47 Design to conductive sulfonated polypyrrole incorporated with hybrid SPVdF- ZnO composite for high energy conversion counter electrode in DSSC

A. SarathkumarMuthuraj^a, M. Sundrarajan^{a*}, M. Balaji^a, S. Jegatheeswaran^a, A. Sangili^a, S. Selvam^b and G. Selvanathan^c

^aAdvanced Green Chemistry Lab, Department of Industrial Chemistry, School of Chemical Sciences, Alagappa University, Karaikudi-600 003, Tamil Nadu, India

^bLaser and sensor Application Laboratory, Pusan National University, Busan 609735, South Korea.

^cDepartment of Chemistry, AVC College, Mayiladuthurai- 609 305, Tamil Nadu, India.

*Corresponding author: drmsgreenchemistrylab@gmail.com and sarath6994@gmail.com

Introduction

Low cost and long life photovoltaic solar cell is one of the most viable renewable energy technologies needed for the future. The development of commercial solid–solid junction type solar cells (e.g., p–n junction based on semiconductor like Si, GaAs, CdS, CdTe etc.) is still limited by cost as well as energy conversion. A new technology of semiconductor electrolyte junction viz. Photo-electrochemical solar cells (PESC) has recently evolved. Dye-sensitization of photo-electrodes has revolutionized the concept of PESC [1]. Here we synthesize conductive sulfonated polypyrrole/SPVdF/ZnO composite and it has been demonstrate as a counter electrode (CE) in dye-sensitized solar cell (DSSC). Polypyrrole has sulfonated, thermally crosslinked with SPVdF, and incorporated with ZnO nanoparticles. In DSSC the composite CE is combined with 1- butyl-3-methyl imidazolium hexafluoro phosphate [BMIM-PF₆] ionic liquidelectrolyte and it show a high light to current conversion efficiency due to the high conductive properties of synthesized electrode [SPPy/SPVdF/ZnO] and electrolyte [BMIM-PF₆].

Synthesis of sulfonated polypyrrole (SPPy)

Polypyrrole was prepared with the help of previous literature [2]. Synthesized PPy powder (0.3 g) was heated in 15mL of concentrated sulfuric acid (H₂SO₄) at 80 °C for 4 hours. After cooling down solution to room temperature, 100 ml of ethanol was added. The black solid was collected by filtration, and washed repeatedly using ethanol until all the unreacted sulfate ions were removed from the solution. The resulting black powder precipitate was filtered, washed and dried in oven at 60°C [3]. Mechanism for the formation of –SO₃H group in PPy is given below.



Synthesis of sulfonated Polyvinylidene fluoride (SPVdF)

PVdF granules were first vacuum-dried for a period of 12 h at a temperature of 60 °C. The sulfonation reaction was carried out in a round-bottom flask containing chlorosulfonic acid (CSA) and PVdF under continuous stirring for 2 h at 50 °C. The obtained black pellets were then collected, washed sequentially with methanol and water and finally dried at 60 °C [4]. Mechanism for The formation of the –SO₃H group in PVdF is given below.

Synthesis and characterization of SPPy/SPVdF/ZnO composite

The SPVdF of 5 g was dissolved in 100 mL of N-Methyl-2-pyrrolidone (NMP) and then the solution was kept on magnetic stirrer at 60°C for 6 hours. The ZnO nanoparticles according to weight ratio (i.e., 1–3 % (w/w)) were dissolved in 20 ml of (NMP) and mixed drop by drop in solution of SPVdF for preparation of SPVdF–ZnO nanocomposite thin film samples. Further, SPVdF-ZnO solution was kept on magnetic stirrer for 12 h to become homogeneous then 4-6 % w/w of SPPy was added and again stirred for 0.5 hours. Now the final solution was kept in sonicator for 10 minutes for better dispersion of ZnO nanoparticles. The prepared solution was poured onto glass plate. The solvent was then allowed to evaporate inside an oven at room at 60°C for 24 hours to yield the SPPy/SPVdF/ZnO composite. The dried composite were further try to a counter electrode in DSSC.

The synthesized composite was characterized by UV- visible, Infrared and Raman spectroscopy, the crystallinity of ZnO nanoparticle in the composite was characterized by XRD techniques. The morphology and elemental analysis of the composite was characterized by SEM with EDX. Electrochemical analysis is carried out by cyclic voltammetry, impedance spectroscopy. Incident photon to current efficiency (IPCE) of prepared SPPy/SPVdF/ZnO composite is measured by I-V characteristic curve and fabricated solar cell efficiency is measured by photo electronic and optoelectronic devices.

Reference

- [1] Suresh Chandra springer, 82 (2012) 5–19.
- [2] Xuotong Zhang, Jin Zhang, Wenhui Song and Zhongfan Liu J. Phys. Chem. B, 110 (2006) 1158-1165.
- [3] Xiaoning Tian, Fabin Sub and X. S. Zhao, Green Chem 10 (2008) 951–956.
- [4] Kingshuk Dutta, Suparna Das and Patit P Kundu, Polymer Journal (2015) 1–9.

4.48 Investigation of Congo red decolourization using clay/polymer composite beads

S. Vahidhabanu, D. Karuppasamy and B. Ramesh Babu

CSIR- Central Electrochemical Research Institute, Karaikudi-630 006, Tamil Nadu.

Email id: vahishappur@gmail.com, karuppasamy_d@yahoo.com, brbabu2011@gmail.com

Sodium alginate/sepiolite nanocomposites hydrogel beads were prepared by the insitu generation of SA nanoparticles during the sol gel transition of the SA/sepiolite suspension. The nanocomposites beads were characterized by FTIR, SEM, and FESEM etc. Removal of Congo red from aqueous solution using this bead was studied in Batch adsorption experiments. Various parameters such as contact time, Dosage, pH, bead size on the CR adsorption were investigated. Pseudo second order kinetics and Langmuir adsorption isotherm fitted well. Desorption studies showed that removal efficiency of CR remained at 97% after ten successive cycles and it shows the high reusability so SA/sepiolite beads were effective and economic adsorbents for removal of organic dye from wastewater.

Keywords: Adsorption, composite beads, Langmuir isotherm, organic dye, sodium alginate, pseudo second order kinetics.

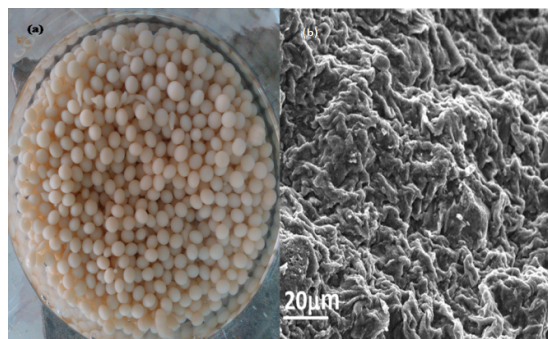


Fig (a) Digital Photograph of synthesized Composite beads (b) SEM images of synthesized composite beads

Alginate and Sepiolite nano composite beads were prepared and their dye adsorption behavior was investigated in batch adsorption studies. The surface morphology of composite beads revealed undulations and folds on the bead surface, effectively increasing the surface area available for dye adsorption. Adsorption isotherm studies exhibits that the Langmuir isotherm described the adsorption process better than the Freundlich isotherm. These beads were also to be reusable and showed more than 97 % dye removal efficiency even after 10 successive adsorption-desorption cycles. All these results indicate that composite beads can be used as an effective adsorbent for the removal of dyes and has the potential to be used in industrial and environmental applications.

4.49 Structure And Vibrational Analysis of Iloperidone

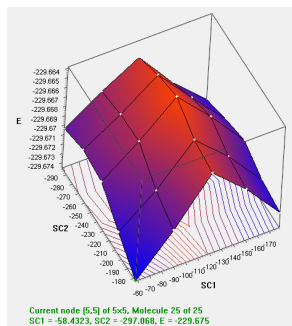
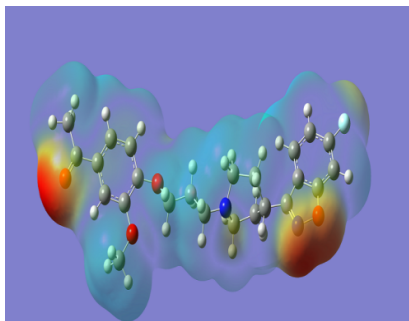
Selvam Karthick^a, Somasundaram Meenakshisundaram^b and Gopalakrishnan Gopu^{*}

^{a, *} Department of Industrial Chemistry, School of Chemical Sciences, Alagappa University, Karaikudi - 630 003.

E-Mail: skarthick.che@gmail.com, nggopi79@gmail.com

Abstract

Theoretical studies of structure, function and reactivity of molecules have involved and occupied in the many research areas such as pharmaceutical research, drug delivery system, chemical synthesis and biological studies for the last fifty years. Theoretical/computational studies in the last few decades have been contributing significantly in chemistry by explanation of experimental results, better understanding of underlying principles and prediction of the unknown experimental outcome. Density functional theory (DFT) methods give mid-level accuracy at mid-level cost and size-dependency and have been the most popular theoretical methods for routine calculations. Hartree-Fock method (HF) and Semi-empirical methods are low cost alternatives with lower reliability. Iloperidone (ILO) is an atypical antipsychotic drug for the treatment of schizophrenia symptoms, that was taken to analysis. Geometry optimization, Electronic structure prediction, Vibrational frequency analysis and all calculations were performed with Gaussian09 package by HF method. All the parameters were allowed to converged to an optimized geometry. In the calculations, with the dihedral angles were varied in steps of 10 °, 20° ... 360° to get the global minima of stable structure. Electron density cubes were generated to find the potential surface. MO editor tool was used to form the molecular orbital diagram for the finalized structure.



Molecular Geometry, Vibrational Frequency analysis, Electrostatic Potentials, Potential Energy Surfaces (PES) and Molecular Orbital Energy of ILO have computed using HF/B3LYP method. Geometry of the ILO have fixed by Optimization and have confirmed by PES and vibrational frequency (absence of imaginary frequencies). So finally, confirmed structure may consider as high stability geometry. Polarity nature also have displayed. Electrostatic Potential layer have visually expressed the activity of ILO depending upon the higher density of electron present in the hetero atoms and Molecular Orbital. This computational study of the ILO molecule may have advantage in realizing the structure, activity and stability of any molecule for in-depth understanding in chemistry world.

References:

- [1] James B. Foresman, Æleen Frisch, Exploring Chemistry with Electronic Structure Methods – Third Edition., *Gaussian Inc.* Wallingford, CT USA (2015).
- [2] H. Bernhard Schlegel, Exploring Potential Energy Surfaces for Chemical Reactions: An Overview of Some Practical Methods, *J Comput Chem*, 24 (2003) 1514–1527.
- [3] H. Feki, A. Ben Ahmed, N. Fourati, Y. Abid, C. Minot, *Journal of Molecular Structure: THEOCHEM*, 895 (2009) 21–25.

4.50 Virtual Screening of High Affinity Guests For Cyclophane Amides

Somasundaram Meenakshisundaram^a, Selvam Karthick^b and Gopalakrishnan Gopu^{*}

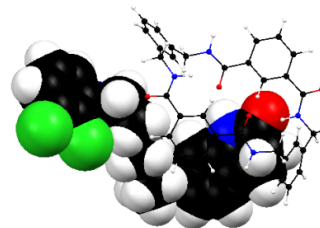
^aResearch and Development Centre, Orchid Chemicals and Pharmaceuticals Ltd., Sozhangannallur, Chennai – 600 119, India

^bDepartment of Industrial Chemistry Alagappa University, Karaikudi-630 003, India.

E-mail: nggopi@gmail.com, mnsk.sundaram2007@gmail.com

Abstract

Supramolecular architecture containing bridged aromatic compounds known as cyclophanes¹ are one of the important central classes of synthetic receptors in molecular recognition. Nowadays, the term “cyclophane” has been widened to include macrocyclic compounds incorporating aromatic ring systems and saturated or unsaturated bridges as alternating components of the ring structure.² Artificial container molecules, such as metal-based coordination cages and organic capsules, provide extensive opportunities for developing new types of functional behavior based on binding of guest molecules in the central cavity³. Cages have potential as drug delivery agents, with recent examples of binding,⁴⁻⁶ transport,⁵ and pH controlled uptake and release of drug molecules.⁵ The protein/Ligand docking software's, which was originally developed for drug discovery, has been used in a virtual screen to identify small molecules that bind with extremely high affinities in the cavity formed by the cyclophane host. This approach provides a powerful predictive tool for virtual screening of large compounds libraries to identify new guests for cyclophanes, thereby greatly simplifying and accelerating the process of identifying guests by removing the reliance on experimental trial-and-error.



References

- [1] Diederich, F. Stoddart, J. F.; Ed.; *Cyclophane in Monographs in Supramolecular Chemistry*; The Royal Society of Chemistry: Cambridge (1994).
- [2] McNaught, A.D.; Wilkinson, A.; *IUPAC Compendium of chemical terminology*, 2nd Ed.; Blackwell, Oxford (1997).
- [3] (a) M. D. Ward and P. R. Raithby, *Chem. Soc. Rev.*, 42 (2013) 1619; (b) M. Yoshizawa, J. K. Klosterman and M. Fujita, *Angew. Chem., Int. Ed.*, 48 (2009) 3418; (c) T. R. Cook, Y.-R. Zheng and P. J. Stang, *Chem. Rev.*, 113 (2013) 734; (d) M. D. Pluth, R. G. Bergman and K. N. Raymond, *Acc. Chem. Res.*, 42 (2009) 1650;

- (e) M. M. J. Smulders, I. A. Riddell, C. Browne and J. R. Nitschke, *Chem. Soc. Rev.*, 42 (2013) 1728; (f) D. Ajami and J. Rebek, *Acc. Chem. Res.*, 46 (2013) 990.
- [4] J. E. M. Lewis, E. L. Gavey, S. A. Cameron and J. D. Crowley, *Chem. Sci.*, 3 (2012) 778.
- [5] (a) J. W. Yi, N. P. E. Barry, M. A. Furrer, O. Zava, P. J. Dyson, B. Therrien and B. H. Kim, *Bio conjugate Chem.*, 23 (2012) 461; (b) B. Therrien, G. Suss-Fink, P. Govindaswamy, A. K. Renfrew and P. J. Dyson, *Angew. Chem., Int. Ed.*, 47 (2008) 3773; (c) O. Zava, J. Mattsson, B. Therrien and P. J. Dyson, *Chem.–Eur. J.*, 16 (2010) 1428.
- [6] W. Cullen, S. Turega, C. A. Hunter and M. D. Ward, *Chem. Sci.*, 6 (2015) 625.

4.51 Photophysical behavior of 6-Perylene imide (6PI) in different solvents and at various pH

Gnanamalar K^{*}, Shanmugapriya RM^{*} and Radha N^{**}

^{**} Asst. Professor, PG and Research Department of Chemistry, Alagappa Govt.Arts College, Karaikudi - 3, India.

^{*} Research scholar, PG and Research Department of Chemistry, Alagappa Govt.Arts College, Karaikudi - 3, India.

Abstract

The single molecule spectra of 5PI and 6PI reveal three different types of emitters, two of which are not observed at the ensemble level. The nature of these two emitter types is not fully uncovered, but evidence is presented that one emitter type is most probably a result of photo-oxidation. Following a suggestion in the literature, the last emitter type may be attributed to twisted conformations in which the amino group is perpendicular to the perylene core. Computational estimation of such conformations, however, casts doubt on this explanation.

- The shape of the emission spectra that are observed in dropcast or spincoated films with a high dye concentration resembles that of the emission spectra in solution.
- The rigidity of the embedding polymer matrix limits the solvatochromic sensitivity, unfortunately, to the extent that the spectra in chemically different polymers are only slightly different. Finally, preliminary results of single molecule excited state deprotonation and reprotonation experiments are presented.

Key words: Fluorophore, Photophysical behavior, single molecule spectra, solvatochromism, Protonations, solvatochromic sensitivity, single molecule excited state.

4.52 Comparative Study on The Removal Congo Red Using Conducting Polymers

A. Vijayakumar, A. Sakthivel, A.Sarathi,N.Raman and K.Arumsunai Kumar

DST – FIST Sponsored Department of Chemistry, VHN Senthikumara Nadar College (Autonomous), Virudhunagar.

E-mail: vijayakumar.a@vhnsnc.edu.in

Polyaniline(PANI) and poly-*o*-toluidine(POT) were synthesised by chemical oxidation of aniline and *o*-toluidine in acidic medium. FTIR spectra were recorded for free and dye loaded polymers. The significant shift in the wave number 3452 cm^{-1} (for PANI shifted to 3447 cm^{-1}) confirmed the interaction between the dye and amino group of the polymer. For POT a similar type of shift was observed (shift in the wave number from 3365 cm^{-1} to 3346 cm^{-1}). However, a minor shift in wave number was observed for the peak at 1595 cm^{-1} is shifted to 1591 cm^{-1} which correspond to the N-H bending vibrations⁵⁵. The results obtained from the FTIR spectra indicated that the adsorption of congo red on the surface of the polymer occurred by the attraction between the negatively charged sulphonated group of dye molecule and positively charged backbone of the contacting polymers.

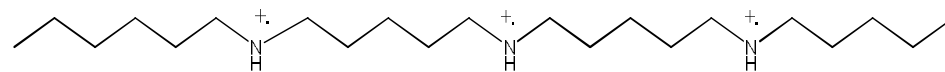
The variation of percentage removal of dye with respect to concentration of dye was more significant when PANI was used as adsorbent. It was observed that the percentage removal of dye decreases with increase in the concentration of dye solution. This is because at lower concentration the ratio of dye molecules to the available surface area is low, subsequently, the adsorption is high. However, at high concentration the available sites of adsorption become fewer and hence the percentage removal of dye is less. In the present study computed values of $1/n$ were found to be fraction, indicating that the adsorption process was favourable for the adsorbents PANI and POT materials. But the low value of 'r' (0.949 and - 0.967) indicates that the adsorption data were not best characterised by Freundlich adsorption isotherm. Hence, the adsorption data were subjected to Langmuir adsorption isotherm. The plot of C_e/q_e Vs C_e was linear. The linearity in the plot shows the formation of monolayer coverage of dyes on the adsorbent surface. The fractional value of R_L indicates that the adsorption obey Langmuir isotherm.

The 'a' value obtained for PANI was high compared to POT. The low monolayer adsorption capacity of POT is due to the presence of methyl group in its structure. The adsorption of Congo red on the surface of the conducting polymers takes place by the attraction between the positively charged amino group and negatively

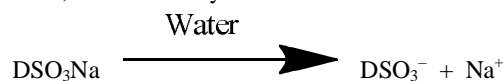
charged sulphonated group from the dye molecule. The presence of methyl group next to amino group neutralise the positive charge on the amino group thereby decrease the attraction between the dye molecule and the surface of the adsorbent. It was observed that the amount of dye adsorbed increased with an increase in adsorbent dosage.

The variation of percentage removal of Congo red with respect to pH can be explained by considering the surface charge of the adsorbent⁵ Under acidic condition, the nitrogen atom present in the constituent polymer is

protonated according to the following reaction:

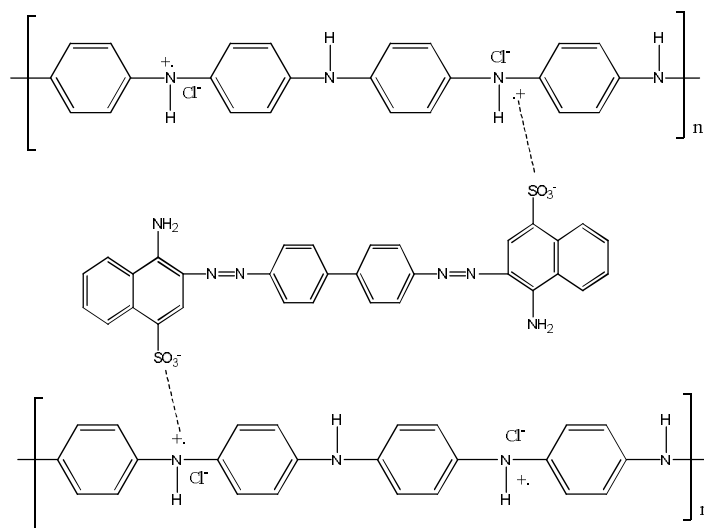


Simultaneously in aqueous solution, the reactive dye molecule is dissociated and converted into dye anions.



The reactive dye anions are migrated from solution to the surface of the polymer matrix. As a result, the adsorption occurs through the electrostatic interaction between the two counter ions.

However, as the pH increases (4-8) deprotonation of nitrogen atom occurs, leading to the depletion of positive charge in the surface of the polymer skeleton. Therefore, the interaction of PANI and POT with the dye molecule is hindered and consequently results in the lower uptake. Congo red contains two sulphonated groups (-SO₃Na). In acidic aqueous solutions, the functional group of CR (-SO₃Na) gets ionized, and the dye exists in anionic form. When PANI emeraldine salt is added to water the -SO₃⁻ group on the dye could lead to chemical interactions with the positively charged backbone of PANI emeraldine salt, and Na⁺ ions interact with the chloride ions that are invariably present in PANI. This will lead to the adsorption of various sulphonated dyes on the surface of PANI. A similar kind of mechanism is possible for the removal of congo red on the surface of POT.



[1]. Azza Khaled, Ahmed El Nemr, Amany El-Sikaily and Ola Abdelwahab *Journal of Hazardous Materials* **165** (2009) 100–110

[2]. M.A.Rauf, S.B.Bukallah, F.A.Hamour and A.S.Nasir, *J. Chem. Eng.*, **137**, 238 (2008).

[3]. Azza Khaled, Ahmed El Nemr, Amany El-Sikaily and Ola Abdelwahab *Journal of Hazardous Materials* **165** (2009) 100–110

[4]. B.H.Hameed and M.I.El-Khaiary, *J. Haz. Mat.*, **159**, 574 (2008)

4.53 Enhanced Cr(Vi) Removal Using Green Synthesized Fe-Nanoparticles Decorated Graphene

Baishnisha Amanulla^a and Sayee Kannan Ramaraj^{a*}

^aPG & Research Department of Chemistry, Thiagarajar College, Madurai-625 009. sayeeekannanramaraj@gmail.com

Abstract:

The present work reports a facile, green and one pot synthesis of iron nanoparticles decorated on graphene using *Nelumbo nucifera* leaf extract. The green synthesized nanocomposites have been characterized

using SEM, EDX, XRD and FT-IR. In addition, the nanocomposite showed enhanced magnetic property, surface area and Cr(VI) adsorption capacity compared to bare iron nanoparticles. This adsorbent exhibits fast Cr(VI) removal with high adsorption capacity under both acidic and neutral conditions. The adsorption kinetics follows the pseudo-second-order model in accordance with the physisorption in nature. The remarkable improvement of Cr(VI) adsorption on FG-nanocomposite was attributed to the good dispersion of Fe-nanoparticles by the graphene network in comparison with other adsorbents. Thus, the FG composite has been demonstrated as a promising separable adsorbent for removing Chromium ions from wastewater.

Keywords: FeNPs-composite, *Nelumbo nucifera*, Cr(VI), Adsorption

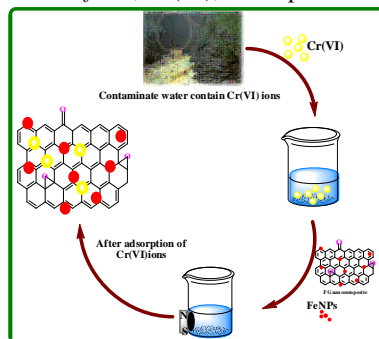


Figure: Removal of Cr(VI) ions from Contaminate water by FG Composite

References:

1. Humera Jabeen, Vimlesh Chandra, Sehoon Jung, Jung Woo Lee, Kwang S. Kim and Seung Bin Kim *Nanoscale*, **2011**, 3, 3583
2. Zhong-Hang Ruan, Jin-Hua Wu, Jian-Fei Huang, Zuan-Tao Lin, Yan-Fang Li, Yong-Lin Liu, Piao-Yang Cao, Yue-Ping Fang, Jun Xie and Gang-Biao Jiang *J. Mater. Chem. A*, **2015**, 3, 4595.

4.54 Preparation of Macromolecule Derivative With Anhydride Salts

R. Sountharya, B. Nivethetha, S. Karthick, G. Gopu*

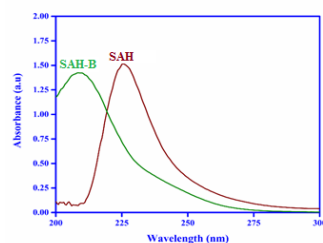
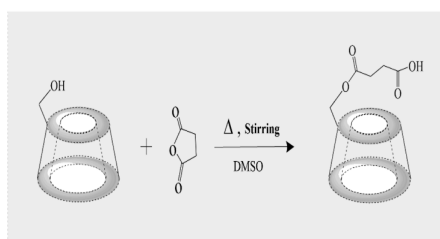
Department of Industrial Chemistry, Alagappa University, Karaikudi - 630 003.

E-Mail: nggopi79@gmail.com, sssoundar307@gmail.com

Abstract

Macrocyclic oligosaccharide consisting of seven glucose units linked by α -1,4 bonds also known as β -Cyclodextrin (β -CD), that has efficient property for accommodate various Drugs, inorganic, organic, and biological molecules into their hydrophobic cavities to form stable host-guest inclusion complexes. The most readily available of the β -CD, shows a low aqueous solubility (18 mg/cm^3 in water at 25°C). This property is a limiting factor in the investigation of the properties of inclusion compounds formed by this cyclic oligosaccharide. Because of that, β -CD and their derivatives are essential for supramolecular chemistry. Preparation of derivative is operated by Succinic anhydride (SAH). The synthesis of β -CD derivatives which are highly soluble in methanol and water. Considering that one, and probably the largest, field of practical utilization of β -CD is based on their solubilizing capacity (mainly in the pharmaceutical industry).

β -CD was dried at 120°C for anhydrous condition. SAH was dissolved in DMSO. To this solution anhydrous β -CD was added and the solution allowed to react under magnetic stirring for 2 hours. The precipitate obtained from ethyl acetate and methanol. The SAH- β -CD (SAH-B) characterized by UV-Visible and FTIR spectral analysis. FT-IR spectra of β -CD presents characteristic peak at 3373.85 cm^{-1} (O-H stretching of alcohol); 2923.56 cm^{-1} (C-H stretching of alkanes). SAH-B shows the different peaks for our desired region in FTIR analysis that is C-H stretching of alkanes and C=O stretching of carbonyl group. The UV spectra of SAH-B and SAH shows the peak for 210nm and 230nm respectively. Preparation, characterization and binding behavior of the β -CD with succinic anhydride was investigated in this work. Finally, we find out the solubility character of modified β -CD is improved than normal β -CD.



Reference

- [1] József Szejtli, Pure Appl. Chem, 76 (2004) 1825–1845.
[2] Alexis K. et.al., Anal. Chem, 64 (1992) 1632-1634.
[3] H. Feki, A. Ben Ahmed, N. Fourati, Y. Abid, C. Minot, Journal of Molecular Structure, 895 (2009) 21–25.

4.55 Synthesis of metal oxide/carbon nanofiber using paraffin wax as precursor for dye adsorption in aqueous media

Indiran Muralisankar^a, Sunderajan Vairam^b, Ramasamy Narayanasamy^{a*}

^aDepartment of Chemistry, Coimbatore Institute of Technology, Coimbatore-641014, Tamil Nadu, India.

^bDepartment of Chemistry, Government College of Technology, Coimbatore-641013, Tamil Nadu, India.

Abstract

Carbon nanotube impregnated with NiO₂ (NCNT-NS) has been used as an efficient adsorbent for the removal of Congo Red (CR) from wastewater. A simple novel technique carried out to prepare nanoporous carbon fiber using nickel acetate used as precursor to pyrolyse paraffin wax. The synthesized nickel nanoporous carbon nanocomposites characterized with XRD, HR-TEM, HR-SEM, FTIR, UV-VIS, VSM, Raman spectra and BET isotherm. The synthesized material subjected to adsorption for methylene blue removal in aqueous medium. XRD analysis confirms the formation of metal oxide nanocomposites. Structural morphology of the composite studied using high resolution scanning electron microscopy (HR-SEM) and High resolution Transmission electron microscopy (HR-TEM). The average size of the synthesized composite is in the range of 50nm. The influence of variables including pH, temperature, and concentration of the dye, amount of adsorbents and contact time, and so forth on the removal of dye was investigated by the batch method. Graphical correlations of various adsorption isotherm models like Langmuir, Freundlich, Temkin, and Dubinin–Radushkevich have been carried out. The adsorption of CR dye has been found to be exothermic and feasible in nature. Various thermodynamic parameters, such as Gibbs free energy, entropy, and enthalpy, of the ongoing adsorption process have been calculated. The kinetic studies suggest the process following pseudo second-order kinetics and involvement of the particle-diffusion mechanism.

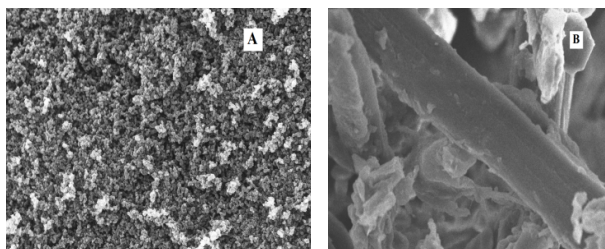


Fig. 1: Field Emission Scanning Electron Microscopy (FE-SEM) of NCNT-NS (a); Higher Magnification imaging of single CNT wrapped with NiO₂ (b).

Keywords: Pyrolysis, analytical techniques, Adsorption studies, kinetics, stability test.

References

- [1] Y.-Y. Li, C.-C. Hsieh, Micro & Nano Letters, (2007), 2(3), 63 –66.
[2] N. Singh and K. Balasubramanian, RSC Adv., (2014), 4, 27691–27701.

4.56 Encapsulation of acenaphthenequinone with p-sulfonatocalix[4]arene

M. Senthilkumar, C. Saravanan, B. M. Ashwin, K. Pramila Selas, P. Muthu Mareeswaran*

Department of Industrial Chemistry, Alagappa University, Karaikudi. Email: kumaransbk@gmail.com

The p-sulfonatocalix[4] arene (p-SC4) has intriguing host-guest properties. It is facile to synthesis and flexible structural features for a host molecule. The negatively charged upper rim, hydrophilic lower rim and hydrophobic cavity made p-SC4 as an important host molecule for variety of guest molecules which are aromatic in nature. The p-SC4 can be utilized as cargo vehicle for drugs since it is not toxic to the biological system. The lower rim intramolecular hydrogen bonding is also keep the flexible cavity in a stable conformation to some extent. Therefore the guest molecule can be excited inside the cavity of p-SC4, since there is no deformation can be envisaged upon excitation of guest inside the p-SC4 cavity. Acenaphthenequinone ACQ is a synthetic precursor for many higher organic compounds and having emission properties along with dione

moiety. In ACQ, the dione moiety is placed in the same ring and interconnected directly. The remaining naphthene rings are attached directly with the dione moiety and the whole compound is aromatic in nature. The excitation of ACQ results in quinone radicals. To study the nature of quinone radicals inside the p-SC4 cavity, the preliminary studies of steady state absorption and emission of ACQ in the presence of p-SC4 should be finished. Therefore, the scope of the present work is studying the interaction of ACQ with p-SC4 using UV-visible absorption and emission spectral techniques.

Photophysical properties of p-Sulfonatocalix[4]arene and Acenaphthenequinone.

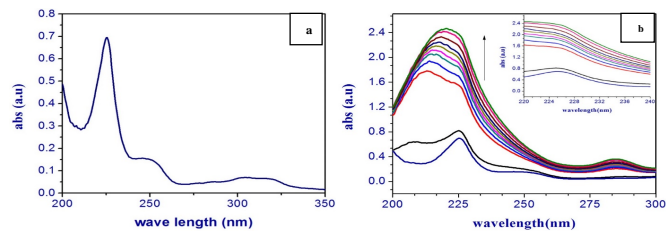


Figure 1. UV-Visible spectrum of ACQ (a). ACQ (1×10^{-5} M) in presence of varies concentration (1×10^{-5} M to 9×10^{-5} M) of p-SC4 (b). Absorption spectra of ACQ Figure. 1a) and the absorption maximum around 225 nm is increased with increase in the concentration (1×10^{-5} M to 9×10^{-5} M) of p-SC4. This indicates the binding between p-SC4 and ACQ (Figure.1b).

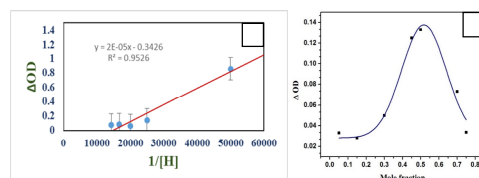


Figure.2 Benesi-Hildebrand plot (a), Job's plot (b) using UV-visible absorption technique.

The binding constant values are calculated by Benesi-Hildebrand equation. Figure.2a is the Benesi-Hildebrand plot for calculating binding constant. From this plot the binding constant value is $1.7 \times 10^4 \text{ M}^{-1}$. The Job's plot (Figure.2b) shows peak at 0.5 mole fraction. This confirms the 1:1 binding of p-SC4 with ACQ.

5.1 Synthesis and Antimicrobial Activity of Novel 5, 5-disubstituted Pyrrolo-β-Carbolines

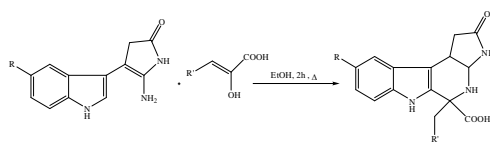
S.Senthilkumar, M.Priya & S.Sudha

Department of Chemistry, Sri Ramakrishna Institute of Technology, Coimbatore-641010, Tamil Nadu, India

E-mail: senswaan@gmail.com

Abstract

Among the four types of carbolines, β-carbolines have received considerable attention among both chemists and biologists, due to their abundant presence in nature along with a broad spectrum of biological activities and pharmacological properties [1-3]. Among the substituted β-carbolines, 5, 5-disubstituted pyrrolo-β-carbolines are the least investigated compounds and only few syntheses are found to be reported in literature. In a continuing effort to develop novel β-carbolines with good antimicrobial activity, a simple high-yielding method for designing β-carboline ring system via Pictet-Spengler (P-S) condensation has been developed and a series of 5, 5-disubstituted pyrrolo-β-carbolines (**4-15**) have been synthesized (**Scheme-1**). The structures of these compounds were established by IR, ¹H-NMR and ¹³C-NMR spectroscopic techniques. Antimicrobial activities of compounds were studied by disc diffusion method. All the newly synthesized compounds were tested against two fungi (*Candida albicans* and *Aspergillus niger*), two Gram positive (*Staphylococcus aureus* and *Bacillus subtilis*) and two Gram negative bacterial strains (*Escherichia coli* and *Pseudomonas aeruginosa*). The results revealed that compounds showed varying degrees of inhibition against the tested microorganisms.



(1-3)

Scheme-1: General synthetic route for 5, 5-disubstituted pyrrolo-β-carbolines (1-1)

The best antibacterial activity was displayed by Compound (**4**) with inhibition zone of 26 mm against *Staphylococcus aureus*. On the other hand compounds (**5&7**) with indolyl and p-hydroxy phenyl substituent at 5-position of β-carboline ring respectively showed strong activity against Gram-positive bacteria *Staphylococcus aureus* and *Bacillus subtilis*. Amongst all the compounds tested, Compound (**7**) is the most potent compound against the Gram negative bacteria *Escherichia coli* and *Pseudomonas aeruginosa*. This indicated the presence of two hydroxyl groups (one at 9-position of β-carboline skeleton and the other at 4-position of phenyl ring) are responsible for the enhanced activity.

Compound (**7**) with hydroxy substitution at 9-position of β-carboline skeleton and 4-position of phenyl ring was found to be the most active of all the tested compounds against *Candida albicans* with good inhibiting zone value. Further it showed almost equipotent antifungal activity against *Candida albicans* as that of reference drug Nystatin.

Compound (**9**) having methoxy group at 9-position and indolyl group at 5-position of β-carboline ring is the most active of all the tested compounds with inhibition zone of 26 mm against *Aspergillus niger*.

Key words: Synthesis, β-carbolines, Pictet-Spengler condensation, antimicrobial activity, Disc diffusion method.

References

- [1] R.Cao, W.Peng, H.Chen, Y.Ma, X.Liu, X.Hou, H.Guan, A.Xu, Biochem Biophys Res Commun 338 (2005) 1557-1563.
- [2] A.Ahmad, K.A.Khan K, S.Sultana, B.S.Siddiqui, S.Begum, S.Faizi, S.Siddiqui, J Ethnopharmacol 35 (1992) 289-294.
- [3] Y.H.Wang, J.G.Tang, R.R.Wang, L.M.Yang, Z.J.Dong, L.Du, X.Shen, J.K.Liu, Y.T.Zheng Biochem Biophys Res Commun 355 (2007) 1091-5.

5.2 Electrocatalytic Reduction of Oxygen at the surface of poly (3-methylthiophene-co-3,4-ethylenedioxythiophene) modified electrode with 1,8-Dihydroxy anthra-9,10-quinone

G. Amala Jothi Grace^a, A. Gomathi^{*b} and C. Vedhi^c

^aDepartment of Chemistry, Chandy College of Engineering, Thoothukudi.

^bDepartment of Chemistry, Sri K.G.S Arts College, Srivaikuntam.

^cDepartment of Chemistry, V.O.Chidambaram college, Thoothukudi.

Abstract:

The glassy carbon electrode was modified with poly (3-methylthiophene-co-3,4-ethylenedioxythiophene) by means of electrodeposition method. The electrochemical and catalytic behaviour of

the copolymer modified electrode with 1,8-Dihydroxy anthra-9,10-quinone (DHAQ) was studied using cyclic voltammetry, chronoamperometry and chronocoulometric techniques. The stability of the copolymer modified electrode was also studied by cyclic voltammetry in acidic, neutral and basic media.

The influence of pH and scan rate (Figure 1A) on the electrochemical behaviour of DHAQ at the modified electrode was studied by cyclic voltammetry in various buffers. Under de-aerated condition, reduction potential of DHAQ at the copolymer modified electrode was shifted toward more negative direction with increasing pH of the media.

The copolymer modified electrode with 1,8-Dihydroxy anthra-9,10-quinone possess good electro catalytic ability for the oxygen reduction. pH 7.0 was chosen as the optimum working pH by comparing the shift in oxygen reduction potential. Under aerated conditions, there is a large enhancement in the cathodic peak current with the disappearance of anodic peak (Figure 1B) which clearly indicates the irreversible electrocatalytic oxygen reduction.

The diffusion coefficient values of anthraquinones at the copolymer modified electrode and the number of electrons involved in oxygen reduction were determined by chronoamperometric and chronocoulometric techniques. These studies showed the involvement of two electrons in the oxygen reduction. The surface morphology of the modified electrode was also characterized by scanning electron microscopy images. Based on these results, this copolymer modified electrode was suggested to use as oxygen sensors.

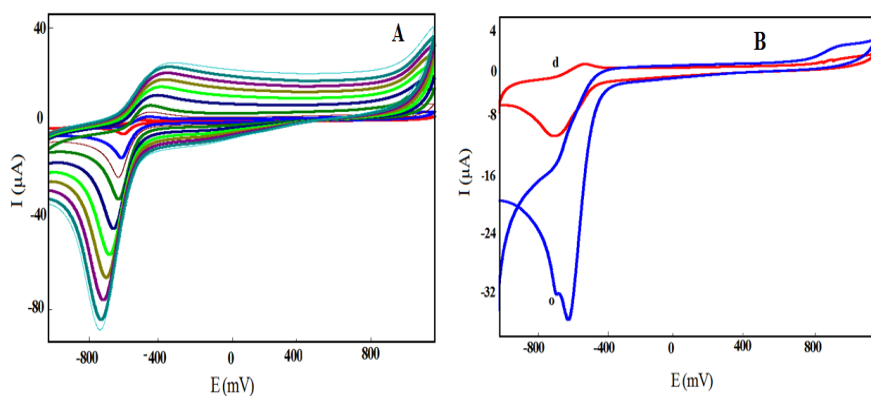


Figure 1. (A). Cyclic voltammograms of DHAQ at METH/EDOT/GCE in pH 5 at scan rates 5, 20, 50, 100, 200, 300, 400, 500, 600, and 700 mVs^{-1} (B). Cyclic voltammograms of DHAQ at METH/EDOT/GCE in the presence (o) and absence (d) of oxygen at pH 7.

Keywords: Oxygen reduction, 1,8- Dihydroxy anthra-9,10-quinone, Voltammograms, Reduction potential, Copolymer modified electrode.

5.3 Green based AgNPs from red seaweed and its defensive effect to control Vibriosis in Brine shrimp: An environmental friendly approach

Lakkakula Satish, Sivasubramanian Santhakumari, Arokiam Sagina Rency, Shanmugaraj Gowrishankar, Shanmugaiah Karutha Pandian, Arumugam Veera Ravi, Manikandan Ramesh
 Department of Biotechnology, Science Campus, Alagappa University, Karaikudi – 630 004, Tamil Nadu, India.
 E-mail: mrbiotech.alu@gmail.com

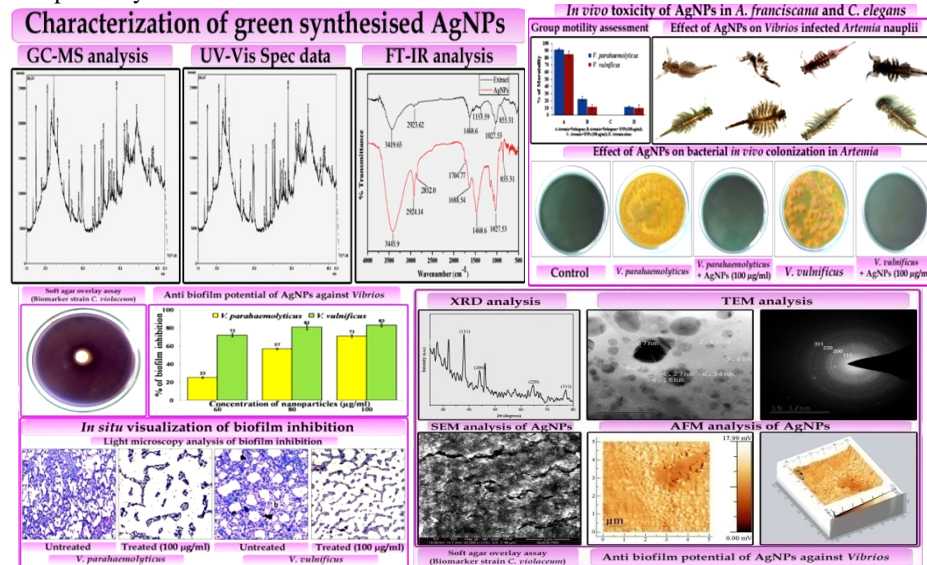
Abstract

Background: Nanomedicine is a prime driving force behind the development of alternative strategies in the arena of antimicrobial discovery. In aquaculture, pathogenic bacteria particularly *Vibrio* spp. adhere to the biotic surfaces and develop as recalcitrant biofilm architectures that embody vital concern in vibriosis infections. As these pathogens are potent biofilm formers, they resist multiple antimicrobials and emerge as difficult-to-treat infections. Hence, it is the need of an hour to develop novel therapeutic agents to combat these biofilm-associated vibriosis infections. This notion has prompted us to explore the inhibitory efficacy of green synthesized silver nanoparticles (AgNPs) from *Gelidiella acerosa* seaweed with immense pharmaceutical values against the biofilm formation of *Vibrio* spp.

Methodology: Spectral characterization of synthesized AgNPs was performed by employing UV-visible, Fourier transform infrared and energy-dispersive spectroscopic techniques followed by X-ray crystallography. Further, the structural characterization was done by scanning electron, transmission electron and atomic force microscopic techniques. These characterized AgNPs (2.8-100 nm) at a concentration of 100 $\mu\text{g/ml}$ tested for antibiofilm effectiveness against multidrug resistant strains viz. *Vibrio parahaemolyticus* and *Vibrio vulnificus* which was divulged through light, scanning electron and confocal laser scanning microscopic analyses.

Results and Discussion: AgNPs comprise a very promising approach for the improvement of new antimicrobial systems. In this study, characterized AgNPs (2.8-100 nm size) at a concentration of 100 $\mu\text{g/ml}$

depicted a profound antibiofilm efficacy against multidrug resistant strains viz. *V. parahaemolyticus* (71%) and *V. vulnificus* (83%), respectively which was divulged through light, scanning electron and confocal laser scanning microscopic analyses.



Interestingly, the AgNPs were proficient enough to disrupt the recalcitrant mature biofilm architecture of aquaculture pathogens. Data of *in vivo* assay using gnotobiotic brine shrimp (*Artemia franciscana*) nauplii unveiled the anti-pathogenic efficacy of AgNPs, as it effectively reduced the pathogenicity and enhanced the survival rate of *in vivo* model upto 100% without any toxicity even at 200 µg/ml concentration. In addition, AgNPs also exhibited the anti-quorum sensing activity by inhibiting the violacein production against biomarker strain *Chromobacterium violaceum*. **Conclusion:** In conclusion, the green synthesized AgNPs from *G. acerosa* could be a starting point for development of promising anti-pathogenic agent against the biofilm-associated infections of drug resistant *Vibrio* spp. in aquaculture environment.

References:

[1]. Gowrishankar S et al. (2015) *Bacillus amyloliquefaciens*-secreted cyclic dipeptide – cyclo(L-leucyl-L-prolyl) inhibits biofilm and virulence production in methicillin-resistant *Staphylococcus aureus*. RSC Adv 5:95788-95804.

Acknowledgements: L. Satish sincerely thanks the UGC (IN) for financial support UGC BSR-SRF (UGC order no. F.4-1/2006 (BSR)/7-326/2011/BSR; dated 25.02.2013).

5.4 Green Synthesis of 5,6-Bis[(2,4-dinitrophenyl)hydrazinylidene]-1,2,3,4-hexanetetrol using Glucose – Urea as Deep Eutectic Solvent

^aD. Ilangeswaran and ^bP.G. Ramesh

^a Department of Chemistry, Rajah Serfoji Govt. College (Autonomous), Thanjavur-613005

^b Department of Chemistry, Swami Dayananda College of Arts & Science, Manjakkudi, Tiruvarur-612610

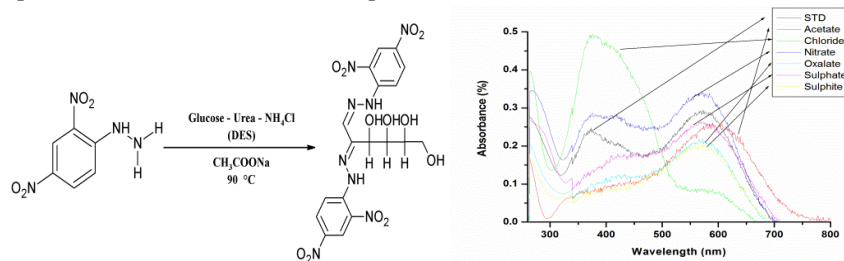
Email: dhailangeswaran@gmail.com, pgrjan2011@gmail.com

Abstract

Deep eutectic solvents (DES) are emerging type of environmentally green solvents. As a new type of solvent, DES has an extremely large number of applications. Even though the problems associated with conventional volatile organic solvents are well studied, the usage of green and bio-renewable solvents still remains a never ending challenge [1]. In this sense, the advantages of using Deep Eutectic Solvents (DES) as reaction medium is highlighted from the fact that they are bio-degradable, non-toxic, recyclable and could be easily prepared using inexpensive raw materials [2-6]. DES have been studied in a variety of applications including metal deposition, metal oxide dissolutions, purification of bio-diesel, bio-transformations, different synthetic processes and metal-catalyzed organic reactions. In recent years, low melting mixtures consisting of carbohydrates, urea and inorganic salts have been introduced as new alternative sustainable solvents for organic transformations [7].

In this work we synthesized osazone of 2,4-dinitrophenylhydrazine {5,6-Bis[(2,4-dinitrophenyl)hydrazinylidene]-1,2,3,4-hexanetetrol} using a deep eutectic solvent (DES) of glucose, urea and NH_4Cl with the percentage composition of 50:40:10. The products obtained were characterized by FTIR, ^{13}C and ^1H NMR spectroscopic techniques. The color of this osazone in DMSO is yellow while the addition of other anions to this solution yielded various color due to the interaction of azomethine group with added anions [8]. The UV-Visible

spectra obtained for this osazone in presence of different anions evidenced this fact.



Scheme: Synthesis of 5,6-Bis[(2,4-dinitrophenyl)hydrazinylidene]-1,2,3,4-hexanetetrol; Figure: The UV-Visible spectra in DMSO for 5,6-Bis[(2,4-dinitrophenyl)hydrazinylidene]-1,2,3,4-hexanetetrol (STD) with different anions

REFERENCES

- [1] *Handbook of Green Chemistry, Vols. 4, 5, and 6, Green Solvents*, Ed. P. T. Anastas; Wiley-VCH: Weinheim, Germany, (2011).
- [2] Qinghua Zhang, Karine De Oliveira Vigier, Sebastien Royer and Francois Jerome, *Chem. Soc. Rev.*(2012), DOI: 10.1039/c2cs35178a.
- [3] A. P. Abbott, R. C. Harris, K. S. Ryder, C. D'Agostino, L. F. Gladden and M. D. Mantle, *Green Chem.*, (2011), 13, 82–90.
- [4] D. Carriazo, M. C. Serrano, M. C. Gutiérrez, M. L. Ferrer, F. del Monte, *Chem. Soc. Rev.* (2012), 41, 4996.
- [5] C. Ruß, B. König, *Green Chem.* (2012), 14, 2969.
- [6] M. Francisco, A. van der Bruinhorst, M. C. Kroon, *Angew. Chem. Int. Ed.* (2013), 52, 3074.
- [7] D. Reinhardt, F. Ilgen, D. Kralisch, B. König and G. Kreisel, *Green Chem.*, (2008), 10, 1170–1181.
- [8] V. K. Gupta, A. K. Singh, S. Bhardwaj, K. R. Bandi, *Sensors and Actuators B* 197 (2014) 264–273.

5.5 PEG assisted two-component access to 3-amino-4-arylidene-1H-pyrazol-5(4H)-ones under catalyst-free conditions

Rathinam Ramesh,^a Pullar Vadivel,^b Kaliyan Bhuvaneshwari^a and Appaswami Lalitha^{*a}

^aDepartment of Chemistry, Periyar University, Periyar Palkalai Nagar, Salem - 636 011, Tamil Nadu, India

^bDepartment of Chemistry, Salem Sowdeswari College, Salem - 636 010, Tamil Nadu, India

*E-mail: lalitha2531@yahoo.co.in, Tel: +91-427-234-5271; Fax: +91-427-234-5124

Abstract

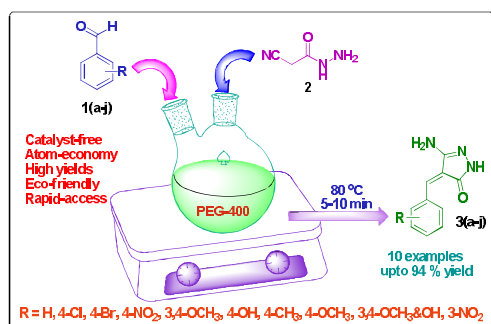
PEG mediated an exemplary and eco-friendly approach has been disclosed for the convenient access of structurally diverse 3-amino-4-arylidene-1H-pyrazol-5(4H)-one motifs via a simple, two-component condensation of multifarious aromatic aldehydes with 2-cyanoacetohydrazide under catalyst-free conditions. Use of recyclable medium, neutral reaction conditions, easy work-up, atom-efficiency and excellent yielding make this protocol as more immense for the greener assembly of privileged 1H-pyrazoles in very shorter reaction times.

Key words: PEG-400, 3-amino-4-arylidene-1H-pyrazolones, catalyst-free, recyclability.

The constantly emergent interest for the development of a convenient and greener methodology motivates the researchers to increase the implements of their arsenal.¹ Recently, tandem reactions have emerged as very attractive techniques for accessing complex organic molecules in a facile and efficient mode.² Nitrogen containing heterocycles such as pyrazoles and pyrazolones having their special interest by the chemists because they constitute an important class of natural as well as unnatural products. Compounds containing pyrazole moieties are well known and they exhibit diverse pharmacological activities such as antimicrobial, antifungal, anti-inflammatory, analgesic, antipyretic, herbicidal and also these derivatives have unique electrical and optical properties.³ Therefore, the design of improved and greener approaches that allow the rapid, cost-effective synthesis of some novel 1H-pyrazole based compounds from 2-cyanoacetohydrazide⁴ would be highly desired.

In continuation of our non-catalytic research with some sustainable alternates,⁵ we have started our experimentation with the two-component reaction of 2-cyanoacetohydrazide **2** (2.0 mmol) and 4-chlorobenzaldehyde **1b** (2.0 mmol) as a model for the synthesis of 3-amino-4-(4-chlorobenzylidene)-1H-pyrazol-5(4H)-one (**3b**) in ethanol. The reaction under reflux conditions without any added catalyst resulted in the formation of **3b** with an insufficient yield (59%) even after 1h.

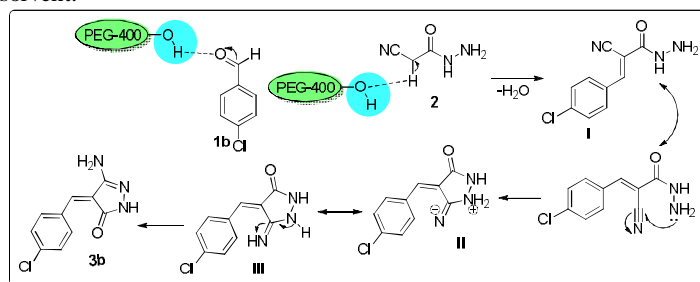
Further, we examined the effect of different solvents such as methanol, 2-propanol, acetonitrile, water, PEG-400 and glycerol on the model reaction at different thermal conditions. From the results obtained, we have selected PEG-400 as a suitable reaction medium due to the increased yield and eco-friendly nature. Next, we have also studied the above model reaction with different temperatures (ranging from RT to 100 °C) and it was found that 80 °C would be the suitable by providing 93 % of **3b** with very shorter reaction time (5 min).



Scheme 1 Uncatalyzed synthesis of 3-amino-4-arylidene-1*H*-pyrazol-5(4*H*)-ones

With the encouraging optimized results in hand, we have checked the generality and effectiveness of the present protocol with a variety of aromatic aldehydes **1(a-j)**. Aldehydes bearing both electron-donating (*methyl*, *methoxy* or *hydroxy*) and electron-withdrawing (*nitro*, *chloro* or *bromo*) substituents gave the corresponding 3-amino-4-arylidene-1*H*-pyrazol-5(4*H*)-ones almost in high yields with shorter reaction times (**Table 2**). The formation of compounds **3(a-j)** were confirmed by IR, ¹H and ¹³C NMR spectral analyses.

A tentative mechanism that accounts for the synthesis of **3(a-j)** is shown in **Scheme 2**. Initially, the aromatic aldehyde (**1b**) was made to react with 2-cyanoacetohydrazide to afford the Knoevenagel adduct *i.e.*, 3-(4-chlorophenyl)-2-cyanoacrylohydrazide (**I**). In the next step, amine (-NH₂) acting as a stronger nucleophile and attacked the nitrile (-CN) carbon of **I** to provide the intermediate **III**. Finally, **III** would be converted into the target molecule (**3b**) by the tautomerisation (*i.e.*, imino to enamino) step which was facilitated by the PEG as an effective greener solvent.



Scheme 2 Plausible mechanistic approach

Typical procedure for the synthesis of 3-amino-4-arylidene-1*H*-pyrazol-5(4*H*)-ones: A mixture of aromatic aldehyde (2.0 mmol) and 2-cyanoacetohydrazide (2.0 mmol) was added to 1.0 ml of PEG-400 in a 25 ml RB flask. The resulting mixture was allowed to stir at 80 °C for the specified time. After completion of the reaction (monitored by TLC), the reaction mixture was cooled to room temperature and treated with de-ionized water (10 ml), well-stirred for a few seconds, and the generated solid was filtered off. The crude products were recrystallized from 95% ethanol to afford the corresponding highly pure 3-amino-4-arylidene-1*H*-pyrazol-5(4*H*)-one derivatives for spectroscopic measurements.

In summary, we have developed a most benign, facile, mild and rapid protocol for the efficient synthesis of some novel 3-amino-4-arylidene-1*H*-pyrazol-5(4*H*)-ones under catalyst-free conditions. PEG-400 assisted this new chemistry would suggest a powerful route for the progress of 1*H*-pyrazole based scaffolds with more sensitive functionalities in the areas of modern synthetic society.

Acknowledgment

R.R. gratefully acknowledge the DST-Inspire Fellowship, New Delhi, India (No: DST/INSPIRE Fellowship/2012/690) for financial support.

References

- [1]. A. Nefzi, J.M. Ostresh, R.A. Houghten, *Chem. Rev.* 1997, 97, 449.
- [2]. T.L. Ho, *Tandem Organic Reactions*; John Wiley & Sons: New York, 1992.
- [3]. (a) S. Fustero, A.S. Fuentes, F.S. Cervera, *Org. Prep. Proced. Int.* 2009, 41, 253; (b) M. Krasavin, I.O. Konstantinov, *Lett. Org. Chem.* 2008, 5, 594; (c) A. Burguete, E. Pontiki, D.H. Litina, R. Villar, E. Vicente, B. Solano, S. Ancizu, S. Silanes, I. Aldana, A. Monge, *Bioorg. Med. Chem. Lett.* 2007, 17, 6439. (d) D. Castagnolo, F. Manetti, M. Radi, B. Bechi, M. Pagano, A. Logu, R. Meleddu, M. Saddi, M. Botta, *Bioorg. Med. Chem.* 2009, 17, 5716; (e) D. Singh, *J. Indian Chem. Soc.* 1991, 68, 16.
- [4]. P. Singh, R. Kumar, B. Yadav, R.S. Khanna, A. Tewari, *RSC Adv.* 2014, 4, 51239.
- [5]. R. Ramesh, A. Lalitha, *RSC Adv.* 2015, 5, 51188.

5.6 A facile and efficient synthesis of fused-pyridine heterocycles in ionic liquid under microwave irradiation

Selvam Chitra,^a Shanmugam Muthusubramanian^{b,*} and Paramasivam Manisankar^{c,*}

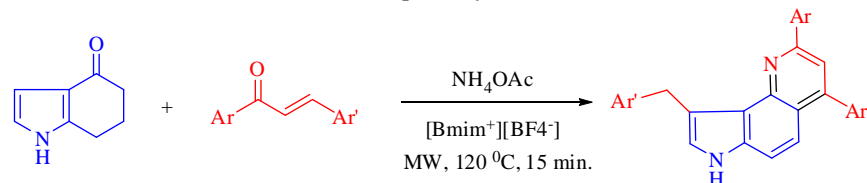
^aDepartment of Chemistry, Seethalakshmi Achi College for Women, Pallathur-630 107

^bDepartment of Organic Chemistry, Madurai Kamaraj University, Madurai-625 021

^cDepartment of Industrial Chemistry, School of Chemistry, Alagappa University, Karaikudi-630 003

Abstract

A efficient and eco-friendly method for the synthesis of pyridine, thienopyridines from the reaction of cyclic ketones and cyclic/acyclic α , β -unsaturated compounds and ammonium acetate using ionic liquid as reaction medium is described. Operational simplicity, high yields and reusability of ionic liquid are the notable features of the present protocol. When 6,7-dihydro-1*H*-indol-4(5*H*)-one is used as the cyclic ketone, an unusual product is formed by a second Michael addition-elimination pathway.



5.7 Synthesis of Newer thiopyridine derivatives and evaluation of their biological properties

P.Muthuraja, S.Prakash, K.Dinesh Christy and P.Manisankar*

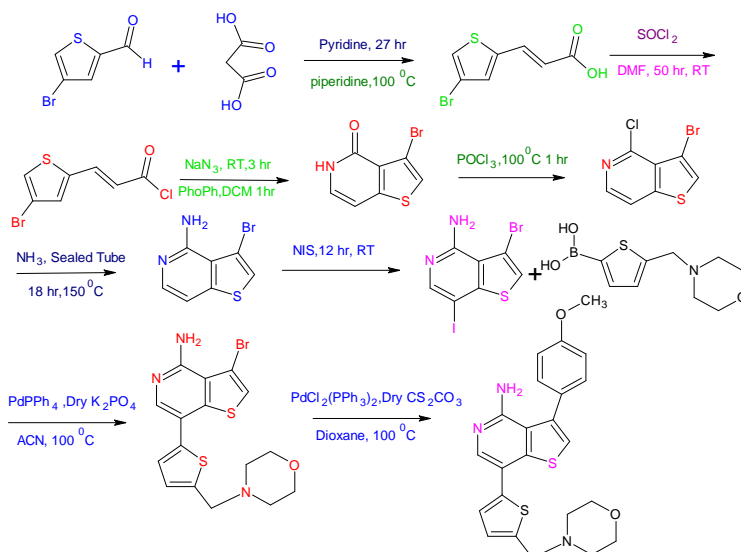
Department of Industrial Chemistry, Alagappa University, Karaikudi – 630 003 Tamilnadu, India.

Phone: +91 4565 228836*E-mail: pms11@rediffmail.com

Abstract

In present study, new scaffolds of 5-bromo-4-[5-(morpholin-4-ylmethyl)thiophen-2-yl]-5*H*-cyclopenta [c] pyridin -1-amine functionalized with different aromatic boronic acid were synthesized. All the synthesized compounds were fully characterized by elemental analysis (CHN), FT-IR, ¹H NMR, ¹³C NMR and mass spectral data. These compounds were computationally evaluated using cheminformatics tools. Six newer thiophene derivatives obeyed Lipinski's rule of five with good biological activity. Six targets among one showed lesser drug likeness and drug score values compared to other thiophene derivatives using OSIRIS property explorer. Except these one derivatives, all other synthesized targets act as drugs. One of the compounds, showed good anti-inflammatory (37.4% at 100 mg/kg p.o.) and analgesic activity (75% at 100 mg/kg p.o.) 1 (3) showed moderate activity against CDK-1 (IC₅₀)=5 microM). The other compounds showed moderate anti-inflammatory (5-20%), analgesic (25-75%) and protein kinase (CDK-5, GSK-3) inhibitory activities (IC₅₀)> 10 microM).

Key words: Thiophene derivatives, Libinski rule, OSIRIS Property Explorer, Mol inspiration software.



Scheme 1. Synthesis of the thiopyridine nucleus

- Reference**
- [1] B.B. Fredholm, A.P. IJzerman, K.A. Jacobson, J. Linden, C.E. Müller, *Pharmacol. Rev.* 2011, **63**, 34.
 - [2] K.A. Jacobson, Z.G. Gao, *Nat. Rev. Drug Disc.* 2006 **5**, 247.
 - [3] B.B. Fredholm, J.F. Chen, S.A. Masino, J.M. Vaugeois, *Annu. Rev. Pharmacol. Toxicol.* 2005, **45**, 385.
 - [4] D. Guo, E.J. van Dorp, T. Mulder-Krieger, J.P. van Veldhoven, J. Brussee, A.P. IJzerman, L.H. Heitman, *J. Biomol. Screen.* 2013, **18**, 309.
 - [5] R. Wilcken, M.O. Zimmermann, A. Lange, A.C. Joerger, F.M. Boeckler, *J. Med. Chem.* 2013, **56**, 1363.

5.8 Anodic bromomethoxylation of styrenes

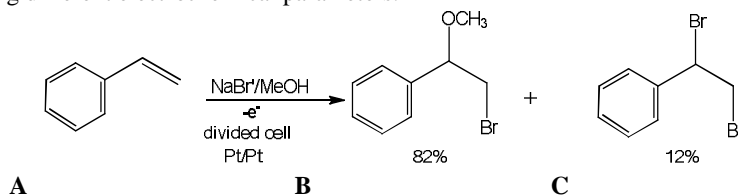
V.M. Shanmugam, K.Kulangiappar, T.Raju and D.Velayutham

Electro organic Division, CSIR - Central Electrochemical Research Institute, Karaikudi – 3. Shanmugam.nmrlab@gmail.com

Abstract

Combining multiple steps without isolating intermediate is important to enhance the power and efficiency of organic synthesis.¹ The integration of chemical reactions enables synthetic transformations that would be otherwise very difficult or impossible, such transformation involving the generation of unstable highly reactive species that are swiftly utilised for a subsequent reaction before they polymerise or decompose. Electrochemical reactions using electron transfer on the surface of the electrode serve as a powerful means of selective oxidation.³ Electrochemistry allows for the selective removal of electrons under mild conditions. However the electrochemical oxidation also often suffers from over oxidation or polymerisation.⁴ For example, the anodic oxidation of alkenes often lead to carbon-carbon bond cleavage.⁵ Herein we report the bromomethoxylation of aryl alkenes via electrochemical oxidation of methanolic solution of aryl alkenes containing 1% NaBr as electrolyte in a divided cell. This paper describes about the various electrochemical parameters studied to get the maximum product yield under mild reaction condition and the probable mechanism also discussed.

Bromomethoxylation of styrene was carried out by anodic oxidation in methanol and NaBr as the bromine source and electrolyte as well. The oxidative reaction was carried out under low current density so as to get 82% of 1-methoxy-2-bromo alkane and 12% of 1, 2-dibromo alkane as products. Selective introduction of two different functional groups, such as hydroxyl, or alkoxy and halogen has attracted sustained attraction in organic synthesis. In the oxidation step both the radicals of different functional groups (i.e. $\text{CH}_3\text{O}^\bullet$, Br^\bullet) are made available in the same environment by electrolysis in the anodic compartment of a divided cell to form the desired product by varying different electrochemical parameters.



Scheme 1: Electrochemical bromomethoxylation of styrene

A - Styrene, B - 1-methoxy-2-bromo-1-phenylethane, C - 1,2-dibromo-1-phenylethane

At first we studied the oxidation of alkene by a two-phase electrolysis in $\text{CHCl}_3/\text{H}_2\text{O}$ solvent where the alkene was present in organic phase while the electrolyte NaBr presents in aqueous phase. The product obtained was 1, 2-dibromo alkane in 98% yield. When the same reaction was carried out in $\text{CH}_3\text{CN}/\text{H}_2\text{O}$ as a solvent the corresponding bromohydrin was obtained as a major product. But 1-Methoxy-2-bromoalkane was isolated in 82% as a major product along with 12% of 1, 2-dibromo-1-phenylethane when 1% NaBr solution of methanol used as solvent to carry out the electrolysis. The electrolysis was monitored by HPLC instrument. The reaction proceeds smoothly and the completion of reaction was observed by the appearance of bromine colour after passing a charge of 2F/mole. The product formation is confirmed by the ^1H NMR, GCMS and FTIR spectroscopic techniques. The process is simple, economic and easy to perform at room temperature condition with high yield.

References

- [1]. Hardee, D.J.; Lambert, T.h. *J. Am. Chem. Soc.* 131, (2009), 7536.
- [2]. Yoshida, J.; Saito, K.; Nokami, T.; Nagaki, A. *Synlett* (2011), 1189.
- [3]. Kirste,.; Schnakenburg, G.; Stecker, F.; Fischer, A.; Waldwogel, S.R. *Angew. Chem., Int. Ed.* 49, (2010), 971.
- [4]. Halas, S.M.; Okyne, K.; Fry, A. *Electrochim. Acta* 48, (2003), 1837.
- [5]. Ogibin, Y.N.; Ilvovskii, A.I.; Nikisin, G.I. *Russ. Chem. Bull.* 43, (1994), 1536.

5.9 Adsorption removal of malachite green dye from aqueous solution by wood apple rind (*Limonia acidissima*)

N.Ramulu^a, S.Krishnaveni^a, T.Rajajeyagantham^b and V.Thirumurugan^a

^aA.V.V.M. Sri. Pushpam College, Poondi (Autonomous), Thanjavur, Tamilnadu, India.

^bM.Kumarasamy College of Engineering, Karur, Tamilnadu, India. Email: ramaravindh1967@gmail.com

Water pollution by dyes is a worldwide problem particularly in textile industry where large quantities of dye effluents are discharged from the dyeing process. Considering both volume and composition, effluent from the textile industry was declared as one of the major sources of wastewater in Asian countries. Dyes are also widely used in other industries such as rubber, paper, plastic, cosmetic etc. The chemical structure of dyes varies enormously, and some have complicated aromatic structures that resist degradation in conventional wastewater treatment process because of their stability to sunlight, oxidizing agents and microorganism. Many of the organic dyes are hazardous and may affect the aquatic life and even the food chain. Dyes are broadly classified as anionic (direct, acid and reactive dyes), cationic (basic dyes), non-ionic and zwitterionic depending on the ionic charge on the dye molecules. Cationic dyes are more toxic than anionic dyes [1]. Removal of color from dye bearing wastewaters is a complex problem because of difficulty in treating such wastewaters by conventional treatment methods [2]. The most useful and economic method is adsorption. Removal of such toxic heavy metal is done by naturally occurring adsorbent like tea leaves, cotton capsule shell, bazarahull, moong shell, Bidi leaves, saw dust, paddy husk [3].

Wood apple shell (WAS) has been used as adsorbent. The wood apple fruit is more popular as medicine than as food. The tannin in it has an astringent effect that once led to its use as a general tonic and as a traditional cure for dysentery, diarrhoea, liver ailments, chronic cough and indigestion. The root juice was once popular as a remedy for snakebites. The unripe fruit is described as astringent and is used in combination with wood apple and other medicines in diarrhoea and dysentery. The ripped fruit is said to be useful in hiccup and infections of the throat [4,5]

Batch biosorption studies

The experiment was carried out by the batch adsorption method in the Erlenmeyer flasks for a predetermined period using orbital shaker. In the adsorption, parameters such as PH, Initial dye concentration, equilibrium time fixation were studied for optimization. The kinetic studies and isotherm study were carried out at different dye concentration, 200 ppm, 250 ppm, 300 ppm, 350 ppm, 400 ppm and 450ppm. by keeping temperature constant at 150 rpm for 2 and half hours. The mechanism of adsorption was investigated by Lagergren's pseudo first order, pseudo-second order. The isotherm study results were fitted in Langmuir and Freundlich isotherms. The measurement of absorbance of colour was done Spectrophotometrically. The equilibrium adsorption capacity was evaluated using the equation

$$q_e = (C_o - C_e) V/m \text{-----(1)}$$

Where q_e (mg/g) is the equilibrium adsorption capacity, C_o and C_e are the initial and equilibrium concentrations (mg/l) of Malachite green dye solution. V is the volume and m is the weight of adsorbent.

Pseudo second order kinetics

The pseudo second order model can be represented in the following form

$$t/q_t = 1/K_2 q_e^2 + 1. t/q_e \text{-----(2)}$$

Where K_2 is the pseudo second order rate constant (g/mg.min). The plots of t versus t/q_t . From the above results pseudo first order has R^2 value was 0.997 and pseudo second order kinetics has R^2 value was 1.0000. Second order q_e experimental value is 93.86 and q_e theoretical value is 92.18mg/g. Second order only q_e experimental and q_e theoretical (mg/g) values are nearly same. From this, It clearly indicates that pseudo second order better fitted than pseudo first order.

Freundlich isotherms

The isotherm was represented by

$$\log q_e = \log K_f + 1/n \log C_e \text{-----(3)}$$

Where q_e is the amount of Malachite green adsorbed at the equilibrium (mg/g), C_e is the equilibrium constant of Malachite green in solution (mg/l), K_f and $1/n$ are constant incorporating factor affecting the adsorption capacity and intensity of adsorption respectively. The R^2 value is 0.9956. It indicates good linearity and obeys the Freundlich isotherm

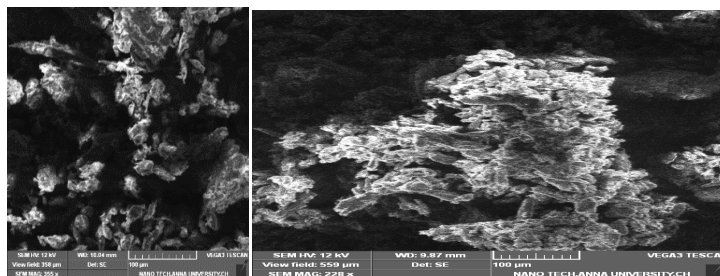


Figure: Before and After adsorption of WAR

Conclusion

The aim of this paper was utilization of natural biosorbent WAR as adsorbent for the removal of Malachite green. Even though pseudo first order kinetic model gave better results, but pseudo second order

kinetic model best fits the kinetics of adsorption. The correlation coefficient $R^2 = 1$ for second order adsorption model and q_e theoretical values are consistent with q_e experimental value showed that pseudo second order adsorption equation fit with whole range of contact time. Among isotherms, Freundlich isotherm was found to be best fitting model with respect to R^2 values. The WAR adsorbent has excellent adsorption capacity compared to any other non-conventional adsorbent. So WAR can be used as a low cost attractive alternative for costly activated carbon.

Reference

- [1]. Nandi, B. K., Goswami, A., Purkait, M. K., 2009. Applied Clay Science. 42, 583–590.
- [2]. K. V. Kumar, V. Ramamurthi and S. Sivasenan, "Dyes and Pigments," vol. 69, pp. 102–107, 2006
- [3]. Marina Trgo, Nediljka Vukojevic Medvidovic and Jelena Peric *Indian J. Chem. Technol* 2011, 18 123
- [4]. D. Ozdes, A. Gundogdu, C. Duran, H. B. Senturk, Sep. Sci. Technol. 45 (2010) 2076–2085.
- [5]. M.M. Sardesai, S.R. Yadav, Flora of Kolhapur District, Shivaji University, press, India (2002)

5.10 Kinetic and statistical studies on degradation of reactive orange -16 dye by electrocoagulation method

K.Diana, R.Koushalyaa, T.Srinithi, N.Maheshwari, G.Madhangi Priyadharshini, V.C.Padmanaban*

Department of Biotechnology, Kamaraj College of Engineering & Technology,
Virudhunagar – 626001. mgdiana2301@gmail.com, vcpadmanaban88@gmail.com

Abstract:

Textile industrial effluents released from the industries poses a threat to the ecosystem, as it causes serious environmental pollution. The environment can be conserved by treating the effluents using various physical, chemical and biological methods. Since conventional methods are less efficient in degrading the large volumes of effluent, electrocoagulation degrades high volumes of dye effluent in short time. The model dye used in this study was Reactive Orange 16 (RO16) and the parameters were optimised as pH 3.0, electrolyte concentration (KCl) as 0.3M and voltage as 20V. The reaction kinetics was also established and was found to follow 1st order kinetics and the rate of the degradation was found to be 2,29,824mg/L.day. The interaction between the factors was studied and the statistical model for the degradation of Reactive Orange 16 dye was developed using Face Centred Central Composite design (CCF). For the developed model, $R^2 = 0.9692$ and adjusted $R^2 = 0.9415$. The end products of the degraded samples were analysed through FTIR.

Keywords: Electrocoagulation, First order kinetics, Reactive Orange 16 (RO16)

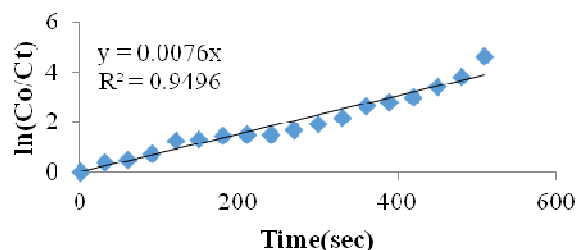


Figure 1. Reaction Kinetics for the degradation of Reactive Orange 16 (RO16)

The significance and adequacy of the model was tested by Analysis of Variance (ANOVA) (Soltani *et al.* 2013). As given in the table 4, the regression model has a high coefficient of determination ($R^2 = 0.9692$). The significance of the model can also be demonstrated by adjusted R^2 value (Amini *et al.* 2008). In this model, the adjusted R^2 was found to be 0.9415. The F-value of the model is 34.9 which implies the model as significant. In this model, A, B, C, C^2 are significant model terms as their P values are low as (<0.0001 , <0.0001 , <0.0001 , 0.0063) respectively. The signal to noise ratio can be determined by "adequate precision" and the desired value should be greater than 4 (Soltani *et al.* 2013).

Reference:

- [1] Amini M., Younesi H., Bahramifar N., Lorestani A. A. Z., Ghorbani F., Daneshi A. and Sharifzadeh M. (2008). *Journal of hazardous materials* 154(1), 694-702.
- [2] Soltani R. D. C., Rezaee A., Godini H., Khataee A. and Hasanbeiki A. (2013). *Chemistry and Ecology* 29(1), 72-85.

5.11 Corrosion inhibition studies on carbon steel in sea water using an aqueous seed extract of *Lablab purpureus*

K Anuradha¹, R Nandhini¹, P Govintha Raju¹ and K Velmanirajan²

¹Department of Chemistry, Alagappa govt. arts college, Karaikudi-3

²Department of Mechanical engineering, Sri Raaja Raajan College of Engg., and Technology, Karaikudi.

Email: anuvmrajan@yahoo.co.in

Abstract

Sea water finds extensive application as coolant in various exothermic reactions. Sea water constitutes a rich source of various commercially important chemical elements. Depending upon the metal /environment combinations different types of inhibitors are used in suitable concentrations. Zinc ions have long been considered as valuable corrosion inhibitors for protection afforded by a cathodic polarization mechanism. In present study the effect of aqueous seed extract of lablab purpureus (LPE) and Zn²⁺ in corrosion inhibition of carbon steel in sea water has been investigated in detail. Hence sea water is chosen as the medium for the present study. Several studies have been published on the use of natural products as corrosion inhibitors. It has been reported that "Compound films" formed by phosphate – chromate mixture are more effective than those of either alone [1-3]. The synergistic effect of halides and organic compound inhibitors are reported often in the literature [4-9]. Several inhibitors such as phosphonic acid [10, 11], Thiourea [12], carboxy methyl cellulose [13], Sodium dodecyl sulphate [14] have been used to control corrosion of carbon steel. Inhibitors for carbon steel in near neutral, aqueous solutions are soluble chromates, dichromates, nitrates, borates, benzoates and salts of carboxylic acids. Corrosion inhibition due to the formation of oxide layer on Cu metal surface in concentrated propionic acid and dilute citric acid [15] have been reported. The LPE used in the present study has been found to be effective in corrosion inhibition of mild steel immersed in sea water. The weight loss study reveals that the formulation consisting of 8 ml of LPE and 15 ppm of Zn²⁺ has 99 % inhibition efficiency in controlling corrosion of mild steel in an aqueous solution containing sea water. The UV-Visible spectrum reveals that a protective film is formed on the metal surface. The FTIR spectrum also reveals the formation of a protective film which consists of Fe²⁺- LPE complex.

Keywords: lablab purpureus, inhibition efficiency, protective nano film, sea water

References:

- [1]. F.N. Speller, Proc. ASTM, 36 (1936) 695.
- [2]. T. Prosekl and D. Thierry, Corr., 60 (2004) 1122.
- [3]. A.C. Bastos, M.G.S. Ferreira and A.M. Simoes, Prog. In Org.Coat., 52 (2005) 339.
- [4]. T. Prosekl and D. Thierry, Corr., 60 (2004) 1122.
- [5]. A.C. Bastos, M.G.S. Ferreira and A.M. Simoes, Prog. In Org.Coat., 52 (2005) 339.
- [6]. R.M. Hudson, Q.L. Loony and G.J. Warning, Br. CorrJ., 2(1967)81.
- [7]. R.M. Hudson and G.J. Warning, Corr. Sci., 10 (1970) 121.
- [8]. R.I. Yurchenko, T.N. Pillipenko and I.S. Pogrebova, Russian, J. Appl. Chem., 78 (2005) 511.
- [9]. C.M. V.B. Almedia and B.F. Giannetti, Matls. Chem. Py, 69 (2001) 261.
- [10]. A. Veres, G. Reinhard and E. Kalman, Br. Corr. J., 27 (1992) 147.
- [11]. S. Rajendran, B.V. Apparao, N. Palaniswamy, Anticorr. Metds. Matls., 49 (2002) 205.
- [12]. J.C. Lin, R.Y. Luem, J.S. Wu and S.L. Lee, Proce. 8th Europ. Sym. Corr. Inhibitors (1995) 123.
- [13]. B.V. Meena, Noreen Anthony, K. Mangayarkarasi, S.J. Rajendran., Electroelum. Soc., 50 (2001) 138.
- [14]. S. Rajendran, S. Mary Reenkala and R. Ramaraj, Corr. Sci., 44 (2002) 2243.
- [15]. C.A. Baah, J.I. Baah, Anti. Corr. Metds. Matls., 47 (200) 105.

5.12 Multistep synthesis of newer 3'-(2-methoxyphenyl)-1'H-spiro[piperidine-4,2'-quinazolin]-4'(3'H)-one derivatives and their biological evaluation

P. Sathiaseelan^{ab}, P.Muthuraja^a, Prakash^a and P.Manisankar^{a*}

^aDepartment of Industrial Chemistry, Alagappa University, Karaikudi – 630 003 Tamilnadu, India.

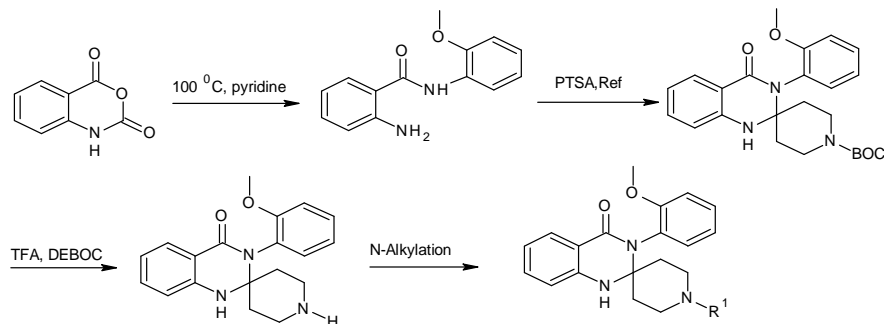
^bDepartment of Chemistry, Bishop Heber College (Autonomous), Trichy - 620017 Tamilnadu, India.

*E-mail: pms11@rediffmail.com, Phone: +91 4565 228836; Fax: +91 4565 225202

Abstract

In the present study, ten new scaffolds of 3'-(2-methoxyphenyl)-1'H-spiro [piperidine-4, 2'-quinazolin]-4'(3'H)-one functionalized with different aryl/alkyl halides were synthesized and computationally evaluated using cheminformatics tools. Newer Spiro piperidine derivatives obeyed Lipinski's rule of five with good biological activity. Three targets among ten showed lesser drug likeness and drug score values compared to other Spiro piperidine derivatives using OSIRIS property explorer. Except these three derivatives, all other synthesized targets act as drugs.

Keywords: Spiro piperidine derivatives, cheminformatics tools, OSIRIS Property Explorer



Reference:

- [1]. Xun-Xiang Guo, Da-Wei Gu, Zhengxing Wu, and Wanbin Zhang, *Chem.Review.* 2015, 115,1622–1651.
- [2]. Hitesh B. Jalani, Amit N. Pandya, Dhaivat H. Pandya, Jayesh A. Sharma, V. Sudarsanam, Kamala K. Vasu , *Tetrahedron Lett.* 2012 ,53 , 4062–4064
- [3]. [Shubhankar Bhattacharyya](#), [Uma Pathak](#), [Sweta Mathur](#), [Subodh Vishnoi](#) and [Rajeev Jain](#) *RSC Adv.*, 2014,4, 18229-18233
- [4]. Wei Xu, Yibao Jin, Hongxia Liu, Yuyang Jiang, and and Hua Fu, *Org Lett.* 2011, 13, 1274-1277.

5.13 Garlic peel derived high capacity hierarchical N-doped porous carbon anode for sodium ion cell

V. Selvamani^a, R.Ravikumar^b, V. Suryanarayanan^{a*}, D. Velayutham^a and S. Gopukumar^{b*}

^aElectrochemical Process Engineering Division, CSIR-Central Electrochemical Research Institute, Karaikudi, 630 006.

^bElectrochemical Power Sources Division, CSIR-Central Electrochemical Research Institute, Karaikudi, 630 006, India.

* e-mail: gopukumar@cecri.res.in & smbtapsun@gmail.com

Abstract

Nitrogen-doped porous carbon synthesised from garlic peel by a simple and cost-effective method has been employed as an anode material for the sodium ion batteries (SIB). The synthesised material has been found to be mesoporous with a high specific surface area (SSA) $\sim 1710 \text{ m}^2 \text{ g}^{-1}$, as calculated with Brunauer–Emmett–Teller (BET) isotherm. Further, Field Emission Scanning Electron Microscopy (FE-SEM) and Transmission Electron Microscopy (TEM) analysis reveal the existence of interconnected micro-pores and voids. The N-doped garlic peel carbon (GPC) exhibits excellent rate capability as well as steady state cycling performance towards sodium and lithium ion shuttlings. Discharge capacities of about 142, 89, 58, 37 mAh g^{-1} have been achieved at various current densities such as 0.5, 1.0, 2.0, 4.0 A g^{-1} respectively in a CR-2032 type Na-ion cell. The high electrochemical performance of the N-doped GPC is mainly attributed to the existence of nitrogen in the carbon matrix and mesoporous structure coupled with a high surface area for accommodating large number of Na ions.

5.14 Preparation, Characterizations and morphological studies of carbonaceous nanoparticle reinforced polymer nano-composites

S. Imthiyas Ahamed¹, R. Janapriyan¹, S. Mohammed Asik¹, R. Mahendran^{2*}, D. Sridharan²,
C. Arunmozhidevan²

¹Department of Chemical Engineering, Anjalai Ammal Mahalingam Engineering College, Kovilvenni - 614 403.

²Department of Chemistry, Anjalai Ammal Mahalingam Engineering College, Kovilvenni-403.

* E-mail: anishmahendran10@gmail.com

The remarkable physico-chemo-mechanical properties of carbon nanotubes make them promising nano-fillers for fabricating polymer nano-composites. In this study, acid treated single walled carbon nanotubes (ATCNTs) were reinforced into sulfonated polyetherimide (SPEI) matrix by solution blending method at various weight ratios of the ATCNTs. The pristine and SPI/ATCNTs composite films were fabricated by phase inversion technique. Hydrophilic groups were incorporated into the CNTs by using nitric acid under ultrasonication and functionalized CNTs were analyzed by FT-IR spectra[1]. The sulfonation of PEI was carried out by using chlorosulfonic acid and analyzed by FT-IR and TGA to conclude the introduction of sulfonic acid

groups in the polymer matrix. The physico-chemical properties of the films were evaluated in terms of ion-exchange capacity, thickness and water uptake is shown

The water uptake and ionic exchange capacity of the films significantly enhanced with respect to the concentration of ATCNTs in the polymer matrix [2], due to the presence of hydrophilic functional groups present in the SPI and functionalized CNTs. Morphological studies of the composite films revealed the agglomeration and dispersion of ATCNTs in the polymer matrix and observed that the agglomeration significantly enhanced by increasing the concentration of ATCNTs in the polymer matrix. Figure 1 shows the FE-SEM images of the SPI-ATCNT 1, SPI-ATCNT 2 and SPI-ATCNT 3 films, which clearly indicate the agglomeration of ATCNTs increased by increasing their concentration by the appearance of tubular shapes of CNTs [3-4].

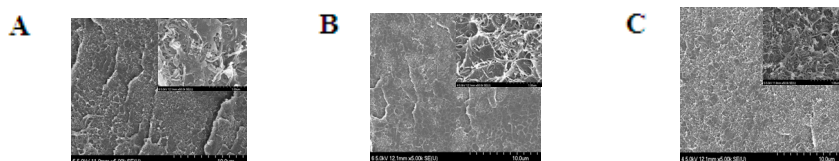


Figure 1. Cross-sectional FE-SEM images of (a) SPI-ATCNT 1, (b) SPI-ATCNT 2 and (c) SPI-ATCNT 3 films.

References

- [1] K. A. Worsley, I. Kalinina, E. Bekyarova and R. C. Haddon, *J. Am. Chem. Soc.*, *131* (50) (2009) 18153–18158.
- [2] X. Zhang, T. Dong, Y. Pu, T. Higashihara, M. Ueda and L. Wang, *J. Phys. Chem. C*, *119* (34) (2015) 19596–19606.
- [3] S. B. Kadambi, K. Pramoda, U. Ramamurty, and C. N. R. Rao. *ACS Appl. Mater. Interfaces*, *7*(31) (2015) 17016–17022.
- [4] J. Zhu, W. Cao, M. Yue, Y. Hou, J. Han and M. Yang, *ACS Nano*, *9* (3) (2015) 2489–2501.

5.15 Preliminary Phytochemical analyses and Antioxidant potential of *Dicranopterislinearis* (Burm.f.) Underw. (Gleicheniaceae)

R. Kalpana Devi Rajesh*, S. Vasantha and A. Panneerselvam

PG and Research Department of Botany and Microbiology, A.V.V.M Sri Pushpam College (Autonomous), Bharathidasan University (Affiliated), Poondi, Thanjavur. *E-mail – kalpanafern@gmail.com

Abstract

Phytochemical analyses and antioxidant potential of *Dicranopterislinearis* (Burm. f.) Underw. was carried out with a view to assess the therapeutic values and or safety of the plant in ethnomedicine. Qualitative phytochemical analyses^[1] was studied in Aqueous, Chloroform, Ethanol, Petroleum ether and Acetone solvent extract to study 13 Phytoconstituents available. Ethanolic fern extracts showed strong positivity to express the 12 phyto-constituents studied except Anthocyanin when compared to other solvent extracts. Ethanolic fern extract showed strong positivity for major phytochemicals like tannin, phenol, flavonoids, terpenoids, quimones and steroids. Chloroform extract performed poorly showing positivity for saponin, phenol and steroids. The Quantitative analysis was performed to quantify, total terpenoids, total tannin, total phenol and total flavonoids and revealed higher concentrations of bioactive constituents comprising terpenoids (97.0 mg/g), total tannin content (30.8 mg TAE/g), total phenol content (28.6 mg GAE/g) and total flavonoid content (8.5 mg QE/g).

Column chromatography were performed using standard protocols. Silica gel (100 - 200 mesh - Fisher Scientific – India) were washed thoroughly using methanol solvent for 3 times. The cleaned silica gel, 10gm of silica gel was carefully poured to column without any air bubbles. Concentrated sample plant extract (10mg/ml) was carefully transferred on to the upper surface of silica gel. The Mobile phase used for extraction was methanol: chloroform (2:1) ratio. The technique to separate the best fraction of fern extract showed maximum antioxidant activity (79.5 %) in fraction V under column chromatography.

Antioxidant activity were determined using DPPH free radical scavenging assay^[2], Hydrogen peroxide scavenging activity^[3] and Ferric Reducing Antioxidant Power (FRAP) reduction assay. The results of DPPH free radical scavenging activity exhibits strong antioxidant activity in ethanolic extract (96.0 %), rather than other four solvent extracts as compared to the standard Butylated Hydroxy Toluene (BHT), Hydrogen peroxide scavenging activity showed 47.45 percentage inhibition of H₂O₂ as compared to the standard Gallic acid and Ferric Reducing Antioxidant Power (FRAP) reduction assay was 141.25 mM Fe (II)/g. The results showed that the plants hold tremendous promise in providing the variable secondary metabolites showing antioxidant property that could enhance the curative process of ill health.

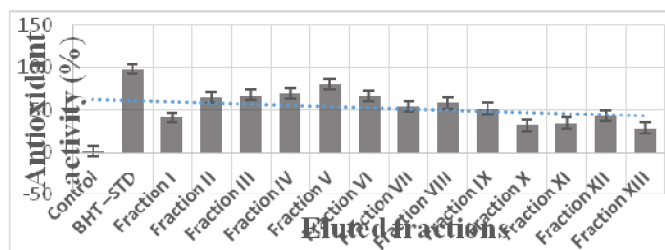


Figure 1. Comparative analysis of various fraction eluted from *Dicranopteris linearis* (Burm. f.) Under solvent extract for antioxidant activity

References

- [1] Savithramma, N., Linga, R.M., Bhumi, G., 2011. J Chem Pharm Res. 3, 2834.
 [2] Lee, C.H., Yang, L., Xu, J.Z., Yeung, S.Y.V., Huang, Y., Chen, Z.Y., 2005. Food Chemistry. 90, 735-741.
 [3] Dehpour, A.A., Ebrahimzadeh, M.A., Nabavi, S.F., Nabavi, S.M., 2009. Grasas Aceites. 60, 405-412.

5.16 Synthesis of phenyl-2-thiocyanatoacrylic acid derivatives

A. Rajan, P. Prakash*

Department of Chemistry, Thiagarajar College, Madurai, Tamilnadu, India. E-mail- kmpprakash@gmail.com

Abstract:

Organic thiocyanates are important synthetic intermediates to access valuable sulfur-containing compounds. Thiocyanate compounds have attracted great attention as interesting intermediates due to its easy transformation into highly valuable molecules applied to both organosulfur and heterocyclic chemistry.¹ Therefore, the synthesis of thiocyanate compounds is the focal point of organic and medicinal chemistry researchers. Herein a simple gram-scale synthesis of 2-thiocyanatoacrylic acid *via* nucleophilic substitution of chloroacetic acid with NH_4SCN in acetonitrile is reported. The reaction proceeds *via* Knoevenagel condensation of 2-thiocyanatoacrylic acid and various aromatic aldehydes in $\text{CH}_3\text{CN}/\text{MeOH}$. The resultant products have been employed for the efficient synthesis of biologically important phenyl-2-thiocyanatoacrylic acid, which was confirmed by UV, IR, $^1\text{H-NMR}$, $^{13}\text{C-NMR}$ spectroscopic techniques.

Keyword: chloroacetic acid, NH_4SCN , phenyl-2-thiocyanatoacrylic acid.

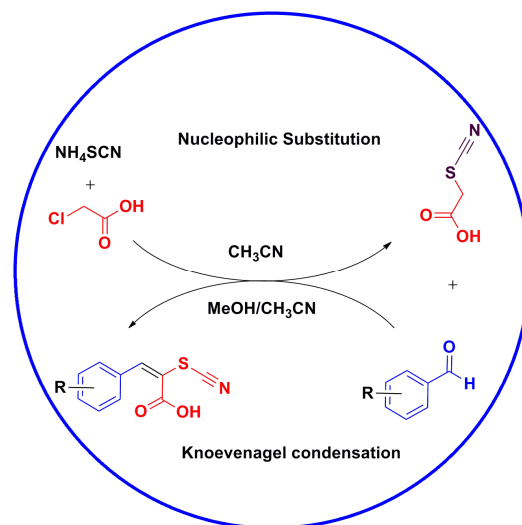


Fig 1: Synthesis of phenyl-2-thiocyanatoacrylic acid

Reference:

- [1]. Fabricio R. Bisogno, Anibal Cuetos, Ivan Lavandera and Vicente Gotor; *Green Chem.*, 2009, 11, 452-454.

5.17 Ionic liquid mediated green synthesis of palladium doped nickel oxide to design efficient catalyst

P. Nithya^a, S. Rajamohamed^b and M. Sundrarajan^{a*}

^a Advanced Green Chemistry Lab, Department of Industrial Chemistry, School of Chemical Sciences, Alagappa University, Karaikudi - 630 003, Tamil Nadu, India.

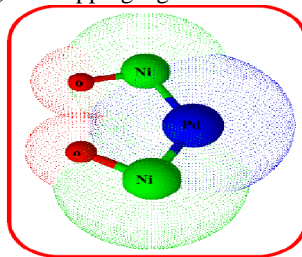
^b Department of Chemistry, Khadir Mohideen Arts & Science College, Adirampattinam - 614 701, Tamil Nadu, India.
Tel: + 91 94444 96151 E-mail: dmsgreenchemistrylab@gmail.com and nithya2291415@gmail.com

Introduction

Green synthesis of nanomaterials finds the edge over chemical methods due to its environmental compatibility. More attention has been devoted on nanoscale magnetic transition metal-based materials, including Fe, Co and Ni due to their superior magnetic properties and their potential applications [1]. Palladium (Pd) described as a good catalyst because of their noble metals inertness, it can adsorb hydrogen and oxygen quite easily and efficiently, and that may be because of their porosity [2]. Herein, we report a facile and eco-friendly method for the synthesis of palladium doped nickel oxide (Pd-NiO) nanoparticles (NPs) using ionic liquid (IL) mediated an aqueous solution of *Justicia adhatoda* (JA), a plant widely found in a large region of India, Sri Lanka as a bio-reductant as well as bio-oxidant. NPs synthesized at room temperature using an ionic liquid (IL) as a mediator for the nucleation and growth process.

Preparation of Pd-NiO catalyst

Palladium doped nickel oxide (Pd-NiO) nanoparticles (structure 1) were prepared by co-precipitation method by nickel chloride used as a precursor with environment benign *Justicia adhatoda* plant extract, palladium chloride and [BMIM] PF₆ (IL) is a capping agent.



Structure 1: Palladium doped nickel oxide nanoparticle

Nickel chloride solution (0.25 N), 0.1 mmol palladium chloride solution and 1 mL of [BMIM] PF₆ (IL) were added to the aqueous solution of *Justicia adhatoda* (JA) plant extract and stirred for 6 hours continuously at room temperature. The resulting samples were filtered, washed with distilled water and dried at 100°C. The powdered sample was calcinated in a muffle furnace at 450°C to get Pd-NiO.

Formation of Pd-NiO NPs and Characterization

The prepared Pd-NiO NPs were characterized by Ultraviolet-visible (UV-vis) spectroscopy, Powder X-ray diffraction (XRD), Transmission electron microscopy (TEM), Energy-dispersive X-ray spectroscopy (EDX), and Fourier transform-infrared spectroscopy (FT-IR). In FT-IR analysis the peaks at 3451, 1552, 1393, 922 and ranges of 425-490 cm⁻¹ indicate the presence of -OH stretching of intramolecular hydrogen bond, C=O stretching and C-C stretching of alkanes, and Ni-O bond stretching vibration respectively [3-5].

The amide linkages between the amino acid residues in the proteins give rise to additional peaks in the infrared region (2900-3700 cm⁻¹) of the electromagnetic spectrum. The bands observed at 3405, 1619, 1392, 1033 and 434 cm⁻¹ have been assigned to stretching vibrations of the primary and secondary amines. The hydroxyl and amine groups of the plant extract JA molecules were found mainly responsible for the reduction and oxidation of Pd and NiO NPs respectively [5-7]. This was confirmed the dual role of the JA, both as a bio-reductant and bio-oxidant. [BMIM] PF₆ (IL) stabilizes the surface of Pd-NiO NPs. In XRD the peak at 45.43°, 43.28°, 62.88°, and 75.47° were conform the crystalline nature and formation of a face-centered cubic structure of the Pd and nickel oxide NPs. Furthermore, the as-synthesized of Pd-NiO NPs demonstrated excellent catalytic activity due to high dispersibility of palladium nanoparticles in to the ferro magnetic nickel oxide NPs [7, 8].

References

- [1] Siavash Irvani, *Green Chemistry*, 13 (2011) 2638.
- [2] L. Zhihua, L. Guojun, H. Phillips, M. Josephine Hill, J. Chang, and A. Ronald Kydd, *Nano Letters*, 12 (2001) 683687.
- [3] H. S. Naiwa Ed., *HandBook of Nanostructural Materials and Nanotechnology*, 15 (2000)
- [4] R. Garima Singhal, B. Kunal Kasariya, A. Ranjan Sharma, Rajendra Pal Singh, *Nanoparticles research*, 13 (2011) 2981-2988.
- [5] F. Davar, Z. Fereshteh, M. Salavati-Niasari, *Journal of alloys and Compounds*, 476 (2009) 797-801.

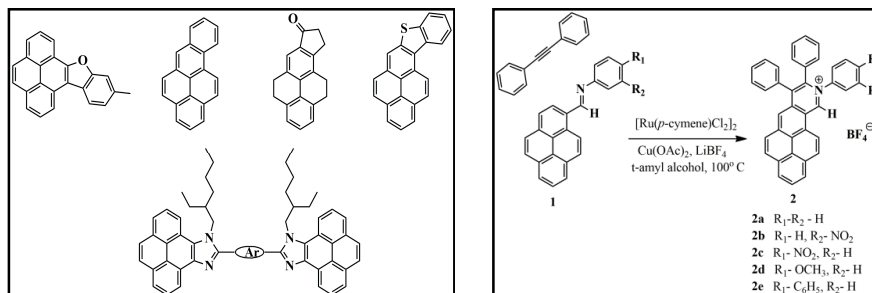
- [6] M. Salavati-Niasari, F. Davar, Z. Fereshteh, *Journal of alloys and Compounds*, **494** (2010) 410-414.
 [7] M. Singh¹, M. Kumar, S. Frantisek, P. Ulbrich, P. Svoboda, E. Santava, M.L. Singla, *Adv. Mat. Letter*, **2** (2011) 409-414.
 [8] W. Szu-Han, C. Dong-Hwang, *Journal of Colloid and Interface Science*, **259** (2003) 282-286.

5.18 Ruthenium (II) Catalyzed Oxidative C-H Activation/Annulation: A Straightforward Route to Pyrene Fused Isoquinolinium Salts

Shanmugam Karthik,^a Joseph Ajantha,^b Shanmugam Easwaramoorthi*^b, Thirumanavelan Gandhi*^a
^aDepartment of Chemistry, School of Advanced Sciences, VIT University, Vellore, 630014, Tamil Nadu, India;
^bChemical Laboratory, CSIR-Central Leather Research Institute, Adyar, Chennai-600020, India
 Email: velan.g@vit.ac.in

Pyrene and its derivatives are versatile π -conjugated PAHs used as a fluorescent probes and organic semiconductors.¹ They are quite famous for its inherent characteristics like high chemical and thermal stability, excimer formation, high photoluminescence,² long fluorescence life time and enhanced charge carrier mobility which make them suitable candidate for optoelectronics. However, its blue light emitting properties is greatly diminished due its high tendency to aggregate i.e., intermolecular π - π stacking at solid state or high concentration, owing to excimer formation, and eventually leading to quenching of fluorescent emission. To overcome this downside, various molecular design strategies have been attempted. This was achieved either by introduction of bulky aryl/alkyl substituents into the pyrene core or incorporating heteroatoms in the extended π -conjugated system of pyrene, thereby overpowering the π - π stacking and enhancing the luminance.

Isoquinolinium cations are one of the most inestimable basis in natural alkaloids³ and are extensively utilized as paints, phase transfer catalyst and insecticides as well as pharmaceuticals.⁴ They are also considered as possible key intermediates for the synthesis of many heterocyclic and bioactive compounds. In recent years, the transition metal catalyzed, directing group facilitated *ortho* C-H bond activation and annulations reactions with alkynes delineated to play a significant role in the synthesis of heterocyclic and polycyclic aromatic hydrocarbons (PAH).⁵



Recently, rhodium and ruthenium catalyzed C-H activation reactions were employed to the synthesis of quinolininium⁶ and cinnolinium salts.⁷ Reports on the synthesis of pyrene-fused heterocyclic compounds are scarce (Scheme 1). In this regard, we wish to establish a straightforward synthetic method for the synthesis of pyrene-fused isoquinolinium salts from pyreneimine and alkynes. Such new isoquinolinium salts may exhibit interesting photophysical properties which will be presented.

Pyreneimines **1** and diphenyl acetylene **4** undergoes catalytic oxidative annulation reaction in the presence of [Ru(*p*-cymene)Cl₂]₂ as catalyst, copper(II)acetate as oxidant, and LiBF₄ as additive in t-amyl alcohol at 100 °C for 24h to give pyrene-fused isoquinolinium salts **2a-2e** in appreciable yields. The synthesized compounds were characterized by spectroscopic techniques such as ¹H NMR, ¹³C NMR, ¹¹B NMR, and HRMS. Detailed studies on photophysical properties of compounds **2a-2e** are in progress.

References

- [1] (a) Mohr, A. et al. *J. Phys. Chem. B*, **2007**, *111* (45), 12985. (b) Cho, H. et al. *ACS Appl. Mater. Interfaces*, **2013**, *5*(9), 3855. (c) Zhang, H. et al. *Chem. Commun.*, **2006**, 755.
 [2] (a) Niko, Y et al. *Tetrahedron* **2012**, *68*, 6177. (b) Sagara, Y. et al. *Adv. Funct. Mater.* **2013**, *23*(42), 5277.
 [3] (a) Laville, R.; Amade, P.; Thomas, O. P. *Pure Appl. Chem.* **2009**, *81*, 1033. (b) Temraz, T. A.; Houssen, W. E.; Jaspars, M.; Woolley, D.R.; Wease, K. N.; Davies, S. N.; Scott, R. H. *BMC Pharmacology*, **2006**, *6*, 10.
 [4] (a) Dehmow, E. V.; Dehmow, S. *Phase Transfer Catalysis, 2nd ed.*; Verlag Chemie: Weinheim, Germany, 1983.
 [5] (a) Duhamel, J. *Langmuir*, **2012**, *28*, 6527, (b) Cho, H.; Lee, S.; Cho, N.; Jabbour, G.; Kwak, J.; Hwang, D.; Lee, C. *Appl. Mater. Interfaces*, **2013**, *5*, 3855.
 [6] Luo, C.-Z.; Gandeepan, P.; Cheng, C.-H. *Chem. Commun.* **2013**, *49*, 8528.
 [7] (a) Muralirajan, K.; Cheng, C.-H. *Chem. Eur. J.* **2013**, *19*, 6198. (b) Zhao, D.; Wu, Q.; Huang, X.; Song, F.; Lv, T.; You, J. *Chem. Eur. J.* **2013**, *19*, 6239.

5.20 Kinetics and thermodynamics of acid catalysed oxidation of dialkyl sulphides by quinolinium dichromate

M.R.K.Hemalatha^a and Dr.T.K.Ganesan^b

^aAssistant Professor, Department of Chemistry, Sri Parasakthi College for Women, Courtallam, Tirunelveli district.

^bAssociate Professor & HOD, PG and Research Department of Chemistry, The American College, Madurai.

Email ID: spc_latha@yahoo.in

Abstract

Introduction: The kinetics and mechanism of oxidation of chromium (VI) has been well studied, chromic acid being one of the most versatile available oxidising agents, reacting with diverse substrates. The development of newer chromium (VI) reagents¹⁻⁶ for the oxidation of organic substrates continues to be of interest. The reagent employed in these investigations, quinolinium dichromate (QDC), $(C_9H_7NH^+)_2 Cr_2O_7^{2-}$ is a useful and versatile oxidant.

Materials and Methods: QDC was prepared by the known literature method⁶. The stock solution was prepared by dissolving QDC in water. The substrates diethyl sulphide (DES), dipropyl sulphide (DPS), dibutyl sulphide (DBS), diisopropyl sulphide (DIPS) and ditertiarybutyl sulphide (DTBS) [TCI, AR] were dissolved in acetonitrile (HPLC grade, E.Merck). Perchloric acid (70%, E.Merck) was the source of H^+ utilized to vary the acid concentration in the reaction media. Kinetics were followed under pseudo-first order conditions at $27 \pm 0.1^\circ C$ spectrophotometrically by measuring the absorbance of QDC at 385 nm in a 1cm cell placed in the cell compartment of LI – 2800 UV – visible spectrophotometer.

Results and Discussion: The stoichiometry of the oxidation of dialkyl sulphides by QDC was found to be 3:2. The reaction order was determined from the plots of $\log k_1$ vs \log (concentration). The order with respect to QDC in the $1.0 \times 10^{-3} - 1.5 \times 10^{-3} \text{ mol dm}^{-3}$ was found to be unity at constant substrate ($[DAS] = 0.02 \text{ mol dm}^{-3}$, acid $[HClO_4] = 0.1 \text{ mol dm}^{-3}$) the order with respect to dialkyl sulphides (DAS) was found to be unity at constant QDC and acid concentration ($[QDC] = 0.001 \text{ mol dm}^{-3}$, acid $[HClO_4] = 0.1 \text{ mol dm}^{-3}$). The effect of perchloric acid concentration was studied between 0.1 to 0.8 mol dm^{-3} at constant oxidant and substrate concentration. The order with respect to acid was found to be 2. The solvent percentage does not affect the reaction rate much. The kinetics was studied at three different temperatures viz. 300K, 308K and 318K. The reaction did not show the polymerization, which indicates the absence of free radical intermediate in the oxidation. The k_2 values for DES, DPS, DBS, DIPS and DTBS in 70:30 (v/v) acetonitrile – water indicate that the reaction is controlled predominantly by steric factor rather than polar effects. The k_2 values are in the order $DES > DPS > DBS > DIPS > DTBS$. Hence k_2 values are analysed in terms of Taft equation and a plot of $\log k$ versus E_s is linear. The acid catalysis of the reaction also supports the mechanism as protonation of oxidant makes it more electrophilic.

Conclusion: The kinetics of oxidation of DES, DPS, DBS, DIPS and DTBS were investigated in acetonitrile – water medium by spectrophotometric method at 300 K. The oxidation of dialkyl sulphides was first order with respect to the dialkyl sulphides and QDC. The reaction was catalyzed by perchloric acid. The reaction did not show the polymerization which indicated the absence of free radical intermediate. The order of reactivity was $DES > DPS > DBS > DIPS > DTBS$.

Keywords: Dialkyl sulphides, Quinolinium dichromate, perchloric acid, oxidation.

Reference:

- [1]. Corey EJ & Schmidt G., Tetrahedron Lett., 20 (1979) 399
- [2]. Bhattacharjee M N, Chaudhuri M K, Dasgupta H S. Roy n & Khathink D T, Synthesis, (1982) 588.
- [3]. Corey EJ, Barette E P & Mariotis P.A., ., Tetrahedron Lett., 24 (1985) 5855.
- [4]. Ciminalle F, Camporeale M, Mello R, Troisi L & Curci R, J Chem Soc Perkin Trans -2 (1989) 417.
- [5]. Sarma GG & Mahanti M K Bull Soc Chim Fr, 128 (1991) 449.
- [6]. Balasubramanian K & Prathibha V, Indian J Chem, 25B (1986) 326.

5.21 Studies on In-Vitro Anti Thyroidal and Antimicrobial Activity of *Aegle marmelos* and *Mukia madaraspatana*

^aK. Murugaiah, ^bR. Venkatachalam, ^cB.Muralidharan

^aResearch Scholar, ^bAssociate Professor, Department of Chemistry, A.V.V.M. Sri Pushpam College, Poondi, Thanjavur

^cBITS, Pilani - Dubai Campus, International Academic City, Dubai-UAE

Email: sdetrkm@gmail.com

Medicinal plants are of great importance to the health of individuals and communities. Medicinal plants have curative properties due to the presence of various complexes chemical substances of different composition. Phytochemicals are secondary metabolites in one or more parts of the medicinal plants. These have the ability to produce a definite physiological action on the human body.

Aegle marmelos(L.) Corr., (Rutaceae) is a popular medicinal plant in the Ayurvedic and Siddha systems of medicine and folk medicines used to treat a wide variety of ailments. The plant, popularly known as the bael tree, is native to the Indo-Malayan region (Hooker JD, 1975) and is currently cultivated in India, Pakistan, Bangladesh, Sri Lanka, Burma and Thailand (Islam R, *et al.*, 1995). The tree is a slender, aromatic perennial, 6.0 – 7.5 m tall and 90 – 120 cm in girth. It flowers from May to July and yields an annual average of 300 – 400 fruits (200 – 250 kg) per tree. Various parts of the tree, including the fruit, possess medicinal properties. The roots are useful for treating diarrhea, dysentery, and dyspepsia (Mazumder, *et al.*, 2006).

Melothria maderaspatana (syn. *Mukia maderaspatana* L.) belongs to the family Cucurbitaceae. The plant is a tendril climber/prostrate herb. The plant was reported to have activities such as hepatoprotective, antirheumatic, diuretic, stomachic (a digestive tonic), gentle aperients, antipyretic and antifatulent, antiasthmatic, antiinflammatory, antidiabetic and anti bronchitis and is used for tooth-ache besides its use in vertigo and biliousness, identification of plants with botanical verifications essential as contamination due to misidentification of planta species or parts in common. Characterizing compound or biomarker is identified from the plant part to assure the identity and quality of the preparation, this need not be responsible for the therapeutic activity. In this present investigation the leaves of *Aegle marmelos* and *Mukia maderaspatana* was collected and extracted using ethanol. The extract was used to evaluate the antithyroidal and anti-microbial activity by *in vitro* methods. The results have been presented and discussed here. There is a growing focus on the medicinal plants use as therapeutic agent because of their limited side effect and retention of appropriate period of activity.

***In-vitro* Anti Thyroidal Activity**

The selected plant *Aegle marmelos* was rich in iodine when compared to *Mukia maderaspatana*. The activity of the enzyme was reduced in presence of the *Aegle marmelos* extract (30.9%) and *Mukia maderaspatana* possess (16.6%) whereas the control contains 40% respectively. In presence of extra iodide recovery in TPO activity was maximum with *Aegle marmelos* when compare to *Mukia maderaspatana* (only 30.9 and 16.6% reduction), moderate.

Many vegetables and plants containing are often consumed but the information on the systemic quantification of different goitrogenic/anti-thyroid components of these vegetables of Indian origin is scanty. Marked variations were noted in the observations apparently for differences in genetic backgrounds and ecological factors and also for presentations of data. Cyanogenic glucosides, glucosinolates and thiocyanate are known as Goitrogenic principles of Cyanogenic plants. Goitrogenic/antithyroidal potential of a plant food depends not only on the nature and the relative concentration for these goitrogenic principles present in it but also on how it is processed as food or the iodine nutritional status of the body.

Raw extract of selected sample reduced TPO activity from 30.9 and 16.6%. Thiocyanate or thiocyanate like compounds primarily inhibit iodine concentrating mechanism of the thyroid, at high concentration thiocyanate inhibits the incorporation of iodide into thyroglobulin by competing with iodide at the thyroid peroxidase level and forming insoluble iodinated thyroglobulin in thyroid²⁴. High concentration of thiocyanate is also responsible for inhibition of TPO catalysed oxidation (I-leads to I²)⁶ while glucosinolates undergo a rearrangement to form isothiocyanate derivatives⁴. Isothiocyanate reacts spontaneously with amino groups to form thiourea that interferes in thyroid gland with organification of iodide and formation of thyroid hormone and this action cannot be antagonized by the iodine. Thus, the *in vitro* inhibition of TPO activity of raw extract seen in the present study appeared to be mediated through thiocyanate or isothiocyanate like anti-thyroid derivatives. In the present study boiled extract of most of the plants studied reduced TPO activity.

***In-vitro* Antibacterial activity**

The evaluation of antimicrobial susceptibility test for *Aegle marmelos* and *Mukia maderaspatana* was conducted for selected pathogenic bacteria and fungus. Five pathogenic bacteria and fungus species were used for this study which was collected from Amphigene Research laboratories. The bacterial species namely *Klebsiella pneumonia*, *Bacillus subtilis*, *Vibrio cholera*, *Proteus vulgaris* and *Enterobacter aerogens* were used to observe the antibacterial activity against the ethanol extract.

The ethanolic extract of *Aegle marmelos* and *Mukia maderaspatana* had high antimicrobial activity against selected bacteria species. The inhibition values of bacterial species against *Aegle marmelos* extract namely, *Klebsiella pneumonia* (12 millimeter), *Bacillus subtilis* (14 millimeter), *Vibrio cholerae* (15 millimeter), *Proteus vulgaris* (17 millimeter), and *Enterobacter aerogens* (15 millimeter) Whereas the *Mukia maderaspatana* leaf extract possess 15 millimeter, 21 millimeter, 22 millimeter, 12 millimeter and 20 millimeter for the above bacterial species respectively.

***In-vitro* Antifungal activity**

The fungus namely *Aspergillus niger*, *Aspergillus fumigates*, *Cunninghamella bertholetiae* and *Penicillium chrysogenum* were used for the following studies and results are recorded and tabulated. The inhibition rate of fungus species against the ethanol extract such as *Aspergillus niger*, *Aspergillus fumigates*, *Cunninghamella bertholetiae* and *Penicillium chrysogenum* are observed and the inhibition rate are

15mm, 18mm, 17mm, 12mm for *Aegle marmelos* whereas the *Mukia maderaspatana* possess 10mm, 14mm, 22mm and 10mm respectively.

This present study shows the Anti-TPO activity of the plant extracts as observed in the present study was consistent with goitrogenic content present in fresh plants. In conclusion, the results showed that the selected plants had in vitro anti-thyroidal activity of selected plant sample, *Aegle marmelos* and *Mukia maderaspatana* possess good activity.

Aegle marmelos and *Mukia maderaspatana* extracts have got profound antibacterial effect and may have the great potential to be used in medicines. An alternative thyroid treatment place more importance on improving lifestyles and nutritional diet, providing spiritual support along with natural thyroid medication and also places a priority on improving functions of other organs that increase thyroid performance. The further study will be carried out for the isolation of bioactive compounds which is responsible for the anti thyroidal activity.

References

- [1]. Hooker JD (1975) The flora of British India. Vol. 1, pp 516–7 Reeve, United Kingdom
- [2]. Mazumder R, Bhattacharya S, Mazumder A, Pattnaik AK, Tiwary PM, Chaudhary S (2006) Antidiarrhoeal evaluation of *Aegle marmelos* (Correa) Linn. Root extract. *Phytother Res* 20, 82–4.
- [3]. Islam R, Hossain M, Karim MR, Joarder OI (1995) Regeneration of *Aegle marmelos* (L.) Corr., plantlets in vitro from callus cultures of embryonic tissues. *Curr Sci* 69, 494–5.

5.22 Primary Phytochemical analysis and Antioxidant activity of *Millingtonia hortensis* Linn., stem bark extracts

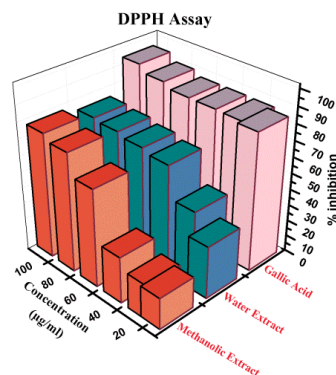
B. Akilanda Easwari and Karuppiyah Muthu*

Department of Chemistry, Manonmaniam Sundaranar University, Tirunelveli – 627 012. TN, India.

E-mail ID: karu.muthu@yahoo.com

Abstract

Millingtonia hortensis Linn., belongs to Bignoniaceae family is commonly known as Indian cork tree, Akash neem, Neem chameli. It is an important medicinal plant in Southern Asia ranging from India, Burma, Thailand and Southern China. The various part of plant has been used as in folklore medicine for the treatment of antipyretic, sinusitis, cholagogue tuberculosis sinusitis, cholagogue, tonic, and asthma. The present study, to determine the primary phytochemical analysis and antioxidant activity of the *Millingtonia hortensis* Linn stem bark extract. The stem bark of *M. hortensis* was extract with increasing order of polarity solvent such as n-hexane, chloroform, ethyl acetate, methanol and triple distilled water (aqueous). The methanol and aqueous extract were screened for in-vitro antioxidant activity by DPPH assay, reducing power assay and hydrogen peroxide radical scavenging assay, nitric acid scavenging assay and total phenolic content respectively. Phytochemical screening revealed that phenols, amino acids, flavonoids, carbohydrates, glycosides compounds are present in methanol and aqueous extract and may be responsible for the activity. It concluded that the methanol and aqueous extract of *M. hortensis* stem bark has moderate antioxidant activity against the standard gallic acid and it can be recommended for the treatment of various diseases.



References

- [1]. R.C. Sharma, A. Zaman, and A.R. Kidwai, *Phytochemistry*, 1968, 7(10), 1891-1892.
- [2]. N. Bunyapraphatsara, G. Blasko, and G.A. Cordell. *Phytochemistry*, 1989, 28(5), 1555-1556.
- [3]. J.B. Harborne, *Phytochemical Methods: A guide to modern techniques of plant analysis*. 3rd edn. Chapman and Hall, New York, 1998, 1–150.
- [4]. K.R. Khandelwal, *Practical Pharmacognosy*, 19th Edition, Pune, India, Nirali Prakashan. 2008, 149–156.
- [5]. S. McDonald, P.D. Prenzler, M. Antolovich, and K. Robards. *Food Chem.* 2001, 73(1), 73-84

5.23 Effect of vigna unguiculata aqueous extract on corrosion inhibition of MS in sea water

K Anuradha¹, R Nandhini², P Govintha Raju² and K Velmanirajan³

¹ Department of Chemistry, Alagappa government arts college, Karaikudi, Tamil Nadu-3,

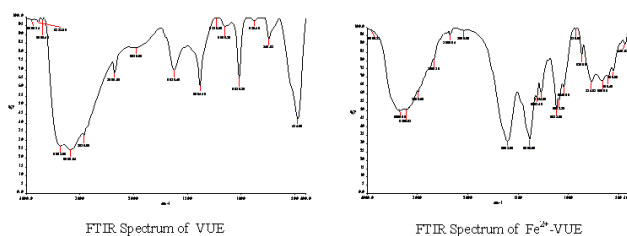
² Research scholar, Department of Chemistry, Alagappa government arts college, Karaikudi-3

³ Department of Mechanical engineering, Sri Raaja Raajan College of Eng.,and Technology, Karaikudi, Tamilnadu.

email: anuvmrajan@yahoo.co.in

Abstract

Sea water constitutes a rich source of various commercially important chemical elements. Sea water finds extensive application as coolant in various exothermic reactions. Depending upon the metal /environment combinations different types of inhibitors are used in suitable concentrations. Zinc ions have long been considered as valuable corrosion inhibitors for protection afforded by a cathodic polarization mechanism. In present study the effect of aqueous seed extract of vigna unguiculata (VUE) and Zn²⁺ in corrosion inhibition of carbon steel in sea water has been investigated in detail. Hence sea water is chosen as the medium for the present study. Several studies have been published on the use of natural products as corrosion inhibitors. It has been reported that "Compound films" formed by phosphate – chromate mixture are more effective than those of either alone [1-3]. Several inhibitors such as phosphonic acid [4, 5], Thiourea [6], carboxy methyl cellulose [7], Sodium dodecyl sulphate [8] have been used to control corrosion of carbon steel. Inhibitors for carbon steel in near neutral, aqueous solutions are soluble chromates, dichromates, nitrates, borates, benzoates and salts of carboxylic acids. Hence sea water is chosen as the medium for the present study. Several studies have been published on the use of natural products as corrosion inhibitors. The VUE used in the present study has been found to be effective in corrosion inhibition of mild steel immersed in sea water. The weight loss study reveals that the formulation consisting of 4 ml of VUE and 10 ppm of Zn²⁺ has 96 % inhibition efficiency in controlling corrosion of mild steel in an aqueous solution containing sea water. The UV-Visible spectrum reveals that a protective film is formed on the metal surface. The FTIR spectrum also reveals the formation of a protective film which consists of Fe²⁺- VUE complex.



Keywords: vigna unguiculata, inhibition efficiency, protective nano film, sea water

References:

- [1]. F.N. Speller, Proc. ASTM, 36 (1936) 695.
- [2]. T. Prosekl and D. Thierry, Corr., 60 (2004) 1122.
- [3]. A.C. Bastos, M.G.S. Ferreira and A.M. Simoes, Prog. In Org.Coat., 52 (2005) 339.
- A. Veres, G. Reinhard and E. Kalman, Br. Corr. J., 27 (1992) 147.
- [4]. S. Rajendran, B.V. Apparao, N. Palaniswamy, Anticorr. Metds. Matls., 49 (2002) 205.
- [5]. J.C. Lin, R.Y. Luem, J.S. Wu and S.L. Lee, Proce. 8th Europ. Sym. Corr. Inhibitors (1995) 123.
- [6]. B.V. Meena, Noreen Anthony, K. Mangayarkarasi, S.J. Rajendran., Electroelum. Soc., 50 (2001) 138.
- [7]. S. Rajendran, S. Mary Reenkala and R. Ramaraj, Corr. Sci., 44 (2002) 2243.

6.1 A study on DNA binding behaviour of a few Schiff base transition metal complexes bearing triazole moiety

Ponya Utthra Ponnukalai and Natarajan Raman*

Research Department of Chemistry, VHNSN College, Virudhunagar-626 001

E-mail: ramchem1964@gmail.com; ponya.phdchem12@gmail.com

Effective Schiff bases comprising of triazole moiety were designed and synthesized. A series of Cu(II), Co(II), Ni(II) and Zn(II) complexes have been prepared. All the synthesized compounds were characterized by various physico-chemical techniques namely, elemental analysis, IR, UV-Vis, ^1H NMR, ^{13}C NMR and magnetic susceptibility. The ^1H and ^{13}C NMR spectral data confirmed the complex formation. The molar conductance data revealed that all the complexes are non-electrolytic in nature. Likewise the synthesized complexes were found to espouse octahedral geometry as shown by the spectral and analytical data. The *in vitro* binding propensity of the Cu(II), Co(II), Ni(II) and Zn(II) complexes with CT-DNA were explored by UV-Vis, Cyclic voltammetry and viscosity measurements. The compounds are subjected to these techniques to reveal the mode of binding of the compounds with CT-DNA.

Generally, there are three types of binding modes viz., covalent, non-covalent and electrostatic binding, out of which non-covalent binding mode is prevalent and much favoured. Further, the non-covalent binding mode is branched into intercalation and groove binding, which is distinguished by the area of the binding of the complexes into DNA structure. The intrusion of the metal complex between the bases of the DNA leads to intercalation whereas the inclusion of metal complex along the groove gives rise to groove binding. The electronic absorption spectroscopy determines the mode of binding and viscosity measurement confirms it by the change in the concentration of DNA after the addition of complex. The variation in the cyclic voltammetric parameters also confirms the intercalation through positive shift of the electrochemical potential. All these investigations when explored in detail on our synthesized Schiff base Cu(II), Co(II), Ni(II) and Zn(II) metal complexes containing 3-amino 1,2,4 triazole strongly evidence intercalation (figure.1) as the binding mode. Thus the preliminary investigations suggest that the complexes possess greater binding efficacy and may be deemed as efficient metallointercalators than the synthesized ligand.

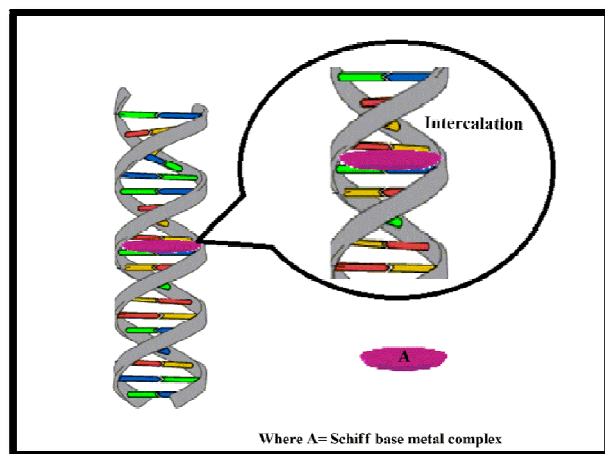


Figure 1. Intercalative binding mode of the synthesized Schiff base metal(II) complex

6.2 Cu(II) Schiff base Metal Complex immobilized on MCM-41 Material as Catalyst for Ullmann-type coupling reactions

M.Malathy, G.Anbarasu and R.Rajavel

Department of Chemistry, Periyar University, Periyar Palkalai Nagar, Salem-636011. drajavel@periyaruniversity.ac.in;

Introduction

Metal complexes with the Schiff bases have been extensively studied because of their attractive chemical and physical properties and due their wide range of scientific applications. Schiff base complexes play a central role in various homogeneous catalytic reactions and the activity of these complexes varies with the type of ligands, co-ordination sites and metal ions. In order to increase the catalytic activity of the Schiff base metal complexes now a day, the anchoring of metal Schiff base complex on mesoporous silica materials has been

developed. Ordered mesoporous silicas are considered as excellent catalyst supports, due to their high surface area, large pore volumes and well ordered arrangement of pores. MCM-41 (pore size 2-3 nm) and SBA-15 (pore size 9 nm) are examples of two well-studied types of mesoporous materials with regards to their use in catalysis. Copper is reported to be active under both homogeneous as well as heterogeneous conditions. Based on the above facts copper Schiff base MCM-41 mesoporous complexes was synthesized, characterization and used as a catalyst for the oxidation of aldehyde.

Results and Discussion

The IR FTIR spectrum of the Cu-Schiff base MCM-41 complex indicates the co-ordination of the ligand with the metal ions through the azomethine nitrogen, phenolic oxygen and chlorine atoms. The FTIR spectra also shows that the hydrogen of the (-OH) may involve in the intramolecular hydrogen bonding between the hydroxyl group oxygen and the nitrogen atom.

The PXRD pattern of the Cu-Schiff base MCM-41 confirmed the mesoporous materials with hexagonal pore arrangement.

The SEM images of Cu-Schiff base MCM-41 complex shows no significant change in the micro structure after the immobilization process had taken place. EDX spectra of the complex show the presence of essential constituents like Cu, Cl along with Si and O, indicates the co-ordination of the compound with the metal ions.

The thermal stability of the catalyst was investigated by thermogravimetric analysis (TGA). The TGA of Cu-Schiff base MCM-41 complex shows that the weight loss occurs when the immobilized complex starts to decompose.

The synthesized Cu-Schiff base MCM-41 catalyst has been successfully applied as a catalyst for Ullmann-type coupling reaction of the aryl halides with aryl halides, phenols, amines and N-heterocyclic amines.

For the coupling reactions the amount of the catalyst, base and the reaction time were set constant. But the reaction was carried out in two different solvents like DMSO and toluene. No product was obtained in the absence of the catalyst. The results revealed that good yield of the product was obtained when the reaction was carried out with DMSO as a solvent. Under this condition the yield of the product was good (85-90 %) and is comparable with the already reported catalytic systems. In the coupling reactions of aryl chlorides with phenols, amines and N-heterocyclic amines, notably low yields of the products were obtained due to the high energy of C-Cl bonds.

6.3 Metal- based biologically active compounds: synthesis, spectral, and biological evaluation of some schiff base metal complexes derived from 2,6-diamino pyridine and cuminaldehyde

R. Jayalakshmi and R. Rajavel*

Department of Chemistry, Periyar University, Salem - 636 011, Tamil Nadu, India.

E-mail: *drrajavelpu@gmail.com, rjchem14@gmail.com

Abstract :

A novel Schiff base metal(II) complexes, ML_2 [$M = Cu$ and Ni], of $(N_2E, N_6E)-N_2, N_6$ -bis(4-isopropylbenzylidene)pyridine-2,6-diamine ligand (HL) containing a hexadentate N_6 -donor system have been successfully synthesized and characterized on the basis of physicochemical techniques. The elemental analysis, molar conductance and spectral studies suggest that metal complexes were electrolytic behaviour(1:1) and octahedral geometry. Schiff base ligand and the metal complexes were tested against Gram positive and negative bacteria.

Keywords: Synthesis, Characterization, Schiff base Metal complexes, Antibacterial activity

Introduction:

The most spectacular advances in medicinal chemistry have been made when heterocyclic compounds played an important role in regulating biological activities. Heterocyclic moieties can be found in a large number of compounds which display biological activity [1]. In this paper we wish to report Synthesis, spectral characterisation and antibacterial studies of metal complexes(Cu(II)and Ni(II)) with 2,6-diamino pyridine and cuminaldehyde.

Results and Discussion:

The analytical and molar conductance data agrees very well with the proposed mononuclear formula and electrolytic nature. Pure ligand showed three intensive bands at 248 nm, 327 nm suggesting the presence of $\pi-\pi^*$ and $n-\pi^*$ transitions. The $\pi-\pi^*$ transition in the complexes (267-276nm) is shifted to a longer wavelength as a consequence of coordination to the metal, confirming the formation of Schiff base metal complexes[2].

Conclusion :

The analytical, molar conductance, vibrational, and electronic spectral study suggested the structures of octahedral arrangement. From the powder XRD datas(Fig 1), we concluded that the Cu complex were nano crystalline structure and the Ni complexe were amorphous nature. The biological activity results solely depend upon the coordination sphere of the central metal ion and the role of the ligand is vital in facilitating the transportation to the target sight.

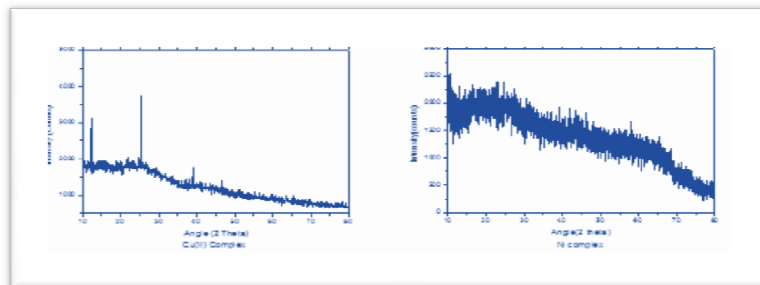


Fig 1 : Powder X-ray diffractogram for Cu and Ni complexes

References :

- [1] T. Rosu, M. Negoiu, S. Pasculescu, E. Pahontu, D. Poirier, A. Gulea, *Eur. J. Med. Chem.* 45 (2010) 774–781.
 [2] S.Y. Uçan, M. Uçan, B. Mercimek *Synth. React. Inorg. Met.-Org. Chem.*, 35 (2005), 417–421

6.4 One-pot synthesis, characterization; HSA and CT DNA binding, *In Vitro* cytotoxicity, and cell imaging studies of surfactant Rhenium(I)-polypyridine complexes

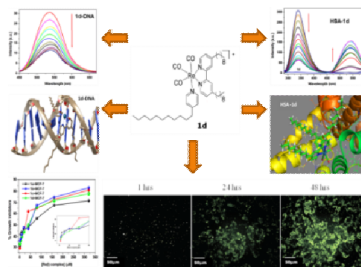
T. Rajendran^{*a,b}, G. Balakrishnan^a, K. Senthil Murugan^a, V.K. Sivasubramanian^{a,c}, M. Ganesan^a, S. Rajagopal^a
^aPost Graduate and Research Department of Chemistry, Vivekananda College, Tiruvadakam West, Madurai-625 234, India.

^bDepartment of Chemistry, PSNA College of Engineering & Technology, Dindigul 624 622, India.

^cDepartment of Chemistry, K.L.N. College of Information Technology, Pottapalayam, Sivagangai 630 611, India

E-mail Address: trajan602012@gmail.com*, mathi1balal@gmail.com

One-pot reaction of $[\text{Re}(\text{CO})_5\text{Br}]$ with 2,2'-bipyridine (**1a**), 4,4'-dimethyl-2,2'-bipyridine (**1b**), 4,4'-di-tert-butyl-2,2'-bipyridine (**1c**), 4,4'-dinonyl-2,2'-bipyridine (**1d**) and 4-Undecylpyridine in dry tetrahydrofuran produced complexes $[\text{Re}(\text{CO})_3(\alpha\text{-diimine})\{\text{py}-(\text{CH}_2)_{10}\text{CH}_3\}]^+$ (**1a-1d**), which were isolated and characterized by ESI-MS and $^1\text{H-NMR}$, IR, UV-vis, and emission spectral techniques. The complexes have been evaluated for their binding affinity with Calf Thymus DNA (CT DNA). The hydrophobic interaction of these complexes with CT DNA is evident from absorption and fluorescence titration experiments. The binding interaction between the complexes **1a-1d** and Human serum albumin (HSA) was studied by absorption, fluorescence and synchronous spectra at room temperature. From the results, it is inferred that complexes **1c** and **1d** had a better binding ability with tryptophan residues of HSA. The *in vitro* cytotoxicity of metal complexes (**1a-1d**) has been evaluated by colorimetric assay (MTT assay). Furthermore, the cellular uptake of complex **1d** has also been studied by laser-scanning confocal microscopy.

**Reference:**

- [1]. G. Balakrishnan, T. Rajendran, K. SenthilMurugan, M. Sathish Kumar, V.K. Sivasubramanian, M. Ganesan, A. Mahesh, T. Thirunalasundari, S. Rajagopal, *Inorg. Chim. Acta* 434 (2015) 51.
 [2]. J. Bhuvaneswari, P. MuthuMareeswaran, K. Anandababu, S. Rajagopal, *RSC Adv.* 4 (2014) 34659.
 [3]. A. Leonidova, G. Gasser, *ACS Chem. Biol.* 9 (2014) 2180.
 [4]. A. Leonidova, V. Pierroz, L.A. Adams, N. Barlow, S. Ferrari, B. Graham, G. Gasser, *ACS Med. Chem. Lett.* 5 (2014) 809.

6.5 Influence of solvent in synthesis of copper(II) biimidazole complex on geometry and Hirshfeld surfaces

^aA. Jayamani, ^aV. Thamilarasan, ^bS. Nagasubramanian, ^aN. Sengottuvelan*

^aDepartment of Industrial Chemistry, Alagappa University, Karaikudi – 630003

^bDepartment of S&H, Sri Raaja Raajan College of Engg. & Tech., Amaravathipur-630301

E-mail: jayamanichem06@yahoo.co.in, nsvelan1975@yahoo.com

Three copper(II) biimidazole complexes $[\text{Cu}(\text{H}_2\text{biim})_2](\text{ClO}_4)(\text{ClO}_4)$ (**1**), $[\text{Cu}(\text{H}_2\text{biim})_2](\text{ClO}_4)_2$ (**2**) and $[\text{Cu}(\text{H}_2\text{biim})_2](\text{ClO}_4)(\text{ClO}_4)$ (**3**) have been synthesized and crystallized using ethanol, acetonitrile and N,N-dimethylformamide (DMF), respectively as solvents. As shown in figure 1, the complex **1** has a five coordinated distorted square pyramid geometry which crystallize in triclinic P_1 space group. The complex **2** has six coordinated octahedral geometry which crystallize in triclinic P_1 space group. The complex **3** has six coordinated octahedral geometry with DMF solvent present in the crystal lattice and crystallize in monoclinic P_21/n space group.

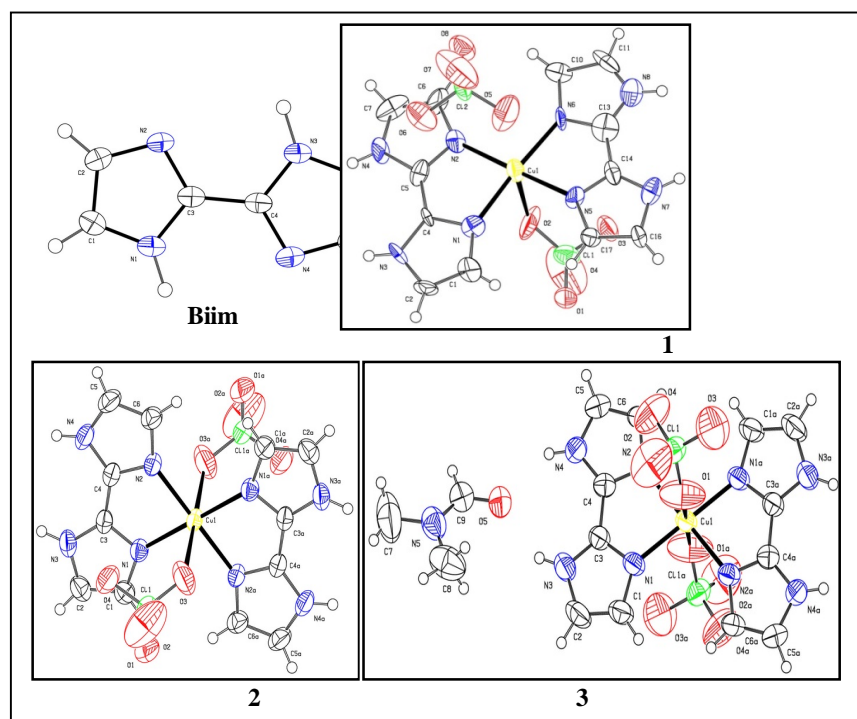


Figure 1. Crystal structures of ligand biimidazole, and copper(II) complexes **1**, **2** & **3**

The main approach was through Hirshfeld surfaces [1], which serves as a powerful tool for elucidating molecular crystal structures, gaining additional insight into polymorphs comparison and identifying common features and trends in specific classes of compounds [2]. Hence we compared the molecular Hirshfeld surface and fingerprint plot analysis of biimidazole in copper(II) complexes **1–3**, with the individual biimidazole, for the purpose of investigating the influence of metals in different environment on the intermolecular interaction around biimidazole. The studies revealed that the solvent molecules for the synthesis of complexes influence the geometry of the complexes and the Hirshfeld surface analysis revealed that the closest contacts of these three complexes were dominated by O–H, H–H, N–H, C–H, π – π (C–C) interactions, and the complexation with copper atom leads to the increase of C–H... π interactions while the decrease of H–H and N–H interactions.

References

- [1] Y.-H. Luo, B.-W. Sun, *Spectrochim. Acta, Part A Mol. Biomol. Spectrosc* 120 (2014) 228.
- [2] Y-H. Luo, Q-X. Mao, B-W. Sun, *Inorganica Chim. Acta* 412 (2014) 60.

6.6 Synthesis, spectral studies and reactivity of Cu(II), Ni(II), Co(II), Zn(II), Cd(II), VO(IV), mixed ligand complexes with 4-oxo-4H-1-benzopyran-3-carboxaldehyde and acetylacetone

V.Pushpa Raja, A. Aarthy Samini, N. Nagarjun C. D. Sheela*

Inorganic DRDO Research Laboratory, Department of Chemistry, The American College, Madurai - 625002.

Email: pushparaj210@gmail.com / arjunchemist92@gmail.com

Abstract

Mixed ligand metal (II) complexes of the type $[ML\{XC(COCH_3)_2\}(H_2O)_n]$ M= Cu^{II}, Ni^{II}, Zn^{II}, Co^{II}, VO^{IV}, Cd^{II}, L=4-oxo-4H-1-benzopyran-3-carboxaldehyde; X=H, Br n=0,1,2 have been prepared and characterized by IR, ¹H NMR, metal estimation, molar conductance, electronic, and mass spectral studies. The conductance data indicates the non-electrolytic nature of the complexes. The halogenations of the parent complexes with N-Bromosuccinimide caused substitution at the γ -position in the acetyl acetone ring. The UV, IR and NMR spectral studies of complexes are consistent with γ -substitution. The redox behaviour of Cu(II) and VO(IV) complexes was studied by cyclic voltametry. The EPR spectrum of Cu(II) complex was recorded at LNT and its salient feature were reported. The in-vitro antimicrobial activity against the bacteria such as *Pseudomonas*, *Staph Aureus*, and fungi *Candida Albican* were studied and compared with that of free ligand by well diffusion technique. The substituted complex shows higher activity than the other compounds. On the basis of above spectral studies it was found Cu(II) complex is square planar, the VO(IV), Zn (II) complexes are square pyramidal while the other complexes (Ni(II), Co(II))are octahedral in geometry.

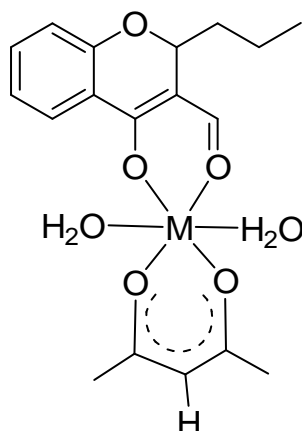


Fig: Metal complexes derived from Formylchromone and Acetylacetone (M= o,Ni,Cu,Zn,Cd,VO)

Reference

- 1) Kavitha.P. Saritha, K. Laxma Reddy, *Journal of Saudi chemical society* 102 (2013)159-168
- 2) Tudor Rosu, Elena Pahontu, *Polyhedron* 29 (2010) 757

6.7 Studies onCu(II),Co(II),Zn(II)complexes of novel Schiff base derived from 2,4-diamino-6-phenyl-1,3,5-triazine and (E)-3-(4-methoxyphenyl)-1-(thiophen-2-yl)prop-2-en-1-one

^aP.Muthukumar, ^aM.Krishnaveni, ^aM.Vathanaruba, ^bP.Tharmaraj

^aDepartment of Chemistry, The American College, Madurai, India -625002

^bDepartment of Chemistry, Thiagarajar College, Madurai, India - 625009

Email: mvruba@gmail.com / mkamc17@gmail.com

Abstract

A Novel Schiff base N,N'-bis(3-(4-methoxyphenyl)-1-(thiophen-2-yl)allylidene)-6-phenyl-1,3,5-triazine-2,4-diamine (BTATA, Fig-1) is synthesized by the condensation reaction of 2,4-diamino-6-phenyl-1,3,5-triazine with the chalcone (E)-3-(4-methoxyphenyl)-1-(thiophen-2-yl)prop-2-en-1-one. Metal complexes of the Schiff base ligand with molecular formula ML_2Cl_2 {where M= Cu(II), Co(II), Zn(II)} have been synthesized by treating the ligand with metal(II) chlorides. The ligand and the metal(II) complexes were characterized by ¹H-NMR, ¹³C-NMR, metal estimation, UV-Visible, IR, EI-Mass and EPR spectral studies. The electrolytic behavior of the complexes is identified from the molar conductance measurements. On comparing IR spectra of the ligand with their metal complexes, stretching band at 1589 cm⁻¹ corresponding to $\nu(C=N)$ group is found to be shifted by 20-10 cm⁻¹ in complexes, indicating the co-ordination of C=N nitrogen. A red shift is observed in

complexes for C-S-C stretching vibration around $823\text{--}810\text{ cm}^{-1}$ in thiophene rings suggested the participation of thiophene $\nu(\text{C-S-C})$ sulphur in coordination [1]. The appearance of non-ligand band in the far IR region at $450\text{--}550\text{ cm}^{-1}$ can be assigned to $\nu(\text{M-N})$ [2] vibration and confirm the interaction between metal and the ligand.

The electronic spectrum of the copper(II) complex exhibits a band at 22935 cm^{-1} which can be assigned to ${}^2\text{B}_{1g} \rightarrow {}^2\text{A}_{1g}$ suggests a square-planar stereochemistry of the compound [3]. The visible electronic absorption spectrum of the cobalt(II) complex shows absorption bands at 16420 and 14792 cm^{-1} which is a typical one for tetrahedral Co(II) complexes. The blue color of the cobalt(II) complex, also suggest tetrahedral stereochemistry. The extended conjugation, the ligand and the complexes are fluorescence in nature.

The electrochemical properties of the metal complexes, particularly with sulphur donor atoms have been studied in order to consider spectral and structural changes accompanying electron transfer. The electrochemical properties of the Cu(II) complex were carried out in the range from $+1.5$ to -1.5 V . The cyclic voltammogram is obtained using a glassy carbon electrode as working electrode and a platinum wire as counter electrode and saturated calomel electrode as reference electrode and tetrabutylammonium perchlorate as supporting electrolyte in DMSO solvent.

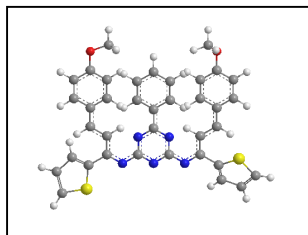


Fig – 1 Structure of the ligand BTATA

The *in-vitro* antimicrobial activity of the synthesized compounds were evaluated against the bacteria such as *Klebsiella Pneumonia*, *Staphylococcus aureus*, *E-coli* and the fungus such as *Candida Albicans* and *Aspergillus Niger* using well diffusion method. The antimicrobial studies reveal that the complexes have more potent activity than the ligand.

References

- [1]. A. P. Mishra, A. Tiwari, Rajendra K. Jain *Adv. Mat. Lett.* **3**(2012)213-219.
- [2]. R. M. Issa, S. A. Azim, A. M. Khedr, and D. F. Draz, *J. Coord. Chem*, **62**(2009)1859-1870.
- [3]. A. B. P. Lever, *Inorganic Electronic Spectroscopy*, Elsevier, Amsterdam (1984)

6.8 Synthesis, Characterization and Antibacterial Study of Ni(II) Complex of 2-(4, 5-diphenyl-1H-imidazol-2yl)-phenol

E. Elanthamilan¹, S. Ebinezer², J. Princy Merlin*, L. Sarala.

*PG and Research Department of Chemistry, Bishop Heber College, Tiruchirapalli-620017, Tamilnadu, India.

Email: elanthamilan1989@gmail.com, ebinezera2d2@gmail.com, pmej_68@yahoo.co.in

Abstract

The ligand 2-(4,5-diphenyl-1H-imidazol-2yl)-phenol abbreviated as DIP were synthesised by the condensation reaction of salicylaldehyde, Benzyl and Ammonium acetate. The complex Ni-DIP were prepared via reaction of $\text{NiCl}_2 \cdot 6\text{H}_2\text{O}$ with DIP. The synthesised ligand (DIP) and complex (Ni-DIP) have been characterised by various analytical (Cyclic Voltammetry) and spectroscopic (IR, UV-Vis, Mass, ^{13}C & ^1H NMR) studies. The synthesised ligand and its Ni^{2+} complex have been screened for their antibacterial activities against two species of bacteria (*Pseudomonas aeruginosa* and *Streptococcus pneumonia*) by well diffusion method. The result showed that the ligand (DIP) is excellent activity than the complex (Ni-DIP).

Key Words: 2-(4, 5-diphenyl-1H-imidazol-2yl)-phenol, Ni^{2+} complex, Antibacterial activity

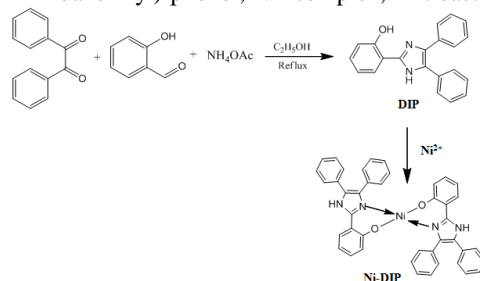


Fig.1. Scheme for the Synthesis of DIP and Ni-DIP.

References

- [1] Florina Ciolan, Luminița Patron, Luminita Marutescu, Mariana Carmenchifiriuc, *Farmacia*, 63, (2015), 86.
[2] Jassim S. Sultan, Sajed M. Lateaf, Dhuha K. Rashid, *Open Journal of Inorganic Chemistry*, 5, (2015), 102.

6.9 Synthesis, DNA interactions and antimicrobial screening of few novel metal(II) complexes with a Schiff base derived from imidazole

Ganesan Kumaravel and Natarajan Raman*

Research Department of Chemistry, VHNSN College, Virudhunagar-626 001

E-mail: ramchem1964@gmail.com; chemistrykumaravel@gmail.com

In the present study, a few imidazole based Schiff base Cu(II), Co(II), Ni(II) and Zn(II) complexes have been synthesized and characterized by elemental analysis, magnetic susceptibility, UV-vis., IR, NMR, EPR and Mass spectral techniques. The molar conductivities of the metal complexes dissolved in DMF (10^{-3} M) at room temperature revealed that all the complexes are electrolytic in nature. The synthesized complexes were found to adopt square-planar geometry as per the spectral and analytical data obtained from UV-Vis data. The EPR spectral data indicate that the exchange interaction is negligible as the observed G value of the Cu(II) complex was greater than 4. The *in vitro* DNA binding studies of all the complexes with CT DNA was carried out by various techniques such as electronic absorption, electrochemical and hydrodynamic measurements which displayed that all the complexes bind to DNA *via* intercalation. Furthermore, the microbial property of the complexes has been verified using disc diffusion method against the Gram-positive bacterial species namely *Staphylococcus aureus* and *Staphylococcus epidermidis*; Gram-negative bacterial species viz., *Pseudomonas aeruginosa*, *Escherichia coli* and *Klebsiella pneumoniae* and the fungal species *Aspergillus niger*, *Aspergillus flavus*, *Culvularia lunata*, *Rhizoctonia bataticola* and *Candida albicans*.

The imidazole based Schiff base was chosen for the investigations owing to its presence in many natural enzymes and proteins, whereas its metal complexes have drawn special attention in the past few decades. They are known to possess powerful antimicrobial activities which were confirmed by the present investigation. The outcome of the *in vitro* antimicrobial screening demonstrated that the complexes possess good biological activity against different microorganisms. The results therefore suggest that all the complexes are better antimicrobial agents than the free ligand.

6.10 Comparative Analysis of Sequences and Predicted Structures of Proteases Produced by *Bacillus pumilus* through *in silico* Approach

Mohana K[#], HariSuthan V[#], Selva Kumar M[#] & Geetha K^{*}

Bioprocess and Downstream Processing Laboratory, Department of Biotechnology, Centre for Research, Kamaraj College of Engineering and Technology, Virudhunagar-626 001, Tamil Nadu, India *geethabt@kamarajengg.edu.in

Extensive sequences of amino acids are cut by proteases into fragments thus regulating many physiological processes. Different proteases have different mode of action, biological processes and consequently also differ in their structures. A total of eight protease sequences from *Bacillus pumilus* was downloaded from NCBI with accession numbers AB211527.1, FJ584420.1, AM748727.1, JXCN01000053.1, JXCO0100017.1, JXCL01000025.1, JXCK01000029.1 and JXCM01000022.1. Physicochemical parameters were computed using ProtParam tool of Expasy (<http://expasy.org/>) server to detect the number of amino acids, molecular weight (MW), isoelectric point (pI), the total number of negatively & positively charged amino acids, instability & aliphatic index & finally, the grand average of hydropathicity. Amino acid number of these proteins ranged from 356-383 with various molecular weight. The range of theoretical pI was identified as 6.71 to 8.75. Variable results were also observed for a number of negatively and positively charged amino acids residues. All the protein sequences showed instability index value of less than 31 stable or unstable and aliphatic index range of 80.08 to 82.32. Wide range of variability was also observed for grand average of hydropathicity (GRAVY) of these proteins.

Superfamily tool on superfamily 1.75 HMM library and genome assessment server were used to find out the family and superfamily of alkaline serine protease protein. The superfamily/family classifications were identified and the physicochemical features were compared through ProtParam. Different superfamilies of protein were found among *Bacillus pumilus*. The alkaline serine proteases were found to contain two domains. The large part of those sequences were related to subtilisin-like superfamily-subtilisins family and the smaller domain was protease pro-peptide/inhibitors superfamily-protease pro-peptide inhibitors family. The secondary structure prediction revealed that the protein consists of 11 α helices and several β sheets. Their topology diagram was generated and depicted in Figure 1.

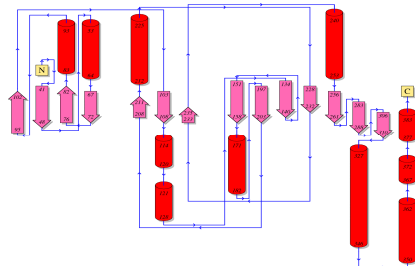


Figure 1: Topology diagram of the *Bacillus pumilis* proteases.

Homology modeling was performed through Protein Model Portal and the quality assessment of these structures was carried out through Ramachandran Plot analysis, Harmony and Prove. The predicted structures were found to be good in quality and no gross or local errors were detected. The structural analysis of all the eight predicted protein structures was carried out using Chimera. The structures of the proteins were overlapped to identify the distribution of active sites. These results will pave way to learn the mechanism of protease action in *Bacillus pumilis*. Further, the proteases will be compared with other classes of bacterial proteases and the uniqueness of the selected group of proteases will be proposed.

6.11 Synthesis of a new series of Cu(II)-Cu(II) homobinuclear and Cu(II)-Zn(II) heterobinuclear side-off complexes: spectral analysis and antimicrobial activity

S. Indira, G. Vinoth and K. Shanmuga bharathi*

Department of chemistry, Periyar University, Salem-11, Tamil Nadu.

E-mail ID: *nksbharathi@periyaruniversity.ac.in, starry.indu@gmail.com.

Abstract

A new class of unsymmetrical compartmental dinucleating ligand was synthesized through the way of Mannich base reactions between the p-tertiarybutylphenol, piperazine and formaldehyde followed by N-methylaniline. Homobinuclear Cu(II) and heterobinuclear Cu(II)-Zn(II) complexes have been synthesized and characterized by elemental and spectral analysis. In the electronic spectra of the homobinuclear complexes a band around 600 nm is due to the d-d transition which is characteristic of square planar geometry. The homobinuclear complexes illustrate an antiferromagnetic interaction (μ_{eff} : about 1.60 BM) at 298K with a broad EPR signal. Variable temperature magnetic moment study of the homobinuclear complexes show $-2J$ value around 190 cm^{-1} . The Cu(II)-Zn(II) complexes have a magnetic moment value close to the spin only value with four hyperfine EPR signals. Electrochemical studies of the complexes reveal that all the binuclear complexes show two irreversible one-electron transfer reduction waves in the cathodic region. Antimicrobial activities were also carried out for the ligands and the complexes.

Keywords: unsymmetrical binuclear complex, side-off, antimicrobial activity.

Introduction:

Involvement of one or more metal ions in various complex biological processes is well established [1]. As an attempt toward this goal, several researchers have synthesized wide varieties of small binuclear copper complexes as models for these metalloproteins and studied their properties on the basis of the spectral, electrochemical and magnetic behaviors of these model complexes [2].

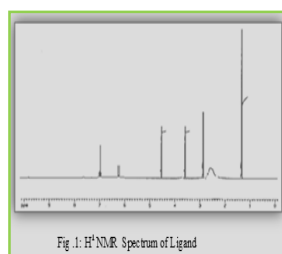
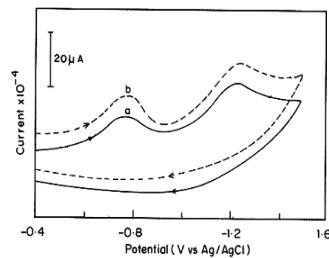
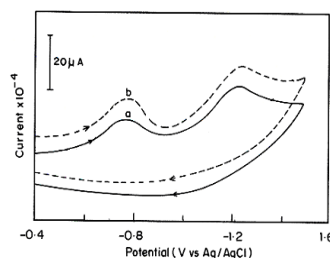


Fig. 1: ^1H NMR Spectrum of Ligand



Results and discussion:

In IR spectrum, the absence of a peak around 3395 cm^{-1} in all the complexes indicates the absence of phenolic $\nu(\text{OH})$ due to deprotonation followed by complexation. The electronic spectra of the ligand were recorded in methanol and it shows an intraligand charge transfer transition at 286 nm Phenolate to metal charge transfer transitions is observed in the range 350-375 nm. The d-d transition for binuclear Cu(II) complexes around λ_{max} at 600 nm is characteristic of square planar geometry. The mass spectrum of the homobinuclear

complex $[\text{Cu}_2\text{L}](\text{Cl}_2)\cdot\text{H}_2\text{O}$ show the molecular ion peak (M^{2+}) at $m/z = 865$. Conductivity values of the binuclear complexes are in the range 150-170 ($\Lambda_m/\text{S cm}^2 \text{mol}^{-1}$) indicating that they are of 1:2 electrolyte types. The cyclic voltammograms for the side-off homo binuclear copper(II) complexes show two step irreversible one electron transfer reductions.

References:

- [1]. Fenton, D. E. In *Advances in Inorganic and Bioinorganic Mechanisms*; Skyes, A. G., Ed.; Academic: London, 1983; Vol. 2, p 187.
 [2]. (a) Casellato, V.; Vigato, P. A.; Fenton, D. E.; Vidali, M. *Chem. Soc. Rev.* **1979**, 8, 199. (b) Sorrell, T. N. *Tetrahedron* **1989**, 45, 3. (c) Vigato, P. A.; Tamburini, S. *Coord. Chem. Rev.* **1990**, 106, 25.

6.12 A Physiochemical Studies of Azo Dyes: DFT based ESIPT process

S. Mohan^a and N. Srinivasan.^{a,b*}

^a Research and Development Centre, Bharathiar University, Coimbatore- 641 046, Tamilnadu,

^b Department of Chemistry, Pachaiyappa's College for Men, Kanchipuram-631 501, Tamilnadu,

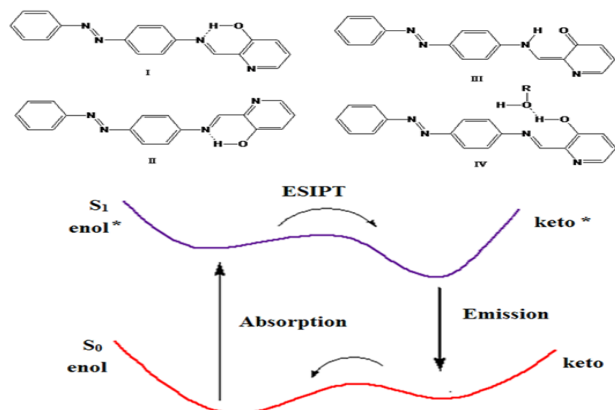
Abstract

Azo compounds are versatile molecules and have received much attention in research in the view of both fundamental and applications. Schiff base ligands are capable of forming stable complexes with metal ions and shows excellent catalytic activity. Atomic emission or mass spectroscopy (ICP-AES, ICP-MS) have been widely used for the detection of heavy metals even at very low concentrations. But these methods are relatively expensive, therefore a series of fluorescence sensors have been developed and development of new fluorescent agents containing chelating groups can help to detect heavy metals more efficiently.

Copper exists in human body, plants and animals in trace amounts; however, high amount can cause serious health problems such as nausea, vomiting and diarrhea as well as damage to liver and kidneys. Therefore, in the view of the biological and environmental importance, considerable attention has been focused on detection of Cu(II) ion by quenching of fluorescence intensity of the employed sensing material.

Metal chelates play an essential role in living organisms and a large number of metal proteins and other metal complexes of biological importance have been studied. Because of the importance of azo-containing Schiff base compounds and in continuance of our previous studies, herein we report a series of azo-linked Schiff bases, their structures were confirmed by elemental, mass, IR and NMR analysis. Photophysical studies of Schiff bases were discussed in detail and the hydroxy Schiff base was developed as a Cu^{+2} selective fluorescence sensor. DFT calculations were carried out by using Gaussian-03 program to supplement the experimental results. An excited state intramolecular proton transfer (ESIPT) in hydroxy Schiff base have been analyzed, found that two distinct ground state isomers of I and II are responsible for the observed dual emission. DFT calculation on energy, dipole moment, charge distribution of the rotamers in the ground and excited states support the ESIPT process

Keywords: NMR, X-ray, ESIPT.



6.13 Studies on Synthesis, Characterization, And Biological Activity of Some Transition Metal Complexes With Isoniazid

S. Radha¹, K. K. Mothilal^{*2}, A. Thamarachelvan³ and A. Elangovan⁴

¹Department of Chemistry, S. B. K. College, Aruppukottai-626101, Tamil Nadu, India

^{*2}Department of Chemistry, Saraswathi Narayanan College, Madurai-625002, Tamil Nadu, India

³Department of Health Sciences, Chettinad Hospital and Research Institute Chennai-603 103, Tamil Nadu, India

⁴Department of Chemistry, Thiagarajar College, Madurai-625009, Tamil Nadu, India

Abstract

A series of five new transition metal complexes of the type, $[M(\text{IAH})_2(\text{H}_2\text{O})(\text{NO}_3)] (\text{NO}_3)$, where M = Mn(II), Co(II), Ni(II), Cu(II), Zn(II) and IAH = isoniazid, have been synthesized with the drug isoniazid (IAH), Nitrate ion and water as ligands. Structural features were obtained from their elemental analyses, molar conductance, IR and UV-Vis spectral, NMR, ESR and Thermal studies. All complexes adopt octahedral geometry around the metal ion. In all complexes, isoniazid was coordinated to the metal *via* N and O atoms. They all show low conductance value indicates non electrolytic nature complexes. The redox properties of the complexes were investigated by cyclic voltammetry. All metal complexes exhibited quasi-reversible single/two electron transfer behavior. The ligand and its metal complexes have been screened for *in-vitro* antibacterial and antifungal properties. The results revealed that all complexes showed significant activity than the parent drug.

Keywords: Isoniazid complexes, Redox behavior, Thermal analysis, Antimicrobial activity.

6.14 Impact of non-aqueous solvent mixtures treatment on the fibre matrix and dyeability of polyester/cotton - a hybrid composite fibre

^aS. Vigneswari, ^bJ. Ethiraj, ^cR. Venkatachalam, ^dV. Ramasamy, ^eG. Gopu and ^fB. Muralidharan

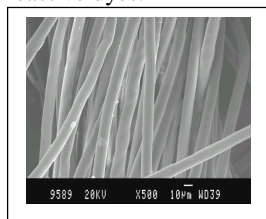
^aDepartment of Chemistry, Raja Duraisingam Govt. Arts College, Sivagangai, T.N., India.

^bDepartment of Chemistry, C. Byregowda Institute of Technology, Kolar, India. ^cDepartment of Chemistry, A. V. V. M. Sri Pushpam College, Poondi, Thanjavur Dt. T.N., India. ^dPeriyar Maniammai University, Vallam, Thanjavur.

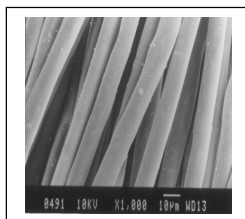
^eDepartment of Industrial Chemistry, Alagappa University, Karaikudi-3, Tamilnadu

^fBITS, Pilani - Dubai Campus, International Academic City, Dubai-UAE. E.mail: vigneswari2020@gmail.com

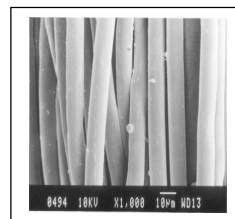
Recent development in textile technologies such as weaving and knitting has resulted in the development of fibre composites with superior handle and mechanical properties. The properties of a composite fibre in addition to their composition can be modified by various physical means. Apart from thermal methods chemical methods also play a key role in making changes in the fibre matrix [1-3]. The present study focuses its attention in terms of treating a hybrid fibre composite i.e. 80:20 Polyester : Cotton blended fabric with Water : Carbon tetrachloride : Sec-Butyl alcohol (W:CTC:sBA = 4.05:91.00:4.95) azeotropic solvent mixture of solvents to improve its physico chemical behaviour. The treated samples were subjected to tearing strength testing, Scanning electron microscopy (SEM), Differential scanning calorimetry (DSC) and X-ray diffraction (XRD) analysis to investigate their mechanical, physical and crystalline properties. The treated and untreated samples were subjected to FTIR studies to study any chemical modification if any was made due to pretreatment. The treated and untreated samples were studied for their dyeing behaviour using disperse and reactive dyes.



SEM photographs of untreated 80:20PCF



W-CTC-sBA - 2 mins pretreated



30 mins pretreated

Conclusion

Tearing strength and weight loss measurements of treated and untreated fibre showed that the solvent treatments have not affected the strength. SEM studies showed that the untreated samples exhibit smooth surface texture. In the treated samples, it appears that as the duration of pretreatment increases, there is progress in attack and erosion propagate inside the fiber resulting in the formation of elongated pits or cavities. This is also supported by the fact that the dye uptake of solvent pretreated composite materials has improved because of development of voids [2,4]. The results from XRD reveals that the solvent treatment disturbs the crystalline distribution, probably creates more cavity and pores resulting in the opening up of the structured assembly [5].

DSC studies shows that the solvent enters into the polymer structure, weakens polymer – polymer interaction, replaces it with polymer – solvent interaction, induces extensive segmental motion and lowers the effective glass transition temperature of material. Results of FTIR studies showed that there is no chemical modification in the polymer. The dyeing method has been found to be time saving with better overall dyeing qualities and cost effective in comparison to conventional methods.

References:

- [1] H. D. Weigmann, M.G.Scott, A.S. Ribnick and R.D. Matkowsky, *Textile Research Journal*, 47(11) (1977)745.
- [2] B. Muralidharan, T. Mathanmohan and J. Ethiraj, *Journal of Applied Polymer Science*, 91(2004)3871.
- [3] Kim Tae-Kyung, Son Young-A, *Dyes and Pigments*, 66 (1) (2005)19.
- [4] B. Muralidharan, S. Vigeswari and S. Laya, *Asian Journal of Textile*, 1(3)(2011) 114.
- [5] H. D. Weigmann and A. S. Ribnick, *Textile Research Journal*, 44(3)(1974)165.

6.15 Synthesis and catalytic activity of novel Cu(II) Schiff base complex immobilized silica

G. Anbarasu, R. Rajavel*

Department of Chemistry, Periyar University, Periyar Palkalai Nagar, Salem-636011, Tamil Nadu, India.

E-mail: drrajavelpu@gmail.com & chemanbarasu@gmail.com

Abstract

Cu(II) Schiff base complex immobilized silica was prepared *via* the one pot reaction of thiophene-2-carbaldehyde with silica functionalized 3-aminopropyltriethoxysilane (APTES) and copper acetate in refluxing ethanol. The formation of this complex was confirmed by FT-IR, XRD, SEM, EDX and ESR analytical techniques. In addition, the catalytic activity of as synthesized Cu(II) Schiff base complex immobilized silica was evaluated through the oxidation of substituted benzylamines to the corresponding imines. The catalyst was easily recovered and reused for next run without any significant loss of its catalytic activity.

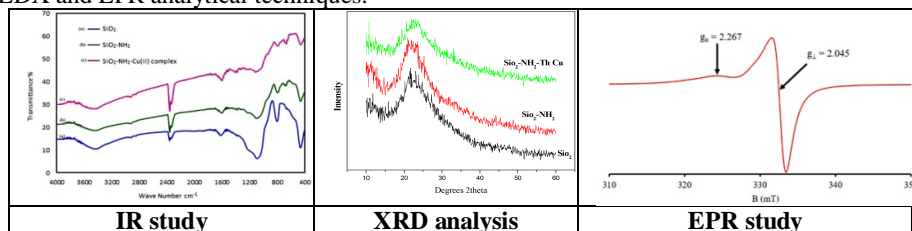
Introduction

In the recent years, transformation of homogenous catalytic process into heterogeneous process involves the anchoring of catalytic active sites on the high surface area of solid support. For this purpose, the immobilization of transition metal complexes on the inorganic and organic supports are one of the better alternatives in the last several decades.¹ Based on this, herein we have synthesized the Cu(II) Schiff base complex immobilized silica and the catalytic efficiency of this catalyst was tested by the oxidation reaction of benzylamines to the imines. Because, imines are important starting material for the synthesis of biologically active compounds such as amides, chiral amines, oxazolidines, hydroxyamines and nitrones.²

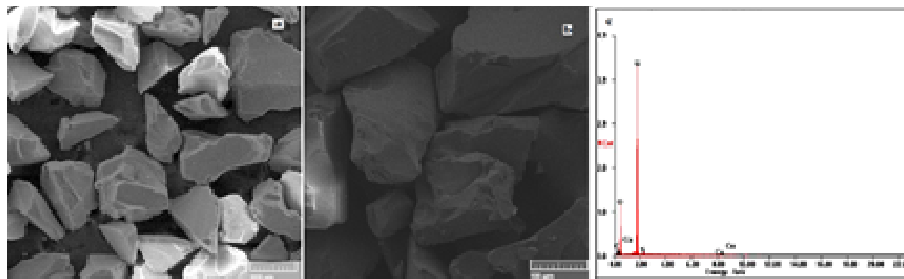
Results and discussion

Characterization of catalyst

The synthesized Cu(II) Schiff base complex immobilized silica was confirmed by IR, XRD, SEM, EDX and EPR analytical techniques.



EPR spectra also proved the presence of Cu(II) ion in the silica functionalized Cu(II) Schiff base complex. The calculated g_{||} & g_⊥ values for the complex were found to be 2.27 and 2.05 indicating the formation of Cu(II) complex.

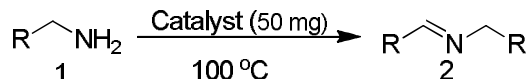


SEM-EDX analysis

By comparing the SEM images of pure silica with Cu(II) Schiff base complex immobilized silica, because of the immobilization of Cu(II) Schiff base complex on pure silica huge surface area was produced and the particle size was also increased. EDX spectrum Cu(II) Schiff base complex immobilized silica also confirmed the presence of copper in the synthesized material.

Catalytic activity

The catalytic activity of the Cu(II) Schiff base complex immobilized silica was evaluated by the oxidation of benzylamines to imines.



In order to optimize the suitable reaction condition for this reaction, initially we have carried out a model reaction of benzylamine in different solvents like ethanol, acetonitrile, toluene, water and benzene under refluxing conditions using 50 mg of Cu(II) Schiff base complex immobilized silica as a catalyst and ethanol was found to be most preferred solvent for this reaction. We have studied the optimum amount of catalyst for this reaction and the product yield was increased with the increasing of catalyst amount up to 50 mg after that remained constant. Under this optimized conditions, we have synthesized a wide variety of imine derivatives in good yields.

Conclusion

In conclusion, we have developed a simple protocol for the synthesis of imine using Cu(II) Schiff base complex immobilized Silica under mild conditions. This material was characterized by FT-IR, XRD, SEM, EDX and ESR analysis. This protocol provides excellent yields in shorter reaction times, mild conditions, easy availability of catalyst and simple work-up procedure are notable advantages of this method. We have also checked the reusability of the synthesized material in this reaction and the catalyst was effectively reused for four times without any change in its catalytic activity.

References

- [1]. F. R. Hartley, Supported Metal Complexes, D. Reiel Publishing Company, Dordrecht, 1985.
- [2]. Nair, V.; Suja, T. D. Tetrahedron 2007, 63, 12247.

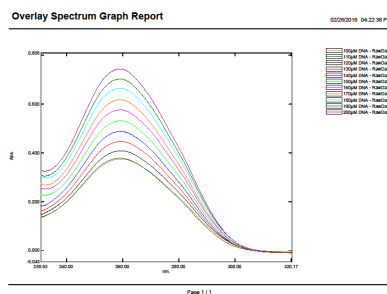
6.16 Synthesis, Analytical, Spectral and DNA Binding Studies of Cu(II) Complex with 1-phenyl-2,3-dimethyl-4-aminopyrazole-5-one and benzoate ion

K.Rajasekar, T. Gomadurai, P. Manikandan, S. Narasimhavarman & B. Sathiyamoorthy
 Department of Chemistry, Government Arts College, Ariyalur-621 713, TamilNadu, India
Yokkesh111@gmail.com and gomadurait@gmail.com

Abstract

Transition metal complex of Cu(II) synthesized from 1-phenyl-2,3-dimethyl-4-aminopyrazole-5-one (4-AAP) and benzoate ion (Benz). Synthesized complex was characterized from their elemental analysis, metal estimation, magnetic moment, molar conductance, IR, UV-Visible and EPR spectral studies. The analytical and spectral data confirmed by the composition of complex. The magnetic moment, UV-Visible, EPR spectral data of the complex suggest a tetragonally distorted octahedral geometry around Cu(II) ion. The non-electrolytic nature (1:0 type) and entry of the ligands into the coordination sphere, functional groups present in the complex were confirmed by the molar conductance and IR spectra. The DNA binding nature of Cu(II) complex with calf thymus DNA (CT-DNA method) was studied by UV-Visible absorption spectral method at 10 different concentrations.

Key Words: 4-AAP, Benzoate ion, Cu(II) complex, EPR, DNA-Binding



DNA-binding absorption spectrum

References

1. N. Raman, A. Kulandaisamy and A. Shanmugasundaram, *Transition Metal Chemistry*, 2001, 26, 131.
2. Paulmony Dharmaraj, Deivasigamani Kodimunthiri, Clarence. D. Sheela and Chappani S. Shanmuga Priya, *J. Seb. Chem. Soc.*, 2009, 74(8-9), 927.
3. B. Anubama, M. Padmaja and C. Gyana Kumari, *E-Journal of Chemistry*, 2012, 9, 389.
4. Pedro M.P.Santos, Alexandra M.M.Antunes, Joao Noronha, Eduara Fernandes and Abel. J.S.C. Vieira, *European Journal of Medicinal Chemistry*, 2010, 45, 2258-2264.
5. N. Raman, S. Johnson Raja, J. Joseph and J. Dhavethu raja, *J. Chil. Chem. Soc.*, 2007, 52(2), 1138.

6.17 Comparative study of biological activity of alanine and valine incorporated schiff-base transition metal complexes

A.Sakthivel, N.Raman, A.Vijayakumar, K.Arunsunai Kumar And A.Sarathi

Department of chemistry, VHNSN College (Autonomous), Virudhunagar – 626 001. Email id: issasakathi@yahoo.com

Abstract

Novel 4-aminoantipyrine incorporating amino acid mixed ligand complexes act as efficient DNA binding and DNA cleaving agents due to the size of the alkyl group present in the amino acid. They are good antimicrobial and oxidative activators. In the present study mixed ligand transition metal complexes of the stoichiometry $[ML(A)_2]$, where $M = Co(II), Ni(II), Cu(II)$ and $Zn(II)$, $L = FFAP$ (furfurylidene-4-aminoantipyrine) and $A =$ amino acid (alanine/valine), have been designed, synthesized.

The synthesized Schiff-base ligand and its complexes of $Co(II)$, $Ni(II)$, $Cu(II)$ and $Zn(II)$ ions were characterized by elemental analysis, molar conductance, 1H -NMR, infrared, electronic spectra and EPR studies. The low molar conductance values of the complexes support the non-electrolytic in nature. In IR spectra, the comparison of shift in frequency of the complexes with the ligand reveals the coordination of donor atom to the metal atom. The mononuclear nature of the complexes is assessed from their magnetic susceptibility values. The electronic and EPR spectra of the metal complexes provide information about the geometry of the complexes and are in good agreement with the proposed Octahedral geometry for complexes.

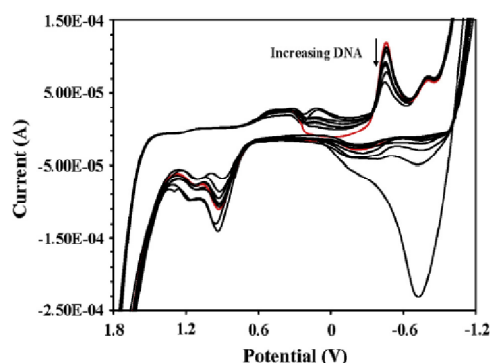


Fig. 1 Cyclic voltammogram of $[Ni(L)(Gly)_2]$ in the absence and in the presence of DNA

The DNA cleavage ability of the complexes was monitored by gel electrophoresis using supercoiled pUC19 DNA. The binding behaviors of the complexes DNA were investigated by absorption spectra, viscosity measurements and cyclic voltammetry.

The interaction of these complexes with CT-DNA indicates that the valine mixed ligand complexes are having higher binding constant than alanine mixed ligand complexes. This analysis reveals that binding constant depends on the size of the alkyl group present in the amino acid. The binding constants of valine mixed ligand complexes are in the order of 10^4 to $10^5 M^{-1}$ revealing that the complexes interact with DNA through moderate intercalation mode. The metal complexes exhibit effective cleavage of pUC19 DNA but it is not preceded via radical cleavage and superoxide anion radical. They are good antimicrobial agents than the free ligand. On comparing the IC_{50} values, $[Ni(L)(Gly)_2]$ is considered as a potential drug to eliminate the hydroxyl radical. The binding constant values (K_b) clearly indicate that valine Schiff-base complexes have very attractive intercalating ability. The results indicate that the complexes bind to DNA through intercalation and act as efficient cleaving agents.

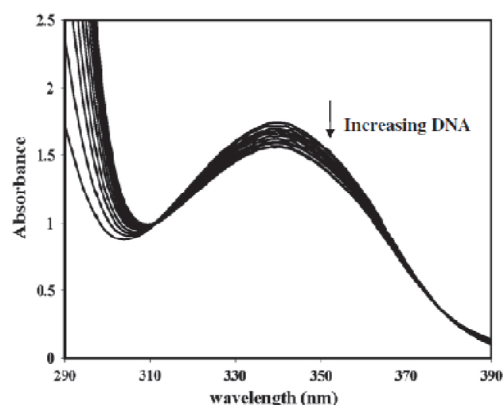


Fig. 2 Electronic spectra of $[\text{Ni}(\text{L})(\text{Gly})_2]$ in the absence and increasing amounts of DNA

The metal complexes were also screened for their antibacterial activities against some pathogenic and non-pathogenic bacterial and fungal strains. The antibacterial and antifungal tests have been carried out using the disc diffusion method. The organisms used in present investigation include the bacteria *Staphylococcus aureus*, *Pseudomonas aeruginosa*, *Escherichia coli*, *Staphylococcus epidermidis*, *Klebsiella pneumoniae* and the fungal species *Aspergillus niger*, *Aspergillus flavus*, *Culvularia lunata*, *Rhizoctonia bataicola* and *Candida albicans*. The effectiveness of the investigated ligand and its metal complexes as good antimicrobial agents has been screened in addition to evaluation of few known antibiotics using streptomycin as standard antibacterial agent and nystatin as antifungal agent. All the complexes are more potent than the ligand towards the specified bacterial and fungal species. Moreover, all the complexes are having antimicrobial activities that are very close to the standard streptomycin and nystatin. Most of the complexes are having better activities towards *P. aeruginosa*, *E. coli*, *S. epidermidis* and fungal species.

References

1. N. Raman, S. Sobha, *Spectrochim. Acta.*, **85A** (2012) 223–229.
2. Z. Guo, R. Xing, S. Liu, H. Yu, P. Wang, C. Li, P. Li, *Bioorg. Med. Chem. Lett.*, **15** (2005) 4600–4603.
3. K. Karaoglu, T. Baran, K. Serbest, M. Er, I. Degirmencioglu, *J. Mol. Struct.*, **922** (2009) 39–45.
4. N. Raman, S. Thalamuthu, J. Dhavethuraja, M.A. Neelakandan, S.J. Banerjee, *J. Chil. Chem. Soc.*, **53** (2008) 1439–1443
5. K. Shanker, R. Rohini, K. Shrivankumar, P. Muralidhar Reddy, Y.P. Ho and V. Ravinder, *Spectrochim. Acta.*, **73A** (2009) 205–211.
6. P. Krishnamoorthy, P. Sathyadevi, A.H. Cowley, R.R. Butorac and N. Dharmaraj, *Eur.J. Med. Chem.*, **46** (2011) 3376–3387.

6.18 Synthesis and spectral characterization of Schiff base complexes of Cu(II), Co(II), Zn(II) and VO(IV) containing 4-(4-aminophenyl)morpholine derivatives: Antimicrobial evaluation and Anticancer studies

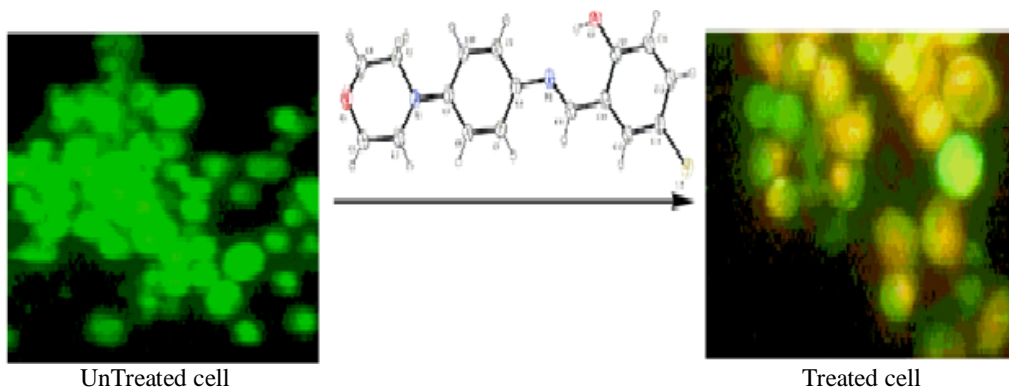
K.Dhahagani^a and G.Rajagopal^{b*}

^aDepartment of chemistry, SACS MAVMM Engineering College, Madurai, Melur 625301, India

^bDepartment of chemistry, Chikkanna Government Arts College, Tiruppur, 641602, India

E-Mail : dhahachem@yahoo.com, rajagopal18@yahoo.com

Abstract: Metal(II) chelates of Schiff bases derived from the condensation of 4-morpholinianiline with substituted salicylaldehyde have been prepared and characterized by ¹H NMR, IR, electronic, EPR, and magnetic measurements. The complexes are of the type $\text{M}(\text{X-MPMP})_2$ [Where M = Cu(II), Co(II), Zn(II), or VO(IV); MPMP = 2-[(4-morpholinophenylimino) methyl] 4-X-phenol, X = Cl, (L₁H), X = Br (L₂H)]. The Schiff bases act as bidentate monobasic ligands, coordinating through deprotonated phenolic oxygen and azomethine nitrogen atoms. The free ligands and metal complexes were screened for their biopotency. Metal complexes exhibit better activity than ligands. Anticancer activity of ligands and their metal complexes were evaluated in human hepatocarcinoma (HepG2) cells. The preliminary bioassay indicates that the Schiff base and its zinc complex exhibit inhibitory activity against the human gastric cancer cell lines.



Key words: Schiff base, Crystal structure, Cytotoxicity Property.

References:

- [1] P.Jaividhya, R.Dhivya, M.A. Akbarsha and M.Palamiandavar, *J.Inorg Biochem.* 114 (2012) 94–105
 [2] X.Y.Qiu, S.Z. Li, A.R Shi, Q.Liand B.Zhai *Chinese J. Struct. Chem.* (2012) 555-561.
 [3] V.T. Kasumo and F. Köksal, *Spectrochim. Acta Part A* 98 (2012) 207-214

6.19 Synthesis, spectral characterization and biological activities of Co^{II}, Ni^{II}, Cu^{II} Schiff base complexes

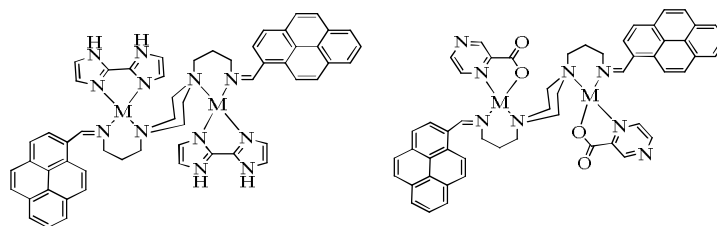
K. Mageswari, R. Regina, A. Surya, V. Thamilarasan, N. Sengottuvelan*
 Department of Industrial Chemistry, Alagappa University, Karaikudi -630 003, India,

Abstract

Metal(II) complexes (**1-6**) such as [Co₂(L)(prz)₂] **1**, [Co₂(L)(biim)₂] **2**, [Ni₂(L)(prz)₂] **3**, [Ni₂(L)(biim)₂] **4**, [Cu₂(L)(prz)₂] **5** and [Cu₂(L)(biim)₂] **6** (where, L = N,N'-bis(pyrenyl)-1,4-bis(3-iminopropyl)piperazine) ligand, prz = pyrazine-2-carboxylic acid, biim = 2,2' biimidazole) were synthesized and characterized. DNA binding properties of the complexes (**1-6**) with calf thymus DNA (CT-DNA) were investigated by UV-visible, fluorescence spectroscopy and computer aided molecular modeling studies. Complexes (**1-6**) exhibit a good binding propensity to bovine serum albumin protein. The ligand and its complexes (**1-6**) have been screened for bacteria such as Gram-positive(G+) (*staphylococcus pneumoniae*, *Bacillus subtilis*) and Gram-negative(G-) (*Escherichia coli*, *pseudomonas aeruginosa*) and fungi (*Aspergillus niger*, *Candida albicans*, *Nigrospora oryzae*, *Trichoderma viride*). Further, the *in vitro* cytotoxic studies of complexes (**1-6**) were tested on human cervical cancer cell line (HeLa).

The intrinsic binding constant K_b of complexes **1 - 6** with CT-DNA obtained from UV-Vis absorption spectral studies were range from 2.65×10^4 - $3.38 \times 10^5 \text{ M}^{-1}$, which revealed that the complexes could interact with CT-DNA through groove binding. The resulting relative binding energy of docked metal complexes **1 - 6** with DNA is found to be -264.52 to -269.30 eV, respectively. The IC₅₀ value of the complexes **1 - 6** is range from 1.36 – 24.2 μM .

Keywords: Metal(II) complexes, Molecular modeling, DNA/Protein interaction, antimicrobial and cytotoxic activities



M = Co, Ni, Cu

Reference

- [1] S. Meghdadi, M. Amirnasr, M.H. Habibi, A. Amiri, V. Ghodsi, A. Rohani, R.W. Harrington, W. Clegg, *Polyhedron*, 2008, **27**, 2771.
 [2] B.A. Uzoukwu, K. Gloe, H. Duddeck, *Synth. React. Inorg. Met. Org. Chem.* 1998, **28**, 819.

7.1 Cellulose aerogel beads: A promising material for future

K. Seeni Meera^{*}, G. Kathirvel, Barbara Milow and Lorenz Ratke

Department of Aerogels, Institute of Materials Research, German Aerospace Centre (DLR), 51147 Cologne, Germany.

^{*}E-mail: kamalmohamed.seenimeera@dlr.de; seenichem86@gmail.com

Telefon: +49-2203 601-4419; Telefax: +49-2203 601-61768

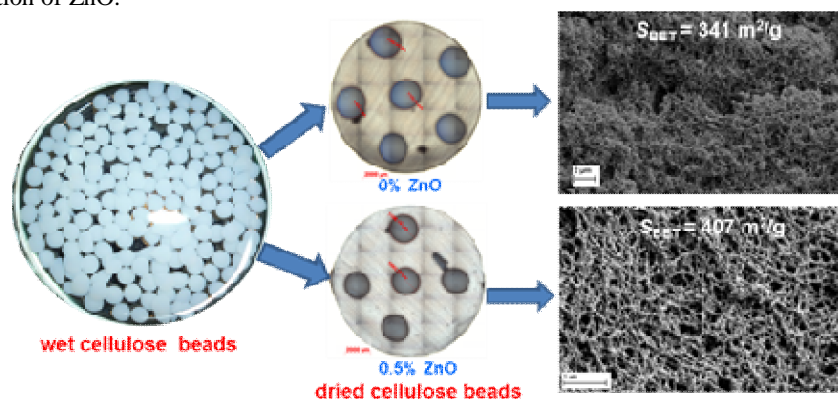
Cellulose is one of the most important polysaccharide, which is available in large quantity in Earth and attracts more researchers in the recent past for the development of new and advanced materials. Cellulose is obtained from various sources like plants (cotton fiber, wood pulp, etc.), animals and bacteria. The most important features and properties of cellulose are high natural abundance, biocompatibility, sustainability, high sorption capacity and hydrophilicity. These excellent properties make cellulose for the development of various types of materials ranging from beads, paper, aerogels, sponges, films, etc. The materials prepared from cellulose have wide applications in various fields like drug delivery, water filtration, biomaterials, separation, etc.

The important form of cellulose is spherical particles or beads called 'cellulose beads'. These beads having particle with diameters in the range of micro- to millimeter scale. These beadshaped particles exhibit several interesting properties like porosity, surface area, density, and fibrous morphology. Microsized beads can be formed by dissolving cellulose in a special solvent and dropping them as beads using a fine nozzle dropper into an anti-solvent followed by regeneration as beads.

The main aim of the present work is to prepare open porous micro-sized beads of cellulose using the mixtures of 7 wt% NaOH and 12 wt% urea with various concentrations of zinc oxide (ZnO). The role and effect of ZnO addition on the properties of cellulose beads were studied using different analytical techniques. It has been observed that such cellulose aerogel beads prepared with lower concentrations of ZnO show shrinkage while drying whereas beads prepared with higher concentrations of ZnO do not exhibit much shrinkage. The dried cellulose aerogel beads were spherical with diameters between 2-2.5 mm.

The skeletal density of all the dried cellulose beads was measured as 1.5 g/cm³. FT-IR spectra reveal that the structure of cellulose I transformed to cellulose II during dissolution and regeneration in a coagulation medium, which was also confirmed from XRD measurements. The beads prepared with NaOH/urea/ZnO aqueous solution exhibit better thermal stability.

We found that the addition of 0.5 wt% ZnO to NaOH/urea mixture greatly increased the surface area of cellulose beads up to 407 m²/g compared to control beads (341 m²/g). Cellulose beads prepared with 0.5 wt% ZnO show higher surface area with large porosity (94%) and increased pore volume of 1.56 cm³/g compared to control cellulose beads (1.48 cm³/g). SEM images indicate that a dense nano-fibrillar network structure was formed in the interior of the cellulose aerogel beads prepared with 0.5 wt% ZnO. These results indicate that the bulk density, surface area, pore volume and pore size of the cellulose aerogel beads can be tuned by changing the concentration of ZnO.



References

- [1]. M. Gericke, J. Trygg, P. Fardim, *Chem. Rev.* **2013**, *113*, 4812-4836.
- [2]. N. Lin, A. Dufresne, *Eur. Polym. J.* **2014**, *59*, 302-325.
- [3]. Q. L. Yang, X. Z. Qin, L. N. Zhang, *Cellulose*, **2011**, *18*, 681-688.
- [4]. L. S. Blachechen, P. Fardim, D. F. S. Petri, *Biomacromolecules*, **2014**, *15*, 3440-3448.
- [5]. K. M. Seeni Meera, K. Ganesan, B. Milow, L. Ratke, *RSC Adv.* **2015**, *5*, 90193-90201.
- [6]. L. Ratke, in *Aerogels Handbook*, eds. M. A. Aegerter, N. Leventis, M. M. Koebel, Springer New York, **2011**, DOI: 10.1007/978-1-4419-7589-8_9, ch. 9, pp. 173-190.
- [7]. S. Hoepfner, L. Ratke, B. Milow, *Cellulose*, 2008, **15**, 121-129.

7.2 Probing the DNA binding and cleavage activities of novel water soluble Cu(II) and Zn(II) complexes having dicarboxylic acids

Ganesan Kumaravel, Narayanaperumal Pravin and Natarajan Raman*

Research Department of Chemistry, VHNSN College, Virudhunagar-626 001. E-mail: ranchem1964@gmail.com

In the present investigation, novel water soluble Cu(II) and Zn(II) complexes were synthesized and characterized by using FTIR, NMR, UV-Vis., elemental analysis, EPR and mass analytical techniques. The molar conductance values indicate that these complexes were non-electrolytes. The UV-Vis. data exhibit that the complexes adopt square-planar geometry. The X-band region EPR spectra of the Cu(II) complexes were recorded in DMSO at LNT. The quoted g factors were relative to the standard marker TCNE ($g = 2.0027$). Frozen solution EPR spectra reveal the axial features ($g_{\parallel} > g_{\perp} > 2.0023$) and suggest a dx^2-y^2 ground state characteristic of square-planar geometry which was axially symmetric. The measure of exchange interaction between the copper centers in the polycrystalline compound can be given by the geometric parameter "G" using relation: $G = (g_{\parallel} - 2) / (g_{\perp} - 2)$. The exchange interaction may be negligible if G is greater than 4. The observed G values of the Cu(II) complexes were 4.12 and 5.02 thereby indicating the negligibility of exchange interaction. The empirical factor $f = g_{\parallel}/A_{\parallel} \text{ cm}^{-1}$ is an index of tetragonal distortion. For small to extreme distortions in square planar complexes, the values of this factor might differ from 129 to 135 which depend on the nature of the coordinated atoms. The f values of the Cu(II) complexes were 159 and 150, indicating significant distortion from planarity. The magnetic moment observed for **1** and **3** are 1.81 BM and 1.83 BM, which are consistent with values expected for copper(II) with the spin $S = 1/2$. The DNA binding studies have been performed using electronic absorption titrations and fluorescence experiments. The experimental evidence reveals that the synthesized complexes interact with calf thymus DNA through intercalation with intrinsic binding constants ranging from 1.3×10^5 to 2.9×10^5 . Moreover, the synthesized complexes have the ability to cleave pBR322 DNA in dose dependent manner.

7.3 A study on extraction of natural dye from bougainvillea bracts and its dyeing properties

J. Ethiraj^{a*}, A.Nagarajan^b, S.Vigneswari^c, G. Gopu^d and B.Muralidharan^e

^aC.Byregowda Institute of Technology, Kolar,India,

^bBangalore Technological Inst. Kodathi Bangalore, India

^cRaja Duraisingam Govt. Arts College, Sivagangai, T.N., India.

^dDepartment of Industrial Chemistry, Alagappa University, Karaikudi-3, Tamilnadu

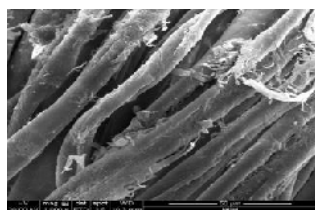
^eBITS, Pilani - Dubai Campus, International Academic City, Dubai, UAE

E.mail: ethiraj96@gmail.com

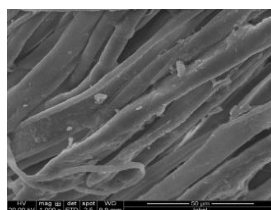
Abstract

Most of the synthetic dyes involve use and release of enormous amounts of hazardous chemicals in the environment during their production and use. Natural dyes are back in use due to their better compatibility with the environment. They are nonhazardous and biodegradable. They possess lower toxicity and allergic property. Thus it is of immense importance to find additional sources of natural dye, which are available in plenty in nature. Majority of synthetic dyes have been found to be carcinogenic and found to cause serious environmental problems and hence are hazardous to mankind. Natural dyes have been found to be eco friendly. The present study deals with extraction of a natural dye from Bougainvillea flower bracts and study of its dyeing behaviour on 100% cotton and 80:20 PET:COTTON using pre mordanting and post mordanting methods at different dyeing temperatures 60°C, 90°C and boil for different time intervals such as 45, 60, and 90 minutes. Potassium dichromate, Potassium permanganate and Ferrous sulphate were used as mordants for dyeing. The dyed materials were assessed for fastness to light, washing, and rubbing. Scanning Electron microscopic study of the dyed samples were also made. The results obtained are presented and discussed.

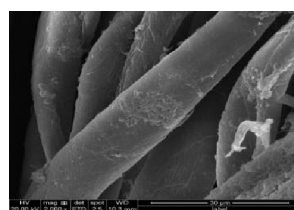
Key Words : Natural Dye, 100% cotton fabric, 80:20 PET:Cotton, Bougainvillea bracts, Mordanting.



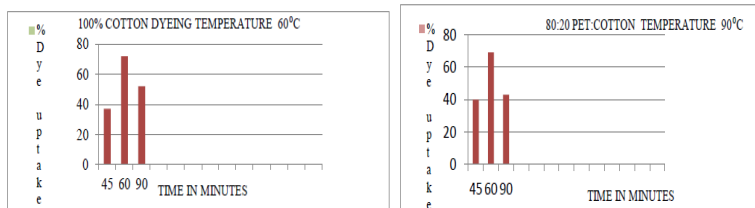
100% COTTON DYED



100% COTTON UNDYED



80:20 PET: COTTON DYED



Conclusion: The present work has been undertaken with a view to study the effect of natural dye extract from boganvillae bracts dyeing on 100% cotton fabric and 80:20 PET: COTTON. The effect of dyeing on various dyeing temperature and dyeing time along with SEM topography, light fastness, wash fastness, computer color matching, rubbing fastness were also subjected. For comparison the undyed fabric was also studied. Studies on surface topography using scanning electron microscope (SEM) shows that the dye enters the surface of the fabric of 100% COTTON and 80:20 PET: COTTON.

References:

- [1]. Lipikachackraborty, supriyachackraborty and C.P.kapse "An Insight to Natural Dyes", *Asian Dyer*. P .36. (2009)
- [2]. B.H.Patel and B.J. Agarwal and H.M.Patel, " Novel padding technique for dyeing Babool dye on cotton", *Colourage*. P 12. (2003)

7.4 Feasibility Studies on the Detection of Onset of Third Phase in the Solvent Extraction Equipment during Reprocessing of Fast Reactor Fuels

M Suba, P.Velavendan, N K Pandey and U Kamachi Mudali

Reprocessing Group, Indira Gandhi centre for Atomic Research, Kalpakkam-603102, India

E-mail address:nkpandey@igcar.gov.in

Fast reactor fuels are reprocessed through aqueous reprocessing route by employing PUREX process (plutonium uranium reduction extraction). This process consist of fuel receipt, chopping, dissolution (nitric acid as dissolvent) and feed clarification, feed conditioning (plutonium valency and nitric acid concentration adjustment), solvent extraction (TBP dissolved in normal paraffin hydrocarbon [NPH] is used as solvent) and partitioning of uranium and plutonium, finally purification and reconversion to respective oxides. During the solvent extraction, process there is a possibility of formation of third phase due to process upsets for example aqueous and organic flow rate variation. This third phase has inherent safety hazard such as criticality and explosion hazard. The criticality hazard is due to the accumulation of fissionable heavy metal ions (plutonium) and explosion hazard due to entrainment of organic phase containing metal ions such as Th and Zr present in aqueous phase this upon waste evaporation circuits. An electrical conductivity measurement based sensor is developed for the detection of formation of third phase in the batch studies [1-2]. The results of this study indicated that third phase (TP) shows higher conductivity as compared to light organic (LO) and homogeneous organic phase (HP) [1]. In order to test the applicability of this conductivity measuring sensor in solvent extraction equipment, simulation experiment extraction studies have been carried out in a single stage mixer settler with and without uranus in nitric acid and 1.09M TBP in NPH is used the solvent as a function of aqueous to organic (A/O) flow ratio.

The conductivity of OPOL was found to be 14-20 $\mu\text{S}/\text{cm}$ at different A/O ratio for 12 M nitric acid feed and this conductivity increased to 460 $\mu\text{S}/\text{cm}$ by changing feed acidity to 15.8 M nitric acid. This is due to formation of third phase and entrainment of the aqueous along with organic phase. Studies with uranus feed indicated for A/O of 0.5 the conductivity of OPOL is around be 11-13 $\mu\text{S}/\text{cm}$ and decreased gradually from 11 $\mu\text{S}/\text{cm}$ to 2.06 $\mu\text{S}/\text{cm}$ with increase of A/O ratio to 1. Conductivity at aqueous and organic phase interface is increased from 2.06 $\mu\text{S}/\text{cm}$ to 170-190 $\mu\text{S}/\text{cm}$. The results of this study is clearly indicated by using two conductivity probes it is feasible to detect the on set of third phase in mixer settler one conductivity probe will be on the organic outlet and another one will be inserted in the aqueous to organic interface therefore it is possible to detect the third phase formation in the solvent extraction equipment.



Figure. 1 Photograph of single stagemixersettler during uranus runs



Figure. 2 Photograph of control unit in experimental study

Key words: conductivity, light phase, single stage mixer settler

References:

- [1]. S Subbuthai, R Ananthanarayann, P Sahoo, A Nageswara Rao and R V Subba Rao, *ibid.*, 295 (2012), 879- 883
- [2]. S. Subbuthai, P. Sahoo, A Nageswara Rao and R. V Subba Rao, *Journal of Radio analytical and Nuclear Chemistry*, 295 (2013), 943-49

7.5 Decolourization and detoxification of distillery spent wash using bacterial consortia – Confirm through structural changes and Ao-Eb fluorescence

Tamilselvi duraisamy¹, Ramarajan selvam², Selvakumar muniraj³, Habibunisha mubarakali⁴ and vasanthymuthunarayanan^{1*}

Department of Environmental Biotechnology, School of Environmental Sciences, Bharathidasan University, Trichirappalli – 620024. tamildhurai@gmail.com

Abstract:

Aim of this study is to isolate the bacterial colonies from the untreated distillery spent wash and enhanced the growth rate of selected bacterial colonies in the suitable medium. The selected strains grow rapidly until they achieved a sustained density of the broth medium in ppm concentrations. The optimal decolourization of melanoidin was achieved at pH7 and temperature is 37°C. The toxicity evaluation with mung bean (*Vigna radiata*) using two concentrations 1% and 5%. It revealed that the raw distillery effluent was environmentally highly toxic as compared to biologically treated distillery effluent.

The isolated bacterial strains (*Pseudomonas* sp., *Bacillus* sp., and *Proteus* sp.) having the ability to degrade and detoxification of melanoidin from the distillery effluent. Catalase production was increased during the process to enhance decolourization of the effluent. Degradation of melanoidin was analyzed by using UV-Visible Spectrometric at 570nm. In HPLC, retention peak reveals the melanoidin reduction and increases of microbial population during the incubation period. Scanning Electron Microscopy showed well structural changes in the 1% and 5% untreated and treated effluent. Finally, fluorescence confirms the growth production of bacterial strains and species identification through confocal microscopy.

The main interest of recycling water is to be related with the management of the effluents by reducing fresh water consumption and waste water treatment costs, small disposal volumes which will minimize the waste disposal costs and reduction. Melanoidin is a water soluble recalcitrant compound which gives color to the distilleries and fermentation industries waste water (Arora et al., 1992). Non enzymatic amino carbonyl reactions produce brown colored pigment called melanoidin, which is known as maillard reaction. High amounts of antioxidants present in melanoidin are found to be the reason for the toxicity to the microorganisms (Chavan, 2006).

Microbiologically, the distillery effluent was reported to be flourishing with a variety of potential microbes (Bacteria). Hence the study reveals that the indigenous microbes have great potential and are likely to be used as bioremediation agents for distillery effluent. Initially screening of 3 different bacterial strains were done in liquid cultures and were used as consortium for biosorption experiments and they have showed different decolourization ability. There was an increase in the decolourization percentage of the medium containing effluent day by day. Decolourization and degradation of distillery spent wash has been a severe environmental concern (Dahiya et al., 2001). The recalcitrance of melanoidin compounds escape various stages of waste water treatment plant and finally, enter the environment. Inspection of literature specified that there is only little study in microorganisms as pollution alleviators and there is none on degradation of melanoidin. The minimum percentage in the consortium was observed at the first day by 14% and it increased up to 95% on the eighth day.

Similarly among the individual cultures the S3 culture was better for decolourization as it went up to 91% of decolourization followed by the S1 with 87% and S2 with 79%. Further up to 100 % germination of *Vigna radiata* was observed with treated wastewater and control (pure water), whereas, only 50 and 10 % germinations were observed for wastewater having dye concentrations 100 and 1,000 mg/l, respectively. The HPLC analysis of dye before and after degradation has five peaks during the retention time 3.00 and 6.50 min, whereas degradation products showed peaks at lower retention time, probably due to degradation of dye into small intermediate products. The consortium has fluoresced well than the individual cells in the 1% treated effluent.

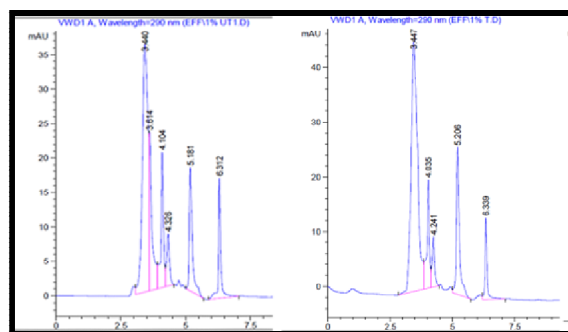


Fig 1. Decolorization of melanoidin in untreated and treated effluent in distillery spent wash.

References

- [1] Arora, M., Sharma, D.K., Behera, *Resources, conservation and recycling*(1992), 347 – 353.
 [2] Chavan, M.N, Kulkarni M.V, Zope V.P, Mahulikar P.P, *Indian journal of biotechnology* (2006),416-421.
 [3] Dahiya , J., Singh , D., Nigam , P ., *Bioresource Technology* 78 (2001), 111-114.

7.6 Biocatalytic Cascade Synthesis of Fine Chemicals-Bio-inspired Metabolic Pathway

Saravanakumar Shanmuganathan

School of Basic & Applied Sciences, Department of Chemistry, Central University of Tamil Nadu, Tiruvarur.
saravanakumar.shanmuganathan@gmail.com

The concepts of green chemistry and sustainable development have become a strategic focus in both the chemical industry and the academic community at large [1]. A prominent feature of this drive towards sustainability is the widespread application of chemo - and biocatalytic methodologies in chemicals manufacture. The key to successful implementation of catalytic methodologies in fine chemicals manufacture is the integration of catalytic steps in multi – step organic syntheses and downstream processing. [2] The ultimate in integration is to combine several catalytic steps into a one - pot, multi - step catalytic cascade process [3]. This is truly inspired by Nature where metabolic pathways conducted in living cells involves an elegant orchestration of a series of enzymatic steps into an exquisite multi - catalyst cascade, without the need for isolation of intermediates [4]. Here I present my work on one – pot multi – step bio-catalytic reactions.

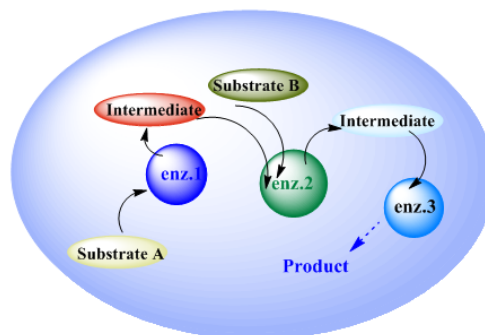


Figure 1. Metabolic Pathway Inspiring Enzymatic Cascade reactions

References

- [1] E.García-Junceda in *Multi-Step Enzyme Catalysis – Biotransformations and Chemoenzymatic Synthesis*, ed. S. G. Burton and M. le Roes-Hill, Wiley-VCH, Weinheim, (2008), pp 41–58.
 [2] H. C. Hailes, P. A. Dalby and J. M. Woodley, *J. Chem. Technol. Biotechnol.*, 82 (2007) 1063.
 [3] P. Domínguez de Marí and S. Shanmuganathan, *Curr. Org. Chem.*, 15 (2011) 2083.
 [4] (a) S. Shanmuganathan, D. Natalia, L. Greiner and P. Domínguez de Marí, *Green Chem.*, 14 (2012), 94; (b) S. Shanmuganathan, D. Natalia, A. van den Wittenboer, C. Kohlmann, L. Greiner and P. Domínguez de Marí, *Green Chem.*, 12 (2010) 2240.

7.7 Effects of dopant HNO₃ on the properties of lead nitrate oxidized polyaniline composite prepared via solid-state polymerization

S. Suganya, J. Dominic, P. Karthikeyan, R. Gowshalyadevi, V. Mangala Gowri and K. K. Satheesh Kumar*
Department of Chemistry, The Gandhigram Rural Institute – Deemed University, Gandhigram – 624 302, Tamil Nadu, India.

*Email: k.k.satheeshkumar@ruraluniv.ac.in / suganya11493@gmail.com Tel.: +91-451-24523771

Abstract

The effects of dopant HNO₃ on the properties of PAN-Pb composite were investigated. PAN-Pb composites were synthesized with the fixed molar ratio of oxidant : monomer (1.25:1), a series of PAN-Pb composite were made by varying the amount of HNO₃ from 0.4 to 1.2 ml at the beginning of solid-state polymerization. The structure and morphology of the samples were characterized by FT-IR, XRD, SEM and Conductivity. It was found that the amount of HNO₃ i.e dopant affects the properties of the synthesized PAN-Pb composite. A maximum electrical conductivity of 0.344×10^{-3} was achieved with the addition of 0.8 ml of HNO₃ at the beginnings of solid-state synthesis of PAN-Pb composite.

1. Introduction

Conducting polymers (CPs) are an innovative material because of their chemical, mechanical, physical and electronic properties [1]. It is an organic material that conducts electricity and has extended π -bonding systems. These polymers are used in many potential applications like electronic devices, sensors, electrodes, super capacitor, electromagnetic shielding, corrosion inhibition [2] and adsorbent etc. PAn has been synthesized either chemically or electrochemically. The most common oxidant was Ammonium persulphate. The other oxidants used are K₂Cr₂O₇, K₂S₂O₈, H₂AuCl₄, FeCl₃, Cu(NO₃)₂, CuSO₄, PbO₂, etc. The conductivity and processability of PAni-Pb can be adjusted through the selection of a suitable dopant and the varying of the oxidation states. In this present study, we have successfully synthesized PAni-Pb composite by solid state polymerization of aniline using lead nitrate as an oxidant and by varying the amount of HNO₃ from 0.4 to 1.2 ml at the beginning of the solid-state polymerization. Recently, solid-state polymerization method attracts more attention due to low cost, reduced pollution and simplicity in processing and handling. The obtained PAni-Pb composites were characterized by FT-IR, EDAX, XRD, SEM and conductivity measured by using the four-probe technique.

2. Synthesis of PAni-Pb

A typical solid-state synthesis of PAni-Pb composite with nitric acid was as follows: 2ml of aniline and 1.4ml of HNO₃ were grinded to mix each other in the mortar. After grinding, the mixture became a white paste and 8.8g of lead nitrate was added and then 0.4ml of HNO₃ was added slowly and continuously grinded for 6hr. Finally, the colour of the powder changes to dark green. The dark green powder was washed with ethanol and deionized water repeatedly until the filtrate was colourless. The obtained PAN-Pb was dried in air oven at 60 °C for 24 hr. The obtained PAni-Pb was labelled as PAni-Pb (1). The same procedure was repeated by changing the amount HNO₃ from 0.6-1.2 ml and the synthesized polymers were labelled as follows: PAni-Pb (2), PAni-Pb (3), PAni-Pb (4) and PAni-Pb (5) respectively.

3. Characterization

Particle size and the morphology of the composites were examined by Scanning electron microscope (VEGA3TESCAN). Infrared spectra were recorded using FT-IR spectrophotometer (JASCO 460 PLUS) to identify the chemical structure of the composites. The conductivity of the composites was measured by using the four-probe technique.

4. Results and discussion

The formation of conducting PAni-Pb composite was confirmed by FT-IR spectra. Fig.1 (a-e) shows the FT-IR spectra of PAN-Pb composite obtained by solid-state polymerization method. The main characteristics peak positions of all PAN-Pb are almost same. The broad band at ~ 3431 to ~ 3464 cm⁻¹ is attributed to the N-H stretching vibration, ~ 803 to ~ 814 cm⁻¹ is arisen to stretching of the aromatic C-H bond. The two bands appear at ~ 1554 to ~ 1565 cm⁻¹ and ~ 1496 cm⁻¹ correspond to the stretching vibration of quinoid and benzenoid ring respectively. The presence of characteristic bands confirms that all PAN-Pb composite is in conducting emeraldine state. The XRD patterns of the PAN-Pb composites were shown in Fig.2. The diffraction peak at $2\theta=24.9^\circ$ arises from the periodicity perpendicular to the polymer chain. The peak at $2\theta=20.5^\circ$ is caused by the periodicity parallel to the polymer chain [3]. The polymer chain (or) characteristic distance between the ring planes of benzene ring in adjacent chains and the close-contact interaction distance as reported of 19.4 \AA is in good agreement with the standard JCPDS values (JCPDS-36-1462) which proves the existence of cubic primitive nature of lead nitrate present in the polymer chain. Fig.3 represents the SEM of PAN-Pb (3). It is well known that the morphology of PAni depends on the polymerization and temperature. As can be seen from the SEM, the formed particle are irregular in shape. Fig.4 shows the elemental compositions of the PAN-Pb (3) composite was found to be C-71%, N-11.85%, O-10.16%, Pb-6.99%, which confirms the formation of PAN-Pb composite. The electrical conductivity of PAN-Pb composite was found to be in the order of PAN-Pb (1) < PAN-

Pb (2) < PAn-Pb (3) > PAn-Pb (4) < PAn-Pb (5).

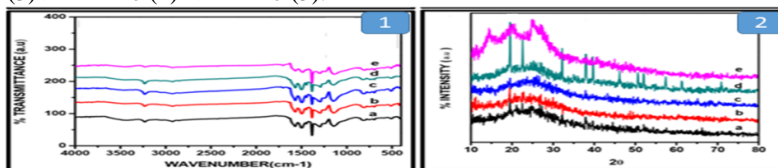


Fig.1 FTIR spectra and Fig.2 XRD patterns of (a) PAni-Pb (1) (b) PAni-Pb (2) (c) PAni-Pb (3) (d) PAni-Pb (4) and (e) PAni-Pb (5) composites

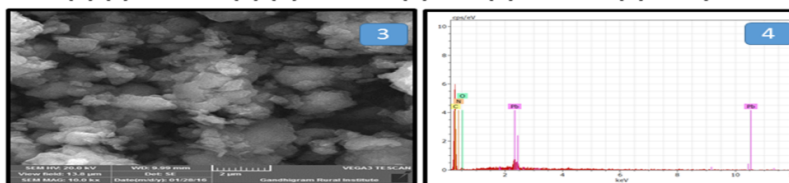


Fig.3 SEM image of PAni-Pb (3) composite

Fig.4 EDAX analysis of PAni-Pb (3) composite

4. Conclusion

In this work, the effect of dopant HNO_3 on the properties of PAn-Pb composite were investigated. These composites were characterized by FT-IR, XRD, SEM, EDAX and Conductivity measurements. The results show that the addition of HNO_3 significantly affects the properties of PAn-Pb composite.

Acknowledgement

One of the authors, **S. Suganya** thanks Department of chemistry, The Gandhigram Rural Institute - Deemed University, Gandhigram for providing lab facilities.

References

- [1]. A.H. Gemeay, I.A. Mansour, Rehab G. El-Sharkawy, A.B. Zaki, *European Polymer Journal*, 41 (2005) 2575
- [2]. D. C. Trivedi, In H.S. Nalwa (ed), Handbook of organic conductive molecules and polymers, Vol.2, *John Wiley, New York*, (1997) p 505.
- [3]. Tang Q, Wu J, Sun X, Li Q, Lin J. Shape and size control of oriented polyaniline microstructure by a self-assembly method. *Langmuir* 25 (2009) 5253

7.8 DPPH radical scavenging antioxidant analysis of leaf extracts of *Dodonaea viscosa*

M. Anandan and H. Gurumalles Prabu*

Department of Industrial Chemistry, School of Chemical Sciences, Alagappa University, Karaikudi -630 003, India

* Tel.: +919443882946; Fax: +91 4565225202 E-mail: hgprabu2010@gmail.com, hgprabhu@alagappauniversity.ac.in

Abstract

Antioxidant activity is one of the promising medicinal activities in most of the plant materials. The aim of this research is to understand the nature of phenolic group responsible for the antioxidant activity. The antioxidant test samples were derived from the extracts of *Dodonaea viscosa* plant source using different solvents. The extracted samples of *Dodonaea viscosa* were subjected to simple preliminary chemical analyses and the results gave positive presence of flavonoids, phenols, quinones, terpenoids, anthraquinones and carbohydrates. UV-VIS analysis discloses that a prominent peak around 660 nm was observed in the extract. FT-ATR results revealed the presence of variety of phytochemicals in the extracts.

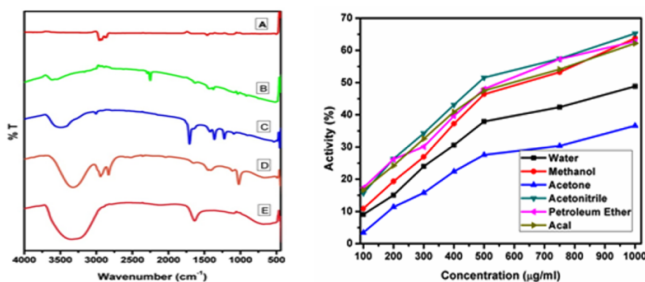


Figure 1. FT-ATR spectrum of extracts obtained from (A) Petroleum Ether, (B) Acetone, (C) Methanol, (D) Acetonitrile, (E) Water; Figure 2. Antioxidant activity of the extracts obtained from Petroleum Ether, Acetone, Methanol, Acetonitrile, Water and ascorbic acid

FT-ATR results showed broad peaks at 3344 , 1450 cm^{-1} and sharp peaks at 2946 , 1647 , 1112 , 1017 cm^{-1} responsible for the O-H stretching, O-H bending, C-H stretching, C=O stretching, C-O-C bending and N-H bending vibrations respectively for the active components present in the crude extracts of *Dodonaea viscosa* [1]. Antioxidant activity of *Dodonaea viscosa* leaf extracts were assessed by DPPH radical scavenging method [2, 3,

4]. Solvents of different polarity were used to obtain the extracts. Both the yield of extraction and the antioxidant activity were strongly dependent on the solvent. DPPH method showed very accompanying results with methanol and acetone extracts. The crude extract possessed a variety of compounds and hence it followed the synergism based effect. Compounds such as flavonoids, phenols, quinones, terpenoids, carbohydrates, tannins, flavones, glycosides, polyenes, and anthraquinones have been found to contribute the overall antioxidant activity. Research findings provided the evidence that crude extracts of leaves contain medicinally important bioactive compounds and it justified their use in the traditional medicines for the treatment of various ailments.

Key words: DPPH radical scavenging, Phytoconstituents, *Dodonaea viscosa*, Antioxidant analysis.

References

- [1] A. Scalbert, *Polyphenolic Phenomena*, INRA Editions, Versailles Cedex, France, (1993).
- [2] A. Apostolou, D. Stagos, E. Galitsiou, A. Spyrou, S. Haroutounian, N. Portesis, I. Trizoglou A. Wallace Hayes, A.M. Tsatsakis, D. Kouretas, *Food Chem. Toxicol.* 61 (2013) 60.
- [3] L.C.N. da Silva, C.A. Silva-Junior, R.M. Souza, A.J. Macedo, M.V. Silva, M.T.S. Correia, *Food Chem. Toxicol.* 49 (2011) 2222.
- [4] J.S. Rathee, S.A. Hassarajani, S. Chattopadhyay, *Food Chem.* 103 (2007) 1350.

7.9 Chemical oxidative polymerization of aniline using zirconium oxynitrate as an oxidizing agent

P. Karthikeyan, J. Dominic, S. Suganya, R. Gowshalyadevi, V. Mangala Gowri and K. K. Satheesh Kumar*
Department of Chemistry, The Gandhigram Rural institute – Deemed University, Gandhigram – 624 302, Tamil Nadu, India.

* Tel.: +91-451-24523771 * E-mail: karthi2011chemistry@gmail.com, k.k.satheeshkumar@ruraluniv.ac.in

Abstract

Zirconium doped polyaniline composite (Zr-PAni) has been synthesized by chemical oxidative polymerization of aniline using Zirconium oxynitrate as an oxidizing agent at room temperature. The synthesized Zr-PAni composite was characterized by Fourier Transform Infra-red spectroscopy (FTIR), X-ray diffraction studies (XRD), scanning electron microscope (SEM), EDAX and conductivity measurement are done by the four-probe technique. The synthesized Zr-PAni composite showed the electrical conductivity of 4.14×10^{-4} S/cm.

Keywords - Composite, Polyaniline, Zirconium oxynitrate, Conductivity, Oxidant

1. Introduction

Hybrid organic – inorganic composite have been widely studied because they can offer combined properties of organic and inorganic material. These materials have variety of applications in the fields electronic, membranes, catalysis, sensors, optics, etc¹. Polyaniline (PAni) is the one among the well known conducting polymers, due to its easy synthesis, low-cost variable conductivity, environmental stability. A number of different metals and metal oxide have been incorporated into conducting polymer host. These materials show better physical, mechanical and chemical properties. In the present work, Zr doped PAni composite was synthesized by chemical oxidative polymerization of aniline using Zirconium oxynitrate as an oxidant at room temperature.

2. Experimental method

Chemical oxidation of aniline was carried out in the presence of HNO₃. About 1ml of aniline was added to the mortar containing 0.7ml of HNO₃. After grinding for 15min, 0.4g of zirconium oxynitrate was added and further grounded for about 2h. The green powder obtained was washed with 1M HNO₃ until the filtrate was colorless. The obtained green powder was dried under vacuum at 80°C for 24h. The obtained composite was labeled as Zr doped PAni (Zr-PAni).

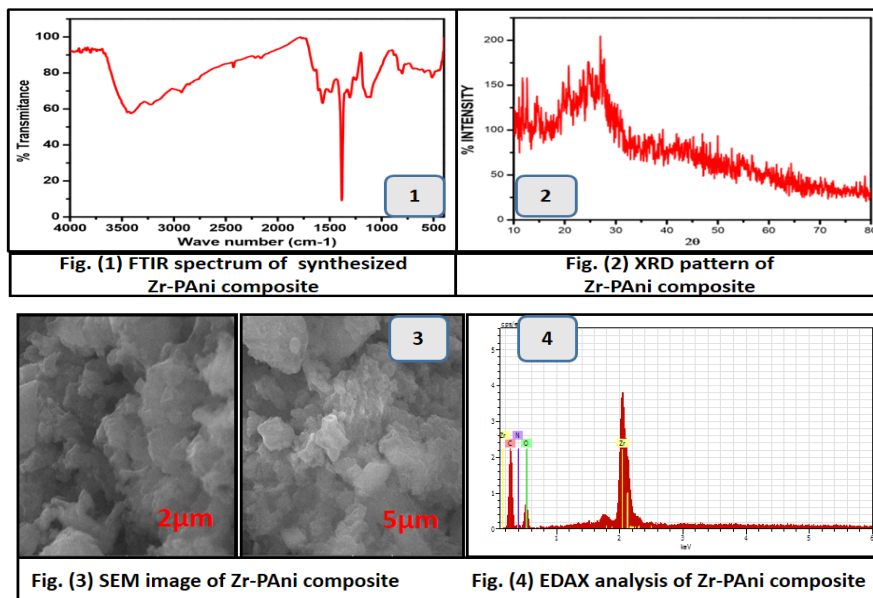
3. Result and discussion

The FT-IR spectrum of Zr doped PAni composite was shown in Fig.1 The main characteristic peaks of Zr doped PAni composite are as follows: ~ 3343, ~ 1569, ~ 1498, ~1306, ~ 1141, ~ 803 and ~ 694 cm⁻¹. The band at ~ 3343 cm⁻¹ is assigned to the N-H stretching vibration. The two bands at ~1569 and ~1498 cm⁻¹ are attributed to the stretching vibration of quinoid and benzenoid units of PAni. The band at ~ 1306 cm⁻¹ can be assigned to the C-N stretching mode of benzenoid unit, while the band at ~ 1141 cm⁻¹ is the characteristic band obtained from stretching vibration of quinoid unit of polyaniline. The band at ~ 813 cm⁻¹ and ~ 694 cm⁻¹ are attributed to C-C and C-H stretching of the benzenoid unit of polyaniline. All these peaks suggest that the obtained polymer is polyaniline. However the observed peaks of Zr doped PAni composite show slight shift in all band when compared to pure PAni, which indicates that some interaction exist between Zr and Nitrogen sites of PAni.

The X-ray diffraction analysis is a powerful tool to provide information with respect to its structure and

nature of the sample. The XRD pattern of pure polyaniline has no characteristic peak and shows a hump at $2\theta=25^\circ$. Therefore it is amorphous in nature². The XRD pattern of Zr-PANI was shown in Fig.2. The Zr-PANI exhibit characteristic diffraction peaks at $2\theta=11.76^\circ$, 12.6° , 19.62° , 23.79° , 24.69° , 27.38° and 78.78° . These diffraction peaks are due to the presence of Zirconium particles in the amorphous polyaniline matrix³.

Fig.3 represents the SEM image of Zr-PANI. As seen in the SEM image, the size and shape of PANi particles are irregular in shape. However based on the EDAX results of Zr-PANI (Fig.4), the following elemental compositions was found: C - 49.31%, N - 8.33%, O - 19.51%, Zr - 22.85%, which confirms that Zirconium particles are dispersed in the PANi matrix. The electrical conductivity of Zr-PANI was found to be 4.14×10^{-4} S/cm.



1. Conclusion

Zirconium doped polyaniline composite (Zr-PANI) has been synthesized by chemical oxidative polymerization of aniline using zirconium oxynitrate as an oxidant at room temperature. The synthesized composite was characterized by FTIR, SEM, XRD, EDAX and conductivity measurement. FTIR study confirms that the obtained polymer composite, some interaction exists between zirconium and nitrogen sites of polyaniline matrix. The diffraction pattern of Zr-PANI show sharper peaks which confirms the presence of zirconium particles in the amorphous polyaniline matrix. The electrical conductivity of Zr-PANI was found to be 4.14×10^{-4} S/cm.

Acknowledgement

One of the authors **P. Karthikeyan** thanks Department of chemistry, The Gandhigram rural institute – Deemed university, Gandhigram for providing lab facilities.

Reference

- [1] C .Sachez., B.Julian, P. Belleville and M. Popall Applications of hybrid organic-inorganic nanocomposites, *J.Mater.chem.*, 15 (2005) 3549
- [2] K.Gupta, P.C.Jana and A.K.Meikkap synthesis electricaltransport and optical properties of polyaniline zirconium nanocomposite. *J.Appl.Phys.*109 (2011) 12373
- [3] Sheng Wang, Chao Liu, Junyan Gong, Xiaobo Zhang, Juan Juan Ma and Zhiwei Tong electrochemical properties of polyaniline/alpha zirconium phosphate` nanocomposite and the effect of pH values *Adv.Mater.Res.*,284-286 (2011) 570-576.

7.10 A Study on the effect of Azeotropic Solvent Mixture pre treatment on the Crystallinity and dyeing behaviour of Polyester/Cotton Composite Fibre

^aS.Vigneswari, ^bJ.Ethiraj, ^cK.Balakrishnan, ^dV.Ramasamy, ^eG. Gopu and ^fB.Muralidharan

^aDepartment of Chemistry, Raja Duraisingam Govt. Arts College, Sivagangai, T.N., India.

^bDepartment of Chemistry, C.Byregowda Institute of Technology, Kolar, India. ^cDepartment of Chemistry, A.V.V.M.SriPushpam College, Poondi,Thanjavur Dt. T.N., ^dPeriyarManiammai university, Vallam,Thanjavur, 613403.T.N.

^eDepartment of Industrial Chemistry, Alagappa University, Karaikudi-3, Tamilnadu

^fBITS, Pilani - Dubai Campus, International Academic City, Dubai-UAE. E.mail:vigneswari2020@gmail.com

Use of Polyester and Cotton composite yarn and fabric materials are attractive due to the combined advantage

of mechanical strength of polyester and water absorbing nature of cotton. [1-3]. The present study aims to assess the effect of an azeotropic solvent mixture Water: Formic Acid : Propionic Acid (W:FA:PA = 18.6:71.9: 9.5) treatment on the molecular orientation, internal and surface modifications in the fibre structure and the dyeability of 80:20 Polyester/cotton blended fabric composite. The treated samples were subjected to tearing strength, scanning electronmicroscopy(SEM), differential scanning calorimetry (DSC) and X-ray diffraction(XRD) analysis to investigate their mechanical, physical and crystalline properties[2]. Changes in the orientation of the polymer crystals due to solvent induced crystallization and surface modifications were observed[3]. Dyeing studies of treated and untreated fibres under different conditions were carried out using disperse and reactive dyes to study the effect on dyeing behaviour of the composite material[4-6].

Dye uptake of 80:20 PCF treated with W-FA-PA :

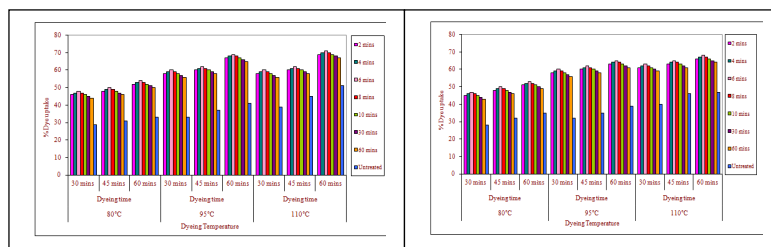


Figure.1. Foron Brilliant Red E-2BL200 F+ Drimarene Brilliant Red K-BL

Figure.2 Foron Blue SE 2R+ Drimarene Turquoise K-2B

pre-treatment has not affected the fastness of dyed fibre samples as well as the stability of dye-fibre bond. SEM studies indicated generation of pits and voids inside the fibre material leading to improved dye uptake. The results of FTIR studies showed that there is no introduction of new functional groups in the fibre matrix. XRD studies revealed the disturbance caused to the crystalline distribution, substantiating solvent induced crystallization which was supported by DSC studies[6].

CONCLUSION

Pretreatment of PET/Cotton composite fabric with Azeotropic solvent mixture was found to improve the dyeing behaviour. As the pre-treatment time increased, the dye uptake increased upto 8-10 minutes pre-treatment duration, beyond which it decreased which may be due to increased irreversible open structure of fibre material during prolonged pre-treatment. Study of wash, light and rubbing fastness properties of treated and untreated fabric material indicated that the solvent

References :

- [1] H.J.Jameel, J.Waldman and L.Rebenfeld, *J. Applied Poly.Sci.*,26(1981) 1795.
- [2] B.Muralidharan and S. Laya, *ISRN Materials Science*, (2011), DOI:10.5402/2011/907493
- [3] B.Muralidharan S. Laya and S.Vigneswari, *Asian Journal of Textile* 1(3), (2011)114. DOI:10.3923/ajt.2011.114.129
- [4] J.J.Lee., N.K.Han, W.J.Lee., J.H.Choi and J.P.Kim, *Color. Technol.*, 119, (2003) 134.
- [5] M.Shingo, K. Katsushi, H. Toshio, and M. Kenji, *Textile Research Journal*, 74,(11) (2004) 989.
- [6] S.Vigneswari, B.Muralidharan, V. Sethuraman and V.Ramasamy, *International Journal of Advanced Scientific and Technical Research* 4(3),(2014) 897.

7.11 Soil conditioning potential of cotton stalk biochar

D.Krishnaveni, S.Priyanga, G.Samuvel, A.N.Senthilkumar*

PG & Research Department of Chemistry, Alagappa Govt. Arts College, Karaikudi-630 003, India.

Abstract

In the present study cotton stalks were used for preparing biochar by slow thermal pyrolysis process at 350°C. The obtained chars (CBC) were subjected to physico-chemical, morphological and functional groups analysis using standard protocols. The prepared CBC was tested as soil conditioner to improve the water holding capacity of soil. Experimental results revealed that the CBC's 9% soil mixture (by mass) served as a good soil amender whose water holding capacity doubled as compared to control treatment.

1. Introduction

Biochar is produced by thermal decomposition of biomass under oxygen-limited conditions. The characteristics of biochar are influenced mainly by the preparation temperature and biomass. Biochars derived from various source materials show different properties of surface area, porosity and the amount of functional groups which influences the properties of biochar. Biochar has been proved to be effective in improving soil properties and increasing crop biomass. Biochar is increasingly receiving attention and highly recommended as soil amendment because it cannot only mitigate climate change by sequestering C from atmosphere into soil [1]

but also improve soil properties and enhance soil fertility by improving moisture and nutrients retention and microbial activity [2]. In the present study cotton stalks were subjected to slow thermal pyrolysis at 350°C. The resulting (CBC) biochars physical and chemical properties were analyzed. Characterized CBC's soil conditioning nature were examined

2. Experimental technique

2.1 Materials and preparation of biochar

Cotton stalks was collected from in and around the farm holdings of Karaikudi, Sivagangai District, Tamil Nadu, India and collected stalks were dried under mild sunlight for 7 days to remove unbound moisture and then shredded. The shredded stalks were pyrolyzed at 350°C. After the pyrolysis biochar was grounded to small granules and pass through 2 mm sieve in order to have the same particle size as that of the soil.

2.2 Physico-chemical characterization

The prepared CBC was mixed with water in the ratio of 1:5 by mass to measure pH and EC in ELICO instrument of model LI 617. The organic carbon was determined by wet digestion method. Total organic carbon (TOC), total nitrogen, phosphorous and potassium content, water soluble cations and exchangeable cations were analysed as reported elsewhere.

2.3 FTIR analysis

Surface functional group of biochar was analysed by fourier transform infrared (FT-IR) spectrometer of BrukerOptik GmbH of model No TENSOR 27. Biochar was pelleted with potassium bromide for experimental use.

2.4 Water holding capacity measurements

Sandy loamy soils were conditioned with various amounts of CBC by mass to assess the effects on the water holding capacity at different mixture rates. The homogenized 2 mm size of 50g soil was filled in 200 ml capacity container and different proportions between 0 -10% were mixed to soil individually. Water was slowly applied to each mixture present in the container, by gentle agitation until super saturation. Then these mixtures were allowed to settle for 24 h to ensure homogeneity and the saturated samples were weighed to determine wet mass. The samples were then dried at 110°C for 24 h using a hot air oven and weighed for dry mass.

3.0 RESULT AND DISCUSSION

3.1 Physico-chemical characteristics of biochar

Physico-chemical parameters of the CBC are given in the Table1. CBC was possessing alkaline pH due to the presence of organic anions, carbonates and other alkali metal ions. Appreciable quantities of dissolved ions were responsible for electrical conductivity (EC) [3] The presence of nitrogen in studied biochar is likely due to amino group as evidenced from FTIR. However, this N content cannot be completely utilized by crops because it exists in inaccessible forms as functional groups in the skeleton of carbon chain. Lower temperature pyrolysis produces higher amount of nitrogen as evident from Table1.

3.2 Water holding capacity

The following equation was used to determine the water holding capacity of CBC

$$\text{Waterholdingcapacity}(\%) = \frac{\text{masswet} - \text{massdry}}{\text{massdry}} \times 100$$

Standard deviation was determined from the three replicate samples for each mixture. The average water holding capacities as a percentage of dry mass are shown in Fig.1. Experimental results revealed that the 9% CBC soil mixture's (by mass) whose water holding capacity doubled as compared to control treatment. It was reported that mixture rates of less than 10% were safe for agricultural purposes to loamy sand soil [4]. The higher water holding capacity was mainly due to its higher carbon and pore space of the studied biochar.

4.0 Conclusion

The study concluded that CBC increased the water holding capacity of sandy loamy soil. 9% addition by mass of CBC enhanced water holding capacity doubly. Hence the biochars can effectively supplement the sandy loamy soil for irrigation purpose.

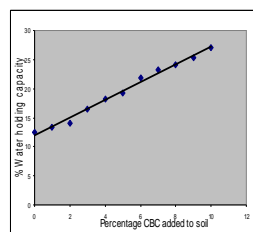


Fig.1: Water holding capacity of CBC

References

- [1] E. Marris, Putting the carbon back: black is the new green, Nature, 442 (2006) 624-626.

- [2] Lehmann, J.: A handful of carbon, *Nature*, 447 (2007) 143-144.
[3] Basile-Doelsch, W.E.E. Amudson, R. Stone, D. Borschneck, J.Y. Bottero, T. Moustier, F. Masin, F. Colin, Mineral control of carbon pools in a colcanic horizon, *Geoderma*, 137 (2007) 437-489.
[4] P. Jha, A. Biswas, B. Lakaria, A.S. Rao, Biochar in agriculture - prospects and related implications. *Current science*, 99 (2010) 1218-1225.

7.12 Strain-free hydrophobic silk fabric coated with Hexamethyldisiloxane (HMDSO) using Plasma Enhanced Chemical Vapour Deposition (PECVD)

K. Vinisha Rani, Bornali Sarma*, and Arun sarma

School of Advanced Sciences (SAS), VIT University, Chennai, Chennai-600127, Tamil Nadu, India.

E-mail: kvinisha.rani2014@vit.ac.in

Abstract:

Natural fibers can become water repellent by depositing fluorinated polymers, through the application of fluorine-containing resins [1]. However, the use of fluorocarbon compounds is undesirable due to their exceptionally high green house effect [2]. Plasma deposition is an environmentally friendly process used to create ultrathin good quality coatings on fabrics at low temperatures. The use of Si-containing monomer precursors is an environmentally friendly technology of surface modification of hydrophobic material like hydrocarbon or fluorocarbon plasma-coatings. Among Si-containing precursors, the most used are tetramethylsilane (TMS), tetraethoxysilane (TEOS) or hexamethyldisiloxane (HMDSO). Both TEOS and HMDSO are non-toxic, non-explosive and much safer than TMS. HMDSO has the further advantage of a higher room temperature vapour pressure than TEOS which allows easier use and optical transparency, which will not affect the colour of the fabric. Using this pure monomer in plasma processes gives the possibility to obtain stable hydrophobic surfaces because of the high retention of methyl groups. Silk fabric with water-repellent properties has great potential in stain-free textile products. This coating makes the silk fabric surface water resistant, preventing it from accidental staining or water damage. A lower surface energy indicates higher contact angle and greater hydrophobicity. HMDSO is a colourless and highly volatile liquid in normal conditions. The depositions of HMDSO on Silk fabric were performed on Plasma enhanced chemical vapour deposition (PECVD) apparatus, operating at 13.56 MHz and room temperature.

In this work, we study the surface modification of silk fabrics using 100% pure hexamethyldisiloxane (HMDSO) as a liquid precursor deposited by plasma enhanced chemical vapour deposition (PECVD) to improve the hydrophobic property. PECVD is an economical and clean, eco- friendly technique, which does not produce waste or appreciable atmospheric emissions. The effect of exposure time 15 mins with different power 100 W and 150 W has been studied. The coatings of silk fabrics were characterized by ATR- FTIR spectroscopy, which confirms the presence of Si containing functional groups in the characteristic peaks at 838 cm^{-1} , 797 cm^{-1} and 1021 cm^{-1} . The surface morphology of untreated and HMDSO coated silk surface are studied by scanning electron microscopy (SEM) which reveals the deposition of HMDSO and surface roughness introduced on the fibers. Fabrics would yield an increase in contact angle and hydrophobicity. The HMDSO coated silk fabric water contact angle increased from 58.9° up to 139.9° showed higher water-repellency. The ageing effects of the fabrics are also observed. Their Contact angle after 100 days does not show any visible changes on the fabrics.

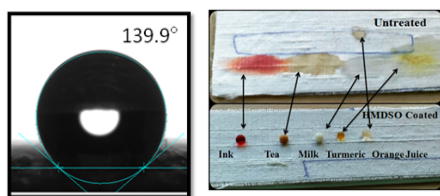


Fig. 1 (a) Contact angle of HMDSO coated fabric and (b) Ageing Effect of untreated and HMDSO coated Silk fabrics with different strains Ink, Tea, milk, Turmeric, orange Juice.

Reference:

- [1] P. Suanpoot, K. Kueseng, S. Ortmann, R. Kaufmann, C. Umongno, P. Nimmanpipug, D. Boonyawan, T. Vilaitong, *Surface & Coatings Technology* 202 (2008) 5543-5549.
[2] Kartick Kumar Samanta, Amish G. Joshi, Manjeet Jassal, Ashwini K. Agrawal, *Surface & Coatings Technology* 213 (2012) 65-76

7.13 Adsorption kinetics and isotherm removal of chromium (VI) ions from aqueous solution by kottikilangu (*Appanogeton natans*)

S. Krishnaveni^a, N. Ramulu^a, T. Rajajeyantham^b and V. Thirumurugan^a

^aA.V.V.M Sri Pushpam College Poondi, (Autonomous) Thanjavur, Tamilnadu, India.

^bM. Kumarasamy College of Engineering, Karur, Tamilnadu, India. Email: skvtmj12@gmail.com

Introduction

Industrial wastewater is considered as one of the major pollutants of the environment. Colored wastewater is produced by various industries, such as textile, dyeing, pharmaceutical, food, cosmetics and healthcare, paper, and leather industries. Many dyes and their breakdown products may be toxic for living organisms. Therefore decolorization of dyes is important before the discharge of effluent. Removal of metals has been attempted extensively using physico-chemical methods such as coagulation, ultra filtration, electro-chemical adsorption, photo oxidation, activated carbon adsorption, etc. In the present study, kottikilangu has been used as an adsorbent whose results showed good absorption in chromium (VI) aqueous solution.

Material and methods

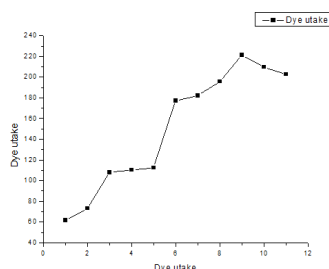
Preparation of an adsorbent

Kottikilangu biomass were obtained from Ponds in Thanjavur, kottikilangu are washed using tap water followed by double distilled water. After washing the kottikilangu were dried under sun light for 72 hours to remove moisture content present. The dried kottikilangu were wash repeatedly with hot water (70⁰ C) to remove any soluble matter present and dried in oven at 85⁰ C for 48 hours. The oven dried kottikilangu were powdered at sieved through 100 mesh sieves and stored air tight polythene bottles for adsorption experiments

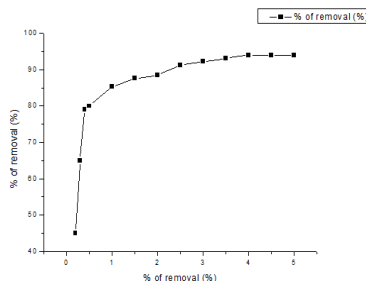
Batch biosorption studies

The experiment was carried out by the batch the adsorption method in the Erlenmeyer flasks for a pre determined period using orbital shaker. In the adsorption parameters such as PH Initial dye concentration, equilibrium time fixation was studied for optimization. The kinetic studies and isotherm studied. The mechanism of adsorption was investigated by lageregen pseudo first order, pseudo-second order. The isotherm study results were fitted in Langmuir, Freundlich isotherms.

Effect of pH



Effect of biosorbent dosage



Conclusion

The aim of this paper was utilization of natural biosorbents kottikilangu as adsorbent for the removal of chromium (VI) ions from aqueous solutions. Pseudo first order kinetic model gave better results but pseudo second order kinetic model best fits the kinetics of adsorption. The correlation coefficient $R^2 = 1$ for second order adsorption model and q_e theoretical values are consistent with q_e experimental value showed that pseudo second order adsorption equation fit with whole range of contact time. Among isotherms Langmuir isotherm was found to be best fitting model with respect to R^2 values. The kottikilangu adsorbent have excellent adsorption capacity. So kottikilangu can be used as a low cost attractive alternative for costly activated carbon.

7.14 Spectral, NLO, Fluorescence, Anti-inflammatory and Biological screening of Thiadiazole based conjugated Ligand and their Metal(II) Complexes

K. Mahalakshmi^a, P. Tharmaraj^{a*}, C.D. Sheela^b

^{a*}Department of Chemistry, Associate professor, Thiagarajar College, Madurai-625009, India

^bDepartment of Chemistry, Associate professor, The American College, Madurai-625009, India

E-mail: kmalardevi@gmail.com

Abstract

Tridentate chelate complexes of ML type (where M= Cu(II), Ni(II), and Co(II)) have been synthesized from triazine based ligand [4,6-bis(5-phenyl-1,3,4-thiadiazole-amine)-2-(4-chlorophenylamino)-1,3,5-triazine] (BPMTDT). Microanalytical data, magnetic susceptibility measurements, IR, ¹H NMR, UV-vis, mass, and EPR spectral techniques were used to characterize the structure of chelates. The electronic absorption spectra and magnetic susceptibility measurements suggest that metal complexes show square pyramidal geometry. The electrochemical behavior of copper(II) complex is studied by cyclic voltammetry. All synthesized compounds

may serve as potential photoactive materials as indicated from their characteristic fluorescence properties. The invitro antimicrobial activities of the ligand and its complexes are evaluated against *Micrococcus luteus*, *Bacillus subtilis*, *Staphylococcus aureus*, *Staphylococcus epidermidis*, *Streptococcus mutans*, *Escherichia coli*, *Enterobacter aerogenes*, *Klebsiella pneumonia*, *Proteus vulgaris*, *Cryptococcus neoformans*, *Pseudomonas aeruginosa*, *Salmonella typhi*, *Serratia marcescens*, *Shigella flexneri*, *Vibrio cholera*, *Vibris parahaemolyticus*, *Aspergillus niger*, *Candida albicans* and *penicillium oxalicum* by well-diffusion method. The second harmonic generation efficiency (SHG) of the ligand and metal complexes has been found to be higher than that of urea and KDP.

Key words: *Metal(II) complexes, Thiadiazole derivative, NLO activity, Anti-inflammatory activity.*

Results and discussion:

IR Spectral studies:

The ligand which exhibits a band at 1646 cm^{-1} is characteristic of (C=N) of thiadiazole ring. In complexes, this strong band is shifted to $1602\text{--}1608\text{ cm}^{-1}$ region corresponding to (C=N) coordination to metal ion. The ligand shows a strong band at 1485 cm^{-1} , which is characteristic of the $\nu(\text{C}=\text{N})$ group in S-triazine. This band shifting to lower frequency of $1448\text{--}1456\text{ cm}^{-1}$ upon complexation indicates that triazine ring nitrogen is one of the coordinating atom in the ligand. In the far IR spectra of complexes, the weak bands appeared at $472\text{--}451\text{ cm}^{-1}$ and $375\text{--}358\text{ cm}^{-1}$ regions can be assigned to $\nu(\text{M-N})$ and $\nu(\text{M-Cl})$ vibrations, respectively, and confirm the interaction between metal and ligand.

References

- [1] S.M.E. Khalil, Journal of coordination chemistry, vol.56, no.12, (2003) 1013-1024.
- [2] V.K. Pandey, S.Tusi, Acta Pharmaceutica, vol.54, no.1, (2004) 1-12.
- [3] K. Naresh Kumar, R. Ramesh, Polyhedron, vol.24, no.14, (2005) 1885-1892
- [4] L.K.Gupta and S. Chandra, Spectrochimica Acta A, vol.65, no.3-4, (2006) 792-796.
- [5] M. Tumer, D. Ekinci, Spectrochimica Acta A, vol.67, no.63, (2007) 916-929.

7.15 Synthesis, spectral characterization and antifungal activities of Some spiroheterocyclic compounds

Elanchezhian. B, Selvanathan. G[#] and Manivannan. N^{*}

Department of Chemistry, A.V.C. College (Autonomous), Mannampandal, Mayiladuthurai, Tamilnadu, India-609305

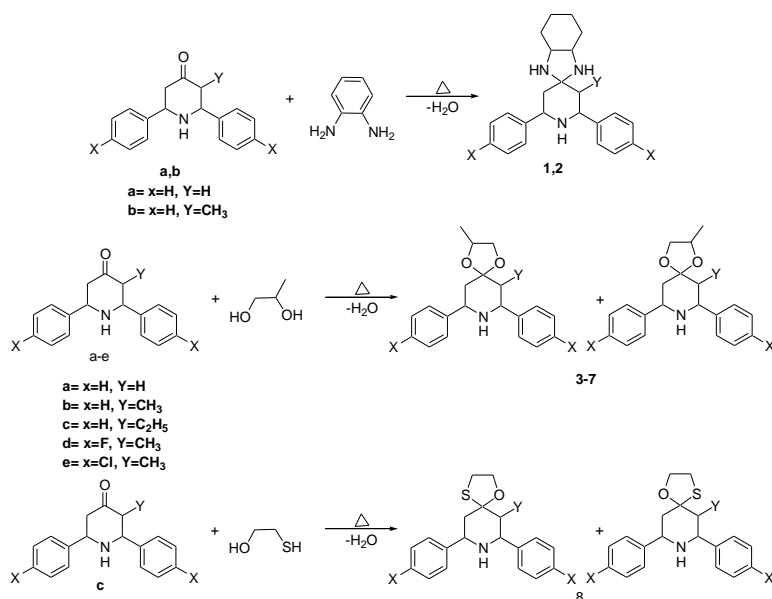
**Department of Chemistry, V.R.S. College of Engineering and Technology, Arasur, Villupuram, Tamilnadu, India-607107*

Corresponding author: selvanathangesan@gmail.com

Abstract

Eight spiro heterocyclic compounds were synthesized by cyclo condensation reaction between 2,6-diarylpiperidin-4-one with o-phenylenediamine, propylene glycol and 2-Mercaptoethanol [1-3]. Compounds were analysed by using spectroscopic methods such as IR, NMR (^1H and ^{13}C) and Mass. The spectral data revealed that the compound adopt chair conformation with equatorial orientation of all the substituents. The newly synthesized compound was tested for their antifungal activity against *Penicillium notatum*, *Candida albicans*, *Mucor indicus*, *Aspergillus niger* and, *Fusarium solani* using micro dilution method [4-7]. Among the compounds tested for their anti-fungal activity 1 and 2 were displayed the most potent inhibitory activity with a MIC value of $7.81\text{ }\mu\text{g ml}^{-1}$ in controlling the growth of *A. niger*, *F. solani* and *C. albicans* respectively. The other compounds also showed considerable antifungal activity with a MIC value ranging between 31.25 and $15.62\text{ }\mu\text{g ml}^{-1}$ against the rest of pathogens.

Keywords: Spiro heterocyclic, Antifungal, Pathogens



References

1. Noller, C. R.; Balliah, V. J. *Am. Chem. Soc.*, 1948, 70, 3853.
2. Manivannan, N.; Stalin Elanchezhian, V.; Selvanathan, G.; Elanchezhian, B. *J. Ultra chem.* 2010, 6, 339.
3. Gao, C.; Hong Ye, T.; Yu Wang, N.; Xiu Zeng, X.; Dan Zhang, L.; Xiong, Y.; Yu You, X.; Xia, Y.; Xu, Y.; Ting Peng, C.; Qiong Zuo, W.; Yuquan Wei, Y.; Ting Yu, L. *Bio. Med. Chem. Lett.* 2013, 23, 4919.
4. Eloff, J. N. *Planta Medica.* 1998, 64, 711.
5. Masoko, P.; Picard, J.; Eloff, J. N., *South African Journal of Botany*, 2007, 73, 173.
6. Balasubramanian, S.; Ramalingan, C.; Aridoss, G.; Kabilan, S. *Eur. J. Med. Chem.* 2005, 40, 694.
7. Rani, M.; Ramachandran, R.; Kabilan, S. *Bioorg. Med. Chem. Lett.* 2010, 20, 6637.

7.16 Physico Chemical Study on the Quality of Surface Water of Kolavai lake in Kanchipuram District, Tamilnadu -Before and After the 2015 Floods

Stephen Jayakumar P¹ and Mary Vergheese. T²

^{1,2}Department of Chemistry, Madras Christian College, Tambaram East, Chennai-600059

Abstract

Lake water is the main source to maintain the water table in rural and urban areas of Tamilnadu. It is also the important source of drinking water for animals for their survival and growth. Unfortunately, because of contamination by industries through discharge of harmful chemicals, disposal of domestic wastes, the disposal of sewage water, plastic wastes etc., the quality of potable water exceeds the minimum desirable drinking water limit and hence not fit for consumption. In the present study the surface water quality of Kolavai lake in Kanchipuram District was analyzed for its drinking water quality during the summer, monsoon and winter seasons of the year 2015. The various Physico-Chemical parameters like pH, turbidity, Conductivity, alkalinity, Dissolved oxygen (DO), Biological Oxygen Demand (BOD), Chemical Oxygen Demand (COD) etc. were studied for the three seasons and were compared. Due to the unprecedented floods that hit Tamil Nadu during the monsoon, it was observed that the surface water quality after the floods was within the WHO permissible limit, it may be due to the excessive runoff of pollutants away from the lakes. The pH level stayed within the desirable limit throughout the year. The electrical conductivity reduced to a great extent, DO was found to be decreased in summers but has shown slightly elevated value during monsoon. Decreased DO level in summers can be attributed to increased temperature in summer. BOD & COD was very high during summer which proves higher level of pollutants in the lake. But by monsoon the value started decreasing and in winter, still less value is observed. A high BOD value indicates the presence of a large number of microorganisms, which shows a high level of pollution. In summer the chloride content was 480 mg/l, a very high level of chloride than the permissible limit of 250 mg/l. It is an indicator of pollution. This amount reduced to 32 mg/l in monsoon and 40 mg/l in winter, which is very well a lower value, suggesting that the water is good for domestic use. It is important for us to take necessary steps to maintain a healthy environment by reducing pollution, so as to ensure optimal water quality.

Key words: Surface Water, Physico-Chemical, BOD, COD.

7.17 Studies on statistical modelling of degradation of Reactive Orange 16 dye by ozonation: central composite design

M. Abaranjitha, G. Abarna, S. Gayathri, G. JananiSree, V. C. Padmanaban*

Department of Biotechnology, Kamaraj College of Engineering and Technology, Virudhunagar – 626 001.
anitha95explorebt@gmail.com, vcpadmanaban88@gmail.com*

Abstract

In the present investigation an attempt was made to degrade Reactive Orange 16, one of the widely used azo dye in the textile industry by ozonation process. The interactive effects of the influencing factors (dye concentration = 100-300ppm; time = 10-60mins; pH = 3-11) on degradation efficiency was critically examined through experimental design optimization by Central Composite Design under the Response Surface Methodology. The results indicated that, the response (% degradation) was affected by all factors individually and interactively. The high correlation coefficients ($R^2 = 0.9676$ & adjusted $R^2 = 0.9384$) obtained by analysis of variance (ANOVA) demonstrated close fit between the experimental and the predicted values. Optimized conditions for the highest desirability of degradation (i.e. 100% degradation) was obtained at pH=11, dye concentration = 100ppm & reaction time of 10mins. The degradation of the azo dye was confirmed through FTIR & UV-Vis Spectrometry. This study showed that rsm could be employed to model degradation attributes of ozonated dye effluent while minimising the number of experiments.

Key words: Ozonation, RSM, FTIR.

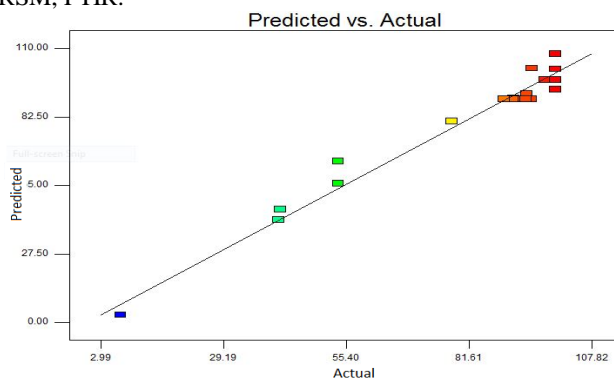


Figure 1. Predicted vs. Actual plot for the degradation of Reactive Orange 16

The significance and adequacy of the model was tested by Analysis of Variance (ANOVA) (Soltani *et al.* 2013). The developed regression model has a high co-efficient of determination ($R^2 = 0.9676$) and adjusted R^2 value ($R^2 = 0.9384$). The significance of the model is justified by above said regression co-efficients (Amini *et al.* 2008). The F-value of the model is 33.16 which implies the model as significant. In this model, A, B, C, AB, AC, C^2 are significant model terms as their P values are low as (<0.0001, <0.0001, 0.0005, 0.0001, 0.0011, 0.001, 0.0113) respectively. The adequate precision value for this model is 22.668.

Reference:

- [1] Amini M., Younesi H., Bahramifar N., Lorestani A. A. Z., Ghorbani F., Daneshi A. and Sharifzadeh M. (2008). Application of response surface methodology for optimization of lead biosorption in an aqueous solution by *Aspergillus niger*, *Journal of hazardous materials*, **154** (1), 694-702.
- [2] Soltani R. D. C., Rezaee A., Godini H., Khataee A. and Hasanbeiki A. (2013). Photoelectrochemical treatment of ammonium using seawater as a natural supporting electrolyte, *Chemistry and Ecology*, **29** (1), 72-85.

7.18 Quality analysis of groundwater in malur taluk of kolar district used for drinking and domestic purposes

*J. Ethiraj^a, Mohammadi Afshan^a, A. Nagarajan^b, S. Vigneswari^c, G. Gopu^d, B. Muralidharan^e

^aC. Byregowda Institute of Technology, Kolar, Karnataka, India.

^bBangalore Technological Institute, Kodathi, Bangalore, Karnataka- India.

^cRaja Duraisingam Govt. Arts College, Sivagangai, T.N., India.

^dDepartment of Industrial Chemistry, Alagappa University, Karaikudi-3, Tamilnadu

^eBITS, Pilani-Dubai Campus, Dubai, UAE. E.mail: ethiraji96@gmail.com

Abstract: Water plays an important and crucial role in our daily lives, be it for domestic, industrial, agricultural and other ecological balances. Much of that water comes from rivers, lakes and other surface water sources.

Wherever water bodies are rare, it has become necessary to exploit groundwater in order to meet the drinking water needs of the ever growing population. When water is polluted it is not only devastating to the environment, but also to human health. Hence it is essential to have a quality analysis of the ground water.

Kolar district is located in Karnataka, about 70kms from the capital Bangalore. Malur taluk in Kolar district is a perennial drought affected area. The dependence on irregular monsoons has forced them to go in massive scale of bore well drilling and water tapping. The same water is used for domestic purposes and consumption without any kind of water treatment. Apart from Bore well and open wells water, drinking water supplied under various schemes such as Metro Water Supply(MWS), National River Water Supply (NRWS), Public Water Supply (PWS) were taken for water quality analysis in the entire Malur taluk and the results obtained have been analyzed and reported in the present study.

Conclusion: The ground water analysis in Malur taluk of Kolar district were collected and carefully analyzed in the lab, which is used for drinking and other domestic purposes. The analysis was done as per the guidelines of ICMR. This report was generated to take remedial activities to ensure safe drinking water in rural area. A total sample of 690 was collected for analysis and carefully analyzed in which 412 samples were potable as per ICMR guidelines and 278 samples were unpotable. In percentage analysis, the potable and unpotable water was analyzed as 59.71%, unpotable 40.29%.

References:

- [1]. Liu, Y. (2005). *Phosphorus Flows in China: Physical Profiles and Environmental Regulation*. Wageningen University, Wageningen, the Netherlands.
- [2]. Liu, Y., Villalba, G., Ayres, R. U., & Schroder, H. (2008). "Global Phosphorus Flows and Environmental Impacts from a consumption Perspective". *Journal of Industrial Ecology*, **12**(2), pp 229-247.

7.19 Extraction and Application of Eco- Friendly Natural dye Obtained from Flower of *Acacia eburnea* (L.f.) Willd on Cotton Fabric

S.Thiyagarajan^a, K.Balakrishnan^a, B.Muralidharan^b

^aDepartment of Chemistry, A. V. V. M. Sri Pushpam College, Poondi, Thanjavur, Tamilnadu-613503, India.

^bBirla Institute of Technology & Science, Pilani, Dubai. E-mail:balki63@gmail.com

Abstract

Now-a-days natural dyes are commonly used for textile industries, due to their harmless effects and harmful consequences of synthetic dyes. Natural dyes work on cotton, silk and wool etc. Their colours are stable and ecofriendly because of no irritating effects on human skin. Different plant parts are used for colouring methods. Nature has given us a number of plants to use them in dyeing processes for safe life. In these processes different mordants are used in combinations which can be natural plant products like lemon juice, tamarind pulp, pomegranate and some chemicals like alum, chrome, stannous chloride, copper sulphate, ferrous sulphate etc. are commonly used. Natural dyeing were found very encouraging, with their non toxic, non allergic and non-carcinogenic soothing harmless effects. Moreover these dyes are cost effective and ecofriendly. In the present study dye extract was prepared from flower of *Acacia eburnea* (L.f.) Willd is used as a source of natural dyes for dyeing of cotton fabric. The bleached cotton fabrics were dyed with different natural mordants using pre-mordanting, post-mordanting and simultaneous-mordanting method. In this method post mordanting method using *Therminalia bellirica* of compound gave good K/S -value than others. The dyed fabrics have show good washing, light, rubbing fastness and perspiration fastness properties.

Keywords: Extraction, natural dyes, flowers, *Acacia eburnea* (L.f.) Willd cotton, textiles.

7.20 Synthesis and characterisation of nylon-6 with *p*-Cresol resin by solution methodology for the thermally stable hydrophobic polymer

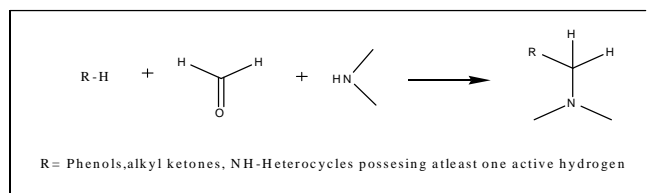
V. Thiruvengadam, M.Malathi*

Condensed Matter Research Laboratory, School of Advance Sciences, VIT University, Vellore-632014

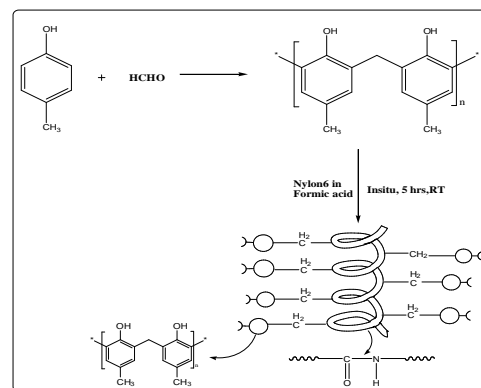
Email.Id: mmalathi@vit.ac.in

Mannich base represents an easily obtained intermediates for the synthesis of other compounds such as heterocycles and amino alcohols. Their derivatives are versatile synthetic intermediates and are employed in diverse types of organic transformations. [1]. It is one of the most widely used reactions in synthetic and medicinal chemistry [2]. Mannich amino alkylation consists of condensation of a substrate with the formaldehyde and a primary or secondary amine [3, 4]. Mannich type condensation of *p*-cresol with formaldehyde and nylon-6 was described. *p*-cresol-formaldehyde resin (PF) is a thermoset resin that has been widely applied by virtue of their excellent properties such as high strength, excellent thermostability and

electrical insulation, and good dimensional stability. Also, this material has intrinsic advantages of flame retardance, ablation resistance and low smoke yield ratio [5]. Although this material has limited its application. Nylon-6 (PA6), is a thermoplastics polymer containing repeated amide units, which serves as a very important plastic because of excellent properties and a wide range of applications [6,7]. Moisture absorption the disadvantage of nylon-6 that leads to problems in dimensional stability and property changes [8]. Hence, we synthesis nylon-6 phenolic resin by Mannich reaction. And the complex was characterised by FT-IR, NMR, TGA–DSC, GPC and Contact Angle Measurement (CA).



Scheme.1. Mannich reaction

Scheme 2. Synthesis of Nylon-6 *p*-cresol resin**Reference:**

- [1] Balasubramanian, K. K.; Selvaraj, S. *J. Org. Chem.* 1980, 45, 3726–3727.
- [2] Arend, M.; Westermann, B.; Risch, N. *Angew. Chem., Int. Ed.* 1998, 37, 1044–1070.
- [3] F.F. “The Mannich Reaction”, *Org. Reaction*, 1, 303 (1942)
- [4] H. Hellmann, G. Opitz, *Angew. Chem* 68, 265 (1956)
- [5] Lei, Y., Wu, Q. and Lian, K. (2006) *J. Appl. Polymer Sci.*, 100, 1642-1650.
- [6] Welgos, R. J. *Encyclopedia of Polymer Science and Engineering*, 2nd ed., Vol. 11; John Wiley and Sons: New York, 1988; p. 445.
- [7] M.I. Kohan (Ed.), *Nylon plastics handbook*, Hanser, New York (1995)
- [8] Huang, M.W.; Zhu, K.J.; Pearce, E.M.; Kwei, T.K. *J Appl Polym Sci* 1993, 48, 563

7.21 Synthesis, Spectral and Antimicrobial studies of some Bis-dimedone derivatives

P. Navamani,^a and N. Srinivasan.^{a,b*}

^aResearch and Development Centre, Bharathiar University, Coimbatore- 641 046, Tamilnadu,

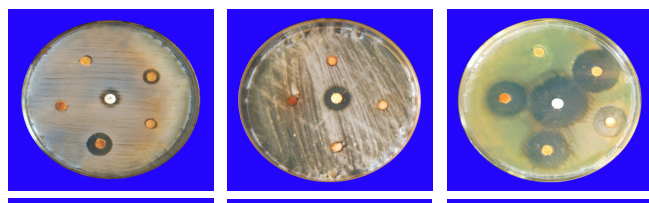
^bDepartment of Chemistry, Pachaiyappa's College for Men, Kanchipuram-631 501, Tamilnadu.

Abstract

Medicinal chemistry is the application of chemical research techniques to the synthesis of pharmaceuticals. Medicinal chemistry explains the design and production of compounds that can be used for the prevention, treatment or cure of human and animal diseases. Bisdimedone derivatives, acridines, acridinediones, xanthene derivatives show antimicrobial activities against certain bacterial and fungal strains. Xanthene, the parent compound of a number of naturally occurring substances. Xanthylium and the carbonyl compound xanthone are derived from xanthene. Xanthenes are important because of their use in medicine and they possess biological activities.

***In vitro* antibacterial and antifungal activity**

The *in vitro* activities of bio active imidazole derivatives were tested in Sabourauds dextrose broth for bacteria by the twofold serial dilution method.^[24-26] The compounds were dissolved in dimethylsulfoxide (DMSO) to obtain 1 mg/ml stock solutions. Seeded broth (broth containing microbial spores) was prepared in NB from 24 hrs old bacterial cultures were suspended in SDB. The colony forming units (cfu) of the seeded broth were determined by plating technique and adjusted in the range of 10^4 - 10^5 cfu/ml. The final inoculum size was 10^5 cfu/ml for antibacterial assay and 1.1 - 1.5×10^2 cfu/ml for antifungal assay and testing was performed at pH 7.4 \pm 0.2. Exactly 0.2 ml of the solution of each test compound was added to 1.8 ml of seeded broth to form the first dilution. One ml of this was diluted with a further 1 ml of the seeded broth to give the second dilution and so on till six such dilutions were obtained. The tubes were incubated in BOD incubators at $37 \pm 1^\circ$ C for bacteria and $28 \pm 1^\circ$ C for fungi.

Anti bacterial activity

7.22 Biotemplate connected on CdO-Polyethylene glycol film for structural and thermal properties

S.Saranya, S.Rajaboopathi, S.Thambidurai*

Department of industrial chemistry, school of chemical sciences, Alagappa university, Karaikudi - 630003, Tamil nadu, India. Email:saranramaiah93@gmail.com

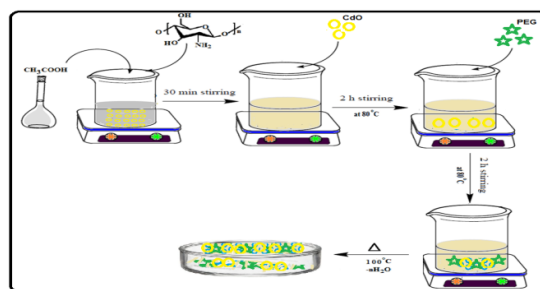
Abstract

In the present study, films can be synthesized by solution costing method using chitosan as a biosurfactant, CdO as a source materials and PEG as film maker. The functional groups of resultant matrix from chitosan, PEG and respective metal oxide were characterized and confirmed by FTIR and UV-Visible spectroscopy. The crystallite size was confirmed by X-ray diffraction analysis (XRD). Gram-positive and Gram-negative bacteria were evaluating the antibacterial activity. The chitosan-CdO particle intercalated PEG films thermal characteristics was analyzed by TG-DTA, the enhanced thermal stability of chitosan based CdO intercalated PEG has higher than chitosan. The results demonstrate that chitosan-CdO intercalated PEG matrix has reinforced effect compared to among the other three components. Therefore, Biotemplate based CdO intercalated to PEG matrix can be promising materials for sensors and super capacitors applications.

1. Introduction

Chitosan is one of the promising natural biopolymer on earth and has been used in wide range of applications with excellent film forming abilities, biocompatibility, non toxicity, good water permeability, metal ion adsorption and high mechanical strength. It is susceptible to chemical modification due to the presence of reactive hydroxyl and amino functional groups. It is used in a wide range of applications such as waste water treatments, separation membranes, drug delivery systems and biosensors. The PEG polymer has a low toxicity and it's used as a lubricating coating for various surfaces in aqueous and non-aqueous environments. The Cadmium oxide (CdO) is an n-type semiconductor with a direct band gap of 2.2 and 2.7 eV. Transparent conducting CdO have been used for many applications, such as gas sensors, photodiodes, phototransistors, photovoltaic solar cells.

2. Experimental details



3. Result and discussion

Chitosan-CdO intercalated PEG matrix has reinforced effect compared to the chitosan-PEG components. The functional groups of resultant matrix from chitosan, PEG and respective metal oxide were characterized and confirmed by FTIR, UV-Vis DRS and XRD analysis. Evaluating the antibacterial activity of chitosan-CdO intercalated PEG matrix and thermal stability was analyzed by TG-DTA. Therefore, chitosan based CdO intercalated to PEG matrix can be promising materials for biomedical and capacitors applications.

4. References

- [1] G.Roberts, Y. Dong, J. Colloid Interface Sci. (2001) 243; 89.
- [2] S.H.Pangburn, PV.Trescony. Biomaterials. (1982) 3; 108.
- [3] O.Victor Sheftel, Indirect food additives and polymers: Migration and Toxicology, (2000) 1114:1116.
- [4] O. Vigil, F. Cruz, Mater. Chem. Phys. (2001) 68; 249.

7.23 Synthesis and characterization of chitosan-SnO₂ particle intercalated PVP films

S.Anusuya, M.Karpuraranjith, S.Thambidurai*

Department of Industrial Chemistry, School of Chemical Sciences, Alagappa University, Karaikudi - 630003, Tamil Nadu. Email: anusekarsanthi@gmail.com

Abstract

In the present study, Biofilms can be synthesized by solution costing method using chitosan as a biosurfactant, tin oxide as a source materials and PVP as film maker. The functional groups of resultant matrix from chitosan, PVP and respective metal oxide were characterized and confirmed by FTIR and UV-Visible spectroscopy. The crystallite size was confirmed by X-ray diffraction analysis (XRD). Gram-positive and Gram-

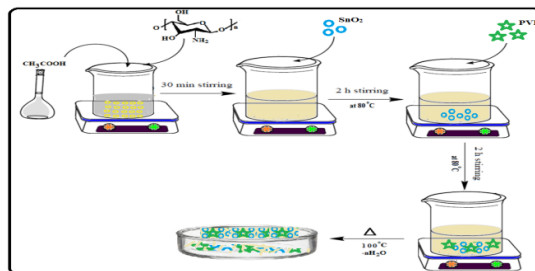
negative bacteria were evaluating the antibacterial activity. The chitosan-SnO₂ particle intercalated PVP films thermal characteristics was analyzed by TG-DTA, the enhanced thermal stability of chitosan based SnO₂ intercalated PVP has higher than chitosan. The results demonstrate that chitosan-SnO₂ intercalated PVP matrix has reinforced effect compared to among the other three components. Therefore, Biotemplate based SnO₂ intercalated to PVP matrix can be promising materials for sensors and super capacitors applications.

Introduction

Chitosan is one of the promising natural biopolymer on earth and has been used in wide range of applications with excellent film forming abilities, biocompatibility, non toxicity, good water permeability, metal ion adsorption and high mechanical strength. It is susceptible to chemical modification due to the presence of reactive hydroxyl and amino functional groups. It is used in a wide range of applications such as waste water treatments, separation membranes, drug delivery systems and biosensors. Tin oxide (SnO₂) is one of the most promising materials, an n-type semiconductor with a wide band gap (E_g = 3.6 eV) and high capacitance, low cost, have been wide range of applications such as energy storage, gas-sensing materials and antireflecting coatings in solar cells.

PVP is used as a [binder](#) in many pharmaceutical tablets; it simply passes through the body when taken orally. However, autopsies have found that [crospovidone \(PVPP\)](#) contributes to pulmonary vascular injury in substance abusers who have injected pharmaceutical tablets intended for oral consumption. This complex is used in various products like solutions, [ointment](#), [pessaries](#), liquid soaps and surgical scrubs.

Experimental details



Result and discussion

Chitosan-SnO₂ intercalated PVP matrix has reinforced effect compared to the chitosan- PVP components. The functional groups of resultant matrix from chitosan, PVP and respective metal oxide were characterized and confirmed by FTIR, UV-Vis DRS and XRD analysis. Evaluating the antibacterial activity of chitosan-SnO₂ intercalated PVP matrix and thermal stability was analyzed by TG-DTA. Therefore, chitosan based SnO₂ intercalated to PVP matrix can be promising materials for biomedical and waste water treatment applications.

Reference

- [1] S. Anandhavelu, S.Thambidurai, Mater. Chem. Phys. 131 (2011) 449–454.
- [2] M. Sharma, Tomar, V. Gupta, Sens. Actuators, B 176 (2013) 675–684.
- [3] J.Gajendiran, V.Rajendran, Mater. Lett. 139 (2015) 116–118.

7.24 Synthesis and characterization of biopolymer connected on copper oxide-polyvinyl alcohol films

S. Muthu, T.Revathi, S.Thambidurai*

Department of Industrial Chemistry, School of Chemical Sciences, Alagappa University, Karaikudi - 630003, Tamil Nadu.
Email:vamuthu94@gmail.com

Abstract

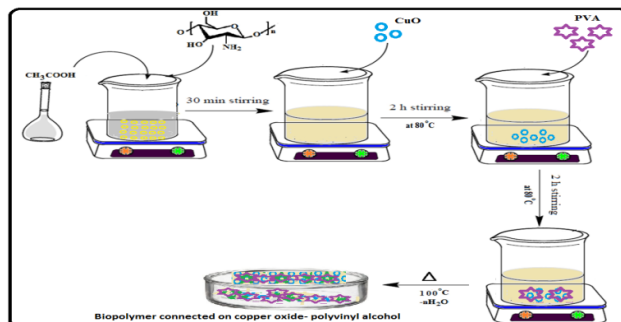
In the present work, biofilms are synthesized by solution coating method. The biofilms using chitosan as biosurfactant, copper oxide as source materials and PVA film maker. The synthesized biofilms were characterized and the amino and hydroxyl groups confirmed by Fourier transform infrared spectroscopy (FT-IR). The crystalline size of biofilms was calculated by X-ray diffraction analysis (XRD). The optical properties of films are analyzed by UV-Vis DRS spectroscopy. The chitosan-PVA and chitosan-CuO-PVA films thermal characteristics were analyzed by TG-DTA, the enhanced thermal stability of chitosan based CuO intercalated PVA has higher than chitosan-PVA. The chitosan-PVA and chitosan-CuO-PVA films exhibited antibacterial activity against gram positive as well as gram negative bacteria. The results demonstrate that biofilms can be promising materials for medical and tissue engineering applications.

Introduction

The development and investigation of new nanocomposite films based on polymer blend natural

attract considerable and increased attentions. Chitosan (CS), a natural polymer extracted by the exoskeleton of crustaceans, is widely investigated because of its good compatibility, biodegradability and antibacterial properties. Poly vinyl alcohol (PVA) is a non toxic water soluble polymer with good physical and chemical properties. It could be blended with different synthetic and natural polymers due to its high hydrophilicity and process ability. The bio inert character of PVA, determined it's broadly use in biomedical field. Copper oxide (CuO) is a semiconductor with band gap of 1.2-2.1eV and exhibits p-type conductivity due to the excess of oxygen or copper vacancies in its structure. The CuO shows good electronic, thermal properties and chemical stability. Therefore, nanostructured CuO has been widely used for various applications.

Experimental details



Result and discussion

Biopolymer connected on copper oxide-polyvinyl alcohol compared to the chitosan-PVA components. The functional groups of resultant matrix from chitosan, PVA and respective metal oxide were characterized and confirmed by FTIR, UV-Vis DRS and XRD analysis. Biopolymers connected on copper oxide-polyvinyl alcohol are thermal stability analyzed by TG-DTA. The results demonstrate that biofilms can be promising materials for medical and tissue engineering applications.

Reference

- [1] S. Anandhavelu, S.Thambidurai, Mater. Chem. Phys. 131 (2011) 449–454.
- [2] K. Pandiselvi, S. Thambidurai, Polymer Degradation and Stability; xxx (2013) 1-9.

7.25 Synthesis and characterization of Polyaniline-CdO composite for better thermal and electrochemical properties

S. Rajaboopathi, S.Thambidurai*

Department of industrial Chemistry, School of Chemical Sciences, Alagappa university, Karaikudi-630003, Tamil nadu.

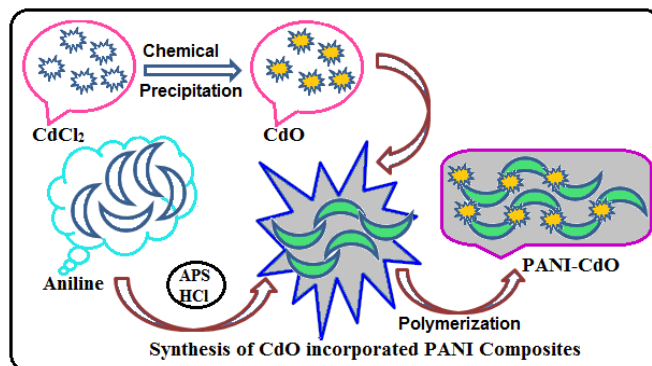
Email:siva.raja2389@gmail.com

Abstract

Polyaniline (PANI) nanofibers as support matrix for metal nanoparticle and the potential material having properties of good suspension ability, high surface areas, less expensive, easily synthesis, good electrical conductivity and main functional group of nitrogen present in the structure and low dimensional systems that provides improved performances for several applications [1-3]. The Cadmium oxide (CdO) is a conducting transparent semiconductor with a direct band gap of 2.5 eV. The CdO has chosen for more number of importance applications, low cost and wide spread availability [4].

In the present work, we aimed to synthesis of CdO decorated PANI composites was synthesized via precipitation followed by in situ chemical oxidative polymerization method using aniline as a monomer and ammonium persulphate as initiator in presence of HCl as a dopant. The FTIR spectra demonstrate the transition metal salt had been incorporated into the polymer chains. The XRD patterns of average crystalline size can be calculated from the Scherer's formula found at 30-40 nm. Surface morphology of CdO-PANI is agglomeration of uniform smooth particles onto the spherical sized PANI surface. Electrical properties of CdO-PANI were found to be increased when compared to pure PANI. Thermal properties CdO decorated PANI has higher thermal stability than pure polyaniline. Thus results indicate that the addition of CdO nanoparticles to the PANI matrix composite has improved electrical and thermal properties.

Key words: Polyaniline, Cadmium oxide, thermal stability, hybrid composite, electrochemical property



References:

- [1] J.J, Li, Mater Lett.(2007) 61: 4894-4896.
- [2] M. Banimahd Keivani, EJournal of Chemistry. (2010) 7: 105-110.
- [3] D. Aussawasathien, J.H. Dong, L. Dai, Synthetic Metals. (2005) 154: 37-40.
- [4] O. Vigil, F. Cruz, Mater. Chem. Phys. (2001) 68; 249–252.

7.26 Biotemplate connected on SnO_2 -graphene hybrid composite for structural, morphological and thermal properties

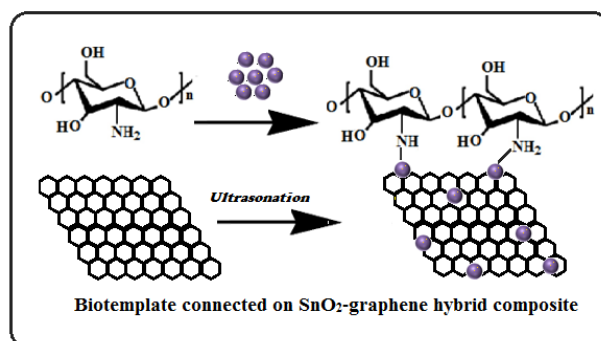
M.Karpuraranjith, S.Thambidurai*

Department of Industrial Chemistry, School of Chemical Sciences, Alagappa University, Karaikudi - 630003, Tamil Nadu.
Email: ranjith3389@gmail.com

Abstract

Chitosan (CS) is one of the promising natural biopolymer on earth used in wide range of applications with excellent film forming abilities, biocompatibility, non toxicity, good water permeability, metal ion adsorption, high mechanical strength, susceptible to chemical modification due to the presence of reactive hydroxyl and amino functional groups. Tin oxide (SnO_2) is one of the most promising materials, an n-type semiconductor with a wide band gap ($E_g = 3.6 \text{ eV}$) and high capacitance, low cost, have been wide range of applications such as energy storage, gas-sensing materials and antireflecting coatings in solar cells. Graphene is a single layer with 2 dimensional structure of carbon atoms. It has extensively interesting research topic for the reason that distinctive property such as the mechanical, thermal and excellent electrical conductivity. It's promising candidate in wide range of applications for storage devices, catalysts, optoelectronic, chemical sensors, ash memory storage devices, transparent conductors and super capacitors.

In the present study, Chitosan- SnO_2 -graphene hybrid composite synthesized by chemical precipitating method using chitosan as a biosurfactant, graphene, tin chloride as a source materials and sodium hydroxide as precipitating agent. The functional groups of resultant matrix from chitosan, metal oxide and graphene were characterized and confirmed by FTIR, and RAMAN Spectroscopy. The crystallite size of the hybrid composite was confirmed by X-ray diffraction analysis (XRD). Surface morphology of the synthesized hybrid composites was analyzed by HR-SEM with EDAX, TEM analysis. The optical property of chitosan- SnO_2 and graphene hybrid composite was analyzed by UV-Vis DRS. The chitosan- SnO_2 particle intercalated graphene layer, thermal stability was analyzed by TG-DTA; the results demonstrate that chitosan- SnO_2 intercalated graphene layer has reinforced effect compared to among the components. Therefore, Biotemplate connected on SnO_2 intercalated to graphene layer can be promising materials for waste water treatment, sensors and super capacitors applications.



Reference

- [1] S. Anandhavelu, S.Thambidurai, Mater. Chem. Phys. 131 (2011) 449–454.
- [2] M. Sharma, Tomar, V. Gupta, Sens. Actuators, B 176 (2013) 675–684.
- [3] J.Gajendiran, V.Rajendran, Mater. Lett. 139 (2015) 116–118.
- [4] S. Anandhavelu, S. Thambidurai, Ionics; 19 (2013) 903-909.
- [5] K. Pandiselvi, S. Thambidurai, Polymer Degradation and Stability; xxx (2013) 1-9.

7.27 Activated carbon-ZnO/Polypyrrole hybrid composite for structural, morphological and thermal properties

S.Nathiya, R.Karthik, S.Thambidurai*

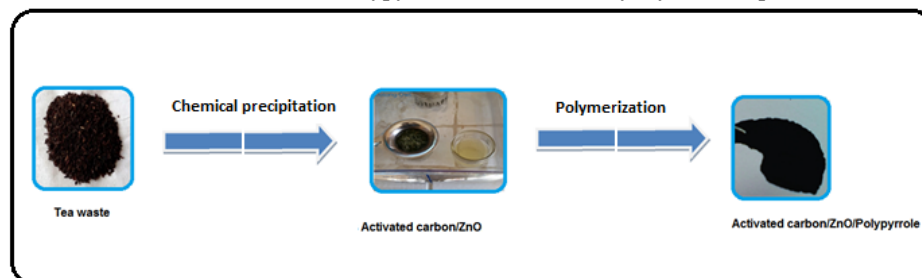
Department of Industrial Chemistry, School of Chemical Sciences, Alagappa University, Karaikudi - 630003, Tamil Nadu.
Email: nathiyamphilchem@gmail.com

Abstract

Nowadays, considering the business cost and energy/ environmental concerns, the use of biomass materials to produce activated carbons (ACs) becomes one of the hot topics. Until now, various biomass materials, such as dates' stones, coconut shells, pitch coke, wood, rice husk, walnut shell and banana peel. AC materials are fabricated by a feasible two-process that consists of carbonization followed by activation. Pyrolysis is occurred in an inert gas atmosphere, such as nitrogen and argon. Whereas, activation is usually carried out via a high temperature process that involves the chemical etching agent of zinc chloride, potassium hydroxide, potassium carbonate and phosphoric acid.

In the present study, Activated carbon-ZnO/Polypyrrole hybrid composite synthesized by chemical precipitation and polymerization method using Tea waste material as a bio mass, Zinc chloride as a source materials and sodium hydroxide as precipitating agent and polymerized with pyrrole. The functional groups of resultant matrix from carbon, metal oxide and nitrogen groups were characterized and confirmed by FTIR Spectroscopy. The crystallite size of the hybrid composite was confirmed by X-ray diffraction analysis (XRD). Surface morphology of the synthesized hybrid composites was analyzed by HR-SEM with EDAX. The optical property of hybrid composite was analyzed by UV-Vis DRS. The Activated carbon-ZnO/Polypyrrole hybrid composite thermal stability was analyzed by TG-DTA; the results demonstrate that activated carbon-ZnO/Polypyrrole hybrid composite has reinforced effect compared to among the components. Therefore, Activated carbon-ZnO/Polypyrrole hybrid composite can be promising materials for waste water treatment, sensors and super capacitors applications.

Key words: Activated carbon, Zinc oxide, Polypyrrole, thermal stability, hybrid composite



Reference

- [1] A. Mohammadi, Y. Yamini, N. Journal of Chromatography A, 1063 (2005) 1-8.
- [2] M. Sharma, Tomar, V. Gupta, Sens. Actuators, B 176 (2013) 675–684.
- [3] S. Anandhavelu, S. Thambidurai, Ionics; 19 (2013) 903-909.
- [4] K. Pandiselvi, S. Thambidurai, Polymer Degradation and Stability; xxx (2013) 1-9.

7.28 Synthesis of novel ionic liquid crystal bearing imidazolium salt

R.Mangaiyarjkarasi, K.Prabhavathi and S.Umadevi *

Department of Industrial Chemistry, Alagappa University, Karaikudi -3, Tamil Nadu, India.
E-mail: umadevilc@gmail.com and mangairajkumarchem@gmail.com

Ionic liquid crystals (ILCs) are fascinating class of materials which incorporate the attractive properties of ionic liquids such as ionic conductivity, high polarizability, low vapour pressure and the interesting features of liquid crystals namely organized structure, anisotropic chemical and physical properties. [1] These

remarkable properties of the ILCs promise potential applications in a variety of fields such as anisotropic ionic conductors, organized reaction medium for organic synthesis as well as the synthesis of mesoporous and nanostructured materials, electrolytes for dye sensitized solar cells and electrochemical applications. [2] Up to date several ILCs exhibiting different mesophase structures namely, hexagonal, cubic, SmA (lamellar) phases have been reported and their ionic conductivity properties have been

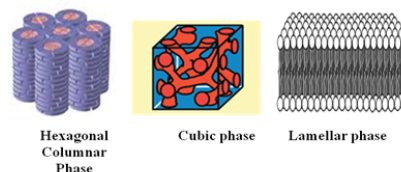
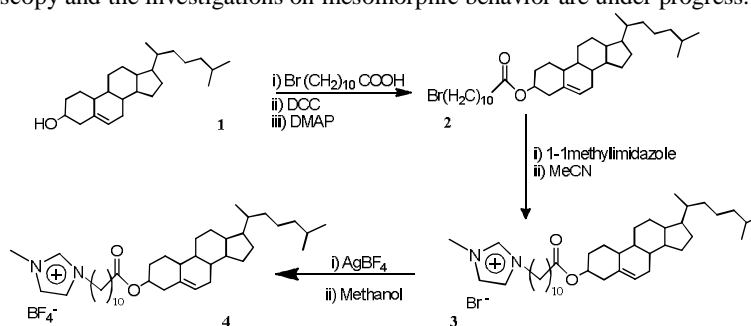


Figure 1: Different mesophase structures exhibited by ILCs

investigated in detail.[3,4,5] However, the other interesting properties of ILCs such as organized reaction medium and as electrolyte for electrochemical reactions are less explored.[6] In this regard we have prepared a new ILCs compound containing an imidazole moiety and intend to employ the mesophase as reaction medium for nanomaterials preparations. Herein, we present the preparation of the compound, its chemical characterization and our preliminary results on mesophase behavior. The calamitic (rod-like) ionic liquid crystal (**4**) with an imidazolium moiety at the end of the molecule is designed and synthesized following a pathway shown in Scheme 1. The synthesized compounds were characterized using infrared and nuclear magnetic resonance spectroscopy and the investigations on mesomorphic behavior are under progress.



Scheme 1: Synthetic pathway for the preparation of calamitic ionic liquid crystal **4**.

References

- [1] K. Binnemans, *Chem. Rev.* 105 (2005) 4148.
- [2] K. V. Axenov, *Materials.* 4 (2011) 206.
- [3] M. Yoshio, T. Mukai, H. Ohno, T. Kato, *J. Am. Chem. Soc.* 9 (2004) 995.
- [4] T. Ichikawa, M. Yoshio, T. Mukai, H. Ohno, T. Kato, *J. Am. Chem. Soc.* 125 (2007) 0663.
- [5] J. Sakuda, M. Yoshio, T. Ichikawa, H. Ohno, T. Kato, *New. J. Chem.* 39 (2015) 4471.
- [6] K. Ching Lee, W. Hsin Huang, J. B Ivan Lin, *Chem. Commun.* (2000) 1911.

7.29 Physico-chemical characterization and identification of halophenols (DBP's) in drinking water sample

Ramarajan Selvam, Selvakumar Muniraj, Tamilselvi Duraisamy, Vasanthy Muthunayanan*, Saravanan Dhandayutham*^{1a}, Ramaswamy Babu Rajendran*²

Department of Environmental Biotechnology, Bharathidasan University, [a] Department of Chemistry National college, Tiruchirappalli 620024. Email: ramjinnaturephd@gmail.com

Abstract:

The US Environmental Protection Agency is developing policy regarding the presence of different drinking water disinfection by-products (DBPs). The hypochlorous and hypobromous acid react with naturally present organic matter to form water disinfection byproducts (DBP's) along with four primary Trihalomethanes such as chloroform (CHCl₃), Bromodichloromethane (CHCl₂Br), Dibromochloromethane (CHClBr₂) and Bromoform (CHBr₃). This study examined the corporation drinking water quality and found the presence of halophenols, one of the disinfection byproducts as a result of disinfection during chlorination.

The water pH value was in the range of 7.98 and the water temperature varied from 63°C. The effects of halide ions, natural organic matter, and drinking water matrix were investigated. The variations of physicochemical parameters as, Electrical conductivity, Total dissolved solids (0±1.22), Dissolved oxygen (DO), Hardness, Calcium, BOD, COD(99±0.08) and major anions namely; Sulphate, phosphate have been

investigated in the main channel of corporation drinking water, Tiruchirappalli, during the year, Jan-2015. The amount of Bromate (81 ± 2.05), Iodate (0.233 ± 0.05), Chlorite (52 ± 1.24) and Chromate (0.098 ± 2.18) was done using UV visible Spectrophotometer.

Here, three extraction solvents are employed for the extraction of disinfection byproducts; the solvents were Hexane, Petroleum ether and Pentane by liquid- liquid extraction method. The two most bountiful classes of DBPs are trihalomethanes (THMs) and haloacetic acids (HAAs) (Krasner et.al 1989). The USEPA has prescribed the maximum permissible level of Trihalomethanes (CHCl_3 , CHCl_2Br , CHClBr_2 , and CHBr_3) to be $80 \mu\text{g/L}$. The Gas chromatographs equipped with capillary columns (DB-WAX, Agilent Technologies, J&W) was employed for the analysis of the drinking water sample.

The analysis shows the presence of 2-bromo-4-chlorophenol. It is commonly accepted that the reaction between chlorine and humic substances, a major component of NOM, is responsible for the production of organochlorine compounds during water treatment. Most chlorine DBPs are produced during oxidation and substitution reactions. The major functional groups of humic substances include acetyl, carboxyl, phenol, alcohol, carbonyl and methoxyl. The reactions proceed much more rapidly at high pH than at low pH.

The formation of such Bromochlorophenol may be due to the reaction between the Chlorine introduced in the form of hypochlorite with phenols and also with the bromine/ bromate present in the water sample. Most chlorine DBPs are produced during oxidation and substitution reactions. The major functional groups of humic substances include acetyl, carboxyl, phenol, alcohol, carbonyl and methoxyl. The reactions proceed much more rapidly at high pH than at low pH.

Chlorine and bromine compounds are reported to be carcinogenic, mutagenic or teratogenic through animal studies (Clifford et.al 1999). The formation of Bromochlorophenol may be due to the reaction between the Chlorine introduced in the form of hypochlorite with phenols to produce monochlorophenols, dichlorophenols or trichlorophenols. This study was conducted to identify DBPs from the corporation drinking water by employing Gas chromatography coupled with Mass Spectrometry.

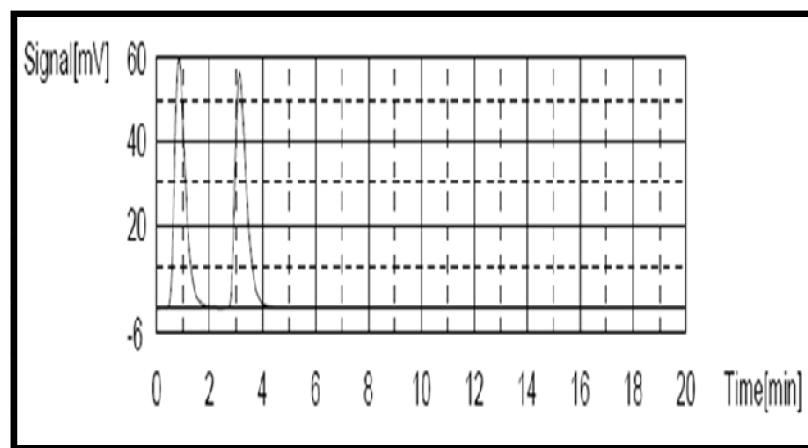


Fig 1. Total Organic Carbon

References

- [1] Clifford P. Weisel, Hekap Kim, Patricia Haltmeier, and Judith B. Klotz, Exposure Estimates to Disinfection By-products of Chlorinated Drinking Water, *Environmental Health Perspectives* (1999), Vol. 107, No. 2, pp. 103-110.
- [2] Krasner SW, McGuire MJ, Jacangelo JG, Patania NL, Reagen KM, Aieta EM. The occurrence of disinfection by-products in US drinking water. *American Water Works Association Journals* (1989) 81:41-53.
- [3] WHO. Guidelines for Drinking-water Quality. Fourth Edition. http://whqlibdoc.who.int/publications/2011/9789241548151_eng.pdf (last accessed 1st September 2014): 2011.

7.30 Design and Performance of a Riboflavin-Alginate Hydrogel beads for In Vitro Anti-Oxidant Activity

G. Sathya, B. Suganya Bharathi, T. Stalin*

Department of Industrial Chemistry, Alagappa University, Karaikudi – 03, Tamilnadu, India.

E-mail: sathyaganesan16@gmail.com and drstalin76@gmail.com

Abstract:

Alginate has a variety of applications due to their biocompatibility and biodegradability character, it treated into various morphologies such as films, capsules, beads or hydrogels. Here, to enhance the antioxidant

activity of a vitamin B₂(Riboflavin) that uses alginate as a carrier matrix. Riboflavin was incorporated in the alginate gel beads as a model bioactive compound. Vitamin B₂ (Riboflavin) loaded calcium chloride cross linked alginate hydrogel beads were prepared by ionotropic gelation followed by freeze-thawing cycles. The crosslinking Process was confirmed by FT-IR and XRD techniques. Scanning Electron Microscope (SEM) and EDX spectra were used to study the morphology and surface elemental composition of the prepared vitamin-alginate gel beads. The antioxidant activity of the prepared riboflavin-alginate gel beads was performed with an aqueous system. The resultant vitamin incorporated alginate gel beads displayed good antioxidant properties.



Fig.1. Riboflavin-Alginate hydrogel beads

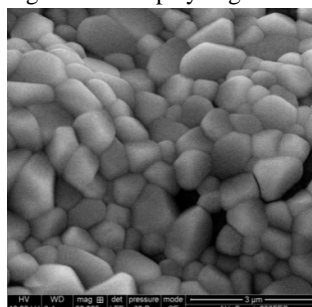


Fig.2. SEM image of Riboflavin-hydrogel beads

Keywords: Calcium alginate, Riboflavin, Hydrogel beads, Anti-oxidant activity.

References:

- [1]. Zhou, Q.; Lin X.; Qian J.; Wang J.; Luo X. *RSC Adv.* **2015**,5, 2100.
- [2]. Elena G. Popa.; Manuela E. Gomes.; Rui L. Reis. *Biomacromolecules.***2011**, 12, 3952-3961.
- [3]. Luo, R.; Venkatraman, S. S.; Neu, B. *Biomacromolecules.* **2013**, 14, 2262–2271.

7.31 Liquid crystal functionalized platforms for electro-optical applications

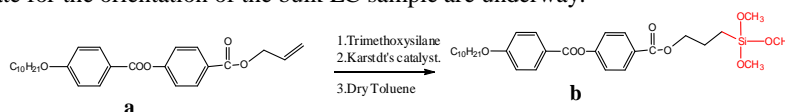
B. Sivarajini, G. Suganya and S. Umadevi*

Department of Industrial Chemistry, Alagappa University, Karaikudi-630 002

E-mail: sivarajini93alu@gmail.com and umadevilc@gmail.com

Liquid crystals (LCs) are self-assembled soft materials with a huge potential for application in a wide variety of fields such as sensing, biomedical, photonics, optoelectronics, electronic conductors, photovoltaic etc. apart from their significant use in display technology.[1,2] For the majority of these LC applications, a pre-oriented well, aligned sample of LC on a suitable substrate is highly crucial. The conventional methods existing so far for the alignment of LCs are effective in orienting the mesophase such as nematic, smectic only and not efficient over a long period of time. Therefore, there is a significant need for formulating simple strategies for effective alignment of these materials on different substrates. An alignment layer made of molecules with a similar shape, i.e., LC molecules itself will provide necessary shape and symmetry compatibility for the bulk LC sample to be aligned. In view of this, we are forming the self-assembled monolayers (SAMs) of tailor-made LC molecules on various substrates and investigating the alignment abilities of these films to orient the bulk LC sample.

Herein, we present the SAM of a rod-like thermotropic LC compound (structure **b**) on a transparent, conductive indium tin oxide (ITO) substrate and the electron transfer properties of the modified substrate across the electrode-electrolyte interface. The preparation of the LC compound, SAM formation on ITO and electrochemical characterization of the SAM modified substrate are described. The vinyl terminal group in the LC compound is converted to a trimethoxysilane moiety through a hydrosilylation reaction (Scheme 1), since trimethoxysilane compounds can be very effectively attached on to ITO surface (Figure 1). All the synthesized compounds are characterized using infrared and nuclear magnetic resonance spectroscopy. Mesomorphic characterization is carried out using a combination of differential scanning calorimetry, X-ray diffraction and polarizing optical microscopy studies. The LC compound displayed a smectic C and nematic phases. The electron transfer behaviour of the LC SAM modified substrate is studied using a cyclic voltammetry technique by employing a potassium ferrocyanide as a redox probe. Studies on alignment properties of the LC SAM modified substrate for the orientation of the bulk LC sample are underway.



Scheme: Synthetic pathway for the preparation of liquid crystals

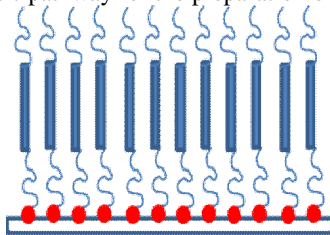


Figure 1: A Schematic representation of LC monolayer functionalized ITO electrode

References

- [1] M. Bremer, P. Kirsch, M. Klasen-Memmer, K. Tarumi, *Angew. Chem. Int. Ed.*, **52**(2013), 8880
 [2] A. M. Lowe, N. L. Abbott, *Chem. Mater.*, **24** (2012), 746; *Liq. Cryst.*, **1**(2013), 29

7.32 Physico-chemical studies and micronutrients status in coastal agriculture land area of Sirkazhi taluk of Nagapattinam district, Tamil Nadu, India

¹A.Arokiyaraj, ²N.Pasupathy, ³A.Vincentraj and ⁴D.Sathya
^{1&2}PG and Research Department of Chemistry, A.V.C.College (Autonomous),
 Mannampandal-609305, Mayiladuthurai, Tamilnadu, India. arochemmyl@gmail.com
³PG and Research Department of Chemistry, Poompuhar College (Autonomous),
 Melaiyur-609 107, Nagapattinam, Tamilnadu, India.sksundharam61@gmail.com
⁴PG and Research Department of Chemistry, Pachaiyappa's College, Chennai-30, Tamilnadu, India.

Abstract

Micronutrients are “trace elements” are essential in small quantities for the growth of plants. Fe, Mn, Zn, Cu, B, Mo, Co and Cl₂ are considered as micronutrients. These micronutrients may produce synergetic and antagonistic effects in plants, if they are present in excess or in deficiency level in the soil. In this study assess the Physico-Chemical parameters and micronutrient status of Fe, Mn, Zn and Cu in Sirkazhi taluk of Nagapattinam district in Tamilnadu state. Surface soil samples depth (0 – 20 cm) numbering 100 from 20 revenue villages, five samples were collected from each revenue village. The study area covers Coastal Agriculture land area of Sirkazhi taluk. The basic physico –chemical parameters pH, EC and OC were calculated in the study area. Assess the micronutrient status by using Atomic Absorption Spectrophotometer. By using the critical levels fixed by earlier workers for DTPA (Diethylene Triamine Penta Acetic acid) extractable micronutrients in Tamilnadu soils, the percentage deficiencies of individual nutrients were calculated in each revenue village. From the results of the analysis of soil samples, concrete suggestions can be made to improve the soil quality and crop production.

Keywords: Micronutrients, Sirkazhi taluk, Soil, Tamil Nadu.

7.33 Synthesis and characterization of PVA modified VO₂ nanocomposites by thermal decomposition method

A. Mohamed Azharudeen^a, B. Kavitha, M. Rajarajan^{a**}, A. Suganthi^{b*}
^aP.G. & Research Department of Chemistry, C. P. A. College, Bodinayakanur- 625513
^bP.G. & Research Department of Chemistry, Thiagarajar College, Madurai- 625009
 Email: azhar5406@gmail.com, rajarajan_1962@yahoo.com

Abstract

Nano-structured vanadium dioxide (VO₂) are fabricated via facile thermal-decomposition method by using PVA (wt %) (Poly vinylalcohol) as a capping agent. The prepared nanocomposites VO₂, VO₂/ 2% PVA, VO₂/ 4% PVA and VO₂/ 6% PVA were characterized through Ultra-violet Diffuse Reflectance spectroscopy (UV-Vis-DRS), Fourier- Transform Infra-red (FT-IR) spectrum, X-ray diffraction (XRD) pattern, Scanning Electron Microscopy (SEM), Energy Dispersive X-ray spectroscopy (EDX) and High resolution Transmission electron microscopy (HR-TEM) techniques. The band gap of the synthesised nanocomposites shifted to the visible region when loading with 2% PVA, 4% PVA and 6% PVA. The bands appear in FT-IR spectrum from 550 cm⁻¹ to 1100 cm⁻¹ are attributed to the stretching vibrations of V-O and the crystal structures are belonging to monoclinic. The SEM image shows that, the aggregation of uniform spheres like structure due to capping effect of PVA. The HR-TEM image reveals that the uniform matrix of PVA incorporated on the surface of VO₂ nanoparticles.

Keywords: Vanadium dioxide nanocomposites, polymer modified, thermal decomposition,

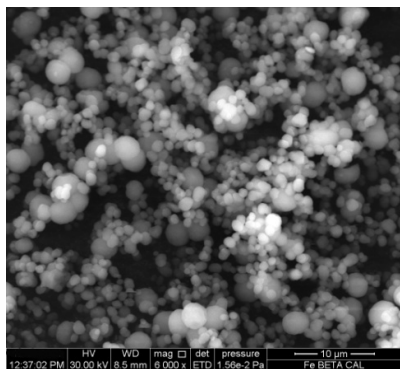


Fig. 1. SEM image of VO₂ / 6% PVA nanocomposites

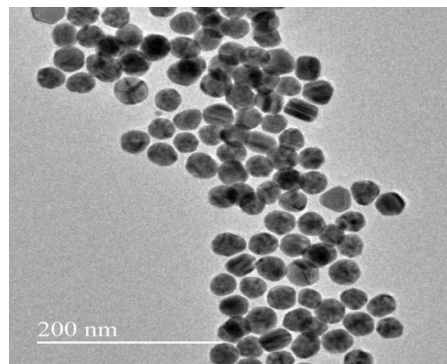


Fig. 2. HR-TEM image of VO₂ / 6% PVA nanocomposites

References

- [1] C. Leroux, G. Nihoul, G. Van Tendeloo, *Physical Review B*, 57 (1998) 5111–21.
 [2] M. Maaza, K. Bouziane, J. Maritz, D. S. McLachlan, R. Swanepool, J. M. Frigerio, *Optical Materials*, 15 (2000) 41–5.

7.34 Antimicrobial activity of some newly synthesized copper (II) 2-(1H-benzo[d]imidazole-yl) methylamino)benzoic acid complex on bacterial and fungal pathogens

R.T. Rajalakshmi^{*}, S. R. Bheeter^a & T. Dons^b

^aP.G & Research Department of chemistry, St. Joseph's College, Trichy

^bP.G & Research Department of Botany, St. Joseph's College, Trichy. *Email : rajichensjc@gmail.com

Abstract

This research involves the preparation of Copper based metallo drugs with the ligand 2-(1H-benzo[d]imidazole-yl) methylamino) benzoic acid. The ligand was prepared through general mannich reaction by the condensation of anthranilic acid with formaldehyde and benzimidazole. The ligand and the copper based metal complex were evaluated for antibacterial and antifungal activity. The [Cu(L₂)Cl₂] complex showed significant antibacterial activity against *Shigella sonnei*, *Klebsiella pneumonia*, *Proteous vulgaris*, *Salmonella typhi*, *Proteous mirabilis* and the antifungal activity against *Curvularia lunata*, *Aspergillus niger*, *Aatternaria solani*, *Bipoaris sps*, *Aspregollus fumigates*. The activity data show that the metal complexes are more potent than the parent ligand. These results collectively support the use of [Cu(L₂)Cl₂] complex as a suitable drug to treat bacterial and fungal infections.

Keywords: Copper(II)complex, 2-(1H-benzo[d]imidazole-yl) methylamino)benzoic acid , antimicrobial studies.

7.35 Synthesis, structural, morphological and electrical properties of Zn_{1-x}Al_xO nanocrystals for thermoelectric applications

T.M.V.Murugu Thiruvalluvan¹, V.Natarajan², S. Valanarasu³, P.Anandan⁴, M.Arivanandhan^{5*},
 R.Chandramohan⁶

¹Department of Physics, Manonmanium Sundaranar University, Tirunelveli, India

²Department of Physics, Dr.Sivanthi Aditanar College of Engineering, Tiruchendur, India

³Department of Physics, Arul Anandar College, Karumathur, Tamil Nadu, India

⁴Department of Physics, Thiru Kolanjiappar Government Arts College, Virudhachalam, India

⁵Center for Nanoscience and Technology, Anna University, Chennai, India

⁶Department of Physics, Sree Sevugan Annamalai College, Devakottai, Tamil Nadu, India

Email: arivucz@gmail.com

Increasing industrial sources and burning of fossil fuel causes CO₂ emission which leads to potential global warming. Hence, it is highly essential to find an alternate way of generating electrical energy instead of burning fossil fuel for solving the energy and environmental problems. Zinc Oxide (ZnO) is a promising direct bandgap semiconductor useful for many applications [1-3]. The thermoelectric properties of Al doped ZnO have been widely studied. The thermoelectric performance of a material can be determined by the dimensionless figure of merit (ZT). The problem with ZnO is its high thermal conductivity at elevated temperature, which

results low ZT of the material. Nanostructuring the material is an efficient way to control the phonon transport, thereby thermal conductivity of the material. Zinc Oxide (ZnO) is a direct bandgap semiconductor useful for many applications. Thermoelectrics is a promising technology to convert waste heat into useful electric energy. The thermoelectric performance of a material can be determined by the dimensionless figure of merit (ZT). The thermoelectric properties of ZnO have been widely studied. The problem with ZnO is its high thermal conductivity at elevated temperature, which results low ZT of the material. Nanostructuring the material is an effective way to control the phonon transport, thereby thermal conductivity of the material.

In the present work, $Zn_{1-x}Al_xO$ nanocrystals were synthesised by sol-gel method with various molar ratios of the precursor solution. The structural properties of the material were studied by X-ray diffraction analysis. The morphology of the synthesized nanocrystals was studied by FE-SEM analysis. The $Zn_{1-x}Al_xO$ nanocrystals were pelletized and the electric properties of the pelletized nanostructured material such as electrical conductivity, carrier concentration, mobility were measured as a function of composition ratio. The electrical conductivity of the $Zn_{1-x}Al_xO$ increased with x up to 0.1 and relatively decreased at higher Al composition ratio. Therefore the electrical properties of the synthesised material can be tuned by varying the Al composition thereby the thermoelectric properties of the material.

References

1. Li Han, Ngo Van Nong, Wei Zhang, Thanh Hung Le, Tim Holgate, Kazunari Tashiro, Michitaka Ohtaki, Nini Pryds, and Søren Linderøth, *RSC Adv.* **4**, 12353 (2014).
2. Li Han, Ngo Van Nong, Thanh Hung Le, Tim Holgate, Nini Pryds, Michitaka Ohtaki, and Søren Linderøth, *J. Alloys Compd.* **555**, 291 (2013).
3. Tsubota T, Ohtaki M, Eguchi K, Arai H. *J Mater Chem* 1997;7:85–90.

7.36 The effect of Zn:ti ratio on the various phase formation and optical properties of zinc titanate nanocrystals

P. Chandrasekaran^a, P. Anandhan^b, A. Raja^c, G. Gopu^d, M. Arivanandhan^e

^aDepartment of Physics, Annamalai University, Annamalai Nagar, Chidambaram, India

^bDepartment of Physics, Thiru Kolanjiyappar Government Arts College, Vridhachalam-606001, India

^cDepartment of Physics, Bharath Institute of Higher Education and Research, Selaiyur, Chennai, India.

^dDepartment of Industrial Chemistry, Alagappa University, Karaikudi, India.

^eCentre for Nanoscience and Technology, Anna University, Chennai-600025, India

Abstract

Titanium dioxide (TiO_2) is a promising material for various applications due to its excellent stability, nontoxicity, low cost and its ability to produce highly oxidizing radicals [1,2]. ZnO is also a potential material in the areas of photocatalysis [3], solar cells [4], and gas sensors [4, 5]. As a consequence, the TiO_2 -ZnO related composite material is highly useful for all the above-mentioned applications and the properties of the composite material can be tuned based on the composition ratio of the source materials. In the present work, $ZnTiO_3$ nanocrystals were synthesized by sol-gel method with different Zn and Ti molar ratios. The synthesized nanocrystals were annealed at different temperatures to study the impact of Zn and Ti molar ratio and annealing temperature on the structural and optical properties of the titanates. The structural, morphological and optical properties of sol-gel synthesized $ZnTiO_3$ nanocrystals were studied by XRD, FESEM and UV-Vis optical spectroscopy. The phase transition of titanates from one phase to another phase as a function of annealing temperature were studied by XRD analysis. Three different phases such as anatase form of TiO_2 , $ZnTiO_3$ and $Zn_2Ti_3O_8$ were observed in the samples calcined at temperature above 600°C. Moreover the $Zn_2Ti_3O_8$ phase was dominated in the samples calcined at 800°C and 1000°C as the diffraction peaks corresponds to $Zn_2Ti_3O_8$ phase was dominant in both the spectra. From the FESEM images, it was observed that the particles are mono dispersed with sizes less than 100 nm at temperature of 400°C. However, when the calcination temperature increases, the particles are grown as large size crystallites. The photoluminescence (PL) of the samples were systematically investigated as a function of Zn to Ti ratio and annealing temperature. The PL results show that the emission wavelength can be tuned based on the Zn and Ti ratio and thus useful for various optical applications.

References

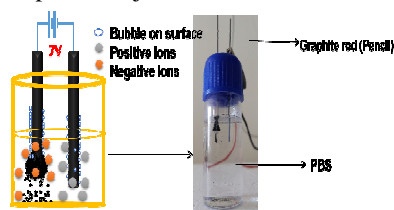
1. Kuo, Y.-L.; Chen, H.-W.; Ku, Y. *Thin Solid Films* 2007, 515, 3461–3468.
2. Yu, J.; Yu, H.; Ao, C. H.; Lee, S. C.; Yu, J. C.; Ho, W. *Thin Solid Films* 2006, 496, 273–280.
3. Georgekutty, R.; Seery, M. K.; Pillai, S. C. *J. Phys. Chem. C* 2008, 112, 13563–13570.
4. Kluth, O.; Schöpe, G.; Hupkes, J.; Agashe, C.; Müller, J.; Rech, B. *Thin Solid Films* 2003, 442.
5. Choi, W. S.; Kim, E. J.; Seong, S. G.; Kim, Y. S.; Park, C.; Hahn, S. H. *Vacuum* 2009, 83, 878–882.

7.37 Dynamic sensing of ascorbic acid, dopamine and uric acid at electrochemically exfoliated graphene oxide-gold nanoparticle by electrochemical methods

Habibulla Imran, Venkataraman Dharuman*

Molecular Electronics Laboratory, Department of Bioelectronics and Biosensors, Science Block, Alagappa University, Karaikudi – 630 004. E-mail: dharumanudhay@yahoo.com

Graphene oxide was prepared from pencil as a graphite rod (dimensions of 60 mm length, 0.6 mm diameter and surface area 20 mm²) electrochemically by applying a constant DC potential +7 V between two pencil electrodes in phosphate buffer saline (pH 7.4) without using ionic liquids, Scheme 1. The formation of GO is confirmed by XRD, FTIR, Raman spectroscopy, Scanning electron microscope (Fig. 1) photoluminescence and UV-Vis spectroscopy. The obtained GO washed and transferred to Dimethylformamide (1.5 mg / 1 ml) and sonicated for 1 hour. The GO immobilized on polished glassy carbon electrode (GCE) by simple drop casting followed by electrochemical deposition of gold nano particles (AuNP) to form GO-AuNP. Both the GO and GO-AuNP modified GCEs are tested for the simultaneous detection of DA, AA, and UA. The peaks are well separated on both the GO-AuNP surfaces, however, significant differences are clear between the two CV profiles, Fig. 2. The GCE-GO-AuNP surface exhibits well defined peaks for all these analytes in CV. The CV peak current increases for the AA, UA and DA. DPV was used for simultaneous detection of the DA, UA and AA and detection limits observed were 20 (UA), 5 (DA) 200 μM (AA). Concentrations of DA, AA and UA in real samples viz., dopamine injection, vitamin C tablets and human urine are evaluated by LSV.



Scheme 1 Electrochemical exfoliation of a pencil to form graphene oxide



Fig. 1 SEM images (A) Pencil graphite rod (B) GO and (C) GO-AuNP.

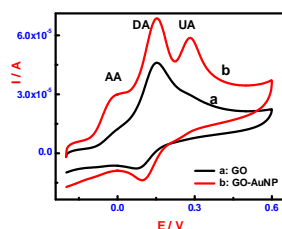


Fig. 2 Simultaneous detection of 1 mM of dopamine, ascorbic acid and uric acid in PBS (pH 7.4) for GO (curve a) and GO-AuNP (curve b).

Keywords: Electrochemical, XRD, FTIR, UV-Vis, dopamine

7.38 Synthesis and characterization of polypyrrole-zirconia-graphene (Ppy-ZrO₂-Graphene) nanocomposite for voltammetric nitrite detection

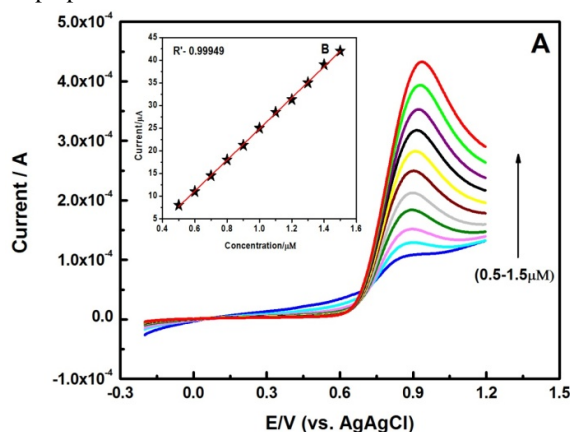
M. Ramya and J. Wilson*

Polymer Electronics Lab, Department of Bioelectronics and Biosensors, Alagappa University, Karaikudi - 630004, Tamilnadu, India. Email: mramya155@gmail.com

Abstract

A novel strategy to fabricate nitrite sensors was developed based on polypyrrole -zirconia - graphene nanotubes (Ppy-ZrO₂-Graphene) composite film on glassy carbon electrode. The Poly pyrrole (Ppy) nanotubes were synthesized by using the complex of methyl orange (MO) / FeCl₃ as a template. Followed by mixing of ZrO₂ and graphene have been performed over the Ppy nanotubes to form Ppy-ZrO₂-Graphene nanotubes. The resulting ppy and Ppy - ZrO₂ - Graphene composite was characterized by X-ray Diffraction (XRD), Fourier transform Infrared spectroscopy (FTIR), Cyclic voltammetry (CV), Electrochemical Impedance spectroscopy

(EIS), and linear sweep voltammetry (LSV). The nanotubular structure with high surface area of Ppy-ZrO₂-Graphene composite film has been highly catalytic activity toward the electrochemical oxidation of nitrite. The modified electrode showed good linear range between 0.5 to 1.5 μ M. In this work, we synthesized high-quality of PPy-ZrO₂-Graphene nanotubes by a simple chemical route using methyl orange as a soft template. The new material can be considered as a high sensitive in voltammetric determination of Nitrite. The proposed sensor shows a novel electrocatalytic activity towards the anodic oxidation of Nitrite with a significant enlargement in peak current and a great decrease in peak potential. The reproducibility, stability and low detection limit of the proposed electrode make it appropriate for use in the electrochemical determination of Nitrate in pharmaceutical and clinical preparations.



References

- [1] A. G. MacDiarmid, *Angew. Chem. Int. Ed.* 40 (2001) 2581.
- [2] A. J. Heeger, *Angew. Chem. Int. Ed.* 40 (2001) 2591.
- [3] Chyong fang hsu, Development of conducting polymer-based antioxidant packaging materials.(2009) page11.

7.39 Cerium doped nickel-oxide nanostructures for riboflavin biosensing and antibacterial applications

P. Muthukumar¹ and J. Wilson^{1*}

¹Polymer Electronics Lab, Department of Bioelectronics and Biosensors, Alagappa University, Karaikudi - 630004, Tamilnadu, India. Email: muthu.oct86@gmail.com

Abstract

A sensitive electrochemical method for riboflavin (RF) detection based on Ce–NiO nanostructures was developed using a hydrothermal assisted chemical route. The created several oxygen vacancies on Ce doping are considered as the key factor for the magnificent electro catalytic behavior of the Ce – NiO sample. The same oxygen vacancies also play an important role in antibacterial applications. Hence dual behavior of this Ce – NiO sample was investigated: (i) RF sensing was characterized by XRD, SEM, cyclic voltammetry (CV), electrochemical impedance spectroscopy (EIS) and square wave voltammetry (SWV) using [Fe(CN)₆]^{3-/4-} and phosphate buffer solution (PBS) for probing the binding interaction between the Ce – NiO and RF. The Ce ions doped into the NiO nanostructure exhibit an excellent performance towards the detection of RF over a wide linear range from 1 mM to 50 nM, with a detection limit of 0.676 nM (3 σ /b). (ii) Investigation of antibacterial activity using both Gram negative and positive bacterial strains. The minimal inhibitory concentration and minimal bactericidal concentration against *B. Subtilis* is found to be 10 μ g ml⁻¹. The diameter of the zone of inhibition for *B. subtilis* and *S. aureus* is quantified to be 22 and 18 mm respectively. Our results confirmed that Ce - doped NiO nanomaterial is a useful platform for electro catalytic and biomedical applications.

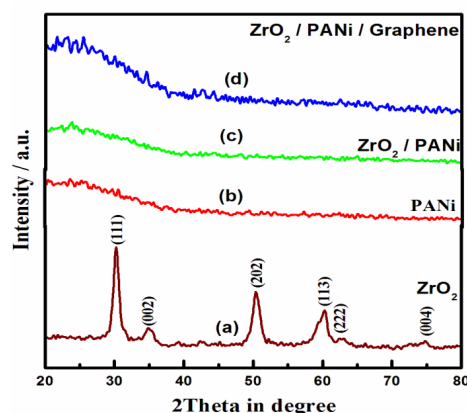
7.40 Synthesis and characterization of polyaniline-zirconia-graphene (PANi -ZrO₂ - Graphene) nanocomposite for voltammetric nitrite detection

P. Thivya¹ and J. Wilson^{1*}

¹Polymer Electronics Lab, Department of Bioelectronics and Biosensors, Alagappa University, Karaikudi - 630004, Tamilnadu, India. Email: ddivyaec@gmail.com

Abstract

A novel strategy to fabricate sensors was developed based on polyaniline/ZrO₂/Graphene nanotubes on glassy carbon electrode. The polyaniline (PANi) nanotubes were synthesized by using the complex of methyl orange (MO)/FeCl₃ as a template. Followed by mixing of ZrO₂ and Graphene have been performed over the PANi nanotube to form PANi/ZrO₂/Graphene nanotubes. The resulting PANi was characterized by fourier transform infrared spectroscopy (FTIR), Cyclic voltammetry (CV), Electrochemical impedance spectroscopy (EIS), X-ray diffraction (XRD) and Linear sweep voltammetry (LSV). The nano tubical structure with high surface area of PANi has been highly catalytic activity toward the electrochemical oxidation of nitrite. The modified electrode showed good linear range between 0.1 to 1mM. In this work, we synthesized high-quality of polyaniline - (PANi-Zro2-Graphene) nanotubes by a simple chemical route. The new material can be considered as a high sensitive in voltammetric determination of nitrite. The reproducibility, stability and low detection limit of the proposed electrode make it appropriate for use in the electrochemical determination pharmaceutical and clinical preparations.



References

- [1] A. G. MacDiarmid, *Angew. Chem. Int. Ed.* 40 (2001) 2581.
- [2] A. J. Heeger, *Angew. Chem. Int. Ed.* 40 (2001) 2591.
- [3] Chyong fang hsu, Development of conducting polymer-based antioxidant packaging materials. (2009) page 11.
- [4] Skotheim. *Handbook of Conducting Polymers Vol I & II.* Marcel Dekker. New York, 1986.

7.41 Synthesis of Pyrano-phenazine derivatives and their evaluation biological activities

P. Veeramani, V. Sethuraman and P. Manisankar*

Department of Industrial Chemistry, Alagappa University, Karaikudi – 630 003

Phone: +91 4565 228836; Fax: +91 4565 225202

*Corresponding Author E-mail: pms11@rediffmail.com

Abstract

The pyrano-phenazine derivatives were synthesized by an efficient procedure using the reaction between benzophenacin-5-ols with the condensation product of an aldehyde with meldrum acid in the presence of a catalytic amount of L-proline at ambient temperature. The procedure is very simple, and products could be separated from the reaction media by simple filtration. High functional-group tolerance both in the benzophenazin-5-ol and aldehyde moieties, facile reaction procedure, medium- to-high yields, and simple separation of the products from the reaction media are the advantages of this route. All Pyrano-phenazine derivative are very good activity in anti biofilm and tumor. All derivatives obeyed Lipinski's rule of five with good biological activity. All targets among two showed lesser drug likeness and drug score values compared to the derivatives using OSIRIS property explorer. Except these two derivatives, all other synthesized targets act as drugs.

7.42 Ag₆Mo₁₀O₃₃/ZnO nanocomposites with high visible light photocatalytic activity for removal of organic pollutant: Optimization by Genetic algorithm

K. Eswaran^a, B. Kavitha^a, P. Manikandan^a, M. Rajarajan^{a**}, A. Suganthi^{b*}

^a P.G. & Research Department of Chemistry, C.P.A. College, Bodinayakanur - 625513, Tamilnadu, India

^b P.G. & Research Department of Chemistry, Thiagarajar College, Madurai - 625009, Tamilnadu, India

Email: eswaran_kamaraj@yahoo.in, rajaramchem1962@gmail.com

Abstract

Photocatalytic removal of toxic dye from aqueous medium is a challenge because of the relatively low efficiency of photocatalysts. There has been sustained interest in a variety of efficient nanomaterials for aqueous treatment. In the present work, an efficient photocatalyst Ag₆Mo₁₀O₃₃/ZnO was synthesized via simple route. The materials were characterized by UV-visible-DRS, FT-IR, XRD, SEM and EDX. The optical band gap was 3.05 eV for ZnO and 2.8 eV for Ag₆Mo₁₀O₃₃/ZnO, which is quite lower than that of bare ZnO. The present investigation describes the applicability of Ag₆Mo₁₀O₃₃/ZnO for removal of Congo red (CR) from aqueous solution. The simultaneous photocatalysis proved to be a better reaction condition for photo degradation of the dye in the presence of Ag₆Mo₁₀O₃₃/ZnO under visible irradiation. A significant removal efficiency of 94 % for CR was achieved in 2 h. An artificial neural network comprising three input variables (pH, catalyst dosage, dye concentration), 10 neurons and an output variable (% dye degradation) was optimized, tested and validated for dye degradation. The network, based on tangent sigmoid and linear transfer functions for the hidden and input/output layers, respectively. The Levenberg–Marquardt back propagation training algorithm, can successfully predict dye degradation.

Keywords: photocatalyst, nanocomposite, congored, degradation, artificial neural network.

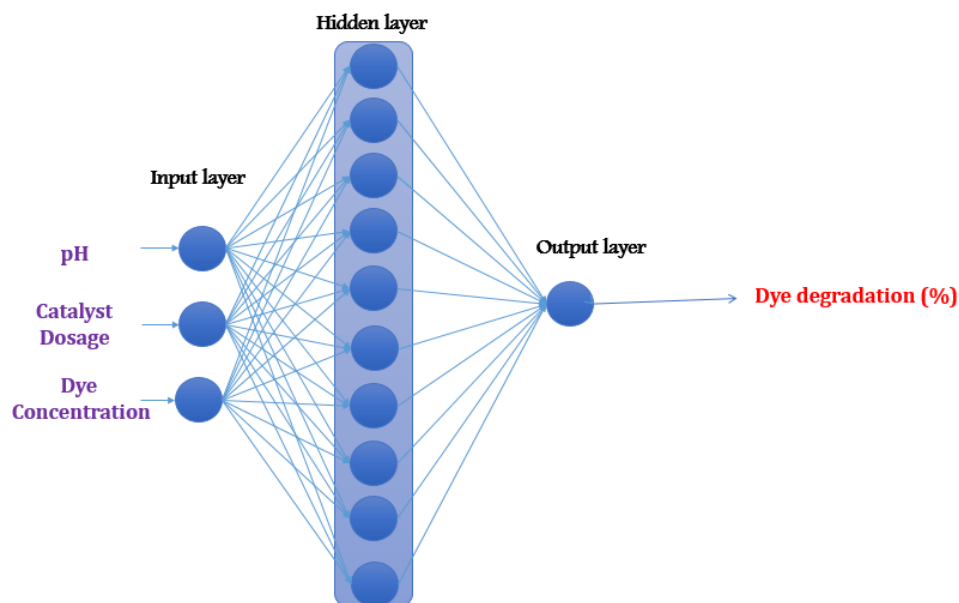


Fig.1 Optimized Artificial Neural Network Model for Degradation of Organic Pollutant

References:

- [1]. K. Buvaneswari, R. Karthiga, B. Kavitha, M. Rajarajan, A. Suganthi, *Applied Surface Science* 356, (2015) 333-340.
- [2]. H. Eskandarloo, A. Badii, M. A. Behnajady, *Industrial and Engineering Chemistry Research*, 53, (2014) 6881–6895.
- [3]. B. Kavitha, D. Sarala Thambavani, *RSC Advances*, 6 (2016), 5837-5847.

7.43 Degradation of Reactive Red 2 Dye With Novel Nanosize Active Charcoal

V. Sreeja^a, J. Anandha Raj^b, C. Vedhi^c

^aDepartment of Chemistry, Vellalar Women College, Erode -630303

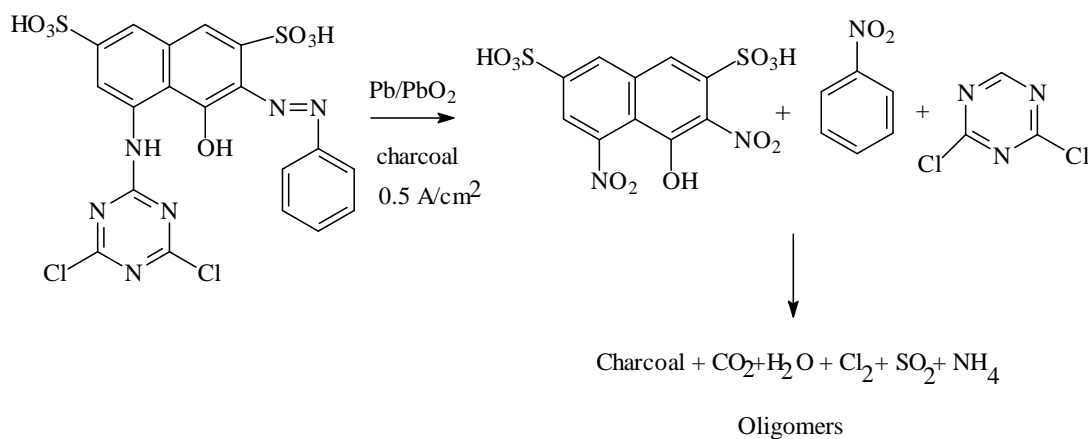
^bDepartment of Industrial Chemistry, Alagappa University, Karaikudi -630 003

^cDepartment of Chemistry, V.O.Chidambaram College, Thoothukudi. Tamilnadu. India

Abstract

Cyclic voltammograms of RR 2 on glassy carbon electrode at different pH, scan rate and concentration were recorded. The effect of pH was studied by varying pH from 1.0 to 9.2. In the pH range studied one sharp anodic peak was prominently seen in the cyclic voltammograms at scan rate 100 mV/sec. One anodic peak around potential 862 mV and one broad cathodic peak centered around -584 mV were observed. The maximum peak current was obtained at pH 1.0. This shows that the electrochemical oxidation of RR 2 is facilitated in acidic media and hence the rate of electron transfer is faster. Environmental problems such as appearance of colour in discharges from various industries, combined with the increasing cost of water for industrial sector, have made the treatment and reuse of effluent increasingly attractive to the industry. Textile industry is one of the oldest industries in India with over 1000 industries. Taking into account the volume and composition of effluent, the textile wastewater is rated as the most polluting among all in the industrial sectors. Electrochemical degradation experiments were conducted to degrade a textile dye. UV-VIS absorption spectrum of 100 ppm reactive red 2 dye was studied from 200 to 800 nm. The typical absorption spectra exhibited two bands at 286 and 526 nm. The absorption band at 286 nm may be due to π - π^* electronic transition of benzene ring. The absorption band at 526 nm associated with conjugation of dye molecules. A laboratory scale bench-top reactor was used to investigate the effect of various operating parameters using stable anode. The influence of operating variables on the mineralization efficiency was studied as a function of the current density, the initial pH, the initial concentration of the dye and the addition of charcoal. Measurement of absorbance was used to discriminate the effect of charcoal in the electro-oxidation process. We found that the decolouring efficiency increased whereas the mineralization efficiency decreased with the increasing concentration of charcoal. Quantitative measurement of organic ions was done by electrochemically. On the basis of the reaction products identified, a possible degradation pathway for the anodic oxidation of RR2 in aqueous solution is proposed.

Key words: Cyclic voltammetry, Reactive Red 2, Lead Electrode, Degradation, Charcoal



7.44. A facile synthesis of magnetic activated carbon/CoFe₂O₄ nanocomposite for the adsorption of congo red dye from water

P. Karthikeyan^a, P. Anjana^a, K.S. Anjali^a, P.S. Anagha^a, B. Ushadevi^b, S. Vairam^b, V. Ranjithkumar^{a*}

^aDepartment of Chemistry, Kongunadu Arts and Science College, Coimbatore – 641029

^bDepartment of Chemistry, Government College of Technology, Coimbatore – 641013

*Corresponding author: mscranjith@gmail.com, Tel: 04222642095 & Fax: 04222644452

Abstract

Activated carbon (AC)/CoFe₂O₄ nanocomposite have been prepared by a simple pyrolytic method using a mixture of oxalates of iron(III) and cobalt (II) was investigated by batch technique. The synthesized nanocomposites were characterized by Fourier transform infrared spectroscopy (FT-IR), X-ray diffraction (XRD), scanning electron microscopy (SEM), energy dispersive x-ray spectroscopy (EDX), transmission electron microscopy (TEM), and vibrating sample magnetometry (VSM). The size of cobalt ferrite nanoparticles formed from oxalate of iron (III) and cobalt (II) precursor was in the range of 6-27 nm. The saturation magnetization (M_s), remanence (M_r) and coercivity (H_c) of the magnetic carbon nanocomposite were found to be 0.2717emu/g, 0.0308emu/g and 338.06 Oe, respectively. The resulting nanocomposite shows extraordinary adsorption capacity and fast adsorption of removal of organic dye, congo red (CR), in water. The adsorption kinetics and isotherm studies were investigated and the results show that the as-prepared AC/CoFe₂O₄ nanocomposite could be utilized as an efficient, magnetically separable adsorbent for the environmental cleanup.

Keywords: Carbon nanocomposites, Magnetic properties, Congo red, Adsorption

5.0 Voight Reaction – Recent Advances and Applications

H. Surya Prakash Rao

Department of Chemistry, Pondicherry University, Pondicherry – 605 014. India
hspr.che@pondiuni.edu.in; hspr@yahoo.com

Voight reaction is for transformation of secondary α -hydroxy ketones into corresponding α -amino ketones. Although discovered as early as 1886, it has not enjoyed wide popularity in organic synthesis as its applicability was restricted to secondary α -hydroxy ketones. In terms of extending the applications of the reaction, we have shown that it takes place on tert- α -hydroxy ketones when present on rigid planar molecular frameworks like phenanthrene, pyrene and acenaphthylene. The reaction is not a simple substitution of the hydroxy group with amines, but goes through imine formation followed by 1,2-C migration. The reaction provides good opportunity for the synthesis of optically active α -amino ketones. We have achieved facile synthesis of some chromatographically separable and optically active tert- α -amino ketones by employing S(-) or R(+)- α -methylbenzylamines in the Voight amination. Details of this work and fall out of research in the area will be covered in the seminar talk.

References:

- (1) RSC Adv. 2012, 2, 6773-6783.
- (2) RSC Adv. 2014, 4, 25747-25758.
- (3) Tetrahedron 2015, 71, 8391-8406.

AUTHOR INDEX

Aarthy Samini A	177	Authidevi P	18	Eswarn K	220
Abaranjitha M	202	Ayeshamariam A	97	Ethiraj J	182,189,196,203
Abarna G	202	Azhagurajan M	28	Ezhilpriya M	27
Abbas Shahul Hameed BH	97	Baby Shanthi A	133	Frank Marken	1
Abdul kathir M	51, 121	Baishnisha Amanulla	149	Ganesan KP	124
Abraham John S	92	Balaji M	60,145	Ganesan Kumaravel	179,189
Akila M	41	Balakrishnan G	175	Ganesan M	175
Akilanda Easwari B	171	Balakrishnan K	196	Ganesan T K	169
Akshay V Salkar	2	Balakrishnan K	204	Ganesh Priya G	134
Alex Mary K	64	Balakumar Vellaichamy	126	Gayathri S	202
Amala Jothi Grace G	153	Balalakshmi C	49	Geetha K	179
Amali Roselin A	12,48,78,118,124,131	Balamurali M	71	Girish Kumar K	86,88
Amarnath TM	48	Bama K	50,73	Gnanamalar K	122,148
Ambika S	51,73	Baranisri T	60	Gnanasundaram I	168
Anaghaa PS	118	Barbara Milow	188	Gomadurai T	184
Anand Tadas	50	Baskar S	47	Gomathi A	53,121, 153
Anandan M	194	Baskaralingam Vaseeharan	140	Gopalakrishnan Balakrishnan	123
Anandan P	28,215	Bharathi K	50	Gopalakrishnan C	38
Anandha Raj J	73,221	Bharathia E	36	Gopalakrishnan Gopu	146, 147
Anandhan N	12,48,78,118,124,131	Bhavanad BVNS	117	Gopinath K	60
Anandhan P	216	Bheeter S R	215	Gopu G	12,20,48,78,118,124,131,150, 82,189,196,203,216
Anandhavelu S	63	Bhuvanalogini G	6	Gopukumar S	163
Anant Achary	47	Bhuvaneshwari S	8,19,36,117	Govintha Raju P	162, 172
Anbarasu G	173, 183	Bornali Sarma	199	Gowri M	35
Angappan S	73	Brundha C	127, 129	Gowri S	58
Anita S	141	Chandramohan G	17	Gowri Shannkari B	46
Anitha AC	82	Chandramohan R	215	Gowshalyadevi R	193,195
Anitha Pushparani J	141	Chandrasekaran P	216	Gurumallesh Prabu H	101,142,194
Anjali KS	118	Chellapandian Kannan	69	Gurunathan K	31,44,48,49,67,83,99,115, 119,131,134,136
Anjana P	118	Chinchu Elezebeth	19	Habibunisha Mubarakali	191
Antony Rajam J	53	Chozhanathmisra M	4,14	Hariharan A	112
Anuradha K	162, 172	Cinnathambi Subramani		HariSuthan	179
Anusha J V	133	Maheswari	30	Hayakawa Y	28
Anusuya S	206	Cristina Delerue-Matos	105,107	Heiner AJ	83,99
Appaswami Lalitha	30, 156	Cyril A	21	Helen Therese	48,49
Archunan G	37,109	Daping He	1	Hemalatha M R K	169
Arivanandhan M	28,215,216	Dhahagani K	186	Ilangeswaran D	155,168
Arockia Selvi J	27	Dhamodharan T K	47	Imran Hussain S	138
Arockiam Sagina Rency	74,154	Dhanalakshmi R	13,25	Imthiyas Ahamed S	163
Arokiyaraj A	214	Dharuman V	12,48,78,83,84,100, 124,131,217	Indira S	180
Arthanareeswari M	27	Diana K	161	Indiran Muralisankar	151
Arumugam A	34,54,55,56,57,58,59,60,111	Dinakaran K	54,112	Isabell S	39
Arumugam Shanmuga Priya	140	Dinesh Christy K	106,158	Ishimwe Francoise	67
Arumugam Veera Ravi	154	Diwakar K	12,13	Iswarya K	73
Arun Prabhu M	44	Dominic J	40,193,195	Ja-an Annie Ho	105
Arun sarma	199	Dons T	215	Janani D	124
Arunadevi R	44	Ebinezer S	178	JananiSree G	202
Arunmozhidevan C	163	Edwinraj S	9	Janapriyan R	163
Arunsunai Kumar K	24,148,185	Elanchezhian B	95,201	Jayabharathi G	17
Ashwin B M	151,123	Elangovan A	182	Jayachandran M	97,103
Asokan K	82	Elanthamilan E	178	Jayalakshmi R	174
		Elavarasan N	62		
		Elena Madrid	1		
		Ellakkiya D	55		

Jayamani A	176	Koushalyaa R	161	Monisha S	47
Jayavel R	28	Krishnan	123	Mothilal K K	182
Jean Claude Nizeyimana	93	Krishnaveni D	197	Muniyandi Ganesan	123
Jegatheeswaran S	31,71,145	Krishnaveni K	26	Muniyappan N	47
Jesny S	86	Krishnaveni M	177	Muralidahrn B	
Jeyachandran Sivakamavalli		Krishnaveni R	33	169,182,196,189,203,204	
	140	Krishnaveni S	159,199	Murugaiah K	169
Jeyakanthan J	90	Kulangiappar K	159	Murugan N	4,14
Jeyanthi V	76	Kumaran R	54	Murugan P	117
John Berchmans L	125	Lakkakula Satish	74,154	Murugavelu M	63
Joseph Ajantha	167	Latha N	35	Murugu Thiruvalluvan. T.M.V	
Kaladevi R	9	Latha R	142		215
Kalaiselvam S	138	Lavanya N	93,94	Muthu Mareeswaran P123,151	
Kalaiselvi C	26	Lokanath NK	90	Muthu S	207
Kalaiselvi K	15	Lorenz Ratke	188	Muthukumar P	177
Kaleeswaran PR	111	Madhangi Priyadharshini G		Muthumariappan S	85
Kaliaperumal Selvaraj	28		161	Muthupandi Kasithevar	98
Kaliyan Bhuvaneswari	156	Magesh Kumar V	51	Muthuraj P	44
Kalpana Devi Rajesh R	164	Mageswari K	187	Muthuraja P 7,90,106,158,162	
Kalyanasundar B	94	Mahalakshmi K	200	Muthusankar G	20
Kalyani R	115,131,134,136	Mahendran R	163	Nachiappan M	90
Kamachi Mudali U	190	Maheshwari N	161	Nagalakshmi M	129
Kamaraj P	27	Malathi M	41,204	Naganathan Dhanalakshmi	84
Kanagavel D	18	Malathy M	173	Nagapriya S	71
Kandasamy P	9	Mamta Prabhugaonkar	2	Nagaraj S	139
Kanmani K	20	Mangaiyarjkarasi R	210	Nagarajan A	189,203
Kannan P	98	Mangala Gowri V	193,195	Nagarajan M	1
Karkuzhali R	23	Manikandan	100	Nagarjun N	177
Karpagam G	75	Manikandan P	184,220	Nagasubramanian S	176
Karpagam J	123	Manikandan Ramesh	154	Nandhini R	162,172
Karpagavinayagam P	141	Manikandan Ramesh	74	Narasimhavarman S	184
Karpuraranjith M	206,209	Manikkaraja C	109	Narayanaperumal Pravin	189
Karthick S	150	Manisankar P		Natarajan Raman 173,179,189	
Karthick SN	31		3,7,41,45,68,90,106,109,119,	Natarajan Suganthi	37
Karthik R	210		21,158,162,219	Natarajan V	215
Karthik R	69	Manivannan N	201	Nathiya D	96
Karthika P	23,89,144	Maniyazagan M	90,103,104	Nathiya RS	16
Karthika V	59	Manjunath R	98	Nathiya S	210
Karthikeyan B	36	Manoj Reddy B	117	Navamani P	205
Karthikeyan M	12,48,	Maragatha J	128	Naveen Kumar G	27
	78,118,124,131	Mariadasse R	90	Naveen S	90
Karthikeyan P		Mariolino Carta	1	Naveenkumar P	76
	4,14,118,193,195	Maruthaiya Karuppaiah	68	Neil B McKeown	1
Karthikumar S	47	Mary Thangam MA	69	Nithya P	144,166
Karuppasamy D	146	Mary Vergheese T	202	Nivethetha B	150
Karuppiah Muthu	43,171	Masilamani K	95	Nivin J	94
Karuppuchamy S		Meenakshi V	54	Oliveira MBPP	107
	62,114,127,128,129,130	Menaka P	57	Padmanaban V C	161,202
Karutha Pandian Divya	83	Meyyathal C	131	Palinci Nagarajan	100
Kasturibai S	67	Mirunalini	39	Pandey N K	190
Kathirvel G	188	Mohamed Azharudeen A	214	Pandimurugan R	42
Kavitha B	44,214,220	Mohammadi Afshan	203	Pandiselvi AR	23
Kavitha C	101	Mohammed Asik S	163	Panneerselvam A	164
Kavitha M	34,57	Mohammed Rafic M	125	Paruthimal Kalaignan G	
Kavitha N	90	Mohan P	5,15	5,9,15,24,32,64,65,67,76	
Kavitha R	121	Mohana	179	Pasupathy N	214
Keerthana S	36	Mohana K	65	Pathanjali GA	1
Kesava M	54	Mohana S	181	Peter J	18
Kiruba R	56	Mohandoss S	120	Ponmudi S	38
Kokila K	62	Mohanraj N	8	Ponmuthuselvi T	102,104

Ponsurya P	97	Ramulu N	159,199	Senthil Kumar A	18
Ponya Utthra Ponnukalai	173	Ramyadevi D	36	Senthil kumar M	45
Prabhavathi K	210	Rani C 72,89,114,137,138,142		Senthil Murugan	123,175
Prabhu	9	Rani Rosaline D	117,133	Senthilkumar A N	197
Pradeepa Prabakaran	22	Rathinam Ramesh	156	Senthilkumar S	24,153
Prakash P	11,21,162,165	Ravikumar R	163	Senthilkumaran M	123,151
Prakash Periakaruppan	98,126	Regina R	99,187	Senthilnathan S	36,119
Prakash S	106,126,158	Revathi T	70,207	Sethuraman V	7,41,63,219
Pramila Selas K	151	Richard Malpass-Evans	1	Shailendera Shukla	8
Premkumar K	90	Roshini Raju	22	Shakkthivel Piraman	65,66,68
Princy Merlin J	178	Rubini K	92	Shalini Menon	88
Priya M	153	Sabine Szunerits	81	Shanmuga Bharathi K	180
Priya P	113	Sachin Kumar	8	Shanmugaiah Karutha Pandian	154
Priyanga S	197	Sakthi Velu K	119,139,140	Shanmugam Easwaramoorthi	167
Priyanka JP	8	Sakthivel A	148,185	Shanmugam Karthik	167
Pullar Vadivel	156	Sakthivel P	108	Shanmugam	
Purnakala Samant	2	Samuvel G	197	Muthusubramanian	158
Pushpa Radhika L	78	Sangeetha C	101	Shanmugam V M	159
Pushpa Raja V	177	Sangeetha S	32,64,65	Shanmugapriya RM	122,148
Pushpa T	115	Sangili A	51,145	Shanmugaraj Gowrishankar	74,154
Radha N	122,148	Sanjeeviraj C	38	Sheela C D	177,200
Radha S	182	Santhi K 72,114,137,138,142		Sinduja B	92
Radhika G	13	Sarala L	178	Sinduja M	47
Raj V	16,113	Saranya S	206	Sirajudheen P	110
Raja A	216	Saranyadevi A	140	Siva Bharathi S	46
Rajaboopathi S	206,208	Saraswathi R	91,125	Sivakumar C	2,77,94
Rajagopal G	186	Sarathi A	148,185	Sivakumar K	92
Rajagopal S	175	Sarathkumar Muthuraja A	145	Sivakumar M	12,13,25,26,79
Rajajeyagantham T	159,199	Saravanakkumar D	97	Sivakumar R	38
Rajalakshmi R T	215	Shanmuganathan		Sivarajini B	213
Rajamohamed S	166	Saravanakumar	192	Sivasakthi S	119
Rajan A	165	Saravanan C	123,151	Sivasubramanian	
Rajan Babu D	28	Saravanan Dhandayutham	211	Santhakumari	154
Rajaraman M	44,51,81,117,133,214,220	Sasikala Sundar	68	Sivasubramanian V K	175
Rajasekar K	184	Sasikumar R	7	Somasundaram	
Rajasekar T S	136	Satheesh Kumar K	40,35,193,195	Meenakshisundaram	146,147
Rajavel R	4,14,173,174,183	Sathiaseelan P	162	Sountharya R	150
Rajendran T	175	Sathishkumar S	4,14	Sowmya Gurusamy	22
Rajesh Madhuvilakku	65,66	Sathiyamoorthy B	184	Sowndharya M	126
Rajeswari K	131	Sathya C	77	Sreeja V	221
Rajeswari P	78	Sathya D	214	Sridharan D	163
Rajeswari R	142	Sathya G	212	Srinithi T	161
Rajkumar P	13,25	Sayee Kannan R	46,149	Srinivasan Alagar	66
Raju T	159	Seeni Meera K	188	Srinivasan G	144
Ramachandran M	79	Seenivasan Rajagopal	123	Srinivasan N	136,181,205
Ramalingam G	31	Sekar C	82,83,84,109	Stalin T	45,90,103,104,119,120,121,1 9,140,212
Raman N	148,185	Sekar K	108	Stanely Britto M	126
Ramar P	47	Sekaran G	27	Stephen Jayakumar P	202
Ramarajan Selvam	191,211	Selva Kumar	179	Suba M	190
Ramasamy Narayanasamy	151	Selvakumar Muniraj	191,211	Subadevi R	12,13,25,26,79
Ramasamy Raja V	117,133	Selvam Chitra	158	Subasree N	27
Ramasamy V	182,196	Selvam Karthick	146,147	Subbulekshmi NL	115
Ramasubramanian S	21	Selvam S	31,60,145	Subramani S	101
Ramaswamy Babu Rajendran	211	Selvamani V	163	Subramani Seethai	43
Ramesh Babu B	146	Selvamurugan M	62	Subramania A	6
Ramesh M	9	Selvanathan G	60,95,145,201		
Ramesh P G	155	Selvarajan S	81		
Ramesh Prabhu Manimuthu	22	Selvi R	78		
		Sengottuvelan N	90,176,187		

Subramanian E	115,133,135	42,63,69,70,206,207,	Veeramani P	219
Subramanian K	112	208,209,210	Velavendan P	190
Sudalaimani S	78	Thamilarasan V	Velayutham D	159,163
Sudha G	135	Thamima M	Velmanirajan K	162,172
Sudha L	21	Thangamuthu Rajendran	Velmurugan A	20
Sudha S	104,153	Thangapandi K	Velrani S	11
Sudhan N	109	Tharanikkarasu K	Veluchamy Kamaraj	
Suganthi A		Tharmaraj P	Sivasubramanian	123
	44,81,117,133,214,220	Thenmozhi U	Venkatachalam R	169,182
Suganya Bharathi B	45,212	Thinakaran N	Venkatesan A	126
Suganya C	48,78	Thirumanavelan Gandhi	Victor Emeka I	104
Suganya G	213	Thirumurugan V	Vidhya R	89
Suganya S	193,195	Thiyagarajan S	Vidhyeswari D	19
Sujatha V	62,126	Umadevi G	Vigneswari S	182,189,196,203
Sumathi D	35	Umadevi J	Vijayakumar A	148,185
Sunderajan Vairam	151	Umadevi S	Vijayan Sri Ramkumar	37
Sundrarajan M		Umamaheswari R	Vimala A	85
	31,50,51,60,71,73,145,166	Usha S	Vinaya Sri T	117
Surendhar A	19	Uttam Kumar	Vincentraj A	214
Surya A	187	Vahidhabanu S	Vinisha Rani K	199
Surya Prakash Rao	152a	Vakula Paranam S	Vinoth G	180
Suryanarayanan V	163	Valanarasu S	Vinothini	138
Swarnalatha S	27	Valarselvan S	Vishnuganth M A	143
Swetha Laxmi K	47	Vasant Naidu	Vishnuprasad	143
Tamil Selvi S	73	Vasantha S	Viswanathan S	
Tamilselvi Duraisamy		Vasanthi C		12,23,48,77,89,102,
	191,211	Vasanthi Muthunayanan		104,105,107,144
Thakur MS	80		Wilson J	96,217,218,219
Thamarachelvan A	182	Vathanaruba M	Yogiananth A	63
Thambidurai S		Vedhi C	Yuanyang Rong	1
		18,53,85,141,153,221		



ADVANCE SCIENTIFIC EQUIPMENT PVT. LTD.

Innovative Solutions • Quality Services

KAILAS ESPLANADE, 'B' WING, 2ND FLOOR, L. B. S. MARG, GHATKOPAR (W), MUMBAI - 400 086. INDIA.
TEL.: (91-22) 2500 2631 / 2500 2632 • FAX : (91-22) 2500 2636 • E-mail : sales@advscientific.com • Web : www.advscientific.com



Product Profile

◆ HORIBA JOBIN YVON S.A.S. --- FRANCE

- Inductively Coupled Plasma Atomic Emission Spectrometer
- Glow Discharge Optical Emission Spectrometer
- Time of Flight Glow Discharge Mass Spectrometer

◆ HORIBA LTD. --- JAPAN

- Laser Scattering Particle Size Distribution Analyzer
- Dynamic Light Scattering Nanoparticle Analyzer

◆ TESCAN BRNO, s.r.o. --- CZECH REPUBLIC

- Conventional & Variable Pressure Scanning Electron Microscope
- High Resolution Schottky Field Emission Scanning Electron Microscope
- Ultra - High Resolution Schottky Field Emission Scanning Electron Microscope
- Combined Focused Ion Beam - Scanning Electron Microscope Systems
- Integrated Mineral Analyzer

◆ SPECTRO A. I. GmbH --- GERMANY

- Combined Polarized / Direct Excitation ED-XRF Spectrometer
- Portable ED - XRF Analyzer
- Micro XRF Analyzer

◆ SKYRAY INSTRUMENT CO. LTD. --- CHINA

- Inductively Coupled Plasma Mass Spectrometer
- Handheld X-Ray Fluorescence Analyzer for Alloy, Mineral, Soil, RoHS

◆ AURORA INSTRUMENTS LTD. --- CANADA

- Atomic Absorption Spectrometer
- Microwave Digestion System

◆ DOTT. GIANNI SCAVINI & C. SNC --- ITALY

- Petroleum Testing Instruments

Branch Offices Delhi • Kolkata • Hyderabad • Chennai • Bangalore • Nagpur • Ahmedabad



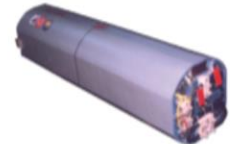
SIMEC 56-15-1



SZ 104



NC 001



SZ 039



FTNC 0155

Power Sources for
HEB
*Aircrafts
Torpedoes
Missiles
Communication
Stationary Applications*



SWA 002



SZ 149



SZ 006



SZ 085

*ISO 9001 : 2000
&
ISO 14001 : 1996
Company*



SZ 101

HIGH ENERGY BATTERIES (INDIA) LIMITED

PAKKUDI ROAD, MATHUR 622 515
Ph : 91-431-2660314 Fax : 91-4339-250516
Email : info@highenergyltd.com
Web Site : www.highenergyltd.com



ISBN 978-81-928690-7-0



9 788192 869070 >

₹ 1000 US \$ 30